

Corresponding State Relations for the Viscosity of Moderately Concentrated Polymer Solutions

L. UTRACKI* and ROBERT SIMHA, *Department of Chemistry, University of Southern California, Los Angeles, California*

Synopsis

Corresponding state relationships are considered for good (toluene) and θ -solvents. The polymers investigated are polystyrene, polymethyl methacrylate, and a copolymer of approximately 49 mole-% of methyl methacrylate with styrene. The choice of the reduced variables $\eta_{sp}/(c[\eta])$ and c/γ permits the construction of master curves, characteristic of a given polymer-solvent system over a wide range of molecular weights. The concentration parameter γ varies with the degree of polymerization less rapidly than c_0 , the concentration for overlap of average coils, particularly in the good solvent. Here γ is independent of temperature. In cyclohexane, γ is proportional to the critical concentration for phase separation. The existence of such universal relations results in an explicit form for the coefficients of the power series expansions of the viscosity as a function of c . In particular the parameter k_1 is predicted to be a slowly decreasing function of molecular weight in the good solvent, but to be almost independent in cyclohexane. This is in accordance with recent observations for polystyrene fractions below 50,000. However, the scatter in the experimental data does not permit a quantitative comparison. Moreover, the results must be sensitive to polydispersity and depend on higher moments of the distribution, as is indicated by the relation between γ and the critical concentration.

Introduction

In the course of investigating hydrodynamic and thermodynamic factors determining the viscosity of polymer solutions, Weissberg et al.¹ and Simha and Zakin² searched for reduced variables which would result in universal or, at least, molecular weight independent representations of the viscosity as a function of concentration for a given polymer-solvent system. Such relations would provide a guide for the further development of theory, besides having an obvious practical utility.

The aforementioned authors studied several polymers in good as well as poor solvents, going as far as θ -solvents. The viscosity variable used was simply the ratio $\eta_{sp}/(c[\eta])$. The reduced concentration was expressed in terms of c_0 , the concentration at which the average polymer coils, treated as equivalent spheres, would start to overlap. If the dimensions of these spheres are taken to be those existing at infinite dilution, they can be approximately related to the intrinsic viscosity.¹⁻³ The choice of these variables yielded relationships for a given polymer nearly independent of

* Permanent address: Polish Academy of Sciences, Polytechnic Institute, Lodz, Poland.

molecular weight in good solvents, at least between 100,000 and 600,000. In poor solvents, on the other hand, the departures appeared to become more pronounced. One problem in this work, of course, was presented by the differences in the molecular weight distributions of the samples, which varied widely in average molecular weight and were of different origin.

In this paper it will first be shown that viscosity-concentration curves for different degrees of polymerization are superimposable, both in good and poor solvents. Secondly, it will be possible to relate the concentration factor in the θ -solvent simply to a thermodynamically significant quantity. The experimental data used are drawn from refs. 1 and 2, augmented by unpublished results of the present authors. Thus a detailed discussion will be given of polystyrene solutions in toluene at two temperatures and in cyclohexane (approximately θ), since a large number of fractions, although of variable or unknown width have been investigated. The data on polymers of methyl methacrylate and its copolymer with styrene encompass only two molecular weights, so that the conclusions are limited. The concentration range extends to about $2/[\eta]$.^{1,2}

Analysis

Our general procedure has been to plot on a double logarithmic scale $\eta_{sp}/(c[\eta])$ vs. c and then to attempt superposition of the curves for different fractions. Figure 1 exhibits the result for polystyrene solutions in toluene at 30^{1,2} and 48°C.¹ (see Table I for the characteristics of the samples).

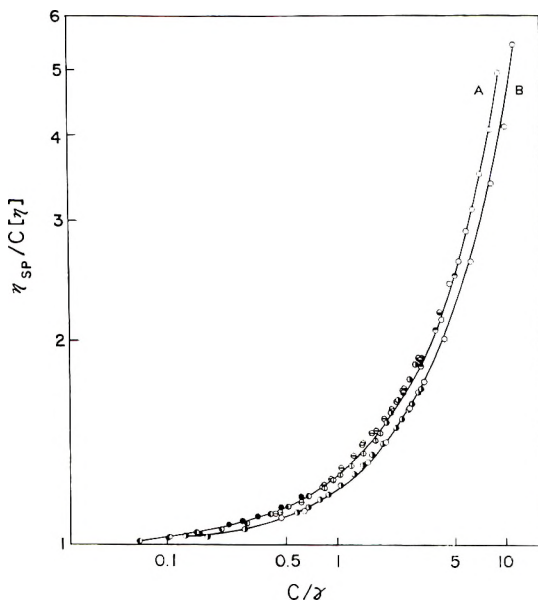


Fig. 1. Reduced viscosity-concentration curves: A, polystyrene in toluene, 30°C. (refs. 1, 2); B, same, 48.2°C. (ref. 1). Solid line for $\bar{M}_n = 146,000$; (○) 1; (●) 3; (◻) 4; (◐) 5; (◑) 6; (◒) 7; (◓) 8; (◔) 9. Numbers refer to Table I.

The curve represents the viscosity-concentration relation for the fraction with $\bar{M}_n = 146,000$. On this master curve are superimposed experimental points for eight other degrees of polymerization, by ascribing to each species a shift factor $\gamma(\bar{M}_n)$ in respect to concentration. Specifically, the following procedure was applied in the placement of points onto curve A, Figure 1 and onto Figure 2 for the upper and lower part two pairs (Nos. 1, 5, 7, and 8, Table I) were selected which cover the appropriate regions of ordinate values. The intermediate portions were subdivided into overlapping sections. Into each of these, experimental points for one particular molecular weight were placed. For 48°C. in toluene, only three molecular

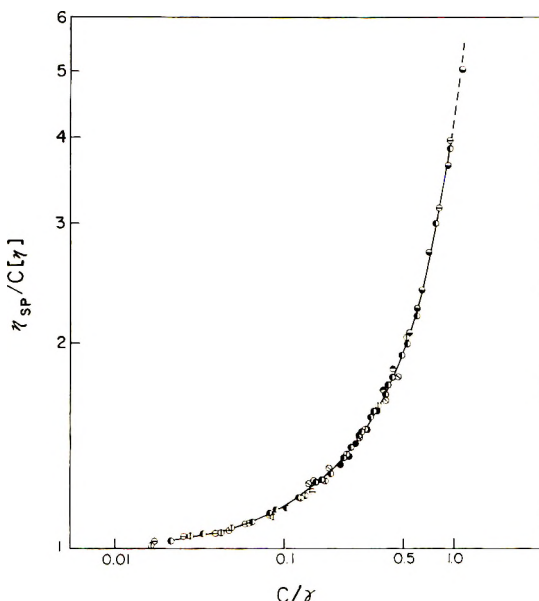


Fig. 2. Reduced viscosity-concentration curves; polystyrene in cyclohexane 34°C. Solid line for $\bar{M}_n = 150,000$; (●) 4; (⊙) 5; (⊕) 6; (●) 8; (⊖) 9; (⊗) 10; (⊙) 11. Numbers refer to Table I.

weights are available. Within this limitation, the factor γ has the same value for a given degree of polymerization as at 30°C. It is impossible to exhibit the complete experimental information available, but Figures 1 and 2 cover the whole range of molecular weights and no systematic deviations are detectable. In the latter the dotted portion of the curve signifies that no experimental datum is available for the reference polymer ($\bar{M}_n = 150,000$) in this range of concentrations. For convenience the γ -values are also tabulated in Table I.

The analogous procedure results in as satisfactory master plots as can be expected for the two fractions of polymethyl methacrylate and the copolymer in good and θ -solvents. The γ -values for these systems are listed in Table II.

TABLE I
 Characteristics of Polystyrene Fractions

No.	Method of prepn.	$\bar{M}_n \cdot 10^{-3}$	\bar{M}_w/\bar{M}_n	Solvent	Temp., °C.	γ	k_1	$[\eta]k_1$	Ref.
1	Thermal	600	?	Toluene	30	0.331	0.38	0.772	1
2	Thermal	146	?	Toluene	30	1	0.37	0.264	1
3	"	58	?	"	30	1.810	0.32	0.119	1
4	"	600	1.6	"	30	0.394	0.34	0.689	2
4	"	600	1.6	Cyclohexane	34	0.457	—	—	2
5	"	167	?	"	34	0.938	—	—	2
5	"	167	?	Toluene	30	0.950	0.37	0.289	2
6	"	45	?	Cyclohexane	34	1.77	—	—	2
6	"	45	?	Toluene	30	2.08	0.40	0.123	2
7	Anionic	150	1.11	"	30	1	0.31	0.227	2
7	Anionic	150	1.11	Cyclohexane	34	1	—	—	2
8	"	40	1.35	Toluene	30	2.26	0.41	0.114	2
8	"	40	1.35	Cyclohexane	34	1.86	—	—	2
9	"	15	?	"	34	2.65	—	—	2
9	"	15	?	Toluene	30	3.63	0.46	0.065	2
10	"	545	?	Cyclohexane	34	0.465	—	—	a
11	"	300	?	"	34	0.708	—	—	a
12	"	36	?	"	34	1.69	—	—	a

^a Unpublished; \bar{M}_n from viscosity data.

 TABLE II
 Characteristics of Polymethyl Methacrylate and Copolymers^a

Polymer	Solvent	Temp., °C.	$\bar{M}_n \cdot 10^{-3}$	γ
			470	1
	Toluene	30	137	1.78
Polymethyl methacrylate			470	1
	4-Heptanone (θ -solvent)	31.8	137	1.95
			630	1
	Toluene	30	217	1.99
Copolymer:				
51.4 mole-% styrene + 48.6 mole-% methyl methacrylate	43.5 vol-% <i>n</i> -heptane, 56.5% methyl isopropyl ketone (θ -solvent)	25	630	1
			217	1.73

^a See ref. 2.

Discussion

Having thus shown that corresponding state variables can be defined in respect to concentration and molecular weight, it is of interest to examine the molecular weight dependence of γ . This permits us to establish whether or not this factor can be related to other characteristic concentra-

tion parameters of the system. Figure 3 shows plots of γ vs. \bar{M}_n for polystyrene and the two solvents. Here no attempt has been made to correct for differences in molecular weight distribution. They can only be conjectural as long as the physical significance of γ is not established or suitable experimental comparisons of polymer fractions, blends, and/or whole polymer are not undertaken. The equations of the two straight lines *B, C* are:

$$\begin{aligned}\gamma (\text{toluene}) &= 19.55 \times 10^2 \bar{M}_n^{-0.640} & (1) \\ \gamma (\text{cyclohexane}) &= 2.596 \times 10^2 \bar{M}_n^{-0.471}\end{aligned}$$

The first equation is derived from a least square analysis. The second actually represents a line drawn parallel to the line *A*. The points defining the latter represent the critical volume fractions v_{2c} for phase separation, as determined by Debye et al.⁴ and Debye and Chu⁵ for a series of relatively narrow fractions ($\bar{M}_w/\bar{M}_n \leq 1.19$). The equation of the least square line *A* is:

$$v_{2c} = 13.82 \times 10^2 \bar{M}_n^{-0.471} \quad (2)$$

The results then suggest that γ in cyclohexane is proportional (or may be taken as equal) to c_c , the concentration for phase separation. It is not possible to examine the validity of such a result in toluene and it will therefore be of interest to see what happens in cyclohexane at $T \neq \theta$.

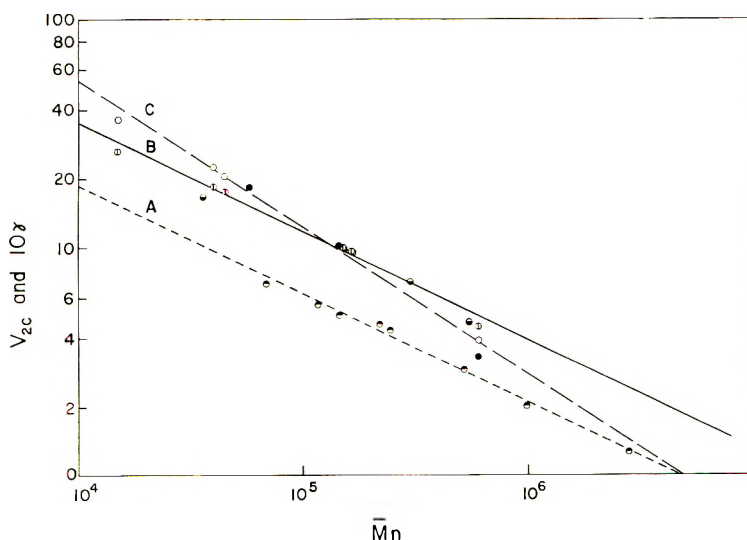


Fig. 3. Concentration parameter γ for polystyrene solutions as a function of \bar{M}_n . *A*, Critical volume fraction v_{2c} for polystyrene-cyclohexane [(●) refs. 4 and 5]. *B*, Cyclohexane, 34°C. [(⊕) ref. 2 (⊙) unpublished data]. *C*, Toluene, 30° and 48.2°C., [(●) ref. 1 (○) ref. 2]. Lines represent eqs. (1) and (2).

It follows from eq. (1) that the previously introduced¹⁻³ variable c_0 and γ are related by the expressions:

$$\begin{aligned} c_0/\gamma &= \text{const. } \bar{M}_n^{-0.082}; \text{ toluene} \\ c_0/\gamma &= \text{const. } \bar{M}_c^{-0.024}; \text{ cyclohexane, } 34^\circ\text{C.} \end{aligned}$$

Thus an appreciable contraction of the c/c_0 scale results in toluene, which is more significant for the higher molecular weights. This would tend to bring the different fractions closer together. In the θ -solvent this effect is minimized. Part of the earlier failure to obtain universal plots is due to the choice of a computed c_0 , whereas the γ 's used in Figures 1 and 2 are not derived from eq. (1) but allowed to scatter to the extent exhibited in Figure 3. Moreover, if γ is related to the critical concentration c_c , it must depend on higher moments of the size distribution and be sensitive to variations in the latter.

The results of Figures 1 and 2, combined with eq. (1), lead to a statement regarding the molecular weight dependence of the parameters k_i , which are defined by the expansions:

$$\eta_{sp}/(c[\eta]) - 1 = \sum_i k_i[\eta]^i c^i$$

Writing for the left-hand side a universal function $f(c/\gamma)$ and expanding $f(c/\gamma) = \sum_i a_i(c/\gamma)^i$, we have

$$k_i = a_i(\gamma[\eta])^{-i} \quad (3)$$

where a_i is independent of molecular weight.

Equations (1) and (3) yield in particular:

$$\begin{aligned} k_1 &= \text{const. } \bar{M}_n^{-0.024}; \text{ cyclohexane} \\ k_1 &= \text{const. } \bar{M}_n^{-0.082}; \text{ toluene} \end{aligned} \quad (4)$$

Experimental data^{2,6} indicate a trend for k_1 to increase in toluene with decreasing \bar{M}_n below about 50,000. Figure 4 shows the data together with a curve, eq. (4), and a proportionality factor fitted to the lowest molecular weight. In the light of the frequently observed scatter in k_1 -values, all that can be said is that the curve, as drawn, is not unreasonable. Figure 5 compares for toluene the product $k_1[\eta]$ with γ as a function of \bar{M}_n according to eq. (3). It appears that the points cluster roughly into three groups, depending upon whether the ratio \bar{M}_w/\bar{M}_n exceeds 2.4, lies between 2.4 and 1.18, or is less than 1.18.

We have also examined the dependence of $k_1[\eta]$ on higher averages. A double logarithmic plots vs. \bar{M}_w does permit the drawing of a single line with moderate scatter. However, there is upward curvature below $\bar{M}_w = 50,000$ and above 700,000. Next, an attempt was made to estimate \bar{M}_z , by extending the procedure of Lundberg et al.⁷ The resulting plot is linear and describes the data for the anionic polymers between \bar{M}_z of 12,000 and 1,300,000 quite well. However, all the thermally or free-radical polymerized samples yield points lying systematically below the line, but could be fitted to a second straight line. This separation

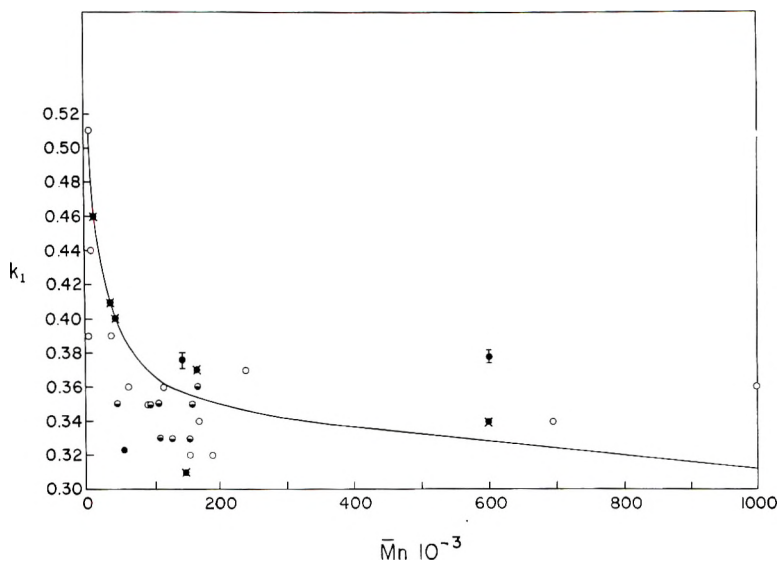


Fig. 4. Parameter k_1 for polystyrene in toluene as a function of \bar{M}_n . [Line, eq. (4)]. (●) 30°C., ref. 1; (◐) 30°C., ref. 2; (○) 25°C., ref. 6, anionic polymer; (◑) 25°C., ref. 6, thermal polymer; (◒) 48°C., ref. 1.

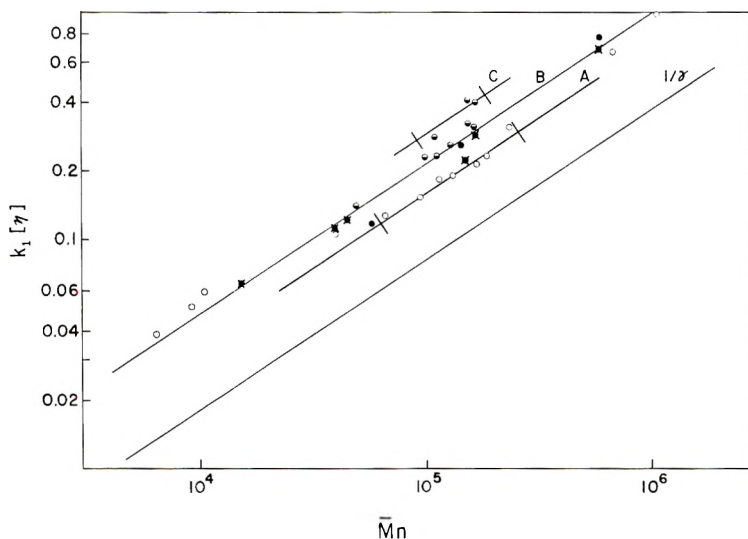


Fig. 5. Product $k_1[\eta]$ as a function of \bar{M}_n ; polystyrene in toluene. Lowest line $1/\gamma$ according to eq. (1). Points are distinguished according to three ranges of polydispersity (see Table I). (●) 30°C., ref. 1; (◐) 30°C., ref. 2; (○) 25°C., ref. 6, anionic polymer; (◑) 25°C., ref. 6, thermal polymer.

into two groups may reflect differences in the molecular weight distribution types. The result is of some interest in spite of the uncertainties of the method used to compute \bar{M}_z and of the data used.

In order to arrive at analytical representations of the master curves, it is preferable to replot them in semilogarithmic form. This is done in Figure

TABLE III
Parameter k_1 ; Polystyrene in Toluene, 25°C.^a

$\bar{M}_n \cdot 10^{-3}$	\bar{M}_w/\bar{M}_n	k_1	$[\eta]k_1$
Anionic Samples			
6.4	1.64	0.51	0.039
9.2	1.50	0.50	0.051
10.5	1.95	0.44	0.060
40	1.35	0.39	0.108
66	1.18	0.36	0.129
95	1.16	0.35	0.154
116	1.08	0.36	0.185
131	1.08	0.33	0.191
170	1.07	0.34	0.218
189	1.11	0.32	0.233
239	1.04	0.37	0.311
694	1.18	0.34	0.661
1000	1.19	0.36	0.980
Thermal Samples			
49	2.41	0.35	0.144
99	1.90	0.35	0.234
111	1.94	0.33	0.235
130	1.96	0.33	0.260
110	2.38	0.35	0.284
161	1.77	0.35	0.312
157	2.23	0.32	0.323
168	2.47	0.36	0.404
157	2.85	0.33	0.407

^a See Ref. 6.

6. Note that Martin's linear empirical relation is obeyed for the θ -solvent in accordance with the earlier observation¹ of its validity in poor solvents. A common tangent appears at the origin. It is possible to fit a four parameter relation to the curves for toluene which reads as follows:

$$\log_{10} (\eta_{sp}/c[\eta]) = Ax + Bx_0 \left\{ 1 - \left[\left(\frac{x}{x_0} - 1 \right)^2 + C \right]^{1/2} \right\}; \quad (5)$$

$$x = c/\gamma$$

The numerical values of the parameters are:

$$30^\circ\text{C}.: A = 8.09 \times 10^{-2}, B = 1.53 \times 10^{-2}, x_0 = 2.124,$$

$$C = 9.47 \times 10^{-2}$$

$$48.2^\circ\text{C}.: A = 7.90 \times 10^{-2}, B = 1.72 \times 10^{-2}, x_0 = 1.750,$$

$$C = 11.1 \times 10^{-2}$$

Equation (5) is derived from the observation that the curves in Figure 6 can be approximated by straight lines for small and large x , respectively. These regions have been bridged by a hyperbolic relation. It should be noted that eq. (5) does not have the correct limit for $c \rightarrow 0$, since the right-hand side reduces to $-BCx_0/2$, considering that C is much less than unity.

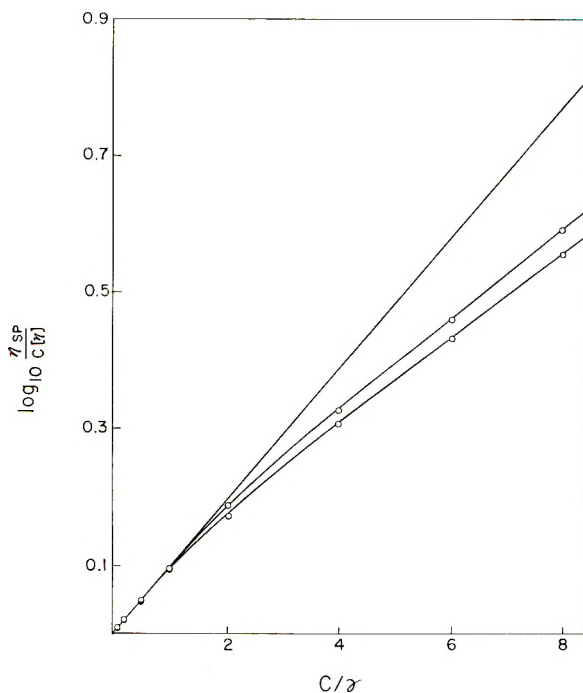


Fig. 6. Comparison of master curves Figs. 1 and 2 in semilogarithmic form, with eq. (5) indicated by points.

This results in a limiting value of $\eta_{sp}/(c[\eta])$ equal to about 0.996. However, for the range of interest here, the extent of agreement between the plotted master curves and the calculated points may be judged from Figure 6.

The next step along the lines discussed in this paper would be a study of universal relations encompassing different polymer-solvent systems. This would include temperature effects. Consideration of these matters will be postponed.⁸

It is a pleasure to acknowledge the support of this work by a grant from the California Research Corp. Some of the numerical computations were carried out at the Jet Propulsion Laboratory, California Institute of Technology, through the courtesy of Dr. R. F. Landel.

References

1. Weissberg, S. G., R. Simha, and S. Rothman, *J. Res. Natl. Bur. Std.*, **47**, 298 (1951).
2. Simha, R., and J. L. Zakin, *J. Colloid Sci.*, **17**, 270 (1962).
3. Simha, R., and J. L. Zakin, *J. Chem. Phys.*, **33**, 1791 (1960).
4. Debye, P., H. Coll, and D. Woermann, *J. Chem. Phys.*, **33**, 1746 (1960).
5. Debye, P., D. Woermann, and B. Chu, *J. Chem. Phys.*, **36**, 851 (1962).
6. McCormick, H. W., *J. Colloid Sci.*, **16**, 635 (1961).
7. Lundberg, J. L., M. Y. Hellman, and H. L. Frisch, *J. Polymer Sci.*, **46**, 3 (1960).
8. Utracki, L., and R. Simha, *J. Phys. Chem.*, in press.

Résumé

On a étudié les relations entre les états correspondants pour un bon solvant (toluène) et des solvants θ . Les polymères étudiés sont le polystyrène, le polyméthacrylate de méthyle et un copolymère d'environ 49 mole-% de méthacrylate de méthyle avec le styrène. Le choix des variables réduites $\eta_{sp}/(c[\eta])$ et c/γ permet de construire des courbes étalons qui sont caractéristiques pour un système donné polymère-solvant sur une large rangée de poids moléculaires. Le paramètre de concentration γ varie moins vite avec le degré de polymérisation que c_0 (la concentration pour recouvrement des pelotes statistiques moyennes) spécialement dans le cas d'un bon solvant. Dans celui-ci γ est indépendant de la température. Dans le cyclohexane γ est proportionnel à la concentration critique de séparation des phases. L'existence de telles relations universelles donne lieu à une forme explicite pour les coefficients du développement en série de la viscosité en fonction de c . En particulier le paramètre k_1 devrait être dans un bon solvant une fonction légèrement décroissante du poids moléculaire, mais presque indépendant dans le cyclohexane. Ceci est en accord avec des observations récentes pour des fractions de polystyrène en dessous de 50.000. Néanmoins les fluctuations des données expérimentales empêchent une comparaison quantitative. De plus, les résultats doivent être sensibles à la polydispersité et encore plus à la distribution, ce qui est démontré par la relation entre γ et la concentration critique.

Zusammenfassung

Beziehungen für übereinstimmende Zustände werden für gute (Toluol) und θ -Lösungsmittel in Betracht gezogen. Als Polymere wurden Polystyrol, Polymethylmethacrylat und ein Copolymeres aus etwa 49 Mol% Methylmethacrylat und Styrol untersucht. Die Wahl der reduzierten Variablen $\eta_{sp}/(c[\eta])$ und c/γ erlaubt die Konstruktion von Einheitskurven, die für ein gegebenes Polymer-Lösungsmittelsystem über einen weiten Molekulargewichtsbereich charakteristisch sind. Der Konzentrationsparameter γ ändert sich mit dem Polymerisationsgrad, besonders im guten Lösungsmittel, weniger rasch als c_0 , die früher verwendete Konzentration für die Überlappung der mittleren Knäuel. Hier ist γ von der Temperatur unabhängig. In Cyclohexan ist γ der kritischen Phasentrennungskonzentration proportional. Das Bestehen solcher universeller Beziehungen führt zu einer expliziten Form für die Koeffizienten der Potenzreihenentwicklung der Viskosität als Funktion von c . Im besonderen wird für den Parameter k_1 die Aussage gemacht, dass er im guten Lösungsmittel eine langsam abnehmende Funktion des Molekulargewichts, in Cyclohexan aber fast unabhängig davon ist. Das steht in Übereinstimmung mit neueren Beobachtungen an Polystyrolfraktionen unterhalb 50000. Die Streuung der Versuchsdaten erlaubt aber keinen quantitativen Vergleich. Ausserdem müssen die Ergebnisse von der Polydispersität abhängen und zwar von höheren Momenten der Verteilung, wie die Beziehung zwischen γ und der kritischen Konzentration zeigt.

Received May 18, 1962

On the Helical Structure of Polytetrafluoroethylene

MACHIO IWASAKI, *Government Industrial Research Institute,
Nagoya, Japan*

Synopsis

The molecular parameters of polytetrafluoroethylene were determined from x-ray diffraction data (Bunn and Howells) as C—C = 1.54 Å, C—F = 1.36 Å, \angle CCC = $114^{\circ}36'$, \angle FCF = $108^{\circ}30'$; each angle of internal rotation around each C—C bond is $16^{\circ}28'$ from the *trans* position. Calculation of the angle of internal rotation for the most stable configuration of the polymer chain was carried out based on the steric and electrostatic interactions. The minimum position of the potential energy seems to be subject chiefly to the steric interaction. The effect of the electrostatic interaction on the minimum position was rather small as compared with the steric interaction. The calculated angle of internal rotation and the fiber period are, respectively, 19° and 16.7 Å, which are in very good agreement with the experimental values $16^{\circ}28'$ and 16.8 Å.

Introduction

Bunn and Howells¹ studied the molecular structure of polytetrafluoroethylene by x-ray diffraction and reported that the polymer chain has a helical structure due to slight distortion from a planar zigzag configuration. They attributed this distortion to overcrowded fluorine atoms attached to the carbon chain. In this connection it may be interesting to calculate the hindering potential energy of the fluorocarbon chain and to compare the minimum position of the potential energy with the observed helical structure.

We have studied the internal rotation of some fluorochloroethanes by electron diffraction² and determined the rotational angles of the *gauche* isomers. It was shown that the observed angles of rotation were in good agreement with the values calculated from the steric and electrostatic interactions (see Table I). Because of this result it was interesting to determine the angle of internal rotation of polytetrafluoroethylene on the same basis of calculation.

TABLE I
Observed and Calculated Rotational Angles^a of the *Gauche* Isomers

Molecule	Observed angle, deg.	Calculated angle, deg.
CF ₂ Cl—CF ₂ Cl	117.5	116
CFCl ₂ —CF ₂ Cl	122	124
CFCl ₂ —CFCl ₂	121	118

^a Rotational angles were measured from the *trans* form for the first and third molecules, and from the C_s form for the second molecule.

Angle of Internal Rotation and Molecular Parameters

Bunn and Howells¹ reported that the fiber period of polytetrafluoroethylene is 16.8 Å, 13 carbon atoms being included, and that the radii of the fluorine and the carbon helices are 1.64 and 0.42 Å, respectively. If we describe a helix by a radius, ρ , a pitch, d , and an angle of rotation around an axis of a helix, θ , the experimental data for the carbon helix of polytetrafluoroethylene gave $\rho = 0.42$ Å, $d = 1.292$ Å, and $\theta = 166^\circ 09'$, where θ was measured from the *cis* position. These parameters can be related to the C—C bond distance, r , the CCC bond angle, φ , and the angle of rotation around the C—C bond, τ , by the following equations:³

$$r^2 = d^2 + 4\rho^2 \sin^2 (\theta/2) \quad (1)$$

$$\cos (\varphi/2) = (1 - d^2/r^2)^{1/2} \sin (\theta/2) \quad (2)$$

$$\tan (\tau/2) = (d/r) \tan (\theta/2) \quad (3)$$

Therefore all the molecular parameters for the carbon skeleton can be determined from the values of ρ , d , and θ as follows: $r = 1.54$ Å, $\varphi = 114^\circ 36'$, and $\tau = 163^\circ 32'$. The C—C bond distance and the CCC bond angle obtained seem to be very reasonable when compared with those of other hydrocarbons. Since the angle of rotation was measured from the *cis* position, it corresponds to $16^\circ 28'$ from the *trans* position. This means that the carbon chain of polytetrafluoroethylene twists $16^\circ 28'$ around each C—C bond from the planar zigzag structure.

Although the x-ray data available are not sufficient to determine a unique set for the rest of the molecular parameters, the C—F bond distance and the FCF bond angle, there exists a correlation between the two parameters which reveal the observed radius of the fluorine helix. The following relation was derived for the fluorine helix by the same treatment used in the derivation of eqs. (1)–(3):

$$4R^2[1 - \cos^2 (\tau/2) \sin^2 \alpha] - 4Rr \cos \alpha + r^2 - d^2 - 4\rho_F^2 \sin^2 (\theta/2) = 0 \quad (4)$$

where R is the C—F bond distance, ρ_F the radius of the fluorine helix, and α the CCF bond angle which is related to the FCF bond angle β by the relation

$$\cos \alpha = -\cos (\beta/2) \cos (\varphi/2) \quad (5)$$

Figure 1 shows the correlation between the C—F bond distance and the FCF bond angle calculated from eqs. (4) and (5). Although any point on the line indicated in Figure 1 reveals the observed radius of the fluorine helix, the combination of 1.36 Å for C—F bond distance and $108^\circ 30'$ for the FCF bond angle appears to be most reasonable for polytetrafluoroethylene since the C—F bond distance and FCF bond angle of CF_2H_2 are 1.358 Å and $108^\circ 17'$ respectively.⁴ This combination also gives the

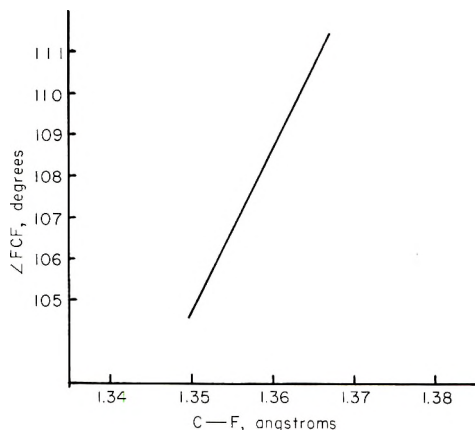


Fig. 1. Correlation between the C—F bond distance and the FCF bond angle. Any point on this line gives the same value as the observed radius of the fluorine helix.

reasonable value $108^{\circ}24'$ for the CCF bond angle. The molecular parameters thus obtained are given in Table II.

TABLE II
Molecular Parameters of Polytetrafluoroethylene

Bond distances		Angles			
C—C	C—F	CCC	FCF	CCF	Rotational ^a
1.54 A.	1.36 A.	$114^{\circ}36'$	$108^{\circ}30'$	$108^{\circ}24'$	$16^{\circ}28'$

^a Rotational angle was measured from the *trans* position.

Hindering Potential

It is said that the internal rotation around a single bond is subject mainly to the steric and electrostatic interactions, so that

$$V = V_{st} + V_{el} \quad (6)$$

where V_{st} is the contribution from the steric interaction and V_{el} is that from the electrostatic interaction. The steric interaction of polytetrafluoroethylene consists of three terms as follows:

$$V_{st} = V(\text{FF}) + V(\text{FC}) + V(\text{CC}) \quad (7)$$

where $V(\text{FF})$, $V(\text{FC})$, and $V(\text{CC})$ are the interactions between fluorine and fluorine, fluorine and carbon, and carbon and carbon, respectively. If the interactions with fluorine atoms attached to neighboring carbon atoms higher than the second are neglected, the $V(\text{FF})$ consists of six terms having interatomic separations different from each other, as shown in (Fig. 2):

$$V(\text{FF}) = (4n - 2)V_t(\text{FF}) + (2n - 1)V_g(\text{FF}) + (2n - 1)V_g'(\text{FF}) \\ + 4(n - 1)V_i(\text{FF}) + 2(n - 1)V_s(\text{FF}) + (2n - 1)V_s'(\text{FF}) \quad (8)$$

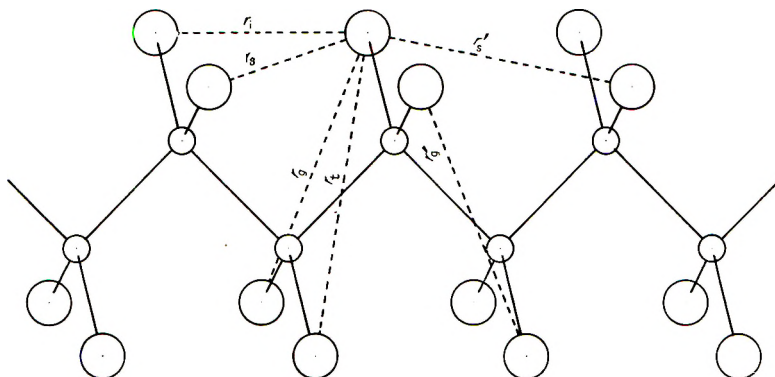


Fig. 2. Possible different fluorine-fluorine distances (r) of the first and second neighbors (dependent on the rotation around the C—C bond); subscripts i , s , g , and t stand for *isotactic*, *syndiotactic*, *gauche*, and *trans*.

where n is the number of monomeric units and V_t , V_g , V_i , and V_s are the contributions from the F—F pairs corresponding to *trans*, *gauche*, *isotactic*, and *syndiotactic* configurations, respectively. Since there are two kinds of *gauche* and *syndiotactic* distances to be distinguished when the carbon chain twists around the C—C bond, V_g' and V_s' are added to eq. (8); $V_g = V_g'$ and $V_s = V_s'$ when the carbon chain is planar. There is no need to take into consideration the nearest F—F distance, which does not change with the rotation around the C—C bond. When $n \gg 1$, the potential energy per monomer unit is:

$$V(\text{FF}) = 4V_t(\text{FF}) + 2V_g(\text{FF}) + 2V_g'(\text{FF}) + 4V_i(\text{FF}) + 2V_s(\text{FF}) + 2V_s'(\text{FF}) \quad (9)$$

The change in both $V(\text{FC})$ and $V(\text{CC})$ with the rotation around the C—C bond may be much smaller than that of the $V(\text{FF})$, for the following reason. For the $V(\text{FC})$, the separation between a carbon atom and a fluorine atom attached to the first neighboring carbon atom does not change with the rotation. If the interactions with fluorine atoms attached to neighboring carbon atoms higher than the second are neglected, the part of the $V(\text{FC})$ dependent on the rotation consists of two terms corresponding to two kinds of *gauche* distances:

$$V(\text{FC}) = V_g(\text{FC}) + V_g'(\text{FC})$$

Since one of the *gauche* distances increases with the rotation around the C—C bond while another decreases, $V(\text{FC})$ may remain almost unchanged with the rotation. For the $V(\text{CC})$, only one term corresponding to the *trans* distance may be of importance. However, since we are interested in a small distortion from the *trans* configuration for which the potential energy would be fairly small, the change of $V(\text{CC})$ with the rotation may be negligible.

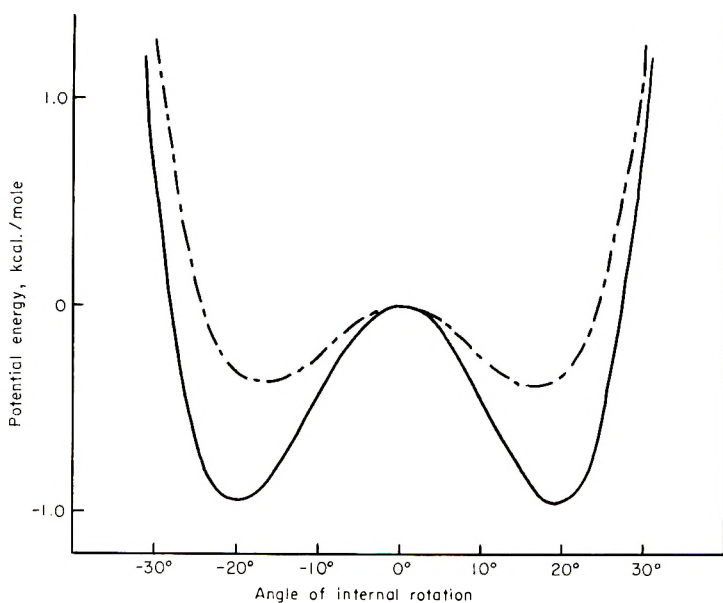


Fig. 3. Hindering potential of polytetrafluoroethylene: (—) total potential energy; (---) steric interaction.

For these reasons both the $V(\text{FC})$ and $V(\text{CC})$ were neglected and only the $V(\text{FF})$ was estimated from the modified Buckingham-type potential proposed by Kreevoy and Mason:⁵

$$V(\text{FF}) = (1.057 \times 10^5) \exp \{-4.608r\} - 125.1/r^6 \quad (11)$$

where the potential energy is in kilocalories per mole and the distance r is angstroms.

For the electrostatic interaction, only the dipole-dipole interaction was estimated:

$$V_{\text{el}} = (\mu_1\mu_2/r^3)(\cos \chi - 3 \cos \alpha_1 \cos \alpha_2) \quad (12)$$

where μ is the bond dipole moment, r the distance between the two dipoles, χ the angle between the two dipoles, and α the angle between the two vectors \mathbf{r} and $\mathbf{\mu}$. The bond dipole moment was estimated by a method described in a previous paper,² the induced moment being taken into account.

With the use of the molecular parameters listed in Table II, the potential energy was calculated as a function of the angle of internal rotation around the C—C bond. As shown in Figure 3, the V_{st} has its minimum value at $17^\circ 30'$ which is in surprisingly good agreement with the observed value of $16^\circ 28'$. The electrostatic interaction energy has a rather small effect on the minimum position of the potential energy, making a small shift of 19° , as shown in Figure 3. The fiber period calculated from this minimum position is 16.7_8 Å, and is in very good agreement with the observed value of 16.8 Å. It is interesting that such a simple calculation agrees so well with

observation. The potential function proposed by Kreevoy and Mason⁵ seems to give very good information at least near the potential minimum.

References

1. Bunn, C. W., and E. R. Howells, *Nature*, **174**, 549 (1954).
2. Iwasaki, M., *Bull. Chem. Soc. Japan*, **32**, 205 (1959).
3. Shimanouchi, T., and S. Mizushima, *J. Chem. Phys.*, **23**, 82 (1955).
4. Lide, D. R., *J. Am. Chem. Soc.*, **74**, 3548 (1952).
5. Kreevoy, M. M., and E. A. Mason, *J. Am. Chem. Soc.*, **79**, 5481 (1957).

Résumé

On a déterminé les paramètres moléculaires du polytétrafluoroéthylène à partir des données de la diffraction aux rayons-x (Bunn et Howells) comme suit: C—C = 1.54 Å, C—F = 1.36 Å, \angle CCC = 114°36', \angle FCF = 108°30', et chaque angle de rotation interne autour de chaque liaison C—C est de 16°28' pour la position *trans*. L'angle de rotation interne pour la configuration la plus stable de la chaîne polymérique a été calculé en se basant sur l'interaction stérique et électrostatique. La position minimale de l'énergie potentielle semble être dépendant surtout de l'interaction stérique. L'effet de l'interaction électrostatique sur la position minimale est plutôt négligeable comparé à l'interaction stérique. L'angle calculé d'interaction interne et l'élément périodique ont une valeur respective de 19° et 16.7₈ Å, qui correspondent très bien aux valeurs expérimentales de 16°28' et 16.8 Å.

Zusammenfassung

Für die Molekülparameter von Polytetrafluoräthylen wurden aus Röntgenbeugungsdaten (Bunn and Howells) folgende Werte bestimmt: C—C = 1,54 Å, C—F = 1,36 Å, \angle CCC = 114°36', \angle FCF = 108°30' und der Winkel der inneren Rotation um jede C—C-Bindung beträgt 16°28' von der *trans*-Stellung. Der Winkel der inneren Rotation für die stabilste Konfiguration der Polymerkette wurde auf Grund der sterischen und elektrostatischen Wechselwirkung berechnet. Die Lage des Minimums der potentiellen Energie scheint hauptsächlich durch sterische Wechselwirkung bestimmt zu sein. Der Einfluss der elektrostatischen Wechselwirkung auf die Lage des Minimums war im Vergleich zur sterischen Wechselwirkung gering. Der berechnete Winkel der inneren Rotation und die Faserperiode betragen 19° bzw. 16,7₈ Å, was mit den experimentelle Werten von 16°28' und 16,8 Å gut übereinstimmt.

Received December 22, 1961

Polyethers. XI. Polymerization of DL-Propylene Oxide with Optically Active Catalyst Systems*†

NAN SHIEH CHU and CHARLES C. PRICE, *Department of Chemistry, University of Pennsylvania, Philadelphia, Pennsylvania*

Synopsis

The polymerizations of L-propylene oxide by aluminum isopropoxide-zinc chloride, ferric chloride-propylene oxide, and diethylzinc-water catalysts have been studied further and analyzed in terms of the source of stereocontrol in producing isotactic crystalline polymer. The polymerization of DL-propylene oxide by optically active complexes of the above catalysts with poly(L-propylene oxide) and with a catalyst formed from triisobutylaluminum and L-propylene glycol failed to produce any evidence for stereopreference by the catalysts for the L- or D-molecules.

INTRODUCTION

A number of suggestions¹⁻³ have been offered to explain the stereocontrol of propagation necessary to account for the conversion of DL-propylene oxide (PO) to crystalline DL-isotactic poly(propylene oxide) (PPO). These have generally involved the concept that the stereocontrol is exerted by catalyst centers owing their selectivity to preferred conformations of adjacent units in the polymer chain in the transition state for propagation. An alternative possibility is that some form of surface asymmetry is built into heterogeneous catalyst sites.

Another interesting question for any stereopolymerization is the degree of tacticity imposed. For example, in isotactic polymerization, what fraction of propagation reactions can occur to produce an asymmetric unit with opposite configuration?

To obtain further information on these questions, we have carried out experiments on the polymerization of DL-propylene oxide employing catalysts which we believe would have to be regarded as initially optically active.

EXPERIMENTAL[‡]

Polymerization of L-Propylene Oxide

A. Aluminum Isopropoxide-Zinc Chloride.^{1b} A solution of 3.5 mg. of fused zinc chloride and 30 mg. of redistilled aluminum isopropoxide in

* Paper presented at the 135th National Meeting of the American Chemical Society, Boston, Mass., April, 1959.

† This study was supported in part by a grant from the California Research Corporation and the American Chemical Society Petroleum Research Fund.

‡ Melting points are by capillary; they are probably several degrees too high.

2.5 ml. of L-propylene oxide^{1a} was flushed with nitrogen, cooled, sealed, and heated to 80°C. for 16 hr.; 1.2 g. of unchanged monomer was recovered by distillation into a Dry-Ice trap, $[\alpha]_D^{20} + 13.6^\circ$ (14% in ether). The residue was dissolved in benzene, washed with dilute hydrochloric acid, dilute bicarbonate, and water, and freeze-dried to yield 0.3 g. of PPO, $[\alpha]_D^{20} - 22.8^\circ$, $\ln \eta_{rel}/c$ 1.19 (0.7% in benzene). When this was dissolved in warm acetone and cooled to -20°C., it gave 0.12 g. of insoluble solid, m.p. 64°C., $[\alpha]_D^{22} - 21.9^\circ$, $\ln \eta_{rel}/c$ 1.90, and 0.16 g. soluble viscous liquid, $[\alpha]_D^{22} - 18.5^\circ$, $\ln \eta_{rel}/c$ 0.38.

Alternatively, a solution of 3 mg. of zinc chloride and 20 mg. of aluminum isopropoxide in 5 ml. (4.3 g.) of L-propylene oxide was sealed and heated at 80°C. for nine days to yield 3.8 g. of opaque white polymer; $[\alpha]_D^{20} - 19.5^\circ$, $[\eta]$ 2.3. A solution of 3.5 g. in warm acetone was cooled to give two crystalline fractions; 1.6 g. ($[\alpha]_D^{20} - 28.6^\circ$, m.p. 70-73°C.), and 0.12 g. ($[\alpha]_D^{20} - 23.9^\circ$, m.p. 64-67.5°C.) and a semisolid soluble residue, 1.57 g. ($[\alpha]_D^{20} - 18.4^\circ$).

B. Iron Catalyst. A solution of 27 mg. of ferric chloride-propylene oxide catalyst⁴ in 3 ml. of L-propylene oxide was sealed and heated at 80°C. for 284 hr. to yield 1.16 g. of polymer, $[\alpha]_D^{20} - 15.7^\circ$, $\ln \eta_{rel}/c$ 2.53. Fractionation from acetone gave 0.47 g., m.p. 73-76°C., $[\alpha]_D^{20} - 23^\circ$, $\ln \eta_{rel}/c$ 4.10, and 0.61 g. of soluble rubber, $[\alpha]_D^{22} - 10^\circ$, $\ln \eta_{rel}/c$ 1.01.

A companion polymerization with DL-monomer gave 1.64 g. of crude polymer, $\ln \eta_{rel}/c$ 2.65, which was fractionated to 0.48 g., m.p. 73-76°C., $\ln \eta_{rel}/c$ 4.11, and 1.1 g. of soluble rubber, $\ln \eta_{rel}/c$ 1.59.

C. Diethylzinc-Water Catalyst.⁵ A solution of 0.14 g. of diethylzinc in 1.5 ml. of heptane was mixed with 3.5 ml. of L-propylene oxide containing 20 mg. of water, sealed under nitrogen, and kept at room temperature for 118 hr. The white, opaque solid was dissolved in benzene and divided into two portions. For one, the polymer was obtained by adding methanol, centrifuging the precipitated zinc, and freeze-drying to yield 1.16 g., $[\alpha]_D^{22} - 22.9^\circ$, $\ln \eta_{rel}/c$ 2.25. Dissolution of 1 g. in warm acetone and chilling to -20°C. gave 0.66 g. of insoluble PPO, m.p. 63-66°C., $[\alpha] - 28.6^\circ$, $\ln \eta_{rel}/c$ 2.75, and 0.28 g. of soluble PPO, $[\alpha] - 5.1^\circ$, $\ln \eta_{rel}/c$ 0.92. The second aliquot of benzene was washed and freeze-dried to yield 1.23 g. $[\alpha]_D^{22} - 22.0^\circ$, $[\eta]$ 2.79. Fractionation of 1 g. gave 0.70 g. of insoluble PPO, m.p. 63-67°C., $[\alpha] - 26.8^\circ$, $\ln \eta_{rel}/c$ 2.86, and 0.26 g. of soluble PPO, $[\alpha] - 3.9^\circ$, $\ln \eta_{rel}/c$ 0.99.

A companion polymerization of DL-monomer gave 2.89 g. of crude polymer, $[\eta]$ 2.32. Fractionation of 1 g. gave 0.18 g. of insoluble PPO, m.p. 61-64°C., $\ln \eta_{rel}/c$ 2.46, and 0.72 g. of soluble PPO, $\ln \eta_{rel}/c$ 1.01.

Polymerization of DL-Propylene Oxide with L-Polymer-Catalyst Complexes

A. Zinc Chloride-Aluminum Isopropoxide. A solution of 56 mg. of zinc chloride and 70 mg. of aluminum isopropoxide (AIP) in 1.5 ml. of L-propylene oxide was sealed and heated for 21 hr. at 70°. After cooling,

15 ml. of DL-monomer was added, and the stirred mixture was divided into seven 2-ml. portions which were sealed under nitrogen and heated to 80°C. The results are summarized in Table I.

Other experiments with this catalyst system are summarized in Table II.

TABLE I
Polymerization of DL-Propylene Oxide by L-Propylene Oxide-Zinc Chloride-Aluminum Isopropoxide Catalyst at 80°C.

Time, hr.	Wt. PPO, g.	Conversion of DL-PO, %	L-Seed, %	Obs. $[\alpha]_D^{20}$	$[\alpha]$ Calcd. for seed
0	0.0574	0	100	-22.8°	—
2	0.0982	5.78	58.6	-14.36°	-13.36°
4	0.1802	10.6	31.85	-7.10°	-7.26°
5	0.2192	12.9	26.18	-5.61°	-5.97°
6	0.2381	14.0	24.10	-3.89°	-5.49°
7	0.2480	14.6	23.14	-4.66°	-5.28°
9	0.510	30.0	11.25	-1.86°	-2.57°
24	0.7336	43.2	7.82	0°	-1.78°

B. Diethylzinc-Water. In a similar manner, a mixture of 140 mg. of diethylzinc in 1.5 ml. of *n*-heptane and 20 mg. of water in 1 ml. of L-propylene oxide was sealed under nitrogen at room temperature overnight. The reaction flask was then opened and 10 ml. of DL-monomer added. The stirred mixture was divided into six 2-ml. aliquots which were resealed under nitrogen. The yields of polymer and optical rotation are summarized in Table III.

C. Aluminum L-Propylene Glycolate-Zinc Chloride Catalyst. The aluminum L-propylene glycolate was made by thorough mixing at -78°C. of different volumes of L-propylene glycol (0.99*M* in CHCl₃) with triisobutylaluminum (0.99*M* in *n*-heptane) in a Pyrex tube. Zinc chloride and DL-propylene oxide were then added in this order. The tube was then sealed and placed in an oil bath at 80°C. for a suitable time. The reaction mixture was dissolved in benzene, and the benzene solution was washed with dilute hydrochloric acid, water, aqueous sodium bicarbonate, and water. The polymer was dried by a freeze-drying technique. The results obtained are summarized in Table IV.

When 7-10% of propylene glycol and triisobutylaluminum in 1:1, 2:1, and 3:1 mole ratio without zinc chloride were used as catalyst for the polymerization of propylene oxide, the catalytic effect was found to decrease with increasing concentration of propylene glycol. In the last two cases, no significant polymerization could be observed, even when the mixture was heated in an oven at 120°C. for two weeks.

No significant polymerization could be observed when 5 g. of DL-propylene oxide was heated with a mixture of 1-methoxy-2-propanol (2 ml., 2.97*M*) and triisobutylaluminum (2 ml., 0.99*M*) as catalyst at 120°C. for one month.

TABLE II
 Polymerization of DL-Propylene Oxide-Aluminum Isopropoxide-Zinc Chloride Catalyst at 80°C.

Time, hr.	Catalyst			DL- Mono- mer, g.	Crude	Polymer		
	1-P-O, mg.	AIP, mg.	ZnCl ₂ , mg.			1st Fraction ^a	2nd Fraction	3rd Fraction
240	850	100	11.7	8.5	9 g. ln η_{rel}/c 1.49 [α] 0.4°	1.1 g. ln η_{rel}/c 1.76 [α] 0°	2.1 g. ln η_{rel}/c 0.533 [α] 0°	4.9 g. ln η_{rel}/c 0.125 [α] -0.3°
90	430	50	5.0	4.3	0.65 g. ln η_{rel}/c 1.51 [α] -3.6°	m.p. 58-61°C. 0.14 g. ln η_{rel}/c 2.48 [α] -3.3°	m.p. 51-55°C. 0.45 g. ln η_{rel}/c 0.69 [α] -2.7°	
44	430	50	7.0	4.3	1.5 g. ln η_{rel}/c 1.84 [α] -2.3°	m.p. 61-63°C. 0.41 g. ln η_{rel}/c 3.05 [α] -0.8°	0.9 g. ln η_{rel}/c 0.76 [α] -0.8°	

^a Fractionated from hot acetone by chilling to -20°C.

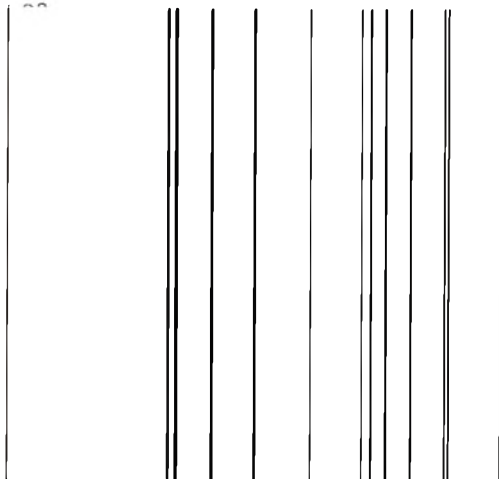
TABLE III

Polymerization of DL-Propylene Oxide by L-Propylene Oxide-Diethylzinc-Water Catalyst at Room Temperature

Time, hr.	Wt. PPO, g.	Conversion of DL-PO, %	L-Seed, %	Obs. $[\alpha]_D^{20}$	$[\alpha]$ Calcd. for Seed
0	0.081		100	-23.1°	—
1	0.1631	9.59	49.66	-11.52°	-11.47°
2	0.2219	13.05	36.50	-8.61°	-8.43°
3	0.3025	17.8	21.77	-6.03°	-6.18°
5	0.4315	25.4	18.77	-4.23°	-4.32°
7	0.5130	30.2	15.78	-3.55°	-3.54°

Optical Activity of the Aluminum Isopropoxide, Zinc Chloride, and L-Propylene Oxide Catalyst

The catalyst prepared in the manner described above (and in Tables I and II) was dried by a freeze-drying technique. This catalyst (0.2144 g.) was then dissolved in benzene (2.14%) and its optical activity was meas-



soluble isotactic polymer varies correspondingly, i.e., two-thirds for diethylzinc and about one-half for iron and aluminum-zinc. Thus, while the diethylzinc catalyst gives the smallest amount of amorphous polymer, this is more completely racemized, i.e., more completely atactic, than that from the other catalysts. All three catalysts produce more insoluble crystalline polymer from L-monomer than from DL-monomer.

The results of polymerization of DL-propylene oxide on various "asymmetric" catalysts, summarized in Tables I-IV, indicate clearly that any asymmetry which may have been attached to catalyst sites is very rapidly lost. The polymer formed from DL-monomer on these "asymmetric" sites, even at very low conversions (Table I, III, and IV) is substantially devoid of any optical activity beyond that of the optically active "seed."

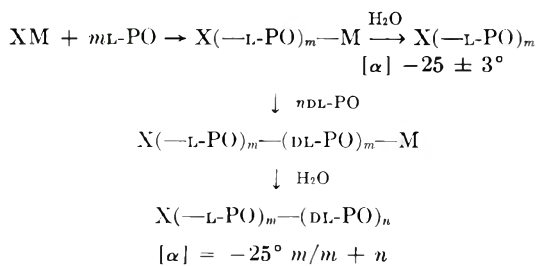
TABLE IV
 Polymerization of DL-Propylene Oxide with Aluminum L-Propylene Glycolate and Zinc Chloride Catalyst
 (Monomer: DL-Propylene Oxide, 2.5 g.; Temp. 80°C.)

Time, days	Catalyst (7-10 wt.-%)		ZnCl ₂ , mg.	Crude	Polymer ^a		
	Al(<i>i</i> -C ₄ H ₉) ₃ , 0.99M, ml. ³	L-PG, 0.99M, ml.			1st Fraction ^b	2nd Fraction ^b	3rd Fraction ^b
5	1	0.5	—	1.6 g.	37 mg. m.p. 56-58°C. ln η_{rel}/c 0.115 ^c	1.04 g. ln η_{rel}/c 0.13	
5	1	1	15-20	2.2 g.	150 mg. m.p. 62-65°C. ln η_{rel}/c 2.09 [η] 3.05	300 mg. m.p. 43-45°C. ln η_{rel}/c 1.92	1.3 g. ln η_{rel}/c 0.265
8	2	3	15-20	2.3 g.	130 mg. m.p. 53-57°C. ln η_{rel}/c 0.637 [η] 0.35	2 g. ln η_{rel}/c 0.20	

^a Crude polymer and all fractions were found to have no detectable optical activity in 2-3% benzene solutions.

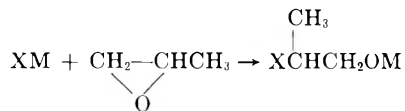
^b From warm acetone by chilling to -20°C.

^c In C₆H₆ (0.3-0.6 g./100 ml.) at 25.0 ± 0.01°C.

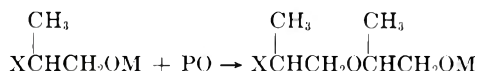


For the case of the aluminum isopropoxide–zinc chloride catalyst, Ebert and Price⁶ have shown that X can be either chlorine or isopropoxyl. This scheme is not intended to indicate that the DL-monomer becomes covalently bonded to the L-polymer. In fact, the experimental evidence reported herein for the aluminum–zinc catalyst indicates that the polymer formed in the early stages has a molecular weight substantially the same as that formed later. Individual polymer molecules must, therefore, proceed through the classical initiation–propagation–termination sequence. The nature of the initiation⁶ and propagation¹ are reasonably well established:

Initiation:



Propagation:



Inadequate information is available on the nature of the termination and/or transfer reactions, although there is some evidence for terminal unsaturation⁷ in high molecular weight poly(ethylene oxide) prepared by aluminum alkyl catalysts. From the experimental data reported herein, we can estimate the ratio of monomer molecules converted to polymer to metal atoms in the catalyst. From our data, this varies from about forty for the diethylzinc catalyst to about 300 for the iron and aluminum–zinc catalysts. Since the viscosity molecular weight indicates number-average molecular weights in excess of 10^5 , there are considerably more metal atoms than one per polymer molecule. If our arguments supporting chain transfer are also correct this indicates that only a very small fraction of the metal atoms present are actually effective as catalyst sites. This is in accord with proposals that the diethylzinc⁸ and iron catalysts⁹ are aggregates with the zinc and iron linked together through oxygen.

The question of whether the asymmetry responsible for stereoselectivity is built into these catalyst aggregates* seems to be answered in the negative, especially by the results with diethylzinc–water. In this case the catalyst

* Corey² has incorrectly ascribed such a proposal to us!

species are generated from the reaction of water with diethylzinc in the presence of monomer and there would be optimum opportunity to build them in a preferred pattern in the presence of L-monomer. The data in Table III indicate that there is no "asymmetric" preference for DL-monomer in catalyst so prepared.

On the other hand, if there were an equal number of D- and L- catalyst sites, then it would seem that the yield of isotactic polymer should be one half as much from L-monomer as from DL-monomer. From diethylzinc catalyst there is actually more isotactic polymer formed from L-monomer than from DL-monomer, while with the iron and aluminum-zinc catalysts about equal weights of isotactic polymer are formed from L- and DL-monomers.

We, therefore, conclude that the asymmetry at the catalyst site must arise from association of the metal oxide aggregate with one or more asymmetric monomer units in the growing polymer chain.

It is of interest to speculate on the degree of stereospecificity for propagation at the various catalyst sites. For completely atactic polymer, $k_{LL} = k_{LD}$, while for highly isotactic sequences, $k_{LL} \gg \gg k_{LD}$. Earlier work on polymerization of L-propylene oxide with potassium hydroxide gave polymer of $DP = 50$, m.p. 56°C . If we assume that endgroups in this polymer can provide the same molar concentration of "impurity" as an equal number of breaks in the isotactic sequence, then the polymers from diethylzinc and aluminum-zinc catalysts with melting points of about $60-65^\circ\text{C}$. probably have isotactic sequences averaging about 100, i.e., $k_{LL} \simeq 100k_{LD}$. Since the degree of polymerization of these polymers is considerably in excess of 1000, they must be stereoblock polymers. Those polymers from the iron catalyst having melting points close to 70°C . presumably have considerably longer isotactic sequences, probably at least 1000.

For the soluble amorphous polymers formed from L-monomer, one may assume that the observed optical rotation would be an indication of the relative number of D- and L- units and thus of the k_{LL} and k_{LD} ratio. On this basis, about one of seven monomer molecules has been inverted in configuration by the aluminum-zinc catalyst sites producing amorphous polymer. For the iron catalyst, the ratio is about one in three, while for the diethylzinc catalyst, $k_{LL} \simeq 1.5k_{LD}$.

One might speculate that the difference between those catalyst sites producing highly crystalline, highly isotactic polymer and those producing amorphous polymer of low tacticity may be the degree of aggregation of the catalyst. The highly aggregated catalyst would be expected to have the tighter steric requirements necessary for isotactic propagation while "monomeric" catalyst molecules may be those responsible for the substantially atactic polymer.*

* Robinson,³ in dismissing possible contributions of cationic centers, seems to have overlooked the fact that L-monomer gives DL-atactic,¹ as well as L-isotactic polymer. The importance he ascribes³ to halogen on the metal is not supported by the high reactivity of the diethylzinc-water catalyst.⁵

References

1. (a) Price C. C., and M. Osgan, *J. Am. Chem. Soc.*, **78**, 4787 (1956); (b) C. C. Price and M. Osgan, *J. Polymer Sci.*, **34**, 153 (1959).
2. Corey, E. J., *Tetrahedron Letters*, No. 2, 1 (1959).
3. Robinson, R., *Tetrahedron*, **5**, 96 (1959).
4. Pruitt, M. E., and J. M. Baggett, U. S. Pat. 2,706,181 (April 12, 1955).
5. Furukawa, J., T. Tsuruta, T. Saegusa, and G. Kakogawa, *J. Polymer Sci.*, **36**, 541 (1959); J. Furukawa, T. Suruta, R. Sakata, T. Saegusa, and A. Kawasaki, *Makromol. Chem.*, **32**, 90 (1959).
6. Ebert, P. E., and C. C. Price, *J. Polymer Sci.*, **46**, 455 (1950).
7. Miller, R. A., and C. C. Price, *J. Polymer Sci.*, **34**, 161 (1959).
8. Sakata, R., T. Tsuruta, T. Saegusa, and J. Furukawa, *Makromol. Chem.*, **40**, 64 (1960).
9. Borkovec, A. B., U.S. Pat. 2,861,962 (Nov. 25, 1958); U.S. Pat. 2,873,258 (Feb. 10, 1959).

Résumé

On a étudié la polymérisation du 1-oxyde de propylène par les catalyseurs suivants: isopropoxyde d'aluminium-chlorure de zinc, chlorure ferrique-oxyde de propylène et zinc diéthylique-eau, et on a analysé ensuite le polymère cristallin isotactique formé en fonction du catalyseur controlant la stéréochimie. La polymérisation d'oxyde de propylène-DL par des complexes optiquement actifs comme les catalyseurs ci-dessus avec le poly(oxyde de propylène-L) et avec un catalyseur formé à partir d'aluminium triisobutylique et de L-propylène glycol ne montre aucune stéréopréférence par le catalyseur pour les molécules L ou D.

Zusammenfassung

Die Untersuchung der Polymerisation von L-Propylenoxyd mit Aluminiumisopropoxyd-Zinkchlorid, Eisenchlorid-Propylenoxyd und Diäthylzink-Wasser als Katalysatoren wurde besonders in Hinblick auf die Aufklärung der Ursachen für die stereospezifische Kontrolle bei der Produktion eines isotaktischen kristallinen Polymeren fortgeführt. Die Polymerisation von DL-Propylenoxyd mit optisch aktiven Komplexen der angeführten Katalysatoren mit Poly(L-propylenoxyd) und mit einem aus Triisobutylaluminium und L-Propylen glykol hergestellten Katalysator ergaben keine stereospezifische Bevorzugung der L- oder D-Moleküle durch die Katalysatoren.

Received August 22, 1961

Revised December 6, 1961

Copolymerization Characteristics of Methyl Acrylate and Methyl Methacrylate. I. Study of Copolymerization Kinetics by a Deuterium Tracer Method

MIKIKO SHIMA* and AKIRA KOTERA, *Department of Chemistry, Faculty of Science, Tokyo University of Education, Otsuka, Tokyo, Japan*

Synopsis

The kinetics of copolymerization for the methyl acrylate-methyl methacrylate system was studied by using monomers which contain deuterium as a tracer. The experiments were made on two series of copolymerizations: methyl acrylate-deuteromethyl methacrylate, $(\text{CH}_2=\text{C}(\text{CH}_3)\text{COOCH}_2\text{D})$, and deuteromethyl acrylate $(\text{CH}_2=\text{CHCOOCH}_2\text{D})$ -methyl methacrylate copolymerization systems. Mass spectrometric analysis was employed for determining the composition of copolymers. The agreement of the experimental results of the two series was reasonable. The monomer reactivity ratios for the methyl acrylate (M_1)-methyl methacrylate (M_2) system were determined as $r_1 = 0.47 \pm 0.09$ and $r_2 = 2.3 \pm 0.5$ at 130°C . These values were compared with those calculated from the Price-Alfrey $Q-e$ scheme.

It is well known that copolymers of methyl acrylate and methyl methacrylate are commercially useful materials. However, the monomer reactivity ratios for the free radical-initiated copolymerization of this system have not been reported. In this system, it is difficult to determine the composition of copolymers by using conventional carbon-hydrogen combustion analysis, because of the similarity in chemical composition of the component monomers.

We have investigated the copolymerization kinetics of this system by using monomers containing deuterium as a tracer, and attempted to determine the monomer reactivity ratios.

EXPERIMENTAL

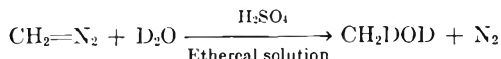
Two series of copolymers were investigated, i.e., methyl acrylate-deuteromethyl methacrylate(MA-DMMA) and deuteromethyl acrylate-methyl methacrylate(DMA-MMA).

1. Preparation of Monomers Containing Deuterium

Deuteromethyl methacrylate $\text{CH}_2=\text{C}(\text{CH}_3)\text{COOCH}_2\text{D}$ was prepared by the following processes.

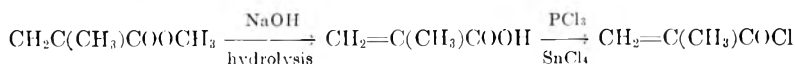
* Present address: Chemistry Department, State University College of Forestry, Syracuse University, Syracuse, N. Y.

Deuteromethanol CH_2DOD was synthesized by treating diazomethane in ether solution with heavy water (D_2O : 99.98%) in the presence of a small amount of sulfuric acid.¹

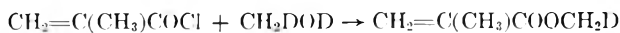


The diazomethane had been prepared by the decomposition of *p*-toluene-sulfomethylnitrosoamide in an alkaline medium.²

Methacrylic acid was prepared by hydrolysis of methyl methacrylate with sodium hydroxide³ and by adding phosphorus trichloride to the methacrylic acid in the presence of tin tetrachloride, methacryloyl chloride (b.p. 39–41°C./70 mm. Hg) was obtained.⁴

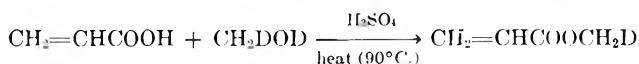


Deuteromethyl methacrylate was prepared by the reaction of methacryloyl chloride with deuteromethanol⁴ and purified by distillation under reduced pressure.



Deuteromethyl methacrylate was diluted with methyl methacrylate. Monomer containing about 4% $\text{CH}_2=\text{C}(\text{CH}_3)\text{COOCH}_2\text{D}$ was used for the copolymerization.

Deuteromethyl acrylate, $\text{CH}_2=\text{CHCOOCH}_2\text{D}$, was prepared by esterification of acrylic acid with deuteromethanol in the presence of sulfuric acid.⁴ The acrylic acid was obtained by hydrolysis of methyl acrylate.



This monomer was diluted with methyl acrylate so as to contain about 2% $\text{CH}_2=\text{CHCOOCH}_2\text{D}$ and was used for the copolymerization.

The methyl acrylate and methyl methacrylate monomers used in these experiments, supplied by Mitsubishi Rayon Company, were distilled twice under reduced pressure in an atmosphere of nitrogen: their boiling points were 28 C./110 mm. Hg and 35.5°C./70 mm. Hg, respectively.

2. Copolymerization Procedure

Polymerization was carried out in sealed ampules. No catalyst was added. Before sealing the tubes were cooled in Dry Ice and ambient air was swept out with dry nitrogen. Polymerizations were carried out thermally in an oil bath maintained at 130°C. When an appropriate conversion took place as indicated by an increase in viscosity, the tubes were taken out of the bath, cooled with Dry Ice, and opened.

The partially polymerized reaction mixtures were dissolved in benzene. The polymers were precipitated by pouring the solution into a large amount of methanol, dried in a high vacuum and finally purified by the frozen benzene sublimation technique of Mayo.⁵ When the polymer solution

was kept in a bath at 0°C. under 1 mm. Hg pressure for about 10 hr. and then heated at 60°C. for 24 hr. in vacuum, a very porous material was obtained. The degree of conversion was determined by weighing the resulting polymer.

3. Analysis

The compositions of the copolymers were determined by measuring the deuterium concentration. About 30 mg. of the polymer was burnt in oxygen at 700°C. and the water produced by the combustion was decomposed with zinc dust. The deuterium concentration in the produced hydrogen was measured by means of Hitachi Model RMDI mass spectrometer,⁶ the accuracy of which was within $\pm 1\%$. Analyses of copolymers were carried out twice for each sample. The deuterium contents shown in Tables I and III are the means values of the measurements.

The deuteromethyl methacrylate used in the MA-DMMA system (series A) contained 0.433% deuterium in hydrogen, and the deuteromethyl acrylate used in DMA-MMA system (series B) contained 0.238% deuterium. The concentration of deuterium in natural hydrogen is 0.015%. The composition of copolymers in series A and in the series B was calculated by using the eqs. (1) and (2), respectively.

$$8 \times 0.433f_2 + 6 \times 0.015(1-f_2)/8f_2 + 6(1-f_2) = c \quad (1)$$

$$8 \times 0.015(1-f_1) + 6 \times 0.238 f_1/8(1-f_1) + 6 f_1 = c' \quad (2)$$

Here, c and c' are the deuterium concentrations, and f_1 and f_2 are the mole fractions of methyl acrylate and methyl methacrylate in the copolymers.

RESULTS AND DISCUSSION

The results of the experiments are summarized in Tables I-IV. The experimental values of the monomer concentrations are shown in Tables II and IV. M_1 and M_2 are the concentrations of methyl acrylate and

TABLE I
Compositions of Copolymers from Deuterium Analyses
(Series A, MA-DMMA System)

Expt. no.	Mole fraction MMA in monomer mixture F_2	D, \bar{c}_i	Mole fraction MMA in copolymer f_2	Conversion, \bar{c}_c
A7	1.0000	0.433	1.000	51.7
A8	0.6707	0.377	0.804	14.4
A9	0.6707	0.377	0.795	19.5
A10	0.5047	0.336	0.692	14.8
A11	0.5047	0.324	0.660	37.4
A12	0.1887	0.157	0.271	48.5
A13	0.1887	0.152	0.260	51.5

TABLE II
Initial and Final Monomer Concentrations for Copolymerization
(Series A, MA-DMMA System)

Expt. no.	M_1^0 , mole/l.	M_2^0 , mole/l.	M_1 , mole/l.	M_2 , mole/l.
A8	0.01576	0.03207	0.01444	0.02663
A9	0.01197	0.02436	0.01055	0.01883
A10	0.02284	0.02328	0.02080	0.01870
A11	0.01917	0.01945	0.01436	0.01020
A12	0.03596	0.008360	0.02049	0.002342
A13	0.03687	0.008574	0.01974	0.002566

TABLE III
Compositions of Copolymers from Deuterium Analyses
(Series B, DMA-MMA System)

Expt. no.	Mole fraction MA in monomer mixture F_1	D, %	Mole fraction MA in copolymer f_1	Conversion, %
B1	1.0000	0.238	1.000	27.5
B2	0.7958	0.137	0.617	4.10
B3	0.7958	0.157	0.700	46.5
B4	0.3630	0.0522	0.211	18.4
B5	0.3630	0.0505	0.202	14.5
B6	0.1060	0.0239	0.0525	8.26
B7	0.1060	0.0255	0.0618	5.41

TABLE IV
Initial and Final Monomer Concentrations for Copolymerization
(Series B, DMA-MMA System)

Expt. no.	M_1^0 , mole/l.	M_2^0 , mole/l.	M_1 , mole/l.	M_2 , mole/l.
B2	0.03007	0.007716	0.02914	0.007139
B3	0.03087	0.007920	0.01843	0.002589
B4	0.01138	0.01997	0.01019	0.01553
B5	0.01205	0.02114	0.01110	0.01739
B6	0.004562	0.03849	0.004368	0.03515
B7	0.002720	0.02295	0.002635	0.02166

methyl methacrylate monomers, respectively at time t . The corresponding initial monomer concentrations, M_1^0 and M_2^0 were determined by weighing the monomers, and the monomer concentrations at time t (M_1 and M_2) were determined from the data of the conversion and the copolymer composition.

The monomer reactivity ratios were obtained by the intersection method of Mayo and Lewis.⁷ From the integrated equation for the copolymer composition, r_2 is expressed as follows

$$r_2 = \frac{\log \frac{M_2^0}{M_2} - \frac{1}{p} \log \frac{1 - p(M_1/M_2)}{1 - p(M_1^0/M_2^0)}}{\log \frac{M_1^0}{M_1} + \log \frac{1 - p(M_1/M_2)}{1 - p(M_1^0/M_2^0)}} \quad (3)$$

where $p = (1 - r_1)/(1 - r_2)$. On the basis of eq. (3), each set of values, M_1^0 , M_2^0 , M_1 , and M_2 in Tables II and IV, yields a straight line plot of r_1 versus r_2 as shown in Figures 1 and 2. If there had been no error in the determination of the monomer concentrations listed in Table II and Table IV, the lines in both Figure 1 and Figure 2 should intersect at a common point characteristic of the true values of r_1 and r_2 . The six experimental determinations are plotted in Figure 1 and in Figure 2. Figure 1 gives the values of $r_1 = 0.50 \pm 0.08$, $r_2 = 2.3 \pm 0.5$, and Figure 2 gives the values of $r_1 = 0.42 \pm 0.06$, $r_2 = 2.2 \pm 0.4$. It seems that the agreement of both experimental results is reasonable, and values of $r_1 = 0.47 \pm 0.09$ and $r_2 = 2.3 \pm 0.5$ are obtained.

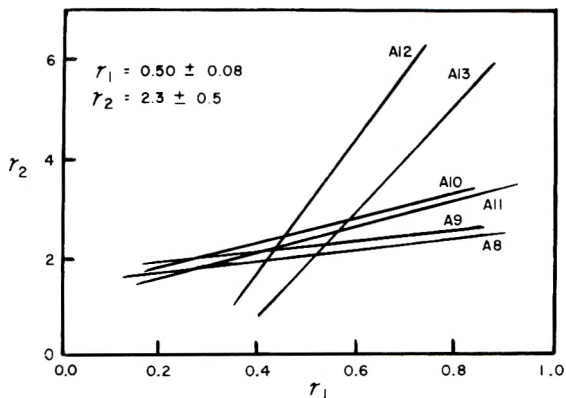


Fig. 1. Plot of r_1 vs. r_2 for the MA-DMMA system.

These reactivity ratios can be compared with those predicted by the Q - e scheme. According to the Q - e scheme of Price,⁸ the copolymerization reactivity ratios are given by eqs. (4) and (5):

$$r_1 = (Q_1/Q_2) \exp \{ -e_1(e_1 - e_2) \} \quad (4)$$

$$r_2 = (Q_2/Q_1) \exp \{ -e_2(e_2 - e_1) \} \quad (5)$$

where Q is related to the specific reactivity of a monomer (resonance factor) and e represents the polar character of the radical adduct (polar factor). Price gave values of $e_1 = 0.6$, $Q_1 = 0.42$ for methyl acrylate and $e_2 = 0.4$, $Q_2 = 0.74$ for methyl methacrylate on the basis of copolymerization experiments with styrene.⁹ On the basis of these data, we obtained the values of $r_1 = 0.504$ and $r_2 = 1.91$ for the present system. Taking the ambiguity in values of Q and e into account, the agreement of the experimentally determined values with the theoretical ones is reasonable.

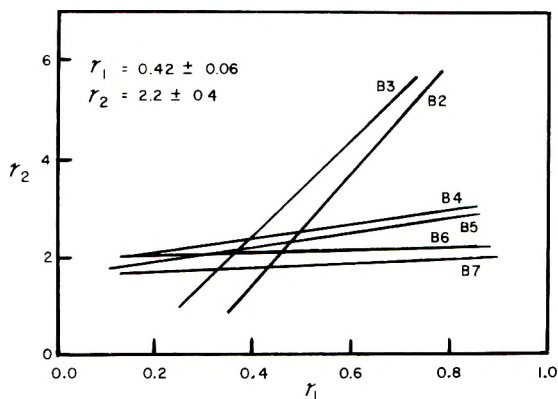


Fig. 2. Plot of r_1 vs. r_2 for the DMA-NMA system.

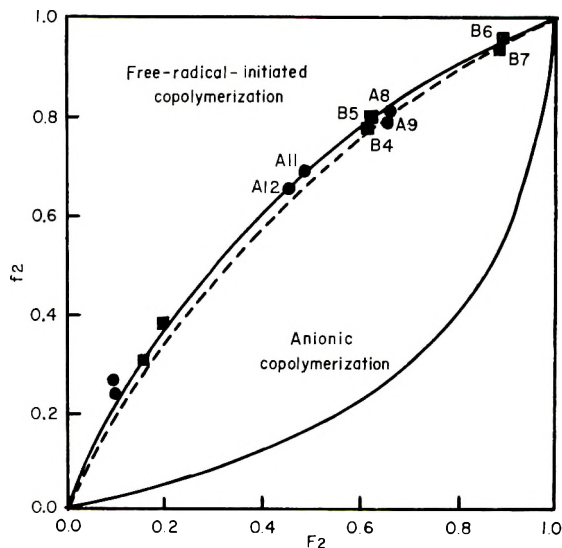


Fig. 3. Copolymer composition curves for methyl acrylate-methyl methacrylate system. (----) curve for the values of r_1 and r_2 calculated from the "Q-e" scheme, ($r_1 = 0.504$, $r_2 = 1.91$); (—) experimental curves for free-radical initiated copolymerization, ($r_1 = 0.47$, $r_2 = 2.3$), and for anionic copolymerization, ($r_1 = 4.5$, $r_2 = 0.1$).

The ionic copolymerization of this system has previously been investigated by Landler.¹⁰ The monomer reactivity ratios in anionic copolymerization (initiated by NaNH_2 in liquid NH_3 solution) have been reported as $r_1 = 4.5 \pm 0.5$ and $r_2 = 0.1 \pm 0.1$; the composition was determined by carbon-hydrogen combustion analysis. In these experiments, as well as in the case of other systems, the monomer reactivity ratios in a free radical-initiated copolymerization were found to differ from those in an ionically initiated copolymerization. Figure 3 illustrates the effect of the difference

in reactivity ratios on the compositions of initial copolymers in the two systems.

The measurements by mass spectrometer in these experiments were carried out at Tokyo Metropolitan University. The authors wish to express their sincere thanks to Professor T. Titani and Professor Y. Horibe of Tokyo Metropolitan University for their kind advice and for the free use of the apparatus located at their university. Thanks are also due to Misses M. Kobayakawa and S. Koda of the university for their kind cooperation in carrying out the deuterium analyses.

References

1. Halford, J. O., L. C. Anderson, and G. H. Kissin, *J. Chem. Phys.*, **5**, 927 (1937).
2. de Boer, T., and H. J. Backer, *Rec. Trav. Chim.*, **73**, 229 (1954).
3. Inoue, R., *J. Chem. Soc. Japan, Ind. Eng. Chem. Sect.*, **45**, 385 (1942).
4. Yoshida, K., and S. Yamaguchi, *Sci. Ind. Japan*, **18**, 532 (1943).
5. Lewis, F. M., and F. R. Mayo, *Ind. Eng. Chem. Anal. Ed.*, **17**, 134 (1945).
6. Titani, T., Y. Horibe, and M. Kobayakawa, *Mass Spectrometric Anal. Japan*, **6**, 27 (1955).
7. Mayo, F. R., and F. M. Lewis, *J. Am. Chem. Soc.*, **66**, 1594 (1944).
8. Alfrey, T., and C. C. Price, *J. Polymer Sci.*, **2**, 101 (1947).
9. Price, C. C., *J. Polymer Sci.*, **3**, 772 (1948).
10. Landler, Y., *J. Polymer Sci.*, **8**, 63 (1952).

Résumé

On a étudié la cinétique de la copolymérisation du système acrylate de méthyle, méthacrylate de méthyle au moyen de monomères contenant du deutérium comme traceur. On a effectué les expériences sur deux séries de copolymérisation, c'est à dire le système de copolymérisation acrylate de méthyle-méthacrylate de deuterométhyle, ($\text{CH}_2=\text{C}(\text{CH}_3)\text{COOCH}_2\text{D}$), et le système acrylate de deutérométhyle ($\text{CH}_2=\text{CHCOO-CH}_2\text{D}$)-méthacrylate de méthyle. On a employé l'analyse spectroscopique de masse pour déterminer la composition des copolymères. Il y a accord raisonnable entre les résultats expérimentaux des deux séries. On a déterminé le rapport des réactivités des monomères du système acrylate de méthyle (M_1)-méthacrylate de méthyle (M_2): $r_1 = 0.47 \pm 0.09$ et $r_2 = 2.3 \pm 0.5$ à 130°C . On compare ces valeurs à celles calculées à partir du schéma Q-e.

Zusammenfassung

Die Kinetik der Copolymerisation des Systems Methylacrylat-Methylmethacrylat wurde mit deuteriummarkierten Monomeren untersucht. Die Versuche wurden an zwei Copolymerisationsreihen ausgeführt, nämlich Methylacrylat-Deuteromethylmethacrylat ($\text{CH}_2=\text{C}(\text{CH}_3)\text{CO}(\text{OCH}_2\text{D})$) und Deuteromethylacrylat ($\text{CH}_2=\text{CHCO}(\text{OCH}_2\text{D})$)-Methylmethacrylat. Die Zusammensetzung der Copolymeren wurde massenspektrometrisch bestimmt. Die Übereinstimmung zwischen den Ergebnissen der beiden Reihen war befriedigend. Die Monomer-Reaktivitätsverhältnisse für Methylacrylat-Methylmethacrylat wurden zu $r_1 = 0,47 \pm 0,09$ und $r_2 = 2,3 \pm 0,5$ bei 130°C (M_1 ; Methylacrylat; M_2 : Methylmethacrylat) bestimmt. Diese Werte wurden mit den aus dem "Q-e-Schema" berechneten verglichen.

Received July 11, 1961

Revised November 27, 1961

Homopolymerization of Maleic Anhydride.

I. Preparation of the Polymer

JOHN L. LANG,* W. A. PAVELICH,† and H. D. CLAREY,
The Dow Chemical Company, Midland, Michigan

Synopsis

Maleic anhydride has been homopolymerized, contrary to accepted beliefs. Polymerization of either molten or dissolved monomer was initiated with the use of gamma-radiation and free-radical initiators. An anhydride having $[\eta] = 0.146$ dl./g. in acetophenone had a molecular weight of 23,100 (free acid), $DP = 199$, by the light-scattering method. The carboxyl group propinquity is responsible for peculiar behavior of aqueous solutions of salts of the poly-acid.

INTRODUCTION

It has been dogmatic for many years that 1,2-disubstituted ethylenes do not homopolymerize. The often-observed reluctance of maleic anhydride to homopolymerize has resulted in the citation of the behavior of this specific compound as the example illustrating this reluctance by many authors in their texts, papers, and lectures.¹⁻¹⁴

The principle reason for this reluctance was supposed to be the steric hindrance imposed by the 1,2-disubstitution of the double bond of the monomeric species. The resonance and polar characteristics of maleic anhydride were also mentioned as contributing to the sterically inherent non-homopolymerizable character.

Although the overwhelming consensus of the literature states that maleic anhydride does not homopolymerize, there are isolated references which, either by themselves or when read in the light of this present work, indicate the possibility of this homopolymerization. Lustig and Wachtel¹⁵ irradiated maleic acid with beta-rays and claimed therapeutic properties for their uncharacterized product in the treatment of cancer in mice. Bartlett and Nozaki¹⁶ determined the codisappearance of both materials in a heated mixture of benzoyl peroxide and maleic anhydride, and postulated the formation of a polymer of $DP = 29$, without isolation or characterization of the product; Marvel and co-workers¹⁷ characterized the product of a similar experiment as mainly cyclic trimer.

Investigation of the system styrene-itaconic anhydride demonstrated that the itaconic anhydride was capable of homopolymerization.¹⁸ Presuming that the resonance and polar factors here are of the same order as in

* Present address: Koppers Research Center, Monroeville, Pennsylvania.

† Present address: Spencer Chemical Company, Merriam, Kansas.

maleic anhydride, the "reluctance" of maleic anhydride toward homopolymerization must depend almost entirely on the steric factor.

The availability of the olefin linkage on the cyclic structure lead to an assumption that maleic anhydride would homopolymerize, and a study was started to accomplish just this. Irradiation by gamma-rays from Co^{60} was selected as the initiation system, because it was felt that a rather drastic treatment might be required to carry out this reputedly impossible polymerization. The solution technique was chosen because it was known that frozen styrene monomer did not polymerize to form crystalline polystyrene.¹⁹ All homopolymerizations of maleic anhydride to this date were carried out in the liquid state. Radiation of the solid monomer seems to be ineffective.¹³

EXPERIMENTAL

Source of Materials

Eastman White Label grade maleic anhydride was used as received for the first fifteen samples. Four samples were prepared from commercial grade material produced by National Aniline Division, Allied Chemical Corp. Resublimed monomer was used for the polymerizations after it was found that the monomer as supplied contained free acid. The maleic anhydride from all sources polymerized. Acetic anhydride was purified by distillation on an 18-plate Oldershaw column. The diacetyl used was Eastman Blue Label grade, redistilled and the fraction used which boiled in the range 87–88°C., at 753 mm. Hg. The α, α' -azobisisobutyronitrile (du Pont) was recrystallized from diethyl ether, m.p. 104.5–105.5°C. Benzoyl peroxide and lauroyl peroxide (Lucidol Div., Wallace & Tiernan Corp.), and benzene (Mallinckrodt, AR grade) were used as received. The other solvents were commercial materials, redistilled to insure that they were dry and reasonably pure.

Sample Preparation

In the initial experiments, the samples were prepared and introduced into washed and dried heavy-walled borosilicate glass ampules, sparged with prepurified nitrogen, and sealed. This procedure produced polymer containing carboxylic acid groups, so a more meticulous method was used to prepare the samples used in the characterization of the polymer. Resublimed monomer and redistilled solvents were placed in clean, dry, heavy-walled borosilicate glass ampules. The whole was immersed in solid CO_2 -trichloroethylene-tetrachloroethylene freezing mixture, and when frozen, evacuated to 1 mm. Hg pressure. The ampule was isolated from the vacuum system and melted. The entrapped gases were expelled mainly during the melting portion of the cycle, which was repeated until no gas was evolved during two successive melting periods. The sample was refrozen, evacuated, and sealed.

Polymerization Procedure

The Co⁶⁰-initiated polymerizations were conducted at the radiation installation of the Nuclear and Basic Research Laboratory of The Dow Chemical Company. Total dosage and dose rate for the individual samples are given in the tables.

The polymerizations initiated by benzoyl peroxide, lauroyl peroxide, and AIBN were conducted in constant temperature baths of conventional design. The polymerizations initiated by ultraviolet-diacetyl were carried out at ambient temperature, using a General Electric mercury vapor arc sunlamp, with RS reflector, 275 w., 110–125 v., 60 cycle alternating current, emitting wavelengths as short as 2800 Å.

The poly(maleic anhydride) was isolated by diluting the reactant solution with butanone and precipitation in dry toluene. Samples used for polymer characterization were reprecipitated. The precipitated polymers were collected in weighed fritted glass Gooch crucibles, washed, and dried under vacuum at 60°C.

Titration was carried out with a Leeds and Northrup in-line pH meter modified to accept Beckman electrodes.

RESULTS

The first irradiation of 25% maleic anhydride in benzene formed a viscous solution. The isolated product was insoluble in toluene, did not melt below 300°C., and had an infrared pattern identical with that expected for the homopolymer of maleic anhydride, with minor contamination by hydrolysis product thereof.

TABLE I
Co⁶⁰-Initiated Polymerization of Maleic Anhydride: Effect of Solvent: Monomer Ratio

Solvent	Solvent: monomer ratio	Temp., °C.	Radiation			Conversion, %
			Intensity, Mrad/hr.	Time, hr.	Total dose, Mrad	
Acetic anhydride	90:10	25	0.195	220.2	43.0	46.7 ^a
Acetic anhydride	75:25	25	0.195	220.2	43.0	98.0
Acetic anhydride	50:50	25	0.195	207.5	40.5	89.2 ^b
Acetic anhydride	10:90	25	0.195	200	39.0	18.4
1,4-Dioxane	80:20	25	0.205	98.9	20.3	17.9
1,4-Dioxane	60:40	25	0.205	98.9	20.3	10.7
1,4-Dioxane	40:60	25	0.205	98.9	20.3	14.7
Benzene	75:25	25	0.195	207.5	40.5	—
Benzene	90:10	25	0.195	207.5	40.5	—
Acetic anhydride	50:50	75	0.206	99.7	20.5	14.4 ^c
None	—	75	0.206	99.7	20.5	56.2 ^d

^a Intrinsic viscosity 0.052 dl./g. (2-butanone).

^b Intrinsic viscosity 0.112 dl./g. (2-butanone).

^c Intrinsic viscosity 0.171 dl./g. (acetophenone).

^d Intrinsic viscosity 0.137 dl./g. (acetophenone).

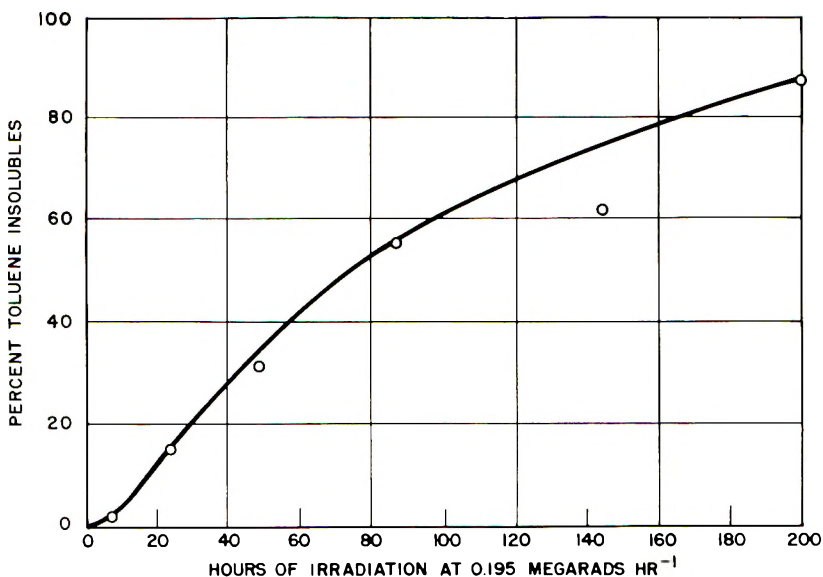


Fig. 1. Rate of polymerization of 1:1 maleic anhydride:acetic anhydride solution.

Having established the validity of the assumption that maleic anhydride would actually polymerize when freed of the restrictions imposed by the crystalline habit of the usual solid form, a study was made of the effect of various solvents and the molten state upon the polymer thereby produced. Solvents used were acetic anhydride, 1,4-dioxane, benzene, and water. These data are presented in Table I. The polymerization proceeds most rapidly in acetic anhydride; conversion rates in 1,4-dioxane and the melt are comparable to one another, but are about one-fourth those where acetic anhydride is used as the solvent.

In experiments conducted to determine the effect of total gamma-radiation dose upon conversion, the amount of product insoluble in toluene recovered after irradiation of 50 wt.-% solutions of the monomer in acetic anhydride was almost directly proportional to the total radiation dose within the limits 0–39 Mrads at a field intensity of ca. 0.195 Mrad/hr., as

TABLE II
Total Radiation Dose vs. Conversion for Polymerization of 1:1 Solutions of Maleic Anhydride–Acetic Anhydride

Field intensity, Mrad/hr.	Total radiation dose, Mrads	Conversion, %	Intrinsic viscosity in acetophenone, dl./g.
0.195	1.56	2.69	0.121
0.195	4.68	15.11	—
0.195	9.36	30.68	0.155
0.195	18.78	55.32	—
0.195	28.08	61.65	—
0.195	39.0	87.08	0.146

shown in Table II and Figure 1. The effect of field intensity upon conversion in the range used for the samples is given in Table III and shown on the graph in Figure 2.

When varying concentrations of maleic anhydride in acetic anhydride were irradiated at a constant field intensity of 0.195 Mrad/hr. for a total radiation dose of ca. 40 Mrads, the conversion increased until the limit of

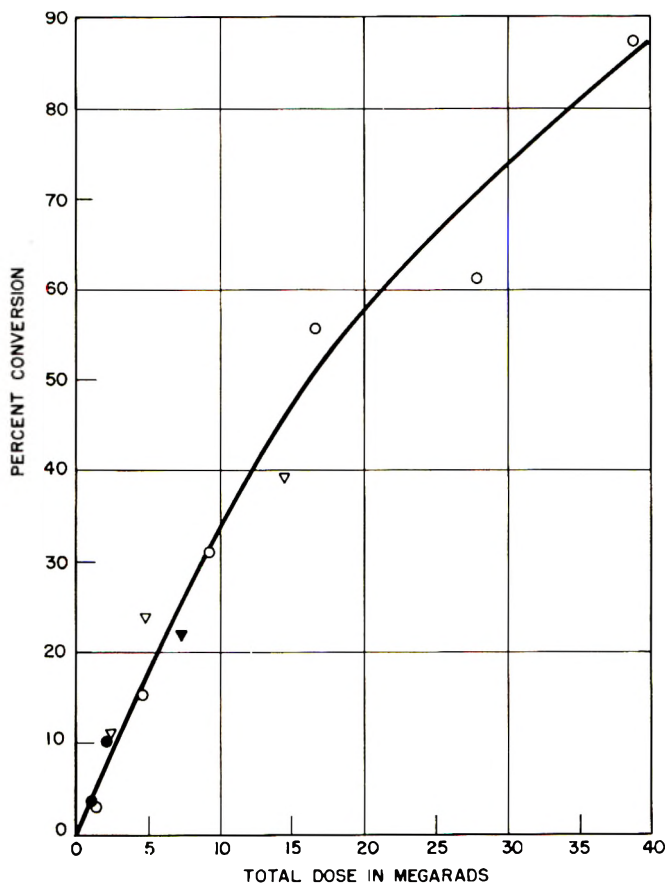


Fig. 2. Field intensity in maleic anhydride polymerization: (O) 0.195 Mrad/hr.; (●) 0.010 Mrad/hr.; (▽) 0.050 Mrad/hr.; (▼) 0.480 Mrad/hr.

solubility of the monomer in the solvent was reached. In saturated solutions, the conversion was diminished somewhat when compared to data for almost saturated solutions. The intrinsic viscosity of the polymer was found to be dependent upon the initial concentration of monomer in the solution irradiated: 10 wt.-% monomer produces polymer having $[\eta] = 0.052$ dl./g.; 50 wt.-% monomer results in a product with $[\eta] = 0.112$ dl./g. with butanone as the solvent in the intrinsic viscosity determinations. As shown in Figure 3, the intrinsic viscosity increased linearly with the initial

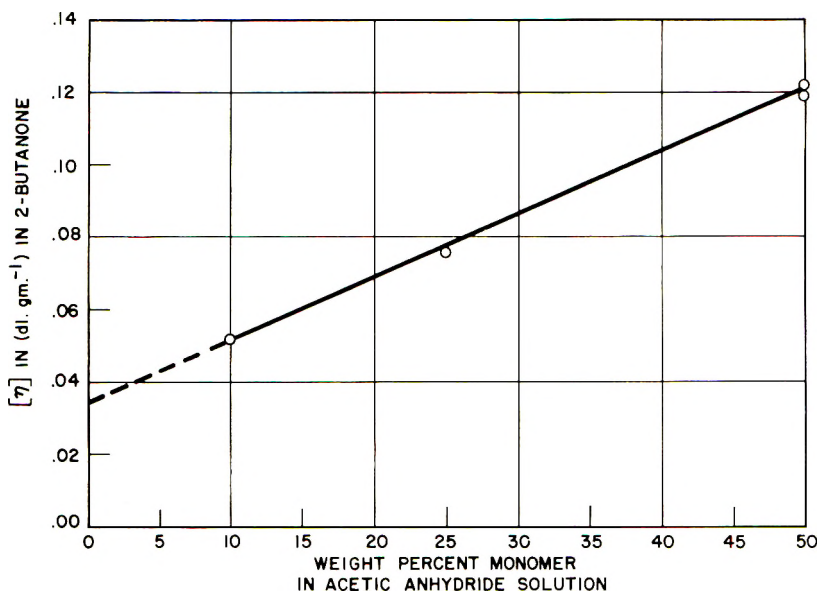


Fig. 3. Intrinsic viscosity of poly(maleic anhydride) prepared at ca. 0.2 Mrad/hr. in solution.

concentration of maleic anhydride in the polymerization mixture up to approximately the limit of solubility in acetic anhydride.

Preliminary free radical-initiated maleic anhydride homopolymerization attempts with the use of lauroyl peroxide and α, α' -azobisisobutyronitrile at 1 wt.-% concentrations in the molten monomer produced miniscule amounts of polymer. With benzoyl peroxide, the free-radical initiator

TABLE III

Effect of Field Intensity and Total Radiation Dose Upon Conversion for Polymerization of 1:1 Solutions of Maleic Anhydride-Acetic Anhydride

Field intensity, Mrad/hr.	Total radiation dose, Mrads	Conversion, %	Intrinsic viscosity in acetophenone, dl./g.
0.010	1.07	3.51	0.155
0.010	2.15	9.63	—
0.010	2.4	11.08	—
0.050	2.4	10.4	—
0.050	2.4	11.47	—
0.050	4.8	23.30	0.183
0.050	4.9	77.01	—
0.100	3.4	17.4	—
0.100	6.8	29.9	0.160
0.400	3.28	9.02	—
0.400	6.48	20.67	—
0.400	11.16	30.62	—
0.480	7.44	22.1	0.137
0.480	14.5	39.2	—

TABLE IV

Sam- ple no.	Initiator	Initiator concn., %	Monomer type	Monomer concn., wt.-%	Solvent	Solvent concn., wt.-%	Temp., °C.	Polymer- ization time, hr.	Con- version, %
43-36	Benzoyl peroxide	4.58	National Aniline	100.0	None	—	60 ± 0.2	48	33.94
27-6	Benzoyl peroxide	5.0	National Aniline	50.0	Acetic anhydride	50.0	70.0 ± 0.2	48	33.6
40-35	AIBN	0.1	Eastman	100	None	—	60-67	169	—
40-34	Lauroyl peroxide	0.1	Eastman	100.0	None	—	60-67	169	—
50-0	Diacetyl-U.V.	1.0	Resublimed	50.0	Acetic anhydride	50.0	25	648	13.34
50-10	Diacetyl-U.V.	1.0	Resublimed	50.0	Acetic anhydride	50.0	25	648	15.99
44-2	C ₆₀ ⁶⁰		National Aniline	100	None	—	75	99.7	14.45

TABLE V
Temperature Effect in the Homopolymerization of Maleic Anhydride

Sample no.	Solvent	Solvent concn., wt.-%	Temp., °C.	Initiator	Initiator concn., % or field intensity, Mrad/hr.	Time, hr.	Total dose, Mrads	Conversion, %
149-43-36	None	—	60 ± 0.2	Benzoyl peroxide	4.58	48	—	33.94
155-27-6	Acetic anhydride	50	70 ± 0.2	Benzoyl peroxide	5.0	48	—	33.6
149-44-1	Acetic anhydride	50	75	Gamma-rays	0.206	99.7	20.54	56.16
100D	Acetic anhydride	50	Ambient	Gamma-rays	0.195	96.3	18.78	55.32
198-35-1	None	—	100 ± 2.0	Gamma-rays	0.200	112.6	22.52	19.52
198-35-2	None	—	125 ± 2.0	Gamma-rays	0.200	112.6	22.52	25.99

concentration was increased to ca. 5%, and 33.94% toluene-insoluble polymer was obtained after polymerization at $60 \pm 0.2^\circ\text{C}$. for 48 hr. In another experiment, 50% maleic anhydride in acetic anhydride was maintained at $70 \pm 0.2^\circ\text{C}$. in the presence of an initial amount of 5.0 wt.-% benzoyl peroxide for 48 hr., resulting in the ultimate isolation of 33.6% polymeric product, having $[\eta] = 0.1211$ dl./g. in acetophenone. The polymer solutions as prepared by initiation with benzoyl peroxide were very dark in color, even black. The precipitated polymer was considerably lighter in color.

The free-radical polymerization initiated by diacetyl-ultraviolet light radiation was carried out for 27 days, 1% diacetyl in a 50% maleic anhydride-acetic anhydride solution being used. Conversions of 13.34 and 15.99% were obtained to a product presumed to be polymeric but not yet characterized as such. The irradiated solutions were a deep purple color at the end of the polymerization period. After precipitation and reprecipitation, the product retained a slight purple tint.

Table IV summarizes the data comparing the various initiator systems used.

The effect of temperature upon the polymerization rate was studied, using both initiation by benzoyl peroxide and by gamma-radiation. As may be seen in Table V, there is no appreciable temperature effect in the range studied when benzoyl peroxide is used as the initiator. Similarly, gamma-radiation initiation with a total dose of ca. 20 Mrads with acetic anhydride as the solvent shows only a slight temperature effect. But when molten maleic anhydride was irradiated with no solvent present, increasing the temperature from 100°C . to 125°C . increased the conversion by one-third at a similar total dose level.

There seems to be a synergistic effect in the combination of maleic anhydride and acetic anhydride. This mixture exhibits both higher polymerization rate and higher molecular weight polymer. Note that the conversion rate is greater in this solvent than in the melt at comparable radiation levels.

Polymer Characteristics

Poly(maleic anhydride) is soluble in water, lower alkyl alcohols, ketones, ethers, and nitroparaffins. It is essentially insoluble in aromatic hydrocarbons, most chlorinated solvents, and the higher paraffins. The hydrolysis product is readily soluble in water, but not readily soluble in the other solvents types mentioned for the poly anhydride. The monosodium salt is water soluble.

The intrinsic viscosity of poly(maleic anhydride) prepared from carefully purified starting materials (Sample PY-100F) was determined in six solvents by standard techniques. These data are given in Table VI.

The intrinsic viscosity of poly(maleic acid) (monosodium salt) was 0.1412 dl./g. at constant ionic strength of 0.14046 meq. of Na^+ /ml., sodium hydroxide being used as the source of the sodium ion.

Since the hydrolyzed polymer is a polyelectrolyte with a high potential

TABLE VI
Intrinsic Viscosity of Polymaleic Anhydride in Various Solvents^a

Solvent	$[\eta]$, dl./g.
Acetonitrile	0.101
<i>N,N</i> -Dimethylformamide	0.120
Acetic anhydride	0.126
Butanone	0.127
Acetophenone	0.146
1,4-Dioxane	0.126

^a Polymer: 100 F prepared at 0.195 Mrad hr. (39.0 Mrads); light-scattering molecular weights 23.1×10^3 .

charge density for every carbon in the main polymer chain, many questions arise concerning its behavior under conditions where these charges are operable. One of these concerns the viscosity of aqueous solutions at various pH values; as can be seen in Table VII, there is no change of great mag-

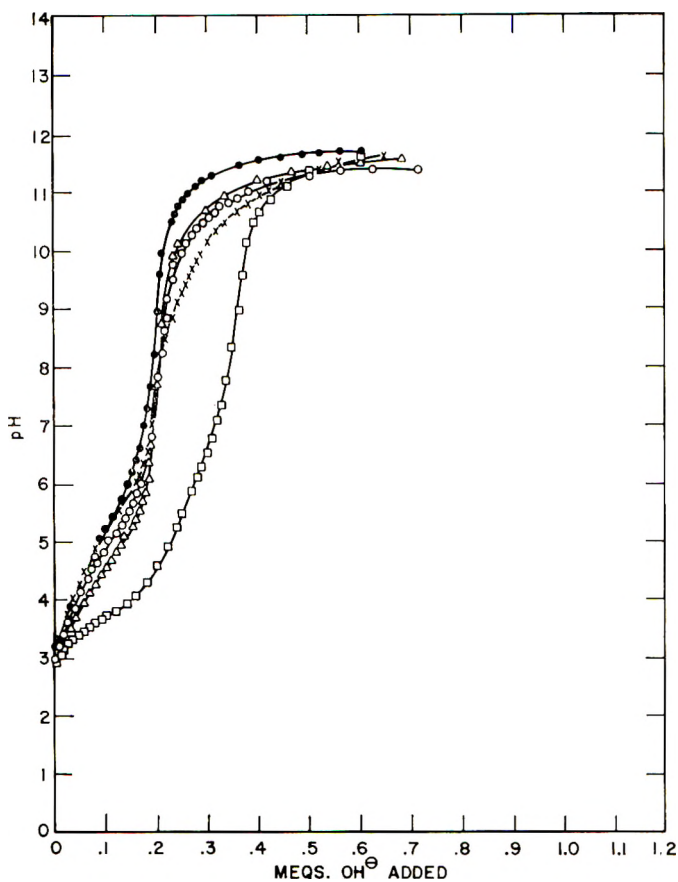


Fig. 4. Titration behavior at 20 ml. 0.02*N* poly(maleic anhydride) with various 0.02*N* bases: (○) NaOH; (▲) KOH; (□) Ba(OH)₂; (×) LiOH; (●) (CH₃)₄NOH.

TABLE VII

The Effect of pH Upon Relative Viscosity at a Poly(maleic Anhydride) Concentration of 0.50 g./l.

NaOH added, meq.	pH	Relative viscosity
0.0	2.66	1.090
0.3583	3.66	1.144
0.7166	4.34	1.185
1.075	4.80	1.211
1.433	5.45	1.240
1.792	8.40	1.222
2.150	9.70	1.176
2.408	10.50	1.124
2.866	11.06	1.053
3.225	11.50	1.031

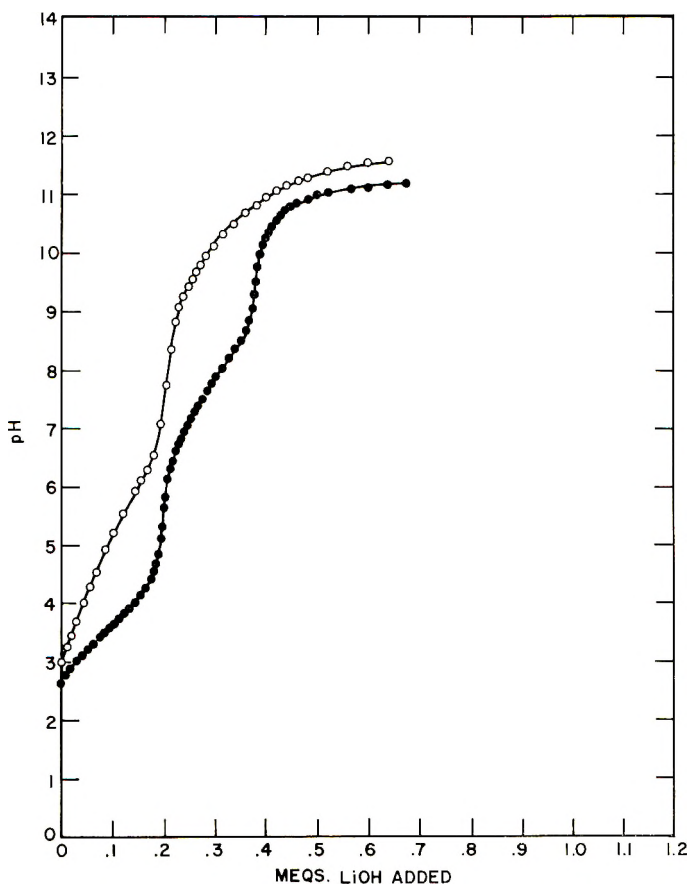


Fig. 5. Titration of 20 ml. 0.02*N* poly(maleic anhydride) with 0.02*N* LiOH in the presence of LiBr: (O) no salt; (●) 0.3*M* LiBr.

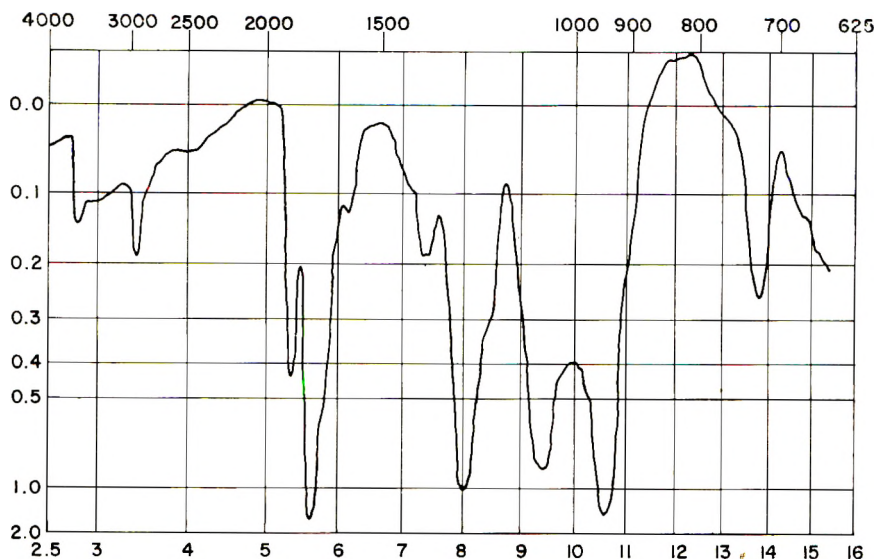


Fig. 7. Infrared spectrum of poly(maleic anhydride).

Potentiometric titrations of poly(maleic anhydride) were carried out with lithium, sodium, potassium, barium, and tetramethylammonium hydroxides. These data, graphed in Figure 4, are the first known examples of neighbor-neighbor interaction by the carboxylic groups of a poly-acid. The potentiometric titration curve is grossly changed when a supporting electrolyte is present to minimize the coulombic long-range repulsions of the poly-acid. The electrolyte was usually one providing an ion common to that of the base. The potentiometric titration curve of poly(maleic acid) at constant volume by lithium hydroxide in both the absence and presence of lithium bromide is shown in Figure 5. Here sufficient common ion has been added to cause great diminution of the neighbor-neighbor interaction.

The viscosity behavior of the acid alone in 1N HCl, and in the presence of varying amounts of sodium ion is shown in Figure 6.

The molecular weight of the polymer whose intrinsic viscosity data are given in Table VI was determined by light scattering, giving a value of 23.1×10^3 , or a \overline{DP} of 199. The melting point of this polymer was ca. 320°C ., with decomposition. The infrared absorption curve of this polymer is reproduced in Figure 7.

References

1. Alfrey, T., and E. Lavin, *J. Am. Chem. Soc.*, **67**, 2044 (1945).
2. Alfrey, T., J. J. Bohrer, and H. Mark, *Copolymerization*, Interscience, New York, 1952, p. 45.
3. Bamford, C. H., W. G. Barb, A. D. Jenkins, and P. F. Onyon, *The Kinetics of Vinyl Polymerization by Radical Mechanisms*, Academic Press, New York; Butterworths, London, 1958, p. 183.

4. Bawn, C. E. H., *The Chemistry of High Polymers*, Interscience, New York, 1948, pp. 14, 15.
5. D'Alelio, G. F., *Fundamental Principles of Polymerization*, Wiley, New York, 1952, pp. 49, 423.
6. DeWilde, M. C., and G. Smets, *J. Polymer Sci.*, **5**, 253 (1950).
7. Flory, P. J., *Principles of Polymer Chemistry*, Cornell Univ. Press, Ithaca, N.Y., 1957, p. 55.
8. Griess, G. A., R. H. Boundy, and R. F. Boyer, *Styrene, Its Polymers, Copolymers and Derivatives*, A.C.S. Monograph No. 115, Reinhold, New York, 1952, p. 862.
9. Küchler, L., *Polymerisations-Kinetik*, Springer-Verlag, Berlin-Göttingen-Heidelberg, 1951, p. 161.
10. Lewis, F. M., and F. R. Mayo, *J. Am. Chem. Soc.*, **70**, 1530, 1535 (1948).
11. Mark, H., and A. V. Tobolsky, *Physical Chemistry of High Polymer Systems*, 2nd Ed., Interscience, New York, 1950, p. 395.
12. Marvel, C. S., *An Introduction to the Organic Chemistry of High Polymers*, Wiley, New York, 1959, p. 62.
13. Restaino, A. J., R. B. Mesrobian, H. Morawetz, D. S. Ballantine, G. J. Dienes, and D. J. Metz, *J. Am. Chem. Soc.*, **78**, 2942 (1956).
14. Wagner-Jauregg, T., *Ber.*, **63**, 3213 (1930).
15. Lustig, B., and H. Wachtel, *Biochem. Z.*, **298**, 330 (1938).
16. Bartlett, P. D., and K. Nozaki, *J. Am. Chem. Soc.*, **68**, 1495 (1946).
17. Marvel, C. S., E. J. Prill, and D. F. Detar, *J. Am. Chem. Soc.*, **69**, 52 (1947).
18. Guile, R. L., and J. C. Drougas, *Dissertation Abstracts*, **21**, 3265 (1961); unpublished thesis.
19. Hansen, A. W., private communication.

Résumé

Contrairement à ce qui était accepté, l'anhydrique maléique a pu être homopolymérisé. La polymérisation du monomère fondu et du monomère en solution a été initiée en utilisant le rayonnement gamma et les initiateurs à radicaux libres. Un polyanhydride ayant $[\eta] = 0.146 \text{ dl/g}^{-1}$ dans l'acétophénone présente un poids moléculaire de 23.100 (acide libre) de $DP = 199$, par la méthode de diffusion lumineuse. La proximité des groupes carboxyles et responsable du comportement particulier des solutions aqueuses des sels du polyacide.

Zusammenfassung

Im Gegensatz zu den üblichen Vorstellungen war es möglich Maleinsäureanhydrid zur Homopolymerisation zu bringen. Die Polymerisation des geschmolzenen oder gelösten Monomeren wurde mit γ -Strahlen oder mit Radikalstartern angeregt. Ein Anhydrid mit $[\eta] = 0,146 \text{ dl/g}^{-1}$ in Acetophenon besass nach Lichtstreuungsmessungen ein Molekulargewicht von 23100 (freie Säure), entsprechend einem DP von 199. Die Nachbarschaft der Karboxylgruppen ist für das eigentümliche Verhalten der wässrigen Lösungen von Salzen der Polysäure verantwortlich.

Received January 17, 1962

Copolymerization Studies. III. Reactivity Ratios of Model Ethylene Copolymerizations and Their Use in Q - e Calculations

R. D. BURKHART and N. L. ZUTTY, *Research and Development Department, Union Carbide Chemicals Company, South Charleston, West Virginia*

Synopsis

Monomer reactivity ratios for the copolymerization of ethylene (M_2) with *n*-butyl acrylate, vinyl chloride, vinyl acetate, and vinyl fluoride have been measured at 1000 atm. The respective values and the experimental temperatures are $r_1 = 11.9$, $r_2 = 0.03$, 70°C.; $r_1 = 3.6$, $r_2 = 0.24$, 90°C.; $r_1 = 1.08$, $r_2 = 1.07$, 90°C.; $r_1 = 0.16$, $r_2 = 4.39$, 160°C. Price Q and e values for ethylene calculated from these reactivity ratios, uncorrected for differences in reaction pressure, are 0.03 and -0.43 , respectively. New Q and e values (Q_0 and e_0) for these four comonomers were calculated on the basis of ethylene rather than styrene as the reference monomer. Assuming that the Q_0 and e_0 values for ethylene are 1.0 and zero, respectively, the monomer's Q_0 and e_0 value are as follows: *n*-butyl acrylate, 33.3, + 1.02; vinyl chloride, 4.2, + 0.37; vinyl acetate, 0.93, ~ 0 ; vinyl fluoride, 0.25, + 0.6. These Q_0 and e_0 values give calculated reactivity ratios which are in reasonable agreement with experimental ones. Good agreement is also obtained when the r_2 value for the vinyl acetate/ethylene copolymerization is compared with the directly determined rate constant ratio for the addition of an ethyl radical to ethylene and to vinyl acetate, respectively, calculated from previously published data.

The free-radical polymerization of ethylene has been studied by a number of workers at autogeneous as well as high pressures.¹⁻³ Although the mechanism for the high pressure, oxygen-initiated reaction has not been precisely established,⁴ it appears that the conventional addition polymerization mechanism is applicable to this high pressure reaction when the usual free-radical initiators are used.⁵ In studying free-radical copolymerizations of ethylene at high pressures, therefore, one is justified in utilizing the scheme proposed by Mayo and Lewis⁶ for relating instantaneous comonomer composition to the instantaneously formed copolymer.

A study of this sort is prompted by a number of considerations. The increasing industrial importance of ethylene copolymers, for instance, demands that accurately known monomer reactivity ratios be obtained. Also, from a theoretical point of view, such a study may be of aid in relating monomer structure to reactivity, since ethylene with its lack of substituent groups is the logical choice for the reference point of such a scheme.

With these views in mind, a study was undertaken to determine the re-

activity ratios involved when ethylene is copolymerized with *n*-butyl acrylate, vinyl acetate, vinyl chloride, and vinyl fluoride under free-radical conditions at 1000 atm. pressure.

EXPERIMENTAL

Monomer Purification and Polymerization Procedure

The experimental equipment and the basic experimental methods have been described previously.⁷ Vinyl acetate and *n*-butyl acrylate (Union Carbide Chemicals Company) were purified by fractional distillation and center cuts retained for use. Vinyl fluoride (E. I. du Pont de Nemours and Company) was treated by passage through Linde #5A molecular sieves before use, and polymerization grade vinyl chloride (Union Carbide Chemicals Company) was used as obtained. Ethylene was treated for oxygen removal by passing through an activated copper column at 180°C. The oxygen level was reduced to 10 ppm by this treatment.

The liquid comonomers were weighed directly into the open autoclave. The autoclave was then sealed and thoroughly purged with high purity nitrogen (Linde Company) before the introduction of ethylene. The gaseous comonomers were admitted from small tared cylinders after the autoclave had been purged with high purity nitrogen. Pressure was maintained throughout the reaction by pumping the solvent, sulfur-free, toluene. Azobisisobutyronitrile (Westville Laboratories) was the catalyst used in the *n*-butyl acrylate, vinyl acetate, and vinyl chloride copolymerizations; the vinyl fluoride copolymerization was catalyzed by di-*tert*-butyl peroxide (Wallace and Tiernan). In all cases, the polymerizations were carried to less than 10% conversion and in most cases, less than 5%.

Polymer Isolation and Analysis

The pure copolymers were isolated as previously described.⁷ Copolymer analyses were carried out by the appropriate elemental analysis. Carbon and chlorine determinations were made in these laboratories, and fluorine analyses were performed by the Clark Microanalytical Laboratories. The reduced viscosities of all copolymers were 0.2 dl./g. or greater.

RESULTS AND DISCUSSION

Figures 1 through 4 show the resulting monomer-polymer composition curves for the four copolymerizations studied. In Table I the reactivity ratios, calculated by the method of Fineman and Ross,⁸ are given.

From these data several interesting points are immediately apparent. The first is that even though four comonomers widely differing in reactivity were copolymerized with ethylene, three of them gave reactivity ratio products (r_1r_2) equal to unity within experimental error and the product for the fourth, butyl acrylate, did not deviate widely from unity. This, of course,

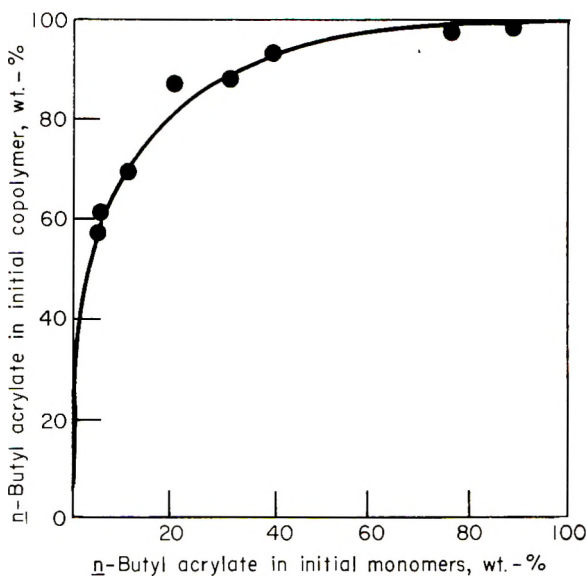
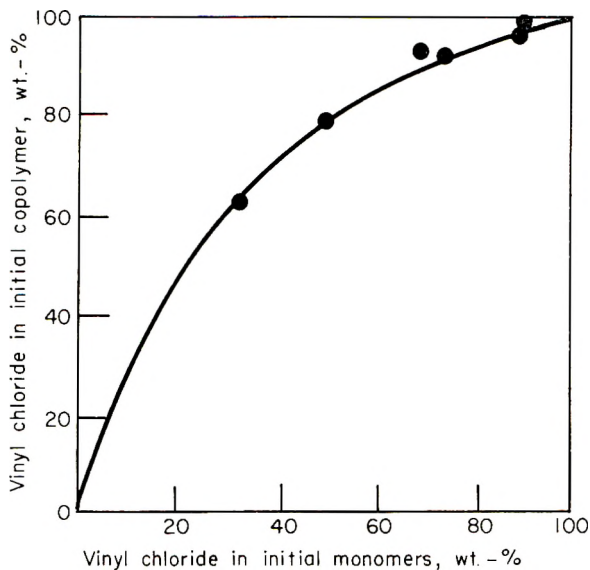
Fig. 1. *n*-Butyl acrylate-ethylene.

Fig. 2. Vinyl chloride-ethylene.

shows that these copolymerizations tend to be ideal and that truly random copolymers, with little alternating tendency, are obtained in ethylene copolymerizations. The implications arising from these phenomena are discussed below in the calculation of structure-reactivity parameters from these reactivity ratio data.

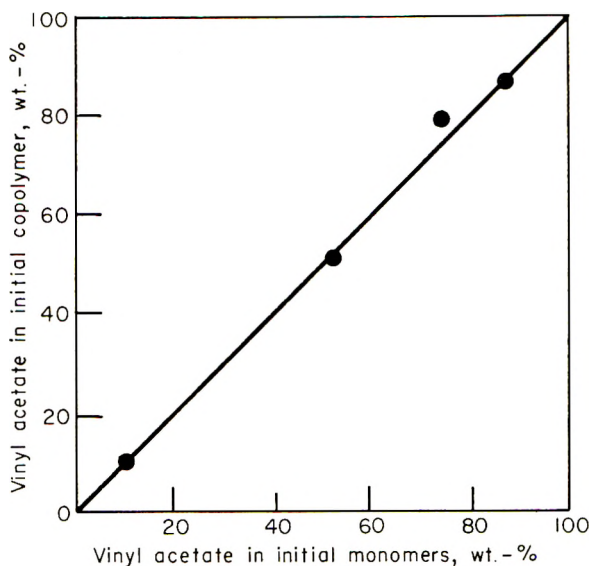


Fig. 3. Vinyl acetate-ethylene.

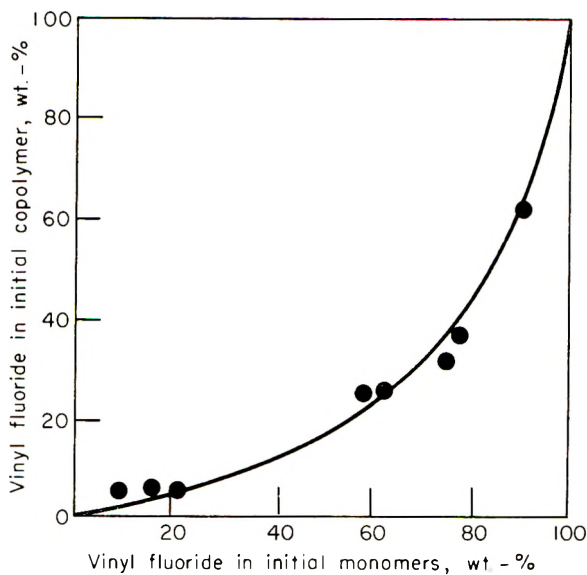


Fig. 4. Vinyl fluoride-ethylene.

Another interesting observation is the wide difference in reactivity of the two vinyl halides, ethylene lying almost midway between vinyl chloride and vinyl fluoride in double-bond reactivity. Although a difference in reactivity between vinyl chloride and vinyl fluoride is to be expected, that one is more and the other less reactive than ethylene is not easily explainable. A third point noticed from these data is that $r_1 r_2 = 1$ for the ethyl-

TABLE I
Reactivity Ratios for Various Monomers Copolymerizing with Ethylene (M_2)

Comonomer	Reaction temp., °C.	r_1	r_2	r_1r_2
<i>n</i> -Butyl acrylate	70	11.9 ± 2.5	0.03 ± 0.01	0.36 ± 0.12
Vinyl chloride	90	3.60 ± 0.30	0.24 ± 0.07	0.85 ± 0.26
Vinyl acetate	90	1.08 ± 0.19	1.07 ± 0.06	1.16 ± 0.21
Vinyl fluoride*	160	0.16 ± 0.05	4.39 ± 0.77	0.70 ± 0.25

* Recent compositional analysis of the vinyl fluoride copolymers by NMR indicates that r_1 might be as much as 15% higher and r_2 15% lower than indicated in Table I.

ene-vinyl acetate copolymerization. This is rare but certainly not unique for a copolymer system.

***Q* and *e* Values for Ethylene Based on Styrene ($Q = 1.0$, $e = -0.8$)**

The calculation of Alfrey and Price⁹ *Q* and *e* values for ethylene from these data presents a problem, since it is known that reactivity ratios are affected by the application of high pressures.⁷ It has been shown, however, that the methyl methacrylate/acrylonitrile and styrene/acrylonitrile copolymerizations tend simply to become more ideal (r_1r_2 tends toward unity) as pressure is increased to 1000 atm., with the result that the *e* values of a comonomer pair tend toward each other with increasing pressure while the *Q* values are relatively unaffected.⁷ The generality of this phenomenon has not been firmly established, but the possible utility of having even approximate *Q* and *e* values for ethylene would seem to justify the inclusion of these calculated values at this point. These are presented in Table II.

TABLE II
Q and *e* Values for Ethylene

Comonomer	<i>Q</i>	<i>e</i>	Reference
<i>n</i> -Butyl acrylate ^a	0.04	-0.41	Alfrey et al. ¹⁰
Vinyl chloride	0.01	-0.57	Thompson and Raines ¹¹
Vinyl acetate	0.03	-0.30	Alfrey et al. ¹⁰
Average	0.03	-0.43	

^a The comparison monomer was actually methyl acrylate.¹⁰

The very low *Q* value for ethylene is certainly to be expected. This finding corresponds with the fact that the activation energy for the addition of an ethyl radical to ethylene is 8.6 kcal./mole,¹² while the addition of an ethyl radical to styrene requires only 4.0 kcal./mole activation energy.¹³

***Q* and *e* Values Based on Ethylene as the Reference Monomer**

It has been suggested that the double bond of ethylene would provide the most reasonable reference point for the *Q*-*e* scheme,¹⁰ however, no quan-

titative data on ethylene copolymerizations have been available heretofore. Indeed, it would seem that ethylene copolymerizations at high pressure might provide a most useful method for the determination of relative monomer reactivities, since the perturbing effects of alternation due to double-bond polarity differences in the comonomers are at a minimum here. It is of interest, therefore, to determine Q and e values for these comonomers using ethylene as the reference monomer.

Since the e value of a vinyl monomer is related to the electron-donating or electron-withdrawing characteristics of the pendant group on the double bond, one may assume that the e value for ethylene is zero. Even though subsequent work may indicate that a slight shift in this e value is desired solely to augment the self-consistency of the scheme, the choice $e = 0$ for ethylene is advantageous and provides a reasonable starting value from which to work. When the Q value for ethylene is chosen to be equal to unity, then the equations relating reactivity ratios to Q and e values become

$$r_1 = (Q_0)_1 \exp \{ -(e_0)_1^2 \} \quad (1)$$

$$r_2 = 1/(Q_0)_1 \quad (2)$$

for ethylene as monomer 2, where the subscript zero denotes the ethylene-based Q - e values.

One important advantage which is obtained with the use of this system instead of the styrene-based system is illustrated in eq. (2). Here it is seen that the Q_0 value for a monomer is a rate constant ratio requiring no adjustment due to differences in double-bond polarity as is required when styrene is used as the reference monomer. A comparison of Q_0 values is therefore a more straightforward measure of monomer reactivity than a comparison of Q values.

It will also be noted that here the copolymerization ideality (the proximity of $r_1 r_2$ to unity) depends only on the e_0 value of the comonomer, and, since ethylene resides at the zero point of the e scale, a relatively large (positive or negative) e_0 value is required to remove $r_1 r_2$ very far from unity. The experimental $r_1 r_2$ values given in Table I bear this out, $r_1 r_2$ being close to unity for ethylene copolymerizations with vinyl acetate, vinyl chloride, and vinyl fluoride; only with *n*-butyl acrylate, whose e value is highly

TABLE III
Comparison of Calculated Q and e Values with Ethylene as the Reference Monomer (Q_0 and e_0) with Q and e Values with Styrene as the Reference

Monomer	Q_0	e_0	Q	e	Reference
<i>n</i> -Butyl acrylate ^a	33.3	+1.02	0.42	+0.6	Alfrey et al. ¹⁰
Vinyl chloride	4.2	+0.37	0.04	-0.17	Thompson and Raines ¹¹
Vinyl acetate	0.93	~0	0.03	-0.3	Alfrey et al. ¹⁰
Vinyl fluoride	0.25	+0.6	—	—	

^a Compared with methyl acrylate.

positive, does the reactivity ratio product vary much from ideality. The Q_0 and e_0 values are given in Table III and compared with Q and e values calculated on the styrene basis ($Q = 1.0$, $e = -0.8$) where possible.

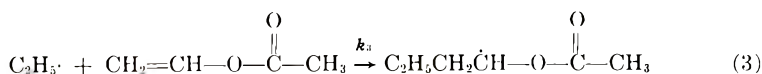
In order to determine if these values are reasonable, reactivity ratios have been calculated for the various copolymerizations possible with the chosen comonomers and compared with experimental values. This comparison is given in Table IV. It will be noted that, although the calculated values refer to high pressure reactions, the degree of agreement is at least sufficient to show that Q_0 and e_0 values are reasonable.

TABLE IV
Reactivity Ratios Calculated from Q_0 and e_0 Values

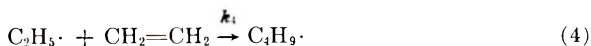
Monomer 1	Monomer 2	r_1		r_2	
		Expt.	Calc.	Expt.	Calc.
<i>n</i> -Butyl acrylate ^a	Vinyl chloride	5.0	4.0	—	0.16
<i>n</i> -Butyl acrylate ^a	Vinyl acetate	9.0 ± 2.5	12.6	0.1 ± 0.1	0.03
Vinyl chloride	Vinyl acetate	2.1	3.7	0.3	0.22

^a Compared with methyl acrylate.

It is of further interest to compare the results obtained here with those recently published by James and MacCallum¹³ on the rates of addition of ethyl radicals to various monomers. When a value of 10^{14} cm.³/mole-sec. is taken as the bimolecular rate constant for the recombination of ethyl radicals,¹² one obtains a value of $k_3 = 1.0 \times 10^7$ cm.³/mole-sec. for the reaction



at 90°C. From the activation energies and frequency factors tabulated by Metcalfe and Trotman-Dickenson,¹² the rate constant for the reaction



is calculated to be 5.0×10^6 cm.³/mole-sec., also at 90°C. The ratio $k_4/k_3 = 0.5$. The directly comparable value (r_2) for the analogous homo- and cross-propagation reactions in the copolymerization of ethylene with vinyl acetate is 1.07. This is quite reasonable agreement, considering the experimental pressure difference which would, if anything, make agreement even closer.

CONCLUSIONS

The high pressure copolymerization of ethylene with *n*-butyl acrylate, vinyl chloride, vinyl acetate, and vinyl fluoride give monomer reactivity ratios from which Q and e values may be calculated on the basis of ethylene as the reference monomer ($Q = 1.0$, $e = 0$). These new Q - e values form

an internally consistent scheme judging from calculated reactivity ratios. Although high reaction pressures have to be used in order to obtain a wide range of copolymer compositions, this practical disadvantage may be offset by the fact that a better reference standard becomes available. The close agreement of the r_2 value for the vinyl acetate/ethylene copolymerization with the directly determined rate constant ratio (k_4/k_3) indicates that data obtained by either method may be useful in attempts to relate monomer structure with reactivity.

The authors wish to acknowledge the assistance of Mr. Ray Haas and Mr. Don Watts in carrying out many of the experiments.

References

1. Laird, R. K., A. G. Morrell, and L. Seed, *Discussions Faraday Soc.*, **22**, 126 (1956).
2. Laita, Z., and Z. Machacek, *J. Polymer Sci.*, **38**, 459 (1959).
3. Lyubetskii, S. G., B. A. Dolgoplosk, and B. L. Erusalimskii, *Vysokomolekulyarne Soedineniya*, **3**, 734 (1961).
4. Ehrlich, P., and R. N. Pittilo, *J. Polymer Sci.*, **43**, 389 (1960).
5. Kadama, S., Y. Matsushima, A. Ueyoshi, T. Shimidzu, T. Kagiya, S. Yuasa, and K. Fukui, *J. Polymer Sci.*, **41**, 83 (1959).
6. Mayo, F. R., and F. M. Lewis, *J. Am. Chem. Soc.*, **66**, 1594 (1944).
7. Burkhart, R. D., and N. L. Zutty, *J. Polymer Sci.*, **57**, 793 (1962).
8. Fineman, M., and S. D. Ross, *J. Polymer Sci.*, **5**, 259 (1950).
9. Alfrey, T., and C. C. Price, *J. Polymer Sci.*, **2**, 101 (1947).
10. Alfrey, T., J. J. Bohrer, and H. Mark, *Copolymerization*, Interscience, New York-London, 1952, p. 91.
11. Thompson, B. R., and R. H. Raines, *J. Polymer Sci.*, **41**, 265 (1959).
12. Metcalfe, E. L., and A. F. Trotman-Dickinson, *J. Chem. Soc.*, **1960**, 5072.
13. James, D. G. L., and D. MacCallum, *Proc. Chem. Soc.*, **1961**, 259.

Résumé

Les rapports des réactivités monomériques pour la copolymérisation d'éthylène (M_2) avec l'acrylate de *n*-butyle, chlorure de vinyle, acétate de vinyle et fluorure de vinyle ont été mesurés à 1000 atm. Les valeurs respectives et les températures expérimentales sont $r_1 = 11.9$, $r_2 = 0.03$, 70°C.; $r_1 = 3.6$, $r_2 = 0.24$, 90°C.; $r_1 = 1.08$, $r_2 = 1.07$, 90°C.; $r_1 = 0.16$, $r_2 = 4.39$, 160°C. Les valeurs Q et e de Price pour l'éthylène calculées aux dépens de ces rapports de réactivités, non-corrigés pour les différences dans la pression de réaction sont 0.03 et -0.43 respectivement. De nouvelles valeurs de Q et e (Q_0 et e_0) pour ces quatre comonomères ont été calculées en utilisant l'éthylène au lieu du styrène comme monomère de référence. Supposant que les valeurs Q_0 et e_0 pour l'éthylène soient 1.0 et zéro respectivement, les valeurs Q_0 et e_0 des monomères sont les suivants: acrylate de *n*-butyle, 33.3, + 1.02; chlorure de vinyle, 4.2, + 0.37; acétate de vinyle, 0.93, ~ 0 ; fluorure de vinyle, 0.25, + 0.6. Ces valeurs de Q_0 et e_0 donnent des rapports de réactivités calculés qui concordent de façon raisonnable avec les valeurs expérimentales. Un bon accord est également obtenu lorsque la valeur r_2 pour la copolymérisation acétate de vinyle/éthylène est comparée avec le rapport des constantes de vitesse directement déterminé dans le cas de l'addition d'un radical éthyle à l'éthylène et à l'acétate de vinyle, respectivement, calculé des données publiées précédemment.

Zusammenfassung

Monomerreaktivitätsverhältnisse wurden für die Copolymerisation von Äthylen (M_2) mit *n*-Butylacrylat, Vinylchlorid, Vinylacetat und Vinylfluorid bei 1000 Atm bestimmt. Die betreffenden Werte sowie die Versuchstemperaturen sind $r_1 = 11,9$, $r_2 = 0,03$, 70°C; $r_1 = 3,6$, $r_2 = 0,24$, 90°C; $r_1 = 1,08$, $r_2 = 1,07$, 90°C; $r_1 = 0,16$, $r_2 = 4,39$, 160°C. Nach Price daraus berechnete Q - und e -Werte betragen ohne Korrektur für Druckunterschiede 0,03 bzw. $-0,43$. Neue Q - und e -Werte (Q_0 und e_0) wurden für die vier Comonomeren mit Äthylen als Bezugsmonomerem an Stelle von Styrol berechnet. Unter der Annahme dass die Q_0 - und e_0 -Werte für Äthylen 1,0 bzw. Null sind, ergeben sich für die Q_0 - und e_0 -Werte der Monomeren folgende Zahlen: *n*-Butylacrylat, 33,3, + 1,02; Vinylchlorid 4,2, + 0,37; Vinylacetat 0,93, ~ 0 ; Vinylfluorid 0,25, + 0,6. Diese Q_0 - und e_0 -Werte liefern berechnete Reaktivitätsverhältnisse, die eine brauchbare Übereinstimmung mit den experimentellen Werten zeigen. Gute Übereinstimmung wird auch beim Vergleich des r_2 -Wertes für die Vinylacetat-Äthylencopolymerisation mit dem direkt bestimmten, aus früher veröffentlichten Daten berechneten, Verhältnis der Geschwindigkeitskonstanten der Addition eines Äthylradikals an Äthylen und Vinylacetat erhalten.

Received December 20, 1961

Revised January 18, 1962

Interfacial Polycondensation. XIII. Viscosity-Molecular Weight Relationship and Some Molecular Characteristics of 6-10 Polyamide

PAUL W. MORGAN and STEPHANIE L. KWOLEK,
*Pioneering Research Laboratory Textile Fibers Department,
E. I. du Pont de Nemours and Company, Inc., Wilmington, Delaware*

Synopsis

Number-average molecular weights were estimated by determination of endgroups on 6-10 polyamide samples prepared by stirred and unstirred interfacial polycondensation procedures under varying conditions. Polymers made by melt and interfacial polycondensation methods obeyed the same dilute solution viscosity relationships. However, polymers from interfacial polycondensation reactions deviated in molecular weight distribution from that found for polymers prepared by the melt method. The deviation, which presents the appearance of broader than random distribution, is believed to result to a considerable degree from the presence of an unusually large low molecular weight fraction rather than a continuous distortion of the distribution curve. The interfacially prepared polyamides having the highest viscosity numbers, obtained by adjusting the concentration ratios of the two reactants, showed the least deviation from random distributions. Evidence was found for branching and even network formation in 6-10 polyamide prepared by interfacial polycondensation as the concentration of the diacid chloride phase was increased. Branching probably occurred through acylation of amide links along the polymer chain to yield imide groups. These groups were cleaved to amide groups in the molten polymer or upon solution in sulfuric acid. Melt-prepared, unfractionated 6-10 polyamide followed the relationship $[\eta] = 1.35 \times 10^{-4} \bar{M}_n^{0.95}$, and a k' factor of 0.43 was found in the equation relating solution viscosity to concentration, $\eta_{sp}/c = [\eta] + k'[\eta]^2c$, for dilute solution determinations in *m*-cresol at 25°C.

INTRODUCTION

Flory¹ first developed relationships for the size distribution of molecules of condensation polymers prepared from bifunctional intermediates. These relationships were based on the premises that there was equal reactivity for all like end groups regardless of the length of the polymer chain and that the end groups reacted randomly. Aliphatic polyamides prepared in a molten state at elevated temperature under nondegradative conditions have been shown²⁻⁵ to possess the molecular weight distribution described by Flory.

The low temperature process of interfacial polycondensation^{6,7} presents an entirely different set of conditions for polyamide formation. It is, therefore, of interest to compare the molecular characteristics and particu-

larly the dilute solution viscosity-molecular weight relationship of these polymers with a typical polymer made by the melt process.

In interfacial polycondensation, as in melt polycondensation, the reactivity of like functional groups at the ends of all but the shortest polymer molecules is presumed to be the same. However, the heterogeneous nature of the interfacial polycondensation procedure could lead to a nonhomogeneous distribution of intermediates and of chain-terminating effects. Some of these restrictions could then result in the nonrandom formation of polymer species. A polymer suitable for study was poly(hexamethylene sebacamide), coded 6-10 polyamide.

RESULTS AND DISCUSSION

Dilute Solution Viscosity

As a preliminary step to the examination of 6-10 polyamide made by interfacial polycondensation, a series of polymers was made by the equilibrium melt method. Table I gives the conditions of preparation, the intrinsic

TABLE I
Intrinsic Viscosity and Molecular Weight Data for 6-10 Polyamide by the Melt Method

Polymerization conditions				Endgroups/10 ⁶ g.				
Temp., °C.	Pressure	Time, hr.	$[\eta]^a$	k'^b	NH ₂	COOH	Total	\bar{M}_n^c
225°C	Sealed tube	2.0	0.770	0.43	31	214	245	8,200
225	Sealed tube	3.0	1.230	0.43	62	86	148	13,500
225	Sealed tube	2.0	1.412	0.44	74	57	131	15,300
250	N ₂ , 760 mm.	2.0						
225	Sealed tube	2.0	2.045	0.42	49	42	91	22,000
250	N ₂ , 760 mm.	2.0						
250	0.1 mm.	0.66						
200	Sealed tube	2.0	2.140		52	32	84	23,800
250	N ₂ , 760 mm.	2.0						
250	1.0 mm.	1.0						

^a Intrinsic viscosity in *m*-cresol at 25°C.

^b Factor for Huggins viscosity equation.

^c Number-average molecular weight calculated from total endgroups with the assumption of two end-groups per molecule.

viscosities in *m*-cresol, and molecular weights by endgroup determinations. Figure 1 shows plots of η_{sp}/c versus c , where η_{sp} is specific viscosity and c is concentration. The value of the k' factor in the Huggins³ equation

$$\eta_{sp}/c = [\eta] + k'[\eta]^2c$$

was found to be 0.43, where $[\eta]$ is intrinsic viscosity. This is appreciably different from the value of 0.11 for 6-6 polyamide in 90% formic acid found

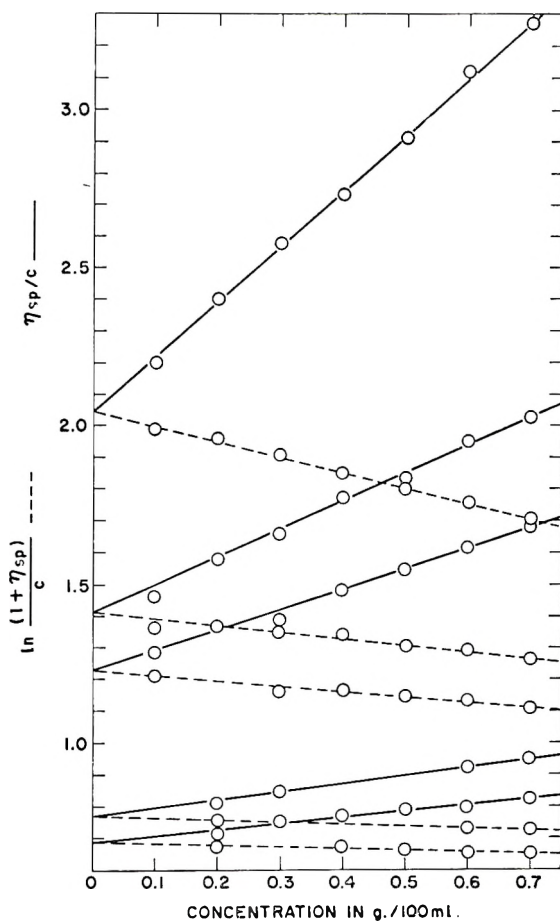


Fig. 1. Solution viscosity (*m*-cresol at 25°C.) vs. concentration relationship for 6-10 polyamide prepared by the melt method.

by Taylor² but is close to the range of 0.35 to 0.40 reported for many linear polymers.^{1b}

The values for k' for 6-10 polyamide made by unstirred⁶ and stirred⁷ interfacial polycondensation procedures were the same as for polymer made by the melt method. Three plots for polymers of similar intrinsic viscosity but made by different interfacial procedures are given in Figure 2; k' values for plots for samples A, B, and C are 0.42, 0.43, and 0.42, respectively.

The plot for sample B (made in the presence of detergent) shows curvature upward at low concentrations suggestive of a polyelectrolyte effect.¹⁵ Other peculiarities of this polymer are discussed later.

Intrinsic Viscosity-Molecular Weight Relationships

Number-average molecular weights \bar{M}_n for unfractionated polymers made by the melt method were determined by a micromodification of the

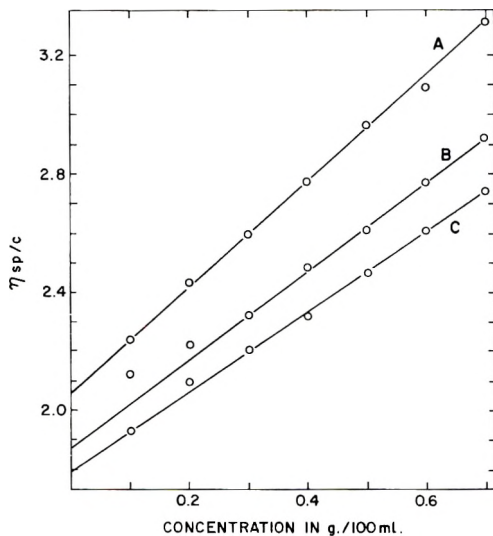


Fig. 2. Solution viscosity (*m*-cresol at 25°C.) vs. concentration relationship for 6-10 polyamide prepared by interfacial polycondensation: (A) stirred method; (B) stirred method with detergent; (C) unstirred method.

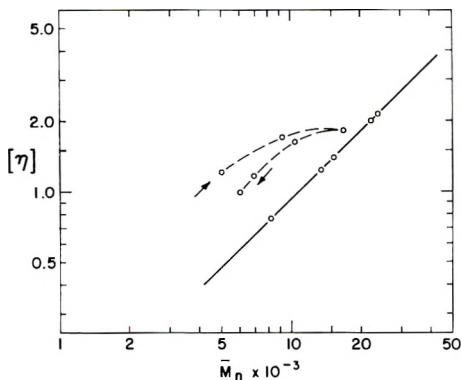


Fig. 3. Relation of intrinsic viscosity in *m*-cresol at 25°C. to number-average molecular weight for 6-10 polyamide: (—) polymers made by melt method; (---) polymers made by unstirred interfacial polycondensation method. Arrows show direction of increasing acid chloride concentration; see Table II.

endgroup methods of Waltz and Taylor.⁹ Figure 3 shows the log-log plot of $[\eta]$ versus \bar{M}_n from which the empirical equations

$$\bar{M}_n = 1.07 \times 10^4 [\eta]^{1.04}$$

or

$$[\eta] = 1.35 \times 10^{-4} \bar{M}_n^{0.96}$$

were obtained.

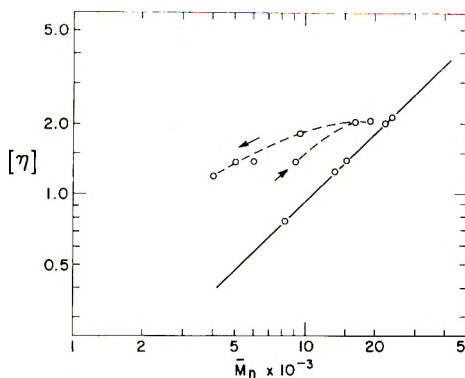


Fig. 4. Relation of intrinsic viscosity in *m*-cresol at 25°C. to number-average molecular weight for 6-10 polyamide: (—) polymers made by melt method; (-----) polymers made by stirred interfacial polycondensation method. Arrows show direction of increasing acid chloride concentration; see Table III.

The exponent a in the second equation usually falls between 1.0 and 0.5. For most polymers the values of a have been in the neighborhood of 0.7,^{1b} but values for various cellulosic materials have approached 1.0. Our value of 0.96 for 6-10 polyamide in *m*-cresol is high compared to several reported values for other aliphatic polyamides.^{2,4,12-14} A high value for a may result in part from a strong polymer-solvent interaction.¹⁰

Number average molecular weights for 6-10 polyamide prepared by interfacial and melt polycondensation processes were compared at the same viscosity number (Tables II and III and Figures 3 and 4). The results show that the polymers from interfacial polycondensation reactions were invariably low in molecular weight for a given intrinsic viscosity. As the concentration ratio of the reactants was varied so as to obtain the highest intrinsic viscosity, the \bar{M}_n of the products approached the \bar{M}_n for polymers made by the melt process at the same intrinsic viscosity. In the stirred system the yield was near a maximum when \bar{M}_n was nearest the value expected for polymer made in a melt system.

As a further check on the molecular weight, \bar{M}_n for the product of procedure B in Paper XII⁷ was determined by the osmotic pressure method in *m*-cresol solution. \bar{M}_n was $19,300 \pm 250$. The polymer contained 27 amine and 88 carboxyl end groups/ 10^6 g., which corresponds to an \bar{M}_n of 17,400. The intrinsic viscosity at 25°C. was 2.19, and a melt polymer of this intrinsic viscosity would have an \bar{M}_n of 24,000. These results uphold the existence of a discrepancy between the value for an interfacial polymer and that expected for a polymer of the same viscosity number made by the melt process.

The deviation described arises from a broader than random distribution of molecular weights. This is not a surprising result from polycondensations carried out under nonequilibrium conditions in two-phase liquid sys-

TABLE II
 Intrinsic Viscosity-Number-Average Molecular Weight Relationship for 6-10 Polyamide
 Made by an Unstirred Interfacial Polycondensation Process^a

Concen- tration ratio, diamine/acid chloride ^b	[η] in <i>m</i> -cresol	Endgroups/10 ⁶ g.			\bar{M}_n ^c	\bar{M}_n for melt polymer of same [η]
		NH ₂	COOH	Total		
0.850	0.99	95	236	331	6,000	10,600
1.70	1.17	98	194	292	6,900	12,500
3.40	1.64	104	90	194	10,400	18,000
6.80	2.00	100	65	165	12,100	22,000
9.00	1.87	42	77	119	16,800	20,000
17.0	1.72	163	55	218	9,200	18,800
34.0	1.21	298	103	401	5,000	12,900

^a Reaction in carbon tetrachloride-water with interface diameter 2.5 in. and rate of film removal 20 ft./min.

^b Diamine at 0.40*M* with 0.80*M* NaOH.

^c Two endgroups per molecule are assumed.

tems from which polymer precipitates instantaneously. A considerable part of the deviation from random distribution is believed to be due to the presence of a low fraction, which has a very high ratio of carboxyl to amine endgroups. The excessively large fraction of low molecular weight polymer probably arises from the trapping of short-chain material in the polymer precipitate, especially on the side of the polymer film away from the liquid interface. Low molecular weight polymer could also form late in the polycondensation experiment as diamine slowly diffuses in to react with acid chloride solution or oligomers occluded in the initial polymer precipitate. Termination with carboxyl groups would result from hydrolysis of the acid chloride function or a failure of diamine to reach acid chloride groups on oligomers.

Although no careful fractionation was undertaken, a number of samples were found to contain fractions of low polymer extractable by acetone or alcohol. Usually these fractions had predominantly carboxyl endgroups. Examples of such extractions are shown in Table VI. Polymers prepared under conditions which gave products with the highest viscosity numbers contained the least amount of extractable material. No attempt has been made to separate cyclic oligomers from the extracts.

It is noteworthy that for the unstirred process the ratio of amine to carboxyl endgroups shifted with changing relative concentration of the reactants (Table II). That is, in the presence of a high relative diamine concentration, a product with a high ratio of amine endgroups was obtained. The unstirred preparations were produced while the reactants were still near to the starting concentrations, and the polymers were removed from the reaction mixture quickly.

The products of stirred preparations show this shift in endgroup ratio to

a much lesser degree (Table III). Undoubtedly, in a stirred preparation under nonoptimum conditions the initial polymer is terminated predominantly with either carboxyl or amine groups, but because of the presence of equivalents of diamine and diacid chloride in the system, continued reaction will produce a modification of the initial endgroup ratio as well as an additional yield of product with the opposite endgroup content.

Redistribution of Molecular Species in Polyamides From Interfacial Polycondensation

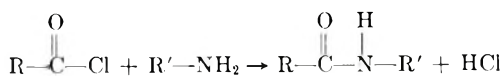
The principle has long been accepted that in polyamidation in a melt above about 200°C. not only is the characteristic distribution of molecular weights achieved in the initial polycondensation but also there is a continual interchange of endgroups and residual moisture with the amide groups along the chain. That is, the polymer species are in equilibrium with themselves and water.^{16,17} Beste and Houtz¹³ showed that interchange along the chains between two amide groups is also possible.

This equilibration process can be used to detect nonrandom distribution of molecular weights in a polyamide and to tell whether the starting distribution is broader or narrower than normal. Requirements for a clear test are that there be no polymer degradation on melting and that there be present and unremoved the amount of moisture needed to maintain the total number of end groups unchanged. The latter condition is not readily achieved. When a polyamide with broader than random distribution is melted and allowed to reach equilibrium without change in \bar{M}_n , the solution viscosity will decrease. The melting of a condensation polymer with a narrow molecular weight distribution will produce a rise in solution viscosity. This result is obtained because the intrinsic viscosity is more dependent on \bar{M}_v than on \bar{M}_n . Large molecules contribute more to the viscosity effect than the same weight of small molecules.

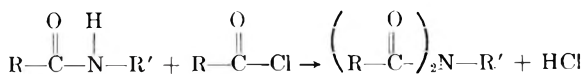
A number of 6-10 polyamide samples made by interfacial polycondensation were dried and melted without stirring at 258°C. (Table IV). In every case except for the highest polymers there was a marked decrease in dilute solution viscosity. The potential viscosity decrease was lessened appreciably by the occurrence of further polycondensation which is shown by the lowered number of end groups in most instances. The points for the equilibrated polymers now fall closer to the line for melt polymers on the \bar{M}_n versus $[\eta]$ plot, and the prior conclusion of a nonrandom distribution is thereby strengthened.

Branching and Network Formation

Evidence for some branching and even network formation was found. The acylation of amide groups along the polymer molecules is proposed as the most likely side reaction. The normal acylation reaction of a primary amine yields an amide:



A second acylation on the amide hydrogen to give an imide is possible when there is no competing amine present and the reaction is not prevented by steric hindrance or low reactivity:



Such a reaction in interfacial polycondensation, where the reactants are multifunctional, would lead to branching and finally to the formation of insoluble networks.

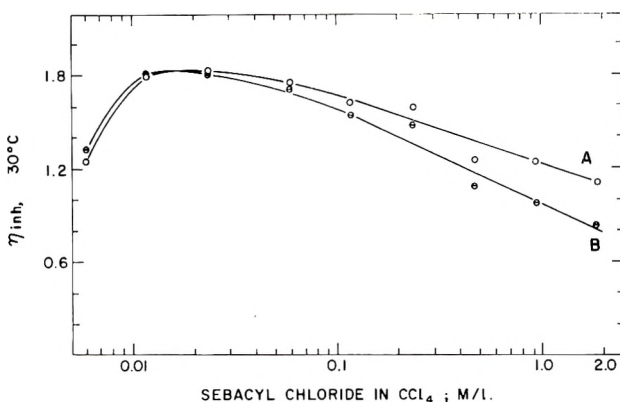


Fig. 5. Relation of product solution viscosity for 6-10 polyamide to concentration of acid chloride in stirred interfacial polycondensation reactions in $\text{CCl}_4/\text{H}_2\text{O}$ with diamine at $0.10M$: (A) η_{inh} determined in *m*-cresol; (B) η_{inh} determined in H_2SO_4 .

Samples of 6-10 polyamide prepared in a carbon tetrachloride–water system were soluble in the usual solvents for aliphatic polyamides. But, as the acid chloride solution used in the preparations was made more concentrated, a divergence of the dilute solution viscosities of the polymers determined in *m*-cresol and concentrated sulfuric acid (Fig. 5) was evident. For 6-10 polyamide made by the melt method and by the interfacial polycondensation method at optimum conditions, there is little difference between the inherent viscosities determined in the two solvents. Such polyamides may be dissolved in sulfuric acid and precipitated by cold water without degradation. Samples showing the viscosity deviations were found to have degraded in sulfuric acid and then gave equal inherent viscosities in the two solvents.

As an example, polymer prepared at a diacid chloride concentration of $0.94M$ in carbon tetrachloride had an inherent viscosity of 1.03 in *m*-cresol and 0.82 in sulfuric acid (see Table IV). Some of this polymer was dissolved in 96% sulfuric acid to form a 5% solution and the polymer was re-

TABLE III
Intrinsic Viscosity-Number-Average Molecular Weight Relationship for 6-10 Polyamide
Made by Stirred Interfacial Polycondensation Process^a

Concentration ratio, diamine/acid chloride	Yield, %	[η] in <i>m</i> -cresol	Endgroups/10 ⁶ g.			\bar{M}_n^b	\bar{M}_n for melt polymer of same [η]
			NH ₂	COOH	Total		
0.054	40	1.22	251	246	497	4,000	13,100
0.11	50	1.37	180	220	300	5,000	14,800
0.21	61	1.38	131	201	332	6,000	15,000
0.43	69	1.83	78	136	224	9,400	20,000
0.85	86	1.86	60	91	151	13,300	20,400
1.7	86	2.05	52	71	123	16,300	22,500
4.3	81	2.13	54	52	106	19,000	23,300
8.5	71	2.10	66	60	126	15,900	23,000
17.0	69	1.38	120	100	220	9,100	15,000

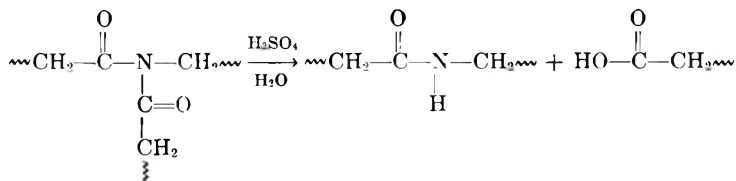
^a See Morgan and Kwolek⁷ for method of preparation. Diamine at 0.10*M* with 0.20*M* NaOH.

^b Two endgroups per molecule are assumed.

covered in ice water in 100% yield. The inherent viscosities in *m*-cresol and sulfuric acid were then both 0.84.

The formation of branch points through imide groups would be expected under any circumstance which permits the initially formed polymer to be in contact with diacid chloride solution for a relatively long time. Insoluble polymers were frequently obtained when chloroform was the solvent and the diacid chloride was concentrated. In carbon tetrachloride this side reaction was never as extensive, possibly because a faster precipitation rate of the polymer and the formation of thinner and less swollen films¹² in this medium reduced the contact with the acid chloride as well as the mobility of the polymer chain ends.

The degradation reaction in sulfuric acid undoubtedly in the rapid cleavage of imide groups to leave an all-amide structure. The polymeric product then is linear and has normal stability and viscosity behavior.



The cleavage reaction yields one new carboxyl end group for each branch point. If there were no losses upon reprecipitation and the ends could be correctly and accurately determined, the degree of branching might be estimated. Further interesting information might be obtained from a

TABLE IV
Melt Treatment of 6-10 Polyamide Prepared by Stirred Interfacial Polycondensation

Concentration ratio, diamine/ acid chloride	As prepared ^a										After melting ^b							
	[η] at 25°C. in		η_{inh} at 30°C.				Endgroups/10 ⁶ g.				[η] at 25°C. in <i>m</i> -cresol				η_{inh} at 30°C.		Endgroups/10 ⁶ g.	
	<i>m</i> -cresol	<i>m</i> -Cresol	<i>m</i> -Cresol	H ₂ SO ₄	NH ₂	COOH	Total	<i>m</i> -Cresol	H ₂ SO ₄	NH ₂	COOH	Total	<i>m</i> -Cresol	H ₂ SO ₄	NH ₂	COOH	Total	
0.054 ^a	1.05	0.95	0.67															
0.11 ^c	1.14	1.03	0.82															
0.11 ^c	1.20	1.12	0.90										0.59					
0.43	1.83	1.59	1.48	78	136	224							1.00		88	145	233	
0.85	1.86	1.61	1.54	60	91	151							1.39		55	77	132	
1.7	2.05	1.75	1.71	52	71	123							1.84		52	56	108	
4.3	2.13	1.82	1.80	54	52	106							1.91		41	42	83	
4.3 ^c	1.75	1.52	1.45										1.74	1.47				

^a Prepared in CCl₄/H₂O. Diamine at 0.10M with 0.20M NaOH (see Morgan and Kwolek⁷).

^b See Experimental section for conditions.

^c All experiments but these are part of the series in Table III and Figure 5.

study of the polyelectrolyte effect on the viscosity of dilute solutions in anhydrous formic acid, as was done for branched polyamides by Schaeffgen and Trivisonno.¹⁵ \bar{M}_w/\bar{M}_n ratios would also be a useful characterization.^{3,11}

The discovery of the branching reaction was made after much of the work was completed and data are not available on the absolute degree of branching or its complexity. Obviously, since some of the polymers are now known to have more than two ends per molecule, some of the calculated molecular weights in Table II and III and Figures 3 and 4 are too low. On the other hand, high degrees of branching can have a counter effect of lowering the dilute solution viscosity for a given molecular weight.¹⁴ The change in solution viscosity brought about by treatment of the polymers with sulfuric acid lessens the difference between the observed \bar{M}_n and that for a sample made by the melt method and having an identical solution viscosity. Even with this adjustment the molecular weights of the polyamides from interfacial polycondensation are consistently low, and the conclusion that there is commonly a deviation from random molecular weight distribution still holds.

Most of the melting and equilibration experiments were done with unbranched polymers. Evidence was obtained that equilibration of the branched polymers leads to a random linear structure (Table IV). This is a reasonable result. One acyl substituent of the imide group is readily hydrolyzed in acid. Therefore, it is expected that hydrolysis by traces of moisture and/or aminolysis by amine chain ends would take place in the melt more readily at the imide group than at other points along the polyamide chain.

Molecular weights of polyamides from interfacial polycondensation processes can be varied or controlled by changing the concentration ratio of the reactants (Figure 5 and Table II and III). However, this leads to branching and nonrandom molecular weight distribution. The molecular

TABLE V
Control of the Inherent Viscosity of 6-10 Polyamide Without Chain Branching

Diacid chloride quality ^a	Inherent viscosity	
	<i>m</i> -Cresol	Sulfuric acid
Best	1.82	1.80
Good	1.60	1.63
Fair	1.53	1.52
Fair + 0.023 mole-% benzoyl chloride	1.03	0.98
Fair + 0.030 mole-% benzoyl chloride	0.76	0.76

^a Prepared at the optimum concentration ratio in CCl₄/H₂O (425/100 phase volume ratio). Diamine at 0.10M with 0.20M NaOH. Medium stirring for 1 min. without detergent. See procedure A of Morgan and Kwolek.⁷

TABLE VI
 Reprecipitation and Extraction of 6-10 Polyamide to Remove Low Molecular Weight Fractions

No.	Treatment ^a	[η] at 25°C. in <i>m</i> -cresol			Endgroups/10 ⁶ g.			\bar{M}_n	
		NH ₂	COOH	Total	From ends group	From [η]			
1	Control; pH adjusted to 7.0	1.48	226	253	7,900	16,100			
2	No. 1 dissolved in 87.5% aqueous phenol and acetone added to turbidity; precipitated in hot water	1.44	194	228	8,800	15,500			
3	Control; pH adjusted to 7.0	1.29	255	264	7,600	13,900			
4	No. 3 extracted 60 hr. with ethanol (91.4% of whole)	1.37	169	180	11,000	14,800			
5	Ethanol extract of No. 3 (8.6%)	0.12	1120	1120	1,800				
6	Control; pH adjusted to 7.0	1.76	52	124	16,100	19,300			
7	No. 6 extracted 120 hr. with ethanol (96.0% of whole)	1.84	40	106	18,900	20,200			
8	Ethanol extract of No. 6 (2.6%)	0.11							
9	Control; pH adjusted to 7.0	1.43	57	154	13,000	15,500			
10	No. 9 extracted 72 hr. with ethanol (94.2% of whole)	1.54	50	141	14,200	16,800			
11	Ethanol extract of No. 9 (4.0%)	0.21							

^a Nos. 1 and 3 prepared in CCl₄/H₂O (170/100 phase volume ratio). Diamine at 0.20M with 0.40M NaOH; 1.0 g. sodium lauryl sulfate; medium stirring for 5 min. Nos. 6 and 9 prepared at the optimum concentration ratio in CCl₄/H₂O (425/100 phase volume ratio). Diamine at 0.10M with 0.20M NaOH; no detergent; medium stirring for 1 min. No. 9 was prepared with poorer quality sebacyl chloride than No. 6.

weight can be varied without the introduction of these faults if the polymerizations are conducted under those conditions which normally yield the highest molecular weight, and the molecular weight is then controlled by the use of impure reactants or, better, by the addition of active monofunctional materials (Table V).

Polyamidation in the Presence of a Detergent

Preceding papers in this series have noted that the addition of sodium lauryl sulfate to interfacial polycondensation reactions caused a shift in the optimum reactant concentration ratio corresponding to an increase in diamine availability. Polymer yields were increased for stirred systems and film formation was disrupted in some unstirred preparations.

Several adverse effects on the properties of the product were found. Traces of detergent were very difficult to remove with water but could be removed with organic solvents such as ethanol. Polymer, containing sodium lauryl sulfate from the reaction or added by soaking clean polymer in a detergent solution, discolored when heated to 258°C. and quickly became infusible and insoluble. Small amounts of detergents added to viscosity determinations did not affect the results. Samples prepared in the presence of detergent contained an exceptionally high proportion of carboxyl endgroups for the conditions employed. Values for \bar{M}_n sometimes showed a much greater deviation than those of preparations without detergent from the \bar{M}_n values expected for melt polyamides of the same intrinsic viscosities. Part of this effect was due to a larger than usual extractable low fraction bearing only carboxyl endgroups (Table VI). The amount of branching, as indicated by divergence of inherent viscosities in *m*-cresol and sulfuric acid, was the same for the highest acid chloride concentrations whether detergent was present or not.

The role of the detergent is best explained at this point as effecting improved stirring and diamine availability but also producing a rapid wetting-out of the polymer fragments by water. The contact of the polymer with water and dilute alkali and diamine probably favors hydrolysis to acid chloride endgroups to carboxyl groups. Improved dispersion of the phases increases the contact of the reactants and consequently the yield, although this additional yield appears to be principally low molecular weight polymer.

EXPERIMENTAL

Interfacial Polycondensation

Polyamides were prepared by the unstirred method⁶ and the stirred procedures⁷ described previously.

Melt Polycondensation

The melt polycondensations were carried out on a 5-g. scale in glass tubes by means of a procedure similar to that of Coffman and co-workers.^{18, 19}

The pH of the 1% aqueous solution of the nylon salt was 7.3,²⁰ Specific conditions for the several polymerizations are given in Table I.

For equilibrating polyamides made by interfacial condensation, the washed sample was thoroughly dried under reduced pressure and placed in a glass polymer tube. The tube was carefully flushed with nitrogen. The sample was then melted at 258°C. for 25 min. at 0.5 mm. pressure. No capillary bleed of nitrogen was used.

Endgroup Determinations

Endgroups were determined by the methods of Waltz and Taylor.⁹ The sample size was reduced to about 0.1 g., and microtitration techniques were used. These changes were necessary in order to conserve the limited supply of polymeric products. The results are believed accurate to ± 3 groups/10⁶ g. for each determination.²

Interfacial polycondensation reactions were quenched by addition of sufficient 3-5% aqueous hydrochloric acid to ensure an acidic system. The mixture was stirred for 1 min. in the blender and the polymer was collected and treated in the following way: (1) thoroughly washed with cold water; (2) soaked in 1% NaOH for 1 hr. or stirred in blender 3 min. (200 ml./5 g. polymer); (3) collected and washed thoroughly with hot and cold water; (4) soaked 3 hr. in distilled water with slow stirring and pH adjusted to 7.0; (5) washed again to remove any salts.

Such elaborate treatment was not necessary with all samples.

For example, with porous samples of 6-10 polyamide, neutralization of the acid with sodium bicarbonate and water washing was sometimes enough to assure a neutral, salt-free product. The purposes of the washing were to remove organic solvent without fractionation, to hydrolyze all acid halide endgroups, to assure that neither amine or carboxyl ends were present as hydrochloride or sodium salts, and to remove all by-product salt or acid.

When the final pH was changed from 7.5 to 6.5, there was a slight shift in the endgroups. Upward in carboxyl groups and downward in amine groups. The total number of endgroups remained the same. Known amounts of hexamethylenediamine dihydrochloride and sodium sebacate added to endgroup determinations produced the expected corresponding change in endgroups, showing that amine hydrochloride ends titrate as acid and sodium carboxylate ends titrate as base.

The treatment of freshly prepared polymers with alcohols was found to convert part of the acid chloride groups to esters. Consequently, the number of titratable carboxyl endgroups was reduced. Alcohol washes or extractions therefore should not be applied until hydrolysis of any acid chloride is complete.

References

- (a) Flory, P. J., *J. Am. Chem. Soc.*, **58**, 1877 (1936); *Chem. Rev.*, **39**, 137 (1946);
(b) *Principles of Polymer Chemistry*, Cornell Univ. Press, Ithaca, N.Y., 1953.
- Taylor, G. B., *J. Am. Chem. Soc.*, **69**, 635, 638 (1947).

3. Beachell, H. C., and D. W. Carlson, *J. Polymer Sci.*, **40**, 545 (1959).
4. Howard, G. J., *J. Polymer Sci.*, **37**, 310 (1959).
5. Griehl, W., and H. Lueckert, *J. Polymer Sci.*, **30**, 399 (1958).
6. Morgan, P. W., and S. L. Kwolek, *J. Polymer Sci.*, **40**, 299 (1959).
7. Morgan, P. W., and S. L. Kwolek, *J. Polymer Sci.*, **62**, 33 (1962).
8. Huggins, M. L., *Ind. Eng. Chem.*, **35**, 980 (1943).
9. Waltz, J. E., and G. B. Taylor, *Anal. Chem.*, **19**, 448 (1947).
10. Carelli, V., A. M. Liquori, A. Mele, and A. Ripamonti, *Chim. e ind. (Milan)*, **37**, 960 (1955).
11. Fendler, H. G., and H. A. Stuart, *Makromol. Chem.*, **25**, 159 (1958).
12. Liquori, A., and A. M. Liquori, *Ann. chim. (Rome)*, **43**, 345 (1953).
13. Beste, L. F., and R. C. Houtz, *J. Polymer Sci.*, **8**, 395 (1952).
14. Schaefgen, J. R., and P. J. Flory, *J. Am. Chem. Soc.*, **70**, 2709 (1948).
15. Schaefgen, J. R., and C. F. Trivisonno, *J. Am. Chem. Soc.*, **73**, 4580 (1951).
16. Brubaker, M. M., D. D. Coffman, and F. C. McGrew, U.S. Pat. 2,339,237 (Jan. 18, 1944) to the Du Pont Company.
17. Reynolds, R. J. W., in *Fibres from Synthetic Polymers*, R. Hill, Ed., Elsevier, New York, 1953, Chap. 5.
18. Coffman, D. D., G. J. Berchet, W. R. Peterson, and E. W. Spanagel, *J. Polymer Sci.*, **2**, 306 (1947).
19. Sorenson, W., and T. W. Campbell, *Preparative Methods of Polymer Chemistry*, Interscience, New York, 1961.
20. Beaman, R. G., and F. B. Cramer, *J. Polymer Sci.*, **21**, 223 (1956).

Résumé

Les poids moléculaires moyens en nombre sont évalués par détermination des groupes terminaux d'échantillons de polyamide 610 préparés par polycondensation interfaciale, avec et sans agitation dans diverses conditions. Les polymères préparés par des méthodes de polycondensation, tant à l'état fondu qu'à l'interface, répondent aux mêmes lois de viscosité des solutions diluées. Toutefois, les polymères produits par polycondensation interfaciale diffèrent par la distribution des poids moléculaires de ceux trouvés pour les polymères obtenus à l'état fondu. On admet que l'écart, qui se trouve être plus large que la distribution statistique normale, est dû à l'importance inusuelle d'une fraction à bas poids moléculaire plutôt qu'à un écart continu de la courbe de distribution. Les polyamides préparés par réaction interfaciale, qui ont la viscosité intrinsèque la plus élevée, et sont obtenus en réglant le rapport de concentration des deux réactifs, diffèrent le moins de la distribution statistique normale. On a démontré la ramification ainsi que la réticulation du polyamide 610 obtenu par polycondensation interfaciale dans la mesure où l'on augmente la concentration de la phase du chlorure de diacide. La ramification provient probablement de l'acylation de liaisons amides tout au long de la chaîne, donnant ainsi une quantité de groupes imides. Ces groupements sont scindés dans le polymère fondu ou dans une solution contenant de l'acide sulfurique. Le polyamide 610 préparé à l'état fondu, non fractionné, à l'équation: $[\eta] = 1.35 \times 10^{-4} \bar{M}_n^{0.96}$ on a trouvé un facteur $k' = 0.43$ dans l'équation de la viscosité relative: $\eta_{sp}/c = [\eta] + k'[\eta]^2 c$ déterminée pour une solution dans le *m*-crésol à 25°C.

Zusammenfassung

Zahlenmittelwerte des Molekulargewichts wurden durch Endgruppenbestimmung an 610-Polyamidproben bestimmt, die durch Grenzflächenpolykondensation mit und ohne Rührung dargestellt worden waren. Polymere aus Schmelz- und Grenzflächenpolykondensation gehorchten der gleichen Beziehung für die Viskosität verdünnter Lösungen. Die Grenzflächenpolykondensate wichen jedoch in ihrer Molekulargewichtsverteilung von den in der Schmelze dargestellten Polymeren ab. Die Abweichung, welche im

Auftreten einer breiteren als der statistischen Verteilung besteht, scheint zum grossen Teil das Ergebnis der Anwesenheit einer ungewöhnlich grossen niedermolekularen Fraktion und nicht einer stetigen Störung der Verteilungskurve zu sein. Die Grenzflächenpolyamide mit der höchsten Viskositätszahl, die durch geeignete Wahl des Konzentrationsverhältnisses der beiden Komponenten erhalten wurden, zeigten die geringste Abweichung von der statistischen Verteilung. Bei den durch Grenzflächenpolykondensation erhaltenen 610-Polyamiden trat bei Konzentrationserhöhung in der Dikarbonsäurechloridphase Verzweigung und sogar Vernetzung auf. Verzweigung tritt wahrscheinlich durch Acylierung der Amidbindungen in der Polymerkette unter Bildung von Imidgruppen ein. Diese Gruppen wurden im geschmolzenen Polymeren oder bei Lösung in Schwefelsäure zu Amidgruppen gespalten. In der Schmelze dargestellte, unfractionierte 610-Polyamide gehorchten der Beziehung $[\eta] = 1,35 \times 10^{-4} \bar{M}_n^{0,95}$ und für die Konzentrationsabhängigkeit der Viskosität $\eta_{sp}/c = [\eta] + k'[\eta]^2c$ ergab sich in verdünnter *m*-Kresollösung bei 25°C der Wert von k' zu 0,43.

Received January 22, 1962

Electron Spin Resonance of Gamma-Irradiated Cellulose*

ROLAND E. FLORIN and LEO A. WALL, *National Bureau of Standards, Washington, D. C.*

Synopsis

Irradiation of purified cellulose with cobalt-60 gamma rays *in vacuo* produces moderate yields of radicals detectable by electron spin resonance. The ESR spectrum is asymmetric, with five partially resolved peaks occupying a total region of about 50 gauss wide and a spectroscopic splitting factor near $g = 2$. The peaks show differing saturation behavior with increasing microwave power. Differences of crystallinity have no obvious effect on the yield or nature of the radical ESR spectrum. The presence of about 8% water during irradiation decreases the yield greatly and modifies the hyperfine structure. For dry cellulose the initial G value for radicals is near 2.8 radicals per 100 e.v. absorbed, but the concentration levels off at doses a little over 6×10^{20} e.v./g. Despite the early falling-off in yield, the radicals in stored irradiated specimens do not decay appreciably in several days. Even upon contact with air the decay is quite slow. Thermal decay is imperfectly second-order, fairly rapid above 120°C., and indicates several radicals of differing lifetimes.

Introduction

Cellulose is degraded very rapidly by nuclear radiation^{1,2} and fairly rapidly by other agents, such as ultraviolet light, acids, and alkaline oxidizing media.³ There are, however, many differences in the mode of action.^{3,4} Although degradation is the predominant reaction from the nuclear irradiation of other polysaccharides and cellulose derivatives, the action on dextran seems to be complicated by crosslinking. Cellulose ethers form visible gel under special conditions of dilute solution, high dose rate, and low total dose.⁵ The γ -irradiation of cellulose is notable also for a large postirradiation decrease in solution viscosity⁶ and for a considerable destruction of sugar recoverable by hydrolysis.⁷ Ultraviolet irradiation of cellulose produces the gases H₂, CO, and CO₂.^{4,8} The occurrence of free radicals in the irradiated cellulose has been demonstrated by electron spin resonance (ESR)^{6,9,10}; the most recent published work shows an unsymmetrical spectrum of about 60 gauss overall width, with hyperfine structure of perhaps five very poorly resolved peaks. Spectra of similar width and usually less resolved hyperfine structure are shown by γ -irradiated starch,^{10,11} many γ -irradiated sugars,^{12,13} and U.V.-irradiated frozen poly-

* This research was supported by the Aeronautical Research Laboratory, Wright-Patterson Air Force Base, Ohio.

hydric alcohols.¹⁴ The present research was undertaken to obtain further information about the amounts and lifetimes of the radicals observed by ESR.

Experimental

The cellulose materials irradiated were purified cotton cellulose, "hydro-cellulose" (type II cellulose of low crystallinity), Whatman No. 40 filter paper, and crude ramie fiber (all obtained through the courtesy of Dr. Florence H. Forziati). Methyl cellulose (Dow Methocel, 15 cpoise viscosity grade) and cellulose acetate (Eastman, acetyl content 39.6–40.4%) were also irradiated and examined. Specimens were placed in Corning-7943 silica tubes and evacuated for 8 to 16 hrs. at 1μ Hg pressure and room temperature, and then for 3 hrs. at 55°C . before irradiation. Some tubes contained break-seals for subsequent addition of water, which was produced by heating weighed amounts of $\text{BaCl}_2 \cdot 2\text{H}_2\text{O}$ in a sidearm that had been evacuated for 1 hr. at -80°C . and then for a few minutes at 0°C . After the crystals had been heated for about 5 min. in a soft flame, the sidearm was quickly sealed off from the main body. Samples were irradiated up to 64 hrs. at a dose rate of about 0.5×10^6 r/hr. in a ^{60}Co gamma facility at $20 \pm 2^\circ\text{C}$. and at -196°C . Heating was done in furnaces having a precision of the order of $\pm 2^\circ\text{C}$., from which the samples were removed briefly for examination. A few samples of filter paper were exposed to ultraviolet rays at a distance of 10 cm. from a Hanovia high-pressure Type L lamp having an output of about 100 mw./cm.² in the wavelength range of 1800–4000 A. at this distance. These exposures were made upon flat sheets in air and bundles of strips in vacuum. Spectra were recorded with a Varian 4500 instrument at about 0.5 mw. microwave power; any higher power saturated and distorted the spectra. Some of the spectra were taken with 100 kc. field modulation. Most spectra shown in the figures here originally contained an intense narrow line from the quartz container, which could be determined separately by inverting the container, tapping to shake the powder out of the tip, and returning the tip to the microwave cavity upside down. A few samples also were examined soon after removal to new containers in the open air. Numbers of radicals were determined from the comparison of doubly integrated areas with copper sulfate pentahydrate, with corrections for geometry as well as large rough empirical corrections for added water.

Results

The ESR spectra obtained resemble closely the published spectrum of Abraham and Whiffen.¹⁰ For a period of a few days after irradiation the spectra show five peaks rather clearly (Fig. 1B). Most of the peak structure is not apparent at high microwave power (Fig. 1A). The methyl and acetate derivatives have poorly resolved but different spectra (Fig. 2). Irradiation in the presence of water gives the same peak locations but different intensities; this change does not occur if the water is added sub-

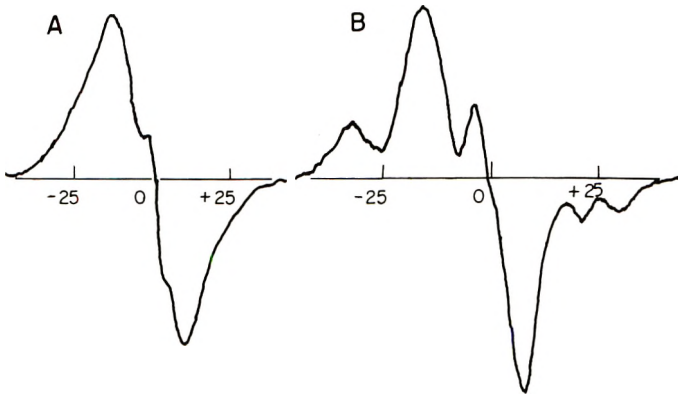


Fig. 1. ESR spectra of purified cotton cellulose irradiated *in vacuo*. Microwave power: (A) 15 mw.; (B) 0.5 mw. Derivative of absorption curve. Numbers are d.c. magnetic field intervals about H_0 .

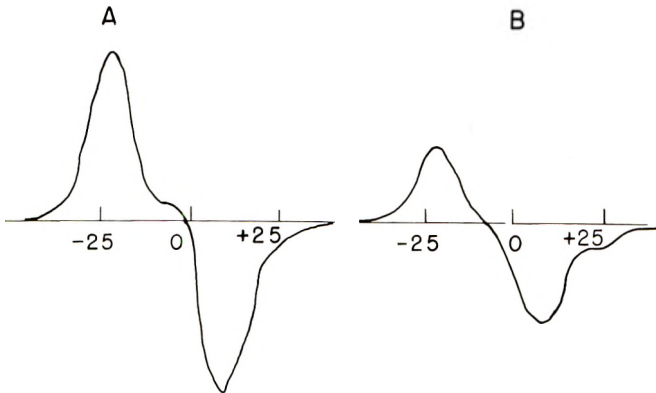


Fig. 2. ESR spectra of irradiated cellulose derivatives, microwave power, 0.5 mw.: (A) methyl cellulose; (B) cellulose triacetate. Conventions same as in Figure 1.

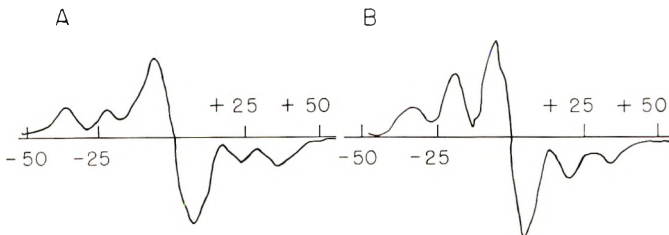


Fig. 3. ESR spectra of ramie irradiated in air: (A) fiber perpendicular to H_0 ; (B) fiber parallel to H_0 . Conventions same as in Figure 1B.

sequently. Ramie fiber spectra show considerable differences with orientation (Fig. 3). The material is especially favorable experimentally because the crystallite axis is identical (within 5°) with the macroscopic fiber axis; however, the promise of deducing significant structural information

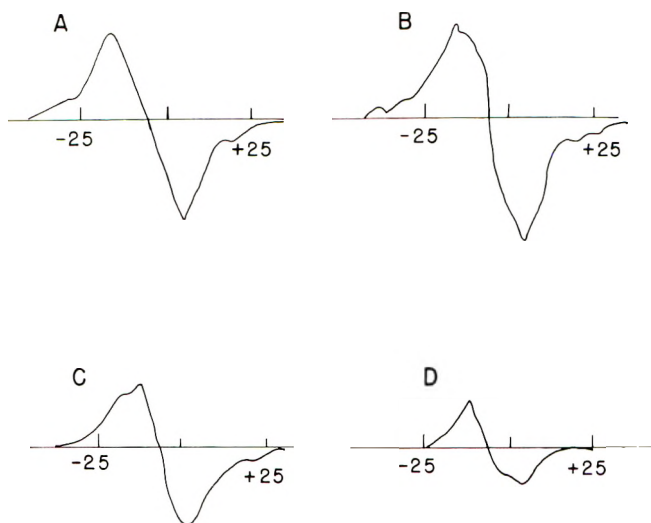


Fig. 4. Thermal decay of ESR spectrum in irradiated cellulose: (A) before heating; (B) after 60 min. at 148°C.; (C) after 100 min. at 148°C.; (D) No. C after 67 min. additional at 208°C.

does not appear great. The changes in spectral shape upon heating, as well as the general asymmetry, appear to indicate several different types of radical species: the principal radical with broad spectrum, and possibly others of narrower spectrum, beginning to emerge as an inflection near -10 gauss (Fig. 4B) and dominant (Fig. 4D). A very narrow spectrum is given in the presence of air at high temperatures (Table I, line 7). Efforts to isolate individual spectra by subtraction, after the fashion of Lawton et al.¹³ were not very successful. Some of the line breadths and peak locations are listed in Table I. Radicals formed by ultraviolet rays have a spectrum of simpler appearance and are probably different in nature, perhaps a single species only. Cellulose acetate and methyl cellulose exhibit two overlapping peaks spaced 10–15 gauss apart.

The initial yields of radicals are high, but the concentration levels off very early (Table II), apparently indicating that radicals are destroyed

TABLE I
Peak Locations, Widths, and Separations

Peak locations, gauss (from DPPH peak)	Peak widths and separations, gauss
Center	Ultimate width, 208°C.
Early narrow center ^a	11.8
Late narrow center ^b	180°C. air
Hyperfine low field	4.2
Hyperfine high field	250°C. char (Pastor)
	6.4
	Acetate separation
	10–15
	Methyl cellulose
	10–15
	separation

^a Mid-point of center peak before heating.

^b Mid-point of center peak after 2.3 hr. at 148°C.

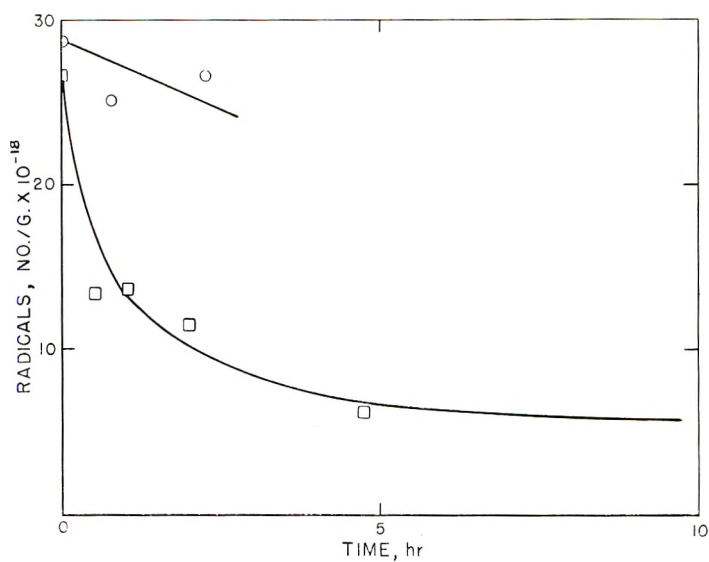


Fig. 5. Thermal decay of cellulose radicals: (○) at 72°C.; (◻) at 103°C.

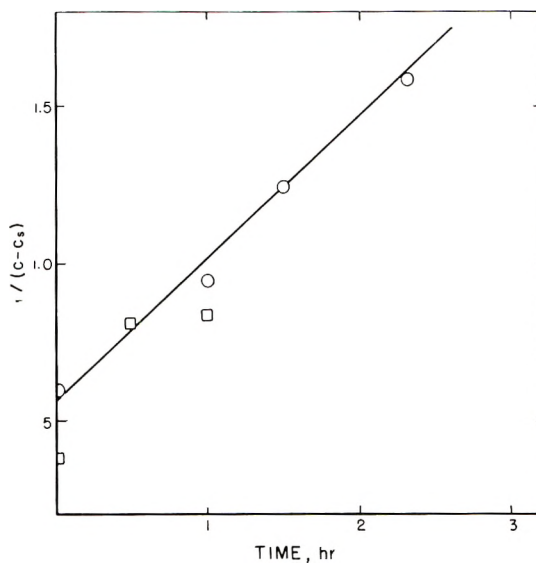


Fig. 6. Decay of radicals at 148°C. Reciprocal of concentration function plotted against time: (○) dry cellulose; (◻) moist cellulose.

during irradiation at rates exceeding by several orders of magnitude the simple thermal decay rates given in Table III. Formation of radicals at -196°C . is considerably slower than is normal, and the accumulation in water and air is slower. Addition of water seems to cause an immediate disappearance of some radicals, after which the remainder disappear somewhat faster than in the dry state. Radicals formed in a wet sample are

just as long-lived as those formed in dry material but their number is small. Exposure to air accelerates the rate of decay approximately ten-fold without any initial precipitous decay. Data, obtained from the measurement of thermal decay, scatter considerably (Table IV, and Figs. 5 and 6). Where there are enough data at a single temperature the pattern suggests a rapid second-order decay until a stable level is reached for the particular temperature. Plots of $1/(C - C_s)$ against time, where C is the concentration and C_s the ultimate stable concentration, are approximately linear (compare Ref. 16). Since the rates at different temperatures involve different surviving radical species, an activation energy calculation would have limited physical significance; in a perfunctory way, the data obtained at 103 and 148°C. imply that $E = 19$ kcal. This value is believed to be low for any single species disappearing measurably at either temperature. In freshly irradiated material, not previously heated, the disappearance rate at 148°C. is quite likely to have been faster than that observed in the samples studied. These necessarily had a previous thermal history because of the manner in which the experiments were conducted. However, even with fresh samples data at short times would not be easily obtained because of the time required for samples to come to the desired

TABLE II
Yields of Radicals in γ -Irradiated Cellulose and Derivatives

Material	Irrad. conditions	Dose, e.v./g. (Spins/g.)		G values
		$\times 10^{-23}$	$\times 10^{-18}$	
Cotton	Dry vac., 20°C.	6.02	17.3	2.88
Cotton	Dry vac., 20°C.	23.8	71-19	0.86 ± 0.05
Hydrocellulose	Dry vac., 20°C.	23.8	22.5	0.95
Ramie	Dry vac., 20°C.	19.3	23	1.24
Cotton	Dry vac., 77°K.	6.15	5.83	0.95
Cotton	Dry vac., 20°C., then water added 8-14%.	19.3	12.8 ^a	0.66 ^a
Cotton	Wet, 20°C., water added 8%	23.8	7.4 ^a	0.31 ^a
Cotton	Air, 20°C.	3.96	2.08	0.53
Paper	U.V., 12 hr., air	—	0.1	—
Methyl cellulose		3.96	3.19	0.81
Cellulose acetate		3.96	6.97	1.76

^a Includes large sensitivity correction because of presence of water.

TABLE III
 Decay of Radicals in Storage^a

Time, days	Relative concn. C_t/C_0	Conditions
110	0.53	Normal
110	0.67	Hydrocellulose
7	0.6	Preheated
0.01	0.80	In air
2.0	0.77	In air
110	0.08	In air
110	1	8% water during irradiation; note initial concn. 0.31% of normal
0.16	0.87	8% water added after irradiation
2	0.69	The same
7	0.26	The same
8	0.14	8% water added after irradiation, then preheated
16	0.14	The same
75	0.33	Methyl cellulose
75	0.63	Cellulose acetate

^a From purified cotton cellulose, irradiated dry, *in vacuo*, unless otherwise indicated.

 TABLE IV
 Levels Reached After Heating

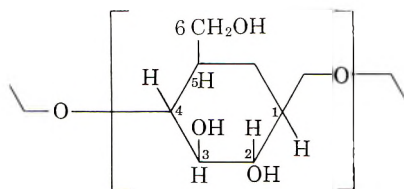
Conditions (temp., °C.; time, hr.)	(Radicals/g.) $\times 10^{-18}$
Original	10-30
72, 2.25	26.8
103, 4.75	6.2
103, 120	1.74
121, 0.7	3.2
148, 2.3	0.84
78, 1, wet	4.9
148, 1, wet	1.33
208, 1.12	0.21
188, 15, air	0.05
250, glucose char (Ref. 21)	0.5

experimental temperature. At the highest temperature, 208°C., low concentrations still remain, even in the presence of air (Table IV).

Discussion

There have been several explicit suggestions as to the structure of radicals in irradiated carbohydrates and the sites of main chain breaks of cellu-

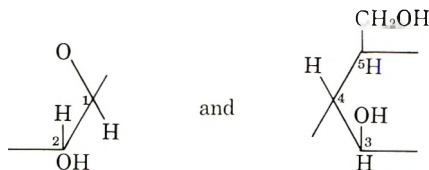
lose.^{3, 4, 8, 12} The chemical evidence seems to indicate that both C₁-O (glycosidic) and C₁-C₂ split during ultraviolet degradation.



It seems likely that the spectrum observed could be due to a collection of different types of radicals. A three-peak spectrum of intensity ratio 1:2:1 could account for a large part of the initial observed intensity. Such a spectrum would correspond to interaction with two equivalent hydrogens, alpha or beta to the odd electron. It is not difficult to write many such radicals formed by bond breaks of C—H, C—C, and C—O in the cellulose unit. Only an approximate equivalence would be required in view of the poorly resolved structure observed. Experimentally, in alcohol radicals the interaction with each proton in an alpha or beta position has been estimated at about 20 gauss.¹⁴ Assumption of this value here would lead to nearly the observed splittings. The meager structure of the spectrum alone does not furnish enough data for a very firm conclusion about the radical structure.

The radicals just discussed are centered near the field for diphenyl picryl hydrazyl (DPPH), corresponding to a spectroscopic splitting factor of $g = 2.0038$. The later surviving radicals are centered at fields 3–5 gauss higher, implying g factors of 0.002 to 0.003 units lower and indicating somewhat more spin-orbit interaction. Small shifts in this direction are found when the free electron is on oxygen or sulfur. The radicals of this class may thus be of the structural type C—O·, formed by breaks of C—O or O—H. The postulate of an assortment of radicals leads to some difficulty in accounting for products. For main chain breaks, Charlesby¹⁷ derived from Saeman's⁷ data a $G_{\text{scission}} = 10$ events per 100 e.v., and a G value of 10 for the destruction of glucose units. From this equivalence it is plausible that each main chain scission is accompanied by the destruction of one glucose unit.

The formation of radicals of any type constitutes the destruction of a glucose unit, although it is possible that some units are re-formed by hydrogen abstraction. From only a few specific sites of bond rupture, namely, the C₁—O linking different glucose units and the C₄—O, chain scission as well as glucose destruction follows. Disruption of bonds at other than these specific sites does not lead to chain degradation without further breaks within the same glucose unit. The apparent equivalence between yield of scission and destruction of glucose units suggests that radiation causes splitting mainly of the C—O type of bond and hence produces radicals of the type:



However, it is likely that the alkali chemical treatment that is used subsequent to irradiation in determining scissions may induce scissions via glucose units already disrupted by radiation.

Although the initial yield of radicals is high, $G_R = 2.8$, it is not as high as the currently favored $G_{\text{scission}} = G_{-\text{glucose}} = 10$. The intermediates for these ultimate gross changes may be less stable kinds of radicals or "hot" radicals of the same kinds as those seen. The rapid falling off in yield with dose, coupled with the stability of radicals once removed from the source, suggests the existence during irradiation of numerous unstable or reactive radicals or excited states, which react as formed with each other and with stable radicals. If many energetically hot or chemically unstable radicals are formed they should endure longer at low temperature. Since the yield of observed radicals from irradiation at -196°C . is only about 0.3 of that found at room temperature, it is likely that the rate of formation of radicals is relatively even less, owing to cage effects. Hence, as in other systems, chain scissions and glucose destruction should be decidedly less at -196°C . If this picture is correct, a higher ultimate steady-state concentration of free radicals can also be expected at -196°C .

The imperfect second-order decay, with leveling off to an unreactive remainder at each temperature, is reminiscent of results with U.V.-irradiated alcohol glasses,¹⁶ and suggests that there are several different radicals, which are isolate rather than existing in close pairs or clusters, and which recombine, primarily by diffusion, with several energies, depending on site and type of radical. Oxygen will react with practically all radicals eventually, and form nonradical products; however, its diffusion is relatively slow. Water may serve as a reactant if present during irradiation, but its principal role if added later must be to facilitate diffusion in noncrystalline regions and to open up the crystalline regions for diffusion. Nevertheless, a few sites must be almost immune to this action of water, in view of the leveling off of decay and the long life of radicals formed with water present. This action of water has analogues in the effect of water on postirradiative changes in starch¹¹ and cellulose⁶ and in the decay of radicals in sugars.^{11,13} In some of these effects the critical water concentrations were tenths of a per cent, and the effect of 3% sorbed water was indistinguishable from that of immersion of the sample.⁶ A study of lower water concentrations would have been interesting here. The crystallinity differences in ramie, cotton, and hydrocellulose had no demonstrable effect on the buildup and decay of radicals in dry cellulose. The relative susceptibility of crystalline and amorphous regions to the action of water could be assessed by experiments with ramie and hydrocellulose.

It may be noted that both the yield of radicals and the rate of decay in air are of the right order of magnitude to explain the postirradiative chain scission of Glegg and Kertesz⁶ and the success of recent procedures for graft polymerization using preirradiated cellulose.¹⁸⁻²⁰

The effect of moisture in facilitating diffusion, which is evident here in accelerated decay of radicals, may have been important also in acrylonitrile graft polymerization,²⁰ where appreciable polymer was formed only in the presence of a swelling solvent such as water or methanol.

In the thermal decay experiments, it may be remarked that the highest temperatures for decay of radicals (Table IV) approach those at which radicals begin to be formed by pyrolysis.²¹

References

1. Bovey, F. A., "Effects of Radiation on Polymers," *Polymer Reviews*, Vol. 1, Interscience, New York-London, 1958, pp. 189-204.
2. Charlesby, A., *Atomic Radiation and Polymers*, Pergamon Press, New York, 1960, pp. 359-361.
3. McBurney, L. F., "Degradation of Cellulose," in *Cellulose and Cellulose Derivatives* (High Polymers, Vol. IV), 2nd ed., Part 1, E. Ott and H. M. Spurlin, Eds., Interscience, New York-London, 1954, pp. 99-182.
4. Beelik, A., and J. K. Hamilton, paper presented at 138th Meeting, Am. Chem. Soc., New York, September 1960.
5. Leavitt, F. C., *Chem. Eng. News*, Nov. 7, 52 (1960).
6. Glegg, R. E., and Z. I. Kertesz, *J. Polymer Sci.*, **26**, 289 (1957).
7. Saeman, J. F., M. A. Mallett, and E. J. Lawton, *Ind. Eng. Chem.*, **44**, 2848 (1952).
8. Flynn, J. H., paper presented at 138th Meeting, Am. Chem. Soc., New York, September 1960.
9. Cambrisson, J., and J. Uebersfeld *Compt. rend.*, **238**, 1397 (1954); Uebersfeld, J., *Ann. phys.*, [13], **1**, 395 (1956).
10. Abraham, R. J., and D. H. Whiffen, *Trans. Faraday Soc.*, **54**, 1291 (1958).
11. O'Meara, J. P., and T. M. Shaw, *Food Technol.*, **9**, 132 (1957).
12. Williams, D., B. Schmidt, M. L. Wolfrom, A. Michelakis, and L. J. McCabe, *Proc. Natl. Acad. Sci.*, **45**, 1744 (1959).
13. Truby, F. K., and W. H. Storey, *J. Chem. Phys.*, **31**, 857 (1959).
14. Gibson, J. F., D. J. E. Ingram, M. C. R. Symons, and M. G. Townsend, *Trans. Faraday Soc.*, **53**, 914 (1957).
15. Lawton, E. J., J. S. Balwit, and R. S. Powell, *J. Chem. Phys.*, **33**, 395 (1960).
16. Alger, R. S., private communication.
17. Charlesby, A., *J. Polymer Sci.*, **15**, 263 (1955).
18. Huang, P. Y. L., B. Immergut, and W. H. Rapson, paper presented at 138th Meeting, Am. Chem. Soc., New York, September 1960.
19. Kobayashi, Y., *Chem. Eng. News*, Nov. 7, 52 (1960).
20. Usmanov, Kh. U., B. I. Aikhodzhaev, and U. O. Azizov, *Vysokomolekulyarnye Soedineniya*, **1**, 1570 (1959).
21. Pastor, R. C., and R. H. Hoskins, *J. Chem. Phys.*, **32**, 264 (1960).

Résumé

L'irradiation de la cellulose purifiée au moyen de rayons gamma de cobalt-60 dans le vide, donne des rendements modérés en radicaux décelables par résonance de spin électronique. Le spectre ESR est asymétrique, avec cinq pics partiellement résolus occupant une région totale d'environ 50 gauss, domaine à l'intérieur duquel le facteur de séparation spectroscopique est voisin de $g = 2$. Les pics montrent différents comporte-

ments de saturation avec une énergie croissante des micro-ondes. Des différences de cristallinité n'ont aucun effet évident sur le rendement ou la nature du spectre radicalaire ESR. La présence d'environ 8% d'eau durant l'irradiation diminue beaucoup le rendement et modifie la structure hyperfine. Pour la cellulose sèche, la valeur initiale de G pour les radicaux est voisine de 2,8 par 100 ev absorbés, mais la concentration reste constante à partir d'une dose un peu supérieure à 6×10^{20} ev/g. En dépit de la diminution initiale de rendement, néanmoins les radicaux formés au sein des spécimens irradiés ne disparaissent pas appréciablement en plusieurs jours. Même au contact de l'air la disparition est plutôt lente. La disparition thermique est de façon imparfaite du second ordre, franchement rapide au-dessus de 120°C , et indique plusieurs radicaux de durée de vie différente.

Zusammenfassung

Bestrahlung von gereinigter Cellulose mit ^{60}Co - γ -Strahlen im Vakuum ergab eine mässige Ausbeute an durch Elektronenspinresonanz nachweisbaren Radikalen. Das ESR-Spektrum ist asymmetrisch mit fünf teilweise aufgelösten Spitzen, die einen Gesamtbereich von ungefähr 50 Gauss mit einem spektroskopischen Aufspaltungsfaktor bei $g = 2$ überstreichen. Die Spitzen zeigen ein unterschiedliches Sättigungsverhalten bei steigender Mikrowellenenergie. Unterschiede in der Kristallinität haben keinen erkennbaren Einfluss auf die Stärke oder Natur des ESR-Radikalspektrums. Die Gegenwart von ungefähr 8% Wasser während der Bestrahlung setzt die Stärke stark herab und verändert die Hyperfeinstruktur. Bei trockener Cellulose liegt der anfängliche G -Wert für Radikale nahe bei 2,8 Radikale pro 100 absorbierten EV, die Konzentration steigt aber bei Dosen wenig über 6×10^{20} EV/g nicht weiter an. Trotz des frühen Abfalls der Ausbeute findet in aufbewahrten bestrahlten Proben während einiger Tage kein merklicher Radikalabfall statt. Sogar bei Berührung mit Luft ist der Abfall recht langsam. Der thermische Abfall ist teilweise zweiter Ordnung, verläuft recht rasch oberhalb 120°C und weist auf das Vorhandensein von Radikalen mit verschiedener Lebensdauer hin.

Received February 6, 1962

Molecular Motion in Polyethylene. III

DAVID W. McCALL and ERNEST W. ANDERSON, *Bell Telephone Laboratories, Incorporated, Murray Hill, New Jersey*

Synopsis

Proton magnetic resonance studies of polyethylene have been extended. The relationship of the rigid fraction (NMR) to the crystalline fraction is discussed, and a case is presented for the relative importance of the rigid fraction (or its complement, the mobile fraction). When the polymer has been swollen by low molecular weight solvents, the NMR spectra yield rather direct evidence that the rigid, and presumably crystalline, regions are unaffected. The nature of the molecular motion is discussed in terms of a model, and it is shown that NMR data imply a rather general type motion.

I. Introduction

Nuclear magnetic resonance measurements on solid polymers have been employed to estimate the fraction of protons held rigidly. That is to say, the resonance can be described, approximately, as a superposition of a broad resonance and a sharper resonance. The intensity of the broad resonance is proportional to the fraction of protons that do not have motional freedom. Usually this fraction is identified with the degree of crystallinity, and this observation has been used successfully as the basis of a method for determining the degree of crystallinity for a number of polymer systems. The necessary requirement is a temperature range that is substantially above the glass transition for the amorphous regions but below the melting point of the crystalline regions.

In Section II of this paper we examine the implications and importance of this technique in relation to the x-ray method for measuring the degree of crystallinity. It is our point of view that the NMR measurement is more important because of the rather direct relationship between many chemical and mechanical properties and molecular mobility factors. In Section III we discuss the resonance behavior of polyethylenes swollen by low molecular weight solvents. Direct evidence is presented to support the view that the crystalline part of polyethylene is not appreciably affected by the presence of solvent. In Section IV the extent of molecular mobility implied by the width of the narrow component is estimated.

II. Degree of Crystallinity

The use of nuclear resonance in measuring the degree of crystallinity has been described by several authors.¹⁻⁸ Briefly, it involves assigning part

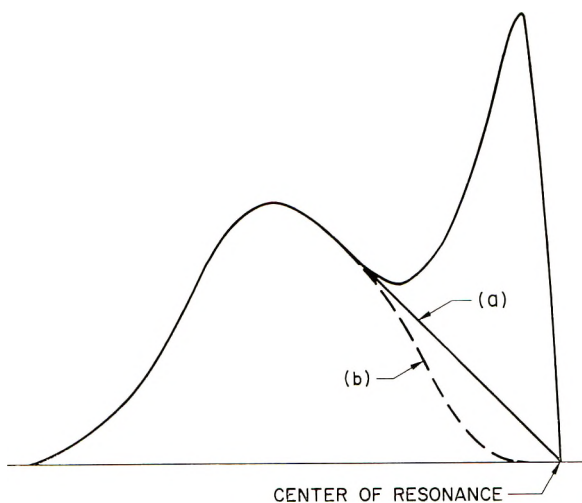


Fig. 1. Half of the derivative of the proton resonance absorption in linear polyethylene (compression-molded). The two methods of decomposing the resonance, for the purpose of determining the mobile fraction, are illustrated: (a) straight line decomposition; (b) low temperature decomposition.

of the resonance absorption to the crystalline regions and measuring the intensity of that part relative to the total intensity.

The decomposition of the resonance has been carried out in two principal ways which are illustrated in Figure 1. The first, called the straight-line method, is employed because it is simple. The second method is based upon the assumption that the crystalline resonance will have the same shape as the total resonance exhibits at low temperatures. The low temperature shape results in somewhat lower calculated crystallinities (perhaps 2-3% lower).

The presence of low molecular weight solvent narrows the narrow resonance but does not affect the broad resonance, and thus swollen specimens can be used to observe the crystalline resonance more clearly. Results of a series of measurements indicate that the straight-line method is more nearly correct but these results are inconclusive. A more convincing test can be made by looking at solution-crystallized linear polyethylene. These preparations appear to be completely crystalline, i.e., there is no narrow resonance component, and the observed shapes are close to that assumed in the straight-line method of decomposition. Therefore, we feel that the straight-line method is to be preferred but the difference between the methods is not great and the evidence in favor of our preference is not conclusive.

Quite apart from difficulties that are inherent in making the assignment (i.e., decomposing the curve), the measurement requires great care because of the fact that the narrow component has a tendency to saturate. (For a discussion of this instrumental effect see Bloembergen et al.⁹) We have found it most satisfactory to plot the apparent degree of crystallinity as a

function of rf level (H_1) and extrapolate to zero H_1 . Typically, this brings the measured crystallinity down by 0–5%. The refinement is probably not significant except in highly crystalline specimens.

Linear polyethylene specimens vary considerably in crystallinity as measured by NMR at room temperature. For example, pellets are 85% crystalline, while compression-molded specimens are found to be 90% crystalline or higher. The pellets are extruded and cooled rapidly. Compression-molded material cools relatively slowly because of the heat capacity of the mold. Annealing at high temperatures ($>120^\circ\text{C}$.) can bring about increases in the degree of crystallinity. Matsuoka¹⁰ has carried out high temperature (about 150°C .) crystallization by applying hydrostatic pressure. The resulting material is 100% crystalline by the NMR method and has a density as high as 0.99 g./cm.^3 . Of course, solution-crystallized material also exhibits 100% NMR crystallinity. However, as Slichter has shown,^{8,11} heat treatment serves to reduce the crystallinity of solution grown specimens.

It is of interest to consider NMR crystallinities of cold drawn linear polyethylene. Up to a draw ratio of 5:1 the NMR crystallinity is substantially unchanged. Above this draw ratio the NMR crystallinity is observed to increase until there is no perceptible narrow resonance at about a draw ratio of 15:1. The figure 15:1 applies to Marlex, type 6000 linear polyethylene (Phillips Petroleum Company) drawn at 22°C . at a rate of 0.2 in./min. The rate and temperature of draw affect the draw ratio that suffices to remove the narrow resonance.

It is doubtful that all of the materials exhibiting 100% NMR crystallinity would be found to be 100% crystalline by x-ray, density, or infrared methods. The x-ray technique is best suited to the measurement of the crystalline fraction, and the rigid fraction (i.e., deduced by NMR) may or may not agree with the x-ray result. It is our belief that the important quantity for the characterization of polymeric materials is not the degree of crystallinity but, rather, the rigid fraction. More pertinent yet is the mobile fraction, as this portion of the polymer tends to dominate the mechanical properties. Of course, the mechanical properties (at small strain) are directly determined by molecular mobility factors and are only related to considerations of crystalline order in a secondary sense. A material in which the molecules are rigidly fixed will be brittle irrespective of the state of order, i.e., whether it is crystalline or glassy, or both.

For these reasons we shall concentrate on the mobile fraction for the remainder of this paper. Mobile fraction is defined as the intensity of the narrow room temperature proton resonance relative to the total intensity of the resonance. This is equal to the fraction of molecular segments which are mobile.

III. Sorption

Sorption, diffusion, and other studies have given indirect evidence in favor of the view that when a semicrystalline polymer absorbs a low molec-

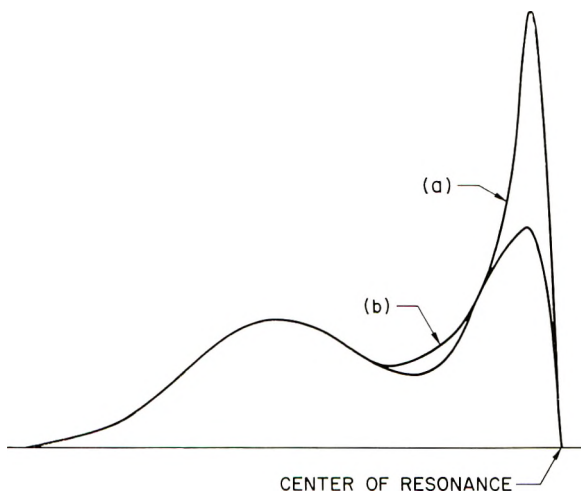


Fig. 2. Half of the derivative of the proton resonance absorption in linear polyethylene (compression-molded) illustrating the effect of carbon tetrachloride on the resonance shape: (a) saturated with CCl_4 ; (b) dry polymer.

ular weight substance the low molecular weight substance enters the amorphous regions only.¹² Nuclear resonance studies of linear polyethylenes that have been swollen by various solvents give direct evidence that this point of view is correct. The experiment, in brief, consists of equilibrating polymer samples with various amounts of a solvent at room temperature. The mobile fraction is then measured as a function of solvent concentration.

Figure 2 shows a comparison of the resonance of a swollen polymer and the resonance of the same polymer before being exposed to the solvent. The solvent used in this example is carbon tetrachloride at saturation concentration (room temperature). Note that the broad resonance is unchanged but the narrow portion is made narrower by the presence of the solvent. However, the integrated intensity of the narrow portion is not affected by the solvent. This is direct evidence that the solvent enters only those regions of the polymer that give rise to the narrow resonance in the unswollen material. We may say that the amorphous regions are plasticized and the crystalline regions are unaffected.

When polyethylene is swollen by exposure to benzene or some other hydrogen-containing substance, similar results are obtained, except that the intensity of the narrow resonance increases owing to the presence of protons in the solvent. The weights of polymer and solvent are known, so the resonance intensity to be attributed to the solvent can easily be calculated and the mobile fraction characteristic of the polymer determined.

For compression-molded linear polyethylene, the mobile fraction was found to be $10 \pm 2\%$ in both swollen and unswollen samples. Pellets of this material may decrease slightly in mobile fraction, say from 15 to 13%. We interpret this change as room temperature annealing enhanced by the solvent, but our results are such that the effects observed are comparable

with experimental error. In this connection, it is worthy of note that the narrow resonances of the swollen polymers show an extreme tendency to saturate (i.e., one must use a low rf field). Thus, it is important that measured mobile fractions be extrapolated to zero radio frequency field.

It is interesting that the rigid crystalline portions of the linear polyethylene remain unaffected, as seen by NMR even though the amorphous volume is increased by a factor as high as 1.5 on swelling in a relatively good solvent. This figure for the swelling ratio is obtained as follows. The mobile fraction is about 10%, and the amorphous density is about 0.8 g./cm.³ compared with the crystalline density of about 1.0 g./cm.³ Thus, the amorphous volume is about 12%. The volume expansion per gram of polymer is about 6% on swelling with benzene, for example, and therefore there is about a 50% increase in the amorphous or mobile volume.

Solution-crystallized linear polyethylene does not exhibit a narrow resonance at room temperature. We have verified this observation for crystals precipitated isothermally from xylene at 70 and 85°C. The solution concentrations ranged from 0.04 to 0.2 wt.-%. When dry crystals are put in contact with carbon tetrachloride at room temperature, however, a mobile fraction of about 1.5% is observed. On removal of the carbon tetrachloride by evaporation the narrow resonance disappears. Note that this solvent effect differs from the effects of heat treatment described by Peterlin¹³ and Slichter.^{8,11} These authors heat-treated solution-crystallized polyethylene and observed the appearance of a narrow resonance. This effect is irreversible at sufficiently high temperatures, however, as the narrow resonance remains on cooling to room temperature. We have no direct evidence that these two effects are related in any way.

Let us now attempt to be more quantitative in our analysis of the narrowing of the resonance induced by solvent absorption. In outline, the approach consists of relating the resonance width to the motional correlation time of the polymer, applying the Eyring theory of rate processes, and analyzing the results in terms of the concentration dependence of the free energy of activation for molecular motion.

The theory of nuclear magnetic relaxation yields^{9,14}

$$\tau_c \cong 10\delta H / \gamma\delta H''^2$$

when

$$\delta H < 3\delta H'' \quad (1)$$

where τ_c is the correlation time for molecular motion, $\gamma = 2.65 \times 10^4$ sec.⁻¹ gauss⁻¹ for protons, δH is the resonance width (in this case the narrow resonance only), and $\delta H''$ is the low temperature limit of δH (which we take to be the width of the broad portion of the polymer resonance). The Eyring theory yields and Arrhenius rate law:¹⁵

$$\tau_c = (h/kT)\exp \left\{ \Delta F^\ddagger / RT \right\} \quad (2)$$

and thus,

$$\delta H \cong (\gamma \delta H''^2 h / 10kT) \exp \{ \Delta F^\ddagger / RT \} \quad (3)$$

By analogy with the analysis of concentration-dependent diffusion¹⁶ (in the same polymer solvent systems) we write,

$$\Delta F^\ddagger = \Delta F_0^\ddagger - cRT\rho \quad (4)$$

where c is the concentration of liquid absorbed by the polymer and ρ is independent of c . Therefore,

$$\delta H = \delta H_0 \exp \{ -\rho c \} \quad (5)$$

In Figure 3 we have plotted $\ln(\delta H_0/\delta H)$ versus c . The slope yields $\rho = 2$, following the convention that $c = 1$ at saturation. The analogous parameter derived from concentration dependent diffusion studies¹⁶ is $\delta = 5$. The system here is carbon tetrachloride in compression-molded linear polyethylene. Neither δ nor ρ is known accurately, but it is safe to

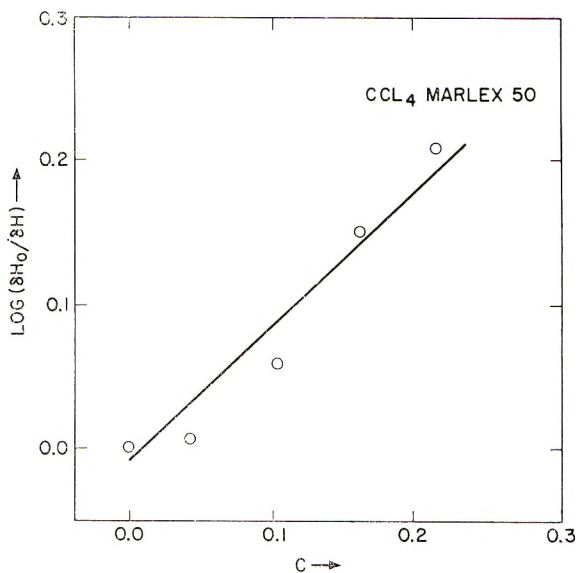


Fig. 3. A plot of $\log(\delta H_0/\delta H)$ vs. c for the system linear polyethylene (compression-molded)-carbon tetrachloride. The units of concentration are chosen such that $c = 1$ at saturation.

say that δ is about 2.5ρ . The activation energy for diffusion is about 18 kcal./mole (at zero concentration) compared with about 6–10 kcal./mole for the nuclear relaxation process. Thus the relative change in activation energy is about the same for resonance width and diffusion, even though the absolute activation energies differ considerably. We anticipate some correspondence between the diffusion and resonance parameters because they are all dependent upon molecular motions.

IV. Resonance Widths

The width of a resonance is a measure of the spread in local field over the sample. The most probable local field is zero and the distribution is symmetrical about this point. When the nuclei are rigidly fixed in space and the nuclei are equivalent to one another, it is a straightforward, if tedious, task to carry through the classical computation of the local field. We compute the field at a typical nucleus. This is the sum over all the local fields contributed by the neighbors. Each nucleus contributes

$$\pm (\mu/r^3) (3 \cos^2\theta - 1) \quad (6)$$

where r is the distance of separation, μ is the nuclear magnetic moment, and θ is the angle between the internuclear vector and the applied magnetic field. The plus or minus sign indicates the spin state of the neighbor, i.e., $m_I = +1/2$ or $m_I = -1/2$, the states being equally probable.

The second moment calculation of Van Vleck¹⁷ is the proper quantum mechanical calculation of the resonance width. If the width is defined as the root second moment, ΔH_2 . Van Vleck's calculation shows that the classical result has the correct form but is too small by the numerical factor $2/3$. The term "second moment" should not obscure the physical meaning. This simply represents the average square of the local field at a typical nucleus. Most line widths are quoted as full widths at maximum slope and $\delta H \cong 2\Delta H_2$.

The rigid lattice result has been experimentally tested in many systems and, in particular, in crystalline polyethylene. Van Vleck's result is entirely consistent with the known molecular parameters and crystal structure. (An earlier suggestion to the contrary³ is in error.)

When molecular rotation, either continuous or jump-wise, takes place, the variables in the local field expression become functions of time, i.e., eq. (6) becomes,

$$\pm [\mu/r^3(t)] [3 \cos^2\theta(t) - 1] \quad (7)$$

For convenience of discussion let us assume that r is constant and only $\theta(t)$ varies with time. (This would be appropriate to the interaction of two protons attached to the same carbon, for example.) We require the time-average local field,

$$(\mu/r^3)(1/T_2) \int_0^{T_2} [3 \cos^2\theta(\tau) - 1] d\tau \quad (8)$$

where T_2 is a time of the order of the time the nucleus resides in a given spin state. If $\theta(\tau)$ varies rapidly with no restrictions on the directions the internuclear vector can assume, the time average can be replaced by the space average:

$$(\mu/r^3) \int_0^\pi (3 \cos^2\theta - 1) \sin\theta d\theta = 0 \quad (9)$$

This is the reason liquids exhibit narrow resonances. Of course, the replacement of the time average is approximate, and some residual width always remains.

There are two interpretations applicable to a partially narrowed resonance such as one observes in molten or amorphous polymers. First, it may be that there are no restrictions on the orientation angle but that the motion is not fast enough to average θ equally over 0 to π in the interval T_2 . Second, it may be that the motion is arbitrarily rapid but θ is restricted in some way. In the first case the resonance width should decrease further with increasing temperature, whereas in the second case the resonance width could be independent of temperature. If the restrictions on θ are temperature-dependent there is no way to choose between the two interpretations.

To get some appreciation for the motion implied by the nuclear resonance widths, we have calculated the width assuming arbitrarily rapid motions subject to the restriction that $\theta > \theta_0$, where θ_0 is to be evaluated from the observed widths. The result is

$$\delta H \cong (\mu/r^3)\cos \theta_0 \sin^2 \theta_0 \quad (10)$$

The ratio of the narrowed resonance width to the rigid lattice width is thus of the order of $\cos \theta_0 \sin^2 \theta_0$. In polyethylene at room temperature the amorphous material exhibits a width of about 0.2 gauss, while the rigid lattice width is about 10 gauss. Thus, $\sin^2 \theta_0 \cos \theta_0$ is roughly 0.02 and $\theta_0 < 10^\circ$. That is, nearly all orientations are accessible to the proton-proton vector, even on the assumption of arbitrarily rapid motions. Even slight restrictions on the rate of fluctuation would require that all orientations be accessible.

Of course, it would be more reasonable to make the restrictions on θ crystallographic in nature. This can be done, but the procedure is cumbersome and the result is nearly the same. One must transform to a local coordinate system, perform the space average, expression (9), and then carry out a "powder average" (i.e., over-all orientations). We omit this calculation.

Therefore, the resonance width observed in the mobile regions of polyethylene at room temperature implies the existence of a very general type motion, and it seems only reasonable to associate this with molecular motion in viscous liquids. For example, the resonance widths observed in polymer melts, solutions, and amorphous regions are comparable with resonance widths observed in liquid glycerine. Every proton-proton vector which is less than, say, 5 Å., must point (almost) equally in all directions in an interval of the order of T_2 , i.e., 10^{-3} -1 sec.

V. Conclusions

The mobile fraction is an extremely important parameter for the characterization of polymers. In fact, we believe that this parameter is superior to the degree of crystallinity for most purposes. Fortunately, the degree of crystallinity and the rigid fraction agree in most systems.

The narrow resonance which appears when solution crystallized material is exposed to carbon tetrachloride could be associated with the molecules on

the lateral surfaces of the single crystal lamellae. The narrow resonances which develop on heat treatment^{8,11,13} of these preparations can also be attributed to lateral surface molecules, as it is known that the lateral surface area must increase by a large amount on heat treatment.¹⁸ This is speculation; we have no direct evidence that the mobile regions are on the lateral surfaces.

The generality of motion implied by the discussion of Section IV leads us to conclude that the amorphous regions must have substantial dimensions. It seems incorrect to describe these regions as defects in any ordinary sense of the word. Of course, some peculiar motion may exist that permits the virtually unrestricted motion of the proton-proton vectors and yet does not require a large mobile region. We have not been able to imagine such a motion.

We are indebted to our colleagues D. C. Douglass, W. P. Slichter, R. Salovey, F. J. Padden, H. D. Keith, S. Matsuoka, and F. H. Winslow for many enlightening discussions of this work. In addition, R. Salovey and S. Matsuoka provided some of the materials studied.

References

1. Wilson, C. W., III, and G. E. Pake, *J. Polymer Sci.*, **10**, 503 (1953).
2. Wilson, C. W., III, and G. E. Pake, *J. Chem. Phys.*, **27**, 115 (1957).
3. McCall, D. W., and W. P. Slichter, *J. Polymer Sci.*, **26**, 171 (1957).
4. Slichter, W. P., and D. W. McCall, *J. Polymer Sci.*, **25**, 20 (1957).
5. Rempel, R., H. Weaver, R. Sands, and R. L. Miller, *J. Appl. Phys.*, **28**, 1082 (1957).
6. Collins, R. L., *J. Polymer Sci.*, **27**, 75 (1958).
7. McCall, D. W., and E. W. Anderson, *J. Chem. Phys.*, **32**, 237 (1960).
8. Slichter, W. P., *J. Appl. Phys.*, **31**, 1865 (1960).
9. Bloembergen, N., E. M. Purcell, and R. V. Pound, *Phys. Rev.*, **73**, 679 (1948).
10. Matsuoka, S., Bell Telephone Laboratories, Murray Hill, New Jersey, private communication.
11. Slichter, W. P., *J. Appl. Phys.*, **32**, 2339 (1961).
12. McCall, D. W., and W. P. Slichter, *J. Am. Chem. Soc.*, **80**, 1861 (1958).
13. Peterlin, A., G. Krasovec, E. Pirkmajer, and J. Levstek, paper presented at I.U.P.A.C. Symposium, Wiesbaden, Germany, October 1959.
14. Gutowsky, H. S., and G. E. Pake, *J. Chem. Phys.*, **18**, 162 (1950).
15. Glasstone, S., K. J. Laidler, and H. Eyring, *Theory of Rate Processes*, McGraw-Hill, New York, 1941.
16. McCall, D. W., *J. Polymer Sci.*, **26**, 15 (1957).
17. Van Vleck, J. H., *Phys. Rev.*, **74**, 1168 (1948).
18. Statton, W. O., and P. H. Geil, *J. Appl. Polymer Sci.*, **3**, 357 (1960).

Résumé

On a développé les études de résonance magnétique nucléaire sur le polyéthylène. On discute la relation entre la fraction rigide (NMR) et la fraction cristalline, et on discute le cas de l'importance relative de la fraction rigide (ou son complément la fraction mobile). Lorsque le polymère a été gonflé par des solvants de bas poids moléculaire, le spectre NMR donne une preuve directe que les régions rigides et probablement cristallines, ne sont pas affectées. On discute la nature des mouvements moléculaires sur la base d'un modèle et on montre que les données de NMR impliquent un mouvement d'un type assez général.

Zusammenfassung

Die Untersuchung der protonmagnetischen Resonanz von Polyäthylen wurde weitergeführt. Die Beziehung zwischen der unbeweglichen Fraktion (NMR) und der kristallinen Fraktion wird diskutiert und die relative Bedeutung der unbeweglichen Fraktion (oder ihres Gegenstücks, der beweglichen Fraktion) in einem bestimmten Fall gezeigt. Bei Quellung des Polymeren in niedermolekularen Lösungsmitteln liefern die NMR-Spektren einen reche direkten Beweis dafür, dass die unbeweglichen, und wahrscheinlich kristallinen Bereiche, unangegriffen bleiben. Die Natur der Molekülbewegung wird an einem Modell diskutiert und es wird gezeigt, dass die NMR-Daten einem ziemlich allgemeinen Bewegungstyp entsprechen.

Received January 22, 1962

Crystallite Orientation in Regenerated Cellulose Filaments. I. Measurement of Orientation by X-Ray Methods*

K. C. ELLIS and J. O. WARWICKER, *Shirley Institute, Manchester,
England*

Synopsis

The theory of the fiber diagram has been considered, and it has been shown that Polanyi's theory can be rewritten in terms of the reciprocal lattice and Ewald's construction. By the use of this theory the opacity at a point of an x-ray diffraction photograph of a fiber has been related to the density of reciprocal lattice points at a point in reciprocal space. The effect of imperfections in the experimental arrangement on the azimuthal intensity distribution in a fiber diagram has been considered and an arrangement has been described with which the distribution of orientation of the crystallites can be obtained from the azimuthal intensity distribution after the application of only two simple conversion factors.

Introduction

The first x-ray diagrams of cellulose fibers were obtained by Nishikawa and Ono¹ in 1913. From these, Nishikawa² concluded that cellulose fibers must contain elementary crystals arranged parallel to the fiber axis. Polanyi^{3,4} and Polanyi and Weissenberg^{5,6} considered the mathematical theory of the fiber diagram and showed that it was possible to measure the degree of dispersion of orientation of the crystallites in a fiber from the x-ray diagram. Because the degree of crystallite orientation affects the mechanical properties of the fiber⁷⁻¹¹ there has been considerable interest in this orientation and many measurements of it have been made by x-ray methods. The earliest measurements relied on visual estimates of the length of the diffraction arc and were of a qualitative nature only. The first quantitative measurements were made by Sisson and Clark,¹² who used a photometer to measure the distribution of optical density around the diffraction circle and then used the breadth of this distribution as a measure of the degree of orientation. Although later workers^{7,8,10,13-19} have introduced refinements both in the experimental procedure and in the interpretation of the experimental data, all the methods have been based on the method of Sisson and Clark and the theory of Polanyi and Weissenberg. In this paper a new approach to the theory is made and the experimental

* The contents of this paper form part of the subject matter of a thesis by K. C. Ellis that has been approved by the University of London for the award of the Ph.D. degree.

arrangement is examined to determine the conditions which are necessary to obtain more accurate values of the orientation.

Basic Theory

Polanyi^{3,4} and Polanyi and Weissenberg^{5,6} in their consideration of the theory of the fiber diagram did not use the concepts of the reciprocal lattice and Ewald's construction. Their theory can however be rewritten in terms of these concepts and is more convenient to use in this form.

The reciprocal lattice point representing a set of crystal planes (hkl) lies at a distance σ_{hkl} from the origin in the direction of the normal to the planes. If the specimen contains many crystallites, as a fiber does, the reciprocal lattice points representing the same set of planes in the many different crystallites that are irradiated by the incident x-ray beam will all lie on a sphere of radius σ_{hkl} centered at the origin and will form on it a coating whose density distribution is identical with the distribution of orientation of the corresponding crystal planes. The reciprocal solid for a polycrystalline specimen consists therefore of a set of concentric spheres. Any one of these spheres is identical, apart from a scale factor, with the "Lagenkugel" of Polanyi and Weissenberg. Such a sphere will intersect the sphere of reflection in a circle that will be identical with Polanyi's circle of reflection. The direction of reflected beams will be given by the usual construction of drawing lines from the center of the sphere of reflection to the reciprocal lattice points that are located on the sphere of reflection. For any one reflection, the diffracted beams will therefore lie on a cone and will strike a plane film placed normal to the incident beam in a circle.

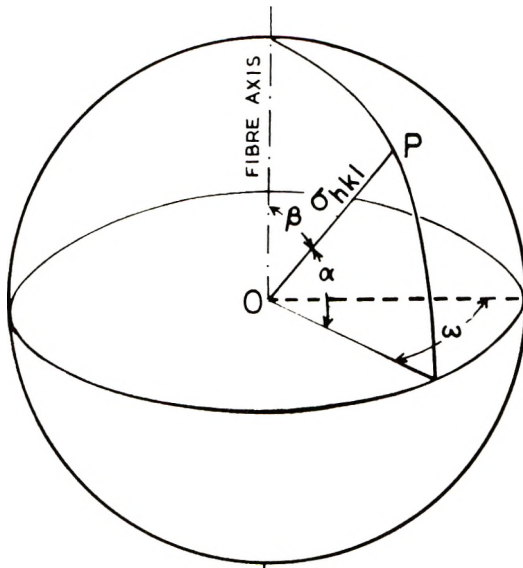
Because of the limited types of orientation that can occur in fibers,²⁰ the reciprocal solid for a fiber specimen will have circular symmetry about the direction of the fiber axis and the density of reciprocal lattice points at a point on a reciprocal lattice sphere will depend only on the angle of latitude, α , of that point. The distribution of orientation of the crystallites in the specimen will therefore be identical with the distribution of density of reciprocal lattice points on a great circle of the reciprocal lattice sphere. With simple photographic methods of recording, this distribution cannot be obtained directly from the photograph. Polanyi³ gave the relations between the angles measured on photographs obtained with a plane film normal to the incident x-ray beam and the angles in reciprocal space. His equations can be written as follows:

(a) With the fiber axis perpendicular to the incident beam

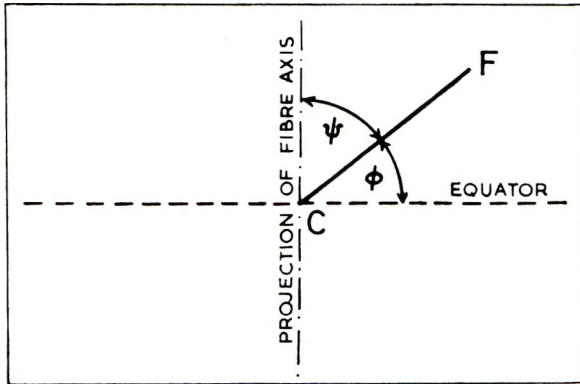
$$\sin \alpha = \cos \theta \sin \phi \quad (1)$$

(b) With the fiber axis inclined at an angle $\pi/2 - \theta$ to the incident beam

$$\cos \beta = 1 - \cos^2 \theta (1 - \cos \psi) \quad (2)$$



(a)



(b)

Fig. 1. (a) Coordinates of the point P on the reciprocal lattice sphere. (b) Angles measured on the film.

Here α and β are the latitude and colatitude, respectively, of the appropriate point P on the reciprocal lattice sphere (see Fig. 1a), θ and ψ are the angles measured on the film (see Fig. 1b), and θ is the Bragg angle.

It can be seen from eq. (1) that $\sin \alpha$ can never be greater than $\cos \theta$ and therefore part of the distribution must be lost if the fiber axis is placed perpendicular to the incident beam. For a diatropic reflection, the part that is lost includes the maximum of the distribution and therefore, for any study of the orientation of these planes, the fiber axis must be inclined

at the appropriate angle to the incident beam. For a paratropic reflection, provided θ is fairly small, the part that is lost is small and relatively unimportant and the fiber axis can be placed perpendicular to the incident beam so that duplicate results can be obtained from the left- and right-hand sides of the photograph. If a counter method of recording is used, the intensity of each diffracted beam is recorded separately, and the positions of the specimen and counter can be varied in such a way that effectively a scan around a great circle of the reciprocal lattice sphere is made.

Polanyi and Weissenberg did not consider the relation between the density of reciprocal lattice points on the reciprocal lattice sphere (in their nomenclature, the density of the coating on the Lagenkugel) and the intensity of the diffracted beam. Baule et al.¹³ assumed that the intensity of the diffracted beam was proportional to the density of reciprocal lattice points but did not justify this assumption. Hermans et al.¹⁵ gave a proof of this relation in which they stated that it was necessary to make the circle of reflection into a band λ of width $\Delta\theta$ because the incident beam is neither strictly monochromatic nor strictly parallel. They did not consider in detail the effect of the nonmonochromatic and nonparallel nature of the incident beam but implicitly assumed that these factors produced a band of constant width to replace the circle of reflection. Consideration of these factors shows that either of them will have this effect only if very simple conditions, not obtaining in practice, are assumed. It is therefore more satisfactory to calculate the relation between the density of reciprocal lattice points and the intensity of the diffracted beam without introducing these factors; corrections for the lack of perfection in the experimental arrangement can then be considered separately.

The relation between the intensity of a diffracted ray and the density of reciprocal lattice points on the reciprocal lattice sphere can be obtained as follows. Let the density of reciprocal lattice points at a point P on the reciprocal lattice sphere be $P(\beta, \omega)$. Then

$$P(\beta, \omega) = \lim_{\Delta A \rightarrow 0} \frac{N}{\Delta A} \quad (3)$$

where N is the number of reciprocal lattice points contained in a small area ΔA at the point P whose polar coordinates are $\sigma_{hkl}, \beta, \omega$.

The energy E diffracted into a small beam defined by ΔA is proportional to N ; i.e.,

$$E = KN \quad (4)$$

Since the area ΔA is inclined at an angle θ to the line joining P to the center of the sphere of reflection (see Fig. 2), the solid angle filled by the diffracted beam is $\Delta\Omega$, where

$$\Delta\Omega = \frac{A \sin \theta}{(1/\lambda)^2} = \lambda^2 \Delta A \sin \theta \quad (5)$$

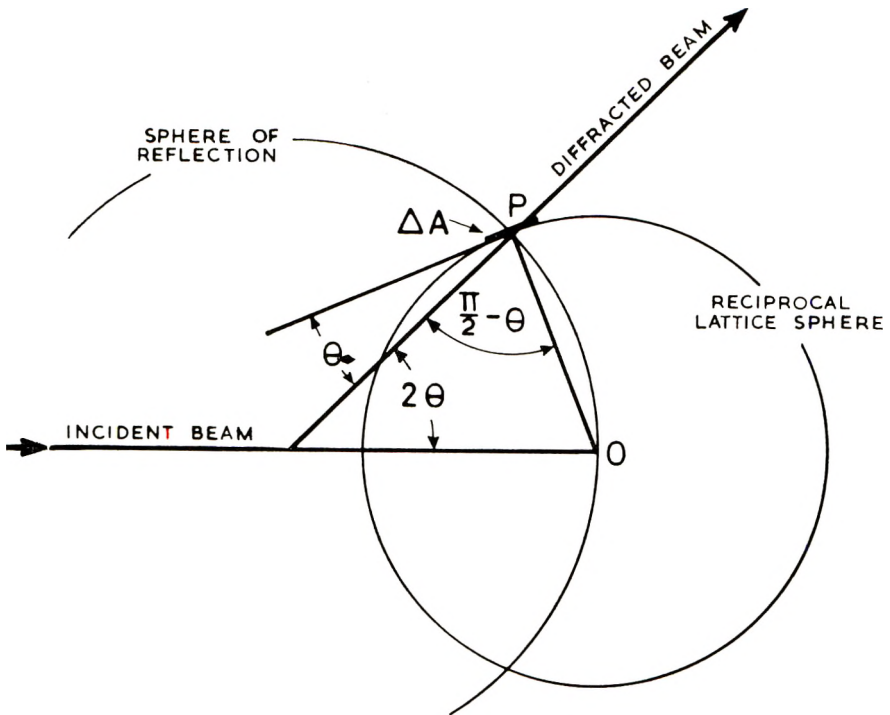


Fig. 2. The reciprocal lattice diagram.

The intensity of the diffracted beam at a distance R from the specimen is therefore I , where

$$I = \frac{E}{R^2 \Delta \Omega} = \frac{KN}{R^2 \lambda^2 \Delta A \sin \theta} \quad (6)$$

The intensity of the diffracted ray will thus be J , where

$$J = \lim_{\Delta A \rightarrow 0} I = \frac{KP(\beta, \omega)}{R^2 \lambda^2 \sin \theta} \quad (7)$$

For any one reciprocal lattice sphere and radiation of one wavelength, θ and λ are constant, so that the intensity of the diffracted ray is proportional to the density of reciprocal lattice points on the reciprocal lattice sphere.

Theory of Corrections

It has been shown that under ideal conditions the intensity of the x-rays diffracted in a particular direction is proportional to the number of crystallites having a corresponding particular orientation. There are however a number of correction factors that have to be considered.

The well-known polarization correction will have no effect on the measurement of orientation since it is given by²¹

$$I_{\text{corr.}} = \frac{2I_{\text{obs.}}}{1 + \cos^2 2\theta} \quad (8)$$

and is independent of α and ϕ .

If a counter diffractometer is used, the intensities of the diffracted beams will be measured at a constant distance from the specimen and the intensity at the point of measurement will be the quantity J that appears in eq. (7). If photographic recording is used, however, this will not be so. It is convenient to use a plane film placed normal to the incident beam when measurements of orientation are required, since the beams diffracted from a particular set of crystal planes [e.g., the (101)] will then strike the film at points on a circle. Then, since the diffracted beam will be inclined at an angle $\pi/2 - 2\theta$ to the film, the small beam defined by the area ΔA of the reciprocal lattice sphere will intersect the film in an area ΔU where

$$\Delta U = s^2 \lambda^2 \sec^3 2\theta \sin \theta \Delta A \quad (9)$$

Here s is the film-specimen distance.

The energy per unit area received on the film will be $KN/\Delta U$ and, since the beam is incident on the film at an angle 2θ , the energy E_a absorbed per unit area in an emulsion of thickness t will be proportional to $(KN/\Delta U)t \sec 2\theta$.²² Therefore

$$E_a = \frac{K'N}{s^2 \lambda^2 \sec^2 2\theta \sin \theta \Delta A} \quad (10)$$

The energy absorbed per unit area at a point P on the film will be E , where

$$E = \lim_{\Delta A \rightarrow 0} E_a = \frac{K'P(\beta, \omega)}{s^2 \lambda^2 \sec^2 2\theta \sin \theta} \quad (11)$$

The quantity required is $P(\beta, \omega)$, and since s and λ are constant for a particular photograph,

$$P(\beta, \omega) \propto E \sec^2 2\theta \sin \theta \quad (12)$$

and at constant θ

$$P(\beta, \omega) \propto E \quad (13)$$

Equations (7) and (13) contain the intensity of the diffracted beam and the energy absorbed per unit area in the film respectively. These are the quantities that have to be measured either by a counter or by a photometer. In both instances it is necessary to consider the relation between the quantity that it is required to measure and the quantity that is actually measured. The size of the receiving slit of the measuring instrument enters into both considerations and will be considered later. When a counter is used to measure x-ray intensity, errors arise from the fact that the x-ray

quanta are randomly distributed with respect to time, and from the resolving time of the measuring apparatus. These two factors have been discussed by many authors and equations are available²³ from which the errors can be calculated. These errors can be considerable when the specimen has a low diffracting power and a highly collimated beam is required. When photographic recording is used, the quantity that is actually measured is the optical density of the film. VanHorn²⁴ has shown that, under suitable conditions of exposure and development, there is a linear relation between the optical density and the absorbed energy, but it is more reliable to calibrate each film with an intensity scale.

The factors that remain to be considered include: (a) the finite size of the aperture of the measuring apparatus, (b) the finite size of the irradiated volume of the specimen, (c) the nonparallel nature of the incident beam, (d) the polychromatic nature of the incident beam, (e) absorption within the specimen, and (f) possible nonuniform distribution of crystallite size.

The effect of these factors is complex and not easily calculated. Ideally they should be considered simultaneously, as they are interdependent, but such a treatment is extremely difficult. Instead they will be considered separately, the aim being to show that under suitable experimental conditions the effect of each on the required intensity distribution is very small.

The effect of factors (a)–(d) can be expressed^{25–27} by an equation of the type

$$I'(x',y') = \int_{-\infty}^{+\infty} \int_{-\infty}^{+\infty} g(x,x',y,y')I(x,y)dx dy \quad (14)$$

where $I'(x',y')$ represents the observed intensity distribution, $I(x,y)$ represents the required intensity distribution, $g(x,x',y,y')$ represents a function of the apparatus, and x,x',y,y' are distances in real space as, for example, the coordinates of a point on the film.

If a reasonable expression is assumed for $I(x,y)$, and $g(x,x',y,y')$ is calculated for simplified conditions that correspond reasonably well with the actual experimental conditions, the expression $g(x,x',y,y')I(x,y) dx dy$ is not usually amenable to direct integration and indirect methods have to be adopted. Calculations of the effect of these factors on the radial intensity distribution in a powder diagram have been made by several authors^{26–29} but their effect on the azimuthal intensity distribution in a fiber diagram has not been calculated. A method that can be used will therefore be illustrated for the finite width and height of the incident beam.

Consider first an ideal, parallel, monochromatic x-ray beam of width $2a$ and negligible height, incident on a specimen of negligible thickness whose dimension in the direction of the width of the incident beam is greater than $2a$. Each ray of the incident beam will produce a diffraction pattern that is identical with the others except for a lateral displacement depending on the position of the incident ray and an intensity scaling factor depending on the intensity of the incident ray. Let the intensity distribution in one of these component patterns be represented by a function $f(x,y)$ and that in the incident beam by a function $g(x)$. The total intensity of all the dif-

fracted rays that strike the point on the film whose coordinates are x' , y' will be $I'(x',y')$, where

$$I'(x',y') = \int_{-a}^{+a} g(x'')f(x' - x'',y')dx'' \quad (15)$$

Now, let $x' - x'' = x$ and $y' = y$ and consider the distribution of intensity along the line $y = C$. Then,

$$I'(x',C) = \int_{x'-a}^{x'+a} g(x' - x)f(x,C)dx \quad (16)$$

If the incident beam were of uniform intensity so that

$$g(x) = c \quad -a \leq x \leq +a \quad (17)$$

where c is a constant.

Then

$$I'(x',C) = c \int_{x'-a}^{x'+a} f(x,C) dx \quad (18)$$

The integral in eq. (18) is equal to the area under the curve $f(x,C)$ between $x = x' - a$ and $x = x' + a$. If a is small, so that the part of the curve lying between these limits may be regarded as a straight line,

$$I'(x',C) = 2acf(x',C) \quad (19)$$

and the observed and required distributions have the same shape.

Normally the incident beam will not be uniform. A better approximation is for $g(x)$ to have a symmetrical form such that

$$g(-x) = g(x) \quad (20)$$

$$g(x_1) \geq g(x_2) \quad x_2 > x_1$$

Let a be small enough that for any range $2a$ of x ,

$$f(x,C) = f(x',C) + m(x - x') + l(x - x')^2 \quad (21)$$

Substituting eq. (21) into (16),

$$I'(x',C) = G_0f(x',C) + mG_1 + lG_2 \quad (22)$$

where

$$G_0 = \int_{x'-a}^{x'+a} g(x' - x) dx = \int_{-a}^{+a} g(x'') dx'' \quad (23)$$

$$G_1 = \int_{x'-a}^{x'+a} (x - x')g(x' - x) dx = - \int_{-a}^{+a} x''g(x'') dx'' = 0 \quad (24)$$

$$G_2 = \int_{x'-a}^{x'+a} (x - x')^2g(x' - x) dx = \int_{-a}^{+a} x''^2g(x'') dx'' \quad (25)$$

Here G_0 is the total intensity of all the incident rays that strike the specimen.

The difference in shape of the observed and required distributions is given by lG_2/G_0 . This quantity is smaller for a beam in which the intensity decreases continuously and symmetrically from the center than for one of the same width but uniform intensity. It will therefore be sufficient to show that the difference in shape of the observed and required distributions

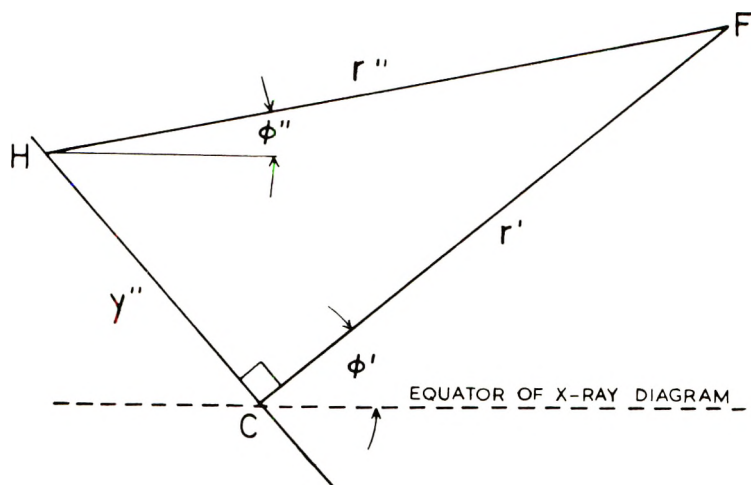


Fig. 3. Diagram used in the consideration of the effect of the finite width and height of the incident beam.

would be small if the incident beam had a uniform intensity and the same total width as the actual beam.

Consider next an ideal, parallel, monochromatic x-ray beam of circular cross section incident on an infinitely thin specimen whose dimensions in all directions perpendicular to the incident beam are greater than the diameter, $2a_0$, of the incident beam. Let the principal ray of the incident beam strike the film at C (Fig. 3). In order to find the intensity at a point F on the film let the incident beam be divided into a number of component beams by planes parallel to CF . If the distance between successive planes is infinitesimal, then each of the component beams can be regarded as a beam of finite width (parallel to CF) but negligible height (perpendicular to CF). If the diameter of the incident beam is small enough, each component beam may be replaced by an ideal ray of intensity $G(y)$ at its center, where

$$G(y) = \int_{-a'}^{+a'} g(x,y) dx \quad (26)$$

$$a'^2 = a_0^2 - y^2 \quad (27)$$

Here $g(x,y)$ represents the intensity distribution in the incident beam, and x and y are measured parallel and perpendicular, respectively, to CF .

If the incident beam has circular symmetry, $G(y)$ will have the same form and magnitude whatever the orientation of the axes and $G(-y)$ will be equal to $G(y)$. The circular beam may therefore be treated as a beam of infinitesimal width but finite height. Each ray in this beam will produce a diffraction pattern in which the intensity distribution can be represented by a function $k(r,\phi)$, where r and ϕ are the polar coordinates of the point on the film at which the intensity is $k(r,\phi)$. Here $k(r,\phi)$ can be expressed in terms of $k(r,0)$, the distribution on the equator:

$$k(r,\phi) = k(r,0)p(\phi) \quad (28)$$

The total intensity received at the point F whose coordinates are r', ϕ' will be $K(r', \phi')$ where

$$K(r', \phi') = \int_{-a_0}^{+a_0} G(y'') k(r'', \phi'') dy'' \quad (29)$$

$$r''^2 = r'^2 + y''^2 \quad (30)$$

$$\tan(\phi' - \phi'') = -y''/r' \quad (31)$$

If a_0 is small enough that the curve $I = p(\phi)$ can be regarded as linear between $\phi = \phi' - \tan^{-1}(a_0/r')$ and $\phi = \phi' + \tan^{-1}(a_0/r')$,

$$\begin{aligned} p(\phi'') &= p(\phi') + q(\phi'' - \phi') \\ &= p(\phi') + q \tan^{-1}(y''/r') \end{aligned} \quad (32)$$

Therefore

$$\begin{aligned} K(r', \phi') &= p(\phi') \int_{-a_0}^{+a_0} G(y'') k(r'', 0) dy'' \\ &\quad + q \int_{-a_0}^{+a_0} G(y'') k(r'', 0) \tan^{-1}(y''/r') dy'' \end{aligned} \quad (33)$$

The nature of $G(y'')$ and $k(r'', 0)$ is such that they are both always positive. In addition, $k(r'', 0)$ will have the same value for y'' and $-y''$, $G(-y'') = G(y'')$ and $\tan^{-1}(-y''/r') = -\tan^{-1}(y''/r')$. Therefore

$$K(r', \phi') = p(\phi') \int_{-a_0}^{+a_0} G(y'') k(r'', 0) dy'' \quad (34)$$

Since the form and magnitude of $G(y'')$ and $k(r'', 0)$ do not depend on ϕ' , the value of the integral in eq. (34) will be a function of r' and a_0 only and the shapes of the observed and required intensity distributions will be the same.

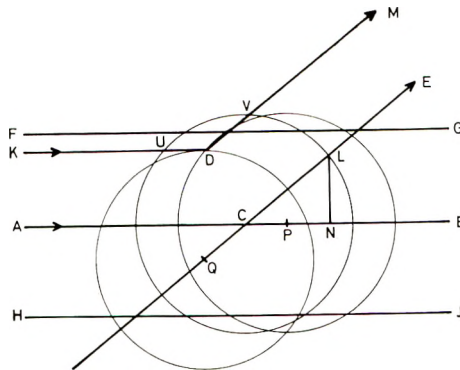


Fig. 4. Diagram used in the calculation of the absorption correction.

It has been shown that no correction will be needed for the finite width and height of the incident beam provided (a) the beam is circularly symmetrical, (b) the intensity of the beam decreases continuously and symmetrically from the center, and (c) the diameter of the beam is so small that

the appropriate sections of the curves $I = f(x, C)$ and $I = p(\phi)$ can be regarded as linear.

Factors (a)–(c) listed before have been considered in the same way and the conditions found to be necessary were of a similar type. Factor (d) was also considered and it was found that this could only directly affect the radial intensity distribution. Indirectly, however, the use of polychromatic radiation could give rise to errors in the measured degree of crystallite orientation because of overlapping reflections. It is therefore desirable to make the radiation as nearly monochromatic as possible.

Methods of calculating the absorption correction have been developed by several authors,^{30–32} but these have not dealt with nonequatorial points in the diagrams obtained with cylindrical specimens. The method of Claassen³⁰ has therefore been adapted to enable the absorption corrections for these points to be calculated.

The method is a graphical one and depends on constructing lines of constant path length within the specimen. A circle of radius R is drawn to represent a section through the specimen normal to the fiber axis at a distance h from the principal ray of the incident beam. In Figure 4 this is drawn about C as center; AC is drawn parallel to the incident beam and CE parallel to the projection of the diffracted beam on the plane of the section. The angle BCE is $2\theta'$ and is given by

$$\tan 2\theta' = \sin \psi \tan 2\theta \quad (35)$$

Two circles of radius R are drawn about P and Q as centers, where P is any point on AC extended and Q is any point on EC extended. Consider the ray diffracted at the point D where these two circles intersect. The path length within the specimen of this ray is $UD + DV \sec \xi$, where ξ is the angle that the diffracted beam makes with the plane of the section and is given by

$$\sin \xi = \cos \psi \sin 2\theta \quad (36)$$

Since $UD = CP$ and $DV = QC$, the path length within the specimen of the ray KDM is $PC + QC \sec \xi$. If now P and Q are moved through distances u and $u \cos \xi$ so that $PC + QC \sec \xi$ remains constant, the point D will trace out a line of constant path length. Lines of this sort can be drawn for a series of values of $PC + QC \sec \xi$ and the section thus divided into regions such that the path length within the specimen for a ray diffracted at any point within one region is approximately constant.

Since the diameter of a fiber specimen is usually greater than the diameter of the incident beam, it is necessary to find that part of the section that is irradiated by the incident beam. If, of this, an area A_n lies in the region for which the path length is l_n , the volume V_n of the specimen for which the path length is l_n is given by

$$V_n = \int_{-r_0}^{+r_0} A_n dh \quad (37)$$

where $2r_0$ is the diameter of the specimen.

The absorption correction factor is then C_A , where

$$C_A = \frac{\sum_n V_n}{\sum_n V_n \exp \{-\mu l_n\}} \quad (38)$$

Here μ is the linear absorption coefficient for the material of the specimen.

The last factor to be considered is a possible nonuniform distribution of crystallite size. This would cause the shape of the radial intensity distribution to vary with the azimuthal angle. It would then be necessary to measure the crystallite orientation from a graph of the area of the peak in the radial intensity distribution against azimuthal angle instead of from the azimuthal intensity distribution.

Experimental

If the degree of orientation of the crystallites in a fiber specimen is to be measured accurately, the experimental arrangement that is used must satisfy the conditions that make the corrections small. The arrangement that we have used does this and will be briefly described. A complete description has been given elsewhere.³³

Photographic recording was used, and each film was calibrated by means of a rotating sector wheel. The camera (Fig. 5) was an improved version of that used by Meredith¹⁸ with the specimen table, beam stop, and film cassette mounted on brass blocks. By assembling the camera with the blocks always in contact, a constant distance of 5 cm. could be maintained between the specimen and the film. The collimator was a lead-glass tube

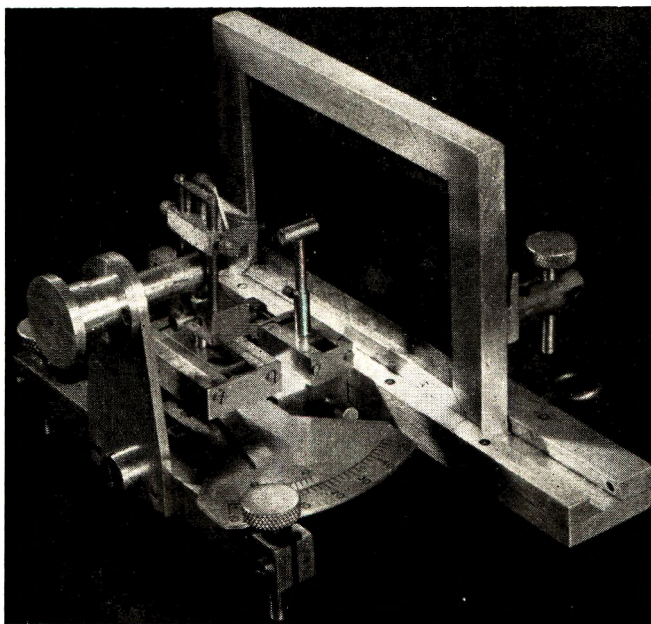


Fig. 5. X-ray camera.

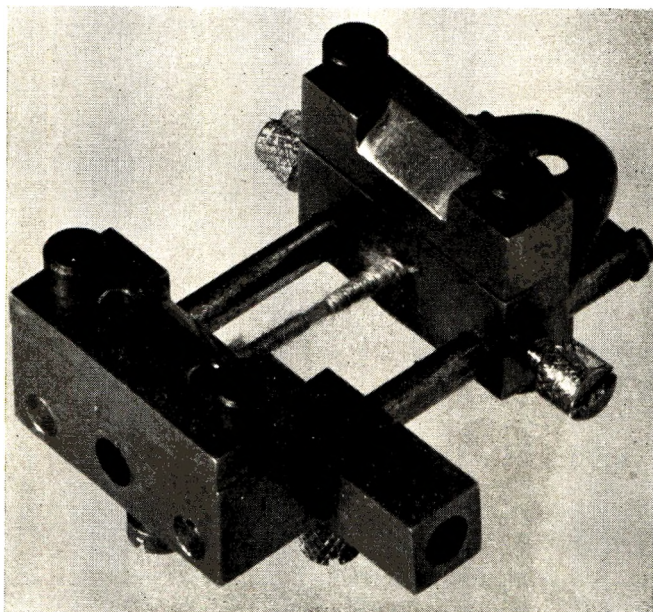


Fig. 6. Specimen holder.

of 0.2 mm. internal diameter and 4 cm. length. The specimen table could be rotated through known angles about a vertical axis so that photographs of the $0k0$ reflections could be taken with the fiber axis inclined at the correct angle to the incident beam (fiber axis horizontal).

The method of preparing the specimens was similar to those described by Berkley and Woodyard^{7,8} and Meredith.¹⁸ A 25-mg. bundle of fibers one inch long was carefully combed to produce a parallel arrangement of fibers and then wrapped with cotton thread. In order that the fibers should be kept straight but not stretched while the wrapping was being applied, the bundle was tensioned by means of a 2-lb. weight. This weight provided a tension of 0.1 g./denier, which is that normally used to remove the crimp from regenerated cellulose filaments when the denier is being measured. The wrapping was applied in three sections, first from one end of the bundle to a point $1/16$ in. from the center, then over the central $1/8$ in., and finally over the remainder. The wrapping on the center section was afterwards removed so that the central $1/8$ in. of the fiber bundle was exposed. The specimen was mounted in a special holder (Fig. 6) and again tensioned by means of a 2-lb. weight. The tension was preserved by means of clamping screws. The holder was provided with two alternative means of mounting so that the fiber axis could be either vertical or horizontal.

The x-ray exposures were made at 25 (kilo volt peak) in order to reduce the proportion of white radiation. Ilford Industrial B film was used and, with an anode current of 20 ma., the normal exposure times were 24 hr. for the 101 reflection and 48 hr. for the 020 reflection. During this exposure a strip of the film was protected by a piece of lead foil and an intensity calibration scale was later recorded on this strip. A nickel-foil β -filter was used for

both the main and the calibration exposures. The films were developed in Ilford ID 19 for 5 min. at room temperature.

The distribution of optical density along the appropriate lines on the film was measured by means of a double beam microdensitometer similar to that described by Taylor.³⁴ The effective slit size at the film was: width, 0.033 mm.; height, 0.15 mm. The optical densities were converted into x-ray intensities by means of the calibration curve obtained from the intensity scale. A radial intensity distribution curve close to the equator or meridian was plotted in order to determine the position of the peak of the appropriate reflection, and a semicircular scan was then made through that point about the center of the pattern. The azimuthal intensity distribution so obtained was used for measuring the crystallite orientation.

The factors that have to be taken into account when considering the effect of experimental conditions on the shape of the azimuthal intensity distribution curve are (1) the size of the photometer slit, (2) the diameter of the incident x-ray beam, (3) the divergence of the incident x-ray beam, (4) the distribution of intensity in the incident x-ray beam, (5) absorption of the x-ray beams within the specimen, and (6) the distribution of crystallite size with respect to azimuthal angle.

Factors (4) and (6) were checked experimentally. The distribution of intensity along a number of radii of the spot produced by the main beam was measured, and it was found that the intensity decreased continuously and symmetrically from the center. The beam was therefore circularly symmetrical. In order to check the distribution of crystallite size with respect to azimuthal angle, radial intensity distribution curves were obtained at several different angles to the equator on the diagrams produced by some representative specimens. No significant difference was found in the shape of these radial distributions and therefore this factor can have had no effect on the shape of the azimuthal intensity distributions. Factors (1)–(3) were each considered by the method that has been described above. It was found that none of the correction factors differed from unity by as much as 1% and they were therefore taken as unity. The absorption correction factors for several values of 2θ and ψ were calculated by the method that has been described above. The values that were obtained

TABLE I
Absorption Corrections for a Normal Fiber Photograph

Diffraction angle, 2θ	Azimuthal angle, ψ	Absorption correction factor, C_A
0	0	3.65
10°	0	3.64
15°	0	3.62
45°	0	3.51
12°	0	3.63
12°	30°	3.65
12°	60°	3.73
12°	90°	3.69

(Table I) were almost constant and the absorption effect could therefore be neglected.

Orientation Coefficient

With the experimental arrangement that we used, the only corrections that need to be applied are those whereby the measured azimuthal angle (ϕ or ψ) is converted into the angle of latitude α or colatitude β , and the measured optical density is converted into x-ray intensity. Once these conversions had been made, the azimuthal intensity distribution curve was identical with the orientation distribution curve. Although for some purposes it might be desirable to study the complete distribution curves, for most purposes it is convenient and satisfactory to use one quantity as a measure of the degree of orientation of the crystallites. Several such quantities, all related to the breadth of the distribution curve, have been suggested.^{12, 15, 18, 19, 35} That suggested by Hermans et al.¹⁵ has theoretical advantages but two serious practical disadvantages. First, it is highly dependent on the high-angle parts of the distribution curve where the error in the intensity measurements is relatively higher and, second, it is a less sensitive measure than the breadth of the distribution curve.¹⁹ For most purposes, that suggested by Kast¹⁰ and Kast and Prietzschk,¹⁹ namely, the reciprocal of the half-breadth of the distribution curve, seems to be the most suitable. We have used three coefficients, the 40, 50, and 60% coefficients, defined as the reciprocals of half the breadth of the distribution curve at 40, 50, and 60%, respectively, of the maximum height, and have found them equally satisfactory.

Conclusion

Provided care is taken with the experimental arrangement, it is possible to measure the degree of crystallite orientation in a fiber specimen directly from the azimuthal intensity distribution curve. The experimental arrangement that has been described is satisfactory for this purpose and has been used to investigate the effect of degree of polymerization on crystallite orientation in regenerated cellulose filaments. The results of this investigation will be described in Part II.

References

1. Nishikawa, S., and S. Ono, *Proc. Tokyo Math.-Phys. Soc.*, **7**, 131 (1913).
2. Nishikawa, S., *Proc. Tokyo Math.-Phys. Soc.*, **7**, 296 (1914).
3. Polanyi, M., *Z. Physik.*, **7**, 149 (1921).
4. Polanyi, M., *Naturwissenschaften*, **9**, 337 (1921).
5. Polanyi, M., and K. Weissenberg, *Z. Physik.*, **9**, 123 (1922).
6. Polanyi, M., and K. Weissenberg, *Z. Physik.*, **10**, 44 (1922).
7. Berkley, E. E., and O. C. Woodyard, *Ind. Eng. Chem. Anal. Ed.*, **10**, 451 (1938).
8. Berkley, E. E., O. C. Woodyard, H. D. Barker, T. Kerr, and C. J. King, *U.S. Dept. Agr. Tech. Bull. No. 949*, 3-14 and 57-61 (1948).
9. Meredith, R., *Shirley Inst. Mem.*, **25**, 41 (1951); or *J. Textile Inst.*, **42**, T291 (1951).
10. Kast, W., *Forschungsber. Wirtschafts- u. Verkehrsministeriums Nordrhein-Westfalen*, No. 35 (1953).
11. Kast, W., *Melliand Textilber.*, **32**, 361-3 and 442-6 (1951).

12. Sisson, W. A., and G. L. Clark, *Ind. Eng. Chem. Anal. Ed.*, **5**, 296 (1933).
13. Baule, B., O. Kratky, and R. Treer, *Z. physik. Chem.*, **B50**, 255 (1941).
14. Kratky, O., F. Schossberger, and A. Sekora, *Z. Elektrochem.*, **48**, 409 (1942).
15. Hermans, J. J., P. H. Hermans, D. Vermaas, and A. Weidinger, *Rec. trav. chim.*, **65**, 427 (1946).
16. Hermans, P. H., *Physics and Chemistry of Cellulose Fibres*, Elsevier, New York, 1949, pp. 244-265.
17. Segal, L., J. J. Creely, and C. M. Conrad, *Rev. Sci. Instr.*, **21**, 431 (1950).
18. Meredith, R., *Shirley Inst. Mem.*, **25**, 25 (1951); or *J. Textile Inst.*, **42**, T275 (1951).
19. Kast, W., and A. Prietzschk, *Kolloid-Z.*, **114**, 23 (1949).
20. Sisson, W. A., *J. Phys. Chem.*, **40**, 343 (1936).
21. *Internationale Tabellen zur Bestimmung von Kristallstrukturen*, Vol. 2, Gebrüder Borntraeger, Berlin, 1935 p. 560.
22. Cox, E. G., and W. F. B. Shaw, *Proc. Roy. Soc. (London)*, **A127**, 71 (1930).
23. Arndt, U. W., in H. S. Peiser, H. P. Rooksby, and A. J. C. Wilson, eds., *X-ray Diffraction by Polycrystalline Materials*, Institute of Physics, London, 1955, pp. 222-226.
24. VanHorn, M. H., *Rev. Sci. Instr.*, **22**, 809 (1951).
25. Spencer, R. C., *Phys. Rev.*, **38**, 618 (1931).
26. Jones, F. W., *Proc. Roy. Soc. (London)*, **A166**, 16 (1938).
27. Klug, H. P., and L. E. Alexander, *X-Ray Diffraction Procedures for Polycrystalline and Amorphous Materials*, Wiley, New York, 1954, pp. 243-257, 494-511.
28. Shull, C. G., *Phys. Rev.*, **70**, 679 (1946).
29. Stokes, A. R., *Proc. Phys. Soc. (London)*, **61**, 382 (1948).
30. Claassen, A., *Phil. Mag.*, **9**, 57 (1930).
31. Bradley, A. J., *Proc. Phys. Soc. (London)*, **47**, 879 (1935).
32. *International Tables for X-Ray Crystallography*, Vol. 2, The International Union of Crystallography, Kynoch Press, Birmingham, England, 1959, pp. 291-312.
33. Ellis, K. C., Ph.D. thesis, Univ. of London, 1960.
34. Taylor, A., *J. Sci. Instr.*, **28**, 200 (1951).
35. Sisson, W. A., *Textile Research*, **7**, 425 (1937).

Résumé

La théorie des diagrammes de fibres a été considérée et on a montré que la théorie de Polanyi pouvait être revue sur la base d'un réseau réciproque et de la construction d'Ewald. Grâce à cette théorie l'opacité en un point déterminé d'un diagramme de diffraction de rayons-X d'une fibre a pu être mise en relation avec la densité des points du réseau réciproque en un point de l'espace réciproque. L'influence des imperfections du montage expérimental sur la distribution azimuthale de l'intensité dans un diagramme de fibre a été examinée; on a décrit un montage permettant l'obtention de la distribution de l'orientation des cristallites à partir de la distribution azimuthale de l'intensité après l'application de deux facteurs de conversion simples.

Zusammenfassung

Die Theorie des Faserdiagramms wurde untersucht und es wurde gezeigt, dass die Theorie von Polanyi im reziproken Gitter und in der Konstruktion von Ewald dargestellt werden kann. Unter Benützung dieser Theorie wurde die Undurchlässigkeit an einem Punkt einer Röntgenbeugungsaufnahme einer Faser zu der Dichte der Punkte im reziproken Gitter an einem Punkt im reziproken Raum in Beziehung gesetzt. Der Einfluss von Unvollkommenheiten in der Versuchsanordnung auf die azimuthale Intensitätsverteilung in einem Faserdiagramm wurde berücksichtigt und es wurde eine Anordnung beschrieben, mit der die Orientierungsverteilung der Kristallite aus der azimuthalen Intensitätsverteilung mittels nur zweier einfacher Konversionsfaktoren erhalten werden kann.

Received October 9, 1961

The Second Newtonian Viscosity Number

E. W. MERRILL, H. S. MICKLEY, A. RAM, and
W. H. STOCKMAYER, *Departments of Chemical Engineering and of
Chemistry, Massachusetts Institute of Technology,
Cambridge, Massachusetts*

Synopsis

The second Newtonian viscosities η_2 of solutions of polystyrene and polyisobutylene were determined in a coaxial cylinder viscometer at shear rates near 10^6 sec.⁻¹. The second Newtonian viscosity numbers $(\eta_2 - \eta_s)/\eta_s c$, where η_s is solvent viscosity and c is polymer concentration, were determined as a function of concentration. For polymer species of viscosity-average molecular weight \bar{M}_v less than 1×10^6 , $\lim_{c \rightarrow 0} (\eta_2 - \eta_s)/\eta_s c$ appears almost identical to intrinsic viscosity $[\eta]$. Above $\bar{M}_v \simeq 1 \times 10^6$, a plateau of constant $(\eta_2 - \eta_s)/\eta_s c$ is found when this function is plotted against c . For good solvents the plateau value: $\{(\eta_2 - \eta_s)/\eta_s c\}_p$ lies below $[\eta]$, but in poor solvents (near the θ temperature) the opposite is true. Correlation of plateau values vs. \bar{M}_v can be achieved in the manner of the Mark-Houwink equation: $[\eta] = K' \bar{M}_v^a$, by writing: $\{(\eta_2 - \eta_s)/\eta_s c\}_p = K'' \bar{M}_v^b$. The sum of $a + b$ of any species in two given solvents is approximately unity. Though the data are inconclusive, it appears that even above $\bar{M}_v \simeq 1 \times 10^6$, the second Newtonian viscosity number tends to approach $[\eta]$ as c approaches zero.

INTRODUCTION

Solutions of random coiling polymers have, in general (if the molecular weight is 10^4 or greater), two different levels of Newtonian viscosity separated by a region of non-Newtonian behavior. The first Newtonian viscosity, found under very low shear rates, is always higher than the second Newtonian viscosity, which generally is found at shear rates exceeding $50,000$ sec.⁻¹. In ordinary capillary viscometers for intrinsic viscosity determination it is impossible to reach the second Newtonian viscosity and, for high molecular weight polymers, it is difficult to establish the first Newtonian viscosity. The complete viscosity-shear rate relation is indicated schematically in Figure 1. Liquids following this kind of relation might appropriately be designated Ostwald-Philippoff (OP) liquids after the discoverers.^{1,2} In Figure 1, it is the second Newtonian viscosity beyond c which is the subject of this report.

No attempt appears to have been made to determine the properties of the viscosity number for polymer solutions, as calculated from the second Newtonian viscosity, prior to 1959.³ Since that time a few papers have appeared concerning variously the second Newtonian viscosity, OP-type liquid behavior over many decades of shear rate, or viscosity numbers and

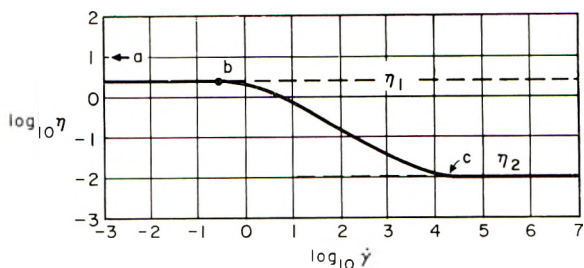


Fig. 1. General characteristics of an Ostwald-Philippoff fluid, on a diagram of $\log \eta$ vs. $\log \dot{\gamma}$ (η = apparent viscosity = shear stress τ divided by shear rate $\dot{\gamma}$), showing first Newtonian viscosity η_1 , and second Newtonian viscosity η_2 , connected by non-Newtonian regime *bc*.

intrinsic viscosities related to the second Newtonian viscosity.⁴⁻⁶ To the limited extent that these references⁴⁻⁶ overlap the studies reported herein, there appears to be reasonable concordance.

EXPERIMENTAL

1. Polymers: Type and Source

Polystyrenes (PST). Anionically polymerized polystyrenes used in this study, which were generously provided by the Dow Chemical Co., are listed in Table IA.

Two whole (wide distribution) polystyrenes were provided by Monsanto Chemical Co., and are described in Table IB.

Polyisobutylenes (PIB). Enjay Company supplied the whole, commercial grades of polyisobutylene listed in Table IIA and the experimental grades listed in Table IIB.

TABLE IA
Anionic Polystyrenes

Dow designation	\bar{M}_v (toluene, 25°C.)
S103	120,000
S105	152,000
S109	190,000
S108	250,000
S 12	(1.27×10^6 , min.) ^a
S114	(4.25×10^6 , min.) ^a

^a These species showed shear rate dependence of $[\eta]$. The zero shear $[\eta]$ was not determined; it is estimated to be 10% higher than the value used.

TABLE IB
Wide Distribution Polystyrenes

Monsanto designation	\bar{M}_v (toluene, 25°C.)
RL 35 K3-3	210,000
Erinoid 2CL/HS	380,000

TABLE IIA
Commercial Polyisobutylenes

Enjay designation	\bar{M}_v^a
LMMH	50,000
L60	855,000
L80	1.13×10^6
L100	1.46×10^6
L120	1.75×10^6
L140	2.17×10^6

^a This is the average from values of $[\eta]$ determined for each species at 30°C. in toluene and cyclohexane.

TABLE IIB
Experimental Polyisobutylenes

Enjay designation	Minimum \bar{M}_v^a
L200	5×10^6
L250	6×10^6
L300	11×10^6 (Un- certain)

^a Determined from average values of $[\eta]$ obtained at 30°C. in both toluene and cyclohexane. Because of extreme shear rate dependence of values and variation in $[\eta]$ for each species according to manipulative procedure, these values are probably lower than true values.

2. Solvents

Reagent grades of solvents (toluene, benzene, cyclohexane, and decalin) from scaled new bottles were used without further purification.

3. Preparation of Solutions

For intrinsic viscosity determination in Ubbelohde viscometers, the initial polymer concentration was adjusted (by previous trials) to give a relative viscosity η_r less than 2.0. Polymer and solvent were allowed to stand together for 3 to 10 days, without agitation, before test.

For the high shear rate determinations on more concentrated solutions, the polymer and solvent were allowed to stand undisturbed in volumetric flasks for 48 hr., then gently mixed in an end-over-end motion, 15 times/min. The high viscosity and slow motion prevented degradation by turbulence.

4. Intrinsic Viscosity Determinations

The viscosity-average molecular weights of the polymers studied were determined, through the use of established correlations of the Mark-Houwink type, by intrinsic viscosity determinations. Ubbelohde dilution viscometers, were used for this purpose. These viscometers had a helical capillary of 25 cm. length, diameter 0.5 mm. with two bulbs permitting measurement at average wall shear stresses of 4.03, 4.73, and 5.65 dyne/

cm.². In all cases kinetic energy corrections were applied. The water bath temperature was controlled to $\pm 0.05^\circ\text{C}$. In all cases double plots of η_{sp}/c versus c and $\ln\eta_r/c$ versus c were made. Failure of these curves to coincide at zero c led to rejection of the run (usually due to contamination).

5. Determination of the Second Newtonian Viscosity

The second Newtonian viscosity of the polymer solutions was measured in a coaxial cylinder viscometer, the design of which is indicated schematically in Figure 2 and has been described in detail by Merrill.⁷ Relevant to this paper are the following details. Liquid under test (black) flows from syringe 6 through port 5 into a narrow (0.006 in.) open-ended annulus, upper end 7, lower end 8, defined by an air-floated, torque measuring stationary cylinder 3 and a rotating cylinder 1, both cylinders being temperature controlled by forced circulation of thermostatically controlled water through channels 9–13 in cylinder 1 and 14–18 in cylinder 3. In general, the circulating water was at 30°C .

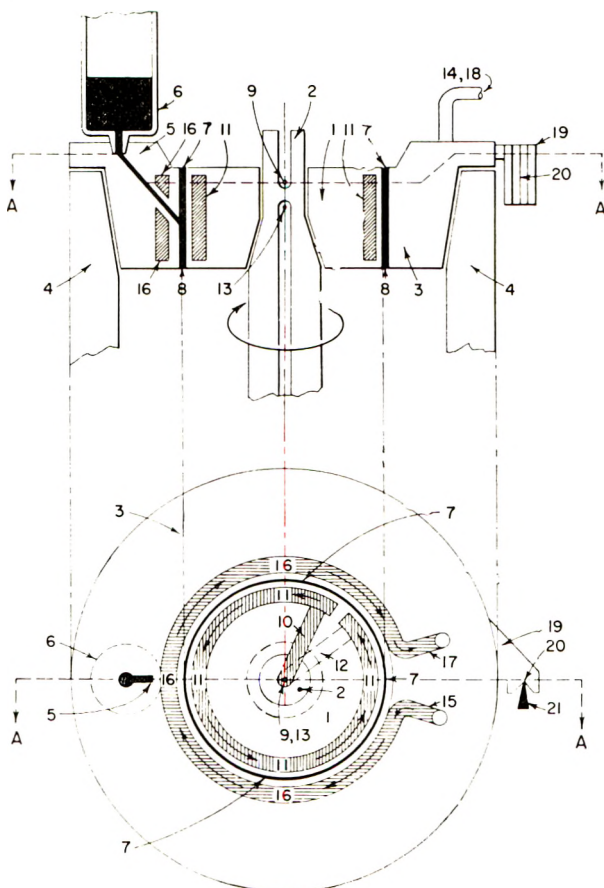


Fig. 2. Side and top elevations of coaxial cylinder viscometer.

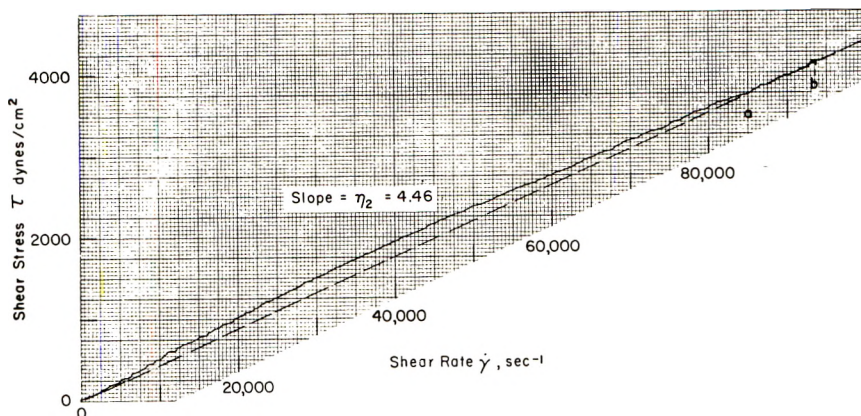


Fig. 3. An original recorder plot of shear stress vs. shear rate for polyisobutylene L80 in decalin at 30°C., conc. $c = 0.35$ g./dl. Second Newtonian viscosity η_2 , found in range ab , is 4.46 cpoise; solvent viscosity $\eta_s = 2.35$ cpoise; thus $(\eta_2 - \eta_s)/\eta_s c = 2.86$ dl./g.

The rotational speed of shaft 2 which carried cylinder 1 was programmed to increase and decrease linearly with time from 0 to 5000 to 0 in 60 sec. and was transduced to an X-Y recorder. The maximum rotational speed corresponded to a shear rate of 96,000 sec^{-1} . Torque on cylinder 3 was sensed by a strain cell and transduced to the other axis of the recorder. In practically all cases, testing of pure solvent in this device preceded testing of polymer solutions. The traces obtained from the recorder showed the linear shear stress versus shear rate relation of the solvent. In the case of solvents, the constant slope was the solvent viscosity η_s . With polymer solutions the second Newtonian viscosity was observed as the value of the slope of a straight segment extrapolating through 0,0. This is shown for a typical solution in an original X-Y recorder plot (Fig. 3). The slope of the dashed line is the second Newtonian viscosity η_2 . In this case, the second Newtonian regime was observed only over the short segment ab . Usually the second Newtonian regime was found at a shear rate exceeding 70,000 sec^{-1} . From the values of η_2 and η_s thus determined the second Newtonian viscosity number, $(\eta_2 - \eta_s)/\eta_s c$, was computed and studied as a function of polymer type, molecular weight, solvent, and polymer concentration. In general, temperature was held constant at 25 or 30°C.

RESULTS

In general, two distinctive types of polymer concentration dependence of the second Newtonian viscosity number were found, according to the molecular weight of the polymer.

Type A

In type A behavior, the second Newtonian viscosity number increased gradually with increase of concentration (but not nearly so steeply as the

increase of the ordinary viscosity number with concentration), and the value of the second Newtonian viscosity number, extrapolated to zero concentration, was very close to the standard intrinsic viscosity. For polymers of styrene and of isobutylene, type A behavior was found for all molecular weights less than approximately one million.

Type B

In type B behavior, the second Newtonian viscosity showed a more or less broad plateau of constancy over a range of concentrations that, according to usual intrinsic viscosity techniques, would be considered as rather high. In general this plateau value of the second Newtonian viscosity number did not correspond to the standard intrinsic viscosity.

Two subcategories of type B can be discerned, although as will be evident more data are needed.

Type B₁. The polymer, dissolved in a relatively poor solvent, shows a plateau value of $(\eta_2 - \eta_s)/\eta_s c$ considerably greater than the standard intrinsic viscosity $[\eta]$. As concentration is decreased below the lower limit of the plateau, the value of $(\eta_2 - \eta_s)/\eta_s c$ drops toward the value of $[\eta]$.

Type B₂. The polymer, dissolved in a good solvent, shows a plateau value of $(\eta_2 - \eta_s)/\eta_s c$ less than the standard intrinsic viscosity $[\eta]$. As concentration is decreased below the lower limit of the plateau, the value of $(\eta_2 - \eta_s)/\eta_s c$ rises toward the value of $[\eta]$.

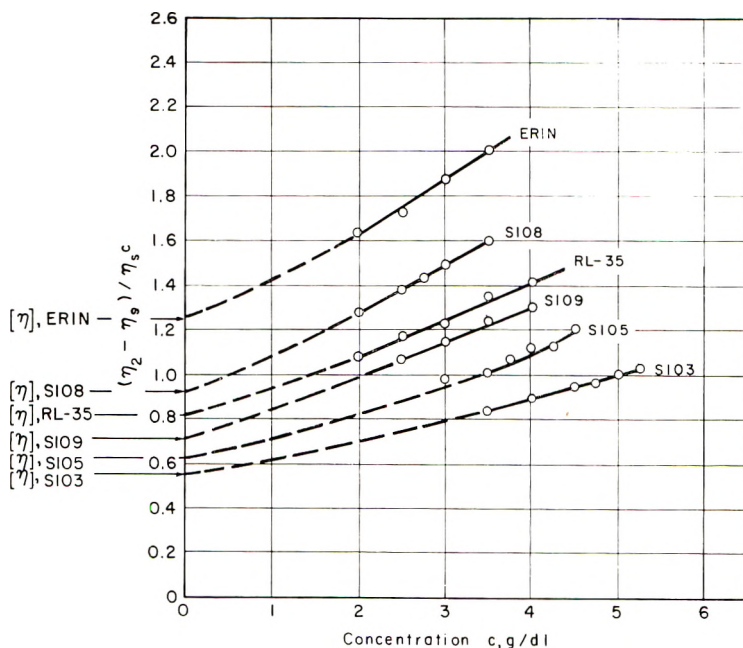


Fig. 4. Second Newtonian viscosity number $(\eta_2 - \eta_s)/\eta_s c$ vs. concentration c for polystyrenes in toluene at 30°C. Standard intrinsic viscosities $[\eta]$ (toluene, 30°C.) are indicated for each species in left margin.

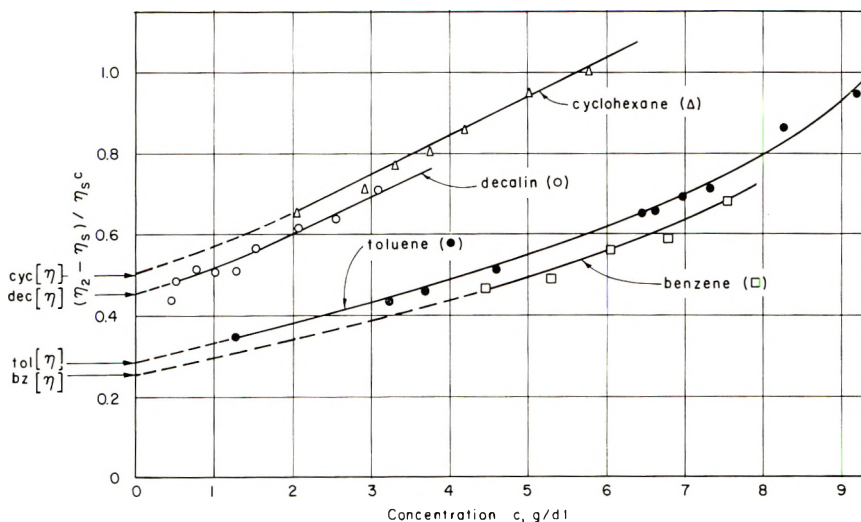


Fig. 5. Second Newtonian viscosity number $(\eta_2 - \eta_s)/\eta_s c$ vs. concentration c for polyisobutylene LMMH in cyclohexane, decalin, toluene, and benzene at 30°C. Standard intrinsic viscosities $[\eta]$ in respective solvents at 30°C. are indicated in left margin.

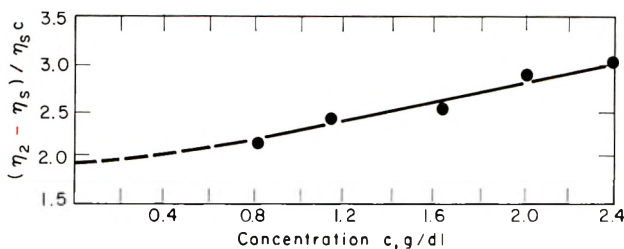


Fig. 6. Second Newtonian viscosity number $(\eta_2 - \eta_s)/\eta_s c$ vs. concentration c for polyisobutylene L60 in toluene, 30°C. Standard intrinsic viscosity $[\eta] = 1.93$.

For polymers of styrene and isobutylene, type B behavior was found above molecular weights of about 1×10^6 , and type B₂ was especially noted in three polyisobutylenes, the molecular weights of which exceeded 5×10^6 .

Illustrative of type A are the curves of $(\eta_2 - \eta_s)/\eta_s c$ for six polystyrene species, dissolved in toluene, shown in Figure 4, for a low molecular weight species of polyisobutylene LMMH in four different solvents, shown in Figure 5, and for a polyisobutylene of high molecular weight, L60, just short of Type B, dissolved in toluene, shown in Figure 6.

For comparison, the respective intrinsic viscosities obtained by Ubbelohde viscometer are shown on the ordinate, and it is clear that there is no significant difference between $[\eta]$ and the value of $(\eta_2 - \eta_s)/\eta_s c$ extrapolated to zero c . Admittedly there is no justification for extrapolating the curves (shown dashed) such that the curves intersect the ordinate at the respective values of $[\eta]$. On the other hand, extensions of the best straight lines through the data points intersect the ordinate at values not much less than the standard intrinsic viscosity. Onset of turbulence in the viscometer

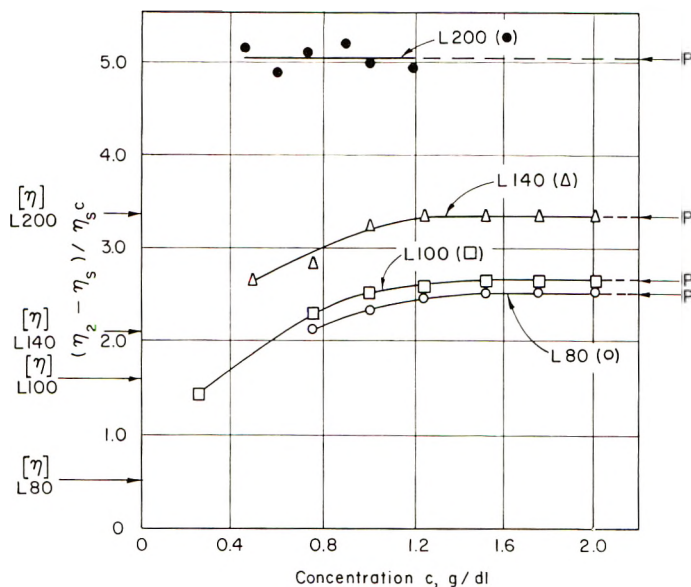


Fig. 7. Second Newtonian viscosity number vs. concentration for polyisobutylenes L80, L100, L140, and L200 in benzene at 30°C., with indication of standard intrinsic viscosities $[\eta]$ (benzene, 30°C.) on left margin, and plateau values P i.e., $\{(\eta_2 - \eta_s) / \eta_s c\}_p$, on right margin.

prevented obtaining data between zero concentration and the lowest value shown.

Typical of type B_1 behavior are the curves shown in Figure 7 for three species of polyisobutylene above 1×10^6 in molecular weight in benzene at 30°C., 24.5°C. being the theta temperature. It appears as if the values of $(\eta_2 - \eta_s) / \eta_s c$ were tending toward $[\eta]$ as concentration decreases below the limit of the plateau shown, but obviously from these data no definite conclusions can be drawn. Because of the onset of turbulence, discussed elsewhere,⁹ it was impossible to obtain data at lower values of c as would have been desired.

In contrast, the curves in Figure 8 for five species of polyisobutylene in decalin (a good solvent) show unmistakably type B_2 behavior, i.e., at concentrations below the lower limit of the plateau, the value of $(\eta_2 - \eta_s) / \eta_s c$ tends to rise toward the standard intrinsic viscosity $[\eta]$. This trend, slight for L80 and L140, becomes very strong for the higher molecular weight species L200, L250, and L300. Decalin solutions yielded more information than cyclohexane solutions because, owing to the high viscosity of decalin, it was possible to achieve greater dilutions before the onset of turbulence. However, cyclohexane solutions of L200, L250, and L300 showed unmistakably the same trend of substantial rise of $(\eta_2 - \eta_s) / \eta_s c$ as did the decalin solutions.

Figure 9 shows the well-defined plateau in the case of two high molecular weight polystyrene species S12 and S114. For S12, the value of $[\eta]$ is so

close to the plateau value of $(\eta_2 - \eta_s)/\eta_s c$ that no rise or fall toward $[\eta]$ would be expected. For S114, it seems likely that, if further dilution had been possible (elimination of turbulence) an upward trend of $(\eta_2 - \eta_s)/\eta_s c$ toward $[\eta]$ would have been found.

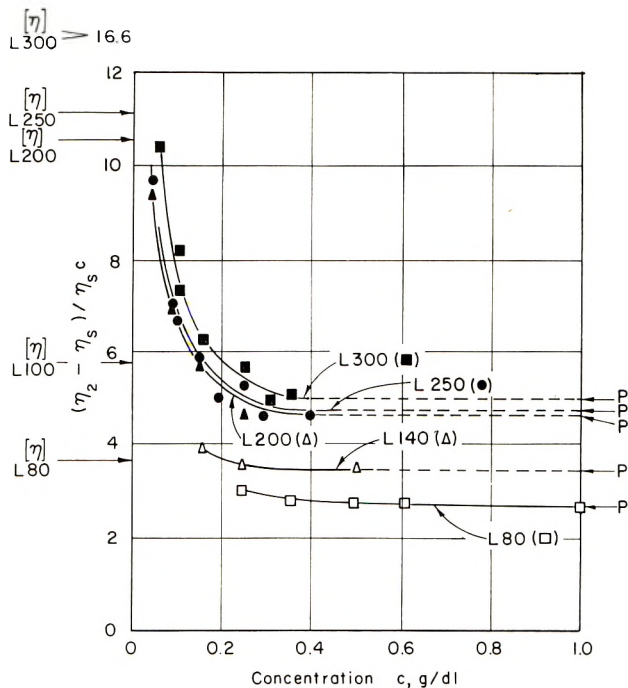


Fig. 8. Second Newtonian viscosity number vs. concentration for polyisobutylenes L80, L140, L200, L250, and L300 in decalin at 30°C., with indication of standard intrinsic viscosities $[\eta]$ (decalin, 30°C.) on left margin, and plateau values P , i.e., $\{(\eta_2 - \eta_s)/\eta_s c\}_p$, on right margin.

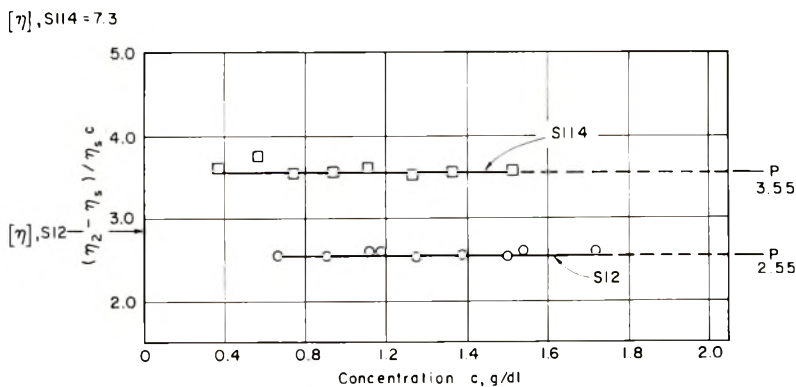


Fig. 9. Second Newtonian viscosity number vs. concentration for polystyrenes S12 and S114 in toluene at 30°C. with indications of standard intrinsic viscosities $[\eta]$ (toluene, 30°C.) on left margin and plateau values P , i.e., $\{(\eta_2 - \eta_s)/\eta_s c\}_p$, on right margin.

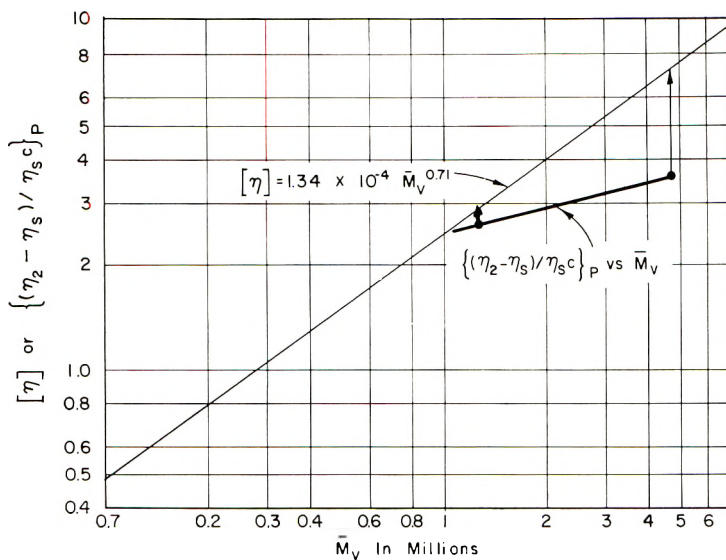


Fig. 10. Log-log plots of intrinsic viscosity $[\eta]$ vs. \bar{M}_v and of plateau value of second Newtonian viscosity number, $\{(\eta_2 - \eta_s)/\eta_s c\}_p$, vs. \bar{M}_v , for two polystyrenes in toluene. Arrows show $[\eta]$ in relation to $\{(\eta_2 - \eta_s)/\eta_s c\}_p$ for each species.

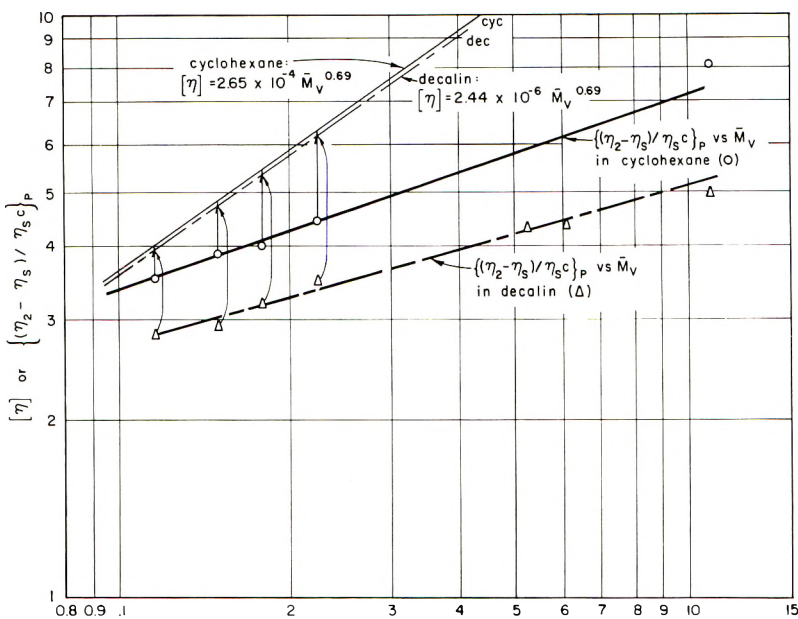


Fig. 11. Log-log plots of intrinsic viscosity $[\eta]$ vs. \bar{M}_v and of plateau values of second Newtonian viscosity number, $\{(\eta_2 - \eta_s)/\eta_s c\}_p$, vs. \bar{M}_v , for polyisobutylenes in cyclohexane and in decalin. Arrows show $[\eta]$ in relation to $\{(\eta_2 - \eta_s)/\eta_s c\}_p$ for each species. Abscissa is \bar{M}_v in millions.

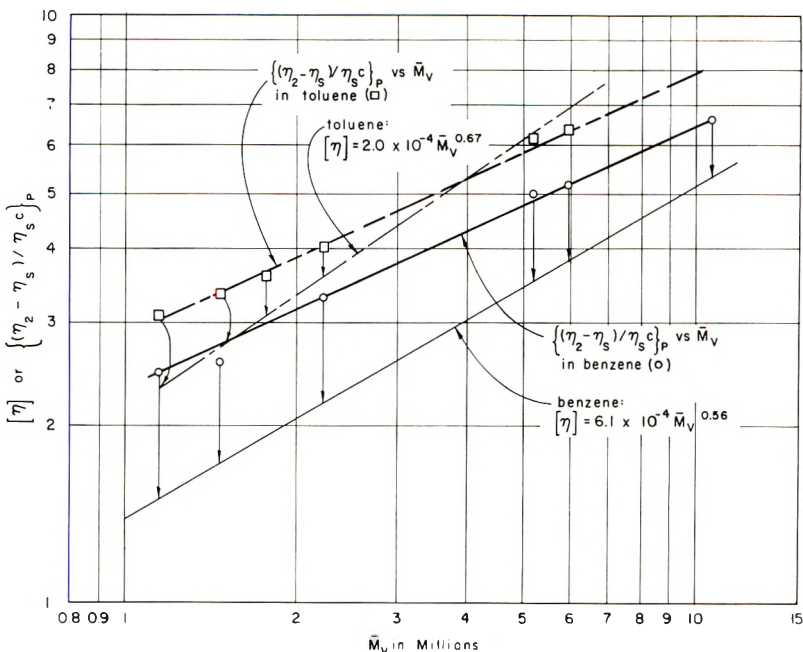


Fig. 12. Log-log plots of intrinsic viscosity $[\eta]$ vs. \bar{M}_v and of plateau values of second Newtonian viscosity number $\{(\eta_2 - \eta_s)/\eta_{sc}\}_p$ vs. \bar{M}_v for polyisobutylenes in benzene and in toluene. Arrows show $[\eta]$ in relation to $\{(\eta_2 - \eta_s)/\eta_{sc}\}_p$ for each species.

The general relationship of the *plateau value* $\{(\eta_2 - \eta_s)/\eta_{sc}\}_p$ to $[\eta]$ and to molecular weight for polystyrene in the “good” solvent toluene is shown in Figure 10. From Figure 10, the tentative conclusion is made that, above molecular weight of 1×10^6 , $[\eta]$ lies above the plateau value $\{(\eta_2 - \eta_s)/\eta_{sc}\}_p$, based on only one point (S114). Figure 11 presents the same kind of information for polyisobutylenes in two “good” solvents (cyclohexane and decalin). In this case, there seems to be no question that $[\eta]$ exceeds $\{(\eta_2 - \eta_s)/\eta_{sc}\}_p$ and that the logarithm of the latter increases linearly with $\log \bar{M}_v$. In contrast, Figure 12 shows that with the mediocre solvent for polyisobutylene, toluene, the plateau value $\{(\eta_2 - \eta_s)/\eta_{sc}\}_p$ exceeds $[\eta]$ up to 4×10^6 molecular weight, where the lines cross, and for the “poor” solvent benzene, the plateau value $\{(\eta_2 - \eta_s)/\eta_{sc}\}_p$ is greater than $[\eta]$ over the range of molecular weights studied (up to 11×10^6).

From Figures 10, 11, and 12, it is easily possible to establish (as the slopes on the log-log plots) the values of b in an empirical equation that reads:

$$\{(\eta_2 - \eta_s)/\eta_{sc}\}_p = K'' \bar{M}_v^b$$

which is written in analogy to the Mark-Houwink equation:

$$[\eta] = K' \bar{M}_v^a$$

Table I summarizes values of b and a for the systems studied.

TABLE I

Polymer	Solvent	Temp., °C.	<i>a</i>	<i>b</i>	<i>a</i> + <i>b</i>
Polystyrene	Toluene	25	0.71	0.25	0.96
Polyisobutylene	Cyclohexane	30	0.69	0.33	1.02
	Decalin	30	0.69	0.28	0.97
	Toluene	30	0.67	0.45	1.12
	Benzene	30	0.56	0.45	1.01

After taking into account the difficulties of the experimental determination of η_2 and scatter in the data, there remains a trend such that the sum of the exponents $a + b$ is near unity.

DISCUSSION

Without further study of macromolecules in fields of high shear rate it is mere speculation to propose a physical model for the data. The original proposal of Merrill,³ viz., that the molecules were hydrodynamically independent, seems difficult to reconcile with these observations of $\{(\eta_2 - \eta_s)/\eta_s c\}_p$ attended by increase or decrease of the second Newtonian viscosity below a certain concentration defining one limit of the plateau. One could hypothesize that in the plateau regimes of the second Newtonian viscosity number, as a consequence of high rotational speeds, the macromolecular coils somehow are distorted in a progressive manner as more macromolecules are added so as to maintain individually the same hydrodynamic resistance and also so as to maintain freedom from entanglement with neighbors.

In any case, there appears to be a trend of the second Newtonian viscosity number to approach under all conditions the standard intrinsic viscosity as concentration is decreased. By the use of more viscous solvents to postpone onset of turbulence, it is expected that the relation between $\lim_{c \rightarrow 0} (\eta_2 - \eta_s)/\eta_s c$ and $[\eta]$ will be definitely established.

The generous financial support of the Film Department of E. I. du Pont de Nemours and Company is gratefully acknowledged, as well as the cooperation of the Dow Chemical Company, Monsanto Chemical Company, and Enjay Company in furnishing valuable experimental samples.

References

- Ostwald, Wo., *Kolloid-Z.*, **36**, 99 (1925); Wo. Ostwald and P. Auerbach, *Kolloid-Z.*, **38**, 261 (1926).
- Philippoff, W., and K. Hess, *Z. physik. Chem.*, **B31**, 237 (1936); W. Philippoff, F. H. Gaskins, and J. G. Brodnyan, *Trans. Soc. Rheology*, **1**, 109 (1957).
- Merrill, E. W., *J. Polymer Sci.*, **38**, 539 (1959).
- Brodnyan, J. G., and E. L. Kelley, *Trans. Soc. Rheology*, **5**, 205 (1961).
- Claesson, S., and U. Lohmander, *Makromol. Chem.*, **44-46**, 461 (1961).
- Passaglia, E., J. T. Yang, and N. J. Wegemer, *J. Polymer Sci.*, **47**, 333 (1960).
- Merrill, E. W., Proceedings of the ASTM Symposium on Non-Newtonian Viscometry, Washington, D.C., October 1960.

8. Merrill, E. W., H. S. Mickley, A. Ram, and G. Perkinson, *Trans. Soc. Rheology*, **5**, 237 (1961).
9. Merrill, E. W., H. S. Mickley, and A. Ram, *J. Fluid Mechanics*, **13**, 86 (1962).

Résumé

On détermine le viscosité seconde de Newton η_2 , de solutions de polystyrène et de polyisobutylène dans un viscosimètre cylindrique coaxial, à une vitesse absolue d'environ 10^5 sec^{-1} . On détermina l'indice viscosimétrique $(\eta_2 - \eta_s)/\eta_s c$ (où η_s = la viscosité du solvant, c = la concentration du solvant, g/dl) en fonction de la concentration. Pour les polymères qui ont un poids moléculaire moyen viscosimétrique de moins de 1×10^6 , la $\lim_{c \rightarrow 0} (\eta_2 - \eta_s)/\eta_s c$ est généralement identique à la viscosité intrinsèque (η) . Au delà de $\bar{M}_v \simeq 1 \times 10^6$ on trouve un plateau de $(\eta_2 - \eta_s)/\eta_s c$ de valeur constante en mettant cette valeur en fonction de c . Pour de bons solvants la valeur du plateau $\{(\eta_2 - \eta_s)/\eta_s c\}_p$ est inférieur à $[\eta]$, mais pour des solvants pauvres (aux environs de la température θ) le contraire est vrai. La relation des valeurs du plateau par rapport à \bar{M}_v , peut être établie par l'équation de Mark-Houwink: $[\eta] = K' \bar{M}_v^a$, en écrivant $\{(\eta_2 - \eta_s)/\eta_s c\}_p = K'' \bar{M}_v^b$. La somme de $a + b$ de toute substance dans deux solvants donnés est approximativement égale à l'unité. Bien qu'une conclusion formelle ne puisse être tirée de ces résultats, il est clair que même au delà de $\bar{M}_v \simeq 1 \times 10^6$, le second nombre de viscosités de Newton tend vers $[\eta]$ quand c s'approche à zéro.

Zusammenfassung

Die zweite Newtonsche Viskosität η_2 von Polystyrol- und Polyisobutylendösungen wurde in einem Koaxial-Zylinder-Viskosimeter bei Schergeschwindigkeiten in der Nähe von 10^5 sec^{-1} bestimmt. Die zweiten Newtonschen Viskositätszahlen $(\eta_2 - \eta_s)/\eta_s c$ (wo η_s = Viskosität des Lösungsmittels, c = Polymerkonzentration in g/dl) wurden in Abhängigkeit von der Konzentration bestimmt. Bei Polymeren mit einem Viskositätsmittelwert des Molekulargewichts kleiner als 1×10^6 scheint $\lim_{c \rightarrow 0} (\eta_2 - \eta_s)/\eta_s c$ praktisch mit der Viskositätszahl $[\eta]$ identisch zu sein. Oberhalb $\bar{M}_v \simeq 1 \times 10^6$ ergibt sich beim Auftragen von $(\eta_2 - \eta_s)/\eta_s c$ gegen c ein Plateau mit konstantem $(\eta_2 - \eta_s)/\eta_s c$. Bei guten Lösungsmitteln liegt der Plateauwert: $\{(\eta_2 - \eta_s)/\eta_s c\}_p$ unterhalb $[\eta]$, bei schlechten Lösungsmitteln (in der Nähe der Θ -Temperatur) ist aber das Gegenteil der Fall. Eine Korrelation der Plateauwerte zu \bar{M}_v kann nach Art der Mark-Houwinkgleichung: $[\eta] = K' \bar{M}_v^a$ in der Form $\{(\eta_2 - \eta_s)/\eta_s c\}_p = K'' \bar{M}_v^b$ erfolgen. Die Summe von $a + b$ für ein beliebiges Polymeres in zwei gegebenen Lösungsmitteln ist angenähert gleich eins. Obgleich noch zuwenig Daten vorliegen, scheint doch auch oberhalb $\bar{M}_v \simeq 1 \times 10^6$ die zweite Newtonsche Viskositätszahl sich bei $c \rightarrow 0$ dem Wert von $[\eta]$ zu nähern.

Received January 25, 1962

On the Ultraviolet Absorption Spectrum of Polyvinyl Alcohol

HOWARD C. HAAS, HELEN HUSEK, and LLOYD D. TAYLOR,
Research Division, Polaroid Corporation, Cambridge, Massachusetts

Synopsis

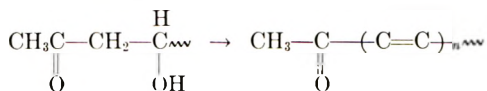
A study of the ultraviolet absorption spectrum of polyvinyl alcohol (PVA) was made. Spectral examination of the solvolysis products of vinyl acetate and 1-methoxyvinyl ester copolymers shows unequivocally that the absorption bands in PVA at 225, 280, and 330 $m\mu$ are related to carbonyl-containing structures. The high intensities of these bands in the solvolyzed copolymers is additional evidence that the absorbing groups

O
||

cannot be unconjugated carbonyl and are probably of the type $-(C=C)_n-C-$. Ultraviolet dichroism measurements tend to confirm this view. The ultraviolet absorbing bands in PVA arise predominantly from two sources: the presence of acetaldehyde, and dissolved air in the vinyl acetate monomer during polymerization. In the case of the latter, the formation of the vinyl acetate-oxygen copolymer and its subsequent decomposition to aldehydic-type products introduce, into the polymer, chain structures similar to those introduced by acetaldehyde. By the careful exclusion of acetaldehyde and air during vinyl acetate polymerization and by a judicious choice of initiator, PVAs having minimal ultraviolet absorptions can be prepared. Treatment of PVA at room temperature with dilute aqueous alkali results in a marked diminution in the intensities of all three absorption bands. Hot dilute acid, while essentially removing the 330 $m\mu$ band, produces no consistent change in the relative intensities of the 225 and 280 $m\mu$ bands.

Various investigators have studied the ultraviolet absorption spectra and the dilute solution viscosity behavior of polyvinyl alcohols (PVA) in attempts to interpret the absorption bands present in the 200-400 $m\mu$ region. In early studies, Marvel and Inskeep¹ suggested that the erratic viscosity behavior of aqueous PVA solutions could be accounted for by a terminal aldehyde group. Clarke and Blout,² however, concluded that the carbonyl was largely ketonic and that α,β -unsaturated ketone residues were responsible for the absorption band at 225 $m\mu$, and β -hydroxy ketone structures for the 280 $m\mu$ band. Takayama³ found that the 280 $m\mu$ band was proportional to the carbonyl content of the PVA when the latter was controlled by the quantity of acetaldehyde present during vinyl acetate polymerization. Similar behavior was observed by Matsumoto et al.,⁴ except that absorption at 280 $m\mu$ was much too high for the quantities of acetaldehyde employed. In this connection, Yamaguchi et al.⁵ insist that the absorption bands at 225, 280, and 330 $m\mu$ should be assigned

to $\text{-(C=C)}_n\overset{\text{O}}{\parallel}\text{C-}$ where $n = 1, 2,$ and 3 respectively. During their studies, Matsumoto and coworkers prepared PVA from polyvinyl acetate (PVAC) which was chain-transferred with acetone and acetaldehyde; they showed that there is no necessary relationship between carbonyl content and absorption at $280\text{ m}\mu$, that the molar absorption coefficient of the $280\text{ m}\mu$ band is much too high for unconjugated carbonyl, and that the more strenuous the hydrolytic conditions employed for hydrolyzing the PVAC, the higher the $280\text{ m}\mu$ absorption, although the carbonyl content remains constant. Their researches imply that the absorbing groups are mainly at the ends of PVA chains and arise from an acetaldehyde chain transfer reaction and dehydration of the resulting terminal β -hydroxy ketone structure.



More recently Lloyd⁶ demonstrated by selective reduction of PVA with the use of Raney nickel and hydrogen and sodium borohydride that the groups responsible for the 280 and $330\text{ m}\mu$ bands must contain both carbonyl and ethylenic unsaturation and also that some unconjugated carbonyl groups are present whose absorption at $280\text{ m}\mu$ is masked by the higher extinction

$\text{-(C=C)}_2\overset{\text{O}}{\parallel}\text{C-}$ groups.

We have made a few observations in this field which we report below. Our results are in general accord with the more recent interpretations.

Experimental

Preparation of PVA

In an initial exploratory series of experiments, several PVAC were prepared under a variety of conditions for the purpose of studying the effects on the ultraviolet absorption spectra of the resulting PVA. Highly purified vinyl acetate monomer, free of acetaldehyde, was employed. PVAC polymers were prepared by bulk and emulsion polymerization in glass tubes sealed under vacuum. The polymers were purified by several reprecipitations from ethanol into water, were dried, and were converted to PVA by being dissolved in methanol, adding a catalytic amount of sodium methoxide, and heating the solutions for 20 min. at about 60°C . The PVA was reprecipitated from water into methanol, washed with methanol, and dried at 40°C . under vacuum. Ultraviolet absorption spectra ($200\text{--}400\text{ m}\mu$) were obtained for molar aqueous solutions (0.44 g. PVA per 10 cc.) by using a Cary Model 14 spectrophotometer the optical system of which was flushed with nitrogen. The details of the polymerizations are given in Table I. Since the spectra in the $200\text{--}400$ region are determined to

TABLE I
Vinyl Acetate Polymerizations

Expt. no.	Polymerization	Catalyst	Temp., °C.	U.V. spectra (PVA), $m\mu$		
				225	280	330
1	Bulk	0.1% benzoyl peroxide	60	0.15	0.03	0.0
2	"	0.3% benzoyl peroxide	60	0.51	0.09	0.01
3	"	0.1% AIBN ^a	60	0.02	0.02	0.0
4	"	G.E. AH-4 lamp	~40	0.03	0.02	0.01
5	Emulsion	H ₂ O, 100 cc.	53	0.04	0.03	0.02
		K ₂ S ₂ O ₈ , 0.05 g. Monomer, 50 g. Dupanol C, 1 g. ^b				

^a Azobisisobutyronitrile.

^b Sodium lauryl sulfate (Du Pont).

some extent by absorption below 200 $m\mu$ and also complicated by some scattered light, smooth curves were drawn over the investigated spectral range and deviations from these curves at 225, 280, and 330 $m\mu$ were noted in optical density units. These numbers are included in Table I as a measure of the absorption at these wavelengths. A typical ultraviolet absorption spectrum is reproduced in Figure 1.

Oxygen and Acetaldehyde Experiments

Many vinyl acetate polymerizations were carried out in the presence of acetaldehyde. Typically, a tube containing 97% monomer, 3% acetaldehyde, and 0.1% AIBN was sealed under vacuum and polymerized at 60°C. The polymers were purified by several reprecipitations from benzene into hexane, dried, and solvolyzed to PVA as before. The three usual

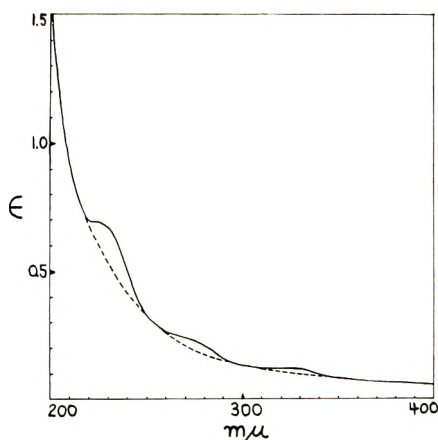


Fig. 1. Typical ultraviolet absorption spectrum (solid line) of an aqueous PVA solution.

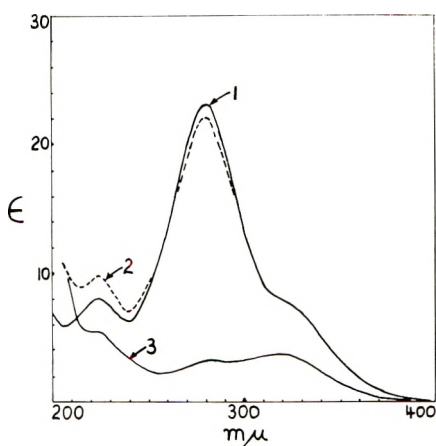


Fig. 2A. Ultraviolet absorption spectra of (1) an aqueous solution of PVA from an acetaldehyde chain-transferred polyvinyl acetate, (2) the same PVA in 0.02% aqueous sodium hydroxide, and (3) the same as (2) after 10 days at room temperature.

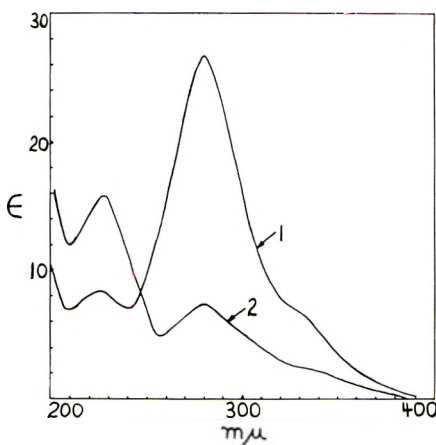


Fig. 2B. Ultraviolet absorption spectra of (1) an aqueous solution of PVA from an acetaldehyde chain-transferred polyvinyl acetate, and (2) the same PVA in 0.02*N* aqueous HCl after heating of the acidic solution for 18 hrs. at 95°C.

absorption bands are always found in high intensity but their relative intensities vary from experiment to experiment. These variations probably depend on the degree of conversion of vinyl acetate to polymer and on small differences in the conditions for solvolysis. In Figure 2A the spectrum of an aqueous solution of a chain-transferred PVA is presented and spectra of the same PVA in 0.02% aqueous sodium hydroxide, taken immediately and after 10 days' standing at room temperature. In Figure 2B the effect of heating a different chain-transferred PVA in 0.02*N* aqueous HCl for 18 hrs. is illustrated.

Oxygen runs were made by saturating pure vinyl acetate monomer containing either 0.1% benzoyl peroxide or AIBN with dry oxygen, by sealing

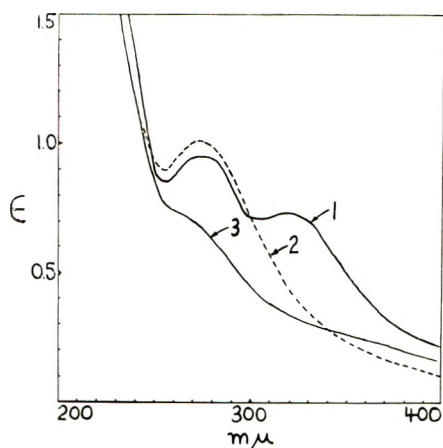


Fig. 3. Ultraviolet absorption spectra of (1) an aqueous solution of PVA from a polyvinyl acetate polymerized under oxygen, (2) the same PVA in 0.02*N* HCl after heating overnight at 95°C., and (3) the same PVA in 0.02% aqueous NaOH after the solution was allowed to stand 10 days at room temperature.

off the tubes, and polymerizing at 60°C. Several runs contained no catalyst, and polymerization was initiated with a General Electric AH-4 ultraviolet source. The PVACs were purified and solvolysed as before. Regardless of the initiating technique, the ultraviolet absorption spectra again showed strong absorption at 225, 280, and 330 $m\mu$, the relative band intensities varying with the experiment. In Figure 3 the spectrum of an aqueous PVA solution prepared from a benzoyl peroxide-initiated oxygen polymerization is reproduced, and the effects of dilute alkali at room temperature and dilute HCl at 95°C. are included. A PVA obtained from a similar PVAC (benzoyl peroxide-initiated, saturated with oxygen) by methanol-HCl solvolysis shows strong absorption at 225 and 280 $m\mu$, but the 330 band is absent.

Copolymerization Experiments

The recent synthesis⁷ of the 1-methoxyvinyl esters should allow the direct introduction of carbonyl groups into the PVA backbone by copolymerization with vinyl acetate. Copolymerization of two such vinyl esters, 1-methoxyvinyl acetate and the 1-methoxyvinyl trifluoroacetate, with vinyl

TABLE II
Copolymerization of Vinyl Acetate with 1-Methoxy Vinyl Acetates

Vinyl acetate, g.	1-Methoxy monomer, g.	Conversion, %	Analyses, ^a %	
			C	H
9.82	0.75 (trifluoroacetate)	~30	53.7	6.5
8.37	0.93 (acetate)	33	55.5	7.0
Polyvinyl acetate			55.8	7.0

^a See Ref. 8.

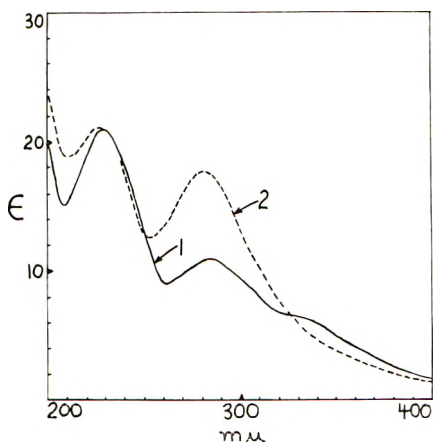


Fig. 4. Ultraviolet absorption spectra of (1) an aqueous solution of the polymer from the alkaline solvolysis of a vinyl acetate-1-methoxy vinyl acetate copolymer, and (2) the same polymer in 0.02*N* HCl after heating overnight at 95°C.

acetate was carried out at 60°C. under vacuum with 0.3% AIBN. The copolymers were purified and the PVAs obtained, as before, by NaOCH₃ solvolysis in methanol. Relevant information is given in Table II.

In Figure 4 the ultraviolet absorption spectrum of the PVA from the 1-methoxyvinyl acetate copolymer and the changes observed upon heating overnight in dilute HCl are given.

Random Oxidation of PVA

A commercial PVA (Du Pont Elvanol 72-60), 2.2 g. in H₂O, was treated with 8.9 g. of *N*-bromosuccinimide and 3.95 g. of pyridine and heated 2 hrs. at 60°C., after the procedure of Saigusa and Oda⁹ for introducing carbonyl groups into PVA. A considerable amount of insoluble product was produced but the soluble portion which was isolated showed very strong absorption at 225 and 280 mμ.

Ultraviolet Dichroism Measurements

The ultraviolet dichroism of oriented PVAs obtained from PVACs prepared in the presence of oxygen and acetaldehyde was studied. Films of these PVAs were cast on glass from water, allowed to dry in air and then stretched about five times their original length over a hot plate. Final stretched film thicknesses were 1.5–2.0 mils. The measurements were made by adapting a Model 11 Cary spectrophotometer to hold a Glan Foucault prism and compensating for the prisms' absorption over the spectral range being used. The oriented films were mounted on a rotatable holder which permitted the precise setting of the stretch direction to be either parallel or perpendicular to the electric vector of the plane-polarized light. A typical set of $d_{||}$ and d_{\perp} curves illustrating the dichroic nature of the ultraviolet absorption bands are reproduced in Figure 5.

Comparison of Du Pont Elvanols 72-60 and 70-05

The ultraviolet absorption spectra of molar solutions of Du Pont Elvanols 72-60 and 70-05 (the same lots used in a previous study¹⁰) in

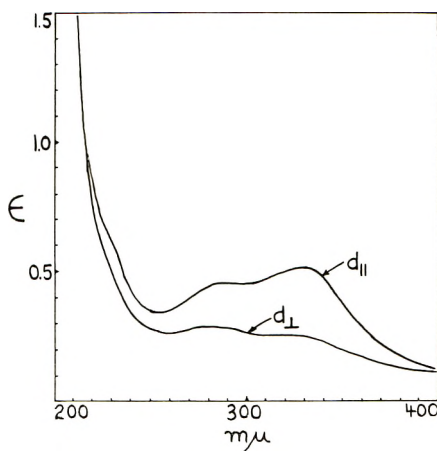


Fig. 5. Polarized ultraviolet absorption spectra of an oriented PVA film with the electric vector direction at 0° (d_{\parallel}) and at 90° (d_{\perp}) to the stretch direction.

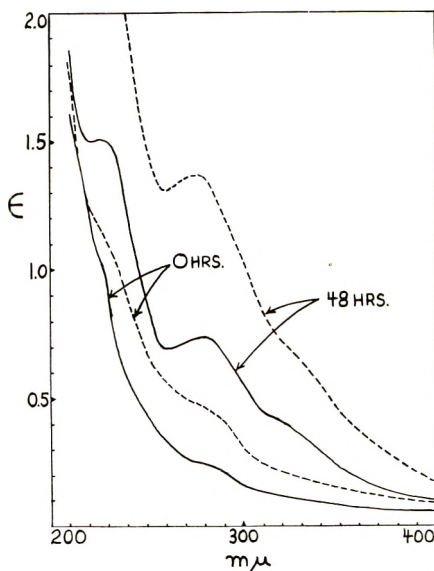


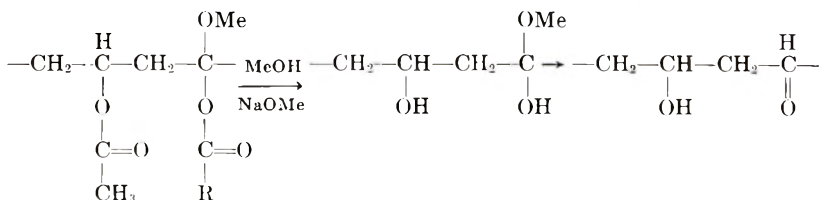
Fig. 6. Ultraviolet absorption spectra of (—) Du Pont Elvanols 72-60 and (---) 70-05 in 0.02*N* aqueous HCl, taken immediately, and after 48 hrs. of heating at 95°C .

0.02*N* HCl were obtained and then the solutions were heated at 95°C . and the spectra taken periodically over a 48-hr. period. The results are presented in Figure 6.

Discussion

From our exploratory vinyl acetate polymerizations it is obvious that the PVAs obtained do contain the three reported ultraviolet absorption bands at about 225, 280, and 330 $m\mu$. The intensity of these bands varies with the polymerization method, although when pure vinyl acetate monomer is employed and the polymerizations are carried out in the absence of oxygen in no instance is the intensity of these bands excessively high. Benzoyl peroxide-initiated vinyl acetate polymerizations (Table I) lead to PVAs having more ultraviolet absorption than the PVAs obtained by the other methods.

Although the varied evidence that these ultraviolet absorption bands are the result of carbonyl and related types of structures is fairly convincing, we thought it would be desirable unequivocally to introduce carbonyl groups into the backbone of the PVA molecule and then inspect the ultraviolet absorption spectra. The copolymerization of the 1-methoxyvinyl esters with vinyl acetate appeared to be a particularly suitable means of accomplishing this. The presence of an acetate group on the double bond should improve the copolymerizability of the 1-methoxyvinyl esters over that of the vinyl ethers and, in addition, on hydrolysis the instability of the hemiacetal structure should readily induce carbonyl formation.



Since PVAs obtained from PVACs which were carefully polymerized with AIBN in the absence of air showed very little absorption in the 200–400 $m\mu$ region (Table I), these conditions were selected for the preparation of the vinyl acetate–1-methoxyvinyl ester copolymers (Table II). Any major ultraviolet absorption should then result from the copolymer structure. We believe that the ultraviolet absorption spectra of the PVAs from these copolymers prove that all these absorption bands are related to carbonyl-type structures. In the spectrum of the PVA from the 1-methoxyvinyl acetate copolymer (Fig. 4), the three normal bands at 225, 280, and 330 $m\mu$ are evident and strong. The positions of the bands in the PVA from the fluorocopolymer are somewhat shifted, but this may have resulted from different relative intensities and band overlap. After treatment with dilute HCl, the normal band positions are observed. Furthermore, the 280 $m\mu$ bands in these spectra cannot result from unconjugated carbonyl groups. Employing a molar extinction coefficient of 63 for unconjugated carbonyl,² the PVA from the 1-methoxyvinyl acetate copolymer should contain 17.6 mole-% of $-\text{CH}_2-\text{C}-$ residues, and this would re-



quire a carbon analysis for the original copolymer of 55.0% versus the observed 55.5%. Also, the 1-methoxyvinyl acetate, because of a higher double-bond electron density, would be expected to enter the copolymer chain at a lower rate than vinyl acetate. In the case of the PVA from the fluorocopolymer, the intensity of the 280 $m\mu$ band is so high that it completely discounts the possibility that this band can be associated with unconjugated carbonyl absorption. Neither of these 1-methoxy monomers homopolymerizes by a radical mechanism, so that the presence of 1,3-diketone structures in the resulting PVAs is very improbable. Incidentally, the 1-methoxyvinyl trifluoroacetate enters the copolymer faster than the 1-methoxyvinyl acetate, probably because of a more positive double-bond character.

Additional evidence that the 280 $m\mu$ band is not due primarily to unconjugated carbonyl absorption and also that unsaturation is probably associated with the carbonyl function is found in the ultraviolet dichroism measurements of Figure 5. Although it is difficult to make dichroism measurements of PVAs with limited ultraviolet absorption, PVAs from PVACs prepared in the presence of acetaldehyde or oxygen show parallel dichroism for all three bands; i.e., absorption of light is greater when the electric vector of the plane-polarized light is parallel with the direction of stretch of the film. This would not be true for unconjugated carbonyl whose C=O double bond would be perpendicular to the chain direction, but it could well be true for the $=(C=C)_n-C-$ series postulated as being



responsible for these absorption bands. Since random oxidation of PVA leads to a large increase in the intensity of the 280 $m\mu$ band (as well as the 225 $m\mu$ band) and the copolymer PVAs show strong 280 $m\mu$ absorption, it seems that even when carbonyl groups are interjected into the middle of a PVA chain the preferred structure, after the formation of the first carbonyl-

conjugated double bond, is $(-C=C-)_2C-\begin{array}{c} \text{O} \\ \parallel \end{array}$ and not $-C=C-C-\begin{array}{c} \text{O} \\ \parallel \end{array}-C=C-$. Cross-conjugated systems, as in phorone, generally absorb at about 265 $m\mu$.

The presence of acetaldehyde during vinyl acetate polymerization leads to the three absorption bands (Fig. 2A), as does the presence of oxygen (Fig. 3). In the case of the latter, the effect probably results from the formation of the vinyl acetate-oxygen copolymer¹¹ and its subsequent decomposition yielding aldehydic types of material¹² which then act as chain transfer agents, much as acetaldehyde, leading to the terminal types of carbonyl structures.

It is pretty certain, however, that while the presence of acetaldehyde and air during vinyl acetate polymerization may account for most of the ultraviolet absorption of PVAs, structures of this type are present in PVA in places other than at the chain ends. Clarke and Blout² reported decreases in the viscosities of PVA solutions in dilute aqueous alkali and postulated

The authors wish to thank Mr. Albert S. Makas for his help in making the ultraviolet dichroism measurements.

References

1. Marvel, C. S., and G. E. Inskip, *J. Am. Chem. Soc.*, **65**, 1710 (1943).
2. Clarke, J. T., and E. R. Blout, *J. Polymer Sci.*, **1**, 419 (1946).
3. Takayama, G., *J. Chem. Soc. Japan, Ind. Chem. Sect.*, **59**, 1432 (1956).
4. Matsumoto, M., K. Imai, and Y. Kazusa, *J. Polymer Sci.*, **28**, 426 (1958).
5. Yamaguchi, K., M. Amagasa, S. Kinumaki, and T. Takahashi, paper presented at the Annual Meeting of High Polymer Chemistry, Tokyo, June 1-2, 1956.
6. Lloyd, D. G., *J. Appl. Polymer Sci.*, **1**, 70 (1959).
7. Wasserman, H. H., and P. S. Wharton, *J. Am. Chem. Soc.*, **82**, 661 (1960).
8. Analysis by C. Fitz, Needham Heights, Mass., and S. M. Nagy, MIT.
9. Saigusa, T., and R. Oda, *J. Chem. Soc. (Japan), Ind. Chem. Sect.*, **57**, 950 (1954).
10. Haas, H. C., and A. S. Makas, *J. Polymer Sci.*, **46**, 524 (1960).
11. Baines, C. E., R. M. Eloffson, and G. D. Jones, *J. Am. Chem. Soc.*, **72**, 210 (1950).
12. Stern, D., and G. V. Schulz, *Makromol. Chem.*, **38**, 248 (1960).
13. Clarke, J. T., R. O. Howard, and W. H. Stockmayer, *Makromol. Chem.*, **44-46**, 427 (1961).
14. Matsumoto, M., and K. Imai, *J. Polymer Sci.*, **24**, 125 (1957).

Résumé

On a fait une étude des spectres d'absorption ultraviolette du PVOAc. L'examen spectral des produits de solvolysé des copolymères acétate de vinyle/ester-1-méthoxy-vinyle montre de manière univoque que les bandes d'absorption du PVOAc à 225, 280 et 330 $m\mu$ sont en relation avec les structures contenant les carbonyles. Les intensités élevées de ces bandes dans les copolymères solvolysés sont une évidence supplémentaire que les groupes absorbants ne peuvent être des carboxyles non conjugués et



sont probablement du type $\text{---}(\text{C}=\text{C})_n\text{---C---}$. Des mesures de dichroïsme ultra-violet tendent à confirmer cette vue. Les bandes d'absorption ultra-violettes dans le PVOAc proviennent de façon prédominante de deux sources, la présence d'acétaldéhyde ou la dissolution d'air dans le monomère, acétate de vinyle, au cours de la polymérisation. Dans le dernier cas, la formation du copolymère acétate de vinyle/oxygène et sa décomposition subséquente en produits de type aldéhydique introduisant dans la chaîne de polymère des structures similaires à celles introduites par l'acétaldéhyde. On a préparé du PVOAc ayant un minimum d'absorption ultraviolette par l'exclusion soignée d'acétaldéhyde et d'air au cours de la polymérisation de l'acétate de vinyle et par un choix judicieux d'initiateur. Le traitement du PVOAc à basse température par de l'alcali dilué en solution aqueuse conduit à une diminution marquée des intensités de chacune des trois bandes d'absorption. L'acide dilué chaud, quoique supprimant essentiellement la bande de 330 $m\mu$ ne produit aucun changement important dans les intensités relatives des bandes de 225 et 280 $m\mu$.

Zusammenfassung

Das Ultravioletabsorptionsspektrum von PVA wurde untersucht. Die Untersuchung der Spektren der Solvolysprodukte von Vinylacetat-1-Methoxyvinylester-copolymeren zeigt eindeutig, dass die Absorptionsbanden im PVA bei 225, 280 und 330 $m\mu$ zu Carbonylgruppen enthaltenden Strukturen zugeordnet sind. Die hohe Intensität dieser Banden in den solvolysierten Copolymeren zeigt zusätzlich, dass die absorbierenden Gruppen nicht unkonjugierte Carbonylgruppen sein können und wahrscheinlich

von folgendem, kürzlich vorgeschlagenem Typ sind: $-(C=C)_n-\overset{\text{O}}{\parallel}{C}-$. Messungen des Ultraviolett-dichroismus bestätigen diese Ansicht. Die Ultraviolettabsorptionsbanden von PVA sind vorwiegend auf zwei Ursachen zurückzuführen, nämlich die Gegenwart von Acetaldehyd oder gelöster Luft im monomeren Vinylacetat während der Polymerisation. Im letzteren Fall führt die Bildung der Vinylacetat-Sauerstoff-Copolymeren und ihre darauffolgende Zersetzung zu aldehydartigen Produkten in die Polymerkette Strukturen ein, die den durch Acetaldehyd gebildeten ähnlich sind. Durch sorgfältigen Ausschluss von Acetaldehyd und Luft während der Vinylacetat-polymerisation und durch eine geeignete Wahl des Starters kann man PVA mit einer minimalen Ultraviolettabsorption herstellen. Behandlung von PVA mit verdünntem wässrigem Alkali bei Raumtemperatur ergibt eine merkliche Verminderung der Intensitäten aller drei Absorptionsbanden. Heiss verdünnte Säure beseitigt zwar im wesentlichen die 330 m μ -Bande, liefert aber keine entsprechende Änderung der relativen Intensität der 225 und 280 m μ -Bande.

Received February 7, 1962

Reaction Kinetics and Tacticity of Macromolecules. II. Acrylic Acid Copolymers

G. SMETS and W. VAN HUMBEECK, *Laboratoire de Chimie
Macromoléculaire, University of Louvain, Belgium*

Synopsis

The influence of steric effects and of the microtacticity of polymeric chains has been examined during the hydrolysis of acid-ester copolymers. Four different acrylic acid-ethyl ethacrylate copolymers have been prepared; their molar acid content was 50, 67, 77, and 85%. The rate of hydrolysis was examined at different degrees of neutralization in buffered aqueous solutions at 113°C. The rate was directly proportional to the content of (acid-ester-acid) triads and was highest where the degree of neutralization was equal to 0.5. The final degree of conversion is, however, limited on account of the existence of different stereochemical structures of these (acid-ester-acid) triads. Conventional and isotactic acrylic acid-methyl acrylate copolymers have also been prepared; their molar acid content was 64.5 and 80.5% for the conventional and 67 and 80% for the isotactic copolymers. From the rates of hydrolysis measured at 103°C. in buffered aqueous solutions, it becomes evident that the isotactic polymers hydrolyze 3 to 5 times more rapidly than the conventional polymers; moreover, the final degree of conversion is much higher. Finally conventional and isotactic acrylic acid-*tert*-butyl acrylate copolymers have been examined; these copolymers hydrolyze only in the presence of mineral acid; any intramolecular functional interaction is absent in both cases. This stability has been explained on the basis of a different mechanism of hydrolysis of these tertiary butyl esters.

It has been demonstrated previously that the hydrolysis of acid-ester and acid-amide copolymers in buffered aqueous solutions proceeds through an intramolecular mechanism by the interactions of neighboring functions.¹⁻⁹ It is the purpose of the present paper to report some new results obtained with acrylic acid copolymers, in which the second component, the comonomer, was characterized by a high steric hindrance either in the main chain (ethyl ethacrylate) or in the side chain ester group (*tert*-butyl acrylate). The behavior of these copolymers will be compared with those of acrylic acid-methyl acrylate copolymers of different tacticities, and it will be shown that besides the microtacticity of the chain the steric effects exert also a predominant effect on the reaction rate.

We shall consider successively the hydrolysis of acrylic acid-ethyl ethacrylate, acrylic acid-methyl acrylate, and acrylic acid-*tert*-butyl acrylate copolymers.

I. EXPERIMENTAL

1. Acrylic Acid-Ethyl Ethacrylate Copolymer

Ethyl ethacrylate was prepared from ethyl hydrogen (2-ethyl)malonate by condensation with formaldehyde, followed by dehydration in the presence of hydrochloric acid; b.p. 137.5–138.5°C.¹⁰

For the preparation of copolymers of a given composition, the r_1 and r_2 copolymerization parameters were determined. The reactions were carried out in benzene in the presence of azobisisobutyronitrile, 1% with respect to the monomer concentration; the total concentration of the monomers was 2 mole/l. Copolymers with an acid content higher than 60% precipitated while formed; those with less than 45% acid remained soluble and were precipitated by being poured in heptane. The yield was always kept lower than 5–10%. The copolymers were analyzed for acid content by conductometric titration.

TABLE I
Copolymerization of Acrylic Acid (M_1) and Ethyl Ethacrylate (M_2)

Fraction of M_1 in monomer	Fraction of M_1 in copolymer
0.83	0.84
0.76	0.80
0.71	0.75
0.58	0.63
0.47	0.54
0.325	0.43
0.20	0.305

From the data given in Table I, $r_1 = 0.9 \pm 0.1$ and $r_2 = 0.45 \pm 0.05$. On the basis of the results, four different copolymers were prepared; their acid contents were 50, 67, 77, and 85 mole-%.

2. Poly-*tert*-butyl Acrylate

tert-Butyl acrylate was prepared in diethyl ether solution from acryloyl chloride and *tert*-butyl alcohol in the presence of dimethylaniline.

Conventional polymer was prepared at 80°C. in dioxane solution in the presence of 1% azobisisobutyronitrile initiator. The polymer was precipitated in a mixture of 4:1 methanol/water and redissolved in dioxane; it was isolated by freeze-drying.

Isotactic polymer was prepared with phenylmagnesium bromide catalyst at -60°C . by the method described by Fox et al.¹¹

Differences in tacticity of the two kinds of polymer were shown by infrared spectrometry, especially at 695 and 863 cm.^{-1} , where the isotactic polymer absorbs more intensely.

3. Acrylic Acid-*tert*-Butyl Acrylate Copolymer

Poly-*tert*-butyl acrylate as partially hydrolyzed in dioxane-water solution in the presence of sulfuric acid. After reaction, the solution was evaporated *in vacuo* and poured in diethyl ether. After redissolution in dioxane and precipitation in diethyl ether, the polymer was isolated by freeze-drying.

The acid content was determined in dioxane solution with 0.1N KOH in methanol, thymol blue being used as indicator.

Two copolymers were prepared from the conventional and isotactic poly-*tert*-butyl acrylate; their acid contents were 40 and 79%.

4. Acrylic Acid-Methyl Acrylate Copolymers

Two conventional copolymers were prepared at 50°C. in benzene solution; the copolymers precipitated while formed. Their acid compositions were 0.805 and 0.645 mole-%.

Isotactic copolymer was prepared in two stages. Isotactic poly-*tert*-butyl acrylate was hydrolyzed to isotactic polyacrylic acid; this acid was dissolved in dioxan and partially methylated with diazomethane. By this method two copolymers were prepared whose acid contents were 0.80 and 0.67 mole-%.

5. Rate of Hydrolysis

Hydrolysis of acrylic acid copolymers was carried out in buffered aqueous solution at different degrees of neutralization of the acid groups, r being the ratio of the concentration of undissociated acid [HA] to neutralized carboxylic $[A^-]$ functions. For all experiments the ester concentration was kept constant at 0.02 mole/l., except when indicated. At r values of 7, 0.5, and 0 the pH was equal to 5, 7, and 8.5, respectively. The influence of H_3O^+ ions was therefore negligible during these experiments.

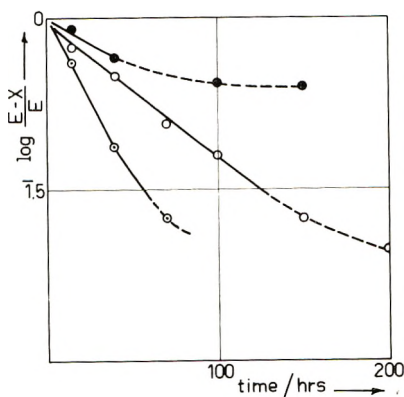


Fig. 1. Rate of hydrolysis of 77/23 acrylic acid-ethyl ethacrylate copolymer: (●) $r = 7$; (○) $r = 0$; (⊙) $r = 0.95$.

The reactions were carried out at 113°C. for acrylic acid-ethyl ethacrylate polymers, and at 103°C. for acrylic acid-methyl acrylate polymers. After a given time the solutions were titrated conductometrically with 0.1N NaOH; the degree of conversion was evaluated by the difference between the conductometric value at zero time and time t (Fig. 1).

The *tert*-butyl acrylate polymers were hydrolyzed at 90°C. in dioxan-water solution (97.3:2.7) in the presence of sulfuric acid at a concentration of 0.0909 mole/l. both of ester and of acid.

II. RESULTS AND DISCUSSION

Acrylic Acid-Ethyl Ethacrylate Copolymers

When the hydrolysis of acrylic acid-ethyl ethacrylate is represented by plotting the percentage of hydrolyzed ester as a function of time, it appears that only a part of the ester groups can be hydrolyzed; the final asymptotic value E is a function only of the composition of the copolymer and is equal to 25, 38, 43, and 45% for copolymers C₅₀, C₆₇, C₇₇, and C₈₅, respectively. (Here the subscript figures e.g., 50, 67, indicate the acrylic acid content in mole per cent.) This limited value, however, is attained more or less rapidly, depending on the degree of neutralization. If E represents the amount of the hydrolyzable ester groups and x the amount of ester hydrolyzed at time t , a plot of $\log (E - x)/E$ as a function of time gives a linear diagram, from which the slope indicates the corresponding apparent first-order rate constant (Fig. 1). The results are given in Table II.

TABLE II
 k_1 Values and Rates of Hydrolysis R of Acrylic Acid-Ethyl Ethacrylate Polymers at 113°C.; [ester]₀ = 0.02 mole/l.

$r = \frac{[H^+]}{[A^-]}$	Acid content of copolymer, mole-%	$k_1 \times 10^6$, sec. ⁻¹	$R \times 10^8$, mole/l. sec.
0	50	2.2	1.1
	67	2.5	1.9 ^a
	77	2.7	2.3
	85	2.6	2.4
0.5	50	4	2
	50	5.9	2.9
0.95	67	5.4	4
	77	5.75	4.95 ^{b,c}
	85	6.11	5.4
	67	3.5	2.6
2	77	2.3	2
3	77	2.3	2
4.6	77	2.4	2.1
7	67	1.3	1
	77	1.55	1.3

^a $R = 2.8 \times 10^8$ mole/l. sec. at [ester]₀ = 0.03 mole/l.

^b $R = 2.5 \times 10^8$ mole/l. sec. at [ester]₀ = 0.01 mole/l.

^c $R = 9.5 \times 10^8$ mole/l. sec. at [ester]₀ = 0.04 mole/l.

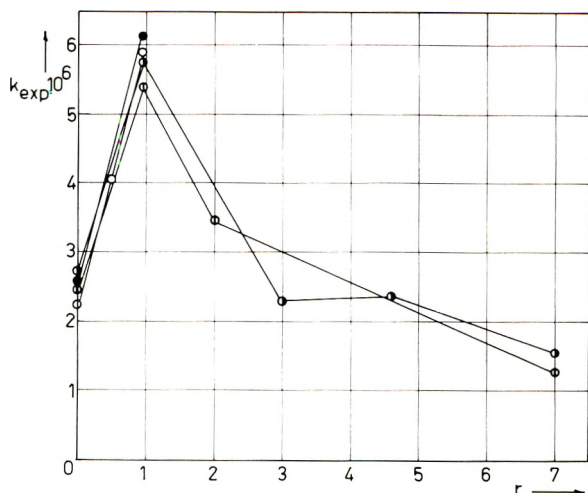


Fig. 2. k_{exp} as a function of r ($= [\text{HA}]/[\text{A}^-]$) for acrylic acid-ethyl ethacrylate copolymers: (○) C₅₀; (⊙) C₆₇; (●) C₇₇; (●) C₈₅.

From the data of Table II it becomes evident that (1) r , for a given degree of neutralization the k_1 constants are about equal for polymers of different chemical compositions; (2) the k_1 values are highest at $r = 0.95$, for which the undissociated and carboxylate groups are about equally distributed (Fig. 2); (3) at $r = 7$, k_1 values are lowest, and, moreover, the amount of hydrolyzable ester groups is smaller than for the other values of r ; (4) the reaction proceeds by an intramolecular mechanism between neighboring groups; indeed, the data of Table II show that the rate of hydrolysis is proportional to the polymer concentration; consequently an acid-ester pair functions as a kinetic entity and not as separately isolated groups.

In the case of copolymer C₇₇ for $r = 0.95$, the energy of activation has been determined by measuring the rate of hydrolysis also at two other temperatures, namely, 90 and 100°C.; the k_1 values were 1.3×10^{-6} and 2.4×10^{-6} , respectively. The corresponding energy of activation is equal to 17 kcal./mole.

Taking into account the values of the copolymerization parameters ($r_1 = 0.9$ and $r_2 = 0.45$), the probabilities of the different propagation sequences P_{121} , P_{122} , P_{221} , and P_{222} can be determined; here, P_{121} indicates the probability that an acrylic acid radical $\cdot M_1$ reacts successively with ethyl ethacrylate M_2 and a new acrylic acid monomer; this value is necessarily equal to the product $P_{12}P_{21}$.

From the point of view of the copolymer composition, the values P_{121} and P_{122} must be multiplied by the molar ratio m_1/m_2 of the monomer in the copolymer in order to show the relative importance of the configurations in the final structure of the polymer. The results of these calculations are given in the Table III.

TABLE III
 Relative Distribution of Triad Configurations

Copolymer acid content, mole-%	[121]	[122] and [221]	[222]
0.5	0.36	0.48	0.16
0.67	0.63	0.32	0.05
0.77	0.77	0.214	0.016
0.85	0.86	0.135	0.005

The values of Table III are valid only for two different units, acrylic acid and ethyl ethacrylate. If the acid units are partially neutralized, a triad configuration, e.g., acid-ester-acid can also be present as carboxylate-ester-carboxylate and carboxylate-ester-acid unit. Although the relative importance of each species could be easily evaluated on the basis of the degree of neutralization α , i.e. the ratio $[A]/[HA] + [A]$, nevertheless the significance is most clear for the data when $r = 0$, at which point only two components, carboxylate and ethyl ethacrylate units, must be considered.

If one takes into account that the rate of hydrolysis is proportional to the overall polymer concentration, it is possible to calculate the rate of reaction for each of the four copolymers at the same concentration of one configuration; the rates are then only a function of the percentage of the other configuration. This has been calculated for a constant concentration of acid-ester-ester triads $[122] = 0.32 \times 10^{-2} \text{ l.}^{-1}$ and of acid-ester-acid triads $[121] = 0.77 \times 10^{-2} \text{ l.}^{-1}$. The results are summarized in Table IV.

 TABLE IV
 Rates of Hydrolysis R of Acrylic Acid-Ethyl Ethacrylate Polymers
 Copolymer

[ac.-est.-est.] = $0.32 \times 10^{-2} \text{ l.}^{-1}$		Copolymer acid content, mole-%	[ac.-est.-ac.] = $0.77 \times 10^{-2} \text{ l.}^{-1}$	
[ac.-est.-ac.] $\times 10^2$	Rate $R \times 10^8$		[ac.-est.-est.] $\times 10^2$	Rate $R \times 10^8$
0.24	0.363	50	1.03	1.17
0.63	0.95	67	0.39	1.16
1.1	1.67	77	0.22	1.15
2.1	3.05	85	0.12	1.08

By plotting these values in a diagram giving the rate of hydrolysis versus the concentration of the configuration (Fig. 3), it can be seen that the rate is directly proportional to the acid-ester-acid triad concentration [ac.-est.-ac.] the plot passing through the origin (curve *a*); on the other hand, the rate is practically insensitive to variation of concentration of acid-ester-ester triads (curve *b*). The slope of curve *a* is equal to 1.45×10^{-6} , so that the rate expression becomes

$$R = 1.45 \times 10^{-6} [\text{ac.est.ac.}]$$

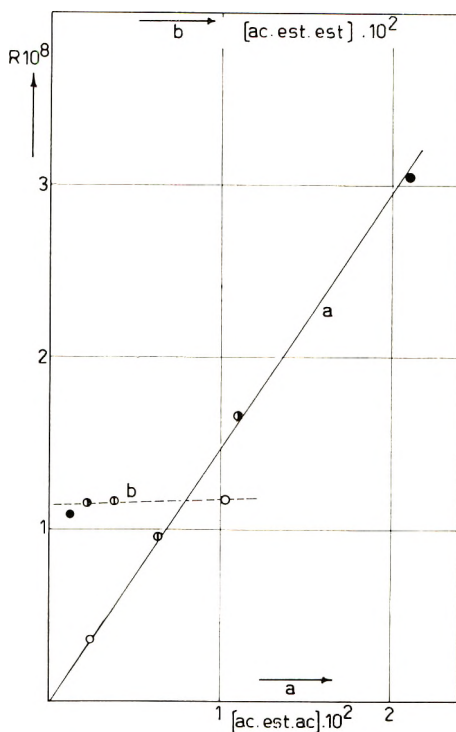


Fig. 3. Rates of hydrolysis of acrylic acid-ethyl ethacrylate copolymers (*a*) at constant $[\text{ac. est. est.}] = 0.32 \times 10^{-2}$ and (*b*) at constant $[\text{ac. est. ac.}] = 0.77 \times 10^{-2}$; (O) C₅₀; (◐) C₆₇; (●) C₇₇; (●) C₈₅.

By comparison of this value with the experimental expression $R_{\text{exp}} = 2.5 \times 10^{-6} [\text{hydrolyzable ester}]$ (for $r = 0$, Table II), it becomes evident that only 58% of the (ac. est. ac.) triad units can be hydrolyzed. This discrepancy must be explained by differences in stereochemical position of the different functions.

The stability of (ac. est. est.) triads with respect to intramolecular hydrolysis must be related to the high steric hinderance due to the direct neighborhood of two ester groups, which prevents the formation of an intermediary anhydride link.

For the other r values, Figure 2 shows clearly that the k_{exp} increase from $r = 0$ to $r = 0.95$, at which value the [acid-ester-acid] configurations have the distribution ($\alpha = 0.51$) 26% (carboxylate-ester-carboxylate), 24% (acid-ester-acid) and 50% (acid-ester-carboxylate). This predominant (acid-ester-carboxylate) configuration must therefore be considered as the most favorable for hydrolysis, probably by the occurrence of a concerted reaction mechanism. Moreover, the activation energy of hydrolysis of 17 kcal./mole is similar to that found by De Loecker and Smets in the case of methacrylic copolymers (16.5 kcal.), for which a similar mechanism has been suggested; in the case of the methacrylic series, however, the optimum

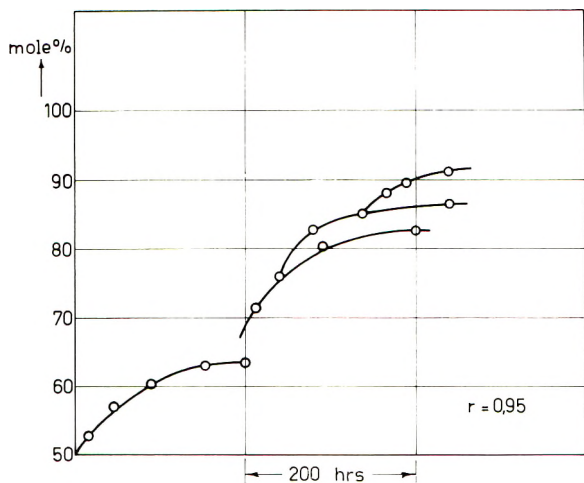


Fig. 4. Influence of the stereochemical composition on successive hydrolyses of different acrylic acid-ethyl ethacrylate copolymers.

value of r was three, and occurred only for polymers of high acid content (72–86.5% acid).

For $r = 0.95$, the role of the stereochemical composition of the copolymers has again been taken in evidence. Figure 4 shows the successive hydrolysis of the copolymers with different acid contents; the diagram is completely similar to that given previously by one of us for methacrylic copolymers. When one of the copolymers (e.g., C_{67}) is hydrolyzed up to the composition of the next copolymer (C_{77}) its rate of hydrolysis is much lower than that of this last copolymer.

At higher r value evidently the concentration of half-neutralized configurations decreases appreciably: e.g., for $r = 7$ it is only 26.5%, while the [ac-est-ac.] configuration becomes most important and represents already 72% of the ester groups. This completely acid configuration must therefore be considered to be quite unfavorable. These considerations at different r values can, however, be accepted only with some restriction; indeed, the partially neutralized polymer should not be considered as a static but as a dynamic system.

As conclusion of this first section, it may be concluded that the hydrolysis of acrylic acid-ethyl ethacrylate copolymers is directly related to the presence of (1,2,1) triads, and that, depending on the degree of neutralization, the following decreasing order of reactivity has been found (acid-ester-carboxylate) > (carboxylate-ester-carboxylate) >> (acid-ester-acid).

The amount of hydrolyzable ester functions is, however, always lower (about 60%) than the total amount of (1,2,1) units; this discrepancy must be explained on the basis of differences in the stereochemical composition of the system.

2. Acrylic Acid-Methyl Acrylate Copolymers

A direct demonstration of the influence of the microtacticity on the reaction kinetics can however be given for acrylic acid-methyl acrylate copolymers of about the same overall chemical composition but different in their tacticity. The preparation of these copolymers was described above in the experimental section.

As for the preceding copolymers, only a part of the ester groups can be hydrolyzed. The limited values are 27 and 43% for the conventional copolymers C_{64.5} and C_{80.5}, respectively; they are noticeably higher (equal to 47 and 60%) for the isotactic copolymers Is₆₇ and Is₈₀, respectively. The rates of hydrolysis and the first-order rate constant k_1 evaluated by the same method as indicated before are summarized in Table V.

TABLE V
Rate Constants k_1 and Rates of Hydrolysis R of Conventional and Isotactic Acrylic Acid-Methyl Acrylate Copolymer Obtained at 103°C.; [ester] = 0.02 mole/l.

Polymer	$r = \frac{[\text{HA}]}{[\text{A}^-]}$	Acid content of copolymer, mole-%	$k_1 \times 10^6$, sec. ⁻¹	$R \times 10^8$, mole/l. sec.
C _{64.5}	0	64.5	5.1	2.7
Is ₆₇		67	14	13
C _{80.5}		80.5	3.1	2.7
Is ₈₀		80	14	17
C _{64.5}	1	64.5	5.4	2.9
Is ₆₇		67	15	14
C _{80.5}		80.5	5.8	5
Is ₈₀		80	61.5	20
C _{64.5}	2	64.5	6.7	3.7
Is ₆₇		67	17	16
C _{80.5}		80.5	7.9	6.8
Is ₈₀		80	19	23
C _{90.5}	3	80.5	9.2	7.9

The data of Table V show that in the case of the conventional polymers (1) the k_1 values are of the same order of magnitude as those for the acrylic acid-ethyl methacrylate copolymers; (2) the k_1 increase with increasing r values, i.e., for lower degrees of neutralization.

This behavior of the acrylic copolymers differs markedly from that of the acrylic acid-ethyl methacrylate copolymers. Methyl acrylate groups react as well with neighboring acid as with carboxylate groups; the acid-ester configuration is even more reactive than a carboxylate-ester pair.

No maximum of k_1 as a function of r could be found; it is therefore not necessary to postulate a concerted mechanism for these acrylic copolymers.

In the case of the isotactic copolymers, (1) the initial rates R and the corresponding k_1 values are 3 to 5 times higher than for the conventional copolymers; (2) the rates and k_1 increase with r and are highest for copolymer Is₈₀.

For copolymer $I_{S_{80}}$ the energy of activation was determined by measuring the rate of hydrolysis at three other temperatures for the same degree of neutralization ($r = 1$). At 90, 95, and 113°C. the k_1 values are, respectively, 7.2, 12, and 32×10^{-6} sec.⁻¹. Consequently the corresponding energy of activation is equal to 16.5 kcal., a value practically identical with that found previously. As already pointed out, the occurrence of a concerted mechanism in this acrylic series is much less evident than with the ethacrylate copolymers; the change of intimate internal mechanism must be directly related to the steric hindrance along the polymeric chain.

These experiments show evidently that the stereochemical composition exerts a direct influence on the intramolecular hydrolysis of the ester function, not only by increasing the rate constant two- to fivefold, but also by increasing the limited ester concentration which can be hydrolyzed.

3. Poly-*tert*-butyl Acrylate

The influence of the steric hindrance of the hydrolyzable groups on the intramolecular reaction mechanism has been also considered in an extreme case, that of poly-*tert*-butyl acrylates.

In this case no differences at all could be detected between the hydrolysis of conventional and isotactic poly-*tert*-butyl acrylate.

In the presence of H_2SO_4 , 0.0909 mole/l., at 90°C. the apparent first-order rate constant is equal to 0.35×10^{-4} for both homopolymers.

Corresponding conventional and isotactic acrylic acid-*tert*-butyl acrylate copolymers were found to be completely insensitive to intramolecular hydrolysis, whatever the value of r used. The copolymers were hydrolyzed only in the presence of strong inorganic acid.

The small acceleration of the sulfuric acid hydrolysis of *tert*-butyl acrylates which can be observed at degree of conversion higher than 30% is due essentially to an increase of the dissociation of the sulfuric acid, as was shown by the increase of conductivity of the solution when the reaction proceeds.

From these results, it is admitted that the hydrolysis of *tert*-butyl ester groups proceeds essentially by an A_{A11} mechanism through an alkyl-oxygen scission.¹² The BAC_2 mechanism usually suggested for neighboring interaction becomes practically impossible on account of the strong steric effect of the *tert*-butyl groups. Evidently the absence of interfunctional reaction excludes automatically any influence of the microtacticity on the hydrolysis of *tert*-butyl acrylate polymers.

III. CONCLUSIONS

Acrylic acid-ethyl ethacrylate copolymers hydrolyze in aqueous medium by an intramolecular mechanism inside of (acid-ester-acid)triad configurations. The rate of hydrolysis is highest when, on the average, half of the acid groups are neutralized; a concerted reaction mechanism has been

therefore postulated. The final degree of conversion is, however, limited for stereochemical reasons related to the microtacticity of the polymeric chains.

The influence of the microtacticity on the reaction kinetics has been demonstrated with conventional and isotactic acrylic-acid-methyl acrylate copolymers of about the same overall chemical composition. Indeed, the isotactic systems hydrolyze 3 to 5 times more rapidly than the conventional ones, and their final degree of conversion is much higher.

In the case of acrylic acid-*tert*-butyl acrylate copolymers, any intramolecular reaction was absent, whatever the degree of neutralization and independently of the type of copolymers used, conventional or isotactic. This stability must be explained by a different mechanism of hydrolysis in the case of these tertiary butyl esters.

References

1. Morawetz, H., and P. E. Zimmering, *J. Phys. Chem.*, **58**, 753 (1954).
2. Morawetz, H., and E. W. Westhead, Jr., *J. Polymer Sci.*, **16**, 273 (1955).
3. Morawetz, H., and Gaetjins, *J. Polymer Sci.*, **32**, 526 (1958).
4. Smets, G., and A. M. Hesbain, *J. Polymer Sci.*, **40**, 217 (1959).
5. De Loecker, W., and G. Smets, *J. Polymer Sci.*, **40**, 203 (1959).
6. Smets, G., and W. De Loecker, *J. Polymer Sci.*, **41**, 375 (1959).
7. Smets, G., and W. De Loecker, *J. Polymer Sci.*, **45**, 461 (1960).
8. Glavis, F. J., *J. Polymer Sci.*, **36**, 547 (1959).
9. Chapman, C. B., *J. Polymer Sci.*, **45**, 237 (1960).
10. Mannich, C., and K. Ritzert, *Ber.*, **57**, 1117 (1924).
11. Fox, T. G, Jr., J. W. E. Goode, and J. D. Stroupe, Brit. Pat. 566,713, to Rohm & Haas Co. (1957).
12. Ingold, C. K., *Structure and Mechanism in Organic Chemistry*, Cornell Univ. Press, Ithaca, N. Y., 1953, pp. 779-82.

Résumé

L'influence d'effets stériques et de la microtacticité des chaînes polymériques a été étudiée dans le cas de l'hydrolyse de copolymères acide-ester. Quatre copolymères différents d'acide acrylique et d'éthacrylate d'éthyle ont été préparés; leur teneur molaire en acide s'élevait à 50, 67, 77 et 85%. Leur vitesse d'hydrolyse a été examinée à différents taux de neutralisation en solution aqueuse tamponnée à 113°C. La vitesse était directement proportionnelle à la teneur en triades (acide-ester-acide) et était la plus élevée lorsque le degré de neutralisation était égal à 0.5. Le taux de conversion final était toutefois limité par suite de l'existence de différentes structures stéréochimiques au sein de ces triades (acide-ester-acide). Des copolymères conventionnels et isotactiques d'acide acrylique et d'acrylate de méthyle ont également été préparés; leur teneur molaire en acide s'élevait à 64.5 et 80.5% pour les copolymères conventionnels, 67 et 80% pour les polymères isotactiques. Au départ des vitesses d'hydrolyse mesurées à 103°C en solution tampon aqueuse, il résulte que les polymères isotactiques hydrolysent 3 à 5 fois plus rapidement que les polymères conventionnels; en outre, le taux de conversion final est beaucoup plus élevé. Finalement, on a étudié des copolymères conventionnels et isotactiques d'acide acrylique et d'acrylate de *tert*isobutyle. Ces copolymères hydrolysent uniquement en présence d'un acide minéral; toute interaction fonctionnelle intramoléculaire est absente dans les deux systèmes. La stabilité de ces composés est expliquée sur la base d'un mécanisme d'hydrolyse différent dans le cas des esters *tert*-butyliques.

Zusammenfassung

Der Einfluss sterischer Effekte und der Mikrotaktizität von Polymerketten auf die Hydrolyse von Säure-Estercopolymeren wurde untersucht. Vier verschiedene Acrylsäure-Athyläthacrylatcopolymere wurden hergestellt; ihr molarer Säuregehalt betrug 50, 67, 77 und 85%. Die Hydrolysegeschwindigkeit wurde bei verschiedenen Neutralisationsgraden in gepufferter wässriger Lösung bei 113°C untersucht. Die Geschwindigkeit war dem Gehalt an Säure-Ester-Säure-Triaden direkt proportional und bei einem Neutralisationsgrad von 0,5 am grössten. Der Endumsatz ist jedoch durch das Vorhandensein von verschiedenen stereochemischen Strukturen dieser Säure-Ester-Säure-Triaden begrenzt. Weiters wurden konventionelle und isotaktische Acrylsäure-Methylacrylatcopolymere hergestellt; ihr molarer Säuregehalt betrug 64,5 und 80,5% für die konventionellen, 67 und 80% für die isotaktischen Copolymeren. Aus den bei 103°C in gepufferter wässriger Lösung gemessenen Hydrolysegeschwindigkeiten ergibt sich, dass die isotaktischen Polymeren 3 bis 5 mal rascher hydrolysiert werden als die konventionellen, ausserdem ist der Endumsatz wesentlich höher. Schliesslich wurden konventionelle und isotaktische Acrylsäure *tert.* Butylacrylatcopolymere untersucht; diese Copolymeren werden nur in Gegenwart von Mineralsäuren hydrolytisch gespalten; in beiden Fällen ist keinerlei intermolekulare funktionelle Wechselwirkung vorhanden. Diese Stabilität wurde durch Annahme eines verschiedenen Hydrolysemechanismus für die tertiären Butylester erklärt.

Received February 6, 1962

Dynamic Properties of Homo- and Copolymers of 4-Methyl-1-Pentene

W. A. HEWETT* and F. E. WEIR, *Shell Development Company,
Emeryville Research Center, Emeryville, California*

Synopsis

Dynamic measurements of homo- and copolymers of 4-methyl-1-pentene have been made with a self-damped torsion pendulum. It has been shown that one can calculate the glass transition temperature of these copolymers by means of an equation suggested by T. Fox. It has also been shown that there is a danger in correlating per cent insolubles with crystallinity in a new polymer system without considering molecular weight.

Introduction

Since the discovery of new methods for the polymerization of α -olefins by Ziegler¹ and the subsequent thorough investigation of these systems by Natta,² many new homo- and copolymer systems have been considered interesting candidates for study. Within this group alone there exists an infinity of combinations and the possibility of obtaining a vast range of physical properties. This study comprises the preparation and dynamic mechanical properties of some homo- and copolymers of 4-methyl-1-pentene.

Preparation

The polymerization of 4-methyl-1-pentene and its copolymerization with other α -olefins have been reported before.³⁻⁵ Table I summarizes the experimental procedure followed in this work. There were five homopolymers of 4-methyl-1-pentene having varying stereoregularity and molecular weight (measured by intrinsic viscosity), two copolymers with 1-hexene having different monomer ratios, and one copolymer of approximately 60:40 4-methyl-1-pentene/1-pentene.

Dynamic Mechanical Properties

In semicrystalline polymers, such as those discussed here, a major amorphous transition which has a great effect on the physical properties of the material always occurs in some range of temperature-frequency. While such materials frequently show other transitions, the major one,

*Present address: IBM Research Laboratory, Monterey and Cottle Roads, San Jose, California.

TABLE I
Preparation of Homopolymers and Copolymers of 4-Methyl-1-Pentene^a

Expt. no.	Monomer ratio	Wt., g.	Heptane, ml.	Catalyst, mmole	Reaction conditions		Yield of solid polymer, %	η at 150° in decalin	Insolubles, ^b %
					Time, hr.	Temp., °C.			
A	100% 4-Methyl-1-pentene	20	100	3.5 Et ₂ AlCl/1.2 γ -TiCl ₃ ^c	24	50	98	5.5	95
B	100% 4-Methyl-1-pentene	20	100	3.5 Et ₂ AlCl/1.2 γ -TiCl ₃ /0.75 ZnEt ₂	24	50	81	1.3	76
C	100% 4-Methyl-1-pentene	189	500	Supported TiCl ₄ /Et ₂ AlCl	90	50	96	6.8	60
D	100% 4-Methyl-1-pentene	39	100	Ti ₂ Al ₂ Cl ₂ ^d /Et ₂ AlCl	24	50	97	4.2	81
E	100% 4-Methyl-1-pentene	400	8400	105 Et ₂ AlCl/35 γ -TiCl ₃ ^c	6	70	80	3.7	93
F	90% 4-Methyl-1-pentene 10% 1-Hexene	180 20	900	28 Et ₂ AlCl/8 γ -TiCl ₃ ^c	17	23	87	7.0	—
G	50% 4-Methyl-1-pentene 50% 1-Hexene	15 15	80	7.2 Et ₂ AlCl/2 β -TiCl ₃ ^c	17	50	93	2.9	—
H	62% 4-Methyl-1-pentene 38% 1-Pentene	74 26	1020	14 Et ₂ AlCl/4 γ -TiCl ₃ ^c	17	23	97	7.2	73

^a Reactions were carried out in suitable vessels that provided adequate shaking or stirring at the desired reaction temperature.

^b Boiling isooctane for 24 hrs.

^c See Ref. 8 for a discussion of the different crystalline modifications of TiCl₃.

^d Stauffer Chemical Company.

analogous to the glass-rubber transition in amorphous polymers, dominates. Below the transition temperature the amorphous regions are locked in, unable to move freely, and the polymer as a whole acts like a brittle material. In this condition it shows such characteristics as low elongation, tendency to brittle fracture, and low impact resistance. Above this temperature it is more ductile, more impact-resistant, and of lower modulus. Evidently, the temperature at which the major transition occurs can be nearly as decisive as the melting point in determining a useful range of application.

There appears to exist a fairly consistent relation between the composition of a copolymer (which is not too blocky) and its glass transition temperature. If a relation also holds for semicrystalline stereoregular copolymers, between their composition and the temperature of their major amorphous transition, a means is afforded of producing materials of any desired transition temperature by copolymerizing different materials.

An equation suggested by Fox^{6,7} for nonpolar materials is

$$1/T_g = W_1/T_{g1} + W_2/T_{g2} \quad (1)$$

where T_g represents the glass transition temperature of the copolymer, T_{g1} and T_{g2} those of the homopolymers, and W_1 and W_2 refer to the weight fraction of the two comonomers. This relation has been found to hold well for the materials studied here.

The means used for the determination of the major transition temperature in this study is that of torsional damping at frequencies near 1 cycle/sec. The torsional pendulum used in the study is one of our own design; it will be described elsewhere.

It is well known that

$$\tan \delta = G''/G' \quad (2)$$

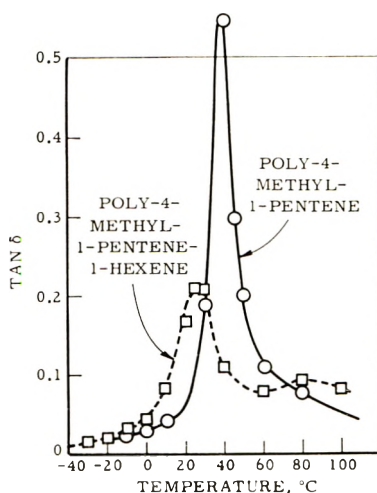
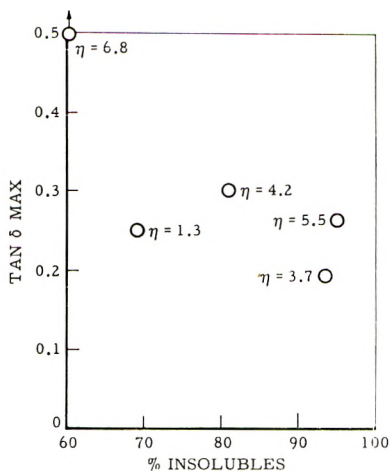


Fig. 1. Plot of $\tan \delta$ versus temperature.

Fig. 2. Plot of $\tan \delta_{\max}$ versus per cent insolubles.

maximizes near the inflection point in a plot of G' (shear modulus) versus temperature, this maximum serving as a convenient measure of the approximate center of a transition which occurs over a range of temperatures. For purposes of this discussion, the temperature of the maximum in $\tan \delta$ at or near frequencies of 1 cycle/sec. will be taken as T_{θ} (see Fig. 1).

Table II shows results of dynamic measurements on the materials. For the homopolymer of 4-methyl-1-pentene, maxima in $\tan \delta$ were found in all cases between 35 and 40°C., averaging 38°C. For three copolymers involving 1-hexene and 1-pentene, good agreement was found between T_{\max} and that calculated from eq. (1). Values for T_{θ} of polymers of 1-pentene and 1-hexene were taken from the literature⁹ for purposes of calculation, which demonstrates the possibility of producing materials with

TABLE II
 T_{θ} of Homo- and Copolymers of 4-Methyl-1-Pentene

Expt. no.	Polymer	T_{\max} , °C.		
		Meas.	Caled.	$\tan \delta_{\max}$
—	Polypropylene	2	—	0.075
—	Poly-1-pentene	—53 ^a	—	—
—	Poly-1-hexene	—50 ^a	—	—
A	Poly-4-methyl-1-pentene	35	—	0.266
B	Poly-4-methyl-1-pentene	38	—	0.250
C	Poly-4-methyl-1-pentene	38	—	0.300
D	Poly-4-methyl-1-pentene	40	—	>0.500
E	Poly-4-methyl-1-pentene	38	—	0.194
F	Poly-4-methyl-1-pentene-1-hexene	28	26 ^b	0.230
G	Poly-4-methyl-1-pentene-1-hexene	—20	—13 ^b	0.310
H	Poly-4-methyl-1-pentene-1-pentene	—6	—5 ^b	0.140

^a Values taken from the literature; see Ref. 9.

^b Calculations based on T_{θ} for poly-4-methyl-1-pentene being 38°C. (311°K.)

a very broad range of properties from the olefin monomers available, and also, lends support to the applicability of eq. (1) to copolymers within this system.

The successful prediction of T_g of the copolymers by means of eq. (1) implies that crystalline and amorphous phases have the same composition if crystallinity exists at all in the system. The presence or crystallinity is certain, since the copolymers all gave differential thermal analysis peaks in the vicinity of the melting point of poly-4-methyl-1-pentene and since the damping peak heights were all too low for a completely amorphous system. This tends to support the view that crystals involving mixed monomer units can form in these systems, as has been suggested by others.¹⁰ A more complete investigation of this point will be the subject of a later communication.

Solubility in iso-octane was determined for the polymers labeled A through E; the data are shown in Table III along with values obtained for $\tan \delta_{\max}$ and intrinsic viscosities (in decalin at 150°C.).

TABLE III
A Comparison of $\tan \delta_{\max}$, Per Cent Insolubles, and Intrinsic Viscosity for Polymers of 4-Methyl-1-Pentene

Expt. no.	$\tan \delta_{\max}$	Insolubles, %	η at 150°C. in decalin
A	0.266	95	5.5
B	0.250	68	1.3
C	>0.500	60	6.8
D	0.300	81	4.2
E	0.194	93	3.7

Since the 38°C. transition is obviously an amorphous transition and would not occur in a purely crystalline material, the height of the curve of $\tan \delta$ at the maximum must be a function of the degree of crystallinity: the greater the peak the lower the crystallinity. Further, the damping peak, arising from motions of segments and not whole molecules, should not be highly dependent on molecular weight. Any measurement which gives crystallinity should correlate to some extent with the damping peak height, and this has been the case in these laboratories with many materials.

Figure 2 shows the extremely poor correlation found when the two measures are compared. Evidently, the very great differences in molecular weight are responsible for a good part of the lack of correlation. The solubility of partially crystalline polymers depends upon molecular weight as strongly, perhaps, as on degree of crystallinity. This dual dependence can cause insolubility measurements to be very misleading. For example, on the basis of insolubility alone one would judge samples A and E to be of approximately the same stereoregularity, but a comparison of the respective damping peak heights indicates that this is very unlikely.

References

1. Ziegler, K., *Angew. Chem.*, **64**, 323 (1952).
2. Natta, G., *Modern Plastics*, December, 169 (1956).
3. "Montecatini" (Societa generale industries mineraria e chemica), Belg. Pat. 545,952 (March 10, 1956).
4. Campbell, T. W., and A. C. Haven, *J. Appl. Polymer Sci.*, **1**, 78 (1959).
5. Campbell, T. W., *J. Appl. Polymer Sci.*, **5**, 184 (1961).
6. Fox, T., *Bull. Am. Phys. Soc.*, [2], **1**, (3) 123 (1956).
7. Wood, L. A., *J. Polymer Sci.*, **28**, 319 (1958).
8. Natta, G., P. Corradini, and G. Allegra, *J. Polymer Sci.*, **51**, 399 (1961).
9. Natta, G., F. Danusso, and G. Moraglio, *J. Polymer Sci.*, **25**, 119 (1957).
10. Reding, F. P., and E. R. Walter, *J. Polymer Sci.*, **37**, 555 (1959).

Résumé

On a fait des mesures dynamiques des homo- et copolymères du 4-méthyl-1-pentène au moyen d'un pendule de torsion à amortissement automatique. On a montré que l'on peut calculer la température de transition vitreuse de ces copolymères en employant une équation proposée par T. Fox. On a aussi montré qu'il est dangereux de mettre en corrélation le pourcentage d'insolubilité avec la cristallinité dans un nouveau système de polymère sans considération du poids moléculaire.

Zusammenfassung

Dynamische Messungen an Homo- und Copolymeren von 4-Methyl-1-penten wurden mit einem Torsionspendel mit Eigendämpfung durchgeführt. Es wurde gezeigt, dass man unter Verwendung einer von T. Fox vorgeschlagenen Beziehung die Glasumwandlungstemperatur dieser Copolymeren berechnen kann. Weiters wurde gezeigt, dass man nicht ohne weiteres den Prozentgehalt an Unlöslichem zur Kristallinität in einem neuen Polymersystem ohne Berücksichtigung des Molekulargewichts in Beziehung setzen kann.

Received February 7, 1962

The Effect of Pressure on the Crystallization of Polyethylene from Dilute Solution

BERNHARD WUNDERLICH, *Department of Chemistry,
Cornell University, Ithaca, New York*

Synopsis

Linear polyethylene has been crystallized isothermally from 0.05% toluene solution at atmospheric pressure and up to 6000 atm. hydrostatic pressure. At atmospheric pressure a high temperature form of unknown structure was found crystallizing above 90°C. Single crystal lamellae crystallized between 75 and 90°C. Dendrites were formed below 75°C. The temperature dividing the dendritic growth from single crystalline growth increases with increasing pressure. The thickness of crystals grown at approximately constant supercooling, but at elevated temperature and pressure increased only slightly. A discussion in the light of present day theories is attempted.

Introduction

In this article the crystallization of linear unfractionated polyethylene from dilute toluene solution is described. In crystallizing at atmospheric pressure, three distinct kinds of crystalline growth have been observed: (a) a high-temperature form, which has not yet been analyzed, (b) a single-crystal crystalline growth, first described by Fischer,¹ Keller,² and Till,³ and reviewed in detail by Keller,⁴ and (c) a dendritic growth at temperatures below that of the single-crystal type of growth, described in detail in a previous publication.⁵

An increase in pressure (up to 6000 atm.) allowed crystallization at elevated temperatures. Also, the increase of pressure could be executed rather quickly, so that an almost instantaneous supercooling was reached, a necessary condition for dendritic growth.

Determination of the morphology of the crystals and the thickness of single-crystal platelets was made by means of interference microscope. The use of this rather new instrument for polymer research and, in particular, for thickness determination of single-crystal lamellae has been described.⁶

Under "Discussion" an attempt is made to fit the observations to current theories of the crystallization of polymers from solution.⁷⁻¹¹

Experimental

Crystallization

Crystallization at atmospheric pressure was done in a regulated ($\pm 0.01^\circ\text{C}$.) water bath. The samples (unfractionated linear polyethylene,

Marlex 50, dissolved in filtered A.R.-grade toluene) were contained in sealed 10–100-ml. ampules. The concentrations were varied from 0.009 to 0.32 wt.-%. In this article, however, all results refer to 0.05 ± 0.01 wt.-% polyethylene in toluene; in this range all variations with concentration are within the error limit of the techniques here employed. The crystallization temperature was obtained by quickly cooling the entire bath from 100°C . to the chosen value. On adding cold water, the time to reach a stable crystallization temperature was 1–2 min. For the faster crystallization a jacketed test tube was used whose constant-temperature circulation jacket could be switched instantaneously to a lower temperature bath ($\pm 0.1^{\circ}\text{C}$).

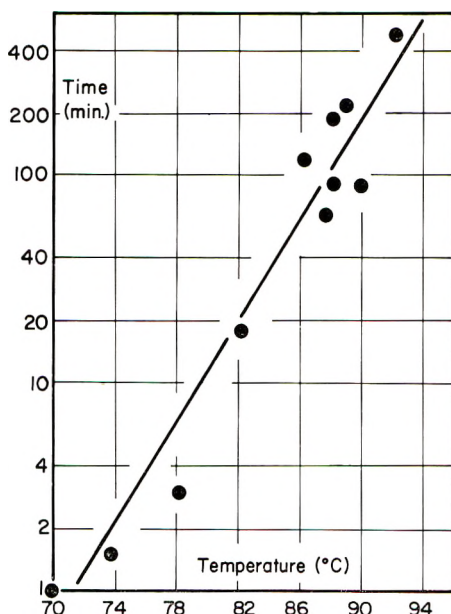


Fig. 1. Appearance time of crystals of polyethylene crystallized isothermally from a 0.05% solution in toluene at given temperatures.

The time to reach constant temperature was 30 sec.; thus this set of experiments (see Fig. 1) was limited to isothermal crystallization at 70°C . or higher.

Appearance times of the first crystals were determined visually and should be interpreted as a rough measure of the crystallization of a certain fraction (10–30%) of the approximately 0.05% concentrated solutions. At the higher temperatures, ten or more times the appearance time was not sufficient to crystallize all the dissolved polyethylene. The differentiation between the crystals grown at high temperature and those precipitated on cooling was made by quenching the ampules filled with partially crystallized solution by a quick transfer from the crystallization bath to ice water. Microscope observation revealed the not isothermally crystallized material as dendrites, as was to be expected from rapid cooling to 0°C .

Crystallization at elevated pressures was done with batches of solutions of approximately 50 ml. enclosed in stainless-steel or brass bellows. The bellows were brought into a 6500-atm. pressure stat especially designed¹² to keep relatively high pressures for extended periods of time with an accuracy of better than $\pm 1.5\%$. The autoclave containing the bellow was thermostatted in a 55-gal. oil bath to $\pm 0.1^\circ\text{C}$. After the sample was heated to the crystallization temperature under atmospheric pressure, the higher pressure was applied within 2 min. by the pumping of hydraulic oil into the autoclave. The pressure was kept constant afterwards by an automatic regulating device (for a detailed description see reference 12). Crystallization at constant temperature was continued for 2–12 hrs.; then cooling at approximately $4^\circ\text{C}/\text{hr}$. at constant elevated pressure was started. This rate of cooling was slow enough (see Fig. 1) to ensure single-crystal growth if the isothermal crystallization temperature picked had been too high for immediate growth of crystals at the applied pressure. The pressure was released when a temperature below 50°C . was reached. The 2 min. rise time for the hydraulic pressure, on the other hand, was fast enough for dendritic growth if the isothermal crystallization temperature picked had been too low for single-crystal growth.

Analysis

Analysis of the resulting crystals was carried by means of an optical interference microscope. The morphology of each sample was noted and, in the case of single-crystal platelets, the thickness was measured according to the method described in reference 6. All samples were mounted in air on a microscope slide, for a maximum difference in refractive index between sample and reference beam. The interference microscope has⁶ for this type of measurement under optimal conditions (widely separated, large, disturbance-free, single crystals) an intrinsic limitation of accuracy of $\pm 6\text{\AA}$. Each single platelet thickness determination was repeated at least five times, and from each crystal preparation five to eighteen different platelets were measured.

Results

Atmospheric Pressure Crystallization

Figure 2 gives the three distinct types of crystalline growth of polyethylene from dilute solution. A finely divided, irregularly structured, strongly birefringent material of considerable thickness, which was beyond the capability of measurement of the interference microscope of $\sim 100,000$ A., results in crystallization at temperatures above 90 – 92°C . This high-temperature material is shown in Figure 2a. After 14 days of crystallization at 94.1°C . a large part of the polyethylene was still not crystallized. The material formed in this way redissolved on slow heating ($\sim 1^\circ/\text{hr}$.) at 97 to 98.6°C .

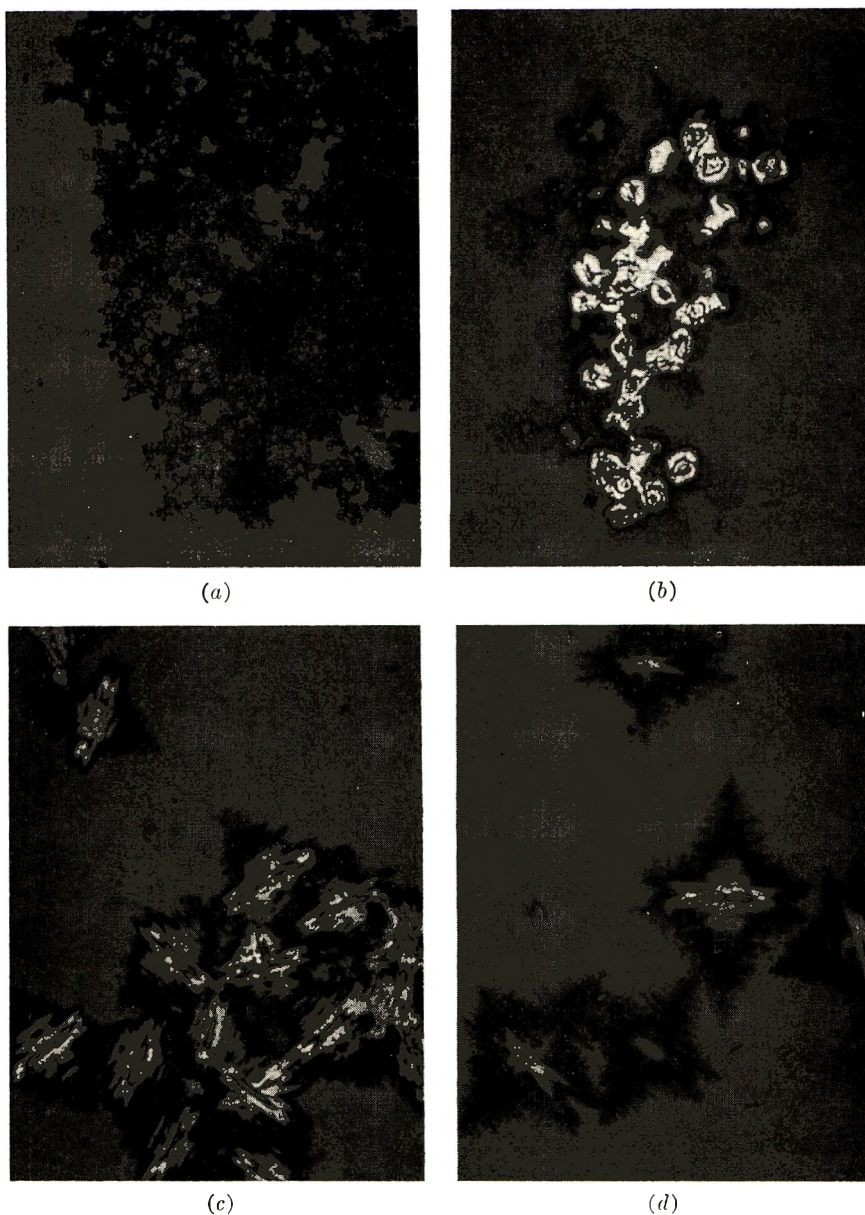


Fig. 2. Interference photomicrographs of polyethylene isothermally crystallized from 0.05% toluene solution at atmospheric pressure. The actual size of the long side of each figure is 0.13 mm. Crystallized at: (a) 94.1°C.; (b) 88.1°C.; (c) 73.8°C.; (d) 70°C.

Crystallization between 78 and 90°C. lead to the well-known single-crystal platelets shown in Figure 2b. Their platelet thickness ranged from 127 Å. for the samples crystallized at 82.3°C. to 150 Å. for the material crystallized at 88.1°C. On relatively quick reheating the turbid

suspension of crystals in toluene cleared completely between 94–95°C. Increasing amounts of material similar to the high-temperature polyethylene formed on slower heating, and persisted up to the dissolution temperature of this high-temperature material.

Crystallization at 73.8°C. and lower led to increasingly feathery dendrites, shown in Figures 2c and 2d. These show the steep-angle six-ended type described previously for this concentration.⁵ The dissolution of the dendrites is a complicated process. Microscopically detectable changes in the structure appear already at approximately 80–85°C. (A complete report on the dissolution of dendrites will be given in the future.)

Figure 1 gives the visually determined approximate appearance times as a function of the temperature of crystals isothermally crystallized from the 0.05% polyethylene solution in toluene. Different preparations varied by a factor of as much as 3, indicating that perhaps heterogeneous nucleation is of considerable importance. Refined data, obtained with better methods of detection and a mote-free solution, are necessary before conclusions may be drawn about the nucleation and subsequent growth kinetics. The appearance times of all types of crystals fitted on the same graph. Dendritic growth was found for appearance times of 2 min. or less, while single-crystal growth was not observed for times longer than approximately 300 min. This result gives the basis for the analysis of samples crystallized under high pressure or when crystallization is incomplete.

High-Pressure Crystallization

Crystallization at elevated pressures gave the results which are summarized, together with the atmospheric pressure results, in Figure 3. Figure 4 shows a cross section at 140.5°C. Figure 4a shows feathery dendrites grown at 5200 atm. This type of dendrite is always found at temperatures and pressures far above the solid dividing line in Figure 3. Figure 4b

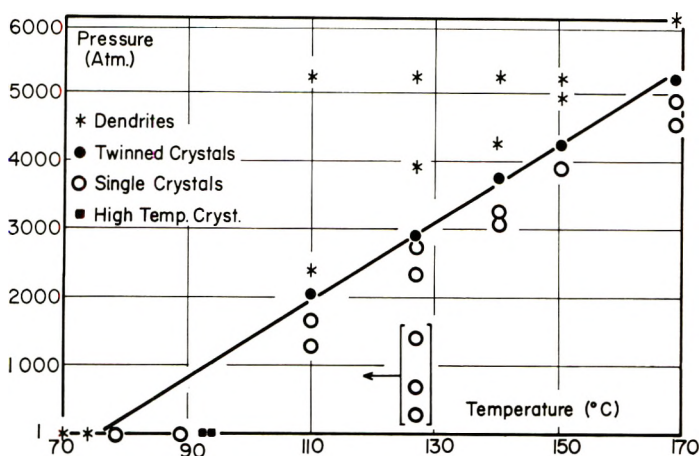


Fig. 3. Morphology of polyethylene crystals grown from 0.05% toluene solution under constant pressure and temperature (see text).

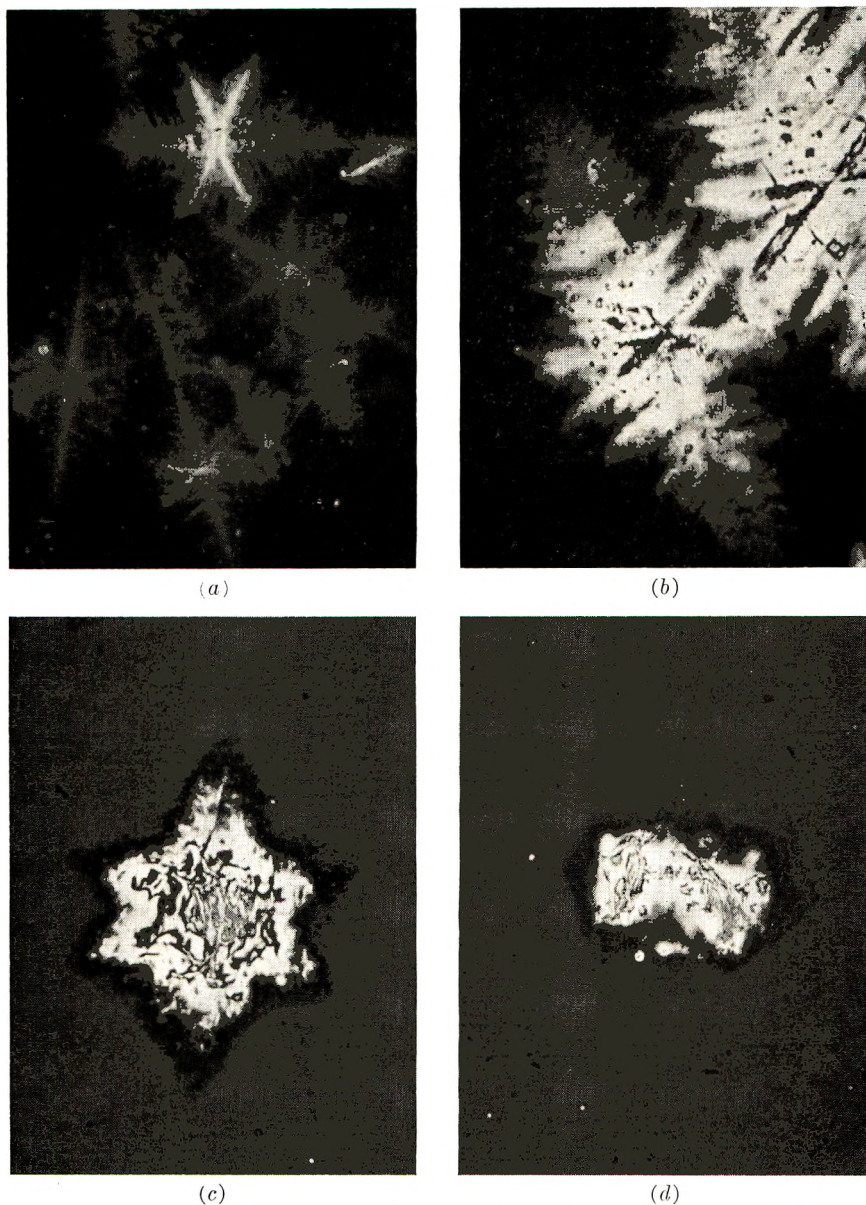


Fig. 4. Interference photomicrographs of polyethylene crystallized at 140.5°C . at varying pressures. The actual size of the long side of each figure is 0.13 mm. Crystallized at: (a) 5200 atm.; (b) 4050 atm.; (c) 3570 atm.; (d) 3230 atm.

shows dendrites grown at 4050 atm., close to the dendrite single-crystal dividing line. Right at the changing point, 3570 atm., an intermediate structure crystallizes (Fig. 4c); these crystals are of a platelet type, but have already the twinning found in the dendrites grown at higher pressures, described previously.¹³ The exact crystallization temperature at lower

pressures is not known although, from a comparison with the time scale of Figure 1, it appears likely that only the values bracketed in Figure 3 have crystallized at appreciably lower temperatures. Figure 4d is an example of a single-crystal cluster grown at 3230 atm., close to the dividing line.

The points in Figure 3 that indicate growth of these six-ended crystals (filled circles) lie on a straight line with a standard deviation of a single determination of $\pm 1^\circ\text{C}.$:

$$t_{\text{cryst}} = 75.2 + (1.79 \times 10^{-2})p$$

The crystallization temperature t_{cryst} is expressed in degrees centigrade, and the crystallization pressure p in atmospheres. Extrapolation to atmospheric pressure gives $75.2^\circ\text{C}.$ for the temperature at which dendritic growth goes over into single-crystal growth. This accords well with the experiments.

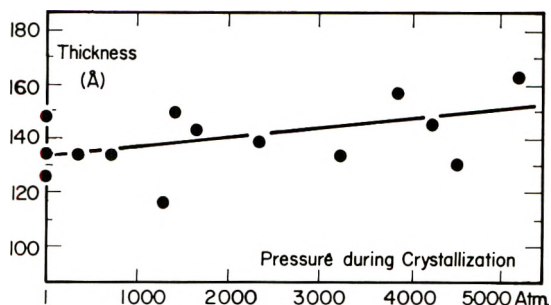


Fig. 5. Thickness of single-crystal platelets of polyethylene grown at various pressures.

Lamella thicknesses of all samples showing large enough crystals for measuring is plotted in Figure 5 as a function of pressure. The obvious result is that despite an increase in temperature of crystallization of approximately $90^\circ\text{C}.$ there has been only a slight increase in thickness. A least-squares expression for all samples results in a thickness of:

$$l = 134 + (3.08 \times 10^{-3})p$$

The thickness l is given in angstroms and the crystallization pressure p in atmospheres. The standard deviation of a single point is ± 12 Å. This relatively large scattering is due partially to the fact that the possible range of crystallization temperature is about $10^\circ\text{C}.$, which will be discussed below, is a critical factor in determining the thickness of the crystals.

The dissolution temperature of all single-crystal samples was 93 – $95^\circ\text{C}.$, comparable to that of the atmospheric-pressure samples. No dependence on the crystallization pressure was found.

Discussion

Discussion of the results centers around three points: (a) the types of growth found at atmospheric pressure, (b) the slope of the line dividing

dendritic growth from single-crystal growth as a function of pressure, and (c) the thickness of single crystals grown at elevated temperature and pressure.

Type of growth. Figure 2 shows that plateletlike growth was achieved only over a limited range of temperature ($\sim 15^\circ\text{C}$). The upper limit under the conditions of this series of experiments was $90 \pm 2^\circ\text{C}$. An upper limit of plateletlike growth is also predicted by the fluctuation theory of Frank and Tosi.¹¹ At this upper limit T' , and up to the maximum dissolution temperature T_m , the thickness to which the lamellae thickness (l^{**}) converges¹¹ is l_0 , which is the equilibrium thickness of a large lamella or the thickness for which the further growth rate is zero.⁹ If l_0 is expressed in number of CH_2 units and if g is the free energy of dissolution per bulk CH_2 unit, then:

$$l_0 g = \sigma_f \times \text{fold area} \quad (1)$$

where σ_f is the fold-surface free energy per square centimeter and the cross-sectional area for polyethylene is $18.5 \times 10^{-16} \text{ cm}^2$. The value g can be expressed in terms of the heat of dissolution per cubic centimeter, Δh_f (approximated by the heat of fusion, $2.8 \times 10^9 \text{ erg/cm}^3$), T_m , and of the supercooling $\Delta T (= T_m - T)$:

$$g = \Delta h_f \Delta T (\text{CH}_2 \text{ volume}) / T_m \quad (2)$$

The volume of one CH_2 unit is $2.31 \times 10^{-23} \text{ cm}^3$. At T' Frank and Tosi¹¹ found that:

$$g = \sigma_s \times \text{average side area} \quad (3)$$

where σ_s is the side-surface free energy of the crystallized polyethylene. The average area of one side is $5.25 \times 10^{-16} \text{ cm}^2$. Identification of T' with the 90°C . found for the upper limit of single crystals and extrapolation of the thickness of lamellae to this temperature ($l^{**} = l_0 \approx 120 \text{ CH}_2$ units) give the ratio 17.0 for σ_f/σ_s . Assuming T_m to be $105\text{--}110^\circ\text{C}$. gives values of $83\text{--}110 \text{ erg/cm}^2$ for σ_f and 4.9 to 6.5 erg/cm^2 for σ_s .

The surface free energy values would correspond to $4400\text{--}5800 \text{ cal./mole}$ of folds. These high values could be rationalized by estimating the effect of the 4,5 *gauche* positions in the folds¹⁴ as being $3200\text{--}4000 \text{ cal.}$ and the torsional strain as $1000\text{--}2000 \text{ cal.}$ The packing of the folds is less perfect. If one takes the folds to be 65% crystalline only,¹⁵ one may find that this adds as much as 1900 cal. to the total (estimated from the density of folds of only $\text{C}_{12}\text{H}_{24}$).¹⁶

Slope of Line. The slope of the dividing line between dendrites and single-crystal platelets is $1.79 \times 10^{-2} \text{ }^\circ\text{C.} \times \text{atm.}^{-1}$ (see Fig. 3). This value can be compared with the change in bulk melting and crystallization temperatures with pressure. Parks and Richards¹⁷ and Matsuoka¹⁸ found a value of $0.02^\circ\text{C.} \times \text{atm.}^{-1}$ for the range from one to approximately 2000 atm. Measurements with paraffins (C_9 to C_{24}) showed that for a wider range of pressure the melting point increase is not strictly linear but be-

comes less at higher pressures. The average of eighteen determinations¹⁹ made on different paraffins in this range from one to 5000 atm. was $1.85 \times 10^{-2} \text{ } ^\circ\text{C.} \times \text{atm.}^{-1}$ ($\pm 0.3 \times 10^{-2}$).

The conclusion which can be drawn from this is that the dividing line between single-crystal and dendritic growth is largely parallel to the maximum melting point versus pressure curve and also very probably parallel to the maximum dissolution temperature versus pressure curve. Single crystals grown at pressures of a constant horizontal distance from the line in Figure 3 thus can be looked upon as being grown at constant supercooling ΔT .

Thickness of Crystals. The thickness of single crystals as a function of pressure is given in Figure 5. As a first approximation this thickness stays constant—in accord with any theory showing an inverse ΔT dependence of the thickness, since ΔT has been kept approximately constant. The deviations of thickness of crystals grown at only slightly different pressures can be explained largely by ΔT differences (see especially the 1-atm. values). The variation in ΔT is estimated to be $\pm 5^\circ\text{C.}$, the crystals being formed at 0 – 10° below T' , which corresponds at atmospheric pressure to an appearance time of 300 to 10 min.

The second approximation shows a slight increase in thickness with pressure, the pressure coefficient l/l_{atm} being $2.3 \times 10^{-5} \text{ atm.}^{-1}$. This is about half the increase which would be expected from a T_m proportionality of the thickness. The pressure coefficient of T_m , which is $T_m/T_{m,\text{atm}}$, is $5.1 \times 10^{-5} \text{ atm.}^{-1}$.

The kinetic theory in its present form¹¹ shows that close to the upper limit of plateletlike growth the thickness is determined by eq. (1). When l_0 is expressed in angstroms, it leads to the expression:

$$l_0 = 2\sigma_f T_m / \Delta h_f \Delta T$$

The ΔT and T_m dependence express properly the observed slight variation. The remaining small discrepancy of $-2.8 \times 10^{-5} \text{ atm.}^{-1}$ may stem from the variation of the ratio $\sigma_f / \Delta h_f$ with pressure. Measurements of polyethylene¹⁷ and paraffins¹⁹ show that increasing pressure increases Δh_f , however, nothing is known about the pressure dependence of σ_f .

The equilibrium theory advanced by Peterlin and Fischer⁷ leads to somewhat less quantitatively usable equations. There the variation in thickness is thought to be caused chiefly by the variation of the longitudinal potential Φ with temperature. This potential decreases with increasing temperature, but increases with increasing pressure. Analysis of experimental data^{17,19-21} shows, however, that the effect of pressure is larger than the effect of increased crystallization temperature, so that, qualitatively, one would expect thinner crystals, owing to an increased Φ .

A third theory, advanced by Huggins,⁸ takes the too close approach of hydrogens within the chains as the reason for a slight helical twist which leads to a structure limit for long-chain crystals. At a chain length cor-

responding to the limit of helical twist which is set by the packing of neighboring chains, reversal of the chain (folding) occurs and relieves the strain.

Experimental x-ray determinations of spacings under pressure²² show that the dimensions along the chain change less than one-tenth as much than those at right angles to the chain. As a first approximation one can take, thus, the H—H distances along the chain as being constant. The intermolecular H—H distances, however, decrease more with change in pressure than the corresponding increase in temperature expands the lattice.²³ One would expect, on the basis of this structural theory, a decrease in twist limit with an increase in pressure of crystallization, contrary to the experimental results.

With respect to the growth of single crystals from solution, at this stage of the development of theories, only the kinetic theory seems to support the experiments presented here.

This research was supported in part by the Office of Naval Research and the Advanced Research Projects Agency. Their support is gratefully acknowledged.

References

1. Fischer, E. W., *Z. Naturforsch.*, **12a**, 753 (1957).
2. Keller, A., *Phil. Mag.*, **2**, 1171 (1957).
3. Till, P. H., *J. Polymer Sci.*, **17**, 447 (1957).
4. Keller, A., *Makromol. Chem.*, **34**, 1 (1959).
5. Wunderlich, B., and P. Sullivan, *J. Polymer Sci.*, **61**, 195 (1962).
6. Wunderlich, B., and P. Sullivan, *J. Polymer Sci.*, **56**, 19 (1962).
7. Fischer, E. W., *Z. Naturforsch.*, **14a**, 584 (1959); *idem.*, *Ann. N. Y. Acad. Sci.*, **89**, 620 (1961); Peterlin, A., and E. W. Fischer, *Z. Physik.*, **159**, 272 (1960).
8. Huggins, M. L., *J. Polymer Sci.*, **50**, 65 (1961).
9. Lauritzen, J. I., and J. D. Hoffman, *J. Research Natl. Bur. Standards*, **64A**, 73 (1960).
10. Price, F. P., *J. Polymer Sci.*, **42**, 49 (1960).
11. Frank, F. C., and M. Tosi, *Proc. Roy. Soc. (London)*, **263A**, 323 (1961).
12. Wunderlich, B., *Rev. Sci. Instr.*, **32**, 1424 (1961).
13. Wunderlich, B., and P. Sullivan, *Polymer*, **3**, 247 (1962).
14. Frank, F. C., private communication.
15. Wunderlich, B., and D. Poland, *J. Polymer Sci.*, to be published.
16. Müller, A., *Helv. Chim. Acta*, **16**, 155 (1933).
17. Parks, W., and R. B. Richards, *Trans. Faraday Soc.*, **45**, 203 (1949).
18. Matsuoka, S., *J. Polymer Sci.*, **42**, 511 (1960).
19. Nelson, R. R., W. Webb, and J. A. Dixon, *J. Chem. Phys.*, **33**, 1756 (1960).
20. Weir, C. E., *J. Research Natl. Bur. Standards*, **53**, 245 (1954).
21. Bridgman, P. W., *Proc. Am. Acad. Arts Sci.*, **76**, 55 (1948).
22. Müller, A., *Proc. Roy. Soc. London*, **A178**, 227 (1941).
23. Kabalkina, S. S., and Z. V. Troitskaya, *Zhur. Strukturnoi Khim.*, **2**, 27 (1961); Kitaigorodskii, A. I., and Yu. V. Mnyukh, *Doklady Akad. Nauk SSSR*, **121**, 2 (1958).

Résumé

On a cristallisé isothermiquement du polyéthylène linéaire à partir d'une solution toluénique à 0.05% à pression atmosphérique et sous pression hydrostatique de 6000 atm. A pression atmosphérique, une structure inconnue formée à haute température a été reconnue qui cristallise au-dessus de 90°C. Des cristaux lamellaires simples ont

cristallisé entre 75 et 90°C. Des dendrites se sont formées en-dessous de 75°C. La température séparant la croissance des dendrites de la simple croissance cristalline augmente avec l'augmentation de pression. L'épaisseur des cristaux croît à refroidissement approximativement constant, mais augmente seulement légèrement à température et pression élevée. On esquisse une discussion à la lumière des théories existant actuellement.

Zusammenfassung

Lineares Polyäthylen wurde isotherm aus 0.05% Toluollösung bei Atmosphärendruck und bei hydrostatischen Drucken bis zu 6000 atm. kristallisiert. Unter Atmosphärendruck wurde eine Hochtemperaturform gefunden, die oberhalb 90°C kristallisiert. Einkristall-Lamellen kristallisieren zwischen 75 und 90°C. Dendritische Kristalle wurden unterhalb 75°C gefunden. Die Temperatur, die dendritisches Wachstum von Einkristallwachstum trennt, steigt mit wachsendem Druck an. Die Dicke der Kristalle, die bei etwa konstanter Unterkühlung, jedoch bei erhöhter Temperatur und erhöhtem Druck gezüchtet wurden, wuchs nur wenig an. Eine Diskussion im Lichte der heutigen Theorien wird versucht.

Received December 26, 1961

Revised February 5, 1962

Grafting Vinyl Polymers onto Cellulose by High Energy Radiation. I. High Energy Radiation-Induced Graft Copolymerization of Styrene onto Cellulose*

R. Y.-M. HUANG, B. IMMERGUT,[†] E. H. IMMERGUT,[‡] and W. H. RAPSON, *Department of Chemical Engineering and Applied Chemistry, University of Toronto, Toronto, Ontario, Canada*

Synopsis

Styrene has been grafted onto cellulose in the form of cotton linters, cotton cloth, and rayon by ionizing radiation. Styrene was brought into intimate contact with cellulose by extension of the "inclusion" technique of Staudinger and Krässig, and graft copolymers were prepared by exposure to high energy electrons or to gamma-rays from Co⁶⁰. Substantial grafting was obtained by irradiation in air, nitrogen, or in vacuum. The products were purified by exhaustive extraction with benzene in a Soxhlet apparatus to remove the polystyrene homopolymer. The graft copolymers were characterized by removing the cellulose backbone by hydrolysis and determining the molecular weights of the residual polystyrene. Molecular weights of the grafted polystyrene were found to be considerably higher than those of the extracted homopolymer polystyrene or the polystyrene formed by irradiating styrene in bulk. Calculations based on the molecular weights of cellulose and polystyrene in the graft copolymer indicate that despite the substantial grafting, only one in 5,000-10,000 anhydroglucose units or one in 10-20 cellulose chains carried a grafted polystyrene chain.

INTRODUCTION

High energy radiation-induced graft copolymerization of vinyl monomers onto various polymeric substrates has been the subject of extensive studies in recent years. Relatively little information has been available, however, on the radiation-induced grafting of vinyl monomers onto cellulose. Magat and Tanner¹ in a Belgian patent describe the use of ionizing radiation to modify cellulosic fibers with vinyl monomers. No mention is made in the patent of the amount of grafting and radiation doses described are very high. Other attempts to graft vinyl monomers directly onto cellulosic fibers by means of high energy radiation have resulted in very low grafting.²

When cellulose is irradiated by high energy radiation, the main effects are

* Presented at the Symposium on Block and Graft Copolymers of Cellulose and Polysaccharides, Division of Cellulose Chemistry, 138th National Meeting, American Chemical Society, New York, N. Y., September 1960.

[†] Present address: Polytechnic Institute of Brooklyn, Brooklyn, N. Y.

[‡] Present address: Interscience Publishers, a Division of John Wiley Sons, Inc., New York, N. Y., and Polytechnic Institute of Brooklyn, Brooklyn, N. Y.

the formation of carbonyl and carboxyl groups and degradation or chain scission.³ Free radicals are also formed during the irradiation, and their presence has been detected by electron spin resonance spectroscopy.⁴ Recently, Florin⁵ has investigated the electron spin resonance of gamma-ray irradiated cellulose and obtained an approximate G (radical) value of 2.6 for dry cotton cellulose. The free radicals which were formed in the cellulose survived for a long time, decaying only moderately in several months.

It should thus be possible to graft monomers such as styrene onto cellulose through free radicals which are formed on the cellulose backbone. In our preliminary experiments on grafting onto cellulose, it was found that styrene could not be grafted to cellulose simply by soaking it in the monomer and exposing to high energy radiation, even at very high radiation doses. This was presumed to be due to the inability of styrene to diffuse into the inner regions of the cellulose to the sites of active free radicals. In order to induce graft copolymerization, it is necessary, therefore, that styrene be present at the sites of free radical formation or be able to diffuse to them before their termination. The "inclusion" technique, which was originally used by Staudinger⁶ and Krässig⁷ to include nonswelling compounds such as benzene into cellulose in order to enhance the esterification of cellulose, was applied in the present work to include styrene into swollen cellulose and thus make it more available for grafting. Substantial grafting of styrene onto cellulose was obtained by irradiating the styrene-included cellulose with high energy electrons or with gamma-rays. This paper reports the factors affecting the amount of grafting and presents data on a quantitative investigation of the graft copolymer and homopolymer formed.

Since initiation of this work, Arthur et al.⁸ and Usmanov⁹ have reported the radiation grafting of acrylonitrile onto cellulose. Okamura et al.¹⁰ have grafted styrene onto cellulose by swelling it in formamide-methanol and then irradiating it in styrene-methanol solution. Kobayashi¹¹ has recently investigated the grafting of styrene onto cellulose by means of a preirradiation technique in the presence of hydrogen peroxide. Chapiro and Stannett¹² have studied the effect of diffusion on the direct radiation grafting of styrene onto hydrophilic polymer substrates.

EXPERIMENTAL

Materials

Purified cotton linters and cotton cloth were used. Cotton linters, kindly provided by the Buckeye Cellulose Corporation, Memphis, Tenn., had an α -cellulose content of 99.7% with an average D.P. of 2170. It was used as obtained. Bleached cotton sheeting was purified by extracting with 95% methanol in a Soxhlet apparatus for 2 hr., boiling in 1% sodium hydroxide, and then washing thoroughly with water.

Styrene monomer (Eastman Organic Chemicals Highest Purity) was purified in the usual manner by removing the inhibitor with 10% sodium hydroxide solution, washing, and drying overnight over calcium chloride. It was then distilled under vacuum and used immediately after distillation.

Technical grade methanol was used for the initial stages of the inclusion treatment, and pure methanol (Fisher ACS Grade) was used for the final stages.

Preparation of Samples

The inclusion of styrene monomer into the cellulose was carried out according to the methods described by Staudinger⁶ and Krässig.⁷ The inclusion method was carried one step further by exchanging the benzene for styrene. A 5-g. portion of cotton linters of known dry weight was treated in a Hydrapulper with distilled water for 10 min. and then allowed to swell for 2 hr. The water was removed under suction and gradually exchanged for methanol. The methanol was exchanged five or six times, 100 ml. of methanol being used each time, and the time between exchanges was 2 hr. The methanol was exchanged twice with benzene by adding 100 ml. of benzene and allowing to stand 6 hr. The benzene was, in turn, finally exchanged twice with styrene. In later experiments, the benzene step was eliminated and the methanol exchanged directly three times with styrene. Cotton cloth was cut into strips 15×10 cm. and included in the same way. The amount of included styrene was usually two to three times the original dry weight of the cellulose. The included samples were placed in test tubes, stoppered in air, and flushed with nitrogen or sealed in vacuum according to the conditions of the experiment. For samples irradiated in vacuum, the tubes were evacuated by freezing and thawing and sealed under vacuum at 10^{-3} mm. In some experiments, additional styrene monomer was added to the included cellulose to study the effect of styrene monomer which was not included.

Polymerization of Styrene Monomer

Styrene monomer (10 ml.) was poured into test tubes and sealed under vacuum as described above or simply stoppered and irradiated in air to the required doses.

Degradation of Cellulose

Cotton cellulose (10 g. portion) was placed in a test tube, stoppered, and irradiated in air.

Irradiation

The irradiation with high energy electrons was carried out on a 2-M.e.v. Van de Graaff accelerator at the High Voltage Engineering Corporation in Burlington, Mass.

The gamma-ray irradiations were carried out at the laboratories of the Commercial Products Division, Atomic Energy of Canada Ltd., Ottawa, Ontario, in a Gammacell 220 Co⁶⁰ gamma-ray irradiation unit which had a central field strength of about 1.4×10^6 r./hr. Details of this irradiation facility are described elsewhere.¹³ The irradiations were performed at room temperature, but the temperature in the irradiation cavity

gradually increased due to the heat generated by absorption until it reached a maximum of 50°C. after 1 hr. of irradiation.

Separation of Homopolymer and Determination of Per Cent Grafting

After irradiation, the test tubes were opened and the contents soaked in 400 ml. of benzene overnight to extract the unreacted styrene and part of the polystyrene homopolymer. The sample was then placed in an extraction thimble and extracted continuously with benzene in a Soxhlet apparatus for 72 hr. The graft polymer was then dried and weighed. The increase in weight was taken to be the amount of grafted polystyrene. The per cent grafting is calculated as the ratio of the weight increase to the weight of the original cellulose (dry basis) $\times 100$. The extracted polystyrene homopolymer was determined gravimetrically by pouring the benzene solution into a large excess of methanol to precipitate the polystyrene. The per cent polymerization of styrene monomer by gamma-irradiation was determined by the same method. The grafting efficiency is defined as the weight ratio of the grafted polystyrene to the homopolymer in the irradiated mixture.

Molecular Weight Determinations

The molecular weight of polystyrene was determined by viscometry in benzene solution in a Cannon-Ubbelohde dilution viscometer, size 50, at 30°C. The average molecular weight was calculated from the intrinsic viscosity by use of the equation $\bar{M}_n = 167,000[\eta]^{1.37}$ by Mayo et al.¹⁴ for unfractionated polystyrene. The molecular weight of cellulose was determined by measuring viscosity in 0.5*M* cupriethylenediamine solution at 25°C. in a Cannon-Fenske viscometer, size 100. The specific viscosities were measured at 0.0625, 0.1250, and 0.2500 g./100 ml. and extrapolated to zero concentration to obtain the intrinsic viscosity. The number-average molecular weight was calculated from the Mark-Houwink equation: $[\eta] = K\bar{M}_n^\alpha$, the constants $K = 1.33 \times 10^4$ and $\alpha = 0.905$ recommended by Immergut, Rånby, and Mark¹⁵ being used.

Hydrolysis of the Graft Copolymer

The styrene cellulose graft copolymers were ground to -40 mesh in a Wiley mill and hydrolyzed for 48 hr. in constant boiling hydrochloric acid. The residue after hydrolysis was washed, dried, and dissolved in benzene and the polystyrene isolated by precipitation into methanol.

RESULTS AND DISCUSSION

The effect of gamma-ray irradiation on cellulose and on the styrene monomer in bulk was investigated, since previously published data have been based on irradiation by Co⁶⁰ sources of lower intensity.

Degradation of Cellulose

The degradation of cotton cellulose in air by gamma-ray irradiation at different dose levels is given in Table I and shown in Figure 1. An approx-

TABLE I
Degradation of Cellulose by Gamma-Irradiation

Total radiation dose, $\times 10^{-6}$, r.	Intrinsic viscosity (CED), [η], 100 ml./g.	DP
0	11.10	1676
0.1	8.45	1252
0.5	5.78	823
1.0	4.06	557
2.0	2.92	387
5.0	1.82	202
10.0	0.98	116
50.0	0.33	35
100.0	0.18	18

imately linear relationship is obtained when DP is plotted against radiation dose on a log-log scale. This shows good agreement with previous work by Blouin and Arthur³ and confirms their conclusion that degradation is a function of total radiation dose and is independent of source intensity.

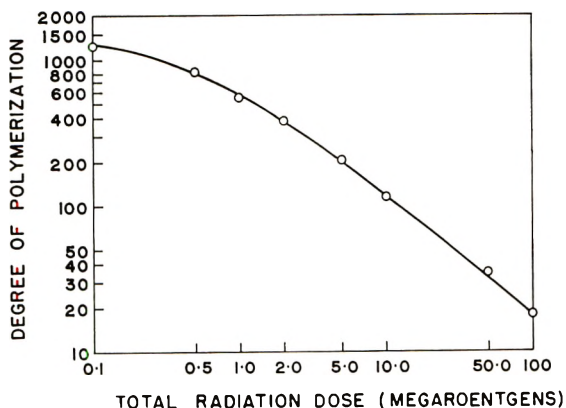


Fig. 1. Degradation of cellulose by gamma-irradiation (Co^{60} source central intensity 1.3×10^6 r/hr.).

Polymerization of Styrene Monomer in Bulk

The per cent polymerization of styrene monomer in bulk is shown in Figure 2 and is compared with the data of Chapiro and Sebban-Dannon,¹⁶ who used an x-ray source with a dose rate of 1.2×10^6 r./hr., and that of Ballantine et al.¹⁷ using gamma-rays from a Co^{60} source of 190,000 rep./hr. No data could be found in the literature for the polymerization of styrene with gamma-rays from a source comparable in intensity to the source used in this investigation. The per cent polymerization per megaröntgen is approximately 1.4. For styrene irradiated in vacuum, the per cent polymerization is higher at low doses, but above 1 Mr the values in vacuum and in air are approximately the same. The reduced efficiency of high intensity sources results from the fact that a higher proportion of primary radicals

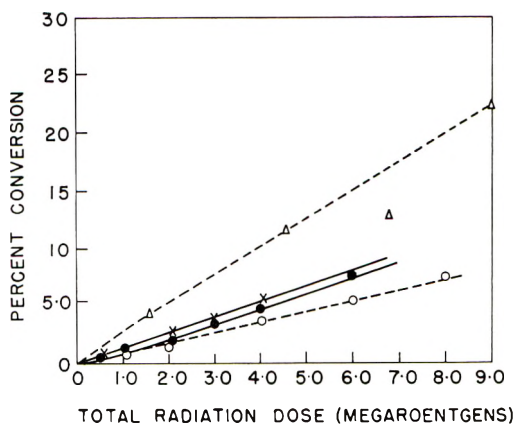


Fig. 2. Polymerization of styrene monomer by gamma-irradiation: (X) irradiated in vacuum; (●) irradiated in air; (Δ) data of Ballantine et al.,¹⁷ gamma-rays, 190,000 rep/hr.; (O) data of Chapiro and Sebban-Dannon,¹¹ x-rays, 1.2×10^6 r/hr.

formed react with growing polymer chains or cross-terminate themselves rather than initiate further polymerization. Under the radiation doses used in our experiments (1–4 Mr) the homopolymerization in styrene is therefore only of the order of 2–6%.

Grafting onto Cellulose by Irradiation with High Energy Electrons

The first part of the investigation was carried out by irradiation with high energy electrons from a 2 M.e.v. Van de Graaff accelerator. The grafting results are shown in Table II. These results show conclusively that very little, if any, grafting can be obtained by simply soaking the cotton cellulose in styrene monomer and irradiating, whereas the included cellulose samples show substantial grafting. An interesting observation was that when the samples were stored after irradiation, the amount of grafted material increased with time, which indicates that the grafting reaction continues even after the irradiation. This is in keeping with the observations of Florin,⁵ who found that free radicals formed by gamma-ray

TABLE II
High Energy Electron-Induced Radiation Grafting of Styrene onto Cellulose

	Radiation dose $\times 10^{-6}$, r	Grafting, %, at various contact times after irradiation		
		2 days	7 days	14 days
Styrene included	0	1.5	6	16
in	0.2	10	36	64
cellulose	2.0	30	56	73
	20.0	55	79	109
Styrene not	0.2	—	0.5	2.2
included	2.0	—	0.1	1.5
	20.0	—	1.2	13.2

irradiation could survive for a long time. Since it was difficult to obtain consistent results in these experiments due to the uneven penetration of the high energy electrons into the samples, later experiments were carried out with gamma-rays from a Co^{60} source.

Grafting onto Cellulose with Gamma-Ray Irradiation

The results of the gamma-ray induced graft copolymerization of styrene onto cotton cellulose are presented in Tables III and IV. As in the case of

TABLE III
Styrene-Cellulose Graft Copolymers formed by Gamma-Irradiation in Vacuum

Graft copolymer sample no.	Radiation dose, $\times 10^{-6}$, r	Grafting, %	Grafting efficiency
4-0	0	1.7	—
4-1	0.25	7.7	2.84
4-2	0.50	14.3	1.91
4-3	1.00	50.0	1.72
4-4	2.00	66.4	1.53
4-5	4.00	51.4	0.99
4-7 ^a	1.00	177.0	
4-8 ^a	1.00	169.2	
4-9 ^a	2.00	158.3	
4-10 ^a	2.00	166.7	

^aPost-irradiation heat treatment, 100°C., 48 hr.

TABLE IV
Styrene-Cellulose Graft Copolymers formed by Gamma-Irradiation in Air

Graft copolymer sample no.	Radiation dose $\times 10^{-6}$, r	Grafting, %	Grafting efficiency	Note
5-1	1.00	27.8	1.59	Styrene included in cellulose
5-3	2.00	82.9	1.39	
5-7	4.00	111.2	1.08	
5-2	1.00	26.4	1.03	Styrene included additional styrene added
5-4	2.00	71.6	1.00	
5-8	4.00	124.9	1.10	
5-5	1.00	107.4	—	Styrene included in cellulose and post-irradiation heat treatment 100°C., 48 hr.
5-6	1.00	110.2	—	
5-10	2.00	197.0	—	
5-20	0.50	4.9	—	Styrene not included
5-21	1.00	4.5	—	
5-22	2.00	3.3	—	
5-23	4.00	4.6	—	
5-24	6.00	4.2	—	

TABLE V
 Radiation Grafting of Styrene onto Cotton Cloth

Radiation dose $\times 10^{-6}$, r	Grafting, %					
	Included cloth			Included cloth suspended in styrene		
	Vacuum	Nitrogen	Air	Vacuum	Nitrogen	Air
0	3.3	4.2	3.4	2.3	4.5	3.7
0.25	14.6	3.9	6.4	16.5	6.6	7.2
0.50	45.8	5.9	—	51.6	8.4	17.0
1.00	53.3	11.9	50.3	50.8	21.6	54.7
2.00	56.6	30.5	50.4	63.8	30.5	64.9
3.00	56.9	41.2	—	72.3	56.5	67.2
4.00	57.6	35.8	54.7	72.3	56.0	70.5

high energy electron irradiation, when styrene was not "included" in the cellulose, very little grafting occurred as compared to the considerable amount of grafting obtained after the inclusion treatment of the cellulose irradiated in vacuum and in air. The presence of air appears to enhance rather than inhibit the grafting reaction at radiation doses above 2×10^6 r. In the low radiation dose range, grafting is more effective in vacuum. Geacintov et al.¹⁸ have found that in ultraviolet-induced grafting onto cellulose a little oxygen enhances the grafting and plays an important role in the intermediate radical mechanism. It is possible that oxygen plays a similar role in our experiments. When the samples irradiated *in vacuo* were subjected to post-irradiation heating in an oven for 48 hr. at 100°C ., the amount of grafting increased sharply. The increased grafting can be attributed to the reaction with remaining free radicals or to peroxide groups which are decomposed and available for further grafting. The results obtained for grafting onto cotton cloth are given in Table V.

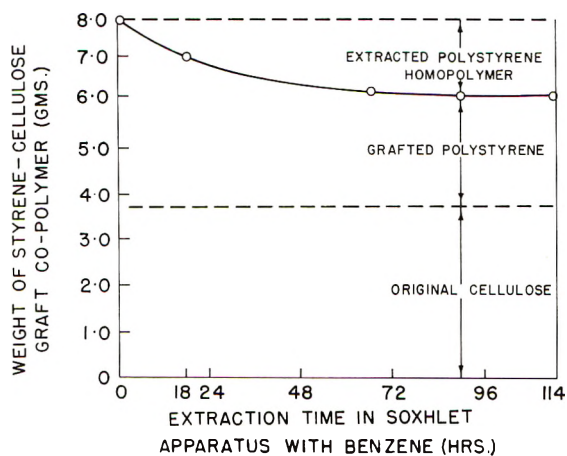


Fig. 3. Extraction curve of styrene-cellulose graft copolymer.

Extraction of the Irradiated Mixture

A typical extraction curve of the irradiated mixture is shown in Figure 3. Most of the nongrafted polystyrene was extracted in the first 48 hr. of cold extraction in benzene followed by Soxhlet extraction. Practically no polystyrene homopolymer could be removed after 72 hr. of extraction. In some experiments, the Soxhlet extractions were continued for one week, but very little further homopolymer could be removed. The grafting efficiency or quantitative ratio of the grafted polystyrene to extracted homopolymer was determined and is shown in Tables III and IV. The grafting efficiency is approximately the same for samples irradiated in vacuum and air at higher grafting values and decreases from 1.7 to 1.0 with increasing radiation dose, i.e., more homopolymer is formed at high radiation doses.

Characterization of the Graft Copolymers and the Polystyrene Homopolymer

Drastic hydrolysis of the cellulose backbone was carried out to isolate and characterize the grafted polystyrene chains. Hydrolysis in constant boiling hydrochloric acid produced a residue which was partly soluble in benzene. Several other methods of hydrolysis were tried, but these yielded only gellike residues which swelled strongly in benzene but did not dissolve. Complete hydrolysis of the cellulose backbone could not be achieved. Results of the hydrolysis and molecular weights of the polystyrene residue are shown in Table VI. The soluble portion was identified as polystyrene by infrared spectrum analysis, but the spectrum failed to show any traces of the grafted endgroups of the hydrolyzed cellulose, due to the fact that the molecular weight of the polystyrene was too high and the endgroups therefore are too few for infrared detection. Microanalysis of one of the hydrolyzed residue samples was made by the Micro-Tech Laboratories, Skokie, Ill. and gave C 91.76% and H 7.84%, which values are close to the calculated values for polystyrene (C 92.18%, H 7.82%).

TABLE VI
Hydrolysis of Styrene-Cellulose Graft Copolymers and Molecular Weights of the Grafted Branches

Graft copolymer sample no.	Grafting, %	Weight loss on hydrolysis, % of original cellulose	Intrinsic viscosity in benzene of soluble residue $[\eta]$, 100 ml./g.	\bar{M}_n
5-1	27.8	93.3	2.42	560,500
5-3	82.9	95.3	2.52	592,400
5-7	111.2	92.9	2.47	576,400
5-2	26.4	93.3	1.94	414,000
5-4	71.6	97.5	2.08	441,300
5-8	124.9	94.3	1.89	399,400

The results of the molecular weight determinations of both the polystyrene homopolymer and the grafted polystyrene are shown in Table VII. It is obvious that the molecular weights of the grafted portion are considerably higher than those of the homopolymer. Previous investigators^{19,20} working with different grafting systems have reported that the chain lengths of the homopolymer are equal to the grafted branches. This, however, does not appear to be the general case, to judge from our experimental results, since the factors affecting the growth of a grafted chain are not necessarily the same as those of the homopolymer chain. It was also observed that the polystyrene homopolymer extracted from the irradiation mixture had a much higher molecular weight than the polystyrene obtained from the gamma-ray irradiation of styrene in bulk. The molecular weight of the extracted homopolymer is of the order of 150,000–200,000, whereas that of the polystyrene formed by irradiation of styrene is approximately 26,000. The high molecular weight of the homopolymer formed within the cellulose layers can be attributed to the fact that the chain termination is less likely to occur due to the restricted movement of the growing chains or to a gel effect. A similar effect has been observed independently by Kobayashi¹¹ in grafting onto cellulose using the preirradiation technique.

The insoluble portion of the grafted polystyrene swelled strongly in benzene but did not dissolve. This may be due to incomplete hydrolysis of the residual cellulose units or to crosslinking. The styrene–cellulose graft copolymer retained the physical appearance of the original cellulose but had widely different solubility properties. The solubility in 0.5*M* cupriethylenediamine (CED) is shown in Figure 4. Solubility in CED decreased with increasing grafting until the graft copolymer became insoluble at high grafting values. The graft copolymer was insoluble in solvents for polystyrene but swelled strongly in them due to the grafted polystyrene chains.

TABLE VII
Molecular Weights of Extracted Polystyrene Homopolymer and Polystyrene Formed by Gamma-Irradiation of Styrene in Bulk

Graft copolymer sample no.	Polystyrene extracted by cold benzene		Polystyrene extracted by benzene in Soxhlet	
	$[\eta]$ in benzene, 100 ml./g.	\bar{M}_n	100 ml./g.	\bar{M}_n
5-1	1.03	173,900	1.60	317,900
5-3	0.86	144,000	1.18	209,500
5-7	1.18	209,500	1.43	272,600
5-2	0.93	160,300	1.14	199,800
5-4	1.02	171,600	1.09	187,900
5-8	0.79	128,000	1.06	180,000
Polystyrene control (bulk radiation polymerization)	0.264 0.262	26,630 26,590		

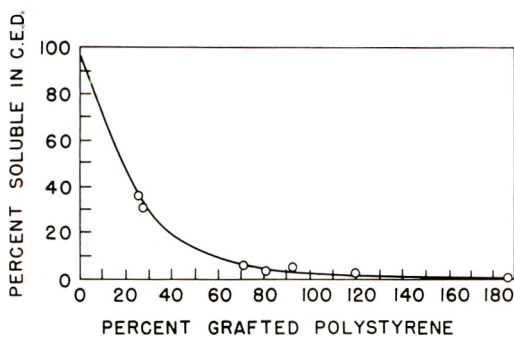


Fig. 4. Solubility of styrene-cellulose graft copolymer in 0.5M cupriethylenediamine.

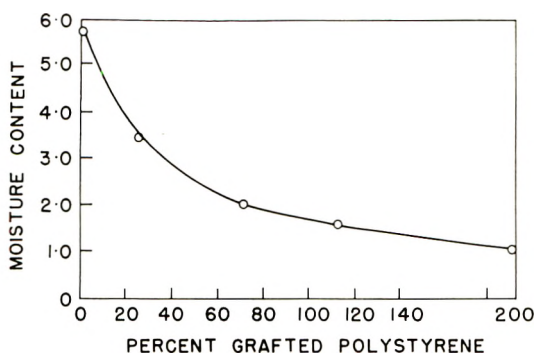


Fig. 5. Moisture absorption of the styrene-cellulose graft copolymer.

It was not wetted by water and even floated on the surface of CED unless it was continuously dispersed by stirring. The moisture absorption characteristics are shown in Figure 5.

Calculation of the Number of Grafted Polystyrene Branches

Calculations of the number of grafted polystyrene chains per cellulose chain and the number of anhydroglucose units having one grafted polystyrene branch were made by using the average molecular weights obtained for cotton cellulose at the respective radiation doses and for the grafted polystyrene. Results of the calculations are summarized in Table VIII. It can be seen that, despite the large weight ratio of grafted polystyrene, as the branches are very long, on the average only one in 10-20 cellulose chains has a grafted polystyrene branch or only one grafted polystyrene branch exists per 4,000-10,000 anhydroglucose units. These calculations lead to the important conclusion that in graft copolymerization onto cellulose or to any other substrate, it is important to be concerned not only with the amount of grafting but also with the distribution of grafted branches and their chain lengths. From the viewpoint of physical properties it may be desirable to produce cellulose graft copolymers having many grafted branches of lower molecular weight.

TABLE VIII
Number of Grafted Polystyrene Branches per Cellulose Chain

Graft co- polymer sample no.	Radiation dose $\times 10^{-6}$, r	Grafting, %	Wt. copolymer, g.	Wt. cellulose, g.	Wt. grafted, polystyrene, g.	\bar{M}_n		Poly- styrene chains per cellulose chain	Cellu- lose chains per polystyrene branch	Poly- styrene branches per anhydro- glucose unit $\times 10^4$	Anhydro- glucose units per polystyrene branch
						Cellulose	Grafted polystyrene				
5-1	1.00	27.8	6.6592	5.2099	1.4403	90,300	560,000	0.045	22	0.81	12,390
5-3	2.00	82.9	9.7583	5.3362	4.4221	62,700	592,400	0.087	11	2.24	4,464
5-7	4.00	111.2	11.4862	5.4377	6.0485	35,640	576,400	0.069	14	3.13	3,194
5-2	1.00	26.4	6.6200	5.2357	1.3843	90,300	414,000	0.057	17	1.02	9,804
5-4	2.00	71.6	9.0013	5.2451	3.7562	62,700	441,300	0.102	10	2.63	3,802
5-8	4.00	124.9	11.8843	5.2856	6.5992	35,640	309,400	0.111	9	5.04	1,984

Proof of Grafting

No direct evidence of a chemical linkage between the cellulose and the polystyrene has as yet been obtained, and work is at present in progress to provide chemical proof. The extraction and solubility data as well as the data on molecular weights of the grafted chains and the polystyrene homopolymer indirectly support the belief that most of the unextracted polystyrene is chemically grafted to the cellulose. In further support of the extraction data, a series of experiments was carried out in which the styrene was included in the usual way and then polymerized *in situ* not by gamma-ray irradiation but by (a) thermal initiation at 100°C. and (b) benzoyl peroxide initiator dissolved in the included styrene. Most of the polystyrene polymerized within the cellulose could be removed by extraction in a Soxhlet apparatus with benzene.

Grafting of polystyrene onto cellulose has been accomplished by swelling cellulose in water, extracting the water with methanol, extracting the methanol with styrene, and subjecting the so-called styrene "included" cellulose to high energy electrons or gamma rays. Because there was no grafting when cellulose immersed in styrene was irradiated, grafting was attributed to the "inclusion" procedure.

We wish to thank Mr. D. Rowat and his associates in the Development Chemistry Section, Commercial Products Division, Atomic Energy of Canada Ltd., for their interest and assistance during the irradiation experiments. One of us (R. Y.-M. Huang) wishes to acknowledge financial assistance in the form of a Rayonier of Canada Ltd. Chemical Engineering Research Fellowship, 1959-60.

References

1. Magat, E. E., and D. Tanner, Belg. Pat. 546,817 (1955).
2. Pan, H.-P., B. E. Proctor, and S. A. Goldblith, *Textile Research J.*, **29**, 422 (1959).
3. Blouin, F. A., and J. C. Arthur, Jr., *Textile Research J.*, **28**, 198 (1958).
4. Abraham, R. J., and D. H. Whiffen, *Trans. Faraday Soc.*, **54**, 1291 (1958).
5. Florin, R. E., personal communication; paper presented to the Division of Cellulose Chemistry, 138th National Meeting, American Chemical Society, September 1960.
6. Staudinger, H., and T. Eicher, *Makromol. Chem.*, **10**, 254 (1953).
7. Krässig, H., and E. Schrott, *Makromol. Chem.*, **13**, 179 (1954).
8. Arthur, J. C., Jr., R. J. Demint, R. J. McSherry, and J. F. Jurgens, *Textile Research J.*, **29**, 759 (1959).
9. Usmanov, Kh. U., B. I. Alkhodzahacv, and V. O. Azizov, *Vysokomolekulyarnye Soedineniya*, **1**, 1570 (1959).
10. Okamura, S., T. Iwasaki, Y. Kobayashi, and K. Hayashi, paper presented at the International Atomic Energy Conference on the Application of Large Radiation Sources in Industry and especially to Chemical Processes, Warsaw, Poland, September 1959.
11. Kobayashi, Y., *J. Polymer Sci.*, **51**, 359 (1961).
12. Chapiro, A., and V. Stannett, *Intern. J. Appl. Radiation and Isotopes*, **8**, 4 (1960).
13. Rice, F. G., and W. D. Smythe, *Ind. Eng. Chem.*, **52**, 5, 52A (1960).
14. Mayo, F. R., R. A. Gregg, and M. S. Matheson, *J. Am. Chem. Soc.*, **73**, 1691 (1951).
15. Immergut, E. H., B. G. Rånby, and H. F. Mark, *Ind. Eng. Chem.*, **45**, 2483 (1953).

16. Chapiro, A., and J. Sebban-Dannon, *J. Chim. Phys.*, **54**, 776 (1957).
17. Ballantine, D. S., P. Colombo, A. Glines, and B. Manowitz, *Chem. Eng. Progr. Symposium Series*, **50**, No. 11, 267 (1954).
18. Geacintov, N., V. T. Stannett, E. W. Abrahamson, and J. J. Hermans, *J. Appl. Polymer Sci.*, **3**, 54 (1960).
19. Mori, Y., Y. Minoura, and M. Imoto, *Makromol. Chem.*, **25**, 1 (1958).
20. Cooper, W., G. Vaughan, S. Miller, and M. Fielden, *J. Polymer Sci.*, **34**, 651 (1959).

Résumé

On a greffé du styrène sur de la cellulose sous forme de linters de coton, des tissus de coton et de rayonne par rayonnement ionisant. On a mis le styrène en contact intime avec la cellulose en utilisant la technique d'inclusion de Staudinger et Krässig, et on a préparé les copolymères greffés par exposition à des électrons à haute énergie ou à des rayons gamma du Co^{60} . On a obtenu un greffage substantiel par irradiation sous air, azote ou sous vide. On a purifié les produits par une extraction minutieuse avec du benzène dans un appareil de Soxhlet pour enlever le homopolystyrène. On a caractérisé les copolymères greffés en enlevant la chaîne cellulosique de base par hydrolyse et en déterminant les poids moléculaires du polystyrène résiduel. On a trouvé que les poids moléculaire du polystyrène greffé étaient considérablement plus grands que ceux du homopolystyrène extrait ou le polystyrène formé en irradiant le styrène en masse. Des calculs basés sur les poids moléculaires de la cellulose et du polystyrène dans le copolymère greffé indiquent que malgré le greffage substantiel, seulement une sur 5000 à 10000 unités anhydroglucoses ou une sur 10 à 20 chaînes cellulosiques portaient une chaîne greffée de polystyrène.

Zusammenfassung

Styrol wurde durch ionisierende Strahlung auf Cellulose in Form von Baumwolllinters, Baumwollzeug und Rayon aufgepfropft. Styrol wurde nach dem "Inclusions"-verfahren von Staudinger und Krässig mit Cellulose in innige Berührung gebracht und Pfcopolymeren durch Einwirkung hochenergetischer Elektronen oder von Co^{60} - γ -Strahlen hergestellt. Gute Aufpfropfung wurde durch Bestrahlung unter Luft, Stickstoff und im Vakuum erhalten. Die Produkte wurden durch erschöpfende Extraktion mit Benzol in einem Soxhletapparat zur Entfernung des Styrolhomopolymeren gereinigt. Die Pfcopolymeren wurden durch hydrolytische Entfernung der Cellulosehauptkette und Bestimmung des Molekulargewichts des zurückbleibenden Polystyrols charakterisiert. Das Molekulargewicht des aufgepfropften Polystyrols war beträchtlich höher als das des extrahierten Styrolhomopolymeren oder das des bei Bestrahlung von Styrol in Substanz gebildeten Polystyrols. Berechnungen auf Grundlage des Molekulargewichts der Cellulose und des Polystyrols im Pfcopolymeren zeigen, dass ungeachtet der guten Aufpfropfung, doch nur eine von 5-10000 Anhydroglukoseeinheiten oder eine von 10-20 Celluloseketten eine aufgepfropfte Polystyrolkette tragen.

Received December 26, 1961

Revised February 5, 1962

Polyethylene Terephthalate Structural Studies

P. G. SCHMIDT, *Film Department, Research and Development Division, Experimental Station, E. I. du Pont de Nemours and Company, Inc., Wilmington, Delaware*

Synopsis

The absorption intensity of a given infrared absorption band, in the infrared spectrum of an oriented polymer is composed of an orientation and a structural factor. A method is discussed, using polarized infrared radiation, which will measure the contribution of each. The ethylene glycol linkage of the polyethylene terephthalate molecule may exist in either of two forms. These forms are rotational isomers. The *trans* form of the molecule is the extended form, the *gauche* form is the relaxed form. The amorphous regions of polyethylene terephthalate films have been found to contain both of these isomers. Polymer orientation is summarized in terms of transition moment types. Orientation parameters characteristic of polyethylene terephthalate films are defined.

I. INTRODUCTION

The object of the work was to determine and measure the effects of orientation on polyethylene terephthalate structure. Infrared methods were chosen for this undertaking, since most orientation processes are reflected in one way or another in the polymer's infrared spectrum. These spectral variations usually occur in the form of absorption band intensity changes. In order to study changes in polyethylene terephthalate structure with changes in orientation, the factors which determine the magnitude of an absorption band intensity had to be isolated and measured.

II. THEORETICAL

A. Absorption Band Intensity Changes

There are two factors which influence the intensity of an absorption band. There is a configurational or structural factor and there is an orientation factor.

Structurally, the intensity of an absorption band is dependent upon the amount of material that it represents. For example, if a film undergoes some treatment that induces crystallization, bands characteristic of the crystalline regions would increase in intensity since there would be more of that structure present; bands characteristic of the amorphous regions would decrease in intensity, since there would be less of that structure

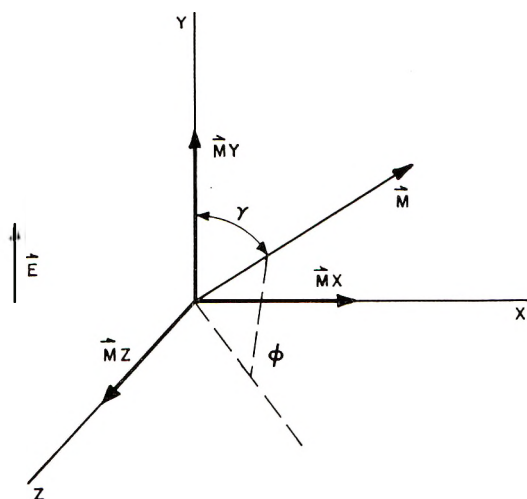


Fig. 1. Transition moment M in xyz coordinates of film: y = machine direction; x = transverse direction; z = normal direction.

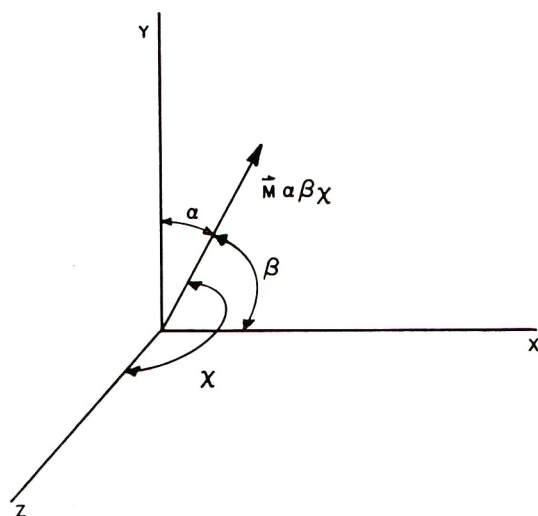


Fig. 2. Electric vector at angles $\alpha\beta\chi$ from xyz film axes.

present. A similar analogy can be made for molecules that undergo isomerization.

The intensity of an infrared band is also dependent upon the orientation of the electric vector of the incident radiation with respect to the absorbing dipole moment. The absorbing dipole moment is called the transition moment. This may best be illustrated by means of the following example. Consider a segment of a polymer chain, e.g., an ester group. Such a group has various normal modes of vibration which can be considered as characteristic group vibrations, such as the carbonyl stretching vibration where the transition moment is along the carbon oxygen bond axis. If we could

analyze one individual carbonyl group with plane-polarized radiation, we would observe a strong absorption band when the electric vector is parallel to the carbonyl bond. Radiation with the electric vector perpendicular to this bond would not be absorbed at all.

Consider this one transition moment located in the boundaries of a film at an angle γ from the y axis (machine direction) and at an angle ϕ from the x axis (transverse direction) in the xz plane (Fig. 1). When the electric vector of the incident radiation is parallel to the machine direction, the absorption intensity A_y , will be proportional to the projection of the absorbing transition moment (M_y^2) along the y axis of the film. Likewise the absorption intensities with the electric vectors parallel to the transverse and normal directions to the film will be proportional to the projections of the transition moment (M_x^2 , M_z^2) along the x and z axes of the film. The absorption intensity with the electric vector of the incident radiation at some angle α from the y axis, β from the x axis, and χ from the z axis (Fig. 2) can be expressed as a function of A_x , A_y , and A_z .

An actual film sample of polyethylene terephthalate contains many carbonyl transition moments oriented in various directions. The absorption intensity in any given direction is determined by the superposition of the contributions from each individual group. The absorption intensity in the y direction, for example, is obtained by integrating M_y^2 over all the individual transition moments in the sample.

General Form of Integrated Expressions. The total absorption intensity in the y direction is given by

$$A_y = \int_{\phi=0}^{\phi=2\pi} \int_{\gamma=0}^{\gamma=\pi/2} G(\gamma, \phi) M_y^2 d\gamma d\phi \quad (1)$$

where $G(\gamma, \phi)$ is the distribution function describing the individual polymer transition moments. In analogy, the total absorption $A_{\alpha,\beta,\chi}$ at any angle in the reference frame (Fig. 2) is given by

$$A_{\alpha,\beta,\chi} = \int_{\phi=0}^{\phi=2\pi} \int_{\gamma=0}^{\gamma=\pi/2} G(\gamma, \phi) M_{\alpha,\beta,\chi}^2 d\gamma d\phi \quad (2)$$

since from Figure 2,

$$M_{\alpha,\beta,\chi} = M_y \cos \alpha + M_x \cos \beta + M_z \cos \chi \quad (3)$$

Then

$$M_{\alpha,\beta,\chi}^2 = M_y^2 \cos^2 \alpha + M_x^2 \cos^2 \beta + M_z^2 \cos^2 \chi + 2M_x M_y \cos \alpha \cos \beta + 2M_x M_z \cos \alpha \cos \chi + 2M_y M_z \cos \beta \cos \chi \quad (4)$$

therefore

$$\begin{aligned} A_{\alpha,\beta,\chi} = & A_y \cos^2 \alpha + A_x \cos^2 \beta + A_z \cos^2 \chi \\ & + \int_{\phi=0}^{\phi=2\pi} \int_{\gamma=0}^{\gamma=\pi/2} 2M_x M_y \cos \alpha \cos \beta G(\gamma, \phi) d\gamma d\phi \\ & + \int_{\phi=0}^{\phi=2\pi} \int_{\gamma=0}^{\gamma=\pi/2} 2M_x M_z \cos \beta \cos \chi G(\gamma, \phi) d\gamma d\phi \\ & + \int_{\phi=0}^{\phi=2\pi} \int_{\gamma=0}^{\gamma=\pi/2} 2M_y M_z \cos \alpha \cos \chi G(\gamma, \phi) d\gamma d\phi \quad (5) \end{aligned}$$

Let us consider under what circumstances these integrands will vanish. The integrands are of the form

$$G(\gamma, \phi) M_x M_z \cos \alpha \cos \beta d\gamma d\phi \quad (6)$$

From Figure 1

$$M_x = M \sin \gamma \cos \phi \quad (7)$$

$$M_z = M \sin \gamma \sin \phi$$

The integrand becomes

$$G(\gamma, \phi) M^2 \sin^2 \gamma \cos \alpha \cos \beta \sin \phi \cos \phi d\gamma d\phi \quad (8)$$

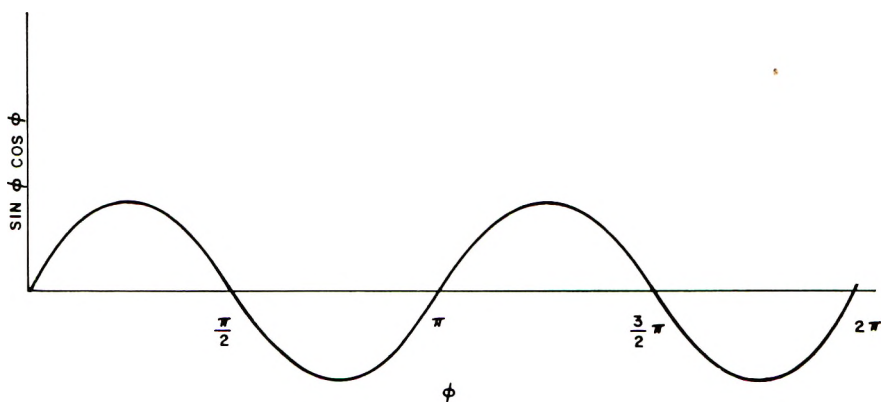


Fig. 3. Graph of $\sin \phi \cos \phi$ vs. ϕ .

Figure 3 is a graph of the function $\sin \phi \cos \phi$. It is obvious that the integrand of $\sin \phi \cos \phi$ (from $\phi = 0$ to $\phi = 2\pi$) is equal to zero. The limitations on $G(\gamma - \phi)$ such that the integral still vanishes are that the function $G(\gamma - \phi)$ be symmetrical about the angles $\phi = 0, \pi/2, \pi,$ and $3/2\pi$; that is, the xy and yz planes are planes of symmetry for the distribution function. This means, in essence, that the absorption intensities are symmetrical about the $x, y,$ or z axes and are independent of the side from which the sample is viewed. In almost all distributions, this is true. Therefore, eq. (5) can be expressed as

$$A_{\alpha,\beta,\chi} = A_y \cos^2 \alpha + A_x \cos^2 \beta + A_z \cos^2 \chi \quad (9)$$

This is the equation for an ellipsoid whose axis lengths are given by $1/A_x^{1/2}, 1/A_y^{1/2}, 1/A_z^{1/2}$, and the length of any line from the origin to a given point of the surface is given by $1/A_{\alpha,\beta,\chi}^{1/2}$ (Fig. 4).

Once the absorption intensities $A_x, A_y,$ and A_z are known, the absorption intensities at any angle α, β, χ can be calculated.

From the symmetry conditions imposed by the distribution function.

$$A_y + A_x + A_z = M^2$$

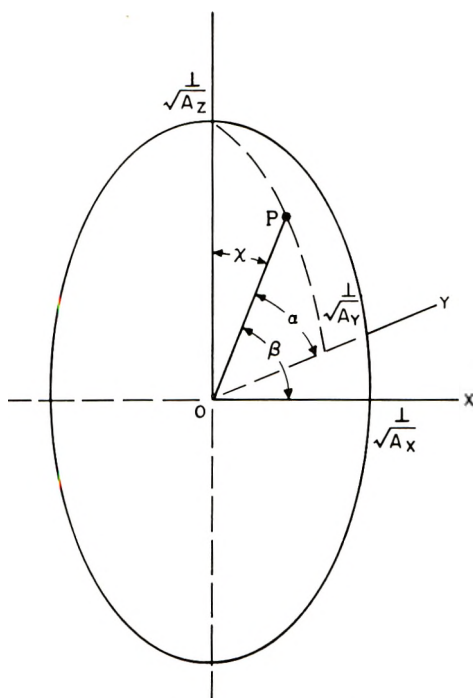


Fig. 4. Intensity ellipsoid.

If the transition moments were randomly oriented, then the sum of the absorption components in the three mutually perpendicular directions still must be equal to M^2 :

$$A_x + A_y + A_z = 3A_0 = M^2 \quad (10)$$

Therefore,

$$(A_x + A_y + A_z)/3 = A_0 \quad (11)$$

The significance of this is as follows. A_0 is the structurally dependent factor of the absorption band. That is, it is the intensity of the band stripped of orientation. Such parameters as A_y/A_0 , A_x/A_0 , A_z/A_0 or $A_{\alpha,\beta,\gamma}/A_0$ are measures of orientation.

Before discussing the techniques of measuring the structural sensitive contribution of an absorption band, along with the parameters characteristic of molecular orientation, a brief digression on the spectrum of polyethylene terephthalate will be made.

B. Spectrum of Polyethylene Terephthalate

The spectrum of polyethylene terephthalate was investigated in the 600 to 1100 cm^{-1} region (Fig. 5). In this region, there exist two types of absorption bands. There are those bands which are both structure- and orientation-sensitive and there are those bands which are orientation-

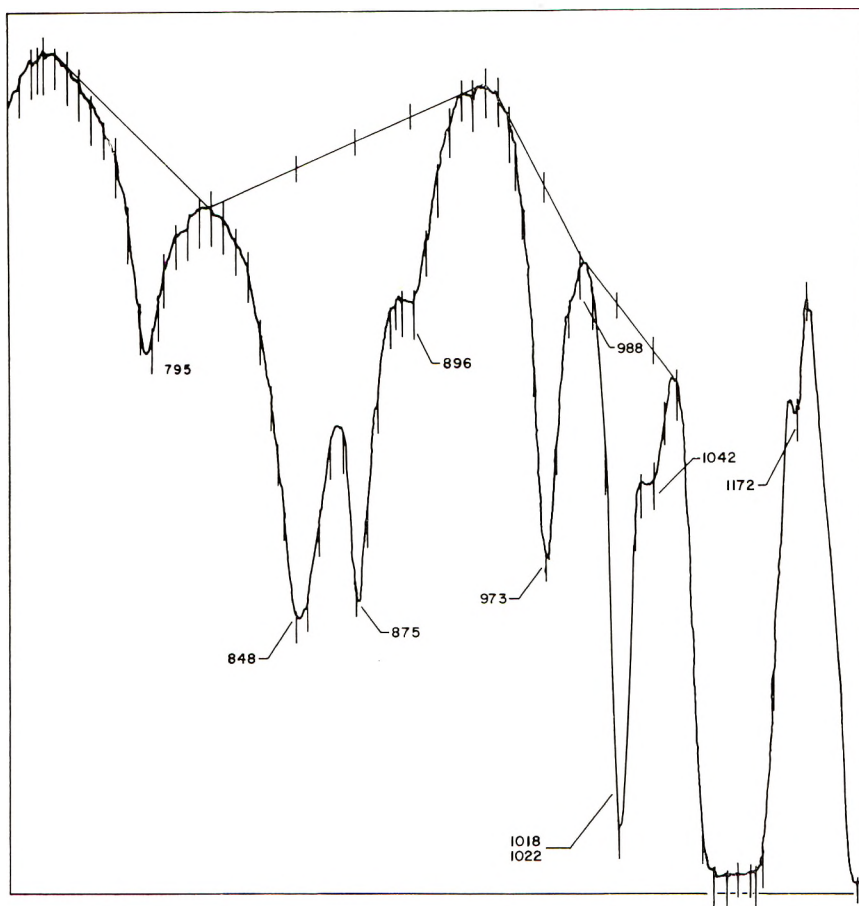


Fig. 5. Infrared spectrum of polyethylene terephthalate (cm^{-1}).

sensitive alone, the structure-sensitive part being dependent only on the amount of polymer present, i.e., film thickness (Table I).

The structure- and orientation-sensitive bands have been postulated to be characteristic of the ethylene glycol linkage. The ethylene glycol linkage is thought to exist in two forms, a *trans* or extended form and a *gauche*

TABLE I
Infrared Bands Investigated in Polyethylene Terephthalate

Structure and Orientation-Sensitive Bands	
<i>Gauche</i> (relaxed), cm^{-1}	<i>Trans.</i> (extended), cm^{-1}
896	848
1042	973
Orientation-Sensitive Bands	
875	
795	

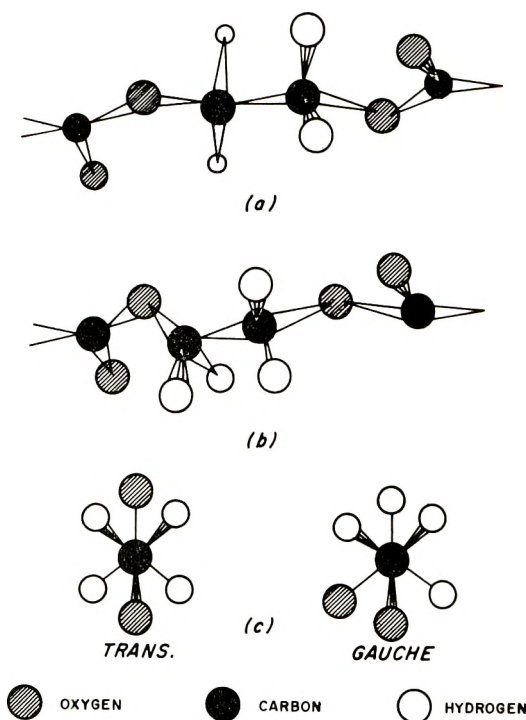


Fig. 6. Diagrams of (a) the crystalline *trans* configuration; (b) the proposed additional *gauche* configuration which is present in amorphous materials; (c) end views.

or relaxed form.¹⁻³ These forms are rotational isomers (Fig. 6). The *gauche* configuration can be produced from the *trans* configuration by a partial rotation about the carbon-carbon bonds.

Miyake³ has demonstrated that the spectral changes produced by drawing and heat setting polyethylene terephthalate films can be interpreted by this rotational isomerization of the ethylene glycol linkage, the *gauche* form in the amorphous regions changing into the *trans* form at crystallization, the *trans* form of the molecule being the form that exists in the crystalline regions.⁵

Miyake, however, did not state whether or not the *trans* form of the molecule may also exist in the amorphous regions of the film. Ward had suggested that it does, but has not been able to justify his position until recently.² Farrow, McIntosh, and Ward,⁶ using NMR measurements, have observed a transition in the amorphous regions of the polymer involving the phenylene carbonyl bond. They attribute this transition to the *trans-gauche* isomerization of the ethylene glycol linkage. Farrow and Ward⁴ have investigated crystallinity in polyethylene terephthalate films by comparing x-ray, infrared, and density measurements. They have shown that reasonable agreement exists between the crystallinities measured by x-rays and density but that poor agreement exists between crystallinities measured by infrared with density or x-ray.

Miller and Willis⁷ have at times noted simultaneous increases in the percentage "amorphous" material and percentage crystalline material for various processing conditions of polyethylene terephthalate films. These measurements were made by use of infrared *gauche* bands along with x-ray techniques.

In summation, many but not all⁸ believe the *trans* form of the molecule to exist in the amorphous regions of the structure. No measurements concerning the amount of this structure have been reported. The reason for this is because infrared methods are believed to be the only way of measuring *trans* structure and the magnitude of the structurally sensitive part of the *trans* absorption bands could not be measured.

III. EXPERIMENTAL

A. Technique to Measure A_z and A_0

In order to determine the contribution of the structurally sensitive part of an absorption band, A_0 , one must determine, A_x , A_y , and A_z . It is a simple matter to determine A_x and A_y , since they are the absorption intensities in the machine and transverse directions of the film. A_z could be measured by cutting a thin section through the film, for example, parallel to the xz plane and analyzing it in an infrared microscope. Such a procedure is usually very tedious and requires a detailed knowledge of the interactions of convergent radiation with microscope geometry and film orientation. A brief discussion of this as applied to axially-oriented samples is given by Fraser.⁹

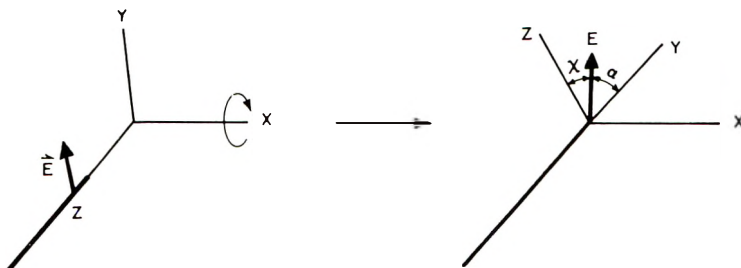


Fig. 7. Tilting references used to calculate A_z .

A_z may easily be measured by rotating the sample about the x axis such that the y axis is at an angle of tilt, α' from the electric vector of the incident radiation (Fig. 7). At this position $\cos \beta$ is equal to zero and $\sin \alpha$ is equal to $\cos \psi$. Equation (9) becomes

$$A_{\alpha,\beta,\chi} = A_y + (A_z - A_y) \sin^2 \alpha \quad (12)$$

Before eq. (12) may be used to calculate A_z and hence A_0 , two modifications must be inserted. The first concerns refraction and reflection; the second, film thickness. Because light is refracted when going through

media of different refractive indices, the angle of sample tilt, α' , is not the same as the angle the electric vector makes with the y axis in the film. The angles α and α' are, however, related through Snell's law.

$$n_1 \sin \alpha' = n_{yz} \sin \alpha \quad (13)$$

where n_1 is the refractive index of air, and n_{yz} is the refractive index of the sample at the angle the electric vector of incident radiation makes with the y axis in the film.

Since the refractive index of air is 1 while the refractive index n_{yz} is of the order of magnitude of 1.6 for polyethylene terephthalate films, there will be a high loss of incident radiation due to reflection. To reduce the amount of reflected radiation, the sample was placed between two hemispheres of potassium bromide. This necessitated the use of an interfacial liquid, which would not absorb in the regions investigated in the film. Nujol is suitable in the 750–1300 cm^{-1} region. All the rays of the slightly converging radiation beam hit the physical surface at right angles where reflection is a minimum and independent of the polarization direction. Furthermore, reflection and refraction at the sample surface is much smaller since the refractive index of the hemispherical material is much closer to that of the sample than the refractive index of air.

The other problem one encounters in measuring the absorption intensities of tilted films is determining the thickness of film for which $A_{\alpha,\beta,\chi}$ is measured. The absorption intensity $A_{\alpha,\beta,\chi}$ is measured in single-beam optics; therefore, the thickness of the sample effectively changes for each angle of tilt. The thickness of the film as measured for $A_{\alpha,\beta,\chi}$, is dependent upon the angle of refraction in the film, which in turn is dependent upon the refractive index of the sample at that angle of tilt. In order that the A_z component of the absorption band be measured for the same thickness of sample as the A_y component, $A'_{\alpha,\beta,\chi}$, the experimental $A_{\alpha,\beta,\chi}$ intensity will have to be corrected for film thickness. This can be accomplished by multiplying $A'_{\alpha,\beta,\chi}$ by the $\cos \alpha$ where α is the angle of refraction in the sample at a particular value of n_{yz} .

$$A'_{\alpha,\beta,\chi} \cos \alpha = A_{\alpha,\beta,\chi} \quad (14)$$

Equation (14) with eqs. (13) and (12) can be expressed as

$$A'_{\alpha,\beta,\chi} [1 - (n/n_{yz})^2 \sin^2 \alpha']^{1/2} = A_y + (A_z - A_y)(n/n_{yz})^2 \sin^2 \alpha'$$

Once n_{yz} can be measured for a given α' , A_z can be determined, and hence, A_0 , the structural intensity of an orientation sensitive band.

Base Lines. A general problem in infrared spectroscopy is that of determining the base line so that reproducible absorption may be measured. Some arbitrary method must be adopted which will give self-consistent results. The base lines employed over the region of the spectrum investigated are as shown in Figure 5. This was found to be the best way of obtaining consistent readings.

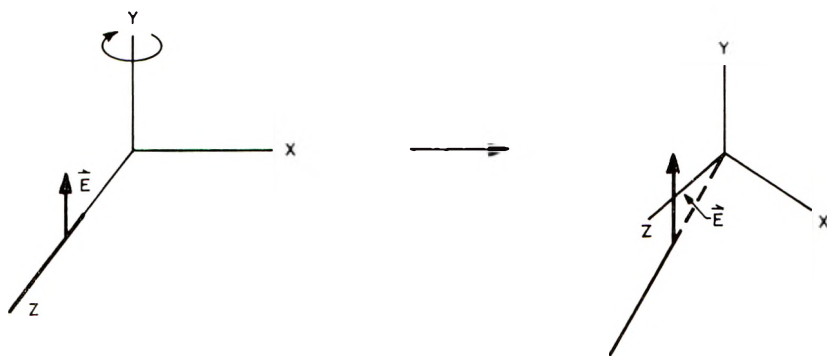


Fig. 8. Tilting references used to calculate n/n_y .

Instrument Conditions. Absorption intensities were measured as peak height rather than integrated band intensities because of the limited amount of time at our disposal. The spectrophotometer was a model 13 Perkin-Elmer spectrophotometer used with single-beam optics. Since peak heights are sensitive to the slit program, a given program was used for all measurements. The polarizer efficiency was assumed to be 100%.

Obtaining n/n_{yz} . The refractive index at the given angle in the film for a given wavelength, n_{yz} , can be computed from a knowledge of the refractive indices in the x , y , and z directions.

For our purposes, we have assumed that the refractive index in the y direction of the film for a given wavelength would be equal to that of the refractive index at the angle of tilt, i.e., $n_y \approx n_{yz}$.

The refractive index n_y at a given wavelength was calculated by measuring the changes in the absorption band intensities for various angles of film tilt. This way the refractive index was measured according to the way the base line above the absorption band was drawn. This assumption should not lead to a very large error in A_z or A_0 , for the birefringence in the thickness direction of the film has been found to be very small.

The refractive index of an absorption band in the y direction of the film was determined by measuring the A_y intensity of the band for two thickness directions. This is illustrated in Figure 8. (Note that in both cases the contributions of A_z and A_x are zero, since $\cos \beta = \cos \psi = 0$.)

The ratio of the absorption intensity A_y at normal incidence to the absorption intensity A_{yp} measured at an angle α' to the direction of the incident radiation is equal to the cosine of the angle that the light beam transverses in the y direction of the film. From this, n/n_y can be computed.

$$A_y/A_{yp} = \cos \alpha = [1 - (n/n_y)^2 \sin^2 \alpha']^{1/2} \quad (15)$$

There are a number of ways that one has in order to check the self-consistency of this method. Firstly, the measurement of the ratio of the refractive index of KBr to a refractive index at a given wavelength for a given absorption band in the y direction of the film must be constant in-

TABLE II
Consistency of n/n_y With Tilting Angle

Tilt	Stretch ratio 4.0 ×					
	1042 cm. ⁻¹	973 cm. ⁻¹	896 cm. ⁻¹	875 cm. ⁻¹	848 cm. ⁻¹	795 cm. ⁻¹
+30°	0.955	0.937	0.972	0.989	0.916	0.805
-35°	0.925	0.938	0.981	0.954	0.877	0.806
+40°	0.905	0.943	0.985	0.985	0.905	0.887
-45°	0.915	0.934	0.951	0.958	0.915	0.836
Avg.	0.925	0.938	0.972	0.971	0.903	0.834

dependent of the angle of measurement. The consistency of these measurements are as shown in Table II.

Secondly, once the value of n/n_y and hence n/n_{yz} is calculated at a given wavelength for a given absorption band, the A_z value for the given absorption band must also be independent of tilt measurement. The consistency of these measurements are as shown in Table III.

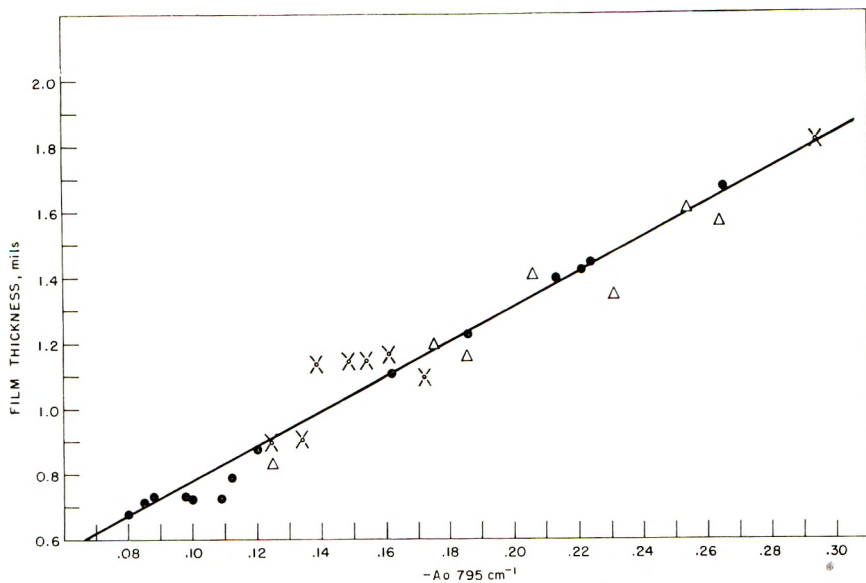
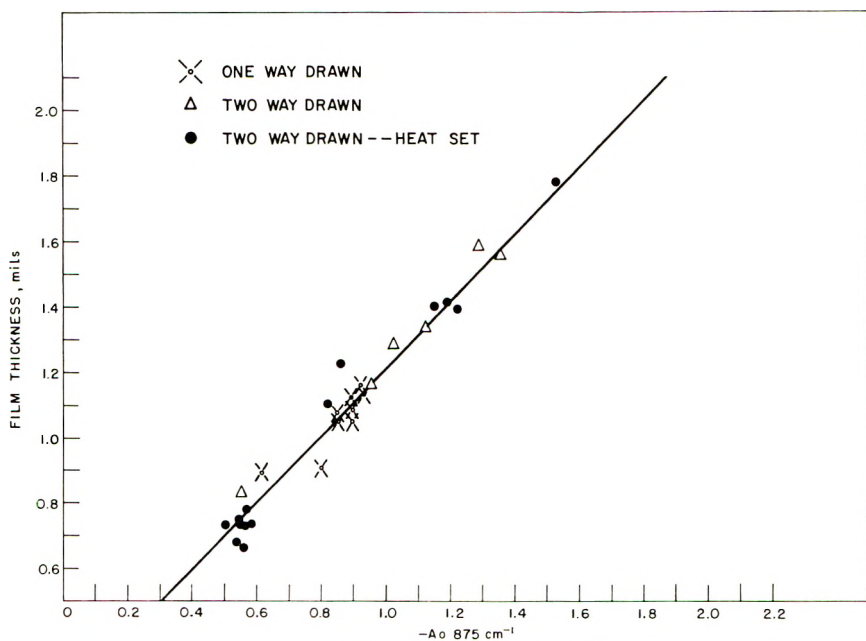
Thirdly, the A_z value for a given absorption band as calculated by tilting the sample about the x axis must be the same as measured and calculated by rotating the sample 90°, such that the x direction of the film is parallel

TABLE III
Consistency of A_z With Tilting Angle

Tilt	Stretch ratio 4.0 ×					
	1042 cm. ⁻¹	973 cm. ⁻¹	896 cm. ⁻¹	875 cm. ⁻¹	848 cm. ⁻¹	795 cm. ⁻¹
+30°	0.312	0.235	0.231	1.551	0.249	0.122
-35°	0.317	0.239	0.253	1.581	0.236	0.138
+40°	0.335	0.209	0.255	1.581	0.230	0.130
-45°	0.328	0.190	0.250	1.511	0.243	0.123
+50°	0.323	0.201	0.248	—	0.257	0.134
Avg.	0.329	0.215	0.247	1.556	0.243	0.129

TABLE IV
 A_z As Calculated For Tilting Measurements About the x and y Axes

	1042 cm. ⁻¹	973 cm. ⁻¹	896 cm. ⁻¹	875 cm. ⁻¹	848 cm. ⁻¹	795 cm. ⁻¹
	Stretch ratio 3.0 × 3.0					
A_y		0.552		0.280	0.389	0.121
A_x		0.342		0.403	0.413	0.155
$A_z(y)$		0.037		1.59	0.072	0.090
$A_z(x)$		0.053		1.49	0.082	0.041
	Stretch ratio 3.5 × 2.5					
A_y	0.285	0.479	0.156	0.462	0.292	0.154
A_x	0.291	0.436	0.161	0.486	0.268	0.161
$A_z(y)$	0.249	0.104	0.203	1.37	0.185	0.115
$A_z(x)$	0.262	0.095	0.205	1.20	0.173	0.100

Fig. 9. A_0 (795 cm^{-1}) vs. film thickness.Fig. 10. A_0 (875 cm^{-1}) vs. film thickness.

to the electric vector of the incident radiation and tilting the sample about its y axis. The consistency of these measurements are as shown in Table IV.

Fourthly, the structural sensitive components of those absorption bands that are only orientation-sensitive (Table I), must be a function of film

thickness only. The consistency of these measurements is as shown in Figures 9 and 10, where the A_0 values for the 875 cm^{-1} and 795 cm^{-1} bands are plotted versus film thickness for a series of differently processed films.

B. Molecular Structure

Figure 11 shows how *trans* and *gauche* polyethylene terephthalate vary for a series of one-way drawn films. As the draw ratio increases, *gauche* polyethylene terephthalate is transformed into *trans* polyethylene terephthalate. Since the amount of crystallinity also increases with draw ratio,¹ we are now in the position to determine whether or not the *trans* form of the molecule also exists in the amorphous regions of the film. Until now, this question could not be resolved, since the structural intensity of an orientation-structural absorption band could not be measured.

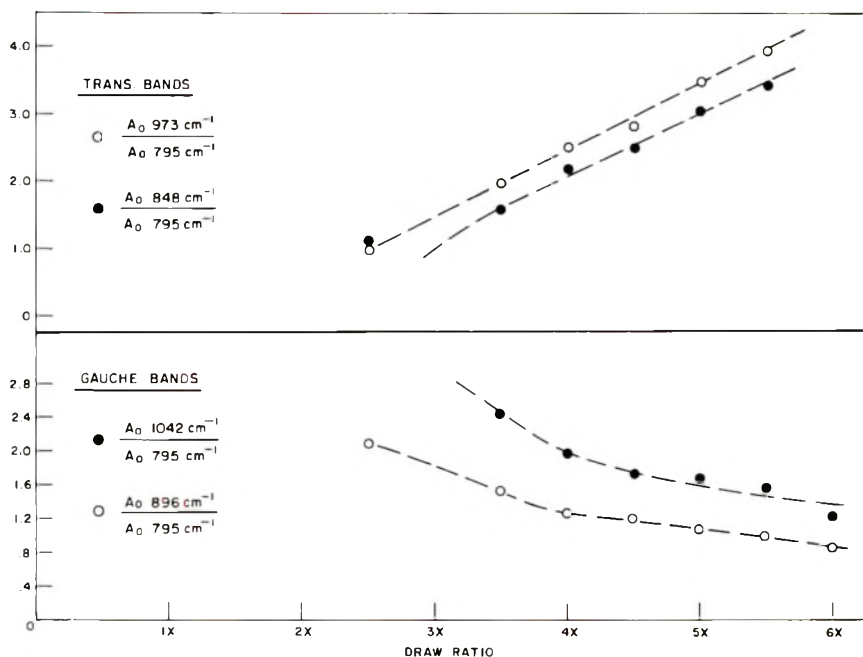


Fig. 11. Variations of *trans-gauche* structure with draw ratio.

Johnson¹⁰ has shown that the density of a film sample of polyethylene terephthalate is a fairly good measure of the per cent crystalline structure when compared to the per cent crystalline structure calculated from x-ray analyses: If the *trans* form of the molecule exists only in the crystalline regions, then for a given percentage crystallinity, that is, a given film density, there should be one and only one value for the amount of *trans* isomer. This will be true independent of the film's previous history. If the *trans* form of the molecule exists in the crystalline and amorphous

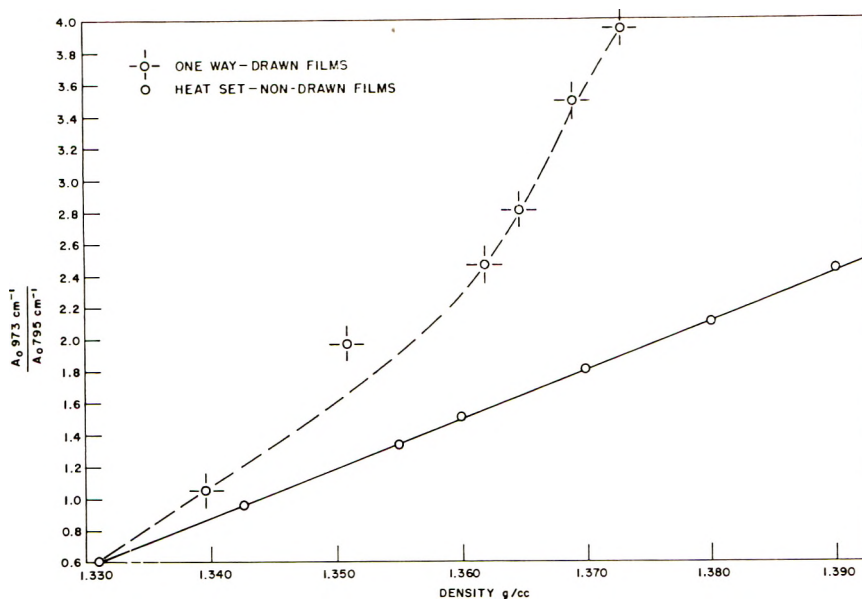


Fig. 12. *Trans* structure as a function of density.

regions, then for a given percentage of crystallinity, that is a given film density, there may be many values for the amount of *trans* structure. The actual amount should be dependent upon film processing. Figure 12 shows how the *trans* content, as measured by the 973 cm^{-1} band, varies with density for a series of heat-set, nonoriented films and a series of one-way drawn films. The line representing the variation of *trans* structure of the heat-set nonoriented films is the result of a least square approximation. It is obvious from Figure 12 that at any given density, that is, at any given per cent crystallinity, there exists an extra or induced amount of structure in the one-way drawn films over that which exists in the heat-set, nonoriented films. This induced *trans* structure must exist in the amorphous regions of the film.

Figure 13 shows how the *trans* content varies for a series of two-way drawn heat-set and nonheat-set films as compared to the heat-set, non-oriented films of corresponding per cent crystallinities. Two points should be noted from Figure 13. Firstly, at any given per cent crystallinity there may be varying amounts of *trans* structure. Secondly, the change of *trans* structure with heat setting for the two-way drawn films almost parallels the change in *trans* content with heat setting for nonoriented films.

Two major assumptions have been made in order to derive these results. The first is that the density is a direct measure of crystallinity. It is realized that this can lead to errors, depending on the sample history (e.g., void content induced). The work of Johnson supports the use of the density/crystallinity relationship. Further, the experimental *trans* con-

tent observed in some of our samples leads to absurd crystallinity results. The second assumption was the use of the A_0 value of the 795 cm^{-1} band as an internal thickness measure. Figure 9 is a plot of this A_0 value versus thickness.

In order to determine a value for the maximum amount of *trans* structure that can exist in a film, the least square line representing the variation of

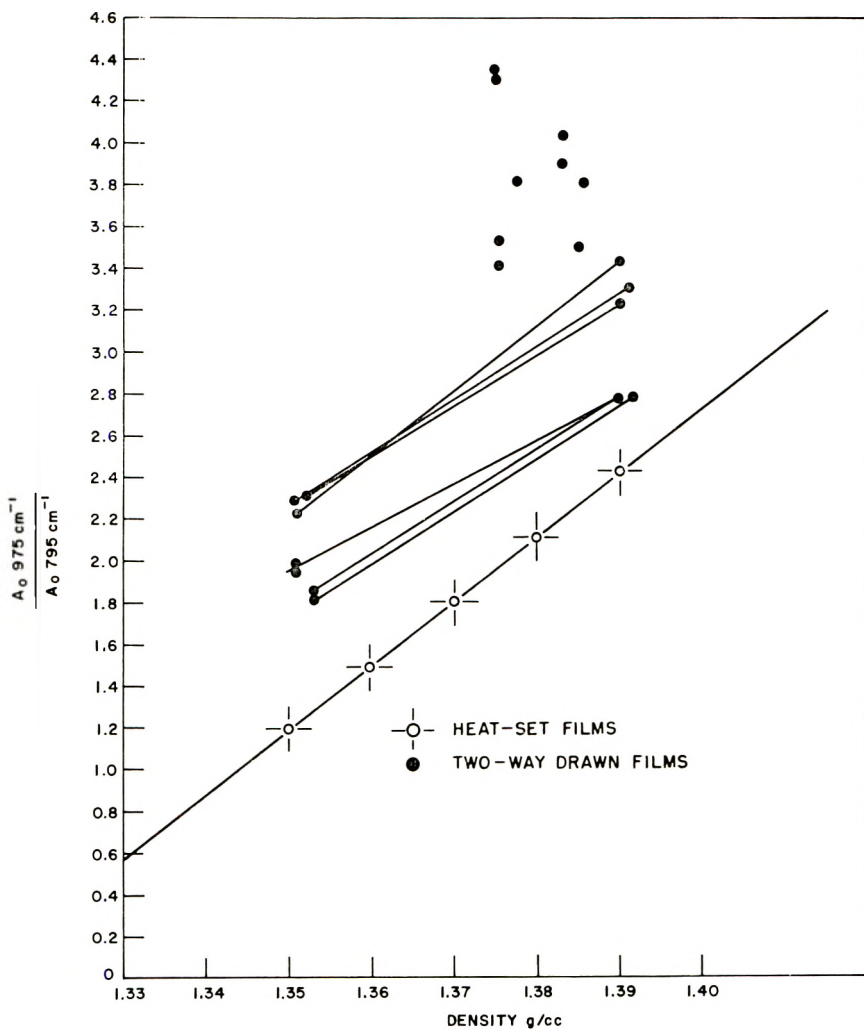


Fig. 13. *Trans* structure as a function of density.

trans structure with density for heat-set, nonoriented films was extrapolated to a density of 1.456. This density is the density of the unit cell of polyethylene terephthalate.⁶ Since the *trans* isomer is the only form that can exist in the crystalline regions, a sample of film which is 100% crystalline must also contain 100% *trans* isomer. The extrapolated value is 4.45.

With the value for the total possible amount of *trans* structure known and with the aid of Johnson's work relating density and per cent crystallinity,¹⁰ one can then calculate the amount of *trans* isomer that exists only in the crystalline regions. The differences between the total *trans* content

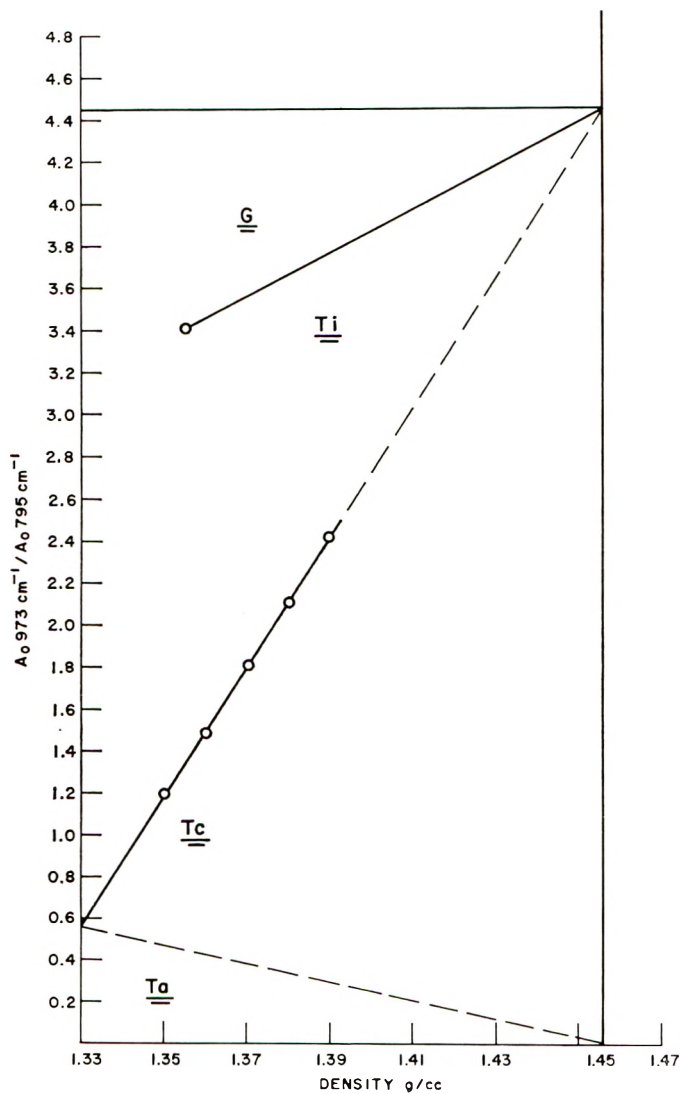


Fig. 14. Phase-type diagram.

for a heat-set, nonoriented film and the *trans* content that exists in the crystalline regions must be equal to the *trans* content in the amorphous regions of these films. Figure 14 displays this graphically. Area T_c represents the *trans* content in the crystalline regions for any given film density, area T_a represents the corresponding amorphous *trans* content. Area T_i represents the induced *trans* content. It is readily observed that an amor-

phous polyethylene terephthalate film contains an equilibrium amount of *trans-gauche* structure.

The *gauche* content for any given film may be determined as the difference in total possible *trans* content and actual *trans* content, the value for the amount of *gauche* being normalized to the *trans* system of measurement.

Once the *trans* content of a processed film is known, one may easily calculate the per cent *trans* structure and per cent *gauche* structure. If one assumes that density is a fairly good measure of the per cent crystallinity, the per cent *trans* crystalline, the per cent *trans* amorphous, and the per cent induced *trans* amorphous structures may also be determined.

The manner in which the *trans* structure changes upon heat setting can be inferred from Figure 14. The *trans* content of a film should change linearly upon heat setting toward the value of the total possible amount of *trans* content, i.e., 4.45.

Since the *trans* form of a molecule can exist in the amorphous regions of the film, and since the *trans* form is the extended form of the molecule, the amount of *trans* structure should be dependent upon the intermolecular forces in the amorphous regions of the film; that is, the tautness of the structure. If this is so, then the amount of *trans* structure should be sensitive to heat relaxation. Table V shows the effects of heat relaxing a $5.5 \times$ drawn film at 100°C . for 2 min. This amount of heating for this period of time is not sufficient to induce appreciable crystallization. While no noticeable change in the per cent crystallinity occurs, the A_0 values for the 973 and 848 cm^{-1} bands decreased in intensity, while the A_0 values of the 1042 and 896 cm^{-1} *gauche* bands increased in value. This corresponds to almost a 50% reduction in the amount of induced *trans* structure.

TABLE V
 A_0 Changes Upon Heat Relaxation, $5.5\times$, Stretch Ratio

	Density, g./cc.	A_0^a			
		973 cm^{-1}	848 cm^{-1}	1042 cm^{-1}	896 cm^{-1}
Not heat-relaxed	1.373	3.96	3.40	1.58	1.02
Heat-relaxed (100°C ., 2 min.)	1.373	2.84	3.00	1.74	1.18

^a A_0 per unit A_0 at 795 cm^{-1} .

C. Molecular Orientation

Once the A_0 value of a given absorption band is measured, the average orientation of that band in any direction of the film can be expressed by parameters such as A_y/A_0 , A_z/A_0 , A_z/A_0 , A_y/A_x , and $A_{\alpha,\beta,\chi}/A_0$. One must note, however, that knowledge of the orientations of the transition moments are of little or no use in determining the orientations of the molecules unless the positions of these transition moments in the molecule are known. Even when the positions of the transition moments in the molecule are known, one must be careful of which transition moment and which

orientation parameter to use in expressing parameters characteristic of axial or uniplanar orientation.* An example will be used to illustrate this point.

Consider a molecule of polyethylene terephthalate in the xyz coordinates of the film (Fig. 15). Let T_1 be a transition moment parallel to the chain axis, T_2 be a transition moment at some angle less than 45° to the chain axis, and T_3 be a transition moment perpendicular to the chain axis. If the film is stretched such that the polymer axis is drawn closer to the y axis of the film, the orientation parameters A_y/A_0 and A_y/A_x will increase for

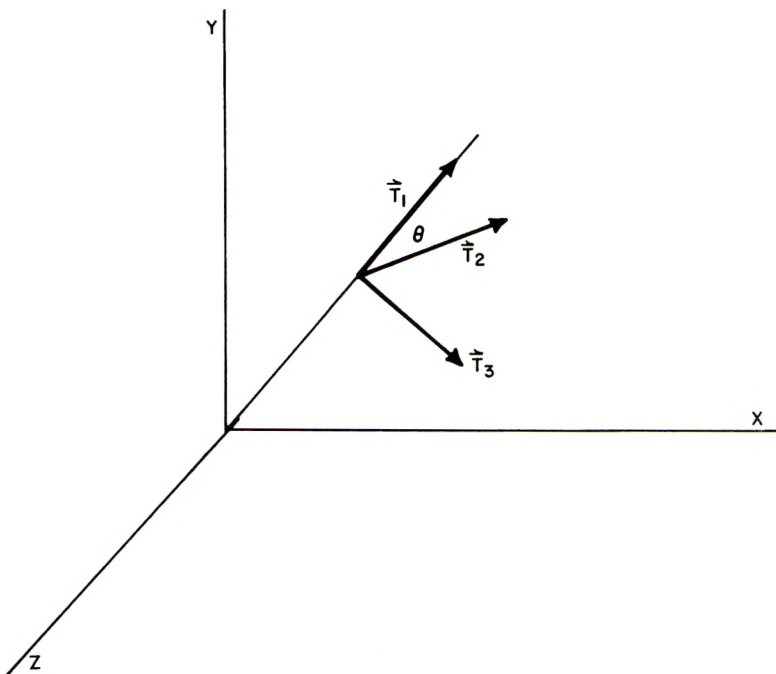


Fig. 15. Polymer molecule in xyz coordinates of film: T_1 = transition moment parallel to molecular chain axis; T_2 = transition moment at an angle θ to molecular chain axis; T_3 = transition moment perpendicular to molecular chain axis.

transition moment types T_1 and T_2 , while parameters A_x/A_0 and A_x/A_y will increase for transition moments time T_3 since this type of moment exhibits perpendicular dichroism. Other orientation parameters may easily be deduced.

If the molecule is held stationary at some angles to the x , y , and z axes but rotated by some angle around its own axis, the orientation parameters for transition moment type T_1 will not change. All orientation parameters for types T_2 and T_3 will change varying amounts except for the A_x/A_y parameter of type T_3 , which will be independent of the amount of rotation.

* Reference axis is the machine direction of the film; reference plane is the plane of the film.

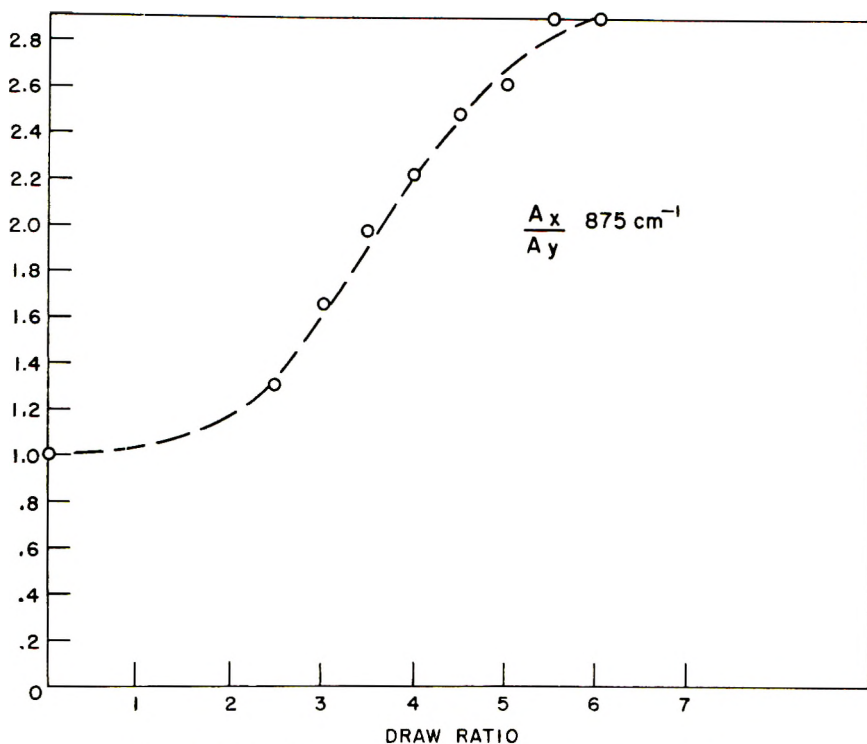


Fig. 16. Molecular axial orientation parameter vs. draw ratio.

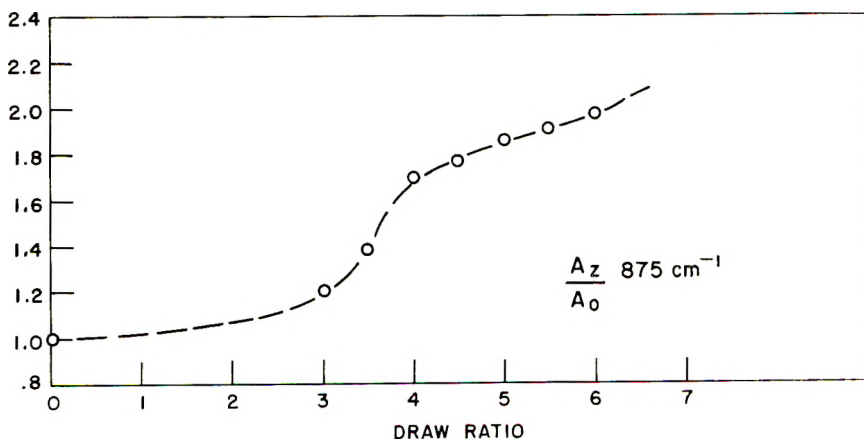


Fig. 17. Molecular uniplanar orientation parameter vs. draw ratio.

It can readily be seen that the A_z/A_0 orientation parameter for type T_3 will be very sensitive to the amount of molecular rotation.

Transition moments of the type T_1 are ideal for obtaining orientation parameters characteristic of the axial alignment of molecules but useless for obtaining orientation parameters characteristic of the uniplanar alignment of molecules. Orientation parameters characteristic of transition

moments type T_2 will change with molecular alignment and with molecular rotation. The mathematical treatment for separating the contribution of each for a given orientation parameter is extremely complicated. For transition moments of type T_3 , the orientation parameter A_x/A_y is characteristic of the alignment of the molecules while the orientation parameter A_z/A_0 is characteristic of the uniplanar orientation of the molecules.

In the regions of the spectrum of polyethylene terephthalate investigated only transition moment types T_2 and T_3 are observed. The transition moment of the 875 cm.^{-1} band is normal to the face of a benzene ring and is a type T_3 transition moment.³ All other bands investigated are of type T_2 . The A_x/A_y orientation parameter of the 875 cm.^{-1} band will be characteristic of the axial orientation of the molecules, while the A_z/A_0 orientation parameters of the 875 cm.^{-1} band will be characteristic of the uniplanar orientations of the molecules.

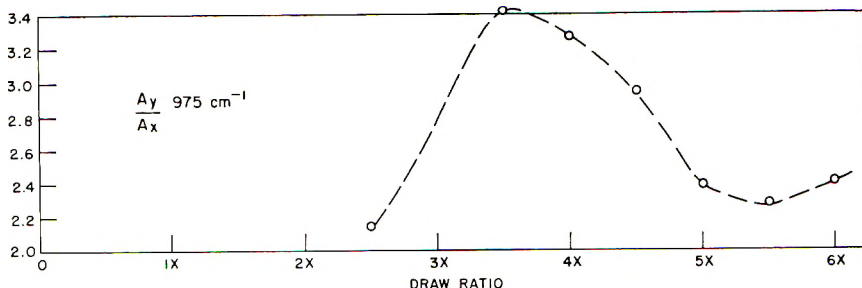


Fig. 18. Dichroic ratio of 975 cm.^{-1} transition vs. draw ratio.

Figures 16 and 17 show how the axial orientation parameters A_x/A_y and the uniplanar orientation parameters A_z/A_0 of the 875 cm.^{-1} band vary for a series of one-way drawn films. Significantly, the axial alignment of the molecules increases with draw ratio, while the uniplanar orientation does not become appreciable until $3.5\times$.

The 973 cm.^{-1} transition moment, like those of the 795 , 840 , 896 , and 1042 cm.^{-1} transition moments, are of type T_2 . Figure 18 shows how the A_y/A_x orientation parameter of the 973 cm.^{-1} band varies for a series of one-way drawn films. The values of A_y/A_x increase up to $3.5\times$, level off, and then decrease for higher draw ratios. This leveling off and subsequent decrease is significant, in that at draw ratios of $3.5\times$ or above, the uniplanar structure of the film becomes appreciable (Fig. 17). For draw ratios up to $3.5\times$, the orientation parameter A_y/A_x of type T_2 transition moments is a function of the axial structure of the film. At draw ratios of $3.5\times$ or above, the orientation parameters of type T_2 transition moments are a function of the axial and uniplanar structure of the film.

These results on the molecular orientation are in direct agreement with the results on the crystalline orientations which were recently published by Heffelfinger and Burton.¹¹

SUMMARY

The division of structure in polyethylene terephthalate films is not simply crystalline and amorphous. There is in addition to this a division of amorphous structure based on the *trans* and *gauche* configuration of the ethylene glycol linkage. A film with a given percentage of crystallization may have varying amounts of *trans-gauche* structure. Likewise, a film with a given percentage of *trans* structure may have varying amounts of crystalline-amorphous structure.

The 875 cm.^{-1} absorption band can be expressed in parameters characteristic of polyethylene terephthalate molecular axial and (or) molecular uniplanar orientation. A_x/A_y of the 875 cm.^{-1} absorption band is characteristic of the molecular axial orientation, while A_z/A_0 of the 875 cm.^{-1} absorption band is characteristic of the molecular uniplanar orientation.

The author wishes to express his appreciation to R. Zbinden of the Pioneering Research Laboratory for his help in the theoretical aspects of this work. The author's appreciation is extended to C. J. Heffelfinger of the Mylar Research and Development Laboratory. His basic work on, and understanding of, Mylar crystalline structure has been most helpful. The author's appreciation is also extended to Professor Bryce Crawford, Jr., of the University of Minnesota. His suggestions and encouragement have been of great value.

References

1. Daniel, W. W., and R. E. Kitson, *J. Polymer Sci.*, **33**, 161 (1958).
2. Ward, I. M., *Textile Research J.*, **31**, 650 (1961).
3. Miyake, A., *J. Polymer Sci.*, **38**, 479 (1959).
4. Farrow, G., and I. M. Ward, *Polymer*, **1**, 330 (1960).
5. Daubeny, R. de P., and C. W. Bunn, *Proc. Roy. Soc. (London)*, **A226**, 531 (1954).
6. Farrow, G., J. McIntosh, and I. M. Ward, *Makromol. Chem.*, **38**, 147 (1960).
7. Miller, R. G. J., and N. A. Willis, *J. Polymer Sci.*, **19**, 485 (1956).
8. Liang, C. Y., and S. Krimm, *J. Mol. Spectroscopy*, **3**, 554 (1959).
9. Fraser, *J. Chem. Phys.*, **21**, 1511 (1956).
10. Johnson, J. E., *J. Appl. Polymer Sci.*, **2**, 205 (1959).
11. Heffelfinger, C. J., and R. L. Burton, *J. Polymer Sci.*, **52**, 289 (1960).

Résumé

L'intensité d'absorption d'une bande d'absorption, dans le spectre infra-rouge d'un polymère orienté, est composée d'un facteur d'orientation et un facteur de structure. On discute une méthode d'utilisation des radiations infra-rouges polarisées qui permet la mesure de la contribution de chacun des facteurs. Le pontage éthylène-glycol de la molécule de téréphtalate de polyéthylène peut exister sous deux formes. Ces formes sont des isomères rotationnels. La forme "trans" de la molécule est la forme étirée, la forme "gauche" de la molécule est la forme relâchée. On trouve que les régions amorphes des films de téréphtalate de polyéthylène contiennent ces deux isomères. On résume l'orientation du polymère en termes de types de moment de transition. On définit les paramètres d'orientation caractéristiques des films de téréphtalate de polyéthylène.

Zusammenfassung

Die Stärke der Absorption in einer Infrarotabsorptionsbande im Infrarotspektrum eines orientierten Polymeren setzt sich aus einem Orientierungs- und einem Struktur-

faktor zusammen. Eine Methode zur Trennung der beiden Beiträge mit Benützung von polarisierter Infrarotstrahlung wird beschrieben. Die Äthylenglykolbindung des Polyäthylenterephthalatmoleküls kann in einer von zwei möglichen Formen existieren. Diese Formen sind Rotationsisomere. Die *trans*-Form des Moleküls bildet den gestreckten, die *gauche*-Form den relaxierten Zustand. Die amorphen Bereiche von Polyäthylenterephthalatfilmen zeigten einen Gehalt an beiden Isomeren. Die Polymerorientierung wird mittels Umwandlungsmoment-Typen dargestellt. Für Polyäthylenterephthalatfilme charakteristische Orientierungsparameter werden definiert.

Received February 8, 1962

Polymerization Induced by Ionizing Radiation at Low Temperatures. III. The Effect of Electron Density on the Polymerization of Substituted Styrenes

CATHERINE S. HSIA CHEN, *Central Research Division, American Cyanamid Company, Stamford, Connecticut*

Synopsis

The solution polymerization in methylene chloride of different methyl-, methoxy- and chloro-substituted styrenes has been studied both at a low temperature ($-65^{\circ}\text{C}.$) and at a higher temperature ($+25^{\circ}\text{C}.$). The rates of the *m*- and *p*-substituted monomers are correlated with the Hammett linear free-energy relationship at both temperatures and the σ^+ constants of Brown and Okamoto. The hypothesis that at low temperatures the polymerization mechanism is cationic and at higher temperatures the mechanism is free-radical is further supported by a negative value for ρ at $-65^{\circ}\text{C}.$ and nearly zero value for ρ at $25^{\circ}\text{C}.$ obtained from the Hammett plots at the respective temperatures. Solid-state polymerizations of undiluted *p*-methylstyrene, *o*-methylstyrene, and α -methylstyrene also have been investigated. It has been found that the termination is unimolecular for *o*-methylstyrene and *p*-methylstyrene. The rates for α -methylstyrene at $-80^{\circ}\text{C}.$ in the solid state are extremely slow. By comparing the results obtained for the solid-state and for the solution polymerizations of *p*-methylstyrene, *o*-methylstyrene, and α -methylstyrene, the hypothesis that the crystal structure plays an important role in determining the rate of solid-phase polymerization and its mechanism is further substantiated by the differences observed. The polymerization of undiluted *p*-methylstyrene at $0^{\circ}\text{C}.$ and at $-15^{\circ}\text{C}.$ in the liquid phase has been undertaken. It has been found that at both temperatures the polymerization is ionic in nature, as evidenced by the dose rate dependences and by the negative activation energy. The polymerization of *p*-methoxystyrene in methylene chloride (~ 3.5 moles/l.) has been undertaken from $-80^{\circ}\text{C}.$ to $25^{\circ}\text{C}.$, covering both solid and liquid phases. In the liquid phase a change of mechanism with change of temperature is again observed. In the solid phase the polymerization is probably of a different nature and is not well understood.

INTRODUCTION

In a previous paper¹ it has been concluded, mostly by means of kinetic methods, that the polymerization of methylene chloride solutions of styrene and of 2,4-dimethylstyrene at low temperatures, induced by ionizing radiation, proceeds primarily by a cationic mechanism. At higher temperatures a free-radical mechanism predominates. In this paper, additional substituted styrenes are investigated in methylene chloride solution, both at a low temperature ($-65^{\circ}\text{C}.$) and at a higher temperature ($+25^{\circ}\text{C}.$). One objective of the present paper is to shed more light on the mechanisms of these polymerization reactions by employing Hammett

linear free energy relationships as well as the σ^+ constants of Brown and Okamoto.^{2,3}

In previous papers,^{1,4} it has been demonstrated that while the polymerization rate of 2,4-dimethylstyrene solutions is severalfold greater than that of styrene solutions at low temperatures, an even greater difference exists in the rates pertaining to polymerization in the solid state. It also has been pointed out that this might be attributed to differences in the crystal structures of the respective monomers. Another objective of the present paper is to test this hypothesis by studying the solid-state polymerization, as well as the solution polymerization of some other substituted styrenes possessing different structural features.

EXPERIMENTAL AND RESULTS

Materials

The methylstyrenes were prepared in these laboratories by methods described elsewhere.⁵⁻⁷

p-Chlorostyrene, α -methylstyrene, and *p*-methoxystyrene were supplied by Monomer-Polymer Laboratories. These monomers were redistilled, and their purity was shown by vapor-phase chromatography to be 99%⁺.

Experimental Methods

The same procedures and radiation source described previously¹ were employed. The rates were apparent rates calculated from the weight of polymer obtained at a given time. The accuracy was estimated to be $\pm 5\%$. The error probably comes primarily from variations of dose rate, which in turn arise from errors in positioning the sample, the variation in the composition of the sample and, perhaps most important, the inherent uncertainty of the energy output of the Van de Graaff generator. According to Goldie et al.,⁸ from 1 to 3 mv., the x-ray output from a 0.25-in. gold target is given by $I = 0.021 V^{3.4}$ (with I in $r/\mu a. \text{ min.}$), in forward direction 100 cm. from the target. We calibrate voltage by activation of silver using photoneutrons emitted by D at or above 2.23 M.e.v. We estimate our error in setting the meter as ± 0.040 M.e.v. The uncertainty in reproducing a previously measured dose rate pertaining to a given set of experimental conditions might be $\pm 2.3\%$.

The solid-phase polymerizations of undiluted *p*-methylstyrene, *o*-methylstyrene, and α -methylstyrene were studied at -80°C. , and the liquid-phase polymerization of *p*-methylstyrene at -15 and 0°C. for various dose rates. When x-rays were used, a dose rate range of 5.0×10^3 to 1.5×10^5 rads/min. was employed; when electrons were used, a dose rate range of 1.25 to 5.0×10^7 rads/min. was employed. In Figure 1 (x-rays), in the lower four lines, log polymerization rate is plotted against log dose rate for the polymerization of *p*-methylstyrene at -80°C. (solid phase), at 0°C. and -15°C. (liquid phase), and for *o*-methylstyrene

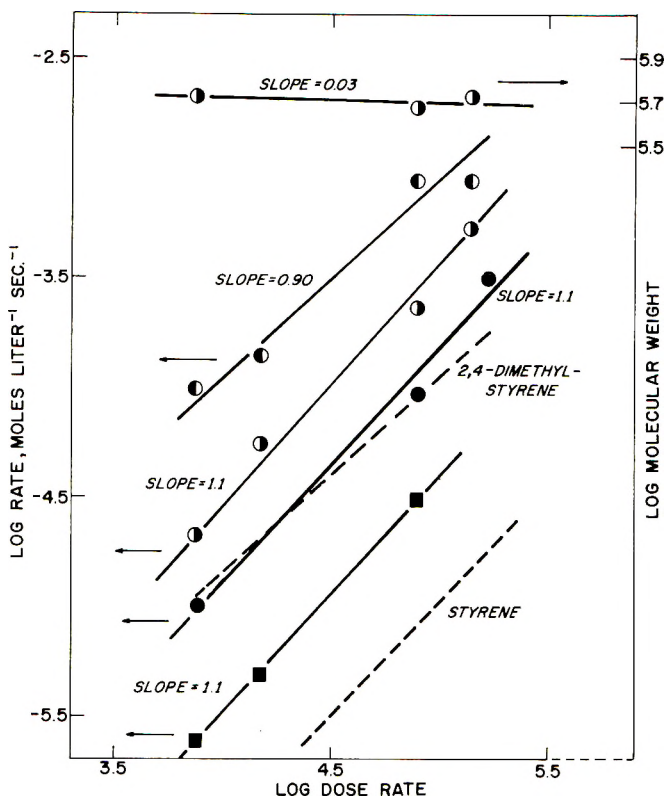


Fig. 1. Polymerization of undiluted methylstyrenes: (●) *p*-methylstyrene, -80°C ., solid; (○) *p*-methylstyrene, 0°C ., liquid; (◐) *p*-methylstyrene, -15°C ., liquid; (■) *o*-methylstyrene, -80°C ., solid.

at -80°C . (solid phase). The dose rate dependences of polymerization rate are the slopes of the best straight lines. It is shown that in all these cases the dose rate dependence is essentially unity. The uppermost straight line, where the slope is essentially zero, represents the dependence of molecular weight on dose rate for the polymerization of *p*-methylstyrene at 0°C . Table I shows the data for polymerization of solid *p*-methylstyrene at -80°C . by electrons and solid α -methylstyrene at -80°C . by x-rays. In the former case, the dose rate dependence is 0.84; in the latter case the rates are extremely small, and the dose rate dependence is not calculated.

A series of experiments was performed where a mixture of *p*-methoxystyrene and methylene chloride ($\sim 50\%$ by volume or ~ 3.4 moles/l.) was polymerized by x-rays at different temperatures, covering both solid and liquid-phase polymerization. The results are shown in Table II and Figure 2. In the liquid phase, from $+25$ to -23.5°C ., the rate decreases with decrease of temperature, $\Delta E_a = 3.7$ kcal./mole; from -23.5 to -40°C ., the rate increases with decrease of temperature, $\Delta E_a = -3.8$ kcal./mole. In the solid phase below -40°C ., the rates are slightly

TABLE I
 Polymerization of *p*-Methylstyrene and α -Methylstyrene in the Solid State
 3 M.e.v. Electrons; 3 M.e.v. Constant Potential X-Rays; Temperature: -80°C .

Monomer	Dose rate, rads/min.	Total dose $\times 10^{-6}$, rads	Polymer yield, %	Dose rate dependence
<i>p</i> -Methylstyrene (electrons)	1.25×10^7	5.0	1.77	Rate $\propto I^{0.84}$
	1.25×10^7	10.0	3.04	
	2.50×10^7	2.5	2.41	
	5.0×10^7	5.0	1.42	
α -Methylstyrene (x-rays)	1.37×10^5	8.23	0.12	
	7.84×10^4	4.70	0.27	
	1.49×10^4	0.92	0	
	7.42×10^3	0.45	0	

higher than those in the liquid state immediately above the melting point, and are independent of temperature, $\Delta E_a = 0$. The molecular weights, represented as intrinsic viscosities, do not vary greatly from -80°C . to 0°C . (both solid and liquid); however, they are considerably lower at 25°C . The chlorine contents of the polymers prepared from -80°C . to -40°C . (solid and liquid) are 0–0.3%, which is within the uncertainty of chlorine analysis (0.3%) and therefore can be neglected. At 25°C ., the chlorine content is considerably higher (1.14%).

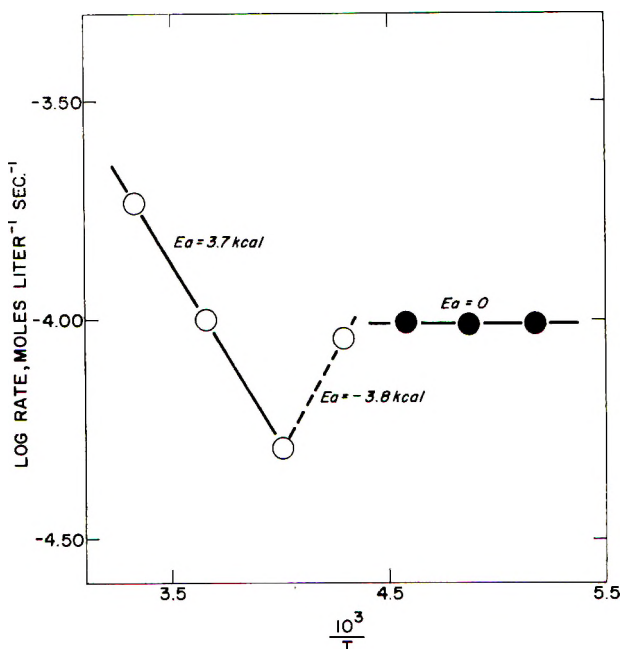


Fig. 2. Polymerization of *p*-methoxystyrene in CH_2Cl_2 at different temperatures: (O) liquid; (●) solid.

TABLE II

Polymerization of *p*-Methoxystyrene in Methylene Chloride
 Dose Rate = 1.10×10^5 rads/min.; Total Dose = 5×10^6 rads; 3 M.e.v. Constant Potential X-Rays

Temperature, °C.	Concentration, moles/l.	Physical state	Polymer yield, %	Rate $\times 10^5$, moles/l. sec. ^a	$[\eta]_{\text{Tot.}}^{30^\circ\text{C.}}$, dl./g.	Cl, %
-80	3.64	solid	4.04	9.87	0.17	0.30
-68	3.43	solid	4.05	9.81	0.18	0.24
-55	3.50	solid	4.07	9.93	0.14	0.0
-40	3.67	liquid	4.01	9.11	0.19	2.20
-23.5	3.48	liquid	2.17	5.30	0.16	—
0	3.49	liquid	3.64	10.1	0.18	—
25	3.47	liquid	7.69	18.7	0.11	1.14

^a Apparent rate calculated based on the per cent polymerization.

The results of polymerization of substituted styrenes in methylene chloride solution at 25°C. and at -65°C. are recorded in Tables III and IV, respectively. It has been shown that, while the other experimental conditions are held essentially constant, the reactivities of the different substituted styrenes are in the following order: at 25°C.: *o*-CH₃ < 2,4-di-CH₃ < *m*-CH₃ < H (styrene) < *p*-Cl \simeq *p*-OCH₃ \approx *p*-CH₃ \leq 3,5-di-CH₃; at -65°C.: *o*-CH₃ < *p*-Cl < *m*-CH₃ < H (styrene) < *p*-CH₃ \simeq 2,4-di-CH₃ < 3,5-di-CH₃. Since at -65°C. a solution of *p*-methoxystyrene in methylene chloride, of the same concentration as other monomers, is a

TABLE III

Polymerization of Substituted Styrenes in Methylene Chloride Solution at 25°C.
 3 M.e.v. Constant Potential X-Rays; Dose Rate = 1.10×10^5 rads/min.; Total Dose = 5.60×10^6 rads

Monomer	Concentration, moles/l. ^a	Polymer yield, %	Rate $\times 10^5$, moles/l. sec. ^b	σ	$\sigma +$	$[\eta]_{\text{Tot.}}^{30^\circ\text{C.}}$, dl./g.	Cl, %
Styrene	3.73	5.16	14.6	0	0	0.05	1.83
<i>o</i> -Methylstyrene	3.55	1.55	3.9	—	—	0.05	1.54
<i>m</i> -Methylstyrene	3.62	5.40	12.8	-0.069	-0.0652	0.05	—
<i>p</i> -Methylstyrene	3.57	8.09	18.9	-0.170	-0.306	0.13	0.81
3,5-Dimethylstyrene	3.76	8.78	19.7	-0.173	-0.130	0.14	—
2,4-Dimethylstyrene	3.12	4.59	10.2	—	—	0.15	—
<i>p</i> -Methoxystyrene	3.47	7.69	18.7	-0.268	-0.764	—	—
<i>p</i> -Chlorostyrene	3.47	8.00	18.1	0.227	—	0.04	26.56

^a Moles of monomer per total volume of the monomer + CH₂Cl₂.

^b Apparent rate.

solid (Table II), the rate is not included in Table IV, all the systems shown forming a liquid phase.

TABLE IV

Polymerization of Substituted Styrenes in Methylene Chloride Solution at -65°C .
3 M.e.v. Constant Potential X-Rays; Dose Rate = 1.10×10^6 rads/min.; Total Dose =
 5.60×10^6 rads

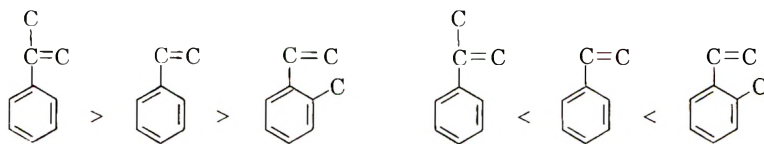
Monomer	Concentration, moles/l.	Polymer yield, %	Rate $\times 10^6$, moles/l. sec.	$[\eta]_{\text{Tot.}}^{30^{\circ}\text{C.}}$, dl./g.
Styrene	3.73	1.94	5.54	0.18
<i>o</i> -Methylstyrene	3.72	0.62	1.70	—
<i>m</i> -Methylstyrene	3.35	1.34	3.37	0.11
	3.47	1.23	3.05	0.12
<i>p</i> -Methylstyrene	3.66	6.19	15.2	0.33
3,5-Dimethylstyrene	3.61	9.64	24.2	0.31
2,4-Dimethylstyrene	3.26	7.33	15.4	0.28
<i>p</i> -Chlorostyrene	3.58	1.10	2.57	0.07

DISCUSSION AND CONCLUSIONS

It has been previously suggested that the crystal structure of the solid monomer plays an important role in determining the rate and mechanism of polymerization in the solid state.^{4,9} The present results support this proposal. For example, the rate of polymerization of solid α -methylstyrene at -80°C . is extremely small compared to the rate for the liquid monomers (Table I). Moreover, the rates of polymerization of solid *o*-methylstyrene are greater than those of solid styrene itself at -80°C ., whereas the reverse is true when the two monomers are polymerized in solution at -65°C . (Fig. 1, Table IV). This means that the relative order of polymerization for styrene, α -methylstyrene and *o*-methylstyrene observed in the liquid state is reversed for polymerization in the solid state.

Liquid or solution:

Solid:



On the other hand, *p*-methylstyrene and 2,4-dimethylstyrene polymerize at a comparable rate, both in the solid state at -80°C . and in solution at -65°C . (Table IV). This demonstrates that the fast rate of polymerization of *o*-methylstyrene is not to be attributed to a chemical effect of the *o*-methyl substituent.

In summary, the above observations show that for some monomers the solid-state polymerization is favored; for other monomers the liquid-

state or solution polymerization is favored; for still other monomers the polymerization is as favorable in the solid phase as in the liquid phase.

The results on liquid-state polymerization of undiluted *p*-methylstyrene show that at both 0 and -15°C . the mechanism is ionic as demonstrated previously for 2,4-dimethylstyrene.¹ As shown in Figure 1 (lines represented by half open circles) based on the available data, the rate is proportional to the first power of the dose rate, both at -15 and 0°C . The molecular weight is essentially independent of the dose rate at 0°C . Also, by comparing the rates at -15 and 0°C ., a negative activation energy is obtained. Moreover, by comparing the rates of polymerization of undiluted *p*-methylstyrene with those of undiluted styrene and 2,4-dimethylstyrene, it can be concluded further that the mechanism is of a cationic nature.

The polymerization of a mixture of *p*-methoxystyrene in methylene chloride (~ 3.5 moles/l.) was studied at -80 to 25°C ., covering both liquid and solid states (Table II and Fig. 2). It should be noted that, as

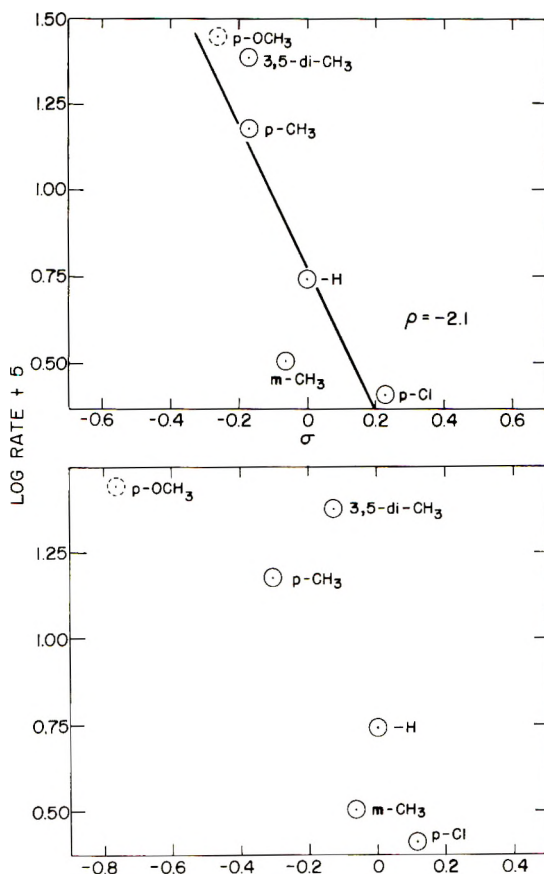


Fig. 3. Apparent polymerization rates of substituted styrenes in CH_2Cl_2 at -65°C . induced by x-rays vs. σ and σ^+ .

with styrene and 2,4-dimethylstyrene in methylene chloride solution,¹ there is a change of mechanism from that of predominantly free radical to that of predominantly ionic. As shown in Figure 2, the values of activation energy are calculated to be 3.7 kcal./mole from 25 to $-23.5^{\circ}\text{C}.$, and -3.8 kcal./mole from -23.5 to $-40^{\circ}\text{C}.$ In the solid phase, the rate of polymerization becomes independent of temperature (-55 to $-80^{\circ}\text{C}.$). It should be noted here that it is not known whether the solid is a solution or a mixture. The molecular weights of the polymers prepared at -80 to $0^{\circ}\text{C}.$ are about the same, as are the chlorine contents; at $25^{\circ}\text{C}.$ the molecular weight is lower and the chlorine content is higher. This may indicate more extensive chain transfer with the solvent, as well as chlorination of the polymer by the solvent by a free radical mechanism at this higher temperature.

The results on the rate of polymerization of substituted styrenes, as summarized in Table III for $25^{\circ}\text{C}.$ and Table IV for $-65^{\circ}\text{C}.$, further support the conclusion that at low temperatures the mechanism is cationic and at higher temperature the mechanism is free-radical. The rates of polymerization of *o*-methylstyrene are small at both temperatures due to steric hindrance of the *o*-methyl group.

The reactivity ratios for several substituted styrenes in their copolymerization under the influence of stannic chloride were previously studied by Overberger and co-workers.¹⁰ It was later shown that these reactivity ratios could be correlated satisfactorily by the σ^+ constants of Brown and Okamoto.¹¹ Consequently, it was of interest to examine the possibility of correlating the rate data obtained in the present study in the same manner. For this purpose it was highly desirable to have data for a highly activating substituent, such as *p*-methoxy. Because of its insolubility in the solvent (solid phase) under the usual conditions, its relative rate was determined by a method of extrapolation. The results of plotting these values of log rate versus the σ^+ constants are shown in Figure 3.

It is unexpected that the σ^+ constants fail to give a reasonable correlation. An attempt was made to apply Hammett's σ constants (Fig. 3). Although the correlation is somewhat better, the deviations are still somewhat larger than one would like in a really satisfactory correlation.

Perhaps the major discrepancy is that *m*-methylstyrene undergoes polymerization at a rate slower than styrene, whereas both the σ and σ^+ constants would predict a faster rate. Even more unexpected is the observation that 3,5-dimethylstyrene, with two *m*-methyl substituents, exhibits an enhanced rate. Obviously, these data cannot be correlated by any value of the substituent constant for the *m*-methyl substituent.

These results would appear to indicate that the rates of polymerization under these conditions do not depend in any simple manner upon the stability of the individual carbonium ions.

In Figure 4, the polymerization rates at $25^{\circ}\text{C}.$ are correlated with σ values and σ^+ values. Six monomers are represented. They are: *p*-methoxystyrene, *p*-methylstyrene, *p*-chlorostyrene, *m*-methylstyrene, 3,5-

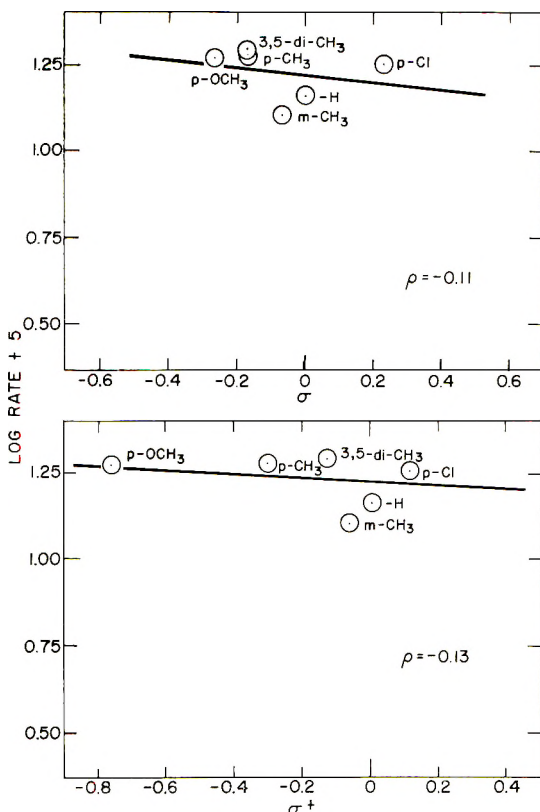


Fig. 4. Apparent polymerization rates of substituted styrenes in CH_2Cl_2 at 25°C . induced by x-rays vs. σ and σ^+ .

dimethylstyrene, and styrene itself. In both σ and σ^+ plots, nearly horizontal lines are obtained with $\rho = -0.10$ and $\rho^+ = -0.13$. This small value of ρ coincides with a neutral reaction mechanism. This again substantiates the contention that at 25°C . the polymerization is by a free-radical mechanism.

Table V presents some data on the molecular weights of polymers prepared from p -methylstyrene at low temperatures. When $\log [\eta]$ is plotted against $\log \bar{M}_w$, the available three points fall on a straight line, from which the relationship between the intrinsic viscosity at 30°C . in toluene and the weight-average molecular weight is derived. The avail-

TABLE V
Data on Molecular Weights of p -Methylstyrene^a

$[\eta]_{\text{Tol.}}^{30^\circ\text{C.}}$, dl./g.	\bar{M}_w	\bar{M}_n
0.22	4.4×10^4	—
1.06	5.2×10^5	2.4×10^5
0.73	2.7×10^5	—

^a Molecular weight obtained by use of the relationship: $[\eta]_{\text{Toluene}}^{30^\circ\text{C.}} = 2.32 \times 10^{-4} \bar{M}_w^{0.64}$.

able data on \bar{M}_w and \bar{M}_n show that the molecular weight has normal distribution (i.e. $\bar{M}_w \approx 2\bar{M}_n$).

The author wishes to express her appreciation for helpful advice and encouragement given by Professor H. C. Brown and Dr. R. F. Stamm.

References

1. Chen, C. S. H., and R. F. Stamm, *J. Polymer Sci.*, **58**, 369 (1962).
2. Brown, H. C., and Y. Okamoto, *J. Am. Chem. Soc.*, **79**, 1913 (1957).
3. Brown, H. C., and Y. Okamoto, *J. Am. Chem. Soc.*, **80**, 4979 (1958).
4. Chen, C. S. H., *J. Polymer Sci.*, **58**, 389 (1962).
5. Marvel, C. S., J. H. Saunders, and C. G. Overberger, *J. Am. Chem. Soc.*, **68**, 1085 (1946); C. S. Marvel, C. G. Overberger, R. E. Allen, and J. H. Saunders, *J. Am. Chem. Soc.*, **68**, 736 (1946); D. T. Mowry, M. Renoll, and W. F. Huber, *J. Am. Chem. Soc.*, **68**, 1105 (1946).
6. Shorygina, P. P., and H. V. Shorygina, *Zhur. Obshchei Khim.*, **5**, 555 (1935).
7. Ramet-Lucas and M. J. Hoch, *Bull. soc. chim.* [5], **2**, 327 (1935).
8. Goldie, C. H., K. A. Wright, J. H. Anson, R. W. Cloud, and J. G. Trump, *ASTM Bull.*, No. **201**, 49 (1954).
9. Morawetz, H., and T. A. Fadner, *J. Polymer Sci.*, **45**, 475 (1960).
10. Overberger, C. G., L. H. Arond, D. Tanner, J. J. Taylor, and T. Alfrey, *J. Am. Chem. Soc.*, **74**, 4848 (1952).
11. Okamoto, Y., and H. C. Brown, *J. Org. Chem.*, **22**, 485 (1957).
12. Hammett, L. P., *Chem. Revs.*, **17**, 125 (1935).
13. Jaffe, H. H., *Chem. Revs.*, **53**, 191 (1953).
14. Taft, R. W., Jr., in *Steric Effects in Organic Chemistry*, M. S. Newman, Ed., Wiley, New York, 1956, Chap. 13.

Résumé

On a étudié à basse (-65°C) et à plus haute température ($+25^{\circ}\text{C}$) la polymérisation de différents styrènes méthyl-, méthoxy- et chlorosubstitués en solution dans le chlorure de méthylène. Les vitesses pour les monomères m et p substitués sont mises en relation avec les relations linéaires de Hammett sur l'énergie libre aux deux températures et avec les constantes σ^+ de Brown et Okamoto. L'hypothèse qu'à basse température le mécanisme de la polymérisation est cationique et qu'il est radicalaire à température plus élevée est confirmée par une valeur négative de ρ à -65°C et par une valeur de ρ proche de zéro à $+25^{\circ}\text{C}$, valeurs fournies par le diagramme de Hammett aux deux températures. On a également étudié la polymérisation à l'état solide du p -méthylstyrène, de l' o -méthylstyrène et de l' α -méthylstyrène non dilués. On a trouvé que la terminaison est monomoléculaire pour l' o -méthylstyrène et le p -méthylstyrène. Les vitesses pour l' α -méthylstyrène à -80°C à l'état solide sont extrêmement lentes. En comparant les résultats obtenus à l'état solide et pour les polymérisations en solution du p -méthylstyrène, de l' o -méthylstyrène et de l' α -méthylstyrène, l'hypothèse suivant laquelle la structure du cristal joue un rôle important dans la détermination de la vitesse de la polymérisation en phase solide est confirmée et son mécanisme est encore étayé par les différences observées. On a étudié la polymérisation du p -méthylstyrène à 0°C et à -15°C en phase liquide. On a trouvé qu'aux deux températures, la polymérisation est de nature ionique ainsi que l'ont mis en évidence les dépendances des vitesses en fonction des doses de radiation et l'énergie d'activation négative. On a étudié la polymérisation du p -méthylstyrène dans le chlorure de méthylène (~ 3.5 moles litre $^{-1}$) dans le domaine de température de -80°C à 25°C couvrant à la fois les phases solides et liquides. En phase liquide on observe à nouveau une variation du mécanisme avec la température. En phase solide la polymérisation semble être différente et n'est pas bien expliquée.

Zusammenfassung

Die Polymerisation verschiedener methyl-, methoxy- und chloresubstituierter Styrole wurde in Methylenchloridlösung bei einer tiefen (-65°C) und einer höheren Temperatur ($+25^{\circ}\text{C}$) untersucht. Für die Geschwindigkeit der *m*- und *p*-substituierten Monomeren besteht bei beiden Temperaturen eine Korrelation mit der linearen Freie-Energie-Beziehung von Hammett und den σ^+ -Konstanten von Brown und Okamoto. Die Annahme, dass bei tiefer Temperatur ein kationischer und bei höherer ein radikalischer Polymerisationsmechanismus vorliegt, wird weiters dadurch unterstützt, dass der aus dem Hammett-Diagramm bei den entsprechenden Temperaturen erhaltene Wert für ρ bei -65°C negativ und bei $+25^{\circ}\text{C}$ fast null war. Polymerisation im festen Zustand von unverdünntem *p*-Methylstyrol, *o*-Methylstyrol und α -Methylstyrol wurde ebenfalls untersucht. Für *o*- und *p*-Methylstyrol wurde ein monomolekularer Abbruch festgestellt. Die Geschwindigkeit ist für α -Methylstyrol bei -80°C im festen Zustand extrem klein. Durch Vergleich der bei der Polymerisation von *p*-, *o*- und α -Methylstyrol in festem Zustand und in Lösung erhaltenen Ergebnisse wurde die Annahme, dass für die Geschwindigkeit und den Mechanismus der Polymerisation in festem Zustand die Kristallstruktur eine wichtige Rolle spielt, durch die beobachteten Unterschiede weiter bekräftigt. Die Polymerisation von unverdünntem *p*-Methylstyrol wurde bei 0°C und bei -15°C in flüssiger Phase durchgeführt. Wie die Abhängigkeit von der Dosisleistung und die negative Aktivierungsenergie zeigt, verläuft die Polymerisation bei beiden Temperaturen nach einem ionischen Mechanismus. Die Polymerisation von *p*-Methoxystyrol in Methylenchlorid ($\sim 3,5$ Mol/Liter) wurde in einem Temperaturbereich von -80°C bis 25°C durchgeführt und erstreckte sich auf die feste und flüssige Phase. In flüssiger Phase wird wieder eine Abhängigkeit des Mechanismus von der Temperatur beobachtet. In fester Phase besitzt die Polymerisation wahrscheinlich einen anderen noch nicht geklärten Charakter.

Received February 13, 1962

NMR Study of Molecular Chain Structure of Polyvinylidene Fluoride

CHAS. W. WILSON, III, *Research and Development Department, Union Carbide Chemicals Company, South Charleston, West Virginia*

Synopsis

Improved resolution of the 40 and 56.4 Mcycle F^{19} NMR room temperature spectra of solutions of polyvinylidene fluoride in dimethylacetamide has resulted in a clearer understanding of the polymer chain structure. The spectra indicate that the structure of polyvinylidene fluoride consists predominantly of head-to-tail sequences of $-\text{CH}_2-\text{CF}_2-$ monomer links, with 5-6% of the monomer links added "backwards" to give occasional $-\text{CF}_2-\text{CF}_2-\text{CH}_2-\text{CH}_2-$ configurations along the chain. Identifying the four principal chemically shifted lines in the NMR spectrum with four specific local chain structures, and applying simple probability theory to compare predicted and observed spectral intensities, it was possible to compute the probabilities of head-to-tail monomer addition (p), head-to-head addition ($1-p$), tail-to-tail addition (q), and tail-to-head addition ($1-q$). The values of both p and q varied somewhat from sample to sample, depending on the temperature and pressure of polymerization; however, both p and q were found to be in the general vicinity of 0.94. This is believed to be the first reported instance in which the relative probabilities of head-to-head, tail-to-tail, head-to-tail, and tail-to-head monomer addition in free-radical polymerization have been determined.

Recent papers¹⁻³ have illustrated the utility of F^{19} NMR chemical shift measurements in compositional and/or structural analyses of fluorine-containing copolymers or homopolymers. In particular, quantitative NMR determination of head-to-head addition of vinylidene fluoride monomer, both in the homopolymer² and in copolymers with hexafluoropropylene,¹ have been most intriguing.

In examining the room temperature 56.4 Mcycle/sec. F^{19} NMR spectrum of a 25% solution of polyvinylidene fluoride in *N,N*-dimethylacetamide, somewhat better resolution was attained than had been previously reported for the homopolymer.² This high resolution spectrum is shown in Figure 1. The spectrum consists of four distinct lines, at the present stage of resolution; each of these four lines is much broader than the lines normally encountered with low viscosity, low molecular weight organic liquids. These lines are designated A, B, C, and D (in the order of increasing magnetic field) in Figure 1. The magnetic field scale in Figure 1 is given in parts per million upfield from an internal CFCl_3 reference.

After comparing the spectra (obtained at both 40 and 56.4 Mcycles/sec.)

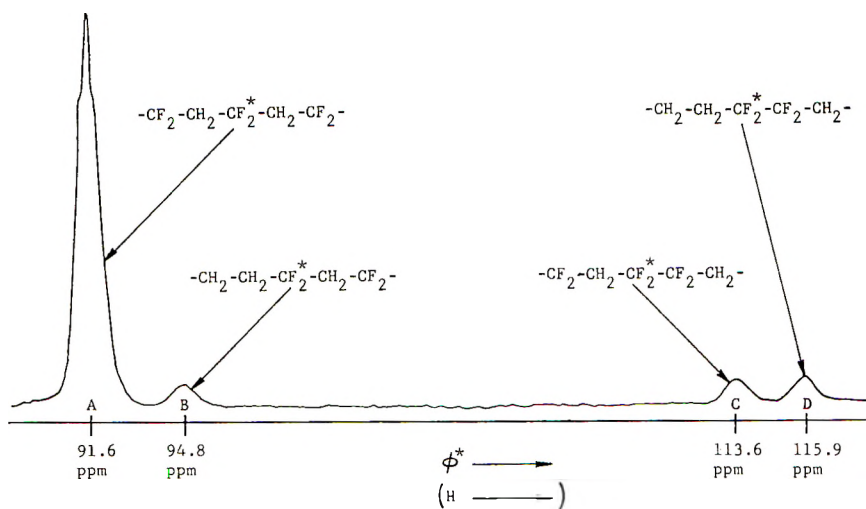


Fig. 1. Room temperature 56.4 Mcycle F^{19} high resolution NMR spectrum of 25% solution of polyvinylidene fluoride in *N,N*-dimethylacetamide. $CFCl_3$ internal reference.

of several samples of polyvinylidene fluoride, including both commercial and experimental polymers prepared under various conditions, several conclusions were possible: (1) each of the four rather broad lines of the spectrum corresponded to chemical shifts, rather than spin-spin couplings, since their spacings were exactly proportional to magnetic field strength, (2) line A, while not completely resolvable, appeared to consist of a 1:4:6:4:1 quintet in the next stage of resolution, with a spacing of about 15 cps between adjacent lines; (3) lines B, C, and D could not be further resolved into component structure, (4) lines B, C, and D were always of nearly equal intensity, and (5) the ratio of the intensity of line A to the other three lines was found to vary somewhat from sample to sample.

Because of the considerable symmetry of vinylidene fluoride, as well as the conventional way in which it has been found to polymerize, it seems most logical to try to account for the spectrum of Figure 1 solely on the basis of various amounts and sequences of head-to-tail, head-to-head, and tail-to-tail structure. (Throughout this discussion $-CF_2-$ will be regarded as the "head" and $-CH_2-$ as the "tail" of the monomer link.)

The work of Naylor and Lasoski² in particular showed convincingly that the spectral region near lines C and D was associated with $-CF_2-CF_2-$ sequences, while the region near lines A and B was due to $-CH_2-CF_2-CH_2-$ structure. The apparent symmetric quintet structure mentioned above for line A is in excellent agreement with the latter conclusion, the principal splitting being presumably due to spin-spin coupling from the four chemically equivalent proton nearest neighbors along the chain. The existence of a pair of chemically shifted lines in each of these

visualize the free-radical polymerization processes leading to the suggested structure of the polyvinylidene fluoride chain. The growing radical can have either the form $R'-CH_2-CF\cdot$ (I) or form $R''-CF_2-CH_2\cdot$ (II); the reactivities of these radical chains is thought to be governed only by the structure of the endgroup on which the unpaired electron is localized, being independent of molecular weight or prior chain structure. Suppose form I adds monomer "head-to-tail" with random probability p (thus perpetuating form I); consequently, form I adds monomer "head-to-head" (converting the radical to form II) with a probability $(1-p)$. Suppose, too, form II adds monomer "tail-to-tail" (converting thereby to form I) with random probability q , also perpetuating itself by "tail-to-head" addition, of course, with probability $(1-q)$. The probabilities of occurrence of the local chain sequences previously associated with lines A, B, C, and D in Figure 1 can then be computed in terms of p and q , and by comparing these with the observed spectral intensities, p and q can be estimated. If A designates the normalized relative intensity of line A, B the intensity of line B, etc., where $A + B + C + D = 1$, then it can be shown that:

$$B = C = q(1 - p)(1 + p - q)/(1 - p + q) \quad (1)$$

$$D = q(1 - p) \quad (2)$$

If a symbol w is introduced, eq. (1) and (2) can be easily reduced to:

$$w \equiv p - q = (C - D)/(C + D) \quad (3)$$

with solutions

$$p = \left[\frac{1}{2} \pm \sqrt{\left(\frac{1-w}{2}\right)^2 - D} \right] + \frac{w}{2} \quad (4)$$

$$q = \left[\frac{1}{2} \pm \sqrt{\left(\frac{1-w}{2}\right)^2 - D} \right] - \frac{w}{2} \quad (5)$$

The plus or minus signs in eqs. (4) and (5) reflect the inability of the NMR spectrum to distinguish from the completed polymer chains in which direction the free-radical propagation occurred, i.e., whether form I or form II of the growing radical chain was favored; other considerations, including its greater stability, indicate that form I should be markedly preferred, so that only the positive sign in eqs. (4) and (5) will be considered.

From the only moderately precise intensity data accumulated thus far for four different polymer samples, lines C and B do appear equally intense, within the $\pm 5\%$ experimental accuracy, in accordance with eq. (1). The computed range of p is from 0.93 to 0.95, whereas the range of q is somewhat larger, from 0.90 to 0.96. The trend is for both p and q to decrease as polymerization pressure and temperature increase. These large values of roughly 0.94 for both p and q indicate clearly that one particular form of

the growing polymer chain radical is strongly favored over the other; most likely this is form I, or $R'-CH_2-CF_2$. The near equality of intensity of spectral peaks B, C, and D, and consequently, the near equality of p and q , emphasizes the fact that radical forms I and II do not differ markedly in their orientational selectivity in adding monomer to the polymer chain.

Finally, a comment on the extent of head-to-head polymerization in polyvinylidene fluoride is in order. The various samples studied here correspond to 5.0–6.2% of the monomer linkages being reversed from their normal head-to-tail sequence, the exact values being dependent upon polymerization conditions. These numbers may be compared with the 8.6–10.6% "head-to-head structure" reported by Naylor and Lasoski.² The apparent factor-of-two difference between these sets of results is due only to the particular choice of reporting the measurements, since it is clear that a random reversal of 5% of all $-CH_2-CF_2-$ linkages in a long head-to-tail sequence corresponds almost exactly to 10% of all $-CF_2-$ units being involved in $-CF_2-CF_2-$ or head-to-head structure.

The NMR instruments used in this study were both standard Varian V-4302 dual purpose spectrometers. Dr. H. F. White kindly permitted the 56.4 Mcycle measurements to be made with his spectrometer.

Discussions with Dr. R. D. Burkhart, Dr. J. P. Henry, Dr. R. D. Lundberg, Dr. F. J. Welch, Dr. N. L. Zutty, and particularly with Dr. A. A. Bothner-By, have been most helpful. Some of the experimental polymer samples were kindly prepared by Dr. R. D. Lundberg. Mr. E. R. Santee, Jr., provided valuable assistance with the experimental measurements and data evaluation.

References

1. Ferguson, R. C., *J. Am. Chem. Soc.*, **82**, 2416 (1960).
2. Naylor, R. E., and S. W. Lasoski, *J. Polymer Sci.*, **44**, 1 (1960).
3. Wilson, C. W., III, *J. Polymer Sci.*, **56**, S16 (1962).

Résumé

Grâce à une résolution améliorée des spectres NMR 40 Mc et 56.4 Mc F^{19} de solutions de fluorure de polyvinylidène dans le diméthylacétamide, pris à température de chambre, on a réussi à mieux comprendre la structure de la chaîne polymérique. Les spectres indiquent que la structure du fluorure de polyvinylidène consiste surtout en séquences tête à queue de chaînons monomériques $-CH_2-CF_2$ avec 5 à 6% de chaînons monomériques additionnés dans l'autre sens de façon à donner de temps à autre le long de la chaîne certaines configurations $-CF_2-CF_2-CH_2-CH_2-$. En attribuant les quatre principales vies déplacées dans le spectre NMR à quatre structures chimiques locales de la chaîne et en appliquant une théorie simple de probabilité pour comparer les intensités spectrales calculées et observées, il a été possible de calculer les probabilités d'addition tête-à-queue du monomère (p) d'addition tête-à-tête ($1-p$) d'addition queue-à-queue (q) et d'addition queue-à-tête ($1-q$). Les valeurs de p et q variaient quelque peu d'un échantillon à l'autre suivant la température et la pression de la polymérisation; cependant on a trouvé que p et q sont tous deux proches de 0.94. Ceci constitue le premier exemple de détermination des probabilités relatives d'addition tête-à-tête, queue-à-queue, tête-à-queue et queue-à-tête, du monomère dans une polymérisation radicalaire.

Zusammenfassung

Die verbesserte Auflösung von 40 Mc und 56,4 Mc¹⁹ F-NMR-Spektren von Polyvinylidenfluoridlösungen in Dimethylacetamid bei Zimmertemperatur ergab ein besseres Verständnis der Struktur der Polymerkette. Die Spektren ergeben für Polyvinylidenfluorid eine Struktur hauptsächlich mit Kopf-Schwanz-Sequenzen von $-\text{CH}_2-\text{CF}_2-$ Monomerbausteinen mit 5% bis 6% "verkehrt" addierten Monomergliedern, die so gelegentlich $-\text{CF}_2-\text{CF}_2-\text{CH}_2-\text{CH}_2-$ Konfigurationen in der Kette bilden. Durch Identifizierung der vier Hauptlinien mit chemischer Verschiebung im NMR-Spektrum mit vier spezifischen lokalen Kettenstrukturen und durch Anwendung einfacher Wahrscheinlichkeitsbetrachtungen beim Vergleich der vorhergesagten und beobachteten Intensitäten des Spektrums war es möglich, die Wahrscheinlichkeit einer Kopf-Schwanz- (p), Kopf-Kopf- ($1-p$), Schwanz-Schwanz- (q) und Schwanz-Kopf-Monomeraddition ($1-q$) zu berechnen. Die Werte für p und q änderten sich von Probe zu Probe je nach Polymerisationstemperatur und -druck ein wenig; p und q lagen aber doch im allgemeinen in der Nähe von 0,94. In der vorliegenden Arbeit wird offenbar zum ersten Mal über die Bestimmung der relativen Wahrscheinlichkeit der Kopf-Kopf-, Schwanz-Schwanz-, Kopf-Schwanz- und Schwanz-Kopf-Monomeraddition bei der radikalischen Polymerisation berichtet.

Received February 16, 1962

Diffusion-Controlled Polymerization of Some Alkyl Methacrylates

A. M. NORTH and G. A. REED, *Department of Inorganic and Physical Chemistry, University of Liverpool, Liverpool, England*

Synopsis

A study has been made of the nonstationary-state free-radical polymerization of methyl, *n*-butyl, isobutyl, and 3,5,5-trimethylhexyl methacrylate in mixed solvents of varying viscosity. It has been found that the termination reaction is diffusion controlled over the complete viscosity range in each case. Values of the ratio k_t/k_p have been obtained for each monomer in ethyl acetate solvent. The relative decreases in this ratio as the size of the alkyl group increases have been compared with decreases calculated (a) on the basis of translational diffusion of macroradicals controlling termination, (b) on the basis that segmental diffusion of the radical chain end in the coiled polymeric free radical is the rate-controlling process in termination. Although it has been necessary to consider an oversimplified model of segmental diffusion, the calculated dependence of k_t on the size of the alkyl group is in accord with that observed experimentally, whereas decreases calculated on the basis of translational diffusion do not agree with those observed. The results are interpreted as signifying that segmental diffusion of the radical chain end is the rate-determining step in the termination of the free-radical polymerization of the alkyl methacrylates, and as providing a simple method of calculating the relative values of the diffusion-controlled termination rate constant for the polymerization of different monomers.

INTRODUCTION

The values of the termination rate constants in the free-radical polymerization of monomers belonging to a given homologous series often differ as the size of the monomer increases. It is usual to explain such differences in radical reactivity either in terms of the inductive or electromeric effect of groups neighboring the reactive carbon atom or in terms of a steric shielding of the reactive center by bulky α -substituents. One such series which has been investigated comprises the alkyl methacrylates.¹ In this case the termination rate constant decreases as the size of the alkyl group increases, an effect which has been ascribed to steric interactions of the bulky ester groups in a radical-radical reaction.

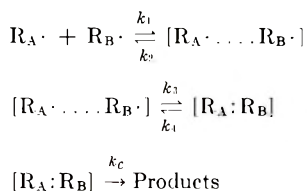
There are two reasons why such a system is worthy of further consideration. In the first place, there is now evidence² that the termination reaction in methyl methacrylate polymerization occurs predominantly by disproportionation. This is a reaction which is subject to less steric interference than the direct combination reaction since the α -methyl and chain methylene groups are both susceptible to hydrogen abstraction. If other

alkyl methacrylates terminate by a disproportionation reaction, the rate constant should not exhibit a great dependence on the size of the ester group. In fact, the disproportionation reaction might be expected to show a dependence on the size of the ester group similar to that of the propagation reaction, which is virtually independent of the size of the ester group.¹ Secondly, it now appears that the termination reaction in methyl methacrylate polymerization is diffusion-controlled.^{3,4} Consequently, if the termination of other alkyl methacrylates is also diffusion-controlled, differences in the measured termination rate constant are not due to differences in the rate of reaction of the radicals involved, but to differences in the rates of the diffusive processes whereby the polymeric free-radicals come into a position suitable for chemical reaction.

The aim of the work reported in this publication was to ascertain whether the termination reaction of the free-radical polymerization of certain alkyl methacrylates is diffusion-controlled, and to ascertain whether the measured differences in the observed rate constants can be correlated with the differences to be expected in the diffusive processes of the various polymeric free radicals.

The simplest test for diffusion control of a termination reaction is a viscosity dependence of either the termination rate constant or some ratio of rate constants involving the termination rate constant.³⁻⁶ Changes in the viscosity of the polymerizing system can be brought about by studying the polymerization to high conversion or by use of solvents themselves inherently viscous. Because of the complications introduced when the viscosity is due to the presence of polymer,^{3,5,6} it is more rigorous to carry out the study in viscous media, i.e., in viscous solvents.

The various diffusive and chemical steps which lead to the removal of free radicals from a system can (for bimolecular termination) be treated as a three-stage process. The first stage is translational diffusion of the centers of gravity of two macroradicals from positions in solution to such proximity that certain segments of each chain can be considered as being in contact. The second stage is a rearrangement of the chains so that the two radical chain ends come sufficiently close for chemical interaction, the third step, to occur. This can be envisaged as,



where $[R_A \cdot \dots R_B \cdot]$ represents a pair of polymeric free radicals with certain unreactive segments in contact, $[R_A : R_B]$ the same pair of radicals with the two reactive carbon atoms in a position favorable for chemical reaction; k_1, k_2 are the rate constants describing translational diffusion forming and destroying $[R_A \cdot \dots R_B \cdot]$ pairs, and k_3, k_4 are rate constants

describing rearrangement, or segmental diffusion of the active chain ends, within such pairs; k_c is the rate constant describing the chemical conversion of free-radical centers "in contact" into inert polymer. For very fast chemical reactions, $k_c \gg k_4$, the rate of conversion of freely propagating radicals to inert polymer is given by

$$d[\text{R}]/dt = k_t[\text{R}]^2 = [k_1k_3'/(k_2 + k_3)][\text{R}]^2$$

where k_t is the observed rate constant for the whole process. For slow translational diffusion $k_t = k_1$, and for slow segmental diffusion $k_t = k_3'$, where $k_3' = k_3K_{AB}$, K_{AB} being the equilibrium constant for the formation of $[\text{R}_A \cdot \dots \text{R}_B \cdot]$ pairs in solution.

One of the problems in any study of diffusion-controlled polymerization reactions is to decide whether translational diffusion or segmental rearrangement is the slower and rate-determining step of the overall termination process. In the case of methyl methacrylate termination, the available evidence^{3,7} suggests that segmental diffusion is the important rate-determining process. Since variation of the ester group in the alkyl methacrylate series might affect the two types of diffusion differently, examination of the values of a series of diffusion controlled termination rate constants might shed further light on this problem.

The polymerization of methyl, *n*-butyl, isobutyl, and nonyl (3,5,5-trimethylhexyl) methacrylate has been studied in solvents of varying viscosity, and the termination reaction found to be diffusion controlled in each case. The variations in the termination rate constants have been compared with those calculated from a simplified picture of the diffusive processes, and best agreement has been found with a model whereby the rate-determining step is segmental diffusion of the radical chain end from a position inside a coiled polymer chain (accessible to monomer and solvent) to a position in solution relatively unhindered by other segments of the same polymer chain (accessible to polymer).

EXPERIMENTAL

Materials

Methyl methacrylate (MMA), B.D.H. purified grade, was freed of inhibitor, dried, and distilled under a nitrogen pressure of 20 mm. Hg. The middle fraction was collected and aliquot portions outgassed on the vacuum line under a pressure of less than 1×10^{-5} mm. Hg, prepolymerized by ultraviolet irradiation, and residual monomer distilled into the polymerization vessels.

n-Butyl methacrylate (BMA), isobutyl methacrylate (IBMA), and nonyl (3,5,5-trimethylhexyl) methacrylate (NMA), supplied by I.C.I. Ltd., were treated similarly, the first distillations being carried out at pressures of 10 mm., 12 mm., and 10^{-4} mm. Hg, respectively.

Ethyl acetate (A.R.) was fractionally distilled over calcium hydride and

the middle fraction collected. Aliquot portions were outgassed and distilled on the vacuum line.

Sucrose acetate isobutyrate, (SAIB), supplied by Eastman Kodak Ltd., was treated with sodium bisulfite and charcoal at 100°C. In order to remove trace impurities which might affect a free-radical polymerization a few milligrams of α, α' -azobisisobutyronitrile were dissolved in aliquot portions of the ester, outgassed, and the azo compound decomposed by ultraviolet irradiation.

Diisooctyl phthalate, supplied by Geigy Ltd., was purified in the same way.

Procedure

Measurements of rates of polymerization were made in thin glass dilatometers with high rates of heat transfer to a water thermostat governed to $30 \pm 0.01^\circ\text{C}$. The movement of the meniscus was observed by means of a cathetometer fitted with an eyepiece scale of 100 divisions. The times of meniscus movement across each scale unit were recorded on a Kymograph with a drum speed of 1 rpm.

Values for the ratio of termination and propagation rate constants, k_t/k_p , were calculated from nonstationary-state measurements of the photo aftereffect using the equation derived by Benson and North.⁸ Irradiation was provided by an Osira 125-w. mercury arc lamp with the outer glass envelope removed, α, α' -azobisisobutyronitrile being used as photosensitizer and dark initiator.

Since the use of initiator to purify viscous solvents led to uncertainties in a calculated rate of initiation, and since the use of molecular weights to evaluate the ratio $k_p/k_t^{1/2}$ required many polymerizations at each viscosity as well as introducing the uncertainties inherent in molecular weight determinations, it was decided that observation of the ratio k_t/k_p provided the most reliable examination of variations in k_t . Since a viscosity dependence of k_p , the propagation rate constant is most unlikely over the range of viscosities studied,^{3,4} the viscosity dependence of the ratio k_t/k_p must be the same as the dependence of the single constant, k_t .

Solvents of varying viscosity but comparable solvent power for polymer were prepared from mixtures of ethyl acetate and SAIB for the lower alkyl methacrylates, and from mixtures of ethyl acetate with diisooctyl phthalate for nonyl methacrylate. The viscosities of the nonviscous solvents were measured in an Ubbelohde viscometer and those of the more viscous media in a falling ball viscometer.

Polymerizations were carried to low conversion of monomer to polymer, so that the monomer concentration was effectively constant throughout any experiment. Furthermore, the viscosity of the system was also found to be unaltered in experiments carried to low conversion.

RESULTS

The viscosities of the mixed solvents used are recorded in Table I.

TABLE I
Viscosity of Mixed Solvents at 30°C.

Solvent components	Vol. fraction monomer	Vol. fraction viscous component	Viscosity, cpoise
SAIB,	0.20	0.00	0.42
ethyl acetate,	0.20	0.20	0.63
monomer	0.20	0.30	0.95
(MMA or	0.20	0.40	1.45
BMA)	0.20	0.50	2.65
	0.20	0.60	5.72
Diisooctyl	0.25	0.35	0.80
phthalate,	0.25	0.60	1.70
ethyl acetate,	0.24	0.76	3.50
NMA	0.25	0.00	0.45

The values of the ratio k_t/k_p for methyl methacrylate and *n*-butyl methacrylate dissolved in SAIB-ethyl acetate mixtures, and for nonyl methacrylate dissolved in diisooctyl phthalate-ethyl acetate mixtures are set forth as a function of solution viscosity in Figure 1. In each case the ratio k_t/k_p increases with increasing solution fluidity, an effect which continues down to viscosities which are in fact lower than those of the pure monomers.

It is interesting to note that the dependence of k_t upon solution viscosity is of power -1 , -0.8 , and -0.7 for methyl, *n*-butyl, and nonyl methacrylate, respectively. To shed further light on the possible reasons for this variation of the viscosity exponent, nonyl and isobutyl methacry-

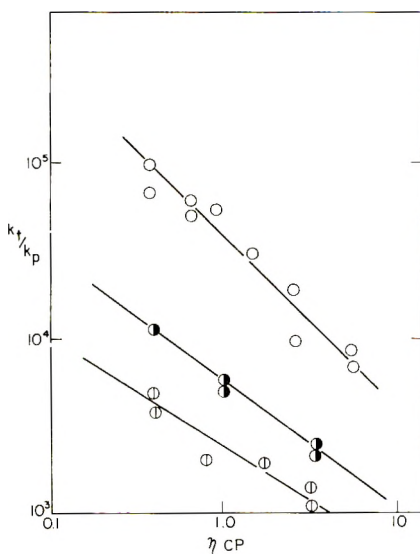


Fig. 1. Ratio k_t/k_p as a function of solution viscosity at 30°C.: (○) methyl methacrylate in SAIB-ethyl acetate; (●) *n*-butyl methacrylate in SAIB-ethyl acetate; (⊕) nonyl methacrylate in diisooctyl phthalate-ethyl acetate.

late have been studied in the SAIB-ethyl acetate system. The values of the ratio k_t/k_p for these two systems are set forth in Figure 2. In both cases a viscosity dependence of the ratio is apparent, but of a smaller negative power than exhibited by the systems plotted in Figure 1.

DISCUSSION

Viscosity Dependence of Termination

For each monomer-solvent system studied, the ratio k_t/k_p , and hence the rate constant k_t , depend upon solution viscosity over the complete range studied. This indicates that the diffusive processes are sufficiently slow compared with the chemical step to be of importance in determining the rate of termination. In the cases where the inverse dependence of k_t upon viscosity is of power less than unity, the problem to be considered is whether the diffusive steps are completely rate-determining, or are of rate comparable with that of the chemical step.

Under conditions when it is not possible to assume $k_c \gg k_4$, the observed termination rate constant can be calculated from the kinetic scheme, assuming a stationary-state concentration of all intermediates, as

$$k_t = \frac{k_1 k_3}{k_2 k_4} \left\{ \frac{[k_4 k_c / (k_4 + k_c)]}{1 + [(k_3 k_c) / k_2 (k_4 + k_c)]} \right\} \quad (2)$$

This can be rearranged to

$$k_t^{-1} = [(k_2 + k_3) / k_1 k_3] + (k_2 k_4 / k_1 k_3) k_c^{-1} \quad (3)$$

Assuming that the rate constants for the diffusive steps are proportional to the solution viscosity to some power, $-m$,

$$k_t^{-1} = a + b\eta^m \quad (4)$$

where a and b are constants.

It is immediately apparent that at a particular viscosity the termination rate constant may appear to depend on a power of viscosity smaller than $-m$. However, over a finite range of viscosities, this dependence must alter, and plots of $\log k_t$ against $\log \eta$ cannot be straight lines.

Although the study of methyl methacrylate yields a value of unity for m for this monomer, the lack of curvature for the other monomers in Figure 1 suggests that the lower powers observed are not due to the diffusive and chemical steps being of comparable rates, but to a lower value of m for the solvent-polymer systems studied.

One of the diffusive processes studied involved movement of the radical chain end in a region of the coiled polymeric species accessible to solvent. If this process is important, it is essential that both solvent components penetrate freely to this region. If one solvent component should be bulky or if the polymer chain side groups should be so arranged that penetration of the polymer coil by solvent is hindered, the environment of

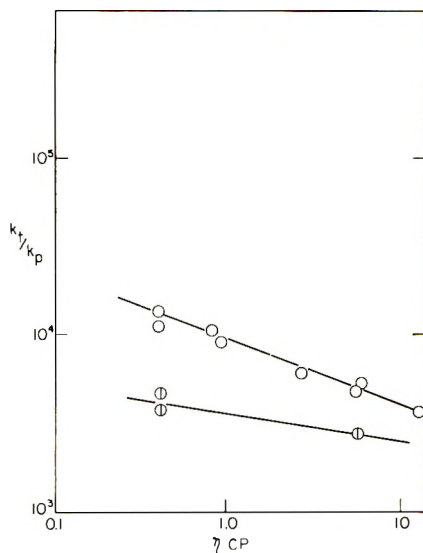


Fig. 2. Ratio k_t/k_p as a function of solution viscosity at 30°C.: (O) isobutyl methacrylate in SAIB-ethyl acetate. (⊙) nonyl methacrylate in SAIB-ethyl acetate.

the radical chain end will be enriched (relative to the bulk of the solution) in the smaller component. Consequently the environment of the chain end will be of lower viscosity than expected from measurements of bulk viscosity. Replacement of diisooctyl phthalate by the bulkier SAIB, or replacement of flexible *n*-butyl side groups by the less flexible isobutyl groups, might both be expected to enhance this phenomenon. As can be seen from Figure 2, in both cases the dependence of k_t upon a measured bulk viscosity is markedly reduced.

The results portrayed in Figure 1 are thus to be interpreted as meaning that the termination reaction is diffusion-controlled over the complete range of viscosities studied. If two solvents of differing viscosity but equal penetrability could be found, an inverse first-power dependence of k_t upon solution viscosity would be expected. There is the added consequence that the diffusive process involving movement of the radical chain end in the polymer coil is the important phenomenon in the case of the higher alkyl methacrylates.

Dependence of Termination on the Size of the Alkyl Group

The values of the ratio k_t/k_p obtained for polymerizations in ethyl acetate as solvent at 30°C. are 7.0×10^4 , 1.1×10^4 , 1.1×10^4 , and 5.6×10^3 for methyl, *n*-butyl, isobutyl, and nonyl methacrylate, respectively. Burnett, Evans, and Melville¹ have shown that the lower alkyl methacrylates exhibit a constant value of k_p , and examination of molecular models shows that there is no steric reason why that of nonyl methacrylate should be greatly different. The ratios k_t/k_p for each monomer can then be used to express the termination rate constant of each methacrylate in

terms of that of methyl methacrylate, $\beta_{\text{MMA}} = 1, \beta_{\text{BMA}} = 6.3, \beta_{\text{IBMA}} = 6.3, \beta_{\text{NMA}} = 12.5$, where $\beta = k_{t,\text{MMA}}k_{p,\text{AMA}}/k_{t,\text{AMA}}k_{p,\text{MMA}} \approx k_{t,\text{MMA}}/k_{t,\text{AMA}}$ the subscript AMA referring to alkyl methacrylate.

It is interesting to note that Burnett, Evans, and Melville¹ obtained a higher value of β_{BMA} in bulk polymerization. Since the viscosity of bulk butyl methacrylate monomer is greater than that of methyl methacrylate monomer, this would be expected for diffusion-controlled termination.

Consider first translational diffusion of the macro-radicals, which can be related directly to D , the self-diffusion coefficient of the polymeric species through a solution containing no gradient of polymer concentration. It has been suggested^{9,10} that the diffusion of polymers can be treated by comparing the polymer molecule with an equivalent hydrodynamic sphere which obeys the Stokes-Einstein relationship. Furthermore the radius of this equivalent sphere has been shown to be proportional to the root-mean-square separation of the chain ends of the polymer coil.

Consequently

$$D_{\text{MMA}}/D_{\text{AMA}} = \sqrt{\bar{r}^2_{\text{AMA}}}/\sqrt{\bar{r}^2_{\text{MMA}}}$$

Use of the Flory relationship¹¹

$$[\eta]M = \Phi(\bar{r}^2)^{3/2}$$

and the data of Chinai and Guzzi¹² yields

$$D_{\text{MMA}}/D_{\text{BMA}} = 1.02$$

for polymeric species of the same degree of polymerization. The small differences in molecular weights of the species involved in the methyl and butyl ester polymerizations carried out in this work would exert a negligible effect on this ratio.

Although comparable data are not available in the literature for nonyl methacrylate, the work of Chinai and Guzzi¹² shows that the polymer chain extension of trimethylhexyl methacrylate must be less than the value they report for *n*-hexyl methacrylate, for which $D_{\text{MMA}}/D_{\text{HMA}} = 1.18$, and greater than that of 2-ethylbutyl methacrylate, for which $D_{\text{MMA}}/D_{\text{EBMA}} = 1.10$.

Consequently, if translational self-diffusion of polymeric radicals were the rate-determining step of the termination process, one would expect $\beta_{\text{BMA}} = 1.02$ and $1.10 < \beta_{\text{NMA}} < 1.18$, values which are not at all in agreement with the observed figures.

An attempt to predict the way in which segmental diffusion of the radical chain end depends on the size of the ester group is more difficult. For a preliminary investigation of this problem we have chosen a model whereby the chain end is considered as a cylinder, the axis of which coincides with the carbon-carbon backbone of the polymer chain, the radius being taken as the distance from the chain to the outer limits of the side groups. This cylindrical chain end is then pictured as diffusing in a "wormlike" fashion

from a most probable position inside a coiled polymeric species into a relatively unhindered position.³ This diffusion must then take place across a polymer segment concentration gradient, through a region where resistance to movement is provided by solvent and in some cases by the other segments of the polymer coil.

For the case when this segmental motion of the radical chain end is rate-determining, the observed termination rate constant is proportional to k_3 . This is provided that the equilibrium constant for pair formation, K_{AB} is the same in every case, an assumption which is inherent and seldom realized in most comparisons of chemical rate constants for reactions in solution. The rate constant k_3 is, in fact, the square of the probability that one radical end reaches the region in which reaction can take place. This probability is directly proportional to the rate of diffusion of the end out of the polymer coil. On the basis of our cylindrical model this rate is (a) inversely proportional to the radius of the cylinder, d , (b) directly proportional to the segment concentration gradient in the region of the chain end, (c) inversely proportional to the distance from the most probable position of the chain end to the region of reaction. Because segment concentration is inversely proportional to the radius of the polymer coil to the power three, the concentration gradient is inversely proportional to the radius to the power four. The distance from the most probable position of the chain end to the outer limits of the coil is directly proportional to the radius of the coil, so that the overall rate of diffusion is inversely proportional to the radius (and hence the root-mean-square separation of the chain ends) raised to the power five. Thus for rate-determining chain end diffusion of two polymeric species of the same degree of polymerization

$$\beta_{AMA} = (d_{AMA}/d_{MMA})^2(\bar{r}_{AMA}^2/\bar{r}_{MMA}^2)^5 \quad (5)$$

Examination of Catalin molecular models, in which the ester side groups have been considered in a variety of configurations, gives for the most probable configurations of the side chains, $\gamma_{MMA} = 1, \gamma_{BMA} = 1.7, \gamma_{IBMA} = 1.6, \gamma_{NMA} = 2.1$, where $\gamma_{AMA} = d_{AMA}/d_{MMA}$.

The corresponding values of β are 1.0, 5.7, 5.1, and 11-23 for methyl, *n*-butyl, isobutyl, and nonyl methacrylate, respectively. These figures are obtained on the assumption that the resistance to chain end diffusion stems from solvent viscosity. If, in tightly coiled polymer chains, the chain segments also impede movement of the radical chain end, these estimates of β must be low, an effect which might be important in the case of the branched chain esters.¹³

Despite the over implication of the diffusion process involved in this preliminary calculation, there is considerable agreement between calculated and observed values of β . Since this represents the first numerical estimate of the way in which the diffusion-controlled termination rate might depend on the chemical nature of the monomer, the method is believed to offer a simple route for the comparison or prediction of other free-radical diffusion-controlled termination rate constants.

A complete summary of the observed and calculated parameters is provided in Table II. It does appear from these data that the rate-determining step of the termination reaction in the free-radical polymerization of the alkyl methacrylates is segmental diffusion of the radical chain ends. From a simplified model of this diffusion it has been possible to calculate decreases in the magnitude of the termination rate constant as the size of the alkyl group increases. These calculated values are in agreement with the observed values.

TABLE II
Calculated and Observed Variations in k_t at 30°C. in Ethyl Acetate as Solvent

Monomer	k_t/k_p $\times 10^{-4}$	$\beta_{\text{obs.}} =$		$\gamma =$ $d_{\text{AMA}}/d_{\text{MMA}}$	$\beta_{\text{calc.}} =$ $\frac{k_{t,\text{MMA}}}{k_{t,\text{AMA}}}$
		$\frac{k_{t,\text{MMA}}k_{p,\text{AMA}}}{k_{p,\text{MMA}}k_{t,\text{AMA}}}$	$\frac{D_{\text{MMA}}}{D_{\text{AMA}}}$		
MMA	7.0	1.0	1.0	1.0	1.0
BMA	1.1	6.3	1.02	1.7	5.7
IBMA	1.1	6.3	1.02	1.6	5.1
NMA	0.56	12.5	1.1-1.2	2.1	11-23

References

1. Burnett, G. M., P. Evans, and H. W. Melville, *Trans. Faraday Soc.*, **49**, 1096, 1105 (1953).
2. Bamford, C. H., W. G. Barb, A. D. Jenkins, and P. F. Onyon, *Kinetics of Vinyl Polymerization by Radical Mechanisms*, Butterworths, London, 1958.
3. North, A. M., and G. A. Reed, *Trans. Faraday Soc.*, **57**, 859 (1961).
4. Benson, S. W., and A. M. North, *J. Am. Chem. Soc.*, **81**, 1339 (1959).
5. Patrick, C. R., *Makromol. Chem.*, **43**, 248 (1961).
6. North, A. M., *Makromol. Chem.*, **49**, 241 (1961).
7. Benson, S. W., and A. M. North, paper presented at Symposium on Recent Advances in Free-Radical Polymerization, American Chemical Society, Cleveland, 1960; *J. Am. Chem. Soc.*, **84**, 935 (1962).
8. Benson, S. W., and A. M. North, *J. Am. Chem. Soc.*, **80**, 5625 (1958).
9. Kirkwood, J. G., and J. Riseman, *J. Chem. Phys.*, **16**, 565 (1948).
10. Debye, P., and A. M. Bueche, *J. Chem. Phys.*, **16**, 573 (1948).
11. Flory, P. J., *Principles of Polymer Chemistry*, Cornell Univ. Press, Ithaca, N. Y., 1953.
12. Chinai, S. M., and R. A. Guzzi, *J. Polymer Sci.*, **41**, 575 (1959).
13. Didot, F. E., S. N. Chinai, and D. W. Levi, *J. Polymer Sci.*, **43**, 557 (1960).

Résumé

On a fait une étude de l'état non-stationnaire du radical libre dans la polymérisation du méthylacrylate de méthyle, *n*-butyle, isobutyle et 3,5,5-triméthylehexyle dans des mélanges de solvants de viscosités variables. On a trouvé que la réaction de terminaison était contrôlée dans chaque cas par la diffusion, et cela sur toute la gamme de viscosité. On a obtenu les valeurs du rapport k_t/k_p pour chaque monomère en utilisant l'acétate d'éthyle comme solvant. On a comparé les diminutions relatives de ce rapport, lorsque le groupe alkyle augmente en grandeur, avec les diminutions calculées en se basant premièrement sur la diffusion par translation des macroradicaux qui règlent la terminaison, en second lieu en se basant sur le fait que la diffusion des segments de la fin de chaîne radicalaire dans le radical libre polymérique est le processus qui contrôle le vitesse de

terminaison. Il est donc nécessaire de considérer un modèle très simplifié de la diffusion des segments. L'influence de la grandeur du groupe alkyle sur la valeur calculée de k_t correspond à ce qui a été observé expérimentalement, quoique les diminutions calculées sur la base de la diffusion par translation ne corresponde pas à ce qui a été observé. Les résultats sont interprétés en considérant que la diffusion des segments de la fin de chaîne radicalaire est l'étape déterminante de la vitesse de terminaison de la polymérisation du radical libre des méthacrylates d'alkyle et fournissent une méthode simple de calcul des valeurs relatives de la constante de vitesse de terminaison contrôlée par la diffusion pour la polymérisation de différents monomères.

Zusammenfassung

Die nichtstationäre radikalische Polymerisation von Methyl-, *n*-Butyl, Isobutyl und 3,5,5-Trimethylhexylmethacrylat wurde in Lösungsmittelgemischen verschiedener Viskosität untersucht. In allen Fällen erwies sich die Abbruchsreaktion im gesamten Viskositätsbereich als diffusionskontrolliert. Werte für das Verhältnis k_t/k_p wurden für alle Monomeren in Athylacetatlösung erhalten. Die relative Abnahme dieses Verhältnisses bei Ansteigen der Grösse der Alkylgruppe wurde (a) mit der auf Grund einer durch Translationsdiffusion von Makroradikalen bestimmten Abbruchgeschwindigkeit und (b) mit der auf der Grundlage der Segmentdiffusion des radikalischen Kettenendes im verknäulten Polymerradikal als geschwindigkeitsbestimmender Prozess beim Abbruch berechneten Abnahme verglichen. Obwohl es notwendig war, ein sehr stark vereinfachtes Modell für die Segmentdiffusion anzunehmen, stimmt die berechnete Abhängigkeit des k_t -Wertes von der Grösse der Alkylgruppe mit der experimentell beobachteten überein, während die für Translationsdiffusion berechnete Abnahme mit der beobachteten nicht übereinstimmt. Die Ergebnisse wurden daher als Beweis für eine Segmentdiffusion des radikalischen Kettenendes als geschwindigkeitsbestimmenden Schritt beim Abbruch der radikalischen Polymerisation von Alkylmethacrylaten betrachtet und liefern eine einfache Methode zur Berechnung der Relativwerte der diffusionskontrollierten Abbruchgeschwindigkeitskonstanten für die Polymerisation verschiedener Monomere.

Received February 15, 1962

Syntheses of Polyanhydrides. XII. Crystalline and High Melting Polyamidepolyanhydride of Methylenebis(*p*-carboxyphenyl)amide*

NAOYA YODA, *Central Research Laboratories, Research Department, Toyo Rayon Co., Ltd., Otsu, Japan*

Synopsis

The acid-catalyzed condensation of formaldehyde and aromatic nitrile has been investigated. Methylenebis(*p*-carboxyphenyl)amide was synthesized in 90% yield by the interaction of *p*-cyanobenzoic acid with formaldehyde under the influence of conc. sulfuric acid. Polycondensation of methylenebis(*p*-carboxyphenyl)-amide was carried out with acetic anhydride at 260–365°C. under vacuum and under a N₂ atmosphere. The linear crystalline polyamidepolyanhydride thus obtained has a melting point at 325–330°C. and exhibits excellent stability towards thermal and hydrolytic degradation. It was confirmed from the experimental evidence that the introduction of the amide linkage in the main chain of the polymer increases the melting temperature of crystallite owing to the formation of intermolecular hydrogen bonds within the molecule of polyanhydride repeating unit. The molecular structure was inferred on the basis of infrared spectra and the x-ray diffraction pattern of the polyamidepolyanhydride. The correlation between cohesion energy per chain unit and crystalline melting temperature of various aromatic and aliphatic polyanhydrides is discussed in detail.

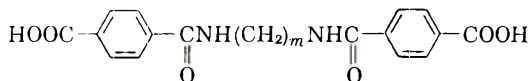
INTRODUCTION

It has been reported in the previous papers of this series that aliphatic,² aromatic,³ and heterocyclic⁴ crystalline polyanhydrides with high melting points and film- and fiber-forming properties could be obtained by polycondensation of corresponding dicarboxylic acids with acetic anhydride. Introduction of ether and thioether linkages in the main chain of aromatic polyanhydrides was found to be effective for lowering melting temperature of crystallite, and easily crystallizable polyanhydrides with high melting points and a good stability towards hydrolytic degradation could be obtained.^{5,6}

The present investigation has been undertaken in order to study the synthesis of high temperature-stable new polyanhydrides which possess amide linkages within a repeating unit. It is reasonably presumed that if aromatic polyanhydrides containing hydrogen-bonded amide linkages within the molecule can be prepared, high melting crystalline polymers with high temperature-resistant properties might possibly be prepared.

* For Part XI of this series see Yoda.¹

The present paper describes the synthesis of a new crystalline polyamide-polyanhydride having a linear polymer structure and showing high melting and thermally stable properties from dicarboxylic acid of the following structure:



where $m = 1, 2, 3, \dots$

Alkylen bisamidodicarboxylic acid was prepared by acid-catalyzed reaction of nitrile with aldehyde in 90% yields. Polycondensation of methylenebis(*p*-carboxyphenyl)amide was carried out with acetic anhydride at 260–365°C. under vacuum and in an N₂ atmosphere to afford high melting crystalline polyamidepolyanhydride as expected.

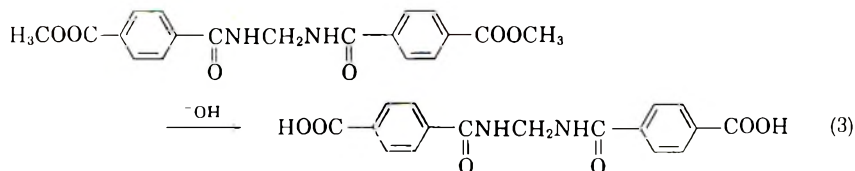
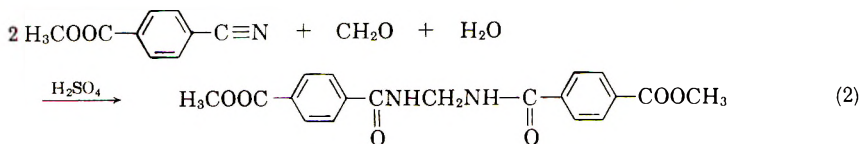
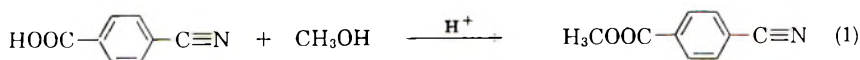
The experimental evidence confirmed that the formation of intermolecular hydrogen bonding within the molecule of chain unit is the main factor for determining high melting of the polymer.

In an attempt to elucidate the relationship between chemical structure and physical properties of these polyanhydrides, the correlation between cohesion energy per chain unit and crystalline melting temperatures of various aromatic and aliphatic polyanhydrides previously reported in the course of this work are discussed in detail.

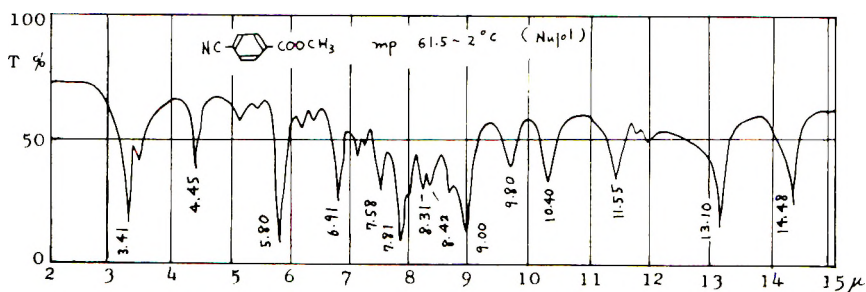
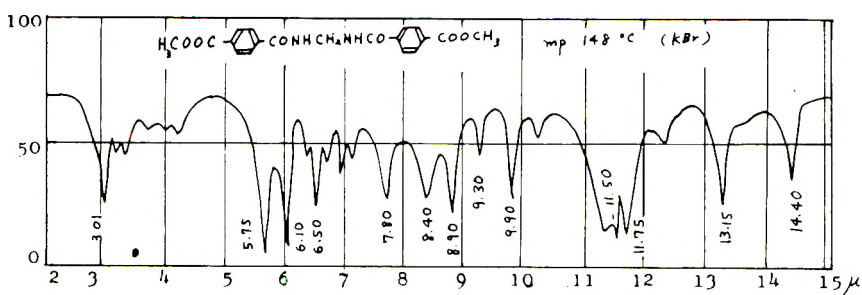
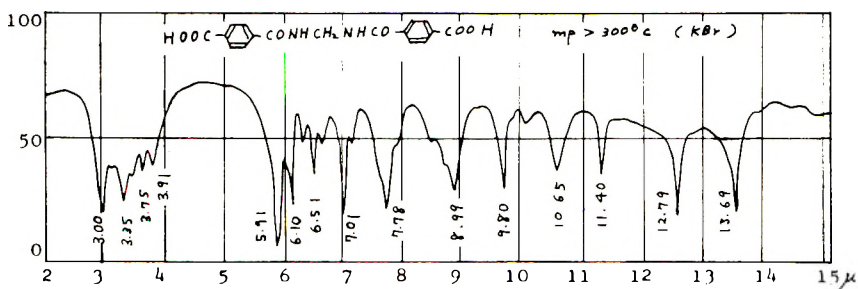
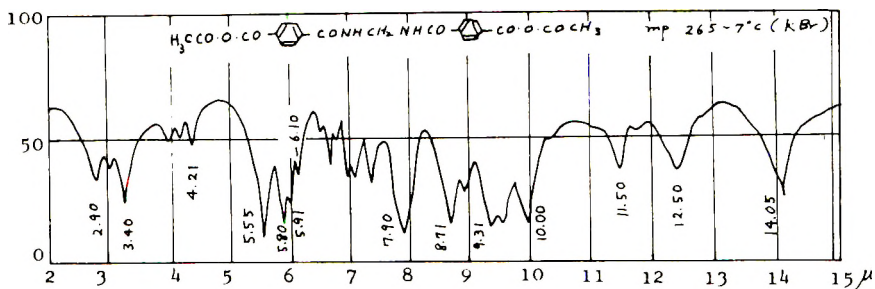
EXPERIMENTAL

Synthesis of Methylenebis(*p*-carboxyphenyl)amide

Acid-catalyzed reaction of nitrile with aldehyde was employed for the preparation of methylenebisamide;⁷ the interaction of methyl *p*-cyanobenzoate with formaldehyde under the influence of conc. sulfuric acid, followed by hydrolysis affords the dicarboxylic acid as shown in eqs. (1)–(3).



The experimental procedure used in the acid-catalyzed reactions to be described consists of adding a mixture of aldehyde and nitrile to an acid

Fig. 1. Infrared spectrum of methyl *p*-cyanobenzoate.Fig. 2. Infrared spectrum of methylenebis(*p*-carbomethoxyphenyl)amide.Fig. 3. Infrared spectrum of methylenebis(*p*-carboxyphenyl)amide.Fig. 4. Infrared spectrum of methylenebis(*p*-carboxyphenyl)amide diacetate.

solution, the reaction temperature being kept at 30°C., and pouring the reaction mixture into an excess of ice and water to precipitate the methylenebisamide reaction product.

Reaction of Methyl *p*-Cyanobenzoate and Formaldehyde. A solution of trioxane (0.025 mole, 0.75 g.) in methyl *p*-cyanobenzoate (0.05 mole, 7.4 g.) was added slowly with stirring to an 85% solution of sulfuric acid (19 ml.) in a 200-ml. three-necked flask. The temperature was maintained at 30°C. by cooling with an ice bath. After 5 hr. the solution was poured into 150 ml. of ice and water. Methylenebis(*p*-carbomethoxyphenyl)amide separated as white crystals which were filtered and recrystallized from 95% ethanol. The yield of product was 49%, melting at 148°C. The infrared spectrum (Fig. 2) shows an ester carbonyl band at $\lambda_{\max} = 5.75 \mu$ and an amide band at $\lambda_{\max} = 6.10 \mu$.

Hydrolysis of Methylenebis(*p*-carbomethoxyphenyl)amide. A 15-g. (0.2 mole) portion of methylenebis(*p*-carbomethoxyphenyl)amide was added to 100 ml. of 10% aqueous sodium hydroxide and refluxed for 2 hr. After the solution was cooled to room temperature, it was acidified and extracted with ether. Upon recrystallization from aqueous ethanol afforded colorless crystals, melting at 310°C. with decomposition. The infrared spectrum (Fig. 3) indicates a carboxyl carbonyl band at $\lambda_{\max} = 5.91 \mu$ and an amide band at $\lambda_{\max} = 6.10 \mu$.

ANAL.: Calc. for $C_{17}H_{14}O_6N_2$ (MW 342.24): C, 59.65%; H, 4.09%; N, 8.18%. Found: C, 58.06%; H, 4.08%; N, 7.89%.

Polymerization of Methylenebis(*p*-carboxyphenyl)amide with Acetic Acid

Acetylation of Methylenebis(*p*-carboxyphenyl)amide. A 10.0-g. (0.03 mole) portion of purified methylenebis(*p*-carboxyphenyl)amide was dissolved in 500 ml. of acetic anhydride and refluxed at 150–160°C. for 5 hr. After the excess of acetic anhydride was removed under reduced pressure, the diacetate was filtered, yielding a crystalline solid melting at 265–267°C. with decomposition. The yield of product was 80%. The infrared spectrum (Fig. 4) indicates the existence of acetate carbonyl absorption bands at $\lambda_{\max} = 5.55 \mu$ and 5.80μ . The amide I group shows a shoulder at $\lambda_{\max} = 6.10 \mu$.

Polymerization of Methylenebis(*p*-carboxyphenyl)amide diacetate. A 15.0-g. portion of purified diacetate of methylenebis(*p*-carboxyphenyl)amide was introduced into a 50-ml. polymerization vessel a glass N_2 inlet tube and connected to a high vacuum pump and heated at 260–365°C./3 mm. Hg.

The detailed polymerization procedure is summarized in Table I.

The polyamidepolyanhydride thus obtained has a melting point at 325–330°C. and is thermally stable. The infrared spectrum of the polyamidepolyanhydride is shown in Figure 5.

The carbonyl stretching vibration of the anhydride group shows two absorption bands at $\lambda_{\max} = 5.59 \mu$ and 5.79μ . The ether linkage of the

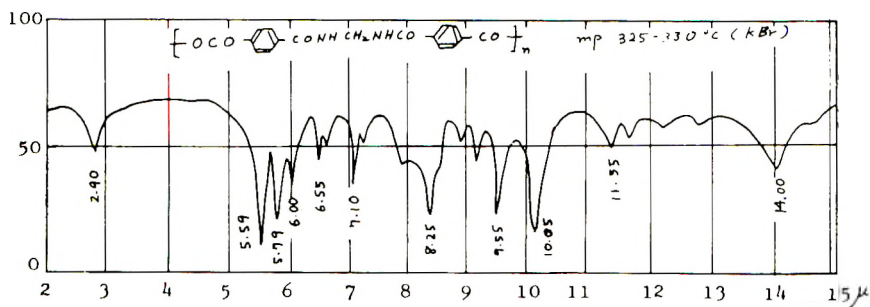
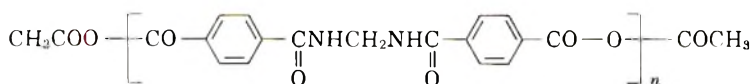


Fig. 5. Infrared spectrum of poly[methylenebis(*p*-carboxyphenyl)amide]anhydride.

anhydride group is also confirmed by absorption band at $\lambda_{\max} = 10.05 \mu$. In addition, amide I band falls as a shoulder in the higher wavelength of carbonyl regions, $\lambda_{\max} = 6.06 \mu$. The intrinsic viscosity of the polymer measured in *m*-cresol at 25.0°C. was 0.140. The product has the structure:



ANAL.: Calc. for $(\text{C}_{17}\text{H}_{12}\text{O}_5\text{N}_2)_n$: C, 62.96%; H, 5.25%; N, 8.64%. Found: C, 61.85%; H, 4.92%; N, 8.62%.

The x-ray diffraction diagram of polyamidepolyanhydride obtained with nickel-filtered $\text{CuK}\alpha$ irradiation shows a discrete Debye-Scherrer ring as shown in Figure 6. It was confirmed that polyanhydride of high crystallinity could be obtained.

TABLE I
Polymerization of Methylenebis(*p*-carboxyphenyl)amide with Acetic Anhydride

Polymerization time, min.	Polymerization temp. and pressure, °C./mm. Hg	Remarks
0	260/20	Diacetate was heated to melt and N_2 gas was introduced
10	265/3	Polymerization starts
20	267/3	Viscosity of the melt increases
50	272/3	"
80	276/3	"
110	305/3	Polymerization proceeds
140	325/3	"
170	360/3	"
200	360/3	Crystalline polymer
230	365/3	Polymerization completed

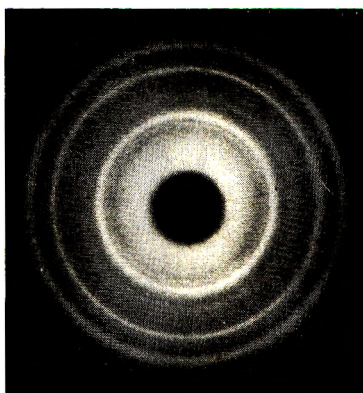


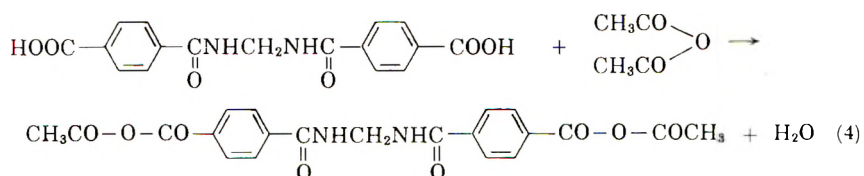
Fig. 6. X-ray diffraction pattern of poly[methylenebis(*p*-carboxyphenyl)amide]-anhydride obtained with the use of $\text{CuK}\alpha$ irradiation (35 kv., 15 ma.).

RESULTS AND DISCUSSION

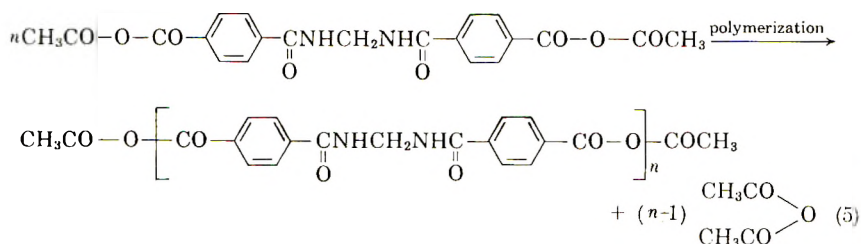
Polymerization Mechanism

In the polymerization dicarboxylic acid of methylenebisamide with acetic anhydride, it is reasonably presumed that the polycondensation reaction proceeds through three steps.

1. Acetylation. Acetylation proceeds as shown in eq. (4).

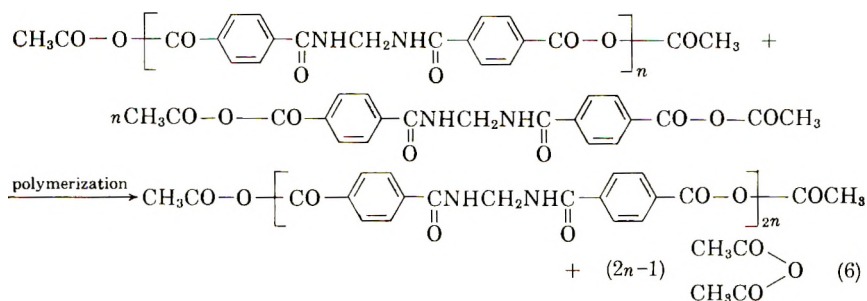


2. Formation of α -Polyamidepolyanhydride. This second step proceeds as shown in eq. (5).



For the α -polyamidepolyanhydride (prepolymer), n is small.

3. Formation of ω -Polyamidepolyanhydride. The last step is as shown in eq. (6).



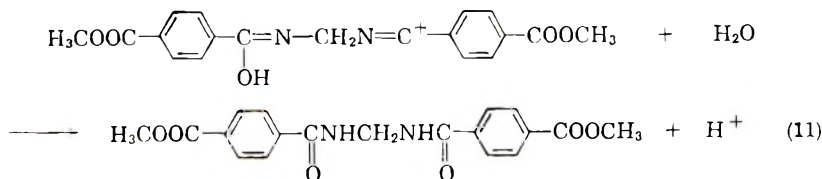
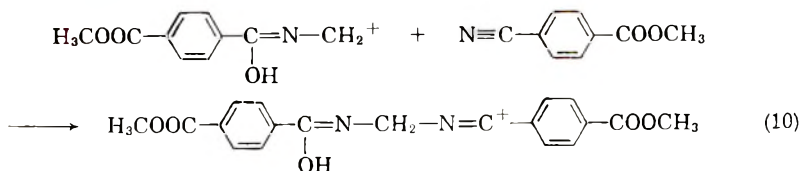
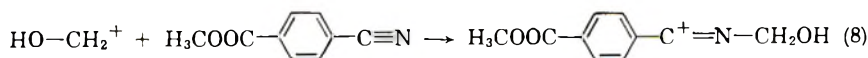
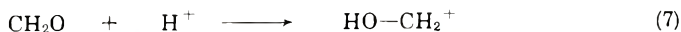
For the ω -polyanhydride, n is large.

In the first step, the diacetate of dicarboxylic acid is formed; this can be separated and purified before polymerization. When it is heated at 160–260°C., acetyl endgroups are split off to afford low-melting crystalline solid in the second step. Finally, upon heating under reduced pressure, polyanhydride having an intermolecularly hydrogen bonding amide group with high molecular weight is formed by a process of dehydration and anhydride interchange involving the elimination of terminal groups between adjacent molecules.

Acid-Catalyzed Carbonium Ion Mechanism of Reaction of Methyl *p*-Cyanobenzoate and Formaldehyde

The reaction of methyl *p*-cyanobenzoate with trioxane appears to proceed by a carbonium ion mechanism and does not involve hydrolysis of the nitrile to amide. This is supported by the fact that (a) amides do not react with formaldehyde under the reaction conditions used for nitriles, and (b) nitriles are not converted to amides by 85% sulfuric acid at a rate comparable to the reaction of nitriles with formaldehyde.

Thus the mechanism may be represented by the following eqs. (7)–



Although equations (10) and (11) represent reversible reactions, the yield of methylenebis(*p*-carboxyphenyl)amide attained was as high as 90%.

Intermolecular Hydrogen Bonding of Polyamidepolyanhydride

As to the possibility of intermolecular hydrogen bonding of polyamidepolyanhydride, it can be seen from Figure 5 that the existence of amide I (6.06μ) and amide II (6.55μ) bands are obvious, and hydrogen-bonding effects give rise to considerable shifts in these bands compared with those of the nonbonded states. By the infrared spectra of the 3μ region with LiF optics, it can be concluded that the amide linkage forms a complete intermolecular hydrogen bond. Thus, the molecular structure and intermolecular hydrogen bonding of amide groups of poly[methylenebis(*p*-carboxyphenyl)amide] anhydride may be represented as shown in Figure 7.

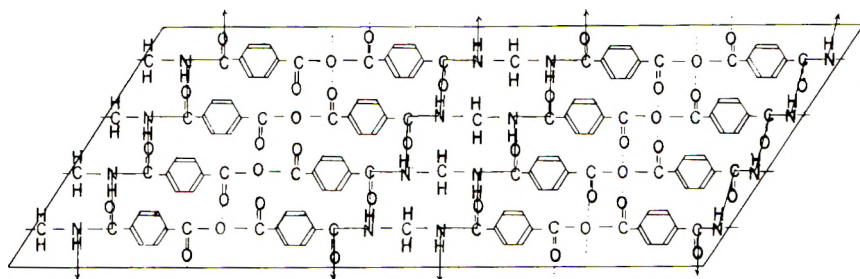


Fig. 7. Molecular structure and intermolecular hydrogen bonding of the amide group in poly[methylenebis(*p*-carboxyphenyl)amide]-anhydride.

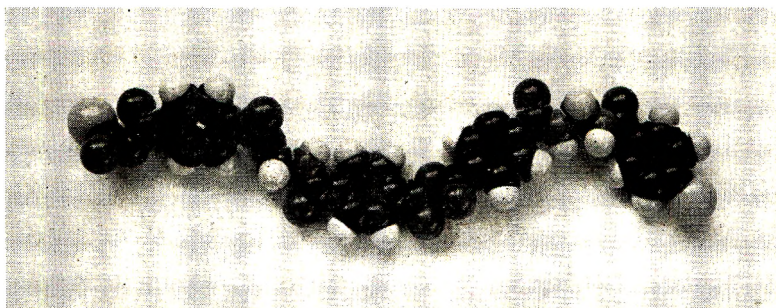


Fig. 8. Stuart molecular model of poly[methylenebis(*p*-carboxyphenyl)amide] anhydride.

It may be suggested that a pleated structure similar to that proposed by Pauling and Corey⁸ for the polypeptide chain might be adopted as the probable configuration of the structure of the polyamidepolyanhydride. The Stuart molecular model of the polymer is shown in Figure 8.

The structural requirements for the polypeptide configuration are the correct bond distances and bond angles, the coplanarity of the atoms com-

prising the amide group, and the formation of close to the maximum possible number of hydrogen bonds with N—H...O distances of approximately 2.8 Å. and with the oxygen atom nearly on the N—H axis. It may be expected for polyamidepolyanhydride that the assumption of the structural requirement of a N—H...O hydrogen bond between adjacent molecules forces the molecules to take the possible configuration illustrated in Figure 7.

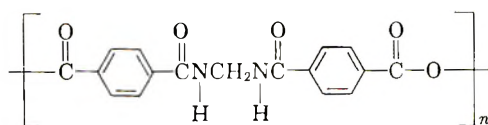
Estimation of Intermolecular Forces of Polyamidepolyanhydride

The physical properties, such as crystalline melting temperatures, of polyanhydrides prepared in the course of this work may depend on some function of cohesion energy of the molecules, on the degree of flexibility of the chains, and on certain shape effects of the degree of departure from cylindrical shape.

The cohesion energy of the chain unit in polyanhydride molecules i.e., the total forces holding the molecule in place in the lattice, may be the most important factor influencing physical properties of the polymers. The cohesion energy E can be measured experimentally as the molar latent heat of evaporation L , and E is expressed by the eq. (12):

$$E = L - RT \quad (12)$$

TABLE II
Molecular Cohesion Energy and Volume Increment of Polyamidepolyanhydride

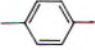



Organic group	Cohesion energy, E , cal./mole	Number of chain unit	Average molecular cohesion energy per chain unit	Volume increment, ml./mole
	3,900	1	—	50.5
	$3,900 \times 2$	2	—	83.9
	$8,500 \times 2$	2	—	36.2
	680	1	—	21.8
Total	29,380	6	4,980	312.5

where the second term is a small correction for the work done on expansion. The cohesion energies of chain units in polyanhydride molecules may be estimated by an additive system, based on the properties of substances composed of small molecules, in which a definite increment is associated with each functional group of atoms.⁹ Table II gives the data for the polyanhydride of methylenebis(*p*-carboxyphenyl)amide. The calculated value of average molecular cohesion energy per chain unit was found to be 4,980 cal./mole.

In order to elucidate the relationship between cohesion energy and crystalline melting temperature of polyanhydrides, figures of cohesion energy of various common aliphatic and aromatic groups for polyanhydrides are summarized in Table III.

TABLE III
Cohesion Energy and Volume Increment for Common Groups^a

No.	Group	Cohesion energy, cal./mole	Volume, cc./mole
1	—CH ₂ —	680	21.8
2		3,900	83.9
3	—CH=CH— CH ₃	1,700	32.0
4	—C— CH ₃	1,900	65.4
5	—Cl	2,800	21.8
6	—Br	3,100	30.5
7	—I	4,200	40.5
8	—CO	2,660	21.6
9	—O—	1,000	7.3
10	—CO—O— (ester)	2,900	28.9
11	—CO—O—CO— (anhydride)	3,900	50.0
12	—S—	2,200	—
13	—CONH—	8,500	36.2
14	—COOH	5,600	36.5
15	 —OC(O)— (carbonate) ^b	4,600	66.2
16	—OH (alcohol)	5,800	14.9

^a Data of Bunn.⁹

^b Calculated value.

Correlations between Melting Point and Cohesion Energy of Polyanhydride Series

The principal factor controlling melting of polyanhydrides appear to be the molar cohesion energy per chain unit. Thus cohesion energies of aro-

matic, aliphatic, and heterocyclic linear crystalline polyanhydrides of various molecular structures prepared in the course of this work have been calculated; these are summarized in Tables IV and V.

The melting points of various types of linear polyanhydrides are now known, and it is possible to plot the melting points against cohesion energy per chain unit as shown in Figure 9.

It is interesting to note that values for aromatic polyanhydrides fall approximately on a straight line and evidently, other things being equal, there is a linear relationship between melting points and cohesion energy per chain unit in aromatic polyanhydrides. When the carbonyl π -electron interacts with the π -orbital of phenylene group, and carbonyl group is directly joined to a benzene ring, the melting points of polyanhydrides are

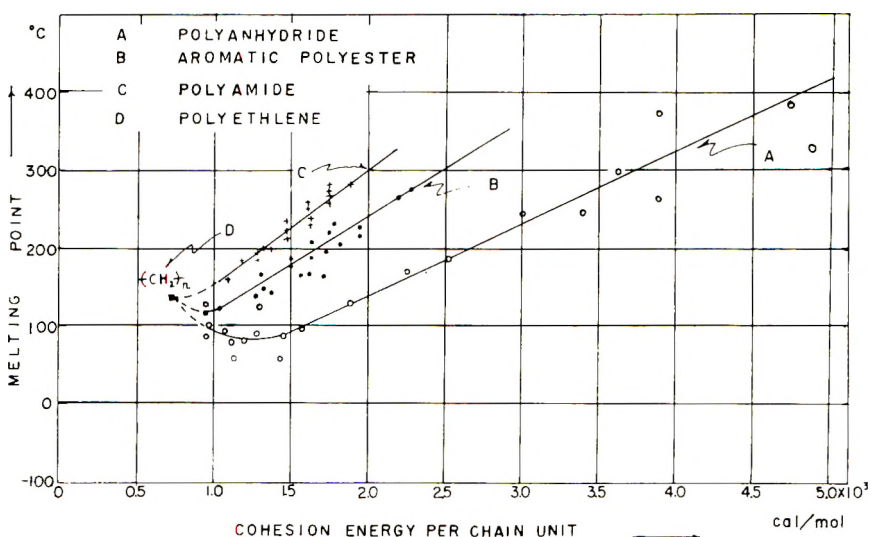
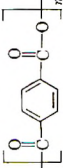
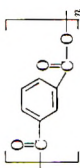
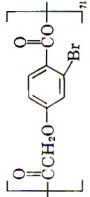
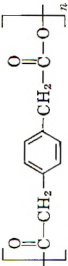
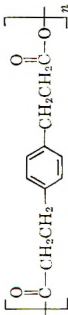
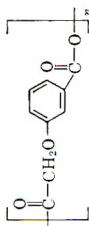


Fig. 9. Cohesion energy per chain unit and melting point of polymers. A (the present study); B ref. 10 C; ref. 9; D ref. 11.

higher than that of polymethylene. It is reasonably presumed that the whole group in the $-\text{C}_6\text{H}_4-\text{CO}-$ or $-\text{CO}-\text{C}_6\text{H}_4-\text{CO}-$ aromatic polyanhydrides is taken as a single unit which owes its rigidity to overlap of π -electron orbitals by resonance effect.

Aliphatic polyanhydrides melt lower than polymethylene, and there is a general decrease of melting point as the proportion of anhydride groups in the chain increases, in spite of the increase of intermolecular forces by the polar anhydride groups.² This suggests that in the anhydride group there is a bond around which rotation is considerably easier than in a CH_2 chain. In *n*-butane, the potential barriers to rotation are about 3,000 cal./mole.¹⁰ Values for potential barriers to rotation in acetone (1,400 cal./mole) and dimethyl ether (2,500–3,100 cal./mole) suggest that the CH_2-CO and CH_2-O bonds are easily rotatable.¹⁰

TABLE IV
Cohesion Energy and Molecular Structure of Various Polyhydrides

No.	Chemical unit	E , cal./mole	Number of chain units	Average E per chain unit, cal./mole	Melting point, °C.
1		7,800	2	3,900	400
2		7,800	2	3,900	259
3		12,580	5	2,516	175-179
4		9,160	6	1,526	90-92
5		10,420	8	1,302	90-29
6		9,480	5	1,896	128-134

7		10,480	8	1,310	127-130
8		14,820	10	1,482	45-55
9		14,820	10	1,482	88
10		16,180	12	1,348	91
11		12,380	11	1,126	75
12		11,020	9	1,224	83
13		8,820	8	1,103	55

TABLE V
Cohesion Energy and Molecular Structure of Various Polyanhydrides

No.	Chemical unit	E_c , cal./mole	Number of chain units	Average E per chain unit	Melt- ing point °C.
1		29,380	6	4,897	325-330
2		11,160	8	1,395	152
3		15,600	7	2,152	215
4		13,600	4	3,400	238-240
5		16,960	10	1,696	196-202
6		10,520	8	1,315	90-2
7		7,670	8	959	67
8		7,770	8	971	188
9		7,670	8	959	78
10		7,670	8	959	135
11		9,770	8	971	103

An increase in chain flexibility and lowering of melting temperatures of the polyanhydrides were also observed for polyetherpolyanhydrides⁵ and polythioetherpolyanhydrides.³

As it may be noted in Tables IV and V and Figure 9, this generalization of correlation between melting temperatures of polyanhydrides and cohe-

sion energy per chain unit throws a valuable light on the further prediction of melting temperature of other types of polyanhydrides.

The author takes pleasure in acknowledging the support and interest of Dr. K. Hoshino, Managing Director of Toyo Rayon Co., Ltd., and Dr. H. Kobayashi, Director of the Research Department, and permission for publication. Sincere thanks are also due to Professor Y. Ishii of Nagoya University for valuable discussions.

References

1. Yoda, N., *Makromol. Chem.*, **56**, 36 (1962).
2. Yoda, N., and A. Miyake, *Bull. Chem. Soc. Japan*, **32**, 1120 (1959).
3. Yoda, N., *Makromol. Chem.*, **32**, 1 (1959); N. Yoda, *Chem. High Polymers Japan*, **19**, 490, 495, 553 (1962).
4. Yoda, N., *Makromol. Chem.*, **55**, 174 (1962).
5. Yoda, N., *Makromol. Chem.*, **56**, 10, 36 (1962); N. Yoda, *J. Chem. Soc. Japan (Ind. Chem. Sect.)*, **65**, 667, 676 (1962).
6. Conix, A., *J. Polymer Sci.*, **29**, 343 (1958); A. Conix, *Makromol. Chem.*, **24**, 76 (1957).
7. Magat, E., B. F. Faris, J. E. Reith, and L. F. Salisbury, *J. Am. Chem. Soc.*, **73**, 1028 (1951); E. Hepp and G. Spiess, *Ber.*, **9**, 1424 (1876); E. Hepp, *Ber.*, **10**, 1649 (1877).
8. Pauling, L., and R. B. Corey, *Proc. Natl. Acad. Sci. U. S.*, **39**, 253 (1953).
9. Bunn, C. W., *J. Polymer Sci.*, **16**, 323 (1955); H. Mark, *Physical Chemistry of High Polymeric Systems*, Interscience, New York, 1950.
10. McCoubrey, J. C., and A. R. Ubbelohde, *Quart. Revs.*, **5**, 364 (1951).
11. Mandelkern, L., M. H. Hellmann, D. W. Brown, D. E. Roberts, and F. A. Quinn, *J. Am. Chem. Soc.*, **75**, 4093 (1953).

Résumé

On a étudié la condensation "acide" du formaldéhyde et d'un nitrile aromatique; on a synthétisé le méthylènebis(*p*-carboxyphényl)amide (90% de rendement) par réaction de l'acide *p*-cyanobenzoïque avec le formaldéhyde en présence d'acide sulfurique concentré. On a polycondensé le méthylènebis(*p*-carboxyphényl)amide en présence d'anhydride acétique à 260–365°C sous vide et sous atmosphère d'azote. Le polyamide-polyanhydride cristallin ainsi obtenu a un point de fusion de 325–330°C et révèle une excellente stabilité vis-à-vis de la dégradation thermique ou homolytique. Par l'expérience on a confirmé que l'introduction de lien amide dans la chaîne principale du polymère augmente la température de fusion du cristallite à cause de la formation de pont hydrogène intermoléculaire entre les molécules d'éléments polyanhydrides. On a déduit la structure moléculaire sur la base des spectres infra-rouges et du diagramme de diffraction des R.X. du polyamide-polyanhydride et on a discuté en détail la relation entre l'énergie de cohésion par unité présente dans la chaîne et la température de fusion des cristallites pour divers polyanhydrides aromatique et aliphatique.

Zusammenfassung

Die säurekatalysierte Kondensation von Formaldehyd mit aromatischen Nitrilen wurde untersucht und Methylenbis(*p*-carboxyphenyl)amid in 90% Ausbeute durch Reaktion von *p*-Cyanbenzoesäure mit Formaldehyd unter Einwirkung starker Schwefelsäure synthetisiert. Die Polykondensation von Methylenbis(*p*-carboxyphenyl)amid wurde mit Essigsäureanhydrid bei 260–365°C im Vakuum und unter Stickstoff durchgeführt. Der Schmelzpunkt des so erhaltenen linearen, kristallinen Polyamidpolyanhydrids liegt bei 325–330°C. Es zeigt eine ausgezeichnete Beständigkeit gegen thermischen und hydrolytischen Abbau. Die experimentellen Ergebnisse bestätigen, dass

die Einführung einer Amidbindung in die Hauptkette des Polymeren den Schmelzpunkt der Kristallite infolge der Bildung von intermolekularen Wasserstoffbindungen im Molekül des Polyanhydridbausteins erhöht. Die Molekülstruktur des Polyamid-polyanhydrids wurde infrarotspektroskopisch und durch Röntgenbeugung untersucht und die Beziehung zwischen Kohäsionsenergie pro Kettenbaustein und Kristallitschmelztemperatur verschiedener aromatischer und aliphatischer Polyanhydride im einzelnen diskutiert.

Received February 13, 1962

The Locus of Adhesive Failure

J. R. HUNTSBERGER, *Fabrics and Finishes Department,
E. I. du Pont de Nemours & Company, Inc., Experimental Station,
Wilmington, Delaware*

Synopsis

The problem of the locus of adhesive failure is discussed. It is proposed that real systems will show departures from regularity and that the interaction between phases is frequently diminished by steric effects leading to interfacial separation. This is counter to some recently proposed views. Estimates of the magnitude of these effects required to lead to interfacial separation are given in terms of failure criteria. Interferometry was used to provide experimental evidence that interfacial separation can occur between poly-isobutylene and a crosslinked alkyd resin. The performance of this system was also shown to be in harmony with the proposed failure criteria.

Introduction

One of the important unresolved problems met in studies of adhesion concerns the locus of adhesive failure. Frequently, the most fruitful avenues for research can be selected only on the basis of unequivocal assignment of such failure as interfacial separation or cohesive failure within one of the adherends or a weaker boundary "interphase."

The purpose of this paper is to present some theoretical considerations and experimental evidence for interfacial separation.

Discussion

There is currently little agreement among various workers in the field of adhesion concerning the locus of failure. Bikerman¹ states that adherends in molecular contact never exhibit interfacial separation. His argument is based on two premises of doubtful validity. First, that the interfacial attraction between the bulk phases is the geometric mean of the attraction between like molecules of each phase. Second, that there is negligible probability that failure could propagate along the interface.

The approximation that the attraction between two dissimilar atoms is the geometric mean of the individual attractions for pairs of similar atoms may frequently be satisfactory for systems in the vapor phase. For condensed phases, however, and especially for solids, restrictions on interatomic spacing and molecular configuration will produce large deviations. Recent work by Girifalco, Good, and Kraus²⁻⁴ has provided an estimate of the magnitude of such deviations for several systems.

Taylor and Rutzler⁵ and Mark⁶ have also indicated that there is little likelihood for one-to-one atomic configurations at the interface.

According to Bikerman, the probability for propagation of interfacial separation is nil. Actually, the biaxial character of residual stresses within most polymeric films attached to rigid substrates is such that the probability is nearly unity that a crack, whatever its initial position, will propagate to the interface. Once this has occurred, both shear and normal components of the internal stress will bias the propagation along the interface. Also, the stresses which occur within the film which result from the strains introduced during the rupture of the bond will be greatest at the interface.

Despite the inherent dangers in extrapolating criteria based on thermodynamics of reversible processes, it may be instructive to consider what values such criteria assume for determining the possibility of interfacial separation.

$$F_{ab} = F_a + F_b - 2\phi(F_a F_b)^{1/2} \quad (1)$$

where F_a and F_b are the surface free energies of phases a and b, and $2\phi(F_a F_b)^{1/2}$ is the energy of interaction between the phases. This latter term is frequently designated as (W_{ADH}) the work of adhesion. The constant ϕ is a function of the molecular characteristics of both phases and is a measure of departure from regularity.

When each phase is comprised of a single component:

$$F_{ab} = F_a - F_b \cos \theta \quad (2)$$

Substituting this value for F_{ab} into eq. (1) gives:

$$2\phi(F_a/F_b)^{1/2} - 1 = \cos \theta \quad (3)$$

Equations (1) and (2) can also be combined to give:

$$W_{ADH} = 2\phi(F_a F_b)^{1/2} = F_b(1 + \cos \theta) \quad (4)$$

For interfacial failure, the energy of adhesion must be less than the energy of cohesion $2F_b$ of the film (assuming that failure will not occur within the substrate phase). Thus, the criterion for interfacial failure is that $\cos \theta < 1$. Consequently, from Equation (3),

$$\phi(F_a/F_b)^{1/2} < 1 \quad (5)$$

represents a criterion for interfacial separation.

From eq. (5) it is evident that for low energy substrates coated with organic polymers only slight irregularity is necessary to permit interfacial separation.

If no restriction is placed on the possibility of failure within the substrate phase, it can be shown that the criterion for interfacial separation becomes:

$$F_{ab} > |F_a - F_b| \quad (6)$$

We can examine these criteria by determining values F_a and F_b for the two phases and finding the minimum permissible value of F_{ab} , and the maximum value of ϕ which would result in interfacial separation.

From Good, Girifalco, and Kraus,³ we find data for a fluorocarbon and benzene. F_a for benzene is 28.2 ergs/cm.² and F_b for the fluorocarbon is 22.8 ergs/cm.²

Using eq. (5), we find that $\phi < 0.90$ corresponds to interfacial separation. Using this value of ϕ in eq. (1) leads to $F_{ab} = 5.5$. The experimental values were given³ as $F_{ab} = 7.9$ and $\phi = 0.85$. When polymers are considered, one would expect lower values for ϕ than are exhibited by low molecular weight liquids.

The arguments presented here indicate that true interfacial separation may occur in practical systems. Frequently, it is very difficult to establish unequivocally whether or not this is actually the case, however, since one would expect that failure would occur very close to the substrate/adhesive interface. Even when failure is cohesive within the adhesive or within a weak "interphase" or boundary layer, only a very thin layer may remain. Such a residual film might be a monolayer or perhaps a few hundred angstroms thick.

The experiments described below were performed in order to establish the locus of failure for one specific system which appeared to fail at the interface.

Experimental

Preliminary experiments with polyisobutylene indicated that this polymer, when peeled from various substrates, failed at the interface. This was true whether high or relatively low molecular weight polymer was used.

In order to provide unequivocal evidence for interfacial separation, it is mandatory that prior to separation intimate interfacial contact is achieved. To insure such approach to the maximum possible interfacial contact, a low molecular weight polyisobutylene was used which exhibited sufficient flow at 25°C. to produce films of high specular gloss. Vistanex LM-MS was fractionated crudely to remove any low molecular weight materials which may have been present. The fractionated polymer was dissolved in spectral grade normal heptane and used without further characterization.

The experiments consisted of casting polyisobutylene on thin substrate films of crosslinked alkyd resin (52% soya, A.N. = 6) of known thickness, allowing sufficient time to insure intimate interfacial contact, then stripping the polyisobutylene from the alkyd and redetermining the thickness of the substrate film plus any residue.

This was accomplished by modifying the interferometric technique described by Miller.⁷ A Perkin-Elmer Spectracord with a reflectance attachment was utilized in the visible wavelength region as an interferometer. The thicknesses of the substrate alkyd films were calculated from the spectral curves by using eqs. (7) and (8):

$$t = (m/2n)\lambda \text{ (for maxima)} \quad (7)$$

$$t = [(2m - 1)\lambda/4n] \text{ (for minima)} \quad (8)$$

where t is film thickness, n is refractive index, λ is wavelength, and m is the order number of the interference peak.

Since n varies as a function of wavelength and we were interested in changes rather than absolute values, n was assumed to be 1.5; thickness values for the films were calculated by extrapolating the data for individual maxima and minima to a fixed arbitrary wavelength of 4600 Å. The precision of this technique was good. The standard deviation for an individual measurement was 4 Å.

The thin (~ 4000 Å.) substrate alkyd films were prepared by casting from dilute solution onto first surface chromed microslides. These films were baked 0.5 hr. at 200°C. and were then extracted at room temperature in reagent grade acetone until further extraction produced no change in thickness (~ 2 months). They were then extracted in n -heptane for two weeks before the final thicknesses of the uncoated substrate films were determined.

Thin (0.001 in.) films of polyisobutylene were cast on the alkyd substrates. These films were allowed to stand for ten days at room temperature in order to achieve maximum or near maximum interfacial contact. They were then stripped from the alkyd by applying cellophane tape to the back and peeling very rapidly. High adhesion between the polyisobutylene and the alkyd was observed during the peeling. After 5 hr. at 25°C. and 50% R.H., the thickness was redetermined. The mean change exhibited by fifty-four samples was -1.3 ± 3.3 Å. (95% confidence limits). Thus, there was no significant change, and true interfacial separation has been demonstrated.

These experiments were based on the premise that the difference in refractive indices of the two films would be sufficiently small compared to the change at the polymer air interface that any polyisobutylene which might remain on the surface of the alkyd could be detected and measured with only a very small error. In order to demonstrate the feasibility of measuring such thin residues, very thin films of polyisobutylene were cast onto premeasured alkyd films from successively more and more dilute solutions from 0.1% to 0.00625% polymer. These very thin films were then dried and the thickness determined. The results are shown in Figure 1. The mean change of duplicate samples is plotted against concentration of the solution from which the polyisobutylene films were deposited. These data show clearly that any residual films would have been detected by the present technique.

The fluid character of the polyisobutylene used for these experiments permitted an estimate of ϕ to be made for the polyisobutylene/alkyd resin system. The contact angle was determined for small droplets of polymer which were placed on the alkyd surface and stored in a desiccator. Measurements were made after three weeks and six weeks to insure that

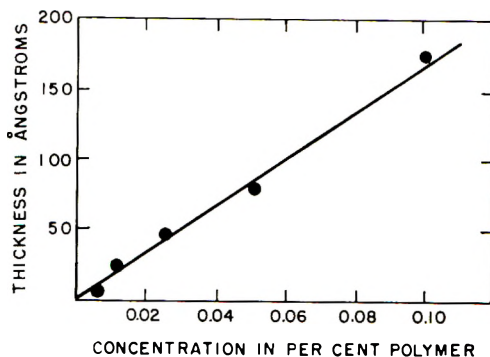


Fig. 1. Thickness of polyisobutylene films vs. concentration of casting solutions.

equilibrium had been reached. There were no significant differences between the three-week and six-week measurements. The contact angle was $17 \pm 1^\circ$. From eqs. (1) and (2), ϕ was determined to be 0.961. The value of F_b for polyisobutylene is 30 ergs/cm.², and F_a for the alkyd is 31 ergs/cm.². These are γ_c values determined by using the method of Fox and Zisman.⁸ From eq. (5), the maximum value of ϕ permitting interfacial separation is 0.985. The finite contact angle (and the associated ϕ values) are consistent with the experimental evidence for interfacial separation.

Conclusions

Separation of adherends at the interface has been demonstrated for one system, and data from the literature appears to suggest that this may be expected for others. The thermodynamic criteria for interfacial separation must be accepted with reservations; but for cases in which the separation rates greatly exceed the relaxation rates of the adhesive, such criteria are probably conservative.

References

1. Bikerman, J. J., *The Science of Adhesive Joints*, Academic Press, New York, 1961.
2. Girifalco, L. A., and R. J. Good, *J. Phys. Chem.*, **61**, 904 (1957).
3. Good, R. J., L. A. Girifalco, and G. Kraus, *J. Phys. Chem.*, **62**, 1418 (1958).
4. Good, R. J., and L. A. Girifalco, *J. Phys. Chem.*, **64**, 561 (1960).
5. Taylor and Rutzler, *Ind. Eng. Chem.*, **50**, 928 (1958).
6. Mark, H., *Problems in Wood Chemistry*, Weizman Science Press of Israel, 1957.
7. Miller, C. D., *J. Polymer Sci.*, **24**, 311 (1957).
8. Fox, H. W., and W. A. Zisman, *J. Colloid Sci.*, **7**, 428 (1952).

Résumé

Le problème de la localisation d'un défaut d'adhésivité est discuté; on admet que des systèmes réels montreront des écarts par rapport à la régularité et que l'interaction entre phases est souvent déterminée par des effets stériques donnant lieu à une séparation interphase. Ceci tient compte de points de vue récemment proposés. On estime que l'ampleur de ces effets donnant lieu à une séparation interphase est donné sur la base de critère de défauts. L'interférométrie a été utilisée afin de prouver expérimentalement

qu'une séparation interphase peut se produire entre le polyisobutylène et une résine alkyde réticulée. On a montré également que la réalisation de ce système est en accord avec les critères de défauts proposés.

Zusammenfassung

Das Problem der Lokalisierung des Bruches von Klebeverbindungen wird diskutiert. Es wird angenommen, dass reale Systeme Abweichungen vom regulären Verhalten zeigen und dass die Stärke der Wechselwirkung zwischen Phasen häufig durch sterische Einflüsse herabgesetzt wird, was zu einer Grenzflächentrennung führt. Diese Annahme steht im Gegensatz zu gewissen neueren Vorschlägen. Eine Abschätzung der Grösse der erwähnten Einflüsse, die zum Auftreten einer Grenzflächentrennung erforderlich ist, wird anhand von Bruchkriterien gegeben. Durch interferometrische Messungen wurde gezeigt, dass Grenzflächentrennung zwischen Polyisobutylen und einem vernetzten Alkydharz auftreten kann. Das Verhalten dieses Systems stand auch mit den angegebenen Bruchkriterien im Einklang.

Received February 21, 1962

Oxidative Crosslinking of Polyethylene by Ultraviolet Light

G. R. COTTEN* and W. SACKS,† *Research Department, Visking Company,
Division of Union Carbide Corporation, Chicago, Illinois*

Synopsis

The mechanism of weathering damage in polyethylene films was studied by measurement of molecular weight (by intrinsic viscosity), content of xylene-insoluble fraction (gel), and carbonyl group concentration (by infrared analysis) in exposed samples. Results obtained indicate that both chain scission β and crosslinking α occur simultaneously. The effect of thickness and crystallinity of the polyethylene films suggest that the ratio β/α may be dependent upon the oxygen concentration at the site of reaction and, therefore, the rate of penetration of oxygen through the film, at constant intensity of absorbed light. The chain scission reaction appears to be favored in highly crystalline regions.

Although poor weathering resistance of polyethylene has been recognized for some time, the mechanism of degradation has not yet been established satisfactorily. A great majority of investigations followed a change in infrared absorption spectra^{1,2} or electrical properties³ as a criterion of the photooxidation taking place. However, such measurements depend largely on the buildup in carbonyl group concentration and do not necessarily correspond to the deterioration in physical properties which, in turn, are closely related to molecular weight and molecular weight distribution within the polymer sample.

In the present work, use was made of Charlesby's technique⁴ for evaluation of the relative magnitudes of chain scission and chain crosslinking reactions when both occur simultaneously. Although this approach has been widely applied to studies of polymers irradiated with high energy radiation, no attempt has apparently been made previously to utilize this technique to study the photochemical degradation of polyethylene that takes place during exposure to strong sunlight or to artificial weathering environments. Since completion of the work to be described, Stephenson and his co-workers⁵ have reported gel formation experiments to estimate the extent of crosslinking relative to chain breakage during the exposure of a high density polyethylene film to 254 m μ ultraviolet light. However, these investigators used inert atmospheres (vacuum or nitrogen) solely. Under these conditions, the proportion of crosslinking to chain scission appeared to vary considerably during the course of their experiment.

* Present address: American Cyanamid Company, Stamford, Conn.

† Present address: Union Carbide Plastics Company, Bound Brook, N. J.

EXPERIMENTAL

Films prepared by blown extrusion with a 2 $\frac{1}{2}$ -in. extruder, were exposed in a Weather-Ometer (Atlas Electric Devices, Chicago) to carbon arc light filtered through a Corex D glass filter. The black body temperature inside the test chamber was 54°C.

Oxygen transmission through the films was measured by the standard A.S.T.M. method (D1434-58), the pressure differential being 1 atm. Intrinsic viscosities of polymer solutions were determined in xylene at 75°C. in an Ubbelohde viscometer. The gel contents in irradiated films were evaluated after a prolonged extraction of approximately 0.25 g. samples with boiling xylene in a Soxhlet extraction apparatus. Results were reproducible to within approximately ± 0.001 g.

Infrared spectra of films were measured on a Perkin-Elmer double-beam spectrometer. The films were coated on both sides with a thin layer of mineral oil to avoid interference patterns.⁶ In a separate experiment it was established that the mineral oil used shows no absorption in regions that were of interest during the present study. Carbonyl group concentrations were calculated from the data of Rugg, Smith, and Bacon.⁷

Results and Discussion

Polyethylene films were exposed in a Weather-Ometer for various periods of time. The chemical change occurring was followed by measuring intrinsic viscosity (or gel fraction) and infrared spectrum. Molecular weight, as measured by intrinsic viscosity, was found to increase rapidly in a 2-mil film. After 100 hr. exposure the molecular weight was approximately

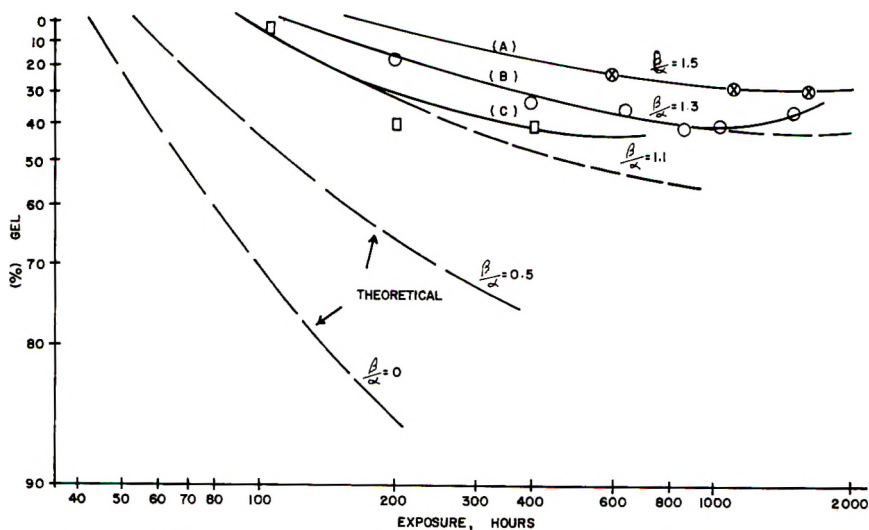


Fig. 1. Gel formation during the exposure of U.C.C. DFD-0100 resin in a Weather-Ometer: (x) 6.0 mil; (O) 2.0 mil; (□) 0.5 mil.

doubled, i.e., if Harris' equation⁸ remained applicable, and after 200 hr. exposure the film contained 18% gel.

The relative magnitude of chain crosslinking α to chain scission β reaction was estimated by measurement of gel content in films exposed for different periods of time. The ratio of chain scission to chain crosslinking frequency, β/α , was evaluated by fitting graphically Charlesby's equation⁴ to experimental results.

The rates of gel formation during irradiation were compared for three films (Fig. 1), and it was found that the chain scission is favored in thicker films. One possible explanation of this phenomenon may be the effect of oxygen concentration at the site of reaction on relative magnitudes of chain scission and chain crosslinking. The effect of oxygen on the course of photooxidation in polyethylene was recognized by Oster, Oster, and Moroson,⁹ who suggested that oxygen aids crosslinking when polyethylene is exposed to near ultraviolet light in the wavelength range of 300–400 $m\mu$. Far ultraviolet light (wavelengths of 200–300 $m\mu$) was stated to give slightly more efficient crosslinking in the absence of oxygen. The latter statement shows some relationship to the work of Alexander and Toms,¹⁰ who found that oxygen aids chain scission reaction in polyethylene exposed to high energy γ -radiation.

The present results on films exposed in a Weather-Ometer indicate that the chain crosslinking reaction is aided by decreasing film thickness and by decreased crystallinity, both of which contribute to high rates of oxygen transmission T . An apparent correlation between β/α and T could be expressed empirically by:

$$A + (B/T)^{1/2} = \beta/\alpha \quad (1)$$

at constant intensity of absorbed light. It is assumed here that the oxygen transmission rate T , as measured by the A.S.T.M. method, bears direct relationship to the rate of oxygen consumption during the photooxidation reaction. The value of constant A was estimated to be 1.0, and that of constant B to be 15 for a resin (U.C.C. DFD-0100, Fig. 2) of density 0.92. The constant A in eq. (1) is supposed to be the value of β/α when the reactions are no longer controlled by the rate of oxygen diffusion. Since the rate of oxygen transmission to a given segment within the film is decreased with increasing distance of that segment from the surface of the film, all results quoted in this work represent only average values. The ratio β/α as calculated from the rates of gel formation is similarly an average value of that at the film surface, assumed to be approximately equal to the constant A , and that at the center of the film. The constant A would be expected to vary with the degree of crystallinity and/or crosslinking in the resin. Such a dependence would conform with the results obtained by Lawton, Balwit, and Powell¹¹ on polyethylenes exposed to a high energy γ -radiation. These authors found that free radicals are trapped in the crystalline regions, or in highly crosslinked areas, and are eventually terminated with the formation

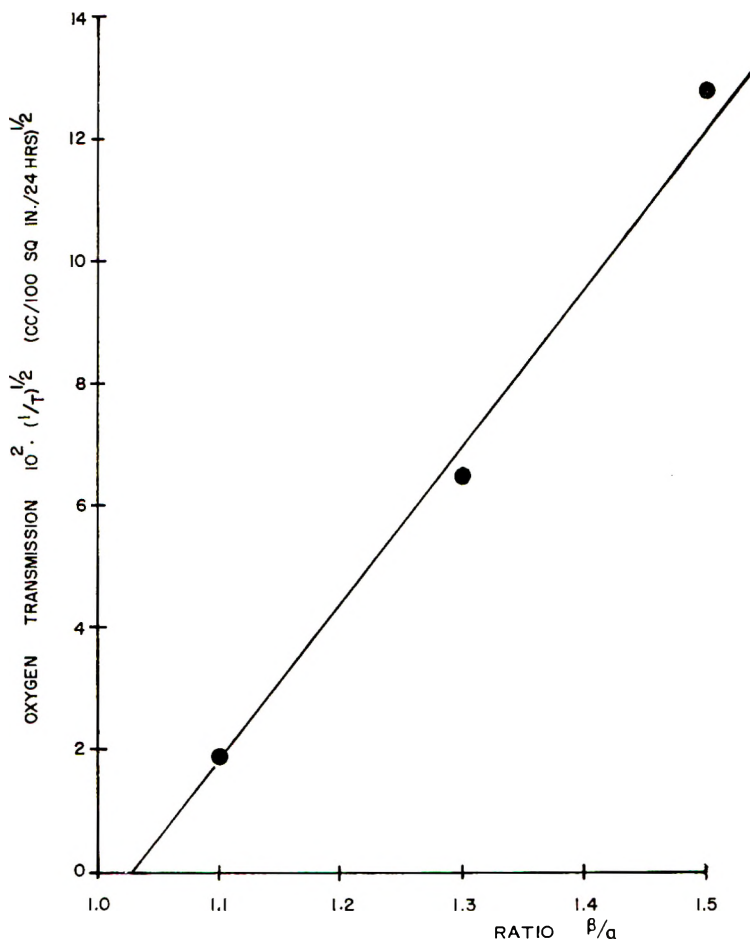


Fig. 2. Variation of β/α with oxygen transmission of film of U.C.C. DFD-0100 resin.

of carbonyl groups. It was also shown that gel is formed predominantly in the amorphous regions.

In our work, several types of polyethylene having different unsaturation and branching values, were exposed in a Weather-Ometer. The rates of gel formation show that the ratio β/α appears to correlate with oxygen transmission. Even with high density (0.94) resin, U.C.C. DBH-502, some gel was obtained when a very thin film was irradiated (Table I).

The results obtained with DBH-502 resin were utilized to evaluate constants A and B of eq. (1). These were calculated to be $A = 1.6$ and $B = 86$.

Another interesting feature shown in Figure 1 is that the experimental line at later stages of reaction, i.e., after some 40% gel was formed, tends to curve upwards, giving less gel fraction than would be expected from the theoretical calculations. Such a trend of results might be caused by: (1) the photoinitiated scission reaction exhibiting self-acceleration, or (2) by a highly crosslinked rigid structure inhibiting further crosslinking reaction.

TABLE I
 Rates of Gel Formation

Resin	Crys- tallinity (from density), %	Oxygen trans- mission, cc./100 in. ² /24 hr.	Thick- ness, mils	Gel content, %, after various exposure times			β/α
				250 hr.	600 hr.	1500 hr.	
Alathon-10 (du Pont)	68	190	1.8	27	44	33	1.3
DFD-0100 (U.C.C.)	67	60	6.0	1	23	32	1.5
		235	2.0	23	38	36	1.3
		2600	0.5	34	45	—	1.1
DYNK-1 (U.C.C.)	66	200	1.8	22	42	37	1.3
DBH-502 (U.C.C.)	77	110	1.8	0	0	0	>2.0
		320	1.0	2	4	—	1.9
		860	0.5	7	12	—	1.7
Marlex-9 (Phillips)	83	58	1.8	0	0	0	>2.0

A further understanding of the reaction was gained from infrared work. Infrared spectra of these films have shown some relationship between carbonyl concentration and time of exposure. The self-acceleration in this oxidation (Fig. 3) is possibly caused by an increase in the ultraviolet

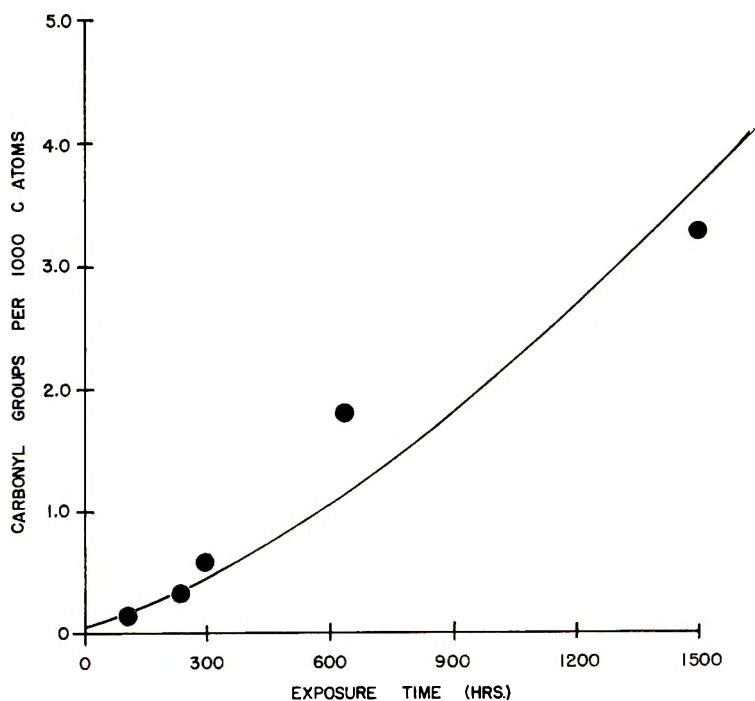


Fig. 3. Buildup of carbonyl concentration with exposure time in U.C.C. DFD-0100 resin.

absorption of these films which, in turn, is somewhat dependent on carbonyl group concentration. Optical density at 310 $m\mu$ was found to increase steadily with the time of irradiation. A 20% increase in absorption was observed after 400 hr. irradiation of a 2-mil thick film made from a DFD-0100 resin. The second possibility was tested by exposing in a Weather-Ometer a low density polyethylene film (2 mils thick) that was initially heavily crosslinked by treating it with a high energy electron beam. The original film contained 60% gel and after 1000 hr. exposure the gel content was reduced to 54%. It is, therefore, concluded that a highly crosslinked structure favors chain scission reaction and possibly both phenomena are responsible for the departure of experimental results from the theoretically predicted line.

TABLE II
Rates of Carbonyl Group Formation in Films Made from U.C.C. DFD-0100 Resin

Thick- ness, mils	Exposure time, hr.	Gel, %	Optical density			Carbonyl group concn., CO groups/ 1000 carbon atoms
			1765 cm. ⁻¹	1725 cm. ⁻¹	1705 cm. ⁻¹	
2	300	26	0.01	0.01	0.02	0.6
	640	36	0.05	0.06	0.13	1.8
	1500	36	0.09	0.15	0.15	3.3
6	250	10	—	0.01	0.03	0.1
	600	24	0.05	0.09	0.11	0.6
	1100	30	0.14	0.27	0.29	1.6

The carbonyl group concentration was found to be appreciably higher in the thinner, more crosslinked films (Table II). This suggests that cross-linking takes place through an oxygen linkage.

The absorption at 1765 $cm.^{-1}$ was assigned to acid anhydride group, the absorption at 1725 $cm.^{-1}$ to ketonic group and that at 1705 $cm.^{-1}$ to carboxylic acid.⁷ No hydroperoxide group was detected during the present experiments by infrared analysis at 3560 $cm.^{-1}$.¹² However, a wide, diffuse absorption band was observed at 1250–1175 $cm.^{-1}$, and this suggests the presence of an ether-type linkage.¹³

References

1. Pross, A. W., and R. M. Black, *J. Soc. Chem. Ind.*, **69**, 113 (1950).
2. Burgess, A. R., *Natl. Bur. Standards (U. S.) Circ.* **525**, 149 (1953).
3. Wallder, V. T., W. J. Clarke, J. B. De Coste, and J. B. Howard, *Ind. Eng. Chem.*, **42**, 2320 (1950).
4. Charlesby, A., *J. Polymer Sci.*, **11**, 513 (1953).
5. Stephenson, C. V., B. C. Moses, R. E. Burks, W. C. Coburn, Jr., and W. S. Wilcox, *J. Polymer Sci.*, **55**, 465 (1961).
6. Dole, M., C. D. Keeling, and D. G. Rose, *J. Am. Chem. Soc.*, **76**, 4304 (1954).
7. Rugg, F. M., J. J. Smith, and R. C. Bacon, *J. Polymer Sci.*, **13**, 535 (1954).
8. Harris, J., *J. Polymer Sci.*, **8**, 353 (1952).

9. Oster, G., G. K. Oster, and H. Moroson, paper presented to Division of Paint, Plastics, and Printing Ink Chemistry, 132nd Natl. Meeting, American Chemical Society, New York City, September, 1957.
10. Alexander, P., and D. Toms, *J. Polymer Sci.*, **22**, 343 (1956).
11. Lawton, E. J., J. S. Balwit, and R. S. Powell, *J. Polymer Sci.*, **32**, 257 (1958).
12. Aggarwal, S. L., and O. J. Sweeting, *Chem. Revs.*, **57**, 678 (1957).
13. Beachell, H. C., and S. P. Nemphos, *J. Polymer Sci.*, **21**, 113 (1956).

Résumé

On étudie le mécanisme d'usure des films de polyéthylène par mesure du poids moléculaire (par viscosité intrinsèque), de la teneur en fraction insoluble dans le xylène (gel) et de la concentration en groupes carbonyles (par analyse infrarouge). Les résultats obtenus montrent que la rupture de la chaîne β et le pontage α interviennent simultanément. L'influence de l'épaisseur et de la cristallinité des films de polyéthylène permet de penser que le rapport β/α peut dépendre de la concentration en oxygène à l'endroit de la réaction, et, donc, de la vitesse de pénétration de l'oxygène à travers le film, pour une intensité constante de la lumière absorbée. Il semble que la réaction de rupture de la chaîne soit favorisée dans les régions de forte cristallinité.

Zusammenfassung

Der Mechanismus der Bewitterungsschädigung von Polyäthylenfilmen wurde durch Molekulargewichtsbestimmung (Viskositätszahl), Messung des Gehalts an xylo-lunlöslicher Fraktion (Gel) und der Karbonylgruppenkonzentration (Infrarotanalyse) an exponierten Proben untersucht. Die Ergebnisse zeigen, dass Kettenspaltung, β , und Vernetzung, α , gleichzeitig auftreten. Der Einfluss der Dicke und Kristallinität der Polyäthylenfilme lässt erkennen, dass das Verhältnis β/α möglicherweise von der Sauerstoffkonzentration am Reaktionsort und daher bei konstanter Lichtintensität von der Geschwindigkeit des Sauerstoffeindringens in den Film abhängt. Die Kettenspaltungsreaktion scheint in hochkristallinen Bereichen begünstigt zu sein.

Received February 23, 1962

Inhibition Kinetics of the Polymerization of Styrene. II. Investigations on the Effect of *s*-Trinitrobenzene*,†

FERENC TŰDÖS, IMRE KENDE, and MÁRIA AZORI, *Central Research
Institute for Chemistry of the Hungarian Academy of Sciences,
Budapest, Hungary*

Synopsis

The kinetics of the polymerization of styrene initiated by azo-bis-isobutyronitrile was investigated in the presence of *s*-trinitrobenzene (TNB). According to the experimental results, the TNB behaves like a weak inhibitor and is transformed into a retarder during the inhibition period. The kinetic laws of this case of inhibition are not known from literature. Therefore, the fundamental kinetic relations of inhibition accompanied by retardation were elaborated. The kinetic equations for the rate of the inhibited polymerization and for the consumption of the inhibitor were deduced. A method was elaborated for the calculation of the length t_i of the inhibition period from the apparent inhibition period t' to be determined by extrapolation from the measured dilatometric data. The experimental results obtained with TNB at 40, 50, and 60°C. can be well interpreted by the deduced kinetic relations. According to the computations, the number of macroradicals deactivated by one TNB molecule amounts to 3.14 ± 0.1 at 40°C., 2.98 ± 0.1 at 50°C., and 2.89 ± 0.2 at 60°C. It is pointed out that this surprising value of the stoichiometric coefficient cannot be interpreted by trivial considerations. Finally, the relative reactivity of the TNB compared to that of the monomer as well as the dependence of this reactivity on temperature were determined.

In 1925, Ostromyslensky¹ observed that the polymerization of styrene is inhibited by aromatic nitro compounds. The effect of these compounds was investigated more exactly by Foord² and later by Schulz.³ It was stated that the retarding effect is enhanced by increasing the number of nitro groups.

Opinions to be found in literature in connection with the inhibition mechanism of the nitro compounds can be divided into two fundamental groups. The earlier investigations carried out by Price and his co-workers⁴ led to the conclusion that the increasing macroradicals attack the aromatic nuclei of the nitro compounds and consequently a substitution reaction takes place on the aromatic nucleus. This conclusion was supported by the fact that polystyrene formed in the presence of an aromatic nitro compound contained nitrogen, whereas the polystyrene formed in a nitro-methane solution did not. A further proof for the occurrence of the substi-

* For Part I, see Tűdös et al.¹⁹

† Presented in part at the Macromolecular Symposium of IUPAC, Moscow, June 1960.

tution in the aromatic nucleus is given by the results of Fieser and his co-workers,⁵ who, by treating nitro compounds with lead tetraacetate, obtained a product methylated in the nucleus. (It is to be noted, however, that the yield of this reaction was very low.)

On the basis of investigations carried out in connection with the polymerization of vinyl acetate and allyl acetate, it was supposed by Bartlett and Kwart^{6,7} as well as by Hammond and Bartlett⁸ that the primary attack takes place on the oxygen atom of the nitro group. To support this hypothesis, these authors point out the fact that the reactivity of the retarder formed from the polynitro compound during the inhibition period is from 8 to 30 times smaller than that of the original nitro compound. Such a marked decrease in the reactivity cannot be explained by a simple substitution reaction taking place in the aromatic nucleus. These authors supposed that the free radicals attack the oxygen atom of the nitro group, thus definitely depriving one of the nitro groups of its nitro character in the course of inhibition.

The investigations of preparative character recently performed by Inamoto and Simamura⁹ as well as by Norris¹⁰ yielded unambiguous evidence for the fact that the macro-radicals attack the nitro groups but not the aromatic nucleus. According to Inamoto's and Simamura's investigations, from the reaction mixture of 2-cyano-2-propyl radicals with nitrobenzene (or *m*-dinitrobenzene), hydrogen cyanide, acetone, and *N*-phenyl-*O,N*-bis-(2-cyano-2-propyl)hydroxylamine (or the corresponding *m*-nitro derivative) can be obtained. Here the formation of the *N*-phenyl compound is the most decisive.

When investigating the reaction of *o*- or *p*-dinitrobenzene or *s*-trinitrobenzene with 2-cyano-2-propyl radicals, Norris¹⁰ succeeded in separating similar *O,N*-disubstituted phenyl-hydroxylamine derivatives. Moreover, he established that the reactivity of the investigated compounds increased in the above order of succession. These results are in contradiction with the results of previous investigations of Gingras and Waters,¹¹ according to which the 2-cyano-2-propyl radicals react neither with *s*-trinitrobenzene nor with 2,4-dinitrochlorobenzene.

Bevington and Ghanem¹² made an effort to elucidate the inhibition mechanism of the nitro compounds. Among others they have established that picric acid does not build in a C—C bond into the polymer.

After the completion of our own investigations, Jackson and Waters' paper¹³ appeared, in which the reactions of the benzyl radical with dinitrobenzene and trinitrobenzene are discussed. According to these investigations, during this reaction benzaldehyde is formed in considerable quantity from the benzyl radical, and during the reduction of the nitro compound, besides the hydroxylamine derivative, aniline and *N*-benzyl aniline derivatives are formed, too. Consequently, in the end products compounds of all states of reduction occur.

Although the inhibitory effect of the nitro compounds is long well known, only a few papers dealing with the inhibition kinetics can be found in the literature.^{6,7,14-16}

Regarding the effect of substituents on the reactivity of nitro compounds, more detailed investigations were performed only in the case of methyl acrylate^{15,16} and vinyl acetate. Concerning styrene, not more than one or two qualitative statements can be found in literature;^{2,3} therefore, it seemed worthwhile to investigate this problem more thoroughly.

In the present paper the effect of *s*-trinitrobenzene is treated. In a following paper¹⁷ the effect of substituents (substituted trinitrobenzenes) will be discussed. Finally, the retarding effect of the mono- and dinitrobenzenes as well as of the aromatic nitroso compounds will be treated.

Experimental

The method employed in the experiments to be described was generally the same as that discussed previously.^{18,19} Azo-bis-isobutyronitrile used for initiation was prepared from technical-grade material. At 40–50°C. a saturated chloroform solution was prepared, then this solution mixed while cooling with ether in excess. The precipitate was purified one or two times in the same way. The *s*-trinitrobenzene (TNB) was prepared from a product of purest grade by recrystallizing three times from absolute ethanol, m.p. 122–122.5°C.

The polymerization was carried out in bulk without any solvent, its progress being followed dilatometrically. The dilatometers used had a volume of 15 ml., by which the contraction could be determined with accuracy to $\pm 1 \mu\text{l}$. In order to ensure better heat transfer, the reservoir of the dilatometer was shaped as a spiral, prepared from a razotherm glass tube having an inner diameter of 5–6 mm. (The experiments described in our previous paper¹⁹ were performed in similar dilatometers.)

The reaction mixtures were prepared in the presence of air, directly in the dilatometers. Then oxygen was removed in the usual way by freezing out and suction (4–5 cycles), whereupon the dilatometers were sealed off under purified nitrogen atmosphere. Until polymerization, the test samples prepared in this way were stored at a temperature of -20°C .

Kinetic Analysis of the Inhibited Process

Under the prevailing experimental conditions, the TNB proved to be an inhibitor of average activity, since during the inhibition period the polymerization proceeded with considerable speed. After the end of the inhibition period, the steady rate of the process is smaller than that of the non-inhibited process. The trend of the inhibited process can be well seen in Figure 1, where $\log m_0/m$ is plotted against t (m and m_0 are the actual and the initial concentrations of the monomer, respectively).

On the basis of the above-described kinetic behavior it has to be supposed that the inhibition effect is exerted by the TNB in two consecutive stages. During the first stage (in the inhibition period) the initial inhibitor is reacting while being transformed into a much (about 25 times) weaker retarder. These data are in good agreement with the results of measurements on vinyl acetate, performed by Bartlett and Kwart,^{6,7} with the difference that

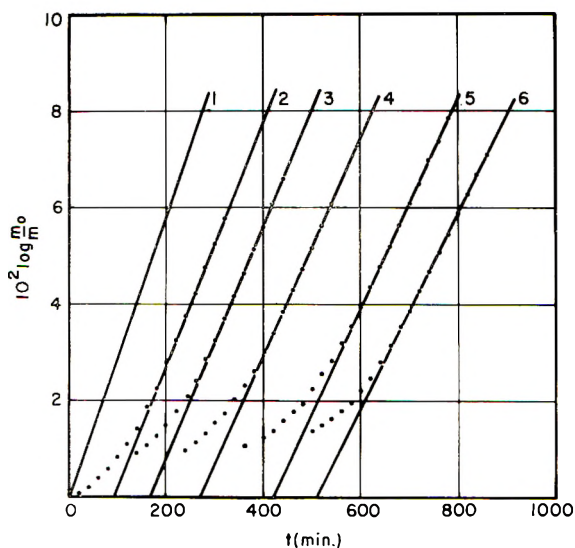


Fig. 1. Kinetic curves in the presence of TNB. Temperature: 50°C. Concentrations: see Table I.

in the case of vinyl acetate the TNB is a much stronger inhibitor. Taking into account the reactivities of the two macroradicals, however, this quantitative difference can be fully understood.

The known kinetic laws of inhibited polymerization²⁰⁻²² proved to be unsuitable for determining the kinetic parameters of the process; therefore, the kinetic laws have been elaborated for the case when, after the inhibition, a secondary, retarded polymerization follows. It is to be mentioned that the first attempts in this direction were carried out some years ago.^{18,23} In the following more detailed computations, for the sake of better understanding, repetitions cannot sometimes be avoided.

The process of initiated polymerization can be described by the following reaction steps which are to be considered nowadays well known:



The processes of inhibition and retardation can be characterized by two equations:



In the above reaction scheme X stands for the initiator, Z for the inhibitor, and Y for the retarder formed from the inhibitor.

The differential equation system of the process can be described as follows by eqs. (6-9):

$$-dm/dt = k_2mr \quad (6)$$

$$-dz/dt = k_5zr \quad (7)$$

$$dy/dt = k_5zr \quad (8)$$

$$dr/dt = 2k_1fx_0 - \mu k_5zr - \mu'k'_5 yr - k_4r^2 \quad (9)$$

In the above equations, the decrease of the concentrations of the retarder and initiator was disregarded as being very slight during the process. Individual concentrations of initiator, inhibitor, and retarder are here represented by the x , r , and y , respectively.

The concentration of the retarder can be easily calculated with the aid of eqs. (7) and (8):

$$y = z_0 - z \quad (10)$$

By using eq. (10) as well as Bodenstein's principle, the concentration of the macroradicals can be determined:

$$r = r_{st} [(1 + \vartheta^2)^{1/2} - \vartheta] \quad (11)$$

where

$$\vartheta = \beta' z_0/(x_0)^{1/2} + (\beta - \beta') z/(x_0)^{1/2} \quad (12)$$

$$r_{st} = (2 k_1 f x_0/k_4)^{1/2} \quad (13)$$

$$\beta = \mu k_5/2(2k_1fk_4)^{1/2} \quad (14)$$

and

$$\beta' = \mu'k'_5/2(2k_1fk_4)^{1/2} \quad (15)$$

where μ and μ' are the stoichiometric coefficients of the inhibitor and of the retarder, respectively,¹⁸ and f is the initiator efficiency.

Introducing the following symbols:

$$\beta z/(x_0)^{1/2} = \varphi$$

and

$$\beta z_0/(x_0)^{1/2} = \varphi_0 \quad (16)$$

$$\beta' z/(x_0)^{1/2} = \varphi'$$

and

$$\beta' z_0/(x_0)^{1/2} = \varphi'_0 \quad (17)$$

and by substituting expression (11) into the differential eq. (7), after integration (with the initial values $t = 0$, $z = z_0$, $y = 0$), we obtain one of the fundamental equations for inhibited polymerization:²²

$$\begin{aligned}
 F(\vartheta) &\equiv \vartheta + (1 + \vartheta^2)^{1/2} + \varphi'_0 \log(\vartheta - \varphi'_0) [(1 + \vartheta^2)^{1/2} + \vartheta] - \\
 &\quad \text{(I)} \quad \text{(II)} \quad \text{(III)} \\
 &(1 + \varphi'^2_0)^{1/2} \log [1/(\vartheta - \varphi'_0)] [1 + \varphi'_0 \vartheta + (1 + \varphi'^2_0)^{1/2} (1 + \vartheta^2)^{1/2}] = \\
 &\quad \text{(IV)} \\
 &F(\vartheta_0) - Bt \quad (18)
 \end{aligned}$$

where $B = k_5 r_{st}$. If $\beta' = 0$ (that is, no secondary retardation occurs) then $\vartheta = \varphi$ and eq. (18) can be written in the following simple form:

$$\begin{aligned}
 F(\varphi) &= \varphi + (1 + \varphi^2)^{1/2} - \log(1/\varphi) [1 + (1 + \varphi^2)^{1/2}] \\
 &= F(\varphi_0) - Bt \quad (19)
 \end{aligned}$$

This equation is identical with one of the fundamental equations for one-step inhibition which had been earlier deduced.²⁴

If $z/(x_0)^{1/2} \rightarrow 0$, then the terms (I - IV) of eq. (18) become much simpler:

$$\begin{aligned}
 \text{(I)} \quad & \lim_{z/(x_0)^{1/2} \rightarrow 0} \vartheta = \varphi'_0 \quad (20)
 \end{aligned}$$

$$\begin{aligned}
 \text{(II)} \quad & \lim_{z/(x_0)^{1/2} \rightarrow 0} (1 + \vartheta^2)^{1/2} = (1 + \varphi'^2_0)^{1/2} \quad (21)
 \end{aligned}$$

Terms (III) and (IV) can be written with good approximation as follows:

$$\text{(III)} \quad \cong \varphi' \log(\vartheta - \varphi'_0) \{ (1 + \varphi'^2_0)^{1/2} + \varphi'_0 \} \quad (22)$$

$$\text{(IV)} \quad \cong - (1 + \varphi'^2_0)^{1/2} \log [2(1 + \varphi'^2_0)/(\vartheta - \varphi'_0)] \quad (23)$$

Summarizing

$$\begin{aligned}
 F(\vartheta) &\cong \varphi'_0 + (1 + \varphi'^2_0)^{1/2} + \varphi'_0 \log(\vartheta - \varphi'_0) \{ (1 + \varphi'^2_0)^{1/2} + \varphi'_0 \} \\
 &\quad - (1 + \varphi'^2_0)^{1/2} \log [2(1 + \varphi'^2_0)/\vartheta - \varphi'_0] \\
 &= F(\vartheta_0) - Bt \quad (24)
 \end{aligned}$$

This form of the fundamental equation is valid with good approximation if the values of $z/(x_0)^{1/2}$ are small (physically, at the end of the inhibition period). Therefore, eq. (24) can be practically used for determining theoretically the length of the inhibition period.

For this purpose, however, the other fundamental equation of inhibited polymerization is also needed. This equation can be deduced in the usual way,⁶ by combining eqs. (6) and (7):

$$dm/dz = (k_-/k_5)(m/z) \quad (25)$$

By solving this differential equation (with the initial conditions ($t = 0, m = m_0$, and $z = z_0$), the following expression is obtained:

$$\log(m_0/m) = (k_-/k_5) \log(z_0/z) \quad (26)$$

Taking into account eqs. (12), (16), and (17), this expression can be written as follows:

$$\begin{aligned} \log(m_0/m) &= (k_2/k_5) \log [(\vartheta_0 - \varphi'_0)/(\vartheta - \varphi'_0)] \\ &= (k_2/k_5) \log [\varphi_0/(\vartheta - \varphi'_0)] \quad (27) \end{aligned}$$

Returning to eq. (24) and separating the constant terms, we can transpose the equation to the following form:

$$\log(\vartheta - \varphi'_0) = [C(\vartheta_0, \varphi'_0) - Bt]/[(1 + \varphi'^2_0)^{1/2} + \varphi'_0] \quad (28)$$

where

$$\begin{aligned} C(\vartheta_0, \varphi'_0) &= F(\vartheta_0) - [\varphi'_0 + (1 + \varphi'^2_0)^{1/2}] - \varphi'_0 \log [\varphi'_0 + (1 + \varphi'^2_0)^{1/2}] \\ &\quad + (1 + \varphi'^2_0)^{1/2} \log 2(1 + \varphi'^2_0) \quad (29) \end{aligned}$$

From eqs. (27) and (28), eq. (30) is obtained:

$$\begin{aligned} \log(m_0/m) &= (k_2/k_5) \{ \log \varphi_0 - C(\vartheta_0, \varphi'_0)/[\varphi'_0 + (1 + \varphi'^2_0)^{1/2}] \\ &\quad + Bt/[\varphi'_0 + (1 + \varphi'^2_0)^{1/2}] \} \quad (30) \end{aligned}$$

by which, as can be unambiguously seen from the assumptions used during the deduction, the period of retarded polymerization which follows the inhibition period is described. Expression (30) is the equation of a straight line the slope of which is given by eq. (31):

$$\frac{d}{dt} \log \frac{m_0}{m} = \frac{k_2 r_{st}}{\varphi'_0 + (1 + \varphi'^2_0)^{1/2}} = W_{ret} \quad (31)$$

where W_{ret} is the velocity of retarded polymerization. If $k'_5 = 0$ (that is, $\varphi'_0 = 0$) then

$$\frac{d}{dt} \log(m_0/m) = k_2 r_{st} = W \quad (32)$$

With the aid of eqs. (31) and (32) the value of the so-called retardation parameter, φ'_0 can be easily determined:

$$\varphi'_0 = (W_{ret}^{-1} - W_{ret})/2 \quad (33)$$

where

$$W_{ret} = W_{ret}/W \quad (34)$$

The apparent length (t') of the inhibition period can be also determined by extrapolating the linear section of the function $\log m_0/m = f(t)$ to the value $\log m_0/m = 0$. Using this method, from eq. (30) the following expression is obtained:

$$t' = \{C(\vartheta_0, \varphi'_0) - [\varphi'_0 + (1 + \varphi'^2_0)^{1/2}] \log \varphi_0\}/B \quad (35)$$

For the true length t_i of the inhibition period, earlier eq. (36) was obtained:²⁴

$$t_i = 2\varphi_0/B \quad (36)$$

and it has been shown that, in case of one-step inhibition, the following relationship exists between t' and t_i :

$$t' = t_i F^* (\varphi_0) \quad (37)$$

[see²⁴ eqs. (24), (43), and (56).]

By using the definition of eq. (36), eq. (35) can be transformed as follows:

$$t' = t_i F^* (\varphi_0, \varphi'_0) \quad (38)$$

where

$$F^* (\varphi_0, \varphi'_0) = (1/2\varphi_0) \{(\varphi_0 + \phi_0) - (\varphi'_0 + \phi'_0) + \varphi'_0 \log [(\varphi_0 + \phi_0)/(\varphi'_0 + \phi'_0)] - \phi'_0 \log [(1 + \varphi_0\varphi'_0 + \phi_0\phi'_0)/2\phi'^2_0]\} \quad (39)$$

and the employed auxiliary functions are:

$$\phi_0 = (1 + \varphi_0^2)^{1/2} \quad (40)$$

$$\phi'_0 = (1 + \varphi'^2_0)^{1/2} \quad (41)$$

If $\varphi'_0 = 0$ (that is, no secondary retardation occurs) then

$$F^* (\varphi_0, 0) = (1/2\varphi_0) \{ \varphi_0 + \phi_0 - 1 + \log [(1 + \phi_0)/2] \} = F^* (\varphi_0) \quad (42)$$

that is, the function $F^* (\varphi_0)$, which has been deduced earlier, is obtained.²⁴ On the other hand, if $\varphi'_0 = \varphi_0$, that is, a retarder having the same reactivity is formed from the inhibitor, then:

$$F^* (\varphi_0, \varphi'_0) = 0 \quad (43)$$

This means that in this case the inhibition period cannot be observed. Of course, this limiting case of no considerable practical significance. For the sake of comparison, some values of the function $F^* (\varphi_0, \varphi'_0)$, at the value $\varphi_0 = 10$, have been computed. The results are shown in Figure 2.

As can be seen, in the beginning the value of the function $F^*(10, \varphi'_0)$ increases with small values of φ'_0 , then it decreases, and with higher values of φ'_0 it rapidly decreases below the value of $F^*(10)$. A more general investigation on this function encounters difficulties. However, it is to be expected that the trend of $F^*(\varphi_0, \varphi'_0)$ is similar also in case of other values of φ_0 .

Equations (38) and (39) can be used for practical calculations for which the following has to be mentioned. The apparent length t' of the inhibition period can be directly determined by extrapolating the linear section of the experimentally obtained function $\log (m_0/m) = f(t)$. However, the true length t_i of the inhibition period can be obtained only by calculation from eqs. (38) and (39). For this calculation, however, the values of the inhibition parameter φ_0 and the retardation parameter φ'_0 are needed. The method of computation of the latter has been shown by eqs. (33) and (34), while the former can be obtained in an analogous way from the initial rate of the inhibited polymerization.

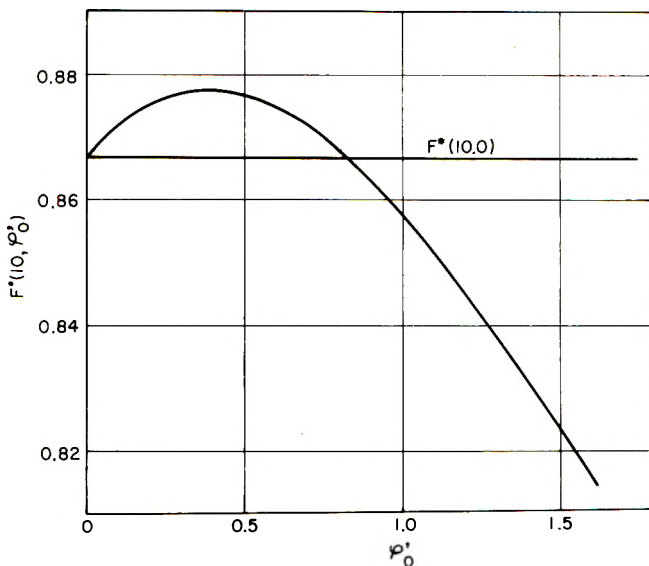


Fig. 2. $F^*(10, \varphi_0')$ plotted against φ_0' .

By substituting the original notations, eq. (36) can be written as follows:

$$t_i = (\mu/2 k_1 f)(z_0/x_0) \quad (44)$$

Consequently, the length of the inhibition period depends linearly on the ratio z_0/x_0 . Although this statement is true in first approximation, in order to make the calculation more exact, the integrated average value of the initiator concentration is used instead of the initial one. As a matter of course, the computation of the average values is performed from $t = 0$ to $t = t_i$ according to the following expression:

$$\bar{x} = (x_0/k_1 t_i) (1 - e^{-k_1 t_i}) \quad (45)$$

Therefore, in these calculations, instead of eq. (44), the following corrected formula was used:

$$t_i = (\mu/2k_1 f)(z_0/\bar{x}) \quad (46)$$

With the aid of this relationship, the value of μ or $2k_1 f$ can be determined. In connection with the investigated system, the value of $2k_1 f$ had been earlier determined with great accuracy, by using two stable free radicals,¹⁹ and the rate constant for the dissociation of the initiator is well known, too;^{25,26} therefore, a possibility arose for an accurate and reliable determination of the stoichiometric coefficient.

The rate constant of the elementary step (4) of inhibition (k_5) can be determined in two ways. Once eqs. (16) and (14) can be used to this purpose. For this calculation the initial rate of polymerization has to be used, the measurement of which can be performed only with limited accuracy; therefore, by this method, the determination can be generally carried out merely with an accuracy of 10–20%.

The other possibility for determining the value of k_5 (that is, the ratio k_5/k_2) is given by the integrated eq. (26). The values of m occurring in this equation can be determined by direct measurements, while those of z can be computed as follows. If the reactivity of the retarder formed from the inhibitor is 1–1.5 orders of magnitude smaller than that of the original inhibitor, then, as can be easily realized, the change with time of the concentration of the inhibitor is described by eq. (19) with a satisfactory accuracy, nearly in the whole of the inhibition period.

The transcendent eq. (19) cannot be advantageously used for series calculations; therefore, the problem has to be further simplified. Earlier it had been shown²⁴ that the following approximation:

$$F(\varphi) \cong 2\varphi - (1/2\varphi) \quad (47)$$

causes an error of not more than 2%, even in the case of the value $\varphi = 1$. Consequently, eq. (19) can be written to a good approximation as follows:

$$2\varphi - (1/2\varphi) = 2\varphi_0 - (1/2\varphi_0) - Bt \quad (48)$$

Taking into account eq. (36), eq. (48) can be written as follows:

$$4\varphi^2 - 4\varphi\tau - 1 = 0 \quad (49)$$

where

$$\tau = \varphi_0 [1 - (t/t_i)] - (1/4\varphi_0) \quad (50)$$

As only the positive radical of eq. (49) has a physical sense, the expression of φ is:

$$\varphi = (1/2)[\tau + (1 + \tau^2)^{1/2}] \quad (51)$$

Consequently, the value of the ratio z_0/z to be found in eq. (26) can be calculated with the aid of the following equation:

$$z_0/z = \varphi_0/\varphi = 2\varphi_0/[\tau + (1 + \tau^2)^{1/2}] \quad (52)$$

Thus, the fundamental kinetic equations of the problem have been deduced. In the following, the applicability of the above equations to the obtained experimental data will be proved.

Experimental Results and Discussion

In the present paper, experiments carried out with TNB at 40, 50, and 60°C. are described. The data of the experiments performed at 50°C. are summarized in Table I.

In Figure 3, the experimentally determined relation $t' = f(z_0/\bar{x})$ as well as the relation $t_i = f(z_0/x)$, obtained by calculation according to the described method, are shown diagrammatically.

As can be seen from the figure, the apparent length t' of the inhibition period is not a linear function of the ratio z_0/\bar{x} , while the values t_i obtained by calculation give a true straight line.

TABLE I
Results at $x_0 = 0.119$ mole/l., 50°C .

No.	$z_0 \times 10^3$, mole/l.	$z_0/\bar{x} \times 10^2$	t' , min.	t_i , min.	k_3/k_2
1	0.881	0.728	92	131	
2	1.545	1.289	166	213	
3	2.254	1.889	269	326	64.4
4	3.299	2.789	418	483	64.1
5	4.022	3.420	508	575	

By the aid of the relation $t_i = f(z_0/x)$ the value of the stoichiometric coefficient was calculated. (The values of the constants used for the calculations are given in Table IV.) According to the experimental results obtained, the value of μ is equal to 2.98 ± 0.1 ; this limit of error was derived from the scattering of the experimental data. Moreover, the probable error of the value $2k_1f$ used for the calculation, which can be estimated to $\pm 2\%$, has to be taken into account, too.

The fact that the value of the stoichiometric coefficient is undoubtedly an uneven number, in contrast to the value which would be expected in the case of a molecule inhibitor, is rather striking. In the literature the only data on the value of the stoichiometric coefficient to be found are those in Bartlett's and Kwart's work.^{6,7} According to their measurements carried out with vinyl acetate, in the case of isomeric dinitrobenzenes, $\mu = 2$, and in the case of TNB, when two nitro groups are consumed, $\mu = 4$.

In our opinion, such an "abnormal" value of the stoichiometric coefficient can be explained by some deeper reason related to the finer mechanism of the inhibition reaction. The fact must not be left out of consideration that, in our previous kinetic computations, the inhibition reaction

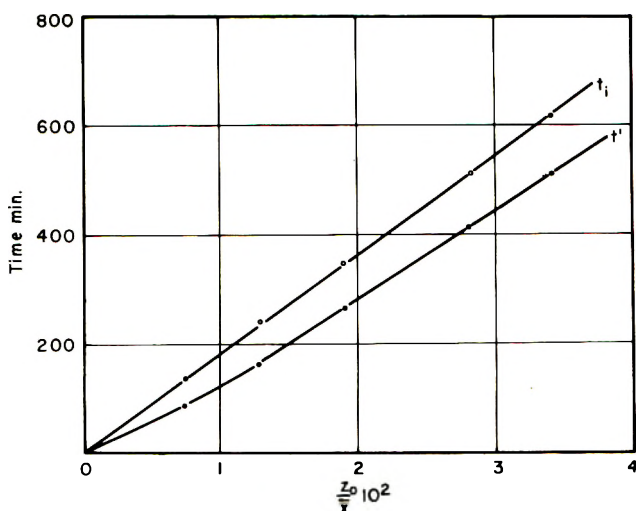


Fig. 3. Dependence of t' and t_i on the values of z_0/\bar{x} .

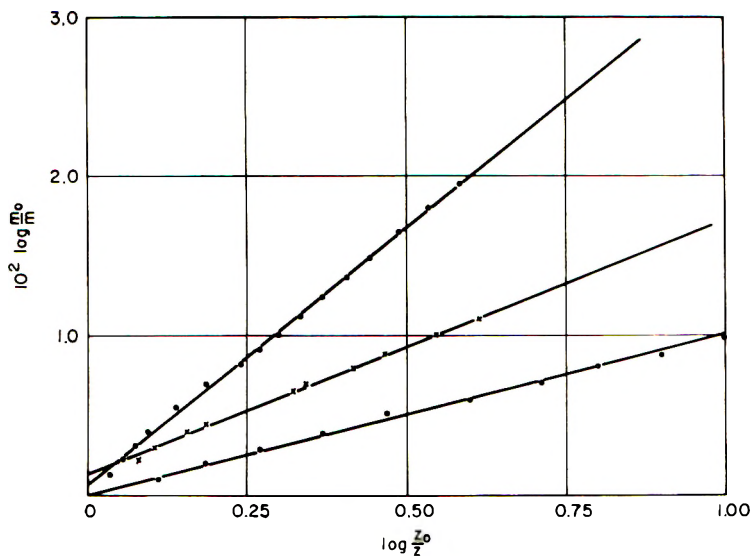


Fig. 4. The relation $\log m_0/m = f(\log z_0/z)$ plotted at different temperatures: (O) 40°C.; (X) 50°C.; (●) 60°C.

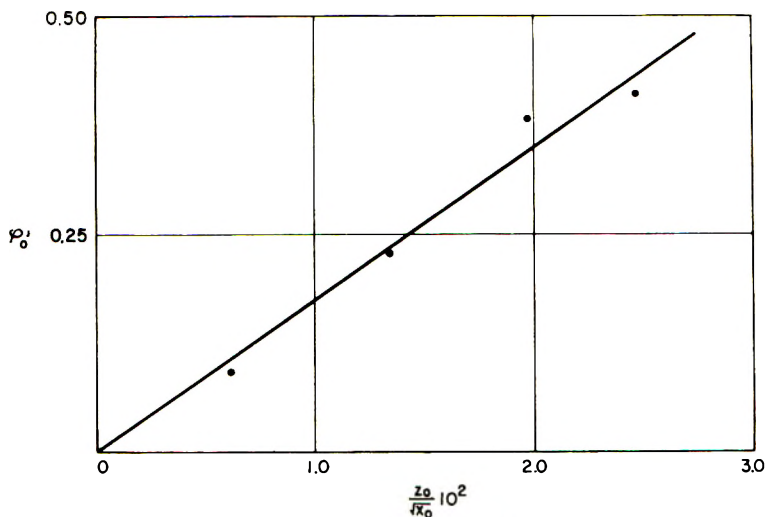


Fig. 5. φ'_0 plotted against $z_0/(x_0)^{1/2}$ at 60°C.

was taken into account fundamentally by a rate expression of the form k_{5zr} , that is, it was supposed that the rate-determining step of the inhibition reaction (or reactions) was that between the macroradical and the inhibitor molecule. By this reaction, however, a free-radical intermediate product can merely be formed; therefore, the rate-determining process must be followed by one or more prompt elementary reactions by which further macroradicals are consumed. Concerning the nature of the further elementary reactions an answer can be probably obtained by investi-

gating substituted TNB derivatives. Our investigations of this kind will be described in a following paper.¹⁷

The reactivity of TNB related to that of the monomer (k_5/k_2) was calculated from the inhibited sections of the kinetic curves by the above-described method. In Figure 4 the relation $\log (m_0/m) = f(\log z_0/z)$ is shown at each temperature.

The satisfying linearity of the graphs proves that the assumption concerning the rate-determining step of the inhibition reaction was right.

In Tables II and III the data of experiments carried out at 40 and 60°C., respectively, are summarized. The values of the constants used in the calculations are to be found in Table IV; these values were calculated from the data of Tüdös,¹⁹ and Tobolsky et al.^{25,26}

In Figure 5, the relation $\varphi'_0 = f[z_0/(x_0)^{1/2}]$ is shown at 60°C. It can be seen that the points plotted on the basis of the experimental data lie with satisfactory accuracy on a straight line.

This fact shows that the hypothesis underlying our previous kinetic computations, according to which during the reaction the inhibitor is transformed quantitatively into a retarder, is really fulfilled.

TABLE II
Results at $x_0 = 0.1207$ mole/l.; 40°C.

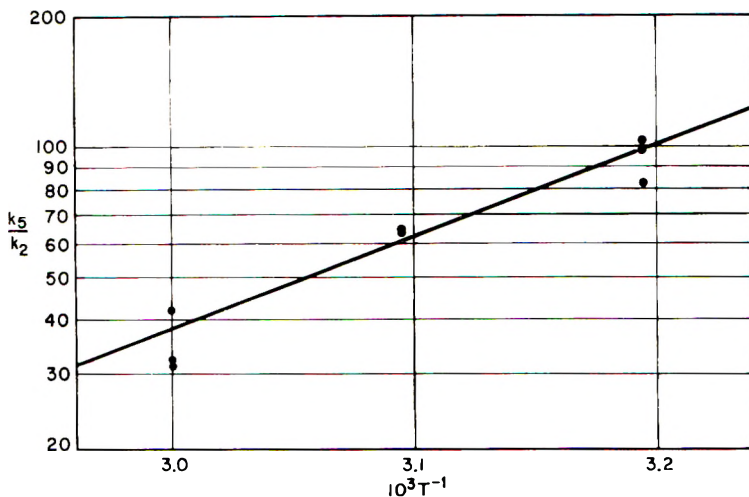
No.	$z_0 \times 10^3$, mole/l.	$z_0/\bar{x} \times 10^3$	t' , min.	t_i , min.	k_5/k_2
6	0.603	5.05	360	461	
7	1.11	9.36	655	775	
8	1.30	10.9	785	914	104.2
9	1.55	13.1	957	1093	98.0
10	1.88	15.9	1210	1360	82.2

TABLE III
Results at $x_0 = 0.0628$ mole/l.; 60°C.

No.	$z_0 \times 10^3$ mole/l.	$z_0/\bar{x} \times 10^2$	t' , min.	t_i , min.	W_{rel}	φ_0	k_5/k_2
11	1.55	2.55	87	123	0.912	0.092	
12	3.37	5.77	193	242	0.798	0.228	31.1
13	4.92	8.69	286	340	0.688	0.382	31.9
14	6.16	11.2	368	428	0.671	0.409	42.2

TABLE IV

Temp., °C.	$k_1 \times 10^5$, min. ⁻¹	$2 k_1 f \times 10^5$, min. ⁻¹	$K \times 10^4$, l. ^{1/2} mole ^{-1/2} min. ⁻¹
40	3.18	3.78	6.58
50	14.1	17.5	19.3
60	62.2	71.5	53.0

Fig. 6. The Arrhenius dependence of k_5/k_2 .

Finally, in Table V the values of μ , β , and β' at different temperatures are summarized.

TABLE V

Temp., °C.	μ	β , $l^{1/2}$ $\text{mole}^{-1/2}$	β' , $l^{1/2}$ $\text{mole}^{-1/2}$
40	3.14 ± 0.1	2460	120
50	2.98 ± 0.1	930	37
60	2.89 ± 0.2	260	17

According to these results, in the temperature interval investigated, the value of the stoichiometric coefficient can be considered practically constant; a possible small increase does not exceed the limit of experimental errors.

The relative reactivity of the inhibitor decreases considerably with the increase of temperature. Formerly a similar tendency was observed in the case of quinones, too.¹³ The dependence on temperature of the relative values of reactivity can be seen in Figure 6.

A satisfactory Arrhenius dependence is exhibited by these data; the values of the Arrhenius parameters are as follows:

$$q_5 - q_2 = -9.5 \pm 3 \text{ kcal./mole}$$

$$\log A_5 - \log A_2 = -4.7 \pm 1.5$$

It is to be mentioned that the error of these values is relatively large. This can be explained by the fact that the determination was made from a temperature interval of but 20°C. Even if the limit of error is taken

into account, the difference $q_5 - q_2$ seems to be larger than the expected value.

The authors wish to express their thanks to Mr. László Sümegi, Miss Ágnes Diószeghy and Miss Edit Fülöp for their assistance in carrying out the experiments.

References

1. Ostromyslensky, J. J., and M. G. Shepard, U. S. Pats. 1,550,323-1,550,324 (1925).
2. Foord, S. G., *J. Chem. Soc.*, **1940**, 48.
3. Schulz, G. V., *Makromol. Chem.*, **1**, 94 (1947).
4. Price, C. C., and P. A. Durham, *J. Am. Chem. Soc.*, **65**, 757 (1943).
5. Fieser, L. F., L. C. Clapp, and W. H. Daudt, *J. Am. Chem. Soc.*, **64**, 2052 (1942).
6. Bartlett, P. D., and H. Kwart, *J. Am. Chem. Soc.*, **72**, 1051 (1950).
7. Bartlett, P. D., and H. Kwart, *J. Am. Chem. Soc.*, **74**, 3969 (1952).
8. Hammond, G. S., and P. D. Bartlett, *J. Polymer Sci.*, **5**, 617 (1950).
9. Inamoto, N., and O. Simamura, *J. Org. Chem.*, **23**, 408 (1958).
10. Norris, W. P., *J. Am. Chem. Soc.*, **81**, 4239 (1959).
11. Gingras, B. A., and W. A. Waters, *J. Chem. Soc.*, **1954**, 1920.
12. Bevington, J. C., and N. A. Ghanem, *J. Chem. Soc.*, **1959**, 2031.
13. Jackson, R. A., and W. A. Waters, *J. Chem. Soc.*, **1960**, 1653.
14. Kice, J. L., *J. Am. Chem. Soc.*, **76**, 6274 (1954).
15. Sinyitsina, Z. A., and G. S. Bagdassarian, *Zhur. Fiz. Khim.*, **32**, 2614 (1958).
16. Sinyitsina, Z. A., and G. S. Bagdassarian, *Zhur. Fiz. Khim.*, **32**, 2663 (1958).
17. Tüdös, F., I. Kende, and M. Azóri, *J. Polymer Sci.*, **A1**, 1369 (1963).
18. Tüdös, F., Dissertation, Leningrad, 1956.
19. Tüdös, F., T. A. Berezsnych, and M. Azóri, *Acta Chim. Hung.*, **24**, 91 (1960).
20. Bamford, C. H., W. G. Barb, A. D. Jenkins, and P. F. Onyon, *The Kinetics of Vinyl Polymerization by Radical Mechanisms*, Butterworths, London, 1958.
21. Bagdassarian, H. S. (*Teoriya Radikal'noi Polymerizatsii*), Izdatelstvo Akademii Nauk SSSR, Moscow, 1959, p. 142.
22. Tüdös, F., and V. Fürst, *Acta Chim. Hung.*, **15**, 389 (1958).
23. Tüdös, F., and N. I. Smirnow, *Acta Chim. Hung.*, **15**, 401 (1958).
24. Tüdös, F., *Magy. Tud. Akad. KKKI Közlemén.* No. 2, 51 (1959).
25. Tobolsky, A. V., and J. A. Offenbach, *J. Polymer Sci.*, **16**, 311 (1955).
26. Van Hook, J. P., and A. V. Tobolsky, *J. Polymer Sci.*, **33**, 429 (1958).

Résumé

La cinétique de polymérisation du styrène initié par l'azobisisobutyronitrile mis en présence de s-trinitrobenzène (TNB) a été examinée. En accord avec les résultats expérimentaux, le TNB se comporte comme un inhibiteur faible et est transformé en retardateur pendant la période d'inhibition. Les lois de la cinétique pour ce cas d'inhibition ne sont pas mentionnées dans la littérature. Par conséquent, les relations cinétiques fondamentales d'une inhibition accompagnée d'un retardement furent élaborées. Les équations cinétiques pour la vitesse de polymérisation inhibée et pour la vitesse de disparition de l'inhibiteur en ont été déduites. Une méthode fut mise au point pour calculer la longueur t_i de la période d'inhibition à partir de la période d'inhibition apparente t' , celle-ci étant déterminée par extrapolation des valeurs dilatométriques mesurées. Les résultats expérimentaux obtenus avec TNB à 40, 50 et 60°C. s'interprètent facilement à partir des relations cinétiques établies. En accord avec les prévisions, le nombre de macroradicaux désactivés par une molécule de TNB s'élève à 3.14 ± 0.1 à 40°C., 2.98 ± 0.1 à 50°C. et 2.89 ± 0.2 à 60°C. respectivement. Il faut noter que cette valeur surprenante du coefficient stoechiométrique ne peut pas être interprétée par des considérations triviales. Enfin on a déterminé la réactivité relative du TNB comparée à celle du monomère de même que l'influence de la température sur la réactivité.

Zusammenfassung

Die Kinetik der durch Azo-bis-isobutyronitril gestarteten Polymerisation des Styrols bei Gegenwart von *s*-Trinitrobenzol (TNB) wurde untersucht. Die Versuchsergebnisse zeigen, dass sich TNB wie ein schwacher Inhibitor verhält und während der Inhibierungsperiode in einen Verzögerer umgewandelt wird. Die Kinetischen Gesetze für ein solches Verhalten sind aus der Literatur noch nicht bekannt. Es wurden daher die grundlegenden kinetischen Beziehungen für eine von Verzögerung begleitete Inhibierung ausgearbeitet. Die kinetischen Gleichungen für die Geschwindigkeit der inhibierten Polymerisation und für den Inhibitorumsatz wurden abgeleitet. Eine Methode zur Berechnung der Länge t , der Inhibierungsperiode aus der scheinbaren, durch Extrapolation der dilatometrischen Messdaten erhaltenen Inhibierungsperiode t' wurde ausgearbeitet. Die mit TNB bei 40, 50 und 60°C, erhaltenen Versuchsergebnisse lassen sich mit den abgeleiteten kinetischen Beziehungen gut darstellen. Die Zahl der durch ein TNB-Molekül desaktivierten Makroradikale wird zu 3.14 ± 0.1 bei 40°C, 2.98 ± 0.1 bei 50°C und 2.89 ± 0.2 bei 60°C berechnet. Dieser überraschende Wert des stöchiometrischen Koeffizienten kann nicht in einfacher Weise erklärt werden. Schliesslich wurde die relative Reaktivität von TNB im Vergleich zu der des Monomeren und die Temperaturabhängigkeit dieser Reaktivität bestimmt.

Received August 1, 1961

Revised February 12, 1962

Inhibition Kinetics of Polymerization of Styrene. III. Investigations on the Effect of Substituted Trinitrobenzenes*

FERENC TÜDÖS, IMRE KENDE, and MÁRIA AZORI, *Central Research Institute for Chemistry of the Hungarian Academy of Sciences, Budapest, Hungary*

Synopsis

In the present paper the effects of substituted derivatives, namely the $-\text{NH}_2$, $-\text{OCH}_3$, $-\text{CH}_3$, $-\text{Cl}$, and $-\text{CO}_2\text{C}_2\text{H}_5$ derivatives of *s*-trinitrobenzene are described on the initiated polymerization of styrene. The investigations were extended to the determination of the relative reactivity k_5/k_2 of the inhibitor as well as of the value of stoichiometric coefficient. It was shown by the values of k_5/k_2 that the Hammett equation can be considered valid within a factor of two. Corresponding to the electron-donating properties of the employed substituents, the values of the stoichiometric coefficient increase from 2.7 to 3.8. This fact as well as other data from literature lead to a mechanism by which these values, which are unexpected in the case of molecular inhibitors, can be interpreted.

In our previous papers,¹ investigations concerning the inhibiting effect of aromatic nitro compounds were briefly summarized. At the same time the kinetic investigations carried out with *s*-trinitrobenzene as the inhibitor in case of styrene at 40, 50, and 60°C. were described. The most unexpected result of our experiments was the value of about 3 of the stoichiometric coefficient μ . In case of molecular inhibitors, according to current conceptions, the value of the stoichiometric coefficient ought to be an even number; consequently, the above-mentioned value cannot be interpreted by trivial considerations. It was concluded that the "abnormal" value of the stoichiometric coefficient has some deeper reason involving the finer mechanism of the inhibition reaction. It was supposed that the inhibitor is consumed by several quick consecutive elementary reactions, the nature of which may be elucidated by investigating substituted derivatives of trinitrobenzene.

Such investigations can also yield an answer to the question of the degree to which the reactivity of the inhibitor, i.e., the value of the ratio k_5/k_2 , is influenced by the individual substituents. In the present paper, the effects of the substituents $-\text{NH}_2$, $-\text{OCH}_3$, $-\text{CH}_3$, $-\text{Cl}$, and $-\text{CO}_2\text{C}_2\text{H}_5$ are described.

* Presented in part at the Macromolecular Symposium of IUPAC, Moscow, June 1960.

Experimental

The method employed was the same as used previously;¹ all experiments were performed at 50°C.

The 2,4,6-trinitrochlorobenzene (PC) was crystallized from ethanol; m.p. 80°C.

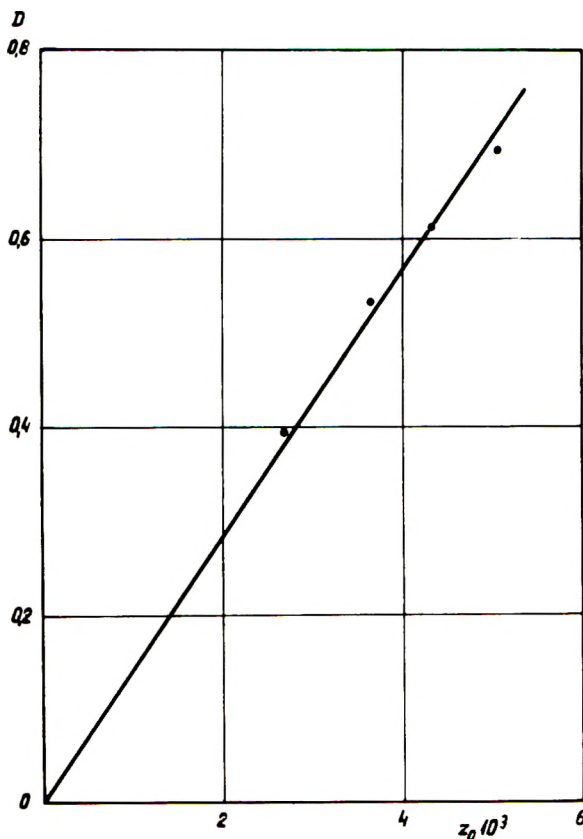


Fig. 1. Optical density of the reaction mixture plotted against the initial concentration of PA.

The ethyl ester of the 2,4,6-trinitrobenzoic acid (TNBE) was synthesized as follows. Trinitrobenzoic acid was prepared by oxidizing trinitrotoluene by published methods.² The acid chloride was prepared by treating the solution of the acid in benzoyl chloride with thionyl chloride.³ The reaction mixture was heated with stirring to 100–150°C. for several hours, then the trinitrobenzoyl chloride was precipitated with petroleum ether and washed with water, m.p. 161–162°C. The esterification was performed by boiling in ethanol. The crude product was recrystallized from chloroform by simultaneous clarification; m.p. 155°C.

The 2,4,6-trinitroaniline (PA) was prepared from picryl chloride with

ammonia in alcoholic medium, with a nearly quantitative yield. The obtained substance was recrystallized from benzene; m.p. 189.5–190°C.

The 2,4,6-trinitroanisole (TNA) was prepared by reacting picryl chloride with sodium methylate according to Chapman.⁴ The crude product was recrystallized from methanol; m.p. 67–68°C.

The 2,4,6-trinitrotoluene (TNT) was prepared from a technical-grade product by recrystallizing it twice from ethanol; m.p. 80.5–81°C.

The investigated compounds behaved more or less like TNB. During the inhibition period the reaction mixture generally darkened. This change was especially striking in the case of PA. This phenomenon is

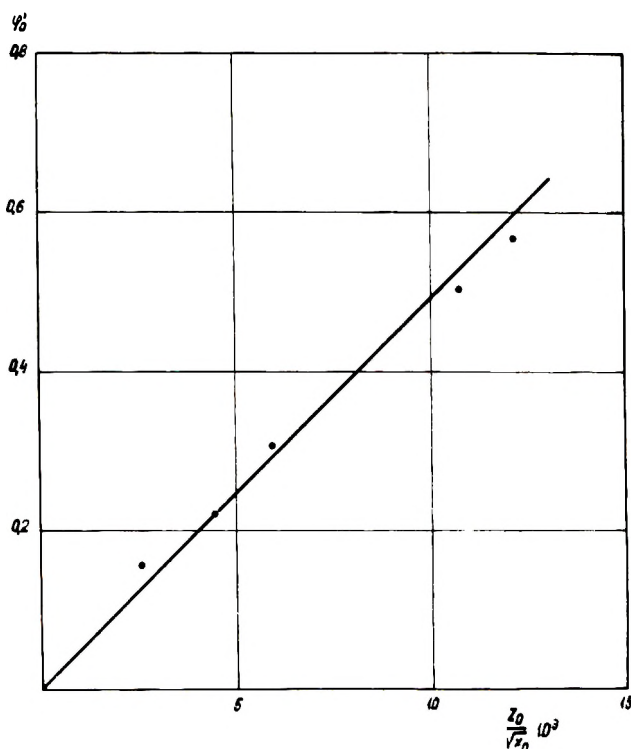


Fig. 2. Dependence of the retardation parameter φ'_0 on the values of the ratio $z_0/x_0^{1/2}$. The data of measurements relate to PC.

evidently connected with the transformation of the inhibitor. After the inhibition period is completed, the optical density D of the reaction mixture depends nearly linearly on the initial concentration of the inhibitor. For the case of PA, this phenomenon is shown in Figure 1.

The absorption was measured with a Pulfrich photometer using an S53 filter, and referred to a cuvet length of 1 cm.

The inhibition-kinetic behavior of PC and TNBE was fully similar to that of TNB. In Figure 2 the retardation parameter φ'_0 is plotted against $z_0/x_0^{1/2}$ for PC.

TABLE I
Inhibition with PC; $x_0 = 0.121$ mole/l.

No.	$z_0 \times 10^3$, mole/l.	$z_0/\bar{x} \times 10^2$	t' , min.	t_i , min.	W_{rel}	φ'_0	k_5/k_2
1	0.898	0.746	98	143	0.856	0.156	—
2	1.75	1.56	182	239	0.802	0.222	—
3	2.60	2.19	278	353	0.740	0.306	—
4	3.75	3.18	406	470	0.616	0.504	59.5
5	4.22	3.60	496	567	0.582	0.568	57.5

TABLE II
Inhibition with TNBE; $x_0 = 0.121$ mole/l.

No.	$z_0 \times 10^3$, mole/l.	$z_0/\bar{x} \times 10^2$	t' , min.	t_i , min.	W_{rel}	φ'_0	k_5/k_2
6	0.732	0.623	84	113	0.903	0.102	—
7	1.584	1.363	192	248	0.846	0.168	—
8	2.305	1.995	295	360	0.813	0.208	59.8
9	3.179	2.762	411	487	0.756	0.283	56.2
10	3.701	3.258	487	569	0.738	0.308	55.6

The data of measurements performed with PC and TNBE are shown in Tables I and II. The kinetic data were treated in the same way as in the case of TNB.¹

The kinetic measurements could be performed with somewhat more

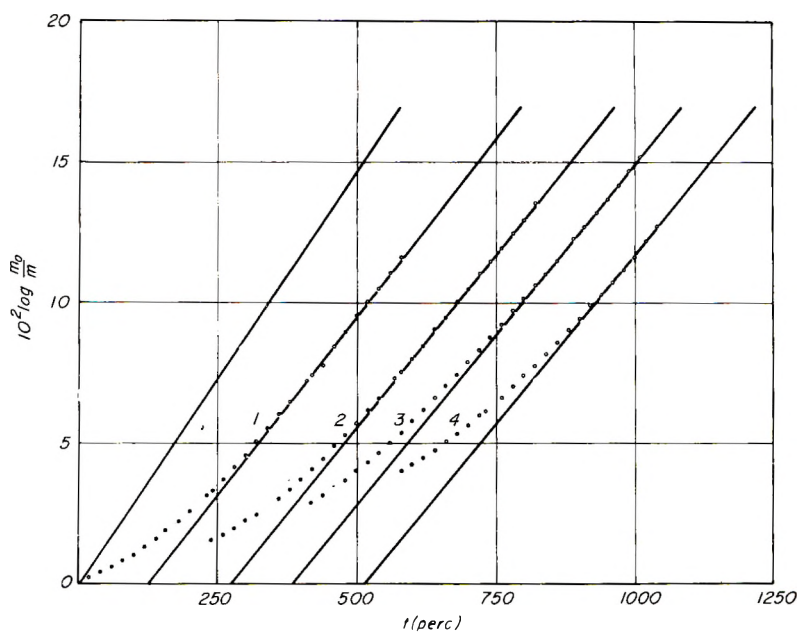


Fig. 3. Kinetic curves in the presence of TNA (the initial concentrations of TNA are given in Table IV): (1) expt. 18; (2) expt. 19; (3) expt. 20; (4) expt. 21.

difficulty and the results evaluated somewhat less exactly in the case of TNA, TNT, and especially in that of PA. The reactivity of these compounds is considerably less than that of the former ones ($k_5/k_2 = 10-20$); therefore, polymerization had to be continued up to a relatively high degree of conversion (30-50%) in order to obtain kinetic curves suitable for extrapolation. Even under such experimental conditions we succeeded in obtaining data which could be kinetically evaluated. One set of measurements for TNA is shown in Figure 3.

In the case of PA, with the two highest inhibitor concentrations, the extrapolations could not be performed, because in case of conversions over 35-40% a Trommsdorff effect⁵ of small degree could be detected. In these cases the true length t_i of the inhibition period was determined from the relation $t_i = f(z_0/x)$ by extrapolation, and these values were used merely for calculating k_5/k_2 .

The data of the experiments carried out with PA, TNA, and TNT are summarized in Tables III, IV, and V, respectively.

TABLE III
Inhibition with PA; $x_0 = 0.121$ mole/l.

No.	$z_0 \times 10^3$ mole/l.	$z_0/\bar{x} \times 10^2$	t' , min.	t_i , min.	k_5/k_2
12	0.949	0.793	169	288	—
13	1.85	1.55	243	373	—
14	2.69	2.28	357	513	—
15	3.66	3.13	498	680	11.5
16	4.33	3.79	—	800	12.1
17	5.06	4.46	—	920	11.7

TABLE IV
Inhibition with TNA; $x_0 = 0.121$ mole/l.

No.	$z_0 \times 10^3$, mole/l.	$z_0/\bar{x} \times 10^2$	t' , min.	t_i , min.	W_{rel}	φ_0'	k_5/k_2
18	1.37	1.14	122	205	0.909	0.095	—
19	2.70	2.28	272	392	0.890	0.116	22.8
20	3.79	3.21	386	530	0.837	0.179	19.1
21	4.78	4.10	514	674	0.789	0.239	18.9

TABLE V
Inhibition with TNT; $x_0 = 0.121$ mole/l.

No.	$z_0 \times 10^3$, mole/l.	$z_0/\bar{x} \times 10^2$	t' , min.	t_i , min.	W_{rel}	φ_0'	k_5/k_2
22	0.909	0.754	101	174	0.428	0.028	—
23	1.89	1.59	194	300	0.315	0.032	—
24	2.73	2.29	270	392	0.230	0.096	—
25	3.37	2.84	354	496	0.212	0.124	14.3
26	4.29	3.64	478	643	0.164	0.132	13.8
27	5.20	4.44	571	745	0.127	0.231	16.6

Some of the relations $\log m_0/m = f(\log z_0/z)$ used in determining the relative reactivity referred to the monomer of the individual inhibitors are shown in Figure 4.

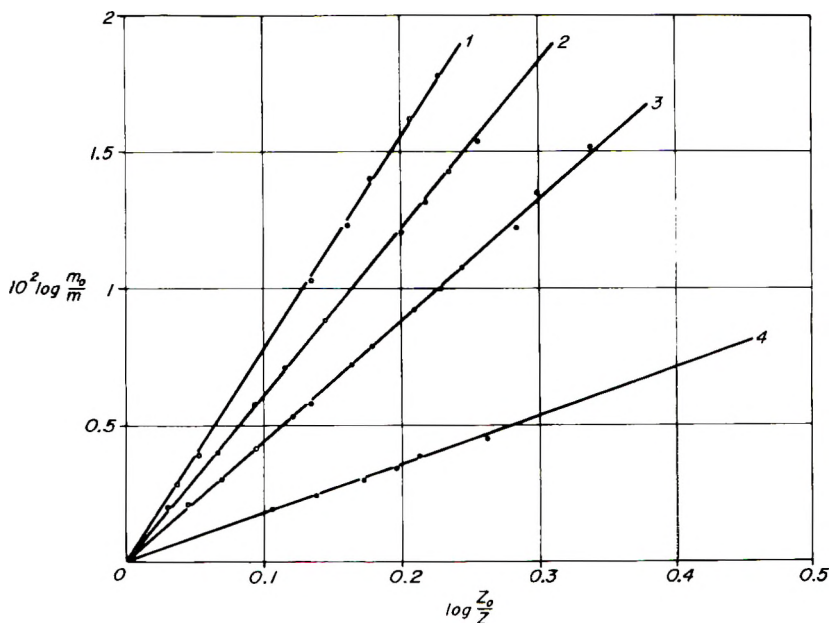


Fig. 4. The relation $10^2 \log m_0/m = f(\log z_0/z)$ in case of the individual inhibitors: (1) PA; (2) TNT; (3) TNA; (4) PC.

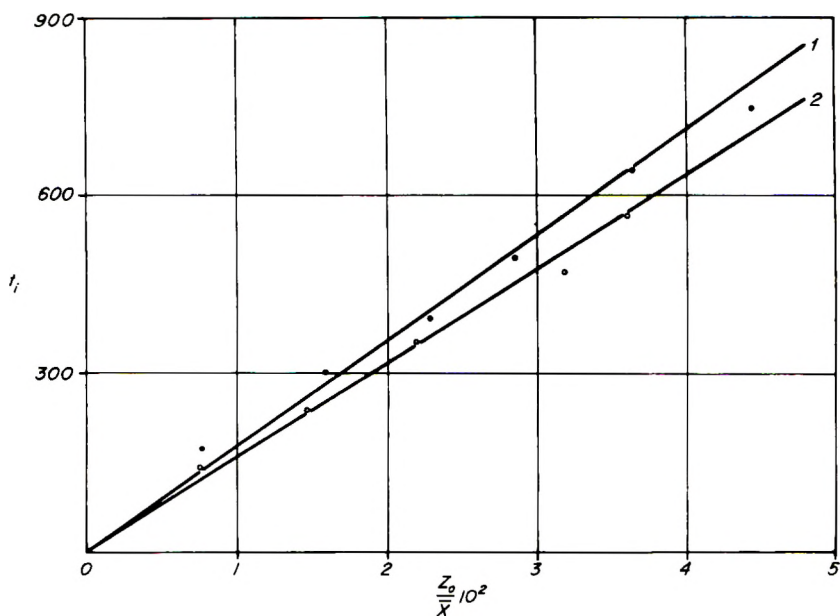


Fig. 5. Dependence of the values of t_i on the ratio z_0/\bar{x} . (1) TNT; (2) PC.

Finally, for two inhibitors, the relation $t_i = f(z_0/\bar{x})$, which was used to determine the stoichiometric coefficient, is shown in Figure 5. The correctness of the former kinetic analysis is again proved by the good linearity of the relations. As can be seen from the figure, the slope of the lines is different for each inhibitor, that is the values of the stoichiometric coefficients are different, too. In Table VI these data as well as the average values of the relative reactivities and of the inhibition and retardation constants are summarized.

Discussion of Experimental Results

The effect of the polar factors is well known in the field of reactions taking place according to an ionic mechanism.⁶ For reactions taking place in the side chain of aromatic compounds, the effect of substituents is described by Hammett's equation.⁷ In case of radical reactions, the effect of the substituents is less known, this being due according to Bagdassarian,⁸ mostly to the difficulties connected with quantitative investigations on radical reactions.

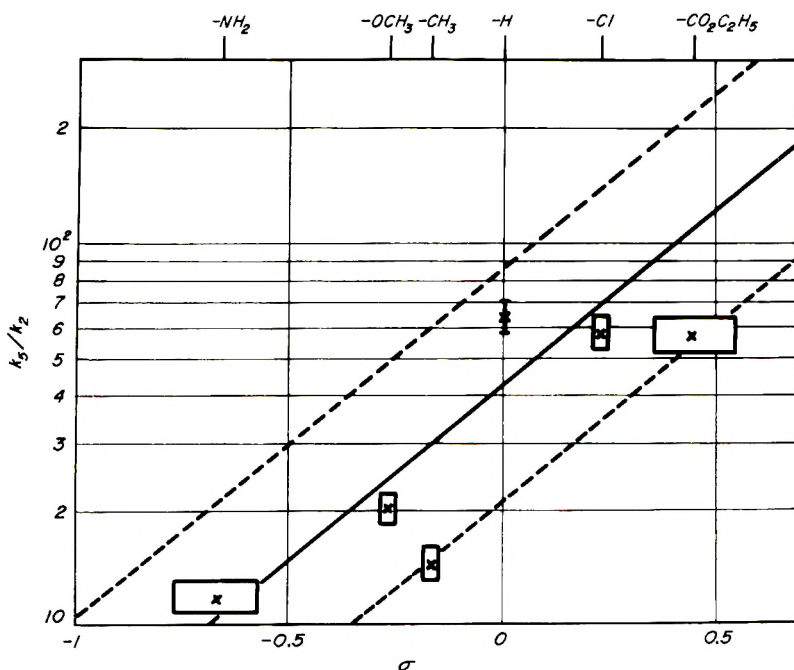


Fig. 6. Dependence of the relative reactivity k_5/k_2 on the Hammett constant.

In some cases,⁹ however, as in that of the dissociation of the tetraphenyl-dibenzoyl-tetrazenes,¹⁰ it was proved that the polar effect caused by the substituents influences considerably the rate of radical reactions. In the field of inhibited polymerization, Sinyicina and Bagdassarian observed that, in the case of the polymerization of methyl acrylate, the reactivity of

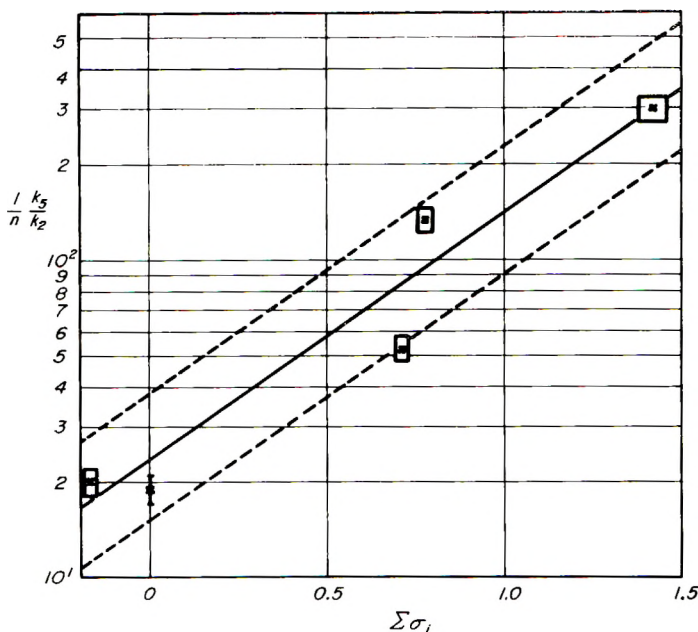


Fig. 7. Hammett-dependence of the values of $(1/n)(k_5/k_2)$ in case of vinyl acetate. From left to right, data for the following inhibitors are given: *p*-nitrotoluene; nitrobenzene; *m*-dinitrobenzene; *s*-trinitrobenzene.

aromatic nitro compounds changes considerably if substituents are introduced into the aromatic nucleus.^{6,11} It has been shown that in the case of *m*-substituted and *p*-substituted nitro compounds, the rate constant of the inhibition reaction can be described by the Hammett equation. In the case of *m*-substitution, the value of the constant ρ characteristic for the reaction is $+0.80$, while it is $+0.75$ in the case of *p*-substitution.

An attempt was made to take into account the effect of the substituent, with the aid of the Hammett equation. In our case, however, this attempt was rendered more difficult by the fact that an *ortho* substitution occurs. If, with rough approximation, *ortho* and *para* sites are considered as being equivalent, then the σ values of the *para*-substituents can be used for the calculations. Further on, in the case of this calculation, also the steric effect caused by the *ortho* substitution must be left out of consideration. Figure 6 showing the relation $k_5/k_2 = f(\sigma)$ was prepared in this way. The pertaining values of σ were taken from the work of McDaniel and Brown.¹²

From Figure 6 it can be seen that in the case of the not too bulky substituents $-\text{H}$, $-\text{NH}_2$, $-\text{CH}_3$, $-\text{OCH}_3$, and $-\text{Cl}$, within a factor of 2, Hammett's equation can be considered valid. Because of the neglect of appreciable factors no better coincidence can be expected. It is to be mentioned that the bases of the quadrangles drawn around the experimental points are equal to the probable errors of the constants and their heights to the maximum error ($\pm 10\%$) of the k_5/k_2 values. On the basis of the figure it can be stated that the reactivity of the individual inhibitors is the

higher the greater is the electron-withdrawing tendency of the substituent. From Figure 6, the value of ρ can be estimated as 1.1; consequently, the reaction taking place between the nitro compound and the polystyrene radical is more sensitive to polar effects than that taking place with the methacrylate radical.

The reactivity of TNBE is considerably smaller than would be expected on the basis of Hammett's equation. Most probably this fact can be explained by the decrease in conjugation as a consequence of the high space requirement of the $-\text{C}(\text{O})\text{C}_2\text{H}_5$ group and the steric hindrance connected with it.

For the sake of comparison, it was investigated whether Hammett's equation is valid for Bartlett's and Kwart's data^{13,14} relating to the polymerization of vinyl acetate. As can be seen from Figure 7, the experimental data fall onto a straight line within a factor of 1.6; the value of ρ is +0.75. In Figure 7 the values of $1/n(k_5/k_2)$, where n is the number of nitro groups are plotted against the algebraic sum of the values of σ . Although the compounds in question involve only *meta*- and *para*-substitutions, the coincidence with Hammett's equation is not better than in our case; the deviations from a straight line are, similarly as in Figure 6, considerably larger than the experimental error.

In connection with this question, it is worthwhile mentioning that, in the case of some substituents, in order to better describe the electrophilic reactions, an extra electrophilic-substituent constant (σ^+) had to be introduced.¹⁵ It is possible that in case of radical reactions, at least for some substituents, substituent constants deviating from the thermodynamic ones ought to be introduced in a similar way. To decide this question, however, numerous experimental data of great accuracy would be required.

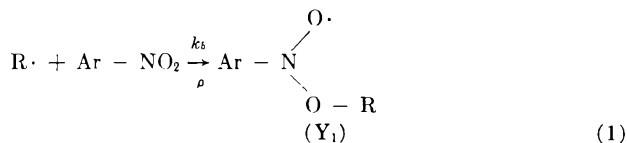
As could be expected, the values of the stoichiometric coefficients were different; according to Table VI, in the case of the tested inhibitors, the values change from 2.7 to 3.8. By a more thorough examination, the trend of the values can be established; the stoichiometric coefficient is increased by electrodonating substituents.

As the value of μ exceeds unity, it follows that the inhibitor is not consumed in a single step but in a sequence of several consecutive reactions. As was shown earlier,¹ the rate-determining step is, however, the reaction of the intact inhibitor molecule with a macroradical. According to

TABLE VI
The Determined Kinetic Constants

Substituent	k_5/k_2	μ	$k_{5.1}/k_{5.2}$	β	β'
$-\text{NH}_2$	11.8	3.78 ± 0.2	0.12	270	—
$-\text{OCH}_3$	20.3	2.96 ± 0.2	1.08	292	17
$-\text{CH}_3$	14.6	3.13 ± 0.2	0.77	255	26
$-\text{H}$	64.2	2.98 ± 0.1	1.04	930	37
$-\text{Cl}$	58.5	2.73 ± 0.1	1.74	820	49
$-\text{CO}_2\text{C}_2\text{H}_5$	57.2	3.15 ± 0.1	0.74	795	76

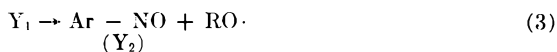
Bartlett's and Kwart's kinetic data,^{13,14} as well as the preparative proofs of Inamoto,¹⁶ Norris,¹⁷ and Jackson,¹⁸ it is the nitro group which is attacked by the macroradical. In compliance with our former kinetic analysis, this reaction is a bimolecular process; consequently, the reaction can be described by the eq. (1);



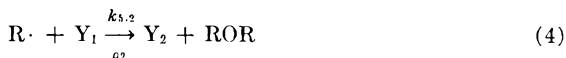
In the case of vinyl acetate, the stoichiometric coefficient amounts to 2^{13,14} therefore, reaction (1) must be succeeded by the following recombination:



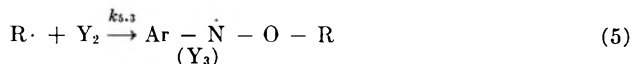
However, in our case, the radical Y_1 must take part in other reactions, too ($\mu \neq 2$). According to Inamoto's and Simamura's hypothesis, Y_1 disintegrates monomolecularly:¹⁴



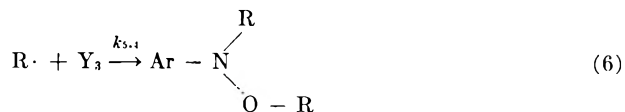
On the other hand, a bimolecular reaction is supposed by Hammon and Bartlett:¹⁹



Finally, according to the studies of Inamoto,¹⁶ Norris,¹⁷ and Jackson¹⁸ in the course of their model reactions, substituted derivatives of hydroxylamine could be separated from the reaction mixture. The latter compounds can not be formed but from the nitroso compound; therefore, two further reactions have to be supposed:



and



As a matter of fact, according to the investigations of Gingras and Waters,²⁰ the corresponding hydroxylamine derivative is produced in nearly quantitative yield by the reaction of nitroso benzene and the 2-cyano-2-propyl radical.

Taking into account reactions (1), (2), and (4)–(6), and by use of the usual symbols,¹ the system of differential equations describing the concentrations of the individual intermediate products can be given as follows:

$$dy_1/dt = k_5 z r - (k_{5.1} + k_{5.2}) y_1 r \quad (7)$$

$$dy_2/dt = k_{5.2} y_1 r - k_{5.3} y_2 r \quad (8)$$

$$dy_3/dt = k_{5.3} y_2 r - k_{5.4} y_3 r \quad (9)$$

and

$$dr/dt = 2k_1 f \bar{x} - k_5 z r - (k_{5.1} + k_{5.2}) y_1 r - k_{5.3} y_2 r - k_{5.4} y_3 r - k_4 r^2 = 0 \quad (10)$$

When Bodenstein's principle:

$$dy_1/dt = 0 \quad (11)$$

$$dy_2/dt = 0 \quad (12)$$

$$dy_3/dt = 0 \quad (13)$$

$$dr/dt = 0 \quad (14)$$

is used, the system of differential equation is transformed into an algebraic one. After performing the corresponding operations, the eq. (15) is obtained:

$$dr/dt = 2k_1 f \bar{x} - 2\{1 + [k_{5.2}/(k_{5.1} + k_{5.2})]\} k_5 z r - k_4 r^2 = 0 \quad (15)$$

Comparing this with eq. (9) in our previous paper,¹ and taking into account that, for the sake of simplicity, in the present case the calculation was carried out with the assumption $k_5' = 0$, the following expression is obtained:

$$\mu = 2\{1 + [k_{5.2}/(k_{5.1} + k_{5.2})]\} \quad (16)$$

Thus, depending on the relative values of the rates of reactions (2) and (4), the stoichiometric coefficient corresponding to the above mechanism may assume values between 2 and 4. It can be thus seen that the experimental results are adequately reflected by eq. (16).

It is to be noted that in the above reaction scheme the monomolecular disintegration of Y_1 , eq. (3), has not been taken into account. This reaction was dismissed from the discussion because each elementary step of the mechanism must be of the same order (that is, each step must be bimolecular). If this were not the case, μ would have to depend on the concentration of the reacting substances, and this is in contradiction with the experimental results. On the other hand, with reaction (3), the value of the stoichiometric coefficient cannot exceed 2, because the radical $RO\cdot$ arising from the disintegration must be very reactive and thus ought to initiate a chain. (In this case, the real inhibitor would be the nitroso compound.)

By the aid of eq. (16), the values of the ratio $k_{5.1}/k_{5.2}$ can be calculated for the different substituents. These data can be found in Table VI. The ratio $k_{5.1}/k_{5.2}$ (similarly to the ratio k_5/k_2) shows probably a Hammett dependence. Theoretically $\rho_1 > 0$ must be expected, because, with respect to the effect of the substituents, reaction (2) is analogous to reaction (1). In

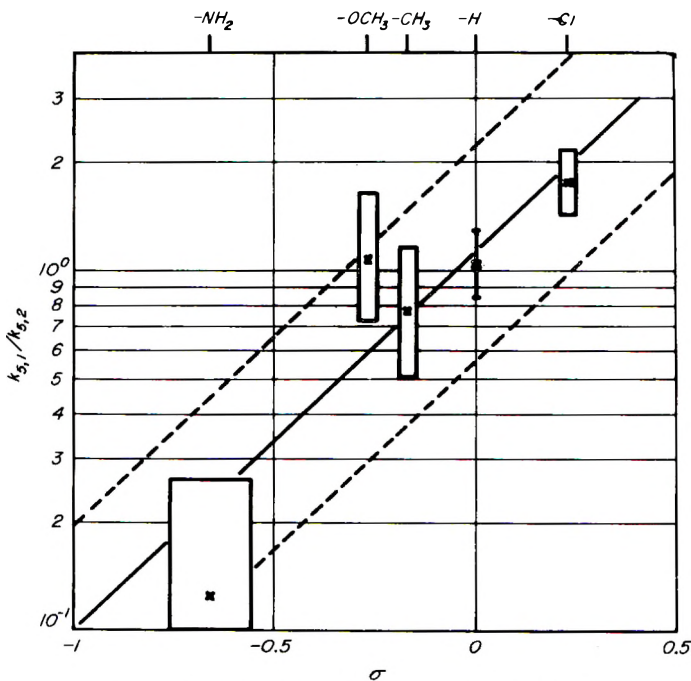


Fig. 8. Hammett dependence of the values $k_{5,1}/k_{5,2}$.

the case of reaction (4), the situation is just reversed. Namely, on introduction of an electron-donating substituent, both the positive charge of the "key" carbon atom and the strength of the N—O bond are decreased. Thus, however, the acceleration of reaction (4) is provoked; consequently, it must be expected that $\rho_2 < 0$. The Hammett dependence of the ratios $k_{5,1}/k_{5,2}$ is shown in Figure 8.

Determined from the diagram, the difference $\rho_1 - \rho_2$ turns out to have the value 1.05; thus, the above statements are qualitatively supported by this figure.

In the case of TNBE, the value of the stoichiometric coefficient amounts to 3.17. Consequently, the rate of reaction (2) is diminished. Taking into account the considerable steric hindrance existing for the substituent $-\text{CO}_2\text{C}_2\text{H}_5$ as well as its deforming effect, this result cannot be considered to be surprising.

The authors wish to express their thanks to Mr. László Sümegei, Miss Ágnes Diószeghy, and Edit Fülöp for their assistance in the course of the experiments.

References

1. Tüdös, F., I. Kende, and M. Azori, *Magy. Tud. Akad. KKKI Közlemén.*, No. 5, 13 (1961); *J. Polymer Sci.*, **A1**, 1353 (1963).
2. *Sintezii Organicheskikh Preparatory*, Izdatelstvo. Inoszt. Literaturi, Moscow, 1949, Vol. I. p. 416.
3. Brown, D. A., and R. F. Hudson, *J. Chem. Soc.*, **1953**, 3352.
4. Chapman, E., A. G. Perkin, and R. Robinson, *J. Chem. Sec.*, **1927** 3015.

5. Trommsdorff, E., H. Köhle, and P. Lagally, *Makromol. Chem.*, **1**, 169 (1948).
6. Jaffé, H., *Chem. Revs.*, **53**, 191 (1953).
7. Hammett, L., *Physical Organic Chemistry*, McGraw-Hill, New York, 1940.
8. Bagdassarian, G. S., *Teoriya Radikal'noi Polimerizatsii*, Izdatelstvo. Akad. Nauk SSSR, Moscow, 1959.
9. Walling, C., *Free Radicals in Solution*, Wiley, New York, 1957.
10. Wilmarth, W. K., and N. Schwartz, *J. Am. Chem. Soc.*, **77**, 4543, 4551 (1955).
11. Sinyitsina, Z. A., and G. S. Bagdassarian, *Zhur. Fiz. Khim.*, **32**, 2663 (1958).
12. McDaniel, D. H., and H. C. Brown, *J. Org. Chem.*, **23**, 420 (1958).
13. Bartlett, P. D., and H. Kwart, *J. Am. Chem. Soc.*, **72**, 1051 (1950).
14. Bartlett, P. D., and H. Kwart, *J. Am. Chem. Soc.*, **74**, 3969 (1952).
15. Brown, H. C., and Y. Okamoto, *J. Am. Chem. Soc.*, **80**, 4979 (1958).
16. Inamoto, N., and O. Simamura, *J. Org. Chem.*, **23**, 408 (1959).
17. Norris, W. P., *J. Am. Chem. Soc.*, **81**, 4239 (1959).
18. Jackson, R. A., and W. A. Waters, *J. Chem. Soc.*, **1960**, 1653.
19. Hammond, G. S., P. D. Bartlett, *J. Polymer Sci.*, **5**, 617 (1950).
20. Gingras, B. A., and W. A. Waters, *J. Chem. Soc.*, **1954**, 1920.

Résumé

Cet article traite de l'influence de dérivés substitués, et notamment $-\text{NH}_2$, $-\text{OCH}_3$, $-\text{CH}_3$, $-\text{Cl}$ et $-\text{CO}_2\text{C}_2\text{H}_5$ du *s*-trinitrobenzène sur la polymérisation du styrène. Les recherches ont été faites en vue de déterminer la réactivité relative k_5/k_2 de l'inhibiteur ainsi que la valeur du coefficient stoechiométrique. On a montré par les valeurs de k_5/k_2 que l'équation de Hammett peut être considérée comme exacte en faisant intervenir un facteur de 2. En accord avec les propriétés électro-donneurs des substituants utilisés, les valeurs du coefficient stoechiométrique augmentent de 2.7 à 3.8. En tenant compte de ce fait ainsi que d'autres données fournies par la littérature, un mécanisme est donné par lequel ces valeurs, quoique surprenantes dans le cas d'inhibiteur moléculaire, peuvent être interprétées.

Zusammenfassung

In der vorliegenden Mitteilung wird der Einfluss substituierter *s*-Trinitrobenzole, nämlich des $-\text{NH}_2$, $-\text{OCH}_3$, $-\text{CH}_3$, $-\text{Cl}$ und $-\text{CO}_2\text{C}_2\text{H}_5$. Derivates, auf die gestartete Styrolpolymerisation beschrieben. Die Untersuchungen wurden auf die Bestimmung der relativen Reaktivität k_5/k_2 des Inhibitors sowie des Wertes des stöchiometrischen Koeffizienten ausgedehnt. Die k_5/k_2 -Werte zeigen, dass die Hammett-Beziehung innerhalb eines Faktors von zwei gültig ist. Entsprechend dem Elektronendonorcharakter des Substituenten nimmt der Wert des stöchiometrischen Koeffizienten von 2,7 auf 3,8 zu. Unter Berücksichtigung dieser Tatsache sowie anderer Literaturdaten wird ein Mechanismus aufgestellt, der diese für molekulare Inhibitoren unerwarteten Werte erklären kann.

Received August 1, 1961

Revised February 6, 1962

Stability of Helical Conformations of Simple Linear Polymers

P. DE SANTIS, E. GIGLIO, A. M. LIQUORI, and A. RIPAMONTI,
*Istituto Chimico, Università di Napoli, Centro Nazionale di Chimica delle
Macromolecole del Consiglio Nazionale delle Ricerche, Sez. III, Naples, Italy*

Synopsis

The potential energy of polyethylene, polytetrafluoroethylene, polyoxymethylene, polyisobutylene, polyvinylidene chloride, and isotactic polypropylene with a helical conformation has been calculated as a function of the angles of rotation around the bonds of the backbone chain. The use of appropriate functions to describe the interaction between nonbonded atoms in the chains, has allowed prediction with surprising accuracy of the most stable conformation for each polymer considered, in spite of the rather drastic assumptions involved in the calculations. The most prominent feature of the potential energy diagrams are discussed with reference to the possibility of predicting the allowed helical conformations for the isolated unperturbed polymer chains considered.

INTRODUCTION

The widely recognized influence of stereochemical factors on the physical properties of linear polymers has stimulated an increasing number of x-ray diffraction studies on crystalline polymers.

Though the detailed crystal structure has been solved only for a few polymers, the chain conformation of a large variety of organic and inorganic polymers has been established with a satisfactory degree of accuracy.

A survey of these data shows that, with only a few exceptions, whenever the configurational identity of the monomeric units along the chain is certain, the conformation is helical. This is, for instance, the case for isotactic vinyl polymers,¹ polyisobutylene,² polyoxymethylene,^{3,4} polytetrafluoroethylene,⁵ polyvinylidene chloride,⁶ and for many inorganic polymers,⁷ such as polymeric sulfur,⁸ selenium,⁹ tellurium,¹⁰ polymeric sulfur trioxide,¹¹ polyphosphonitrilic chloride,¹² and several polyphosphates.¹³⁻¹⁵

A number of methods, mostly based on a theory first formulated by Eyring,¹⁶ have been recently proposed to describe the geometry of helical conformation of linear polymers. However, no attempts seem to have been made thus far to explain the stabilities of the different helical conformations established for the various crystalline polymers investigated.

The main difficulty of such a study is due to the lack of a satisfactory

method for calculating the contribution of the interaction between non-bonded atoms to the conformational potential energy of a polymer molecule.

It appears, however, that a rather easy classification of the known helical conformations can be made in terms of size and mode of alternation of substituents to the backbone chain without considering the mode of molecular packing.⁷ These considerations have encouraged us to make an attempt to explain the relative stabilities of the different conformations by considering intramolecular interactions between nonbonded atoms in the chain only. The use of approximate functions to describe the interactions between pairs of nonbonded atoms has allowed prediction of the most stable helical conformations to be expected for a number of simple linear polymers.

The excellent agreement with the experimental results obtained for polyethylene, polytetrafluoroethylene, polyoxymethylene, polyisobutylene, polyvinylidene chloride, and isotactic polypropylene indicates that this approach, in spite of the drastic approximations implied, might be extended with confidence to more complex polymers.

CONFORMATIONAL POTENTIAL ENERGY OF A HELIX

It is a well established concept that a linear polymer may take up a very large number of conformations by varying the angles of rotation around the bonds of the skeleton.

The helix belongs to a special class of conformations satisfying a very restrictive condition: i.e., equivalence of the monomeric units along the chain, which requires that the angles of rotation around the chemically equivalent skeleton bonds must be identical. It is therefore safe to postulate that the energetically most stable helical conformation of an infinite polymer chain with fixed structural parameters, i.e., bond lengths and bond angles, should be predicted by locating the deepest minimum in the potential energy as a function of the angles of rotation around the bonds of the backbone chain.

Considering only chains containing chemically equivalent atoms or pairs of chemically equivalent atoms in the skeleton (one- and two-atom chains, respectively), the conformational potential energy should be calculated as a function of one or two angles of internal rotation.

Obviously such a calculation involves (a) a suitable choice of bond angles and bond lengths and (b) appropriate potential energy functions to describe the interactions between nonbonded atoms.

While structural parameters collected for simple molecules can be used with some confidence for making reasonably accurate assumptions about bond angles and bond lengths, at least for simple polymers, the correct choice of (b) clearly constitutes a major difficulty.

In fact, the present knowledge of the factors hindering free rotation around single bonds is unfortunately so poor that an exact calculation of the conformational potential energy as a function of the angles of rotation

around the C—C bonds has not yet been possible, even for the simplest hydrocarbon molecules. However, approximate calculations of the potential barriers of hindered rotation for a number of ethane derivatives, based on the most commonly accepted model of Van der Waals interactions between nonbonded atoms, have given rather consistent results.¹⁷

Such a model was therefore adopted in the present calculations of the conformational potential energy of a number of one-atom and two-atom chain helices as a continuous function of one or two angles of internal rotation respectively.

The most stable helices were established from the positions of the deepest minima in one- and two-dimensional plots of the potential energy. It should be pointed out that the degree of accuracy required in this procedure is considerably less than that necessary to predict the barrier heights hindering rotation in small molecules for the same kind of potential function for the interaction between nonbonded atoms.

METHOD OF CALCULATION

a. Distances between Nonbonded Atoms

The polymers considered can be classified according to Hughes and Lauer¹⁸ as one-atom chains:



and "two-atom" chains:



where A and B represent nonequivalent atoms or atomic groups in the chain.

Distances between pairs of nonbonded atoms in the helix were calculated from the corresponding atomic coordinates, as a function of one or two angles of rotation for one- and two-atom chains, respectively.

Relations derived by Shimanouchi and Mizushima¹⁹ and Hughes and Lauer¹⁸ between cylindrical coordinates of the skeleton atoms and structural parameters of one- and two-atom chains as a function of the angles of rotation, were found very convenient for the above purpose.

For a one-atom chain with a bond length l and a bond angle θ the cylindrical coordinates of the second backbone atom are:

$$r = [2l^2(1 + \cos \theta)/(3 + \cos \theta - \cos \psi + \cos \psi \cos \theta)^2]^{1/2} \quad (1)$$

$$\varphi = \cos^{-1}[(1/2)(-\cos \theta + \cos \psi - \cos \theta \cos \psi - 1)] \quad (2)$$

$$z = [l^2(1 - \cos \psi)(1 - \cos \theta)/(3 + \cos \theta - \cos \psi + \cos \psi \cos \theta)]^{1/2} \quad (3)$$

being the first atom at $r, 0, 0$. ψ is the angle of rotation around the skeleton bonds measured from the *cis* conformation.

For a two-atom chain, —A—B—A—B, with identical bond lengths $l = \text{AB} = \text{BA}$ and bond angles $\theta = \widehat{\text{ABA}} = \widehat{\text{BAB}}$ as has been throughout

assumed, putting the first A atom at $r_1, 0, 0$, the cylindrical coordinates (see Fig. 1a) of the next equivalent A atom are

$$r_1 = \{ [2l^2(1 - \cos \theta) - z_1^2] / 2(1 - \cos \varphi_1) \}^{1/2} \quad (4)$$

$$\varphi_1 = \cos^{-1} \{ (1/2) [\cos^2 \theta (1 + \cos \psi_1 \cos \psi_2) - \sin^2 \theta (\cos \psi_1 + \cos \psi_2) + 2 \cos \theta \sin \psi_1 \sin \psi_2 + \cos \psi_1 \cos \psi_2 - 1] \} \quad (5)$$

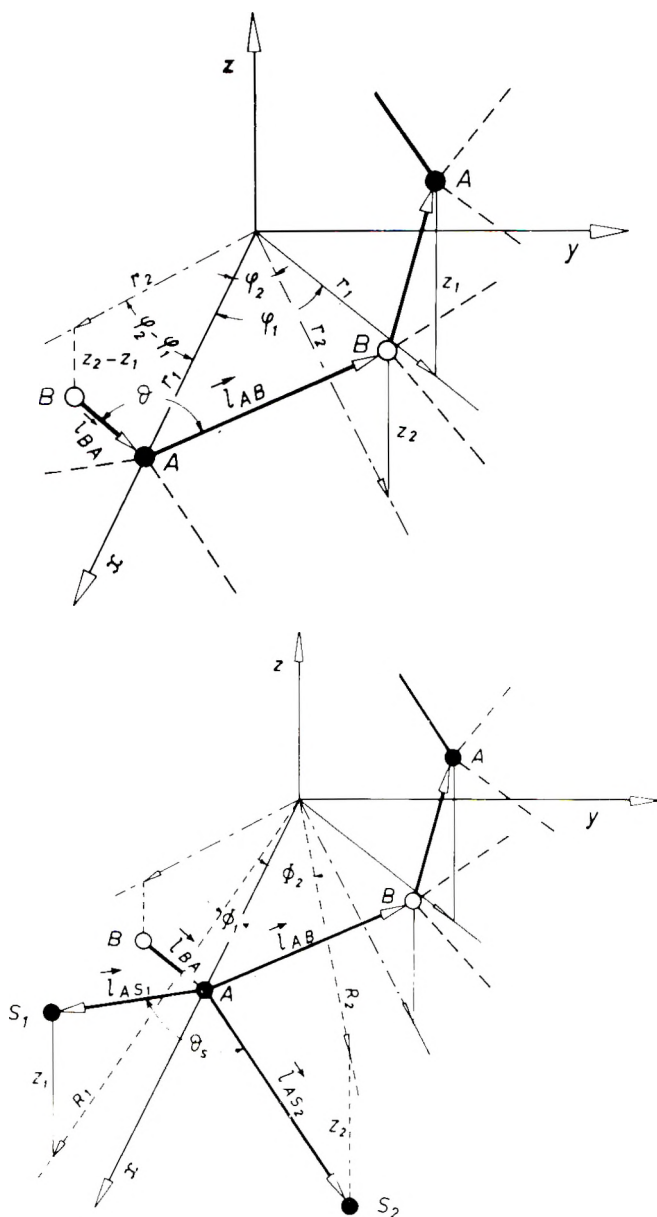


Fig. 1. Cylindrical coordinates of (a) a helix; (b) substituents S_1 and S_2 .

$$z_1 = \left\{ l[(\cos^2 \theta - \cos \varphi_1 - \sin^2 \theta \cos \psi_1)^{1/2} + (\cos^2 \theta - \cos \varphi_1 - \sin^2 \theta \cos \psi_2)^{1/2}] \right\} / (1 - \cos \varphi_1)^{1/2} \quad (6)$$

whereas those of the B atom are

$$r_2 = r_1 \quad (7)$$

$$\varphi_2 = \cos^{-1} [(2r_1^2 - z_2^2 - l^2)/2r_1^2] \quad (8)$$

$$z_2 = [l^2(\cos^2 \theta - \sin^2 \theta \cos \psi_2 - \cos \varphi_1)/(1 - \cos \varphi_1)]^{1/2} \quad (9)$$

ψ_1 and ψ_2 being the angles of rotation around the two nonequivalent AB and BA skeleton bonds. It may be noticed that $r_1 = r_2$ follows from the assumed identity of bond angles.

The cylindrical coordinates of the substituent atoms directly connected to the backbone were derived as follows. Let x, y, z be an orthogonal reference frame with origin at the foot of the perpendicular from the first atom to the helical axis; the x axis lies on this perpendicular, the z axis is on the helical axis, and the y axis is so chosen as to make the system right-handed (see Fig. 1b). Let us denote B,A,B the consecutive atoms of a two-atom chain with coordinates r_1 ($\varphi_2 - \varphi_1$), ($z_2 - z_1$); $r_1, 0, 0$; r_1, φ_2, z_2 . If S_1 and S_2 are two substituents directly bonded to atom A, their cylindrical coordinates will be R_1, Φ_1, Z_1 and R_2, Φ_2, Z_2 respectively.

Let \vec{l}_{BA} and \vec{l}_{AB} be two vectors of magnitude $|l|$ joining atom B and atom A and atom A and the consecutive atom B, and \vec{l}_{AS_1} and \vec{l}_{AS_2} two vectors of magnitude $|s|$ equal to the lengths A— S_1 = A— S_2 of the bonds connecting the atom A to S_1 and S_2 . Putting:

$$\begin{aligned} \vec{l}_{AB} &= ai + bj + ck \\ \vec{l}_{BA} &= \alpha i + \beta j + \gamma k \\ \vec{l}_{AS_1} &= u_1 i + v_1 j + w_1 k \\ \vec{l}_{AS_2} &= u_2 i + v_2 j + w_2 k \end{aligned} \quad (10)$$

it may easily be shown that

$$\begin{aligned} a &= r_1(\cos \varphi_2 - 1); \quad b = r_1 \sin \varphi_2; \quad c = z_2 \\ \alpha &= r_1[1 - \cos(\varphi_2 - \varphi_1)]; \quad \beta = -r_1 \sin(\varphi_2 - \varphi_1); \quad \gamma = -(z_2 - z_1) \\ u_1 &= R_1 \cos \Phi_1 - r_1; \quad v_1 = R_1 \sin \Phi_1; \quad w_1 = Z_1 \\ u_2 &= R_2 \cos \Phi_2 - r_1; \quad v_2 = R_2 \sin \Phi_2; \quad w_2 = Z_2 \end{aligned} \quad (11)$$

From Fig. 1 it may be seen that

$$\begin{aligned}
 \vec{l}_{AB}l_{AS_1} &= \vec{l}_{AB}l_{AS_2} = -ls \cos(\theta_s/2) \cos(\theta/2) \\
 \vec{l}_{BA}l_{AS_1} &= \vec{l}_{BA}l_{AS_2} = ls \cos(\theta_s/2) \cos(\theta/2) \\
 \vec{l}_{AS_1}l_{AS_1} &= \vec{l}_{AS_2}l_{AS_2} = s^2
 \end{aligned} \tag{12}$$

being the plane through the B, A, and B atoms perpendicular to the plane through S₁, A, and S₂. θ_s denotes the bond angle S₁— \widehat{B} —S₂. Substituting eq. (10) in eq. (12) yields

$$\begin{aligned}
 au + bv + cw &= -ls \cos(\theta_s/2) \cos(\theta/2) \\
 \alpha u + \beta v + \gamma w &= ls \cos(\theta_s/2) \cos(\theta/2) \\
 u^2 + v^2 + w^2 &= s^2
 \end{aligned} \tag{13}$$

the two solutions of which give $u_1, v_1, w_1, u_2, v_2, w_2$. The cylindrical coordinates of S₁ and S₂ can thus be obtained with the aid of eq. (11). A similar procedure can be followed in order to derive the coordinates of the substituents bonded to the B atom of the chain.

The atomic coordinates of all the atoms of the helix can be obtained from eqs. (4), (5), (6), (7), (8), (9), and (13) through screw operation. The above relations can be used for a one-atom chain through obvious simplifications.

The required distances between nonbonded atoms can therefore be calculated for the one- and two-atom chains after inserting in the above relations the values of the corresponding bond angles and bond lengths.

TABLE I
Bond Angles and Bond Lengths Used for the Calculation of the Intramolecular Distances

Polymer	Skeleton bond length, A.	Skeleton bond angle	Sidegroup parameters
Polyethylene	1.54	110°	$\overline{CH} = 1.00$ A.; $\widehat{HCH} = 110^\circ$
Polytetrafluoroethylene	1.54	116°	$\overline{CF} = 1.38$ A.; $\widehat{FCF} = 110^\circ$
Polyoxymethylene	1.43	110°	$\overline{CH} = 1.00$ A.; $\widehat{HCH} = 110^\circ$
Polyisobutylene	1.54	114°	$\overline{CH} = 1.00$ A.; $\widehat{HCH} = 110^\circ$ $\overline{CMe} = 1.54$ A.; $\widehat{MeCMe} = 110^\circ$
Polyvinylidene chloride	1.54	114°–120°	$\overline{CH} = 1.00$ A.; $\widehat{HCH} = 110^\circ$ $\overline{CCl} = 1.78$ A.; $\widehat{ClCCl} = 110^\circ$
Isotactic polypropylene	1.54	114°	$\overline{CH} = 1.00$ A.; $\widehat{HCH} = 110^\circ$ $\overline{CMe} = 1.54$ A.; $\widehat{HCMe} = 110^\circ$

Admittedly it seems rather difficult to predict accurately the bond angles in a carbon backbone chain in view of the reported evidence of large deviations from the tetrahedral values for several polymers. For example, the helix found in the stable crystal lattice of polytetrafluoroethylene⁵ implies a C—C—C angle of 116° and that of polyisobutylene² and isotactic polypropylene²⁰ a value of at least 114° . These values were therefore adopted in the calculations for these polymers. In the case of polyvinylidene chloride, for which a drastic increase of the bond angles of the backbone chain could be expected,⁶ both values of 114° and 120° were taken in turn.

Values of bond angles and bond lengths used to calculate the distances between nonbonded atoms for all the polymers considered are given in Table I.

b. The Number of Monomeric Units per Turn and the Monomer Repeat of a Helix

The most widely used parameters to characterize a given helical conformation are the number of monomeric units per turn and the monomer repeat

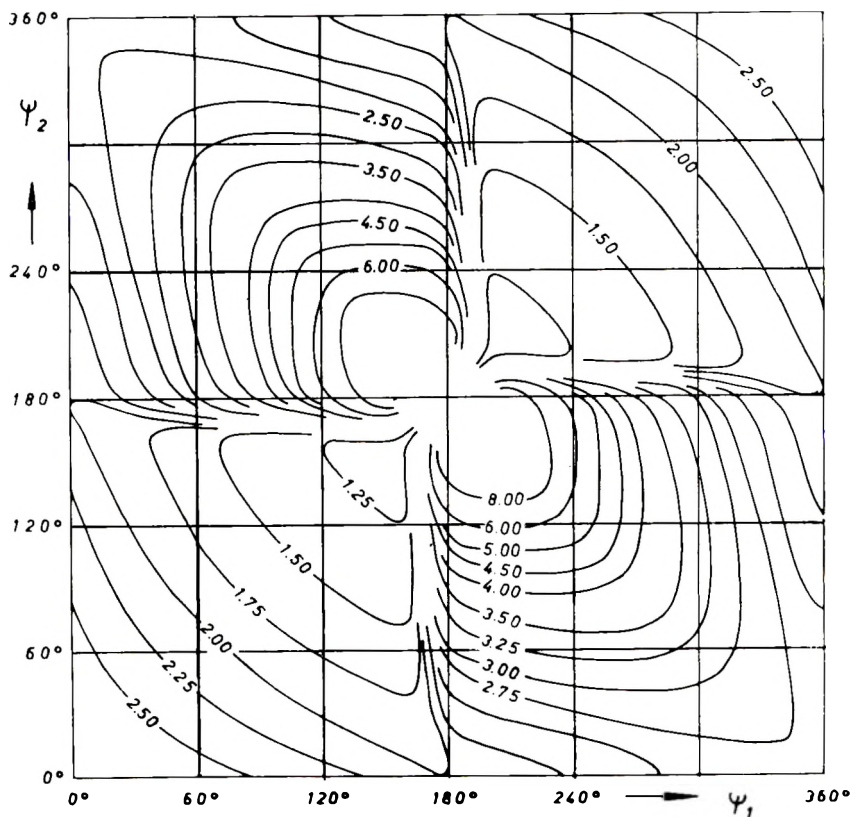


Fig. 2. Plot of the number of monomeric units per turn as a function of ψ_1 and ψ_2 for a two-atom helical chain with equal bond angles of 114° .

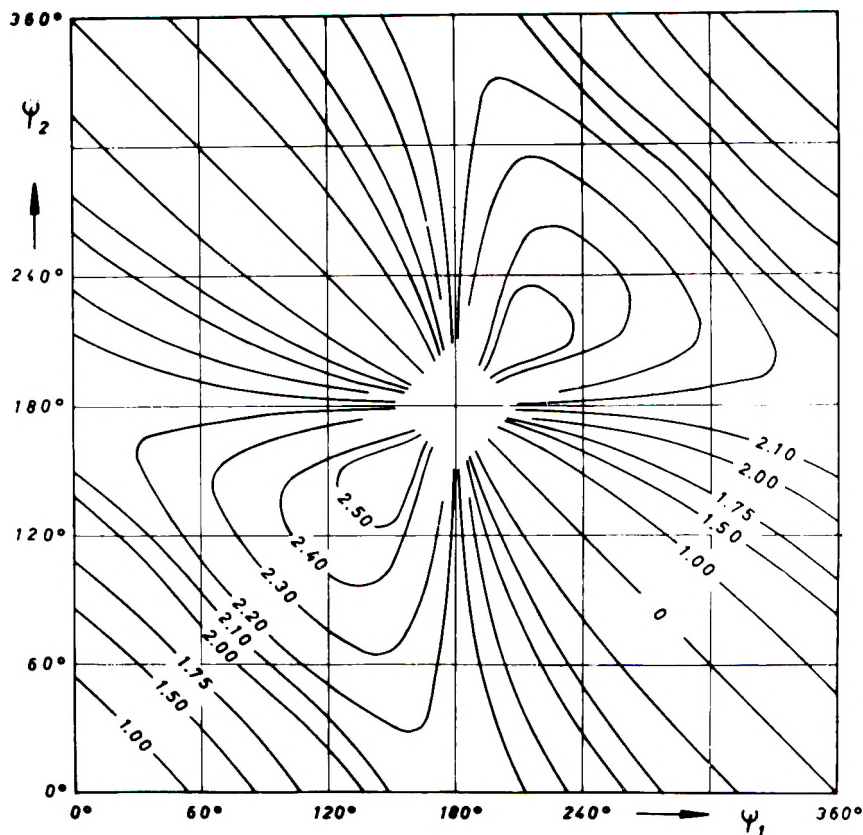


Fig. 3. Plot of the monomer repeat on the helical axis as a function of ψ_1 and ψ_2 for a two-atom helix with equal bond angles of 114° .

repeat on the helical axis. These are in fact related to the most prominent features of the x-ray diffraction photographs of chain polymers. For one- and two-atom chains the numbers of monomeric units per turn may be expressed as $K = 2\pi/\varphi$ and $K_1 = 2\pi/\varphi_1$, φ and φ_1 being the azimuthal angles around the helical axis given by eqs. (2) and (5). For a chain with fixed bond angles, K depends on the angle of rotation ψ , whereas K_1 depends on both ψ_1 and ψ_2 . In Figure 2 a two-dimensional plot of $K_1(\psi_1, \psi_2)$ which was calculated for a bond angle $\theta = 114^\circ$ is shown. Contour lines join identical values of K_1 .

The diagonal $\psi_1 = \psi_2$ joins the representative points of uniform helices and separates helices related by a dyad perpendicular to the chain axis. Doubling the K_1 values along this diagonal gives the number of monomeric units per turn K of a one-atom chain. This arises from having set in the calculation of the plot of figure 2 $\theta = \theta_1 = \theta_2$ as in a one-atom chain. The diagonal $\psi_1 = 2\pi - \psi_2$ separates enantiomorphous helices with identical number of monomers per turn.

The monomer repeat on the axis of a one- or two-atom helix can be

calculated from eqs. (3) and (6) as a function of the angles of rotation after replacing numerical values of bond lengths and bond angles. In Figure 3 a plot of z_1 is shown which was calculated by setting $l = 1.54$ A. and $\theta = 114^\circ$. The symmetry of this plot is the same as that of K_1 shown in Figure 2. Halving the z_1 values lying on the diagonal $\psi_1 = \psi_2$ obviously gives the monomer repeat of a one-atom helical chain having the above bond lengths and bond angles.

c. Potential Functions of Pairwise Interactions

Several potential functions have been proposed in the attempt to describe the interactions between nonbonded atoms. Apparently the best results in the calculation of potential barriers hindering rotations in simple molecules have been obtained by using semiempirical functions consisting of an attractive and a repulsive term.

The potential functions proposed by Mason and Kreevoy¹⁷ were employed in the present calculations in order to describe the F----F, CH₃----CH₃, and Cl----Cl interactions. The potential function for the H----H interactions was derived from the data of Hirschfelder and Linnett²¹ the appropriate force law being assumed to be similar to that between two hydrogen atoms in the triplet state ³Σ. The potential functions for the F----F, CH₃----CH₃, Cl----Cl interactions were derived on the basis of molecular beam scattering and transport data of neon, methane, and argon. The O----O interactions were described by

TABLE II
Van der Waals Interaction Functions

Interaction	Interaction energy (when r is in Angstrom units), kcal./atom pair
H.....H ^a	$3.7164 \times 10^3 \exp \{-3.0708r\} - 89.52r^{-6}$
F.....F ^b	$7.20 \times 10^3 r^{-9.99} \quad (1.7 \leq r \leq 2.30 \text{ A.})$ $1.057 \times 10^5 \exp \{-4.608r\} - 125.10r^{-6} (r \geq 2.30 \text{ A.})$
CH ₃CH ₃ ^b	$2.390 \times 10^4 r^{-7.37} \quad (r \leq 3.20 \text{ A.})$ $2.739 \times 10^5 \exp \{-3.329r\} - 2.942 \times 10^3 r^{-6} (r \geq 3.20 \text{ A.})$
Cl.....Cl ^b	$1.300 \times 10^4 r^{-7.87} \quad (2.18 \leq r \leq 3.00 \text{ A.})$ $2.208 \times 10^5 \exp \{-3.621r\} - 1.430 \times 10^3 r^{-6} (r \geq 3.00 \text{ A.})$
C.....C ^c	$3.012 \times 10^5 r^{-12} - 327.20r^{-6}$
C.....H ^d	$(3.347 \times 10^4 \exp \{-1.5354r\} - 589.00)r^{-6}$
C.....CH ₃ ^d	$(2.879 \times 10^5 \exp \{-1.6645r\} - 1235)r^{-6}$
C.....Cl ^d	$(2.5798 \times 10^5 \exp \{-1.8105r\} - 1111.2)r^{-6}$
H.....CH ₃ ^d	$3.1905 \times 10^4 \exp \{-3.1999r\} - 2089r^{-6}$
H.....Cl ^d	$2.8645 \times 10^4 \exp \{-3.3459r\} - 1702r^{-6}$
O.....H ^d	$1.982 \times 10^4 \exp \{-3.8395r\} - 497.61r^{-6}$
O.....C ^d	$(1.785 \times 10^5 \exp \{-2.304r\} - 202.2)r^{-6}$

^a Data of Hirschfelder and Linnett.²¹

^b Data of Mason and Kreevoy.¹⁷

^c Data of Bartell.²²

^d The mixed interaction functions were minimized by using the following values of the Van der Waals radii: $R_H = 1.20$ A.; $R_C = 1.70$ A.; $R_F = 1.35$ A.; $R_{Cl} = 1.80$ A.; $R_{CH_3} = 2.00$ A.; $R_O = 1.35$ A.

means of the F---F potential function, whereas for the C---C interaction the function proposed by Bartell²¹ was used.

The repulsive terms of the mixed interactions were determined by averaging geometrically the respective repulsive terms of the two different chemical species. An attractive term $-Ar^{-6}$ was then added to the repulsive term, and the complete function was minimized at the Van der Waals distances between the two atoms in order to obtain the value of A .

The potential functions used are given in Table II.

d. Calculation of the Conformational Potential Energy

The conformational potential energy of one-atom and two-atom helices was calculated by adding up all the non-negligible contributions due to interactions between the not directly bonded atoms of an infinite helical chain.

Denoting by $E_\alpha, E_\beta, E_\gamma, \dots$, the interaction energies (referred to the monomeric unit) between the substituents bonded to the first neighboring, to the second, to the third neighboring skeleton atoms, etc., of an infinite chain, we may write the total energy as

$$E = E_\alpha + E_\beta + E_\gamma + \dots \quad (14)$$

As the term corresponding to the interactions between the substituents bonded to the sixth neighboring atoms was always very small, terms higher than the fifth were neglected in the summation of eq. (14).

A program was written for an IBM 650 electronic computer to calculate the intermolecular distances, the contribution due to all the interactions and the total conformational potential energy as a function of rotation angles around the bonds of the backbone chain. One- and two-dimensional plots of conformational potential energy were drawn from the numerical data for one- and two-atom chain respectively.

The minima were located by interpolation, and from the corresponding values of ψ or the pair of values ψ_1 and ψ_2 the number of monomers per turn and the monomer repeat of the most stable helical conformations were derived as described above. These parameters allowed a convenient comparison between the helical conformations predicted theoretically with those established through interpretation of the x-ray fiber photographs.

RESULTS

Polyethylene

Figure 4 shows the variation of potential energy of an infinite polyethylene helix as a function of the internal rotation angle around the C—C bonds. The deepest minimum at $\psi = 180^\circ$ corresponds to the most stable *trans*-planar conformation.²³

The two minima at $\psi = 90^\circ$ and $\psi = 270^\circ$ as well as those higher at $\psi = 60^\circ$ and $\psi = 300^\circ$ are symmetric and correspond to helices.

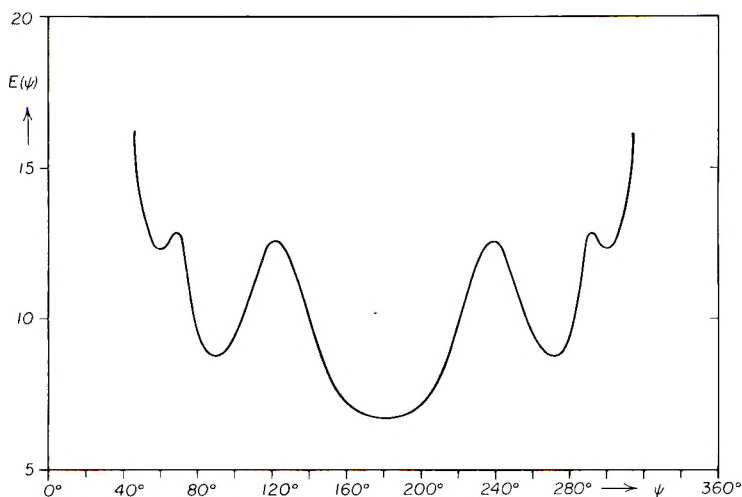


Fig. 4. Conformational potential energy of a helical polyethylene chain.

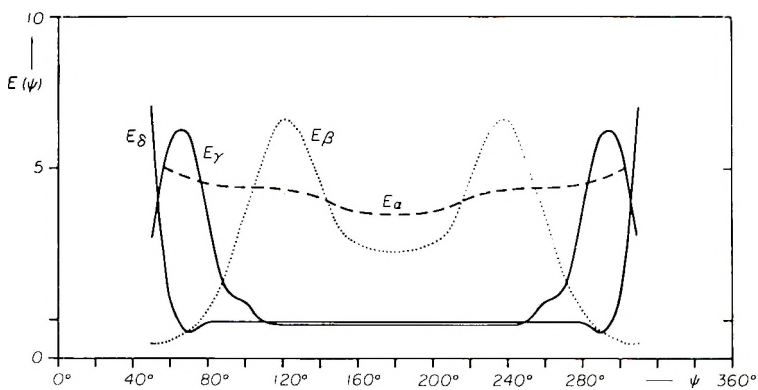


Fig. 5. Variation of the E_{α} , E_{β} , E_{γ} , and E_{δ} contributions to the total potential energy with the internal rotation angle for a helical polyethylene chain.

It is interesting to note that the existence of two minima at $\psi = 60^{\circ}$ and $\psi = 90^{\circ}$, instead of a single at $\psi = 60^{\circ}$, as it is usually assumed for the gauche conformation of hydrocarbon molecules, is due to contribution of the interaction energy E_{γ} (see Fig. 5). Therefore it does not appear justified to neglect this contribution as is frequently done for the calculation of the statistical conformations of normal hydrocarbons.

Polytetrafluoroethylene

The potential energy of the helical conformation of polytetrafluoroethylene, plotted in Figure 6 against the rotation angle ψ , shows three minima at $\psi = 60^{\circ}$, $\psi = 90^{\circ}$, and $\psi = 165^{\circ}$ and symmetric ones corresponding to the enantiomorphous conformations. The deepest minimum

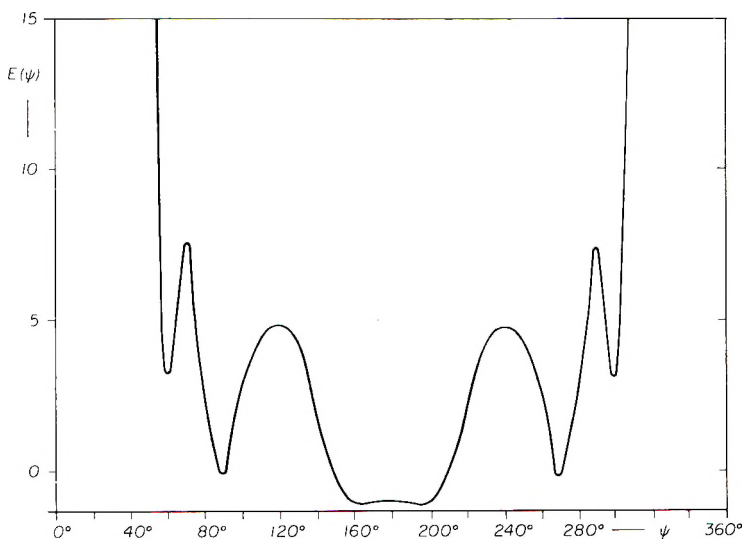


Fig. 6. Conformational potential energy of a helical polytetrafluoroethylene chain.

at $\psi = 165^\circ$ corresponds to a helical conformation with $K = 2.17$, in good agreement with the structure of polytetrafluoroethylene below 20°C ., characterized by a helix with 13 monomeric units in 6 turns ($K = 2.18$).⁵ The minimum at 60° is deeper than that which occurs for polyethylene because of the sharper maximum of E_γ at $\psi = 70^\circ$.

The fact that the potential energy shows a larger number of pronounced minima than that of polyethylene is likely to be related to the occurrence of several crystalline transitions in the polytetrafluoroethylene.

In view of the small energy barrier which separates the two minima at $\psi = 165^\circ$ and $\psi = 195^\circ$ corresponding to the right-handed and left-handed helices, respectively, the room-temperature transition may be tentatively explained. Above 20°C . the chains might consist of a mixture of stretches of left-handed and right-handed helices. In order to avoid too short contacts between the fluorine atoms the different helices should join through bonds in *trans* conformation. Obviously the extensions of the enantiomorphous helices and consequently the number of the junctions should change with the temperature. According to this possibility, the room-temperature transition might be ascribed to a disorder in the molecular chains rather than to a rotation of the helices around their axes.²⁴

Polyoxymethylene

Recently Tadokoro, Yasumoto, Murahashi, and Nitta³ found that the radial intensity distribution of the x-ray fiber diagram is consistent with a uniform helix with 9 monomeric units ($\text{CH}_2\text{—O}$) in 5 turns ($\psi = 77^\circ 23'$), assuming bond lengths $\overline{\text{CO}} = \overline{\text{OC}} = 1.43$ A. and bond angles $\widehat{\text{COC}} = \widehat{\text{OCO}} = 110^\circ 53'$. This structure has been reexamined by Carazzolo,⁴ who

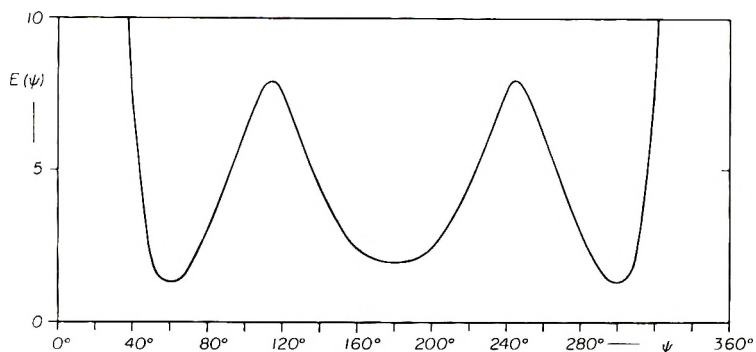


Fig. 7. Conformational potential energy of polyoxymethylene considered as a one-atom helical chain.

also found another crystalline modification containing twofold helices with an angle of rotation $\psi = 63^\circ$ and with $\widehat{COC} = \widehat{OCO} = 112^\circ$.

On the basis of these results and in view of the drastic approximations in the potential function for O.....O interaction the calculation of the potential energy was carried out considering this polymer as a one atom chain. As may be seen in Figure 7, where the conformational potential energy is shown as a function of ψ , the deepest minimum occurs at $\psi = 67^\circ$.

The lack of side groups attached to alternate atoms of the chain is responsible for the fact that the gauche conformation is energetically preferable to the *trans*-planar one in contrast with what happens for polyethylene and polytetrafluoroethylene.

Analogous reasoning can be applied to explain the marked flexibility of the molecular chain and the existence of a number of crystalline helical conformations. It must be noted that the repulsions between the lone pair electrons of the oxygen atoms might be a nonnegligible factor in determining the stability of the polyoxymethylene helices. Nevertheless the results of the present calculation which predicts a helix with $K = 1.92$ are in rather good agreement with the existence of a twofold helix in one of the crystalline modifications of this polymer.

Note added in proof: As a part of a research in progress the potential energy of the helical conformation of polyoxymethylene has been calculated as a function of two internal rotation angles. The map of the potential energy shows the deepest minimum along the diagonal $\psi_1 = \psi_2$ in agreement with the above conclusions.

Polyisobutylene

The interpretation of the x-ray fiber diagram of stretched polyisobutylene² has led to the conclusion that the stable conformation is characterized by a S_5^8 helix with 8 monomeric units in 5 turns ($K_1 = 1.60$). This agrees satisfactorily with the occurrence of a minimum of the potential energy at $\psi_1 = \psi_2 = 85^\circ$ ($K = 1.75$) as can be seen in Figure 8, where the potential energy is shown as a function of ψ_1 and ψ_2 . Furthermore the map shows a

minimum about as deep at $\psi_1 = 155^\circ$, $\psi_2 = 45^\circ$ and two other minima at $\psi_1 = 205^\circ$, $\psi_2 = 85^\circ$, and $\psi_1 = \psi_2 = 160^\circ$ beyond the symmetric ones corresponding to the isoenergetic conformations.

The minimum at $\psi_1 = 155^\circ$, $\psi_2 = 45^\circ$ corresponds to a helix intermediate between the S_6^8 and the *cis*-planar one. The conformation with $\psi_1 = \psi_2 = 160^\circ$ corresponds to a uniform helix with $K_1 = 1.10$ similar to that with 8 monomeric units in 7 turns, proposed by Fuller, Frosh, and Pape²⁵ and resulted in disagreement with the x-ray pattern. Finally the conformation with $\psi_1 = 205^\circ$ and $\psi_2 = 85^\circ$ is a fourfold helix similar to that found for isotactic poly- α -olefins with bulky sidegroups. Poly-3-methylbutene-1,²⁶ for instance, has a helical conformation with $K_1 = 4$.

Polyvinylidene Chloride

The conformational potential energy of the helical polyvinylidene chloride chain is plotted in Figures 9 and 10 for values of the bond angle $\widehat{C-C-C}$ of 114° and 120° , respectively. Although the absolute values of

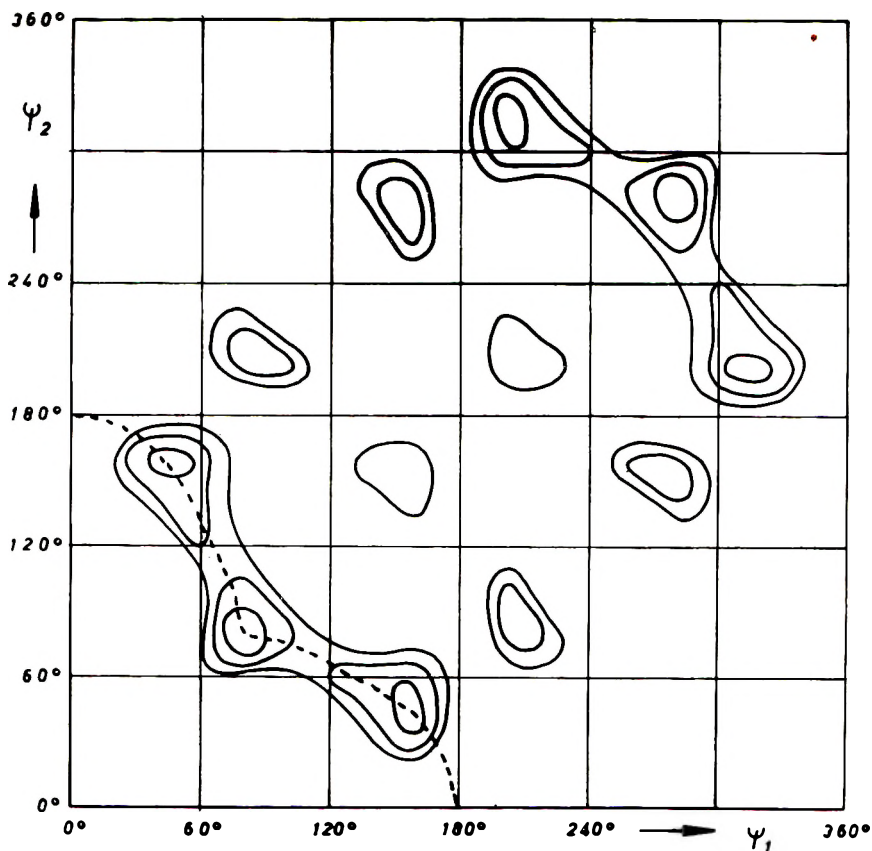


Fig. 8. Conformational potential energy of a helical polyisobutylene chain. Isoenergetic contour lines are drawn at intervals of 10 kcal./monomeric unit.

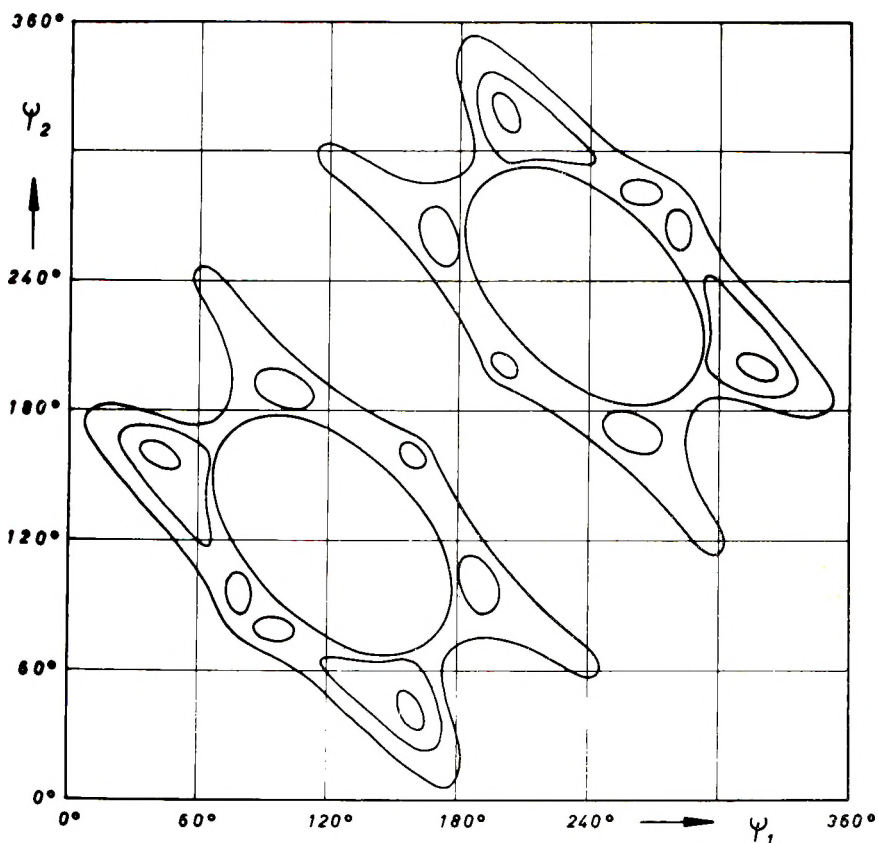


Fig. 9. Conformational potential energy of a helical polyvinylidene chloride chain with equal skeleton bond angles of 114° . Isoenergetic contour lines are drawn at intervals of 4 kcal./monomeric unit.

the energy are rather different, the minima fall in the same region of the graphs.

The behavior of the function is similar to that of polyisobutylene because of the analogy of the structure of the monomeric units. However, the replacement of the two methyl groups with chlorine atoms determines the occurrence of the deepest minimum at about $\psi_1 = 165^\circ$, $\psi_2 = 30^\circ$, (where $\theta = 120^\circ$) in agreement with the conformation found for polyvinylidene chloride in the crystal lattice.⁶ In fact, the interpretation of the x-ray fiber photograph has led to the conclusion that the chain conformation corresponds to a helix with $K_1 = 2$ and with the angles of rotation around the two nonequivalent bonds close to 0° and π , similar to that first proposed by Reinhardt.²⁷

Isotactic Polypropylene

Because of the different groups bonded to the alternate atoms of the vinyl polymer chain the mirror plane $\psi_1 = \psi_2$ in the map of the confor-

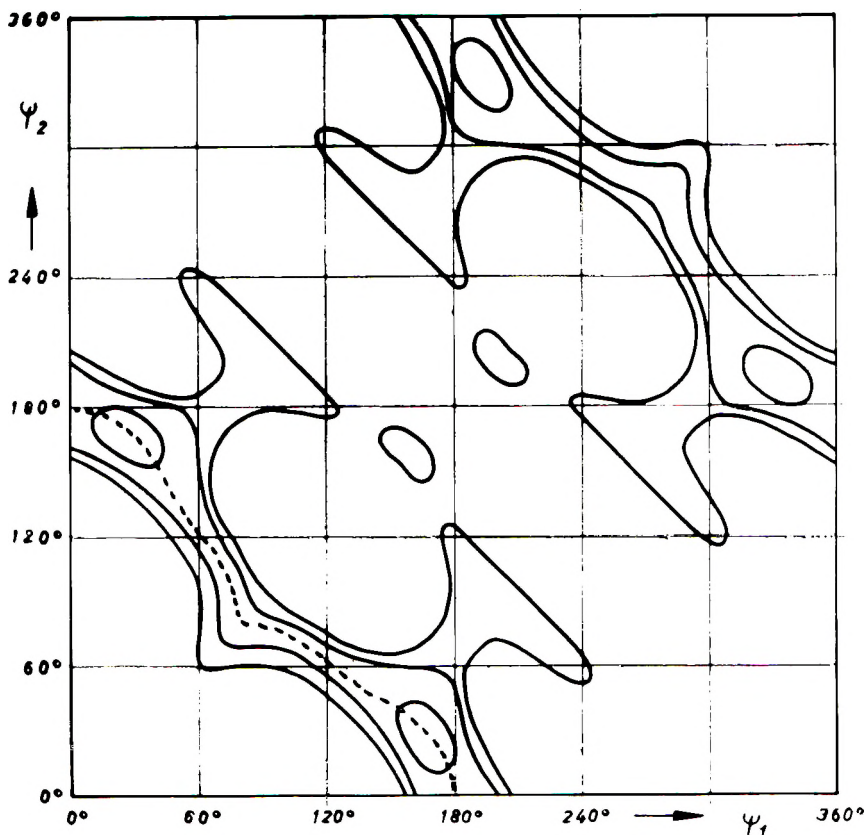


Fig. 10. Conformational potential energy of a helical polyvinylidene chloride chain with equal skeleton bond angles of 120° . Isoenergetic contour lines are drawn at intervals of 4 kcal./monomeric unit.

mational potential energy disappears, as may be seen in Figure 11, where the potential energy of isotactic polypropylene is plotted as a function of ψ_1 and ψ_2 .

The energy minima are at $\psi_1 = 183^\circ, \psi_2 = 62^\circ$; $\psi_1 = 80^\circ, \psi_2 = 100^\circ$; $\psi_2 = 60^\circ, \psi_2 = 160^\circ$ beyond those corresponding to the enantiomorphous conformations.

The deepest minimum is at about $\psi_1 = 183^\circ, \psi_2 = 62^\circ$ and corresponds to a helix with $K_1 = 3.10$, in good agreement with that established for crystalline isotactic polypropylene.²⁰ These results are consistent with those of a calculation carried out for this polymer by Natta, Corradini, and Ganis,²⁸ who used a similar approach.

DISCUSSION

In Figures 12 and 13 the most significant helical parameters, namely the number of monomers per turn K_1 and the monomer repeat z_1 on the chain axis predicted for the polymers considered on the basis of the above de-

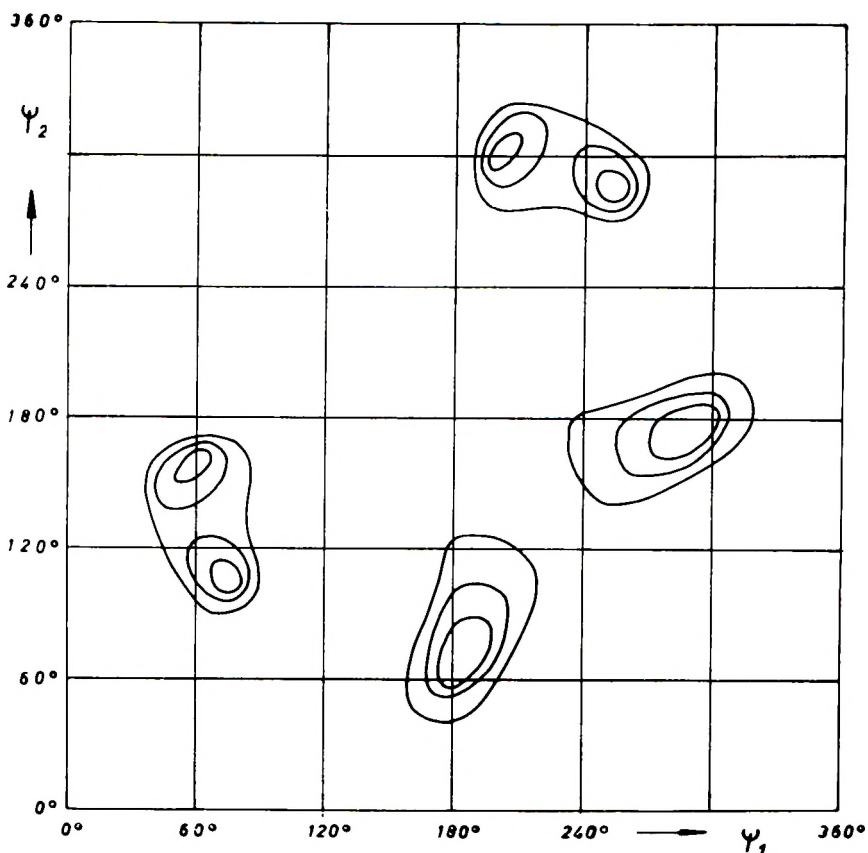


Fig. 11. Conformational potential energy of a helical isotactic polypropylene chain. Isoenergetic contour lines are drawn at intervals of 1 kcal./monomeric unit.

scribed calculations are compared with the corresponding values established by x-ray diffraction. For the sake of uniformity in the plots the K values for polyethylene and polytetrafluoroethylene have been halved and the z values have been doubled. This is equivalent to considering these helices formally as two-atom chains. The agreement is most satisfactory, particularly if one considers the rather drastic assumptions on which the above described theoretical approach is based. The safest conclusion which may be drawn is that, at least for the polymers considered, the helical conformations found in the crystalline state are markedly determined by intramolecular interactions. This appears particularly interesting in view of the increasing tendency to assume that polyolefins and vinyl polymers retain their helical conformation, at least in short sections of the chain, also in the noncrystalline state.²⁹⁻³¹

In this connection it may be worthwhile to discuss some other interesting features of the potential energy diagrams.

In the case of polyisobutylene, for instance, the potential energy diagram indicates that two nonuniform helices (with $\psi_1 = 155^\circ$, $\psi_2 = 45^\circ$, and

$\psi_1 = 45^\circ$, $\psi_2 = 155^\circ$) related to each other by a dyad perpendicular to the chain axis should have about the same energy as the uniform helix ($\psi_1 = \psi_2 = 85^\circ$) present in the crystallized polymer. Such a "conformational degeneracy" might imply that the two enantiomorphous uniform helices present in the crystal might not be the only conformations populated in the unperturbed isolated molecule as it has been thus far assumed.^{29,30}

The uniform helices might be further stabilized in the crystal with respect to the other conformers by the more favorable packing. In fact a sixfold conformational degeneracy might explain the remarkable flexibility

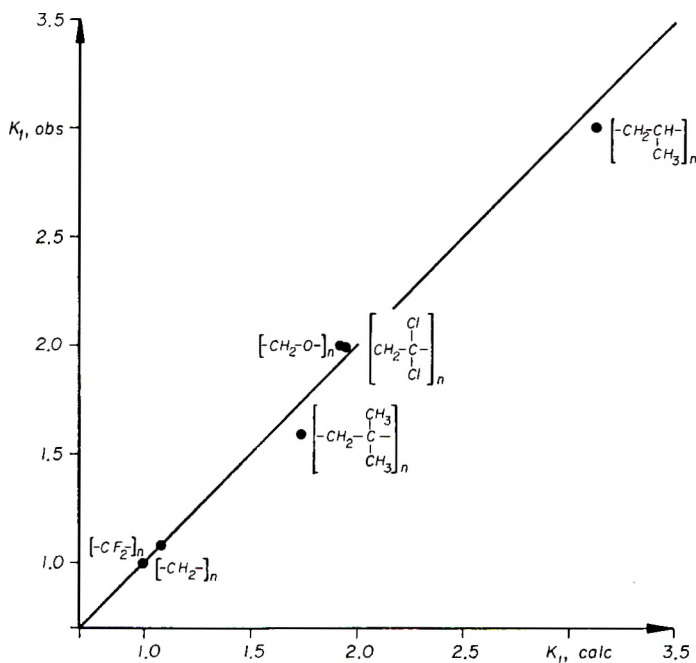


Fig. 12. Comparison of experimental and theoretically predicted values of the numbers of monomeric units per turn K_1 . For polyethylene and polytetrafluoroethylene see text.

of polyisobutylene molecules in terms of a rather wide spectrum of population of isomeric helical segments in the isolated chain. On stretching, the nonuniform helical segments should tend to be converted into the uniform ones, which are the only conformers present in the crystallized polymer. The path of such a transition, which is indicated in the diagram of Figure 8 as a continuous line and in Figure 14 as a profile, does not appear to be hindered by a large potential barrier to take place as easily as it would be required. The conversion from a right-handed to a left-handed helix appears to be much more hindered.

It is interesting to compare the situation of polyisobutylene with that of polyvinylidene chloride. From the conformational energy profile (Fig. 15)

of this polymer it appears that the conformational degeneracy is reduced, since the energy minimum corresponding to the uniform helix is higher.

This might provide the basis for an explanation of the markedly different physical properties of polyisobutylene and polyvinylidene chloride.

It should be pointed out that linear polyphosphonitrilic chloride, a typical rubber which crystallizes on stretching like polyisobutylene, has

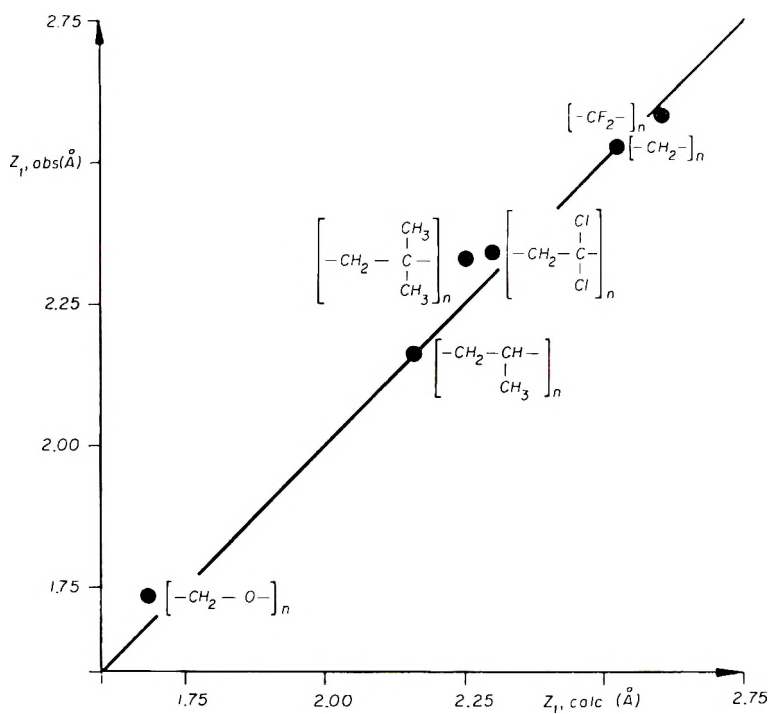


Fig. 13. Comparison of experimental and theoretically predicted values of the monomer repeat on the helical axis. For polyethylene and polytetrafluoroethylene see test.

been found to have in the crystal a helical conformation similar to that of polyvinylidene chloride, namely a nonuniform helix with $\psi_1 = 156^\circ$ and $\psi_2 = 14^\circ$.¹² The molecular flexibility of this polymer might be connected with a conformational degeneracy similar to that of polyisobutylene, if one assumes that the variation of resonance energy with angles of rotation due to π - d bonding in polyphosphonitrilic chloride is shifted with respect to that of Van der Waals interactions. Unfortunately, this hypothesis rests upon qualitative considerations because of the lack of sufficient knowledge about both energy terms.

All the calculations have been carried out for simple polymers not containing true asymmetric centers either in the backbone or in the side chain. This is the reason for the presence of the mirror plane $\psi_1 = 2\pi - \psi_2$ in the two-dimensional conformational energy plots of Figures 8-11. Such a

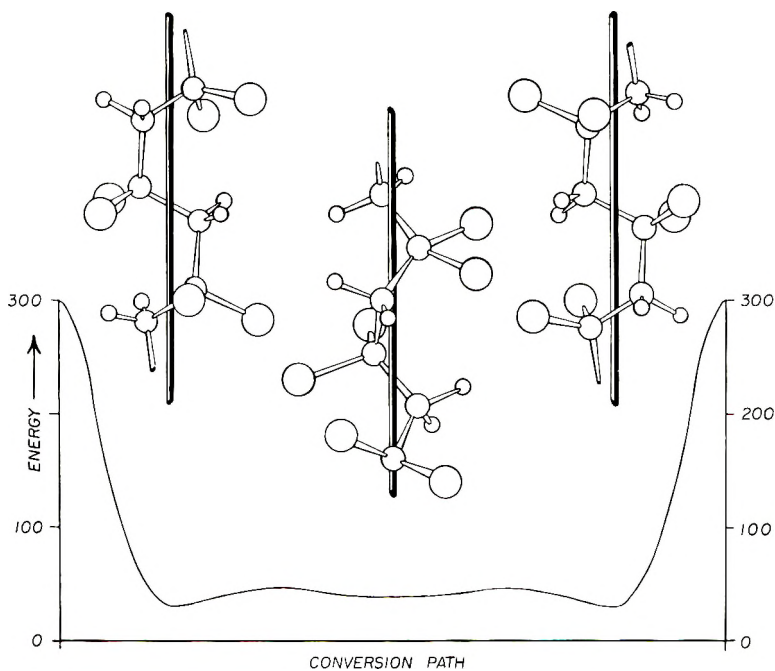


Fig. 14. Conformational energy profile of an infinite helical polyisobutylene chain. The conversion path corresponds to that indicated in the diagram of Fig. 8 by means of a broken line. The helical chains with $\psi_1 = 155^\circ$, $\psi_2 = 45^\circ$; $\psi_1 = \psi_2 = 85^\circ$ and $\psi_1 = 45^\circ$; $\psi_2 = 155^\circ$ are represented.

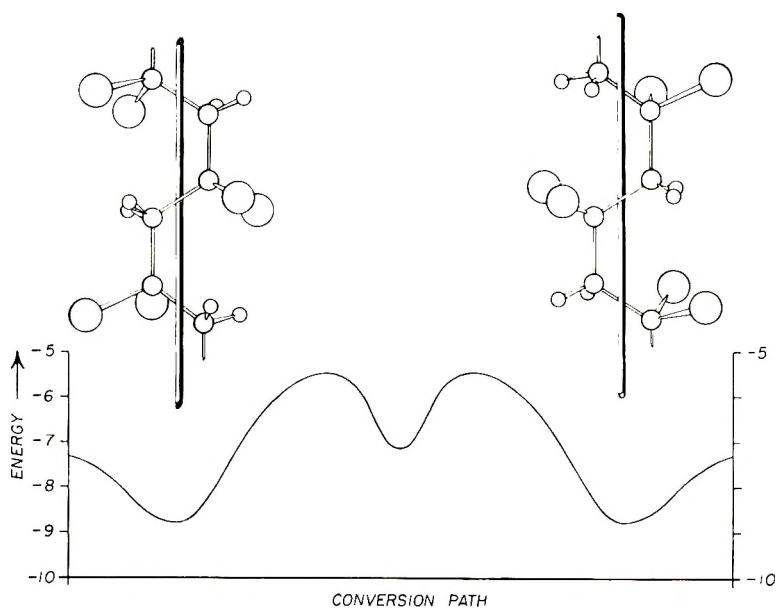


Fig. 15. Conformational energy profile of an infinite helical polyvinylidene chloride chain. The conversion path corresponds to that indicated in the diagram of Fig. 10 by means of a broken line. The helical chains with $\psi_1 = 165^\circ$, $\psi_2 = 30^\circ$, and $\psi_1 = 30^\circ$, $\psi_2 = 165^\circ$ are represented.

plane would generally disappear when the monomeric units contain asymmetric atoms, the enantiomorphous helices being no longer necessarily isoenergetic. The extent of such an energy "splitting," which controls the relative stability of helices of one hand with respect to helices of opposite hand, may be predicted to be large when the asymmetric atoms are in the skeleton. It should decrease as the asymmetric atoms are moved in a side chain far from the skeleton. It is hoped that an extension of the present study to optically active polymers may provide some useful criterion to correlate the stability of asymmetric conformations to the increase in optical rotation often observed in this interesting class of macromolecules.³²

Note added in proof: This method of calculation of the potential energy has been extended to the conformational analysis of polypeptides. The results obtained using the above reported functions to describe the interaction between pairs of nonbonded atoms in the chains and a semi-empirical function for intramolecular hydrogen bonds are in good agreement with experiments. They will be published shortly.

References

1. Natta, G., paper presented at 16th Congr. Intern. Chim., Paris; *Experientia Suppl.*, **7**, 21 (1957).
2. Liquori, A. M., *Acta Cryst.*, **8**, 345 (1955).
3. Tadokoro, H., T. Yasumoto, S. Murahashi, and I. Nitta, *J. Polymer Sci.*, **44**, 266 (1960).
4. Carazzolo, A., private communication.
5. Bunn, C. W., and E. R. Howells, *Nature*, **174**, 549 (1954).
6. Coiro, V., P. De Santis, A. M. Liquori, and A. Ripamonti, paper presented at 9th Congr. Nazl. Soc. Chim., It., Naples, 1962, to be published.
7. Liquori, A. M., *Chimica Inorganica*, IV Corso estivo di Chimica, Varenna, 1959; p. 311, *Ed. Accad. Nazl. Lincei Roma* (1961).
8. Liquori, A. M., and A. Ripamonti, *Ric. Sci.*, **29**, 2186 (1959).
9. *Strukturbericht*, **1**, 27 (1931).
10. Huggins, M. L., *J. Chem. Phys.*, **13**, 37 (1945).
11. Westrick, R., and H. MacGillivray, *Acta Cryst.*, **7**, 764 (1954).
12. Giglio, E., F. Pompa, and A. Ripamonti, *J. Polymer Sci.*, **59**, 293 (1962).
13. Corbridge, D. E. C., *Acta Cryst.*, **8**, 520 (1955).
14. Corbridge, D. E. C., *Acta Cryst.*, **9**, 308 (1956).
15. Jost, K. J., *Z. Anorg. Chem.*, **296**, 154 (1958).
16. Eyring, H., *Phys. Rev.*, **39**, 746 (1932).
17. Mason, E. A., and M. M. Kreevoy, *J. Am. Chem. Soc.*, **77**, 5808 (1955).
18. Hughes, R. E., and J. L. Lauer, *J. Chem. Phys.*, **30**, 1165 (1959).
19. Shimanouchi, T., and S. Mizushima, *J. Chem. Phys.*, **23**, 82 (1955).
20. Natta, G., and P. Corradini, *Atti Accad. Nazl. Lincei, Mem. Classe Sci. Fis. Mat. Nat.*, **4**, 73 (1955).
21. Hirschfelder, J. O., and J. W. Linnett, *J. Chem. Phys.*, **18**, 130 (1950).
22. Bartell, L. S., *J. Chem. Phys.*, **32**, 827 (1960).
23. Bunn, C. W., *Trans. Faraday Soc.*, **35**, 483 (1939).
24. Clark, E. S., and L. T. Muus, *Acta Cryst.*, **13**, 1104 (1960).
25. Fuller, C. S., C. J. Forsch, and N. R. Pape, *J. Am. Chem. Soc.*, **64**, 154 (1942).
26. Natta, G., P. Corradini, and I. W. Bassi, *Atti Accad. Nazl. Lincei, Rend. Classe Sci. Fis. Nat.*, **19**, 404 (1955).
27. Reinhardt, R. C., *Ind. Anal. Chem.*, **35**, 422 (1943).
28. Natta, G., P. Corradini, and P. Ganis, *Makromol. Chem.*, **39**, 238 (1960).
29. Volkenstein, M. V., *J. Polymer Sci.*, **29**, 441 (1958).

30. Hoeve, C. A. J., *J. Chem. Phys.*, **32**, 888 (1960).
31. Lifson, S., *J. Chem. Phys.*, **30**, 964 (1959).
32. Pino, P., and G. P. Lorenzi, *J. Am. Chem. Soc.*, **82**, 4745 (1960).

Résumé

On a calculé l'énergie potentielle du polyéthylène, du polytétrafluoroéthylène, du polyoxyméthylène, du chlorure de polyvinylidène et du polypropylène isotactique à conformation hélicoïdale, comme une fonction des angles de rotation autour des liaisons de la chaîne principale. L'emploi de fonctions appropriées pour décrire l'interaction entre les atomes non-liés dans les chaînes, a permis de prévoir avec une précision surprenante la conformation la plus stable pour chaque polymère considéré, malgré les grossières approximations de calcul. On discute les traits les plus caractéristiques des diagrammes d'énergie potentielle en relation avec la possibilité de prévoir les conformations hélicoïdales permises pour les chaînes polymériques isolées nonperturbées qui sont considérées.

Zusammenfassung

Die potentielle Energie von Polyäthylen, Polytetrafluoräthylen, Polyoxymethylen, Polyisobutylen, Polyvinylidenchlorid und isotaktischem Polypropylen mit Helixkonformation wurde als Funktion des Rotationswinkels um die Hauptkettenbindungen berechnet. Die Verwendung geeigneter Funktionen für die Wechselwirkung zwischen nichtgebundenen Atomen in den Ketten erlaubte für jedes der untersuchten Polymeren, ungeachtet der bei der Berechnung eingeführten recht drastischen Annahmen, eine überraschend genaue Angabe der stabilsten Konformation. Die hervorstechendsten Merkmale der Potentielle-Energie-Diagramme werden auch in Hinblick auf die Möglichkeit einer Vorhersage der erlaubten Helixkonformationen für die isolierten, ungestörten Polymerketten diskutiert.

Received February 21, 1962

Molecular Orbital Theory of Reactivity in Radical Polymerization. Part III*

K. HAYASHI, T. YONEZAWA, S. OKAMURA, and K. FUKUI,
Faculty of Engineering, Kyoto University, Kyoto, Japan

Synopsis

The chemical reactivity in diene type polymerization and degradative chain transfer is discussed by the theory previously proposed by the present authors. In addition to this, a molecular orbital procedure to calculate Q and e values is presented. Further, the stabilization energy and the reactivity ratios in various copolymerizations are calculated. The results coincide with experiment satisfactorily.

Introduction

It has been shown in our previous papers,^{1,2} that the chemical reactivity in radical polymerization can be discussed in terms of the magnitude of stabilization energy due to π conjugation between a monomer and a radical in the transition state. Several problems in the process of radical polymerization such as initiation, termination, and propagation have been successfully interpreted by our procedure.

In the present paper the validity of our theory is further tested by the treatment of diene-type polymerization and degradative chain transfer. In addition to these extensions, a molecular orbital investigation is made on the Q - e scheme which was proposed by Price and Alfrey³ to obtain the relative rates in radical copolymerization. It can be shown by the present investigation that Q , e values obtained by quantum mechanics coincide with those assigned empirically by Price and are useful in calculation of the copolymerization rates.

Further, the stabilization energy obtained by the perturbation theory, expressed in units of kilocalories/mole, and reactivity ratios in various copolymerizations are calculated.

The molecular orbital parameters adopted in the present calculation are the same as those in our previous papers.

Diene-Type Polymerization

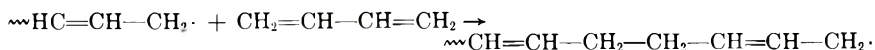
It is well known that diene-type monomers such as butadiene, isoprene, and chloroprene, have two conjugated double bonds; hence a branching reaction can occur to the remaining double bond in a polymer chain.

* Presented at the 7th Annual Meeting of the Chemical Society of Japan, Tokyo, April 1954.

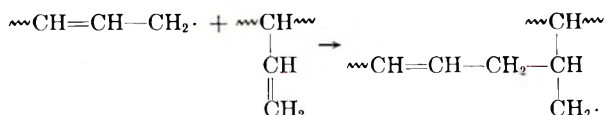
In general, the reactivity in the branching reaction is found to be very small in comparison with that in the normal propagation. The activation energy of the former is larger by 7.1 kcal./mole than that of the latter.⁴

In the case of butadiene, the propagation, the branching initiation, and the branching propagation occur as follows:

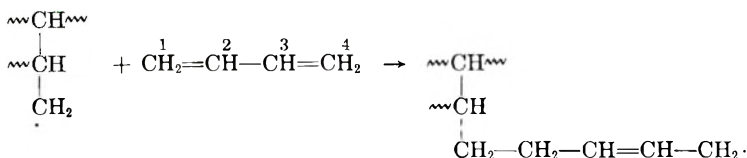
Propagation



Branching initiation:



Branching propagation

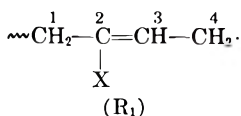
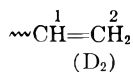
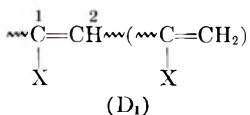
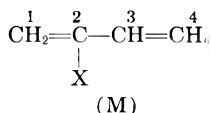


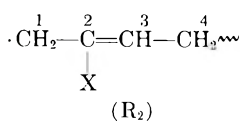
The stabilization energies in these reactions are obtained in units of $-(\Delta\beta)^2/\beta$ as: propagation 0.8944; branching initiation 0.7071; branching propagation 1.3416.

The results show that the possibility of initiation of the branching reaction is less than that for the normal propagation, but once it starts, the branching propagation follows much more easily.

Since isoprene and chloroprene have a methyl group or a chlorine atom, respectively, at position 2, the reactions above become much more complex.

In the present treatment, calculations are made on the normal propagation of isoprene and chloroprene and the branching initiation of isoprene. The monomer, residual double bonds in a polymer, and two kinds of adduct radicals involved in these reactions are as follows:





The letters in the parentheses are the abbreviations representing the monomer, the double bond, and the radical.

The results of the calculations are listed in Tables I and II. The cases which do not appear in these tables are left out of account since they only very rarely take place.

TABLE I
Several Types of Propagation of Isoprene and Chloroprene and Their Reactivities

Type of propagation	Attacking radical	Position of attack		Stabilization energy, kcal./mole	
		Monomer	Radical	Isoprene	Chloroprene
1,4	R ₁	1	4	0.8843	0.9020
1,2	R ₁	1	2	0.8582	0.8477
4,1	R ₂	4	1	0.8939	0.9025
4,3	R ₂	4	3	0.8939	0.8939

TABLE II
Reactivity in Branching Initiation of Isoprene

Double bond	Attacking radical	Position of Attack		Stabilization energy $-(\Delta\beta)^2/\beta$, kcal./mole
		Monomer	Radical	
B ₁	R ₁	2	4	0.7256
B ₁	R ₁	2	2	0.7046
B ₁	R ₂	2	3	0.7128
B ₂	R ₁	1	4	0.7540
B ₂	R ₁	1	2	0.6363
B ₂	R ₂	1	3	0.7081

The results listed in Table I indicate that the reactivity of two monomers in four types of propagation decreases in the order:

$$4,1 \sim 4,3 > 1,4 > 1,2$$

The identical reactivity of the positions 1 and 3 in radical R₂ may be ascribed to uncertainty of the steric circumstances and inductive effect of the polymer chain. Taking these effects into consideration, the 4,1 type of propagation would be expected to proceed more easily than 4,3. It has been demonstrated by experimental data of infrared spectra that in polyisoprene, 89% of the units are composed of 4,1 and 1,4 type, 6% of 3,4 type and 5% of 4,3 type; in polychloroprene, 95.9% originates from 4,1 and 1,4, and 2% from 4,3.^{5,6} These experimental results agree with the present results.

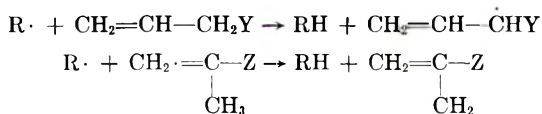
The magnitude of stabilization energies in Table II shows that the branching reaction in isoprene will take place less easily than the propagation as in the case of butadiene.

Degradative Chain Transfer

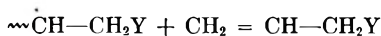
Degradative chain transfer is believed to occur in the radical polymerization of some specific monomers in which the atoms to be replaced easily by a radical are located on a carbon atom α to the ethylenic double bond and the double bond itself is not conjugated.

Monomers such as allyl acetate,⁷ allyl halides, and some α -methyl type monomers⁸ belong to this species.

In the course of polymerization of these monomers, a new radical having no ability to initiate the propagation is produced in the following way:



Hence the occurrence or nonoccurrence of the degradative chain transfer may be theoretically checked if one compares the reactivity of an adduct radical with the radicals produced from a monomer in propagation:



or in chain transfer:



TABLE III
Degradative Chain Transfer to Some Monomers

Monomer ^a	$(\Delta E)_{rs}$, kcal./mole		Possibility of degradative chain transfer
	Propagation	Chain transfer	
$\text{CH}_2 = \text{CH}-\text{CH}_2\text{X}^b$	1.0000	0.7071	+
$\text{CH}_2 = \text{CH}-\text{CH}_2-\text{CH} = \text{CH}_2^b$	1.0000	0.6443	?
$\text{CH}_2 = \text{CH}-\text{CH}_2\text{Cl}^b$	1.0000	0.6942	+
$\begin{array}{c} \text{CH}_3 \\ \\ \text{CH}_2 = \text{C}-\text{X} \end{array}$	0.9603	0.7541	+
$\begin{array}{c} \text{CH}_3 \\ \\ \text{CH}_2 = \text{C}-\text{CH} = \text{CH}_2 \end{array}$	0.8843	0.9574	-
$\begin{array}{c} \text{CH}_3 \\ \\ \text{CH}_2 = \text{C}-\text{C}\equiv\text{N} \end{array}$	0.8484	1.0860	-

^a X denotes the substituent which does not enter into conjugation.

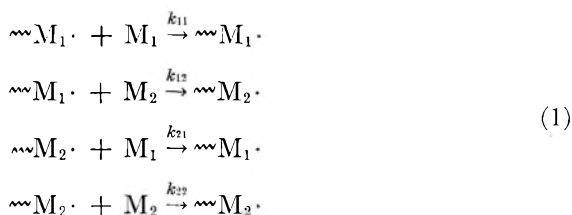
^b These monomers are treated as if they are ethylene for simplicity.

If the stabilization energy $(\Delta E)_{rs}$ of the former is larger than that of the latter, we can conclude that the degradative chain transfer takes place. The results of calculation are cited in Table III where plus and minus signs denote the experimental evidence whether the degradative chain transfer takes place or not. It is found that the degradative chain transfer occurs in these monomers in accordance with experiments, in except isoprene and methacrylonitrile (listed for comparison).

Molecular Orbital Analysis of $Q-e$ Scheme

Alfrey and Price³ have proposed an empirical formula that gives the values of r in copolymerization in terms of the specific reactivity of a monomer, Q , and its polar factor, e .

The propagation step in radical copolymerization consists of the following four elementary reactions:



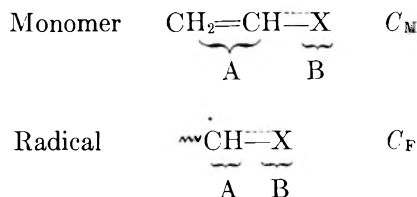
In these equations M_1 and M_2 denote the two kinds of monomers in copolymerization. According to the $Q-e$ scheme, the corresponding reactivity ratios are,

$$\begin{aligned}
 r_1 &\equiv k_{11}/k_{12} = (Q_1/Q_2) e^{-e_1(e_1-e_2)} \\
 r_2 &\equiv k_{22}/k_{21} = (Q_2/Q_1) e^{-e_2(e_2-e_1)}
 \end{aligned} \tag{2}$$

The theoretical basis of this scheme has been studied by Evans⁹ and co-workers. The specific reactivity Q of a monomer is thus given by eq. (3):

$$Q = \exp \{k[(C_F - C_M)/RT]\} \tag{3}$$

where T is the absolute temperature of the system, R is the gas constant, and C_F and C_M represent the stabilization energies when the conjugation across the single bond takes place between π electrons localized in the two parts A and B in a monomer and a radical:



The molecular orbital calculations of these energies were carried out. The values thus obtained, are given in units of $-\beta$ and are summarized in Table IV. For $k = 0.4$, $T = 333^\circ\text{K}$., and $\beta = -20$ kcal./mole in eq. (3),

TABLE IV
 Conjugation Energies of Monomers and Adduct Radicals

Monomer	Conjugation energies, $-\beta$	
	C_M	C_F^a
Styrene	0.4244	0.7208
Butadiene	0.4720	0.8284
Acrylonitrile	0.5228	0.8128
Isoprene	0.7100	1.1084
Methacrylonitrile	0.7490	1.1749
Chloroprene	0.7714	1.1652
Vinyl chloride	0.3101	0.6569
1,2-Dichloroethylene	1.0362	0.6569
Vinylidene chloride	0.5595	0.6825
Trichloroethylene	1.5346	0.6825
Vinylidene cyanide	0.9938	1.3823
Fumaronitrile	0.9922	0.8128
Propylene	0.2570	0.3028

^a This value is identical with the localization energy of the radical.

 TABLE V
 Calculated Q Values

Monomer	Calculated		Experimental Q
	Q	Q^a	
Styrene	80.811	1.00	1.00
Vinyl chloride	4.418	0.057	0.024
Butadiene	71.96	0.92	1.33-0.8
Acrylonitrile	32.59	0.417	0.44
1,2-Dichloroethylene	0.00105	1.346×10^{-4}	—
Vinylidene chloride	7.585	0.097	0.2
Trichloroethylene	0.024	3.115×10^{-4}	—
1,2-Dicyanoethylene	0.116	1.485×10^{-3}	—
Vinylidene cyanide	106.24	1.36	—
Isoprene	119.67	1.53	—
Chloroprene	209.94	2.69	1.7

^a Relative value to styrene.

the Q values theoretically calculated are given in Table V, together with the values assigned by Price for the sake of comparison.

The formula to express e value has been given by Alfrey and Price⁴ as

$$e = q' / \sqrt{rDkT} \quad (4)$$

where r is the distance of separation in the activated complex, D is the effective dielectric constant, and q' is related to the formal charge at the carbon atoms to be attacked in a monomer or a radical.

Inserting the appropriate values in this equation ($r = 2.4-2.5$ A., $T = 333^\circ$ K., $D = 10-20 \times 4.77 \times 10^{-10}$ e.s.u.), we obtain a simplified formula

$$q' = 3q \quad (5)$$

TABLE VI
 Calculated e Values for Monomers

Monomer	Calculated		Empirical e
	e	e'^a	
Styrene	0	-0.80	-0.80
Butadiene	0	-0.80	-0.80
Vinyl chloride	+0.584	+0.30	+0.2
Acrylonitrile	+0.689	+0.50	+1.2
Methacrylonitrile	+0.947	+0.99	+0.7
1,2-Dichloroethylene	+1.192	+1.45	—
Vinylidene cyanide	+0.742	+0.60	+0.60
Trichloroethylene	+1.177	+1.42	—
Isoprene	+0.235	-0.36	—
Chloroprene	+0.248	-0.33	-0.2

^a Relative value obtained from the equation: $e'_{\text{calc.}} = 1.88e_{\text{calc.}} - 0.80$.

 TABLE VII
 Calculated e Values for Radicals

Radical	Calculated	
	e	e'^a
Styrene	0	-0.8
Butadiene	0	-0.8
Acrylonitrile	+0.725	+0.57
Vinyl chloride	+0.944	+0.98
Vinylidene chloride	+1.180	+1.43
Methacrylonitrile	+1.503	+2.04
Isoprene	+0.179	+0.93
Chloroprene	+0.666	+0.46

^a Relative value obtained from the equation: $e'_{\text{calc.}} = 1.88e_{\text{calc.}} - 0.80$.

 TABLE VIII
 Molecular Orbital Calculation of Reactivity Ratios r

Monomer 1	Monomer 2	r	r			
			From $Q-e$ (Price)	From $Q-e$ (calc.) ^a	From $Q-e$ (calc.) ^b	Ob- served
Styrene	Vinyl chloride	r_1	20.2	7.2	7.2	17
Styrene	Vinyl chloride	r_2	0.02	0.04	0.02	0.02
Styrene	Vinylidene chloride	r_1	1.63	3.31	3.31	1.85
Styrene	Vinylidene chloride	r_2	0.086	0.040	0.011	0.085
Styrene	Chloroprene	r_1	0.368	0.252	0.252	0.05
Styrene	Chloroprene	r_2	1.89	3.12	2.32	7

^a e of a radical is not distinguished from e of a monomer.

^b e of a radical is distinguished from e of a monomer.

TABLE IX
 Calculated Reactivity Ratio

Radical	Monomer	$(\Delta E)_{\text{TS}}$, $-(\Delta\beta)^2/\beta$	Difference of $(\Delta E)_{\text{TS}}$, $-(\Delta\beta)^2/\beta$	r	
				calc.	Obs.
Butadiene	Butadiene	0.8944	+0.2030	0.477	0.35
	Acrylonitrile	1.0974			
Acrylonitrile	Acrylonitrile	0.8169	+0.7307	0.074	0.04
	Styrene	1.5476			
Acrylonitrile	Acrylonitrile	0.8169	+0.8046	0.054	0
	Butadiene	1.6215			
Styrene	Styrene	0.9323	+0.0248	0.915	0.78
	Butadiene	0.9571			
Styrene	Styrene	0.9323	+0.2481	0.408	0.41
	Acrylonitrile	1.1804			
Vinyl chloride	Vinyl chloride	0.9358	+0.2360	0.427	0.02
	Acrylonitrile	1.1718			

Butadiene	Propagation	0.8944	-0.1873	1.98	prop. >
Butadiene	Branching	0.7071			branching
Butadiene	Propagation ^a	0.8944	+0.4472	0.197	—
Butadiene	Branching ^a	1.3416			
Maleic anhydride	Maleic anhydride	0.8267	+2.1672	3.7×10^{-4}	0
Maleic anhydride	Styrene	3.0939			
Vinyl chloride	Vinyl chloride	0.9358	+0.5921	0.108	0.29
Vinyl chloride	Maleic anhydride	1.5279			
Maleic anhydride	Maleic anhydride	0.8267	+1.7459	1.71×10^{-3}	0
Maleic anhydride	Vinyl chloride	2.5716			
Butadiene	Termination	2.1518	-1.2574	98	term. \gg prop.
Butadiene	Propagation	0.8944			
Styrene	Termination	3.2786	-2.3463	5.15×10^3	term. \gg prop.
Styrene	Propagation	0.9323			

^a Propagation: branching = 1.98:1.

Then it is assumed that the formal charge is expressed in terms of the total π -electron density q_r at the position of attack in a monomer or a radical as is shown in eq. (6):

$$q' = q_r^{-N/n} \quad (6)$$

where N is the number of total π electrons and n is the number of atoms in the conjugated system. The calculated results are summarized in Tables VI and VII. It may be stressed that the different polar factors for the monomer and the radical derived from it are obtained by the present treatment.

The composition of reactivity ratios r on some monomer pairs are calculated in two different ways from the molecular orbital $Q-e$ values. The same polar factor is adopted in both the monomer and the radical in the first attempt, and, in the second trial, e of the radical is distinguished from that of the monomer. The agreement with experiments observed in Table VIII seems satisfactory. So far as the extent of agreement is concerned, no marked improvement is obtained by adopting the distinguished polar factor for an adduct radical in the $Q-e$ scheme.

The correlation of calculated Q and e values with monomer structure is shown in Figure 1, where the Q values are plotted along the abscissa and the e values along the ordinate. Both calculated and experimental Q and e values are plotted for vinyl chloride, vinylidene chloride, butadiene, and chloroprene. We can observe in the figure that a similar trend of shifts takes place when the hydrogen atom is replaced by the chlorine atom in these monomers.

Hence it may be pointed out as a conclusion that the agreement of the Q and e values calculated theoretically with Price's values is good, and a molecular orbital calculation makes it possible to estimate even the Q

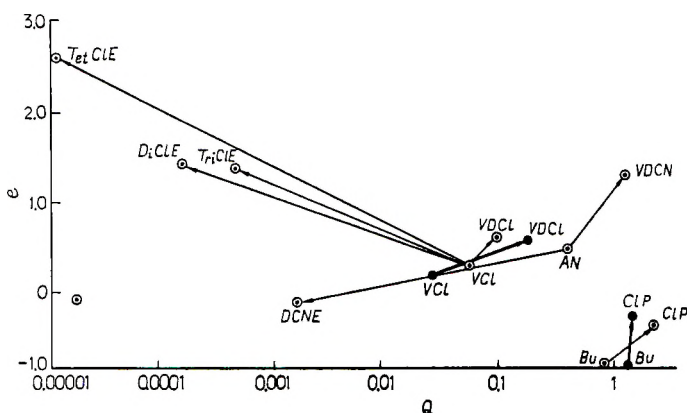


Fig. 1. Influence of substituents in $Q-e$ diagram: (—) calculated and (---) Price's values for butadiene (Bu), chloroprene (ClP), acrylonitrile (AN), vinylidene cyanide (VDCN), dicyanoethylene (DCNE), vinyl chloride (VCL), vinylidene chloride (VDCI), dichloroethylene (DiCIE), trichloroethylene (TriCIE), and tetrachloroethylene (TetCIE).

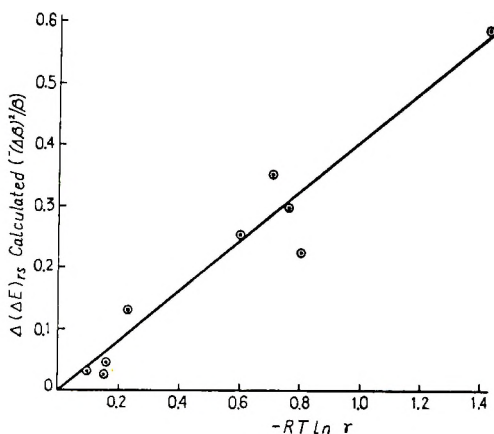


Fig. 2. Reactivity ratio and $(\Delta E)_{rs}$ of copolymerization.

values of tetrachloroethylene and dichloroethylene which are too small to determine experimentally.

Theoretical Calculation of the Reactivity Ratios

In the previous paper,² we derived the equation to combine the reactivity ratio with the difference of the stabilization energies:

$$-RT \ln r = (\Delta E)_{rs^2} - (\Delta E)_{rs^1}$$

where $(\Delta E)_{rs^1}$, $(\Delta E)_{rs^2}$ are stabilization energies represented in units of $-(\Delta\beta)^2/\beta$ in the reactions of two monomers M_1 and M_2 with their polymer radicals, respectively.

This difference is plotted against experimental values of $(-RT \ln r)$ in Figure 2. From the slope of the line in the figure, the magnitude of $-(\Delta\beta)^2/\beta$ is estimated as 2.44 kcal./mole, which yields a value for $\Delta\beta$ of ca. 7 kcal./mole, i.e., ca. $1/3 (-\beta)$.

For this value of $-(\Delta\beta)^2/\beta$, the reactivity ratios in copolymerization are calculated directly by the molecular orbital theory, and Table IX shows the results which agree well with experimental values.

References

1. Yonezawa, S., K. Hayashi, C. Nagata, S. Okamura, and K. Fukui, *J. Polymer Sci.*, **14**, 312 (1954).
2. Hayashi, K., T. Yonezawa, C. Nagata, S. Okamura, and K. Fukui, *J. Polymer Sci.*, **20**, 537 (1956).
3. Alfrey, T., Jr., and C. C. Price, *J. Polymer Sci.*, **2**, 101 (1947).
4. Morton, M., and P. P. Salatiello, *J. Polymer Sci.*, **6**, 225 (1951).
5. Richardson, W. S., and A. Sacher, *J. Polymer Sci.*, **10**, 353 (1953).
6. Richardson, W. S., *J. Polymer Sci.*, **13**, 229 (1954).
7. Bartlett, P. D., and R. Althul, *J. Am. Chem. Soc.*, **67**, 816 (1945).
8. Hart, R., and G. Smets, *J. Polymer Sci.*, **5**, 55 (1950).
9. Evans, M. G., J. Gergely, and E. C. Seaman, *J. Polymer Sci.*, **3**, 866 (1948).

Résumé

On discute de la réactivité chimique dans la polymérisation de type diénique et le transfert de chaîne dégradant sur la base de la théorie proposée précédemment par les auteurs de cet article. De plus, on propose une méthode d'orbitale moléculaire pour calculer les valeurs Q et e . On calcule, ensuite l'énergie de stabilisation et les rapports de réactivité dans diverses copolymérisations. Les résultats concordent de façon satisfaisante avec l'expérience.

Zusammenfassung

Die chemische Reaktivität bei der Dienpolymerisation und die verzögernde Kettenübertragung werden anhand der früher von den Autoren angegebenen Theorie diskutiert. Ausserdem wird ein Molekülorbital Verfahren zur Berechnung von Q - und e -Werten entwickelt. Die Stabilisierungsenergie wird berechnet und die Reaktivitätsverhältnisse bei verschiedenen Copolymerisationen ermittelt. Die Ergebnisse stimmen gut mit den experimentellen Werten überein.

Received March 8, 1962

Molecular Interpretation of Glass Temperature Depression by Plasticizers

EDMUND A. DIMARZIO,* *American Viscose Corporation, Research and Development Division, Marcus Hook, Pennsylvania, and*
JULIAN H. GIBBS, *Department of Chemistry, Brown University, Providence, Rhode Island*

Synopsis

The view that the glass transition is basically thermodynamic in nature is used to derive an expression for glass temperature depression by plasticizers. The second-order transition temperature is given as that temperature at which the configurational entropy first becomes zero as we cool the polymer-diluent system. The concentration of plasticizer, size of the plasticizing molecule, and its flexibility are found to be the main determinants of glass temperature depression. Available experimental data confirm the predictions of the theory, and it is thereby concluded that the thermodynamic view is sufficient to explain glass temperature depression. It is pointed out that data exist which contradict the free volume theory, as applied to glass temperature depression.

I. INTRODUCTION

In this paper an expression will be derived for the variation of the glass temperature of a plasticized high polymer as a function of its plasticizer content. It will be shown that, in conformity to experimental results, the size and stiffness of the plasticizing molecules, as well as the actual amount of plasticizer, affect the glass temperature.

There are two important reasons for investigating glass temperature depression by plasticizers, one a practical reason, the other concerned with theory.

In the first place, the glass temperature is a useful quantity. Thus, for example, knowledge of the glass temperature of any amorphous polymer implies, by virtue of the Williams-Landel-Ferry relation,¹ knowledge of variation of viscosity with temperature. In addition many properties of a particular polymer can sometimes be correlated with glass temperature depression due to plasticization. The work of Lel'chuck and Sedlis² is an example. These authors were able to relate such seemingly unrelated quantities as elastic modulus, electrical resistance, permeability to moisture, and limiting strength to glass temperature depression in polyvinyl chloride plasticized by various materials.

The second reason for investigating plasticization phenomena is that

* Present address: Bell Telephone Laboratories, Murray Hill, New Jersey.

they provide additional experimental tests of the theory³⁻⁵ of the glass transition on which the present derivation will be based and also of alternative views on the glass transition.

The theory utilized in the present derivation is that which relates the glass transition to an underlying second-order transition which would be present in the supercooled amorphous phase even if the latter were allowed to come to internal (metastable with respect to the crystal) equilibrium. The equilibrium second-order transition temperature, T_2 , is the lower limit, reached in experiments of infinite time scale, to the range of values obtainable for the glass-transition temperature T_g . This equilibrium second-order transition temperature T_2 is the temperature at which the configurational entropy first becomes zero as the polymer is cooled. That such a temperature, unequal to absolute zero, exists is indicated both by extrapolation of experimental thermodynamic data through and below T_g ⁶ and by the statistical mechanical theory in question. The existence of values of T_g lying above T_2 by amounts dependent on experimental time scales is attributed, by the theory, to the increase in relaxation times attendant upon the decrease in the number of configurations available to the system as the system is cooled toward T_2 , where the number is of order unity

TABLE I
Plasticizing Efficiency of Various Plasticizers in PMMA and PS

Plasticizer	Molar volume	$-(dT_g/dv)_0$		Sites per molecule		Number of flexible bonds per molecule
		PS	PMMA	PS	PMMA	
CS ₂	60.28	674.	—	1.2	2.8	0
CH ₂ Cl ₂	63.57	483.	—	1.3	3.0	0
Acetone	73.33	—	353.	1.5	3.4	0
CHCl ₃	79.69	485.	214.	1.6	3.7	0
Methyl acetate	79.89	512.	417.	1.6	3.7	1
C ₆ H ₆	88.8	351.	248.	1.8	4.2	0
Butyl alcohol	91.60	—	265.	1.9	4.3	2-3
CCl ₄	96.45	426.	—	1.95	4.5	0
Ethyl acetate	97.78	497.	374.	2.0	4.6	2
C ₆ H ₅ NO ₂	102.8	386.	294.	2.1	4.8	0
C ₆ H ₅ CH ₃	106.3	346.	235.	2.2	5.0	0
Propyl acetate	115.1	—	369.	2.3	5.4	3
Methyl salicylate	128.5	395.	—	2.6	6.0	2-3
n-Butyl acetate	131.7	378.	366.	2.7	6.2	4
Phenyl salicylate	171.4	333.	—	3.5	8.1	2-4
β-Naphthyl salicylate	214.	257.	—	4.3	10.	2-4
Tricresyl phosphate	311.	316.	—	6.3	14.6	3-6

($S = 0$). The reader is referred to the earlier papers of this series for a detailed discussion of the quantitative equilibrium theory,^{4,5} its conformity with experimental results other than those discussed here,^{4,7} and the qualitative interpretation it provides for the concomitant rate effects.⁴ He is also referred to one of these⁴ for the meaning and the justification of comparing theoretically predicted variations in T_2 (attendant upon variations in the amount and type of plasticizer in this case), with the corresponding experimentally observed variations in T_g (but see below also).

Now an alternative interpretation, which is based exclusively on free volume considerations, of the depression of the glass transition on plasticization has recently appeared.⁸ It should be pointed out that data exist which are contrary to this interpretation. According to eq. (10) of the paper by Kelley and Bueche,⁸ two polymers which have the same glass temperature in their undiluted states will have their glass temperatures depressed identical amounts by identical quantities of the same plasticizer. Jenckel and Heusch⁹ have measured glass temperature depression by plasticizers for both polystyrene (PS) and polymethyl methacrylate (PMMA) which have nearly the same glass temperature (100°C.). It was found that a particular plasticizer was always (for the 7 plasticizers tested in Table I) less effective in plasticizing PMMA than it was in plasticizing PS.

As will be shown, the statistical mechanical theory correctly predicts that a plasticizer should be less effective in plasticizing PMMA than in plasticizing PS.

II. DERIVATION OF THE RELATION

We seek an expression for the entropy of a homogeneous mixture of long chain polymers of degree of polymerization r_A with short chain polymers of degree of polymerization r_B . With the use of the quasilattice model an expression is readily obtained; accordingly our discussion will be given in the context of this model.

The configurational entropy S is the important quantity determining the second-order transition temperature; energetics are important only to the extent that they affect the configurational entropy. Now intermolecular attractions between polymer segments affect the entropy in two separate but related ways. In the first place, an infinitely large attraction between segments would imply that no empty lattice sites⁴ exist in the polymer and that, therefore, there is no entropy contribution due to possibilities of permutation of holes and polymer segments. In a real polymer, intermolecular attractions are finite, and consequently an entropy contribution due to the introduction of holes exists. The extent to which this affects the curves for glass temperature as a function of plasticizer content has been displayed in Figure 6 of a previous paper⁴ for the case of polystyrene plasticized by styrene and is reproduced in Figure 2 of this paper. One sees that the effects of holes are minor and predictable in terms of the curves

which do not include this effect. For this reason, we will simplify our work by assuming no holes in our lattice calculation. In the second place, the statistics for athermal mixtures are different from those for mixtures which are not athermal.¹⁰ However, the difference, in the context of this problem is slight, and it does not seem worthwhile to introduce an extra parameter for a correction which is small. Thus, we will use the zeroth approximation,¹⁰ according to which there is a completely random arrangement of the molecules.

The number of ways to pack a binary mixture of molecules A and B is given as eq. 10.10.5 of reference 10. From this equation, we obtain after some labor the expression of eq. (1) for the configurational entropy:

$$\begin{aligned} \frac{S}{k r_A N_A} = & \frac{(z-2)}{2(1-v)} \ln \left[\frac{(z-2)r_B + 2v}{z r_B} \right] \\ & + \frac{v}{r_B(1-v)} \ln \left[\left(\frac{[z-2]r_B + 2v}{z v} \right)^{\frac{z_1 z_2}{2}} \right] \\ & + \frac{v(r_B - 3)}{r_B(1-v)} (\ln [1 + (z-2) \exp \{-\Delta\epsilon_B/kT\}] + f_B \Delta\epsilon_B/kT) \\ & + \ln [1 + (z-2) \exp \{-\Delta\epsilon_A/kT\}] + f_A \Delta\epsilon_A/kT \quad (1) \end{aligned}$$

where

$$f_i = \frac{(z-2) \exp \{-\Delta\epsilon_i/kT\}}{1 + (z-2) \exp \{-\Delta\epsilon_i/kT\}} \quad i = A, B$$

The various quantities used in the above equation are defined as follows. N_A and N_B are the total numbers of A type molecules and B type molecules, respectively; k is, of course, Boltzmann's constant, and T is the temperature in degrees Kelvin; the volume fraction of plasticizer v is defined by

$$v = r_B N_B / (r_A N_A + r_B N_B) \quad (2)$$

r_A and r_B are really the number of lattice site occupiers per molecule. This means that when application to a real system is made, r_A and r_B become multiples of the degrees of polymerization, the multipliers being the number of site occupiers per monomer unit.

The degree of polymerization r_A of the high polymer component has been set equal to infinity in eq. (1). It is both a prediction of the theory and a result of experiment that glass temperatures are independent of molecular weight, providing the degree of polymerization is sufficiently high.⁴

Actually, eq. (1), which is a modification of Guggenheim's equation, is correct for all r_B including r_B equal to 1 and 2. For this reason z_1 and z_2 are defined as follows. z_1 is the number of sites available to the second segment of the molecule after the first segment has been located on the lattice. Thus z_1 is equal to the coordination number of the lattice z when r_B is greater than or equal to 2, but it is equal to 1 if r_B equals 1. z_2 is the

number of sites available to the third segment of the molecule after the first and second segments have been located on the lattice. Thus, z_2 is equal to $z - 1$ if r_B is greater than or equal to 3, but it is equal to 1 if r_B is equal to 1 or 2.

The last two terms of eq. (1) represent contributions to the entropy arising from the multitude of energy-dependent conformations available to a molecule once its posture in space has been determined by location of the first three segments.^{4,11} The terms are energy-dependent because we have assumed that each segment can occupy $z - 1$ positions relative to the coordinate system formed by the previous three segments of the chain and that one of these is favored by an energy $\Delta\epsilon$ ($\Delta\epsilon_A$ for the A type molecule and $\Delta\epsilon_B$ for the B type molecule). This assumption has proved successful when a tetrahedral lattice with a coordination number of 4 is used.⁴ In this paper, we will assume the tetrahedral lattice. Inspection of the last term of eq. (1) shows that if $\Delta\epsilon_A$ were equal to zero, we would have a contribution of $\ln 3$ per segment, while if $\Delta\epsilon_A$ were equal to infinity,

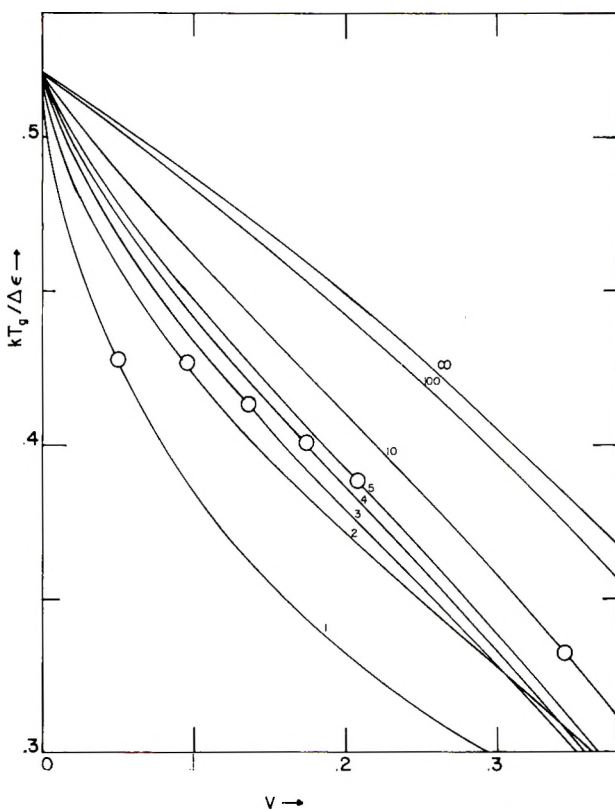


Fig. 1. Predicted glass temperature of a linear high polymer as a function of the volume fraction of plasticizer for perfectly flexible linear plasticizing molecules. The number labeling each curve is the number of sites on the lattice that the plasticizer molecule occupies: (O) points correspond to a mole fraction of 0.05.

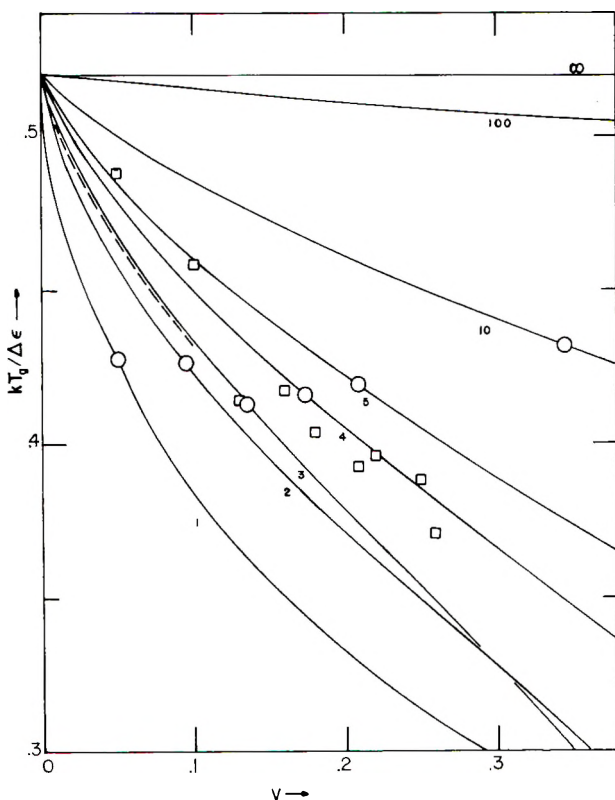


Fig. 2. Glass temperature vs. volume fraction of plasticizer for the case of plasticizing molecules with a stiffness energy equal to that of the high polymer: (O) as for Fig. 1; (□) data points of Kelley and Bueche⁸ for polystyrene plasticized by diethylbenzene; (---) both a best-fit curve to the data of Alexandrov and Lazurkin¹² for polystyrene plasticized by styrene (assumed to occupy two sites on the lattice) and the predicted curve of the theory when volume variations are allowed.

we would have a contribution of zero per segment. This result is what one would expect. f_i is the fraction of segments belonging to the i type molecules which are in the ($z - 2 = 2$) high energy wells.

In accordance with the prescription of the theory, the second-order transition temperature is obtained by setting the entropy equal to zero. This gives an equation for the second-order transition temperature in terms of the variables r_B , v , $\Delta\epsilon_A$, and $\Delta\epsilon_B$.

Strictly speaking, then, $\Delta\epsilon_A$ should be determined from this equation ($S = 0$) applied to the case of the pure homopolymer ($v = 0$) with the second-order transition temperature of the pure homopolymer substituted for T in the expression (1) for the entropy, which is now equated to zero. However, the true value for the second-order transition temperature is unknown. What is known is the value of the glass transition temperature measured in experiments of the usual time-scales of the order of minutes to hours. The easiest procedure, then, for comparing theoretically pre-

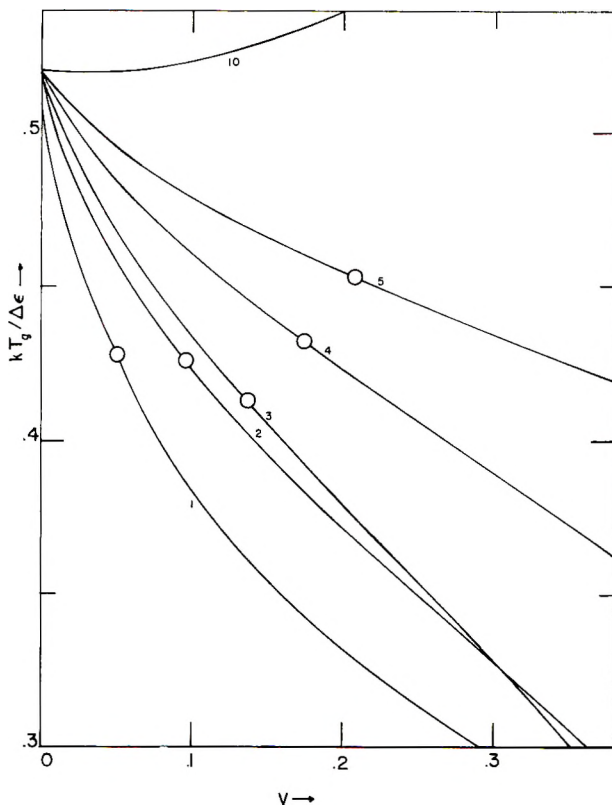


Fig. 3. Glass temperature vs. volume fraction for perfectly stiff plasticizing molecules: (O) as for Fig. 1.

dicted variations in T_2 with experimentally observed variations in T_g is to use the glass transition temperature T_0 of the pure homopolymer in this equation for $\Delta\epsilon_A$. Equation (1), equated to zero and applied to the more general case where $v \neq 0$, will, with a value of $\Delta\epsilon_A$ thus determined substituted into it, then become an equation for T_g rather than T_2 . What we are doing here is to superimpose, for comparison purposes, the theoretical curve for T_2 as a function of v onto the experimental curve for T_g as a function of v , the superposition being chosen such that the two curves coincide at $v = 0$ (pure homopolymer). We are only concerned with the slopes and shapes of the curves, and not with their absolute magnitudes (since $\Delta\epsilon_A$ is not known independently of our procedure for fixing it). Therefore this superposition procedure is entirely acceptable as long as two conditions hold. First T_2 and T_g must not be so far apart on the absolute scale that our choice of $\Delta\epsilon_A$, according to the condition $T_2 = T_g$, is so badly in error that the slopes and shapes of the theoretical curves are distorted. Second, the quantitative relation between T_g and T_2 , whatever it is, must be essentially the same for the various degrees and types of plasticization considered (i.e., over the whole of the curves being compared).

If either of these assumptions were false, and there is independent evidence that neither is, the error involved in making it would show up as a disagreement between theory and experiment in the present comparisons.

Now equation (1) equated to zero at the glass temperature (T_0 for the pure homopolymer) and applied to the case ($v = 0$) of pure homopolymer yields $\Delta\epsilon_A = 1.92 kT_0$. Substitution of this expression for $\Delta\epsilon_A$ and T_0 for T into the general ($v \neq 0$) expression (1) equated to zero yields an expression for the glass temperature T_g of the polymer-diluent system from which it can be seen that the glass temperature depression by diluent is a function of only three quantities, the length of the diluent molecule, its stiffness energy, and, of course, its concentration. In Figures 1-3 we have plotted the glass temperature, actually $kT_g/\Delta\epsilon_A$ as a function of volume fraction of polymer for plasticizer molecules of various lengths and stiffness energies. We could equally well have used $0.521T_g/T_0$ as the ordinate instead of $kT_g/\Delta\epsilon_A$. Each curve is labeled with the number of site occupiers, r_B . Figure 1 displays the curves for the case of perfectly flexible molecules ($\Delta\epsilon_B = 0$). For Figure 2, we have displayed the results when the stiffness energy of the plasticized molecule equals that of the plasticizer molecule, and finally in Figure 3, we assumed infinitely stiff molecules ($\Delta\epsilon_B = \infty$). The encircled points on each curve give the glass temperature and volume fraction for a mole fraction of 0.05. The broken line in Figure 2 gives the predicted curve for plasticization by a two-site occupier when volume effects arising from finite molecular interaction are considered (see reference 4 for details).

III. COMPARISON OF PREDICTED BEHAVIOR WITH OBSERVED BEHAVIOR

We will consider that there is agreement between theory and experiment if each of the three variables v , r_B , $\Delta\epsilon_B$ which we have implicated as determinants of glass temperature depression, are in fact observed to determine glass temperature depression in the manner indicated. It is then sufficient to predict (a) the variation of T_g with v for constant $\Delta\epsilon_B$, r_B ; (b) the variation of T_g with r_B for constant v and $\Delta\epsilon_B$; and (c) the variation of T_g with $\Delta\epsilon_B$ for constant v and r_B .

A. Glass Temperature Depression as a Function of the Amount of Plasticizer

We must first mention that the glass temperature depression of a high molecular weight polystyrene plasticized by styrene has been successfully predicted by the theory. The predicted curve with the experimental points of Alexandrov and Lazurkin¹² is given in Figure 6 of reference 4. In Figure 2 we have reproduced this predicted curve as the broken line. No parameters were used to fit the data. In fact, the two parameters of the theory were determined by the value of the glass temperature of polystyrene ($\Delta\epsilon_A$) and the change in the expansion coefficient above and below

the glass temperature (hole energy). The styrene unit was considered to have the same intermolecular attraction as a monomer unit of polystyrene and it, as well as the monomer unit of the chain, was considered to occupy two sites on the lattice.

The points enclosed by squares in Figure 2 represent the data given by Kelley and Bueche⁸ for polystyrene plasticized by diethylbenzene. Since the ratio of the molecular volume for diethylbenzene (M.V. = 154) to that of styrene (M.V. = 114) is 1.35, it is not unreasonable to assume that diethylbenzene occupies three sites on the lattice. The curve for plasticization by a trimer is seen to fall below most of the data points, but if we were to include the effect of hole energy, we would obviously get a good fit to the data.

Jenckel and Heusch⁹ have measured the glass temperature depression of PS by 15 different plasticizing agents and of PMMA by 10 different plasticizers. If one converts their data from glass temperature vs. weight fraction to glass temperature versus volume fraction, then each of their experimental curves is included among the spectrum of curves of Figures 1-3.

Thus, if one were willing to choose $\Delta\epsilon_B$ and r_B arbitrarily, one could find a curve which fits the data for each plasticizer. There is little point in doing this, however.

Reference to eq. (1) or Figure 1 shows that adding 0.5 vol. % of a dimer to a pure polymer lowers the glass temperature about 10°C. for polystyrene. Thus, a small amount of low molecular weight impurity can cause a large reduction in the glass temperature. It would seem that if the purity of a high polymer is suspected one should not measure the glass temperature directly. It is more sensible to dilute the polymer to a point where the variation of glass temperature with composition is not as marked and then extrapolate to the glass temperature of the pure polymer by means of an appropriate curve in Figures 1, 2, or 3.

We conclude that on the basis of the above-mentioned experiments and others¹³ that the theory does predict correctly the variation of glass temperature with amount of plasticizer.

B. Glass Temperature Depression as a Function of the Size of the Plasticizing Molecule

The observed variations of glass temperature depression are displayed in Table I. Plasticizers are listed in column 1. The second column gives the molar volume obtained by dividing the molecular weight by the density at room temperature. The third and fourth columns give a measure of the plasticizing efficiency for the material in PS and PMMA. We have used the equation

$$(dT_g/dv)_0 = (dT_g/dw)_0 (dw/dv)_0 = (dT_g/dw)_0 (d_1/d_2) \quad (3)$$

which relates the initial slope of the glass temperature versus volume fraction curve to the initial slope of the glass temperature versus weight fraction (w) curve. d_1 and d_2 are the densities of plasticizer and polymer

respectively. The value of $(dT_g/dw)_0$ was taken from Table 2 of reference 9 and the densities of the diluents were obtained from standard sources. We have used values 1.05 and 1.18 for the densities of PS and PMMA, respectively. In the fifth column we have used the fact that a monomer of polystyrene occupies two sites and that, therefore, a site has a molar volume of 49.5. The number of sites per molecule for each plasticizer is obtained by dividing its molar volume by 49.5. The numbers of the sixth column differ from those in the fifth because the number of sites of a monomer of PMMA is 4 rather than 2. The number of sites per monomer equals the number of flexible bonds per monomer for a high polymer.

Since a particular molecule appears twice as large to PMMA as it does to PS, we predict (from Figs. 1, 2, and 3) that the molecule would be less effective in plasticizing PMMA. A comparison of columns 3 and 4 shows this to be the case.

An alternative theory⁸ of glass temperature depression does not predict this effect.

Next, the theory predicts that as we increase the volume of an inflexible molecule (0 in column 7) the plasticizer efficiency decreases. For PS this is seen to be the case. For PMMA the data are inconclusive.

Finally, we predict that for a homologous series in which the stiffness energy is a constant the plasticizer efficiency decreases as we increase the molecular weight. The 4 homologs of the methyl acetate series shown in the table do indeed have this property for both polymers. The three homologs of the salicylate series also show the predicted behavior.

The data of Ueberreiter and Kanig¹⁴ on the self-plasticization of a heterogeneous polystyrene by its low molecular weight components provide a quantitative measure of glass temperature variation with the size (length) of the plasticizing molecule. These authors observed that the glass temperature is a function of the number-average molecular weight. This is also a prediction of our theory.⁴ It follows that the quantitatively correct prediction of glass temperature as a function of number average molecular weight which we have given in Figure 1 of our previous paper⁴ is equivalent to a quantitatively correct prediction of glass temperature as a function of the size of the plasticizing molecule when the stiffness energies of polymer and plasticizer are equal.

We, therefore, conclude on the basis of experiment that if the volume fraction and stiffness energy of the plasticizers are held constant, the plasticizing efficiency decreases as we increase the size of the plasticizer molecule. This is in agreement with the theory.

C. Glass Temperature Depression as a Function of Stiffness of the Plasticizer Molecule

Examination of columns 3 and 4 of Table I shows that, all other things being equal, a flexible molecule has a larger plasticizing efficiency than a stiff molecule. Thus, for example, $-(dT_g/dv)_0$ for methyl acetate is larger

than the corresponding quantity for the plasticizer immediately above it in the table.

Wurstlin and Klein¹⁵ have made a study of plasticization of polyvinyl acetate by a host of plasticizers. They concluded that the least efficient plasticizers were molecules with the largest amount of steric hindrance. Jenckel and Heusch⁹ have, on the basis of their measurements, only part of which were reproduced in Table I, concluded that the more elongated molecules were better plasticizers than the compact ones. Since the more elongated molecules suffer less steric hindrance, we can interpret this result as also agreeing with the prediction of the theory.

The authors wish to thank Dr. H. W. Wyckoff and Dr. J. Hermans, Jr. for their helpful suggestions. One of us (J. H. G.) wishes to acknowledge partial support from a National Institutes of Health research grant.

References

1. Ferry, J. D., *Viscoelastic Properties of Polymers*, Wiley, New York, 1961, Chap. 11.
2. Lel'chuck, Sh. L., and V. I. Sedlis, *Zhur. Priklad. Khim.*, **30**, 412 (1957).
3. Gibbs, J. H., *J. Chem. Phys.*, **25**, 185 (1956).
4. Gibbs, J. H., and E. A. DiMarzio, *J. Chem. Phys.*, **28**, 373 (1958).
5. DiMarzio, E. A., and J. H. Gibbs, *J. Chem. Phys.*, **28**, 807 (1958).
6. Kauzman, W., *Chem. Revs.*, **43**, 219 (1948).
7. DiMarzio, E. A., and J. H. Gibbs, *J. Polymer Sci.*, **40**, 121 (1959).
8. Kelley, F. N., and F. Bueche, *J. Polymer Sci.*, **50**, 549 (1961).
9. Jenckel, E., and R. Heusch, *Kolloid-Z.*, **130**, 89 (1953).
10. Guggenheim, E. A., *Mixtures*, Oxford Univ. Press, London, 1952.
11. Flory, P. J., *Proc. Roy. Soc. (London)*, **A234**, 60 (1956).
12. Alexandrov, A. P., and J. S. Lazurkin, *Compt. rend. acad. sci. U.R.S.S.*, **43**, 376 (1944).
13. Stuart, H. A., *Die Physik der Hochpolymeren*, Vol. IV, Springer-Verlag, Berlin, 1956, Chap. 9.
14. Ueberreiter, K., and G. Kanig, *J. Colloid Sci.*, **7**, 569 (1952).
15. Wurstlin, F., and H. Klein, *Kunststoffe*, **42**, 445 (1952).

Résumé

Le fait que la transition vitreuse est un phénomène fondamentalement thermodynamique, a été utilisé pour dériver une expression pour l'abaissement de la température de transition vitreuse, par les plastifiants. On donne la température de transition du second ordre comme étant la température à laquelle l'entropie première de configuration devient nulle lorsqu'on refroidit le système polymère-diluant. On trouve que la concentration en plastifiant, la dimension de la molécule plastifiée et sa flexibilité sont les facteurs déterminants de la diminution de la température de transition vitreuse. Des faits expérimentaux valables appuient les hypothèses de la théorie, et l'on peut dès lors en conclure que la conception thermodynamique est suffisante pour expliquer l'abaissement de la température de transition vitreuse. On remarque qu'il existe des preuves qui contredisent la théorie du volume libre, lorsque celle-ci est appliquée à la diminution de la température de transition vitreuse.

Zusammenfassung

Unter dem Gesichtspunkt, dass die Glasumwandlung im wesentlichen thermodynamischer Natur ist, wird ein Ausdruck für die Herabsetzung der Glasumwandlungstemperatur durch Weichmacher abgeleitet. Die Temperatur der Umwandlung zweiter

Ordnung wird als diejenige Temperatur festgelegt, bei der die Konfigurationsentropie beim Abkühlen des Polymer-Verdünnungsmittelsystems zuerst null wird. Die Weichmacherkonzentration, Grösse der Weichmachermolekel und ihre Biegsamkeit erweisen sich als Hauptbestimmungsstücke für die Herabsetzung der Umwandlungstemperatur. Die vorhandenen Versuchsergebnisse bestätigen die Aussagen der Theorie, was zu dem Schluss berechtigt, dass der thermodynamische Gesichtspunkt zur Erklärung der Erniedrigung der Glasumwandlungstemperatur ausreicht. Es liegen Daten vor, die im Widerspruch zur Anwendung der Theorie des freien Volumens auf die Umwandlungspunktdepression stehen.

Received February 16, 1962

Studies on Biocolloids and Polyelectrolytes—The Plant—Gums Viscosity of Azrehtic Acid

V. K. KULSHRESTHA, *Department of Physical Chemistry, Jadavpur University, Calcutta, India**

Synopsis

Azrehtic acid (ARA) has been obtained by the electro dialysis of an aqueous solution of the gum of *Azadirachta indica* in an acidic medium. The viscosity of this gum acid has been investigated under different experimental conditions, i.e., with dilution in aqueous and in isoionic concentration of added electrolyte (HCl), and with change in pH. It is observed that the reduced viscosity of the aqueous solutions increases rapidly with dilution and the reduced viscosity-concentration curve is concave upwards instead of being linear as in the case of linear polymers. The viscosity of aqueous ARS solutions follows the equation, $\eta_{sp}/C = A/(1 + B\sqrt{C})$ where A , B , and D are constants ($A = 0.03$, $B = 0.1845$, and $D = 0.05$), as well as the equation $\eta_{sp}/C = aC^b$, in which a and b are constants and equal to 0.2113 and -0.4375 , respectively. It is observed that in isoionic concentrations of added electrolyte (HCl, 2.20×10^{-4} g.-equiv./l.), the sharp rise in the η_{sp}/C versus C curve vanishes, and the curves show well defined maxima which shift to higher concentrations of the gum acid as the electrolyte concentration increases and ultimately vanish at sufficiently high concentration of the added electrolyte (HCl, 2.20×10^{-3} g.-equiv./l.), and the η_{sp}/C versus C curves become linear. The viscosity of azrehtic acid at constant solute concentration increases rapidly when the pH is increased by the addition of NaOH, becomes maximum at a pH of about 6, after which it falls rapidly and becomes constant after a pH of 12. The viscosity also decreases when the pH is decreased on addition of HCl and becomes constant after a pH of 2.0. All these phenomena have been explained on the basis that azrehtic acid behaves as a poly-electrolyte.

INTRODUCTION

Azrehtic acid, a polyelectrolyte, has been obtained by the electro dialysis of the gum of *Azadirachta indica*.¹ This gum has been in pharmaceutical use in India for centuries and is a complex polysaccharide made up of L-arabinose, L-fucose, D-galactose, and D-glucuronic acid² and is associated with different cations such as Ca^{+2} , Mg^{+2} , K^+ , and Na^+ . Until recently, practically nothing was known about the physical properties of azrehtic acid. In one of the papers by the author,¹ the electrochemistry of this acid has been discussed. In the present communication the viscosity of azrehtic acid has been investigated under different experimental conditions, i.e., dilution, effect of counterions, and pH.

* Present address: Institut für makromolekulare Chemie, der Universität Freiburg, i. Br., West Germany.

EXPERIMENTAL

Preparation and purification of azrehtic acid have been described elsewhere.¹ All the viscosity and pH measurements were performed at $35 \pm 0.05^\circ\text{C}$. with a modified Ostwald viscometer³ having an efflux time of 220.1 sec., with the solvent. Since LT_0/V was greater than 400 (where L is the length of the capillary of the viscometer in centimeters, T_0 is the efflux time of the solvent in seconds, and V is the volume in milliliters), no kinetic energy correction was made. In the range of the dilute solutions used the difference in the density of the solution and the solvent used was insignificant, therefore, no density measurements were done for the determination of viscosity. All the solutions were made in conductivity water with a specific conductance of $1-2 \times 10^{-6}$ mho.

Great care was taken to keep the capillary of the viscometer vertical and extremely clean.

pH measurements were carried out with the help of a Cambridge pH meter using the glass electrode.

RESULTS AND DISCUSSIONS

Variation of Viscosity of Azrehtic Acid (ARA) with Dilution

The results of viscosity measurements of aqueous ARA solutions at various dilutions are given in Table I and the values of the reduced viscosity η_{sp}/C have been plotted against concentration C as shown in Figure 1.

TABLE I
Variation of Reduced Viscosity of Azrehtic Acid with Dilution

Concentration, g./100 ml.	Reduced viscosity, η_{sp}/C
0.025	1.071
0.050	0.780
0.075	0.653
0.100	0.572
0.150	0.473
0.200	0.418
0.250	0.382
0.300	0.346
0.400	0.300
0.500	0.275
0.600	0.253
0.800	0.236
1.000	0.214

It is evident from Table I and Figure 1 that η_{sp}/C rises rapidly as the concentration of ARA is reduced, which indicates some increase in the hydrodynamic volume unit. This type of behavior is characteristic of a poly-electrolyte and distinguishes it from other neutral polymers.⁴⁻¹¹ While

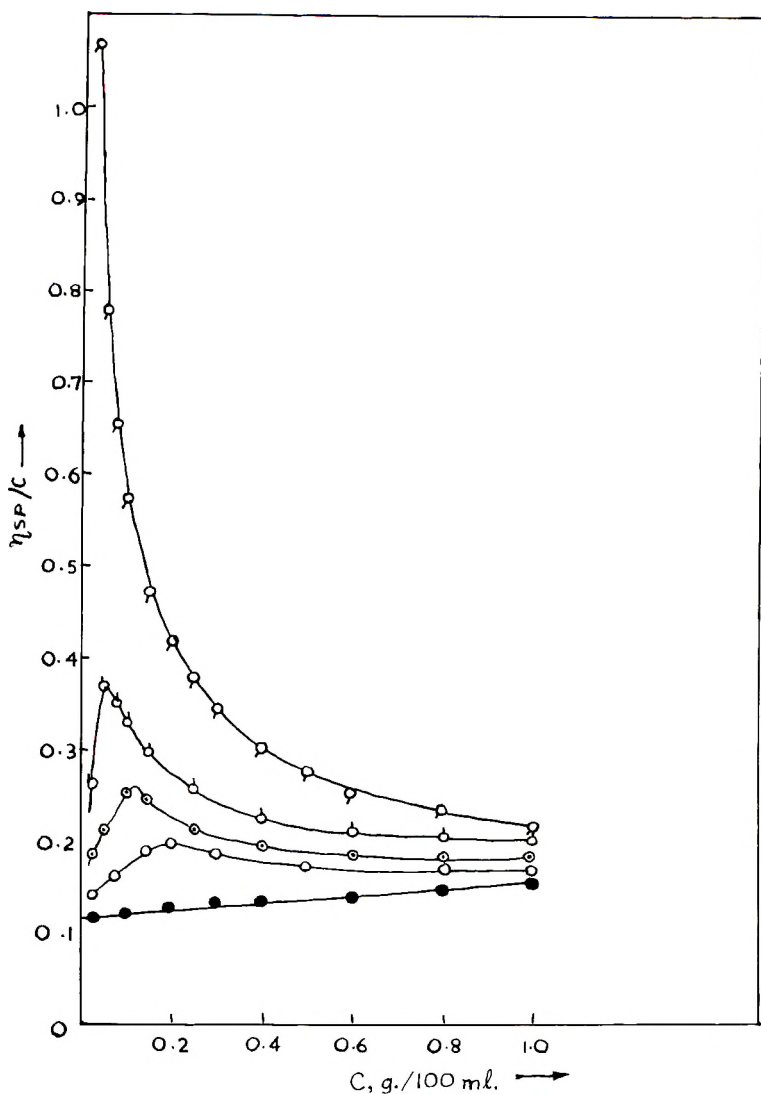


Fig. 1. Reduced viscosity versus concentration for azrehtic acid; viscosity in presence of HCl: (○) nil; (◊) 2.20×10^{-4} g.-equiv./l.; (◐) 3.30×10^{-4} g.-equiv./l.; (◑) 5.50×10^{-4} g.-equiv./l.; (●) 2.20×10^{-3} g.-equiv./l.

for a neutral polymer a plot of η_{sp}/C versus C is a straight line with a positive slope in dilute solutions, with a polyelectrolyte it is not linear and rises rapidly with dilution.

The peculiar viscous behavior of ARA can be explained as due to the increased coulombic repulsion with increasing extent of dissociation with dilution along with the folding and unfolding properties of high polymers. The polymer of azrehtic acid contains a large number of carboxyl (COOH) groups in its backbone which ionize to COO^- and H^+ , the former charge

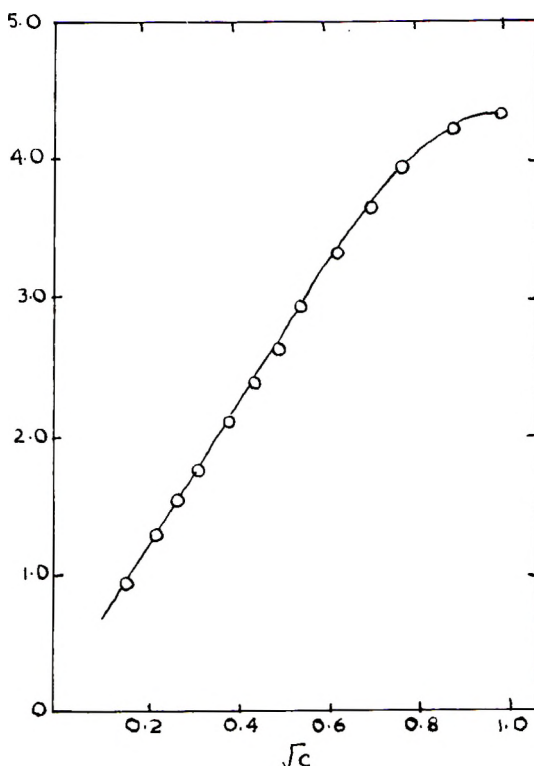


Fig. 2. Reciprocal reduced viscosity vs. \sqrt{c} for azrehtic acid. Ordinate: C/η_{sp}

centers remaining in the backbone of the molecule. When the solution of ARA is diluted, some of the ionizable groups are dissociated, and the polymer chain becomes charged. The repulsion between similarly charged centers on the chain causes it to take up a more stretched out configuration. As the solution is diluted more and more, the number of ionizable groups increases, the chain becomes more charged and extended resulting in a rapid increase in viscosity upon dilution, since the reduced viscosity of a polymer solution is a function of the volume of the dissolved units.

Kuhn, Künzle, and Katchalsky,¹² by mathematical analysis, have predicted a sharp rise of reduced viscosity at higher dilutions for polyelectrolytes. Arnold and Overbeek¹³ theoretically also obtained the same results in the case of polymethyl methacrylate and used Debye's¹⁴ equation for their calculations.

As the solutions are made more concentrated, some of the oppositely charged ions will be drawn back on the polymer chain owing to high charge density on the polyion, thereby neutralizing some of the charged centers of the polyion. Due to the decreased intermolecular coulombic repulsions, the polyion takes up a less extended configuration and thereby the viscosity decreases. This continues till finally the limit is reached when none of the groups are dissociated and the coiling and the viscosity are maximum.

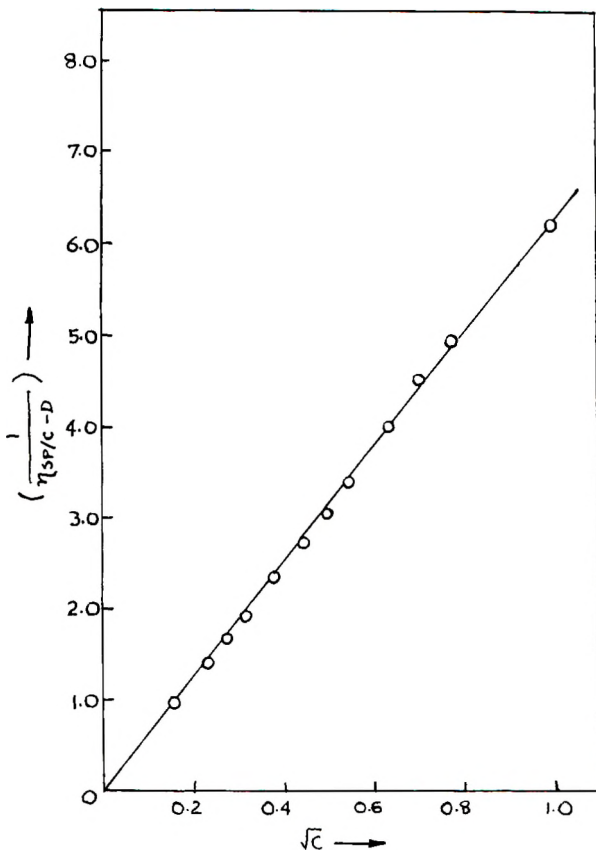


Fig. 3. $(1/\eta_{sp}/C - D)$ vs. \sqrt{C} for azrehtic acid.

A number of relations have been proposed to represent the viscometric behavior of polyelectrolytes in salt-free solutions. The equation

$$\eta_{sp}/C = A/(1 + B\sqrt{C}) \quad (1)$$

first proposed by Fuoss et al.¹⁵ does not fit the present data and the plot of C/η_{sp} versus \sqrt{C} is not a straight line, as shown in Figure 2. Similar deviations have been reported by other workers.^{7,16,17} Fuoss¹⁶ modified eq. (1) to

$$\eta_{sp}/C = [A/(1 + B\sqrt{C})] + D \quad (2)$$

where A , B , and D are constants, to fit the viscometric behavior of various polyelectrolytes studied by him. The term A is a measure of electrostatic interaction; The term D equals η_{sp}/C when C becomes infinite. The term $B\sqrt{C}$ appears to be electrostatic in nature.^{8,16} Equation (2) has been found to hold good in the case of azrehtic acid, a straight line being obtained when $1/(\eta_{sp}/C - D)$ is plotted against \sqrt{C} as shown in Figure 3.

The values of the constants used were $A = 0.03$, $B = 0.1845$, and $D = 0.05$.

The equation of Schaeffgen and Trivisano,¹⁷ eq. (3), does not hold for azrehtic acid and indicates that there is a large amount of uncoiling in the case of azrehtic acid when it is diluted.¹⁹

$$\eta_{sp}/C = [A/(1 + BC)] + D \quad (3)$$

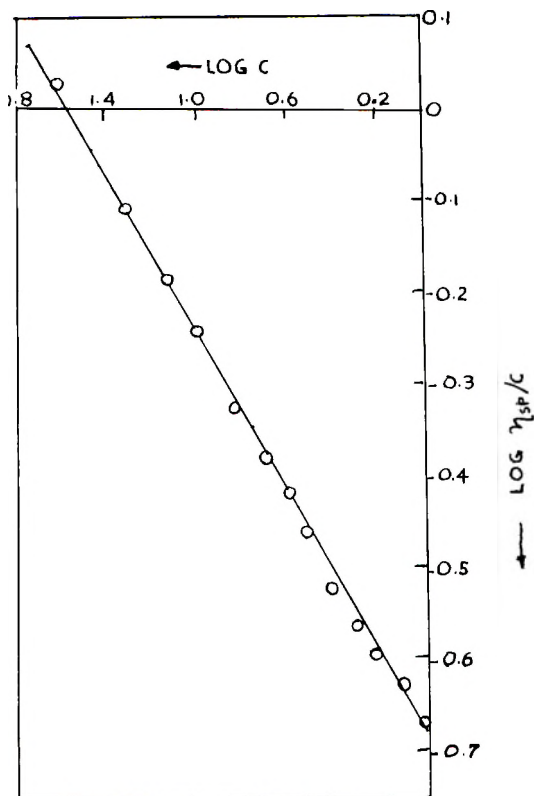


Fig. 4. $\text{Log } \eta_{sp}/C$ vs. $\text{log } C$ for azrehtic acid.

It is further noted that the equation

$$\eta_{sp}/C = aC^b \quad (4)$$

proposed by Wiley, Smith, and Ketterer⁷ holds for ARA. These authors studied the viscometric behavior of potassium *p*-vinylbenzene sulfonate and found eqs. (3) and (4) to hold good for this compound. It is very interesting to note that while the viscosity of ARA does not follow eq. (3), it obeys eq. (4), a straight line being obtained when $\text{log } \eta_{sp}/C$ is plotted against $\text{log } C$ as shown in Figure 4. The values of the different constants are $a = 0.2113$ and $b = -0.4375$.

Effect of Addition of Electrolytes on the Reduced Viscosity of Azrehtic Acid

Various η_{sp}/C versus C curves for ARA in presence of different amounts of HCl are given in Figure 1. It has been found that by the addition of 3.30×10^{-4} g.-equiv./l. of HCl the sharp rise in the η_{sp}/C versus C curve vanishes, the curve showing a well defined maxima which appears when the stoichiometric concentration of hydrogen ions from the polymer becomes nearly equal to that of the added HCl. With increasing HCl concentration, the maximum shifts towards higher ARA concentration, till at last it vanishes completely at 2.20×10^{-3} g. equiv./l. of HCl, and the curve resembles that of a neutral polymer. These results can be explained by the "folding chain" theory of Fuoss in conjunction with mass action or common ion effect. From the point where the maximum lies, if we go towards higher concentration of ARA we find it to behave as a polyelectrolyte.

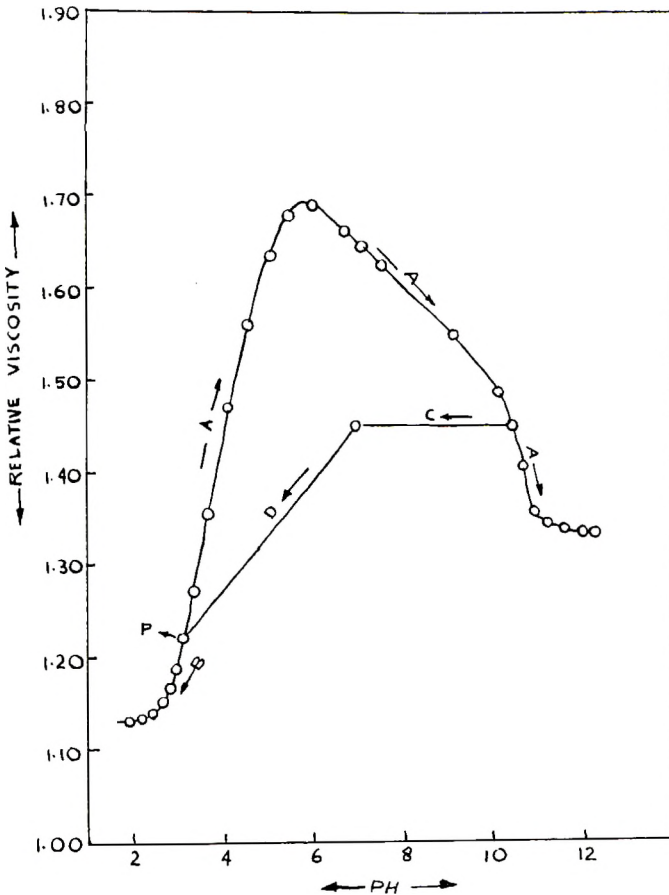


Fig. 5. Relative viscosity vs. pH of azrehtic acid: (A) pH increase with NaOH; (B) pH decrease with HCl; (C) pH decrease with HCl; (D) dialysis; (P) starting point.

But if we move towards lower concentrations of ARA, it behaves as neutral polymer since in this region the electrolyte concentration is sufficiently high to suppress the dissociation, and the molecule curls up completely and behaves as a neutral polymer.

Effect of pH on the Viscosity of Azrehtic Acid

The variation of the relative viscosity of ARA solutions was measured with change in pH by the addition of NaOH or HCl. The concentration of the solute was kept constant at 1%. The results are given in Table II and graphically represented in Figure 5.

From Table II and Figure 5, it is evident that there is a marked effect of pH on the viscosity of ARA solutions. The pH of 1% ARA solution is 3.14 and its relative viscosity 1.220. On increasing the pH by addition of NaOH, the viscosity rises rapidly and becomes maximum at a pH of about 6.00, after which it falls rapidly with rise in pH and becomes constant at a pH of about 12.00. On decreasing the pH by the addition of HCl, the viscosity decreases and becomes constant at about a pH of 2.00. Thomas and Murray²⁰ also observed that the viscosity of Arabic acid changed with pH.

TABLE II
Change in the Relative Viscosity of Azrehtic Acid with pH

pH	Relative viscosity
1.90	1.130
2.12	1.131
2.44	1.140
2.68	1.152
2.80	1.165
2.98	1.186
3.14	1.220
3.35	1.273
3.70	1.352
4.22	1.474
4.60	1.559
5.02	1.629
5.48	1.675
6.00	1.680
6.70	1.653
7.04	1.644
7.50	1.622
9.10	1.550
10.14	1.488
10.44	1.450
10.70	1.405
10.98	1.358
11.20	1.346
11.58	1.340
12.00	1.335
12.22	1.335

At the outset it appears that the viscosity of ARA is pH-dependent, but careful analysis reveals that this is not so. When the pH of 1% ARA solution was changed from 10.44 to 7.50 by neutralizing the acid, it was found that the curve is not retraced and the viscosity remains nearly constant. If, after bringing the pH back to 7.45, the solution is dialyzed, the original viscosity of the solution is restored. If the viscosity was dependent mainly on pH as suggested by Thomas and Murray²⁰ for Arabic acid, the original curve should have been retraced when pH is decreased. But this is not the case.

The characteristic curve in Figure 5 can be explained by the folding chain theory of polyelectrolytes. The ionogenic groups in the chain of ARA are COOH. On the addition of NaOH, the acid is converted into the sodium salt, which dissociates more and more, and the effective charge on the polymer increases. Therefore, the viscosity increases. The viscosity of ARA is maximum near about the neutralization point, where the polymer chain is stretched to its maximum. The fall in viscosity on further addition of NaOH beyond the neutralization point can be explained by the folding chain theory in conjunction with mass action or common ion effect. The same holds good when the pH is decreased by the addition of HCl.

The author is grateful to Prof. S. N. Mukherjee for his keen interest, constant encouragement, and help during the present investigations, and to the Council of Scientific and Industrial Research, Government of India, for financial help.

References

1. Kulshrestha, V. K., *J. Polymer Sci.*, **58**, 809 (1962).
2. Mukherjee, S., and H. C. Shirivastava, *J. Am. Chem. Soc.*, **77**, 422 (1955).
3. Canan, M. R., *Ind. Eng. Chem. Anal. Ed.*, **16**, 708 (1944).
4. Fuoss, R. M., *Science*, **108**, 545 (1948).
5. Fuoss, R. M., and U. P. Strauss, *J. Polymer Sci.*, **3**, 246, 602 (1948).
6. Goldacre, R. J., and I. J. Lorch, *Nature*, **166**, 497 (1950).
7. Wiley, R. H., N. R. Smith, and C. C. Ketterer, *J. Am. Chem. Soc.*, **76**, 720 (1954).
8. Ferry, J. D., D. C. Udy, F. C. Wu, D. E. Heckler, and D. B. Fordyce, *J. Colloid Sci.*, **6**, 429 (1951).
9. Mock, R. A., and C. A. Marshal, *J. Polymer Sci.*, **13**, 263 (1954).
10. Staudinger, H., *Die hochmolekularen Organischen Verbindungen*, Springer, Berlin, 1932, Part 11D.
11. Heidelberger, M., and F. E. Kendal, *J. Biol. Chem.*, **95**, 127 (1932).
12. Kuhn, W., O. Künzle, and A. Katchalsky, *Helv. Chim. Acta*, **31**, 1994 (1948).
13. Arnold, R., and J. Th. G. Overbeek, *Rec. Trav. Chim.*, **69**, 192 (1950).
14. Debye, P. J., *J. Chem. Phys.*, **14**, 636 (1956).
15. Fuoss, R. M., and U. P. Strauss, *Ann. N. Y. Acad. Sci.*, **51**, 836 (1948).
16. Fuoss, R. M., and G. I. Cathers, *J. Polymer Sci.*, **2**, 12 (1947); *ibid.*, **4**, 96 (1949).
17. Schaeffgen, J. R., and C. F. Trivissono, *J. Am. Chem. Soc.*, **73**, 4580 (1951).
18. Oth, A., and P. Doty, *J. Phys. Chem.*, **56**, 43 (1952).
19. Fuoss, R. M., and A. S. Fuoss, *Ann. Rev. Phys. Chem.*, **4**, 64 (1953).
20. Thomas, A. W., and H. A. Murray, *J. Phys. Chem.*, **32**, 676 (1928).

Résumé

L'acide azrechtique (ARA) a été obtenu par électrodialyse d'une solution aqueuse de gomme *Azadirachta indica* en milieu acide. La viscosité de cette gomme acide a été

étudiée dans différentes conditions expérimentales c.à.d. par dilution dans un milieu aqueux et à concentration isoionique d'un électrolyte étranger (HCl), et à des valeurs de pH différentes. On observe que la viscosité réduite des solutions aqueuses augmente rapidement par dilution et la courbe viscosité réduite-concentration est concave au lieu d'être linéaire comme dans le cas des polymères linéaires. La viscosité de solutions aqueuses ARA suit l'équation; $\eta_{sp}/C = A/1 + B\sqrt{C}$ où A , B et D sont constants. $A = 0.03$, $B = 0.1845$ et $D = 0.05$ de même l'équation, $\eta_{sp}/C = aC^b$ dans laquelle a et b sont constants et sont égaux à 0.2113 et 0.4375 respectivement. On observe que pour des concentrations isoioniques d'un électrolyte ajouté (HCl, 2.20×10^{-4} g. équiv./l.), la rapide augmentation dans la courbe représentant η_{sp}/C en fonction de C disparaît et les courbes montrent des maxima bien définis, qui changent à des concentrations plus élevées en gomme acide, de même lorsque la concentration en électrolyte augmente et finalement disparaît pour des concentrations suffisamment élevées en électrolyte ajouté (HCl 2.20×10^{-3} g. équiv./l.) et les courbes η_{sp}/C en fonction de C deviennent linéaires. La viscosité de l'acide azrechtique à concentration constante en soluté croît rapidement lorsque le pH augmente par suite de l'addition de NaOH, atteint un maximum à un pH d'environ 6, puis diminue rapidement pour devenir constant au pH 12. La viscosité également décroît lorsque le pH décroît par addition de HCl et devient constante à un pH 2.0. Tous ces phénomènes ont été expliqués en admettant que l'acide Azrechtique se comporte comme un polyélectrolyte.

Zusammenfassung

Azrechtinsäure (ARA) wurde durch Elektrodialyse einer wässrigen Lösung des Harzes *Azadirachta indica* in saurem Medium erhalten. Die Viskosität dieser Harzsäure wurde unter verschiedenen experimentellen Bedingungen, nämlich bei Verdünnung mit Wasser und mit einer isoionischen Konzentration an zugesetztem Elektrolyt (HCl) sowie bei pH-Änderung untersucht. Die reduzierte Viskosität der wässrigen Lösungen nimmt bei Verdünnung rasch zu und die Kurve reduzierte Viskosität gegen Konzentration verläuft konkav nach oben anstatt linear wie im Falle linearer Polymerer. Die Viskosität wässriger ARA-Lösungen befolgt die Gleichung $\eta_{sp}/C = A/1 + B\sqrt{C}$ wo A , B und D Konstante mit den Werten $A = 0,03$, $B = 0,1845$ und $D = 0,05$ sind, oder die Gleichung $\eta_{sp}/C = aC^b$ wo a und b Konstante mit den Werten $a = 2113$ und $b = 0,4375$ sind. Bei isoionischer Konzentration des zugesetzten Elektrolyten (HCl, $2,20 \times 10^{-4}$ Mol/l.) verschwindet der scharfe Anstieg in der Kurve η_{sp}/C gegen C und die Kurven zeigen gut definierte Maxima, die sich mit zunehmender Elektrolytkonzentration zu höheren Harzsäurekonzentrationen verschieben und schliesslich bei genügend hoher Konzentration des zugesetzten Elektrolyten (HCl, $2,20 \times 10^{-3}$ Mol/l.) verschwinden und eine lineare Abhängigkeit des η_{sp}/C von C liefern. Die Viskosität der Azrechtinsäure nimmt bei konstanter Konzentration mit Erhöhung des pH durch NaOH-Zusatz rasch zu, erreicht bei einem pH von etwa 6 ein Maximum, nach welchem sie rasch abfällt und nach einem pH von 12 konstant wird. Die Viskosität wird auch bei pH-Abnahme durch zugesetzte HCl herabgesetzt und wird nach einem pH von 2 konstant. Alle diese Erscheinungen werden durch das Verhalten von Azrechtinsäure als Polyelektrolyt erklärt.

Received March 13, 1962

Copolymerization of Styrene and Styrene Derivative with an Aluminum Alkyl-Titanium Trichloride Catalyst*

C. G. OVERBERGER and S. NOZAKURA,† *Department of Chemistry,
Institute of Polymer Research, Polytechnic Institute of Brooklyn, Brooklyn,
New York*

Synopsis

Copolymerizations of styrene with *p*-*tert*-butyl-, *o*-methyl-, 2,6-dimethyl-, and *p*-fluorostyrene were carried out with an alkyl aluminum-titanium trichloride catalyst. Overall composition of the product indicated that substituted styrenes were less reactive than expected for a conventional free-radical or ionic mechanism in solution. This fact led to a suggestion of a special steric interaction of the penultimate monomeric unit in the propagation step for this heterogeneous system. A styrene-*p*-*tert*-butylstyrene copolymer was fractionated, showing that it was composed of two or more copolymers of different compositions. The similar situation holds for the other cases except for 2,6-dimethylstyrene, which did not homopolymerize and did not copolymerize. The result was explained by the assumption of either multiactivity of the catalyst due to differences in site activity or a diffusion-controlled process.

In a heterogeneous transition metal catalyst type such as titanium trichloride and triisobutylaluminum, the polymerization probably occurs mainly on the surface of the transition metal portion of the complex.² There is a possibility that absorption or coordination of the monomer on the complex will be subject to a selective steric factor due to a penultimate steric effect due to the structure near the growing end of the polymer chain. Because of the rigidity of the intermediate and the transition state in this polymerization process, these penultimate effects may be much greater than are usually found with homogeneous free radical or ionic catalysis. It is also clear that the complex may have considerable ionic character, and hence polymerization on the complex will be subject to polar effects.

One approach to study of these factors in catalyst systems is the use of copolymerization. Copolymerization of ethylene and propylene with heterogeneous catalysts was studied extensively by Natta and his co-workers,³⁻⁵ and it was shown that the copolymerization can give linear, amorphous copolymer free of homopolymers not only by using transition

* Part XVIII in a series of papers concerned with ionic polymerization. For the previous paper in this series, see Overberger and Davidson.¹

† Post-doctoral Research Associate, 1960-1961. Present address: Faculty of Science, Osaka University, Nakanoshima, Osaka, Japan.

metal halides which are soluble in hydrocarbon solvents but also by using solid, crystalline and insoluble transition metal halides, such as titanium di- and trichlorides. It has been observed that by the use of a catalytic system with a crystalline component, the copolymers containing more than 85 mole-% of propylene show slight crystallinity due to the existence of isotactic sequences of propylene. With the use of noncrystalline components, such as vanadium oxychloride, tetrachloride, and titanium tetrachloride, as a part of the catalytic system, the copolymers are amorphous even if they contain a high percentage of propylene.

Reding⁶ reported crystalline copolymers of 3-methylbutene and 4-methylpentene over the entire range of copolymer composition. However, in the binary copolymerization of styrene, allyltrimethylsilane, and 3-butenyltrimethylsilane, which was carried out by Murahashi and co-workers,⁷ the crystalline part of the product was shown to be composed of two kinds of crystalline copolymers.

It is convenient to compare the copolymerization behavior of a heterogeneous catalyst with that of conventional free radical and ionic copolymerization in solution. Since α -olefins have not given linear high polymer in free radical or ionic systems, styrene and styrene derivatives may be advantageous monomers for the present purpose.

Natta and his co-workers studied the copolymerization of styrene with a number of styrene derivatives.⁸ On the basis of the assumption that the product was a copolymer, the monomer reactivity ratios were measured and the product r_1r_2 was found to be almost always near unity in the cases of copolymerization of styrene with *p*-methyl-, *m*-methyl-, *p*-ethyl-, *p*-fluoro-, *p*-chloro-, and *p*-bromostyrene. It is clear, however, that these monomer reactivity ratios represent some average value of copolymer composition and do not necessarily afford a measure of the monomer reactivity. No fractionation data were reported, so that the nature of the alleged copolymers is not known. Recently, Hodes and Drucker⁹ also reported the copolymerization of *p*-methylstyrene and *o*-methylstyrene, resulting in the formation of crystalline copolymer.

In a preceding paper,¹⁰ copolymerization of styrene with *p*-methylstyrene in the presence of titanium trichloride-triisobutylaluminum catalyst was found to lead to the formation of two or more amorphous copolymers of different compositions. However, copolymerization with *p*-*tert*-butyl- or *p*-*n*-butylstyrene indicated less copolymer formation. These data led to a conclusion that steric and polar requirements, especially the former, for the coordination of the monomer with the catalyst sites of a solid surface might be more selective in regard to reactivity than in a free-radical or ionic polymerization in solution.

The primary object of the present work was to study the steric and polar effects in more detail. Radioactive styrene- α -C¹⁴ was used, except for the copolymerization with *p*-fluorostyrene, to facilitate the analysis of copolymer composition. *p*-*tert*-Butylstyrene was used, since the steric requirements of the monomer used favor penultimate activity. *o*-Methylstyrene

and 2,6-dimethylstyrene were chosen to see if there were normal frontal steric effects compared to *p*-methylstyrene. *p*-fluorostyrene was also used because of its opposite polar effect to the alkyl group types and smaller steric requirements. Copolymerization of these monomers by typical homogeneous anionic catalysts is being undertaken for the purpose of comparison and will be reported in the future.

RESULTS

Homopolymerization and Copolymerization of Styrene, *p*-*tert*-Butylstyrene, *o*-Methylstyrene, 2,6-Dimethylstyrene, and *p*-Fluorostyrene

A comparison of reactivities of styrene derivatives is shown in Table I. The catalyst used was found to have a very high stereospecificity towards styrene, which was shown from the fact that only 1.0–1.7% of polystyrene was extractable with hot methyl ethyl ketone. *p*-*tert*-Butylstyrene and *o*-methylstyrene polymerized but were definitely less reactive than styrene. 2,6-Dimethylstyrene did not yield any polymer under these conditions. On the other hand, *p*-fluorostyrene showed higher reactivity than styrene. Polystyrene, poly-*o*-methylstyrene, and poly-*p*-fluorostyrene showed high crystallinity, as is already known.¹¹ Poly-*p*-*tert*-butylstyrene, however, showed low crystallinity only after it was annealed at 200°C.

TABLE I
Homopolymerization of Styrene, *p*-*tert*-Butylstyrene, *o*-Methylstyrene, 2,6-Dimethylstyrene, and *p*-Fluorostyrene^a

Monomer	Polymerization temp., °C.	TiCl ₃ , g.	Al/Ti ratio	Monomer, mmole	Time, hr.	Conversion, %
Styrene	74	0.11	3.8	20.0	1.5	9.8
	74	0.12	3.4	20.0	21	24.6
<i>p</i> - <i>tert</i> -Butylstyrene	74	0.12	3.6	13.8	1.5	4.8
	74	0.12	3.6	14.0	21	8.7
	74	0.12	3.7	14.1	21	8.6
<i>o</i> -Methylstyrene	74	0.08	4.8	17.2	1.5	3.0
	74	0.11	3.7	17.5	21	8.4
	74	0.11	3.7	19.1	21	12.0
2,6-Dimethylstyrene	74	0.09	4.4	15.8	21	0
	74	0.11	3.7	17.3	21	0
	74	0.13	3.1	17.0	21	0
Styrene	75	0.10	3.8	21.0	1	10.8 ^b
	75	0.11	3.7	20.8	1	14.3 ^b
	75	0.11	3.9	21.8	1	13.3 ^b
	75	0.11	3.8	21.1	1	13.0 ^b
<i>p</i> -Fluorostyrene	75	0.11	3.6	18.8	1.08	26
	75	0.11	3.8	18.8	1	24

^a Solvent, heptane 20 ml.

^b The part of the products extractable by hot methyl ethyl ketone was 1.6, 1.7, 1.6, and 1.0%, respectively.

Preliminary copolymerization of styrene and the styrene derivatives was carried out with monomer mixtures at 50:50 mole-% and the results are shown in Table II. Conversions were kept low, except in the case of *p*-fluorostyrene, to assure constancy of monomer concentrations during the copolymerization. The higher conversions obtained in the *p*-fluorostyrene copolymerizations should not affect the results seriously, since an experiment carried out to lower conversion (10.9%) (Table V) showed nearly the same composition.

TABLE II
Copolymerization of Styrene (M_1) with Styrene Derivatives (M_2)^a

M_2	Al/Ti ratio	Time, min.	Conver- sion, %	M_1 mole-%		$[\eta]$
				Monomer	Polymer	
<i>p</i> - <i>tert</i> -Butyl- styrene	3.7	40	2.7	50.2	83.8 ± 1.4	3.06 ^b
	3.7	50	3.6	50.2	74.2 ± 1.2	2.82
<i>o</i> -Methyl- styrene	3.5	40	5.4	49.9	87.9 ± 1.4	3.56 ^b
	3.4	50	9.4	49.9	83.8 ± 1.4	3.94
2,6-Dimethyl- styrene	3.9	100	6.9	49.7	92.6 ± 1.5	2.90 ^b
	3.8	80	5.7	49.7	93.6 ± 1.6	2.50
<i>p</i> -Fluoro- styrene	3.7	41	22.7	49.8	61	11.6 ^c
	4.2	41	20.1	49.8	59	10.1

^a Copolymerization was carried out in 16 ml. of heptane at 74°C. (except 75°C. for *p*-fluorostyrene) with 0.09–0.12 g. of titanium trichloride.

^b Intrinsic viscosity in xylene at 25°C.

^c Intrinsic viscosity in tetrahydrofuran at 30°C.

An interpretation of the copolymer composition data must allow for an isotope effect¹² in the polymerization of styrene- α -C¹⁴. Thus the activity of thermal polystyrene and isotactic polystyrene, which were polymerized to low conversions from the same batch of styrene- α -C¹⁴ polymer, give an activity of 92.8 ± 1.5% in the isotactic case and 94.1 ± 0.7% in the atactic case. Therefore, the alleged copolymerization product with 2,6-dimethylstyrene is nearly pure polystyrene.

The reluctance of this monomer to enter the growing polymer chain is clearly demonstrated in the data in Table II.

Fractionation of a Styrene-*p*-*tert*-Butylstyrene Copolymer

The results of the fractionation of a styrene-*p*-*tert*-butylstyrene copolymer are summarized in Table III. The toluene-soluble part of the copolymer showed no crystallinity as observed in an x-ray powder pattern and relatively low styrene content by radioactive analysis. Fractions obtained on fractionation of the toluene-insoluble part showed crystallinity and very high styrene contents. There was an increase in the intrinsic viscosity as well as in the styrene content in the middle of the fractions. A plot of intrinsic viscosities versus percentage styrene gave the copolymer compo-

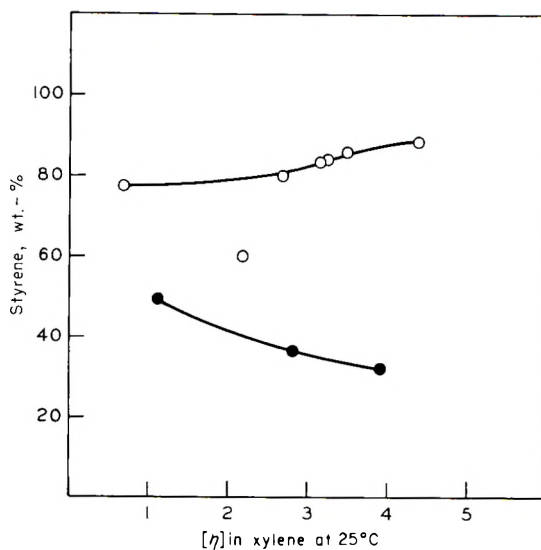


Fig. 1. Fractionation of a copolymerization product of styrene-*p*-*tert*-butylstyrene: (●) toluene-soluble at room temperature; (O) toluene-insoluble at room temperature.

sition distribution shown in Figure 1. It is interesting that the fractions of the toluene-soluble part had considerably higher intrinsic viscosities than the toluene insoluble portion.

TABLE III
Fractionation of a Styrene-*p*-*tert*-Butylstyrene Copolymer^a

	Fraction	Fraction, %	Styrene, mole-%	$[\eta]^b$	Crys- tallinity by x-ray ^c
Insoluble in toluene	1-1	3.7	90.5 ± 1.1	3.46	Low
	1-2	4.5	89.2 ± 1.1	3.26	Low
	1-3	3.4	88.9 ± 1.2	3.14	Low
	1-4	19.9	88.8 ± 1.0	3.16	Low
	1-5	5.5	92.0 ± 1.1	4.83	Low
	1-6	18.5	86.2 ± 1.0	2.67	—
	1-7	13.5	69.4 ± 0.8	2.12	—
	1-8	3.2	83.9 ± 1.2	0.67	Low
Soluble in toluene	2	8.8	41.9 ± 0.5	3.88	None
	3	6.6	47.4 ± 0.5	2.80	None
	4	11.4	59.6 ± 0.7	1.09	None
Total		99.0			

^a Polymerization was carried out at 74°C. for 45 min. in 80 ml. of heptane, with 0.51 g. of titanium trichloride, 2.12 g. of triisobutylaluminum, and 18.7 g. of a monomer mixture (48.6 mole-% styrene). 7.4% conversion. The original copolymer had 77.8 mole-% of styrene.

^b Intrinsic viscosity was measured in xylene at 25°C.

^c Samples were annealed at 150°C. *in vacuo*.

Fractionation of Styrene-*o*-Methylstyrene Copolymer

In this case also, the copolymer was first fractionated into two parts, the toluene-soluble part and the insoluble part, both of which were fractionated

TABLE IV
Fractionation of a Styrene-*o*-Methylstyrene Copolymer^a

	Fraction	Fraction, %	Styrene, mole-%	$[\eta]^b$	Crystallinity by x-ray ^c
	1-1	1.7	(Insoluble)		Medium
	1-2	5.6	86.2 ± 1.2	5.00	Medium
	1-3	2.4	85.3 ± 1.1	4.09	—
	1-4	4.1	79.5 ± 1.0	2.95	Medium
Insoluble in toluene	1-5	4.6	84.6 ± 1.1	3.70	Low
	1-6	5.0	85.8 ± 1.1	3.92	Low
	1-7	12.4	87.8 ± 1.1	5.52	Medium
	1-8	14.0	82.0 ± 1.1	3.53	Medium
	1-9	14.1	83.8 ± 1.1	2.21	—
	1-10	4.7	81.5 ± 1.1	0.75	Medium
Soluble in toluene	2	1.7	66.6 ± 0.8	3.95	Low
	3	8.6	67.2 ± 0.9	1.95	Low
	4	4.6	66.0 ± 0.9	0.80	None
	5	3.7	71.2 ± 0.9	0.36	None
	6	3.1	—	—	None
	Total		89.9		

^a Polymerization was carried out at 74°C. for 65 min. in 80 ml. of heptane, with 0.51 g. of titanium trichloride, 2.05 g. of triisobutylaluminum, and 19.22 g. of a monomer mixture (50.3 mole-% styrene). 12.3% conversion. The original copolymer had 79.2 mole-% of styrene.

^b Intrinsic viscosity was measured in xylene at 25°C.

^c Samples were annealed at 150°C. *in vacuo*.

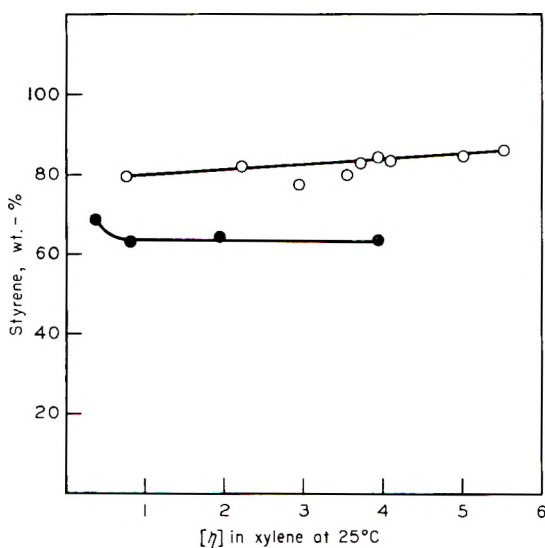


Fig. 2. Fractionation of a copolymerization product of styrene-*o*-methylstyrene: (●) toluene-insoluble at room temperature; (○) toluene-soluble at room temperature.

further as shown in Table IV. The soluble part showed a lower styrene content than the insoluble part. Fractionation of the insoluble portion again showed peculiar irregularity in intrinsic viscosities and styrene content simultaneously. Consequently, a plot of intrinsic viscosity versus percentage styrene fell on two curves as shown in Figure 2. An interesting fact in this case is that not only the fractions of the insoluble part but also those of the soluble part showed some evidence of crystallinity.

Fractionation of a Styrene-*p*-Fluorostyrene Copolymer

Two crude fractionation procedures were attempted: the first, successive extraction by various solvents and the second an ordinary precipitation method preceded by toluene treatment. The results are shown in Table V.

Stereoregular poly-*p*-fluorostyrene was found soluble in hot methyl ethyl ketone, hot toluene, and cold tetrahydrofuran, whereas isotactic polystyrene is not soluble in hot methyl ethyl ketone but is soluble in hot

TABLE V
Fractionation of a Styrene-*p*-Fluorostyrene Copolymer^a

Fraction	Fraction, %	F, %	Sty- rene, mole-%	[η] ^b	Crystallinity by x-ray ^c
A. Solvent Extraction					
Heptane (boiling)	0.5	—	—	—	—
MEK (boiling)	20.9	8.14 8.09	52	2.93	None
THF (room temperature)	70.0	6.75 7.04	60	6.57	Medium
Residue	6.7	7.11 6.93	59	7.00	Low
Total	97.9				
B. Precipitation Method					
2 (insol. in THF)	4.3	6.79	61	—	Low
3	6.2	7.02	59	7.80	Medium
4	6.3	6.52	62	6.41	Medium
5	14.1	7.00	59	4.02	Medium
6	11.2	7.86	54	4.00	Low
7	14.1	8.01	53	8.32	Medium
8	8.6	7.98	53	3.70	Low
9	22.7	8.91	47	6.80	None
10	5.2	9.22	45	1.96	None
1 (Sol. in toluene)	5.7	9.18	45	1.50	None
Total	98.4				

^a Copolymerization was carried out at 75°C. for 41 min. with 0.48 g. of titanium trichloride, 2.13 g. of triisobutylaluminum, 80 ml. of heptane, and 19.4 g. of a monomer mixture (49.8 mole-% styrene). 10.9% conversion. The original copolymer had 61 mole-% of styrene.

^b Intrinsic viscosities were measured in tetrahydrofuran at 30°C.

^c Samples were annealed at 150°C. *in vacuo*.

tetrahydrofuran. Thus, if there is any amount of nearly pure stereoregular poly-*p*-fluorostyrene or polystyrene, the former would fall mainly in the methyl ethyl ketone fraction and the latter in the residue. In fact, fractionation A did not show much difference of composition among three main fractions, although there was a definite difference between the methyl ethyl ketone fraction and the others.

Fractions obtained in fractionation B, which was carried out with tetrahydrofuran as a solvent and methanol as a precipitant, showed considerable irregularity in intrinsic viscosities. However, the styrene content changed quite regularly, indicating that the fractionation was governed mainly by copolymer composition and not by molecular weight. From the results of the two fractionations, it is clear that the product is not a copolymer of homogeneous composition.

Effect of Al/Ti Ratio on Styrene-*p*-*tert*-Butylstyrene Composition

The molar ratio of triisobutylaluminum and titanium trichloride was changed in the copolymerization of styrene and *p*-*tert*-butylstyrene, the amount of titanium trichloride being kept practically constant. The results are summarized in Table VI. With decreasing Al/Ti ratio, yields increased gradually and the percentage of the toluene-insoluble part in the copolymer decreased gradually. However, the percentage of styrene and the intrinsic viscosity of both parts remained practically constant over a tenfold change of the Al/Ti ratio. It is also noteworthy that the intrinsic viscosity of the toluene-soluble parts showed fairly high values ($[\eta] = 3-4$).

TABLE VI
Effect of Al/Ti Ratio on Styrene-*p*-*tert*-Butylstyrene Copolymerization^a

TiCl ₃ , g.	Al/Ti ratio	Conver- sion, %	Tolu- ene-in- soluble portion, %	Insoluble portion		Soluble portion	
				Styrene, mole-%	$[\eta]^b$	Styrene, mole-%	$[\eta]^b$
0.19	3.9	11.0	60.4	92.9 ± 1.1	5.35	52.7 ± 0.6	3.33
0.20	1.2	12.5	59.2	92.0 ± 1.2	5.92	53.2 ± 0.7	4.14
0.19	0.70	13.2	50.4	92.8 ± 1.1	5.17	57.1 ± 0.7	4.33
0.19	0.33	16.7	46.2	91.4 ± 1.1	5.14	54.5 ± 0.7	4.30

^a Polymerization was carried out at 75°C. for 45 min. with 120 ml. of heptane and 7.0 g. of a monomer mixture (styrene 50.6 mole-%).

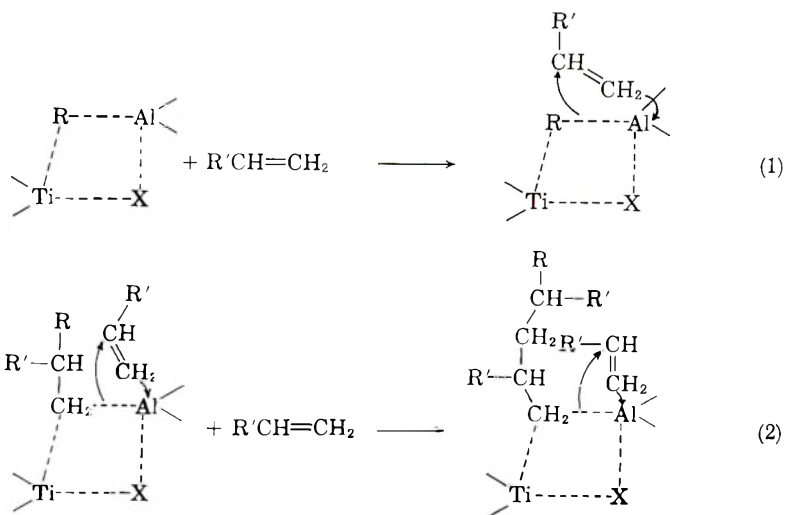
^b Intrinsic viscosities were measured in xylene at 25°C.

DISCUSSION

2,6-Dimethylstyrene did not homopolymerize under the conditions used and also did not copolymerize with styrene. This may be due to an ordinary frontal steric effect in the condensation step of the monomer with the transition metal by the *ortho*-substituents. This is probably the main

reason why *o*-methylstyrene is less reactive than *p*-methylstyrene, which is known to have the same order of reactivity.¹⁰

A typical representation of the growing site is indicated in eqs. (1) and (2):



where X represents a halogen.

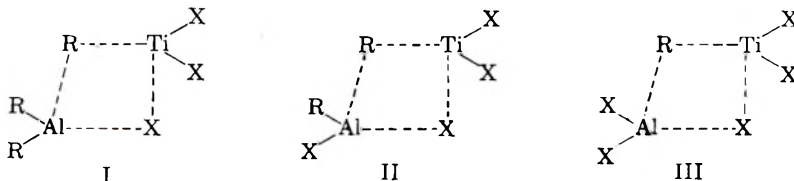
In the case of the heterogeneous catalyst with titanium trichloride, the complex may be formed on the solid surface of the titanium compound. Hence, the presentation or coordination of the monomer will be restricted to one side of the bridge-bond structure. The R group of the first monomeric unit at the growing end will be removed from the coordinating monomer. However, there is a good possibility that the penultimate unit will come closer to the coordinating monomer and the second R group, especially a bulky *para* substituent, will exhibit a spatial interference with the monomer. A steric effect of this kind will account for the low reactivity of *p*-*tert*-butylstyrene in copolymerization than one would predict for a free radical or conventional ionic mechanism. *p*-*t*-fluorostyrene was more reactive than styrene in homopolymerization perhaps because of the electron-withdrawing *p*-fluoro substituent, but was slightly less reactive in the case of copolymerization.

Fractionation of the product showed peculiar irregularities in intrinsic viscosities and copolymer compositions. This phenomenon is not too unreasonable granted that fractionation may be affected by copolymer composition and stereoregularity as well as molecular weight, although qualitative examination of x-ray powder patterns did not reveal any strong support for major differences of stereoregularity among various fractions.

The toluene-soluble part of the styrene-*p*-*tert*-butylstyrene copolymers showed a considerably lower styrene content and was found to be amorphous. This appears to point to a possibility of a cationic propagation, which could result from one of the catalyst components. However, this

possibility is almost definitely excluded by the facts that the catalyst has an extremely high stereospecificity for styrene (>98%) and intrinsic viscosities of the toluene-soluble part showed fairly high values, certainly much higher than one can obtain in a conventional cationic system. A similar situation holds in other cases. Thus, we suggest a multiactivity of the catalyst, due to differences in site activity.

The catalyst site is represented in structures I-III.



where R is alkyl and X is a halogen. Again, the complex may be coordinated on the solid surface of the titanium trichloride. Even if aluminum trialkyl is used as one of the components, alkylaluminum chloride will be produced in minor amounts as the result of surface reaction or reaction with titanium tetrachloride which is present in the trichloride. The alkyl-aluminum chloride thus formed will complex with the titanium compound as shown in II and III. The electron density of the bridge-bond carbon probably decreases from I to II to III. In other words, the active site I will be more anionic than II, and III will be less anionic than II. When these active sites operate in the copolymerization of monomers having more or less different polarities, copolymers of different compositions may result. It is also possible that the valence of titanium in the complex will contribute to multiactivity.

The effect of the aluminum/titanium mole ratio (Table VI) is of considerable interest from this point of view. The decrease of the Al/Ti ratio resulted in only the increase of the toluene-soluble part; the properties of both the soluble and the insoluble parts remained practically unchanged. This shows that the Al/Ti ratio changed the proportion of the various active sites but did not change the nature of the individual active sites.

Since this is a heterogeneous system, the role of diffusion cannot be discounted. The reaction takes place in the direct vicinity of a polar surface and the possibilities of local concentration effects can not be excluded. We feel, however, that at the very low conversion of polymer, a diffusion-controlled process plays only a minor role and that differences in reactivity can be ascribed to chemical structure.

EXPERIMENTAL

Monomers

p-*tert*-Butylstyrene was prepared according to the procedure of Mowry¹³ from commercial *tert*-butylbenzene. The reduction of the ketone, however, was carried out with lithium aluminum hydride rather than catalytically.

p-*tert*-Butylphenylmethylcarbinol was obtained as colorless prisms, m.p. 71.5–72.0°C. after recrystallization from pentane (lit.:¹³ m.p. 67–68°C. by catalytic reduction of *p*-*tert*-butylacetophenone). *p*-*tert*-Butylstyrene was purified by repeated distillation through an 18-cm. helix-packed column, b.p. 92–93°C./10.5 mm., n_D^{25} 1.5238 (lit.:¹³ b.p. 99–100°C./14 mm., n_D^{25} 1.5245).

o-Methylstyrene was prepared from *o*-toluidine according to the procedure of Hirschberg¹⁴ b.p. 53.5–54.5°C./10 mm., n_D^{25} 1.5414 (lit.:¹⁴ b.p. 104.6°C./100 mm., n_D^{20} 1.5437 by the same procedure).

2,6-Dimethylstyrene was prepared also by following the Hirschberg method, starting from 2,6-dimethylaniline, b.p. 65–67°C./10 mm., n_D^{20} 1.5269 (lit.:¹⁴ b.p. 68–69°C./10 mm. by the same procedure).

p-Fluorostyrene was prepared according to the Mowry¹³ method from *p*-fluoroacetophenone. The reduction of ketone was carried out with lithium aluminum hydride, b.p. 52.0°C./22 mm., n_D^{25} 1.5135 (lit.:¹⁵ b.p. 44–45°C./15 mm., n_D^{25} 1.5131 by dehydration of *p*-fluorophenylmethylcarbinol with potassium hydroxide at 250°C.).

Styrene- α -C¹⁴ was prepared according to the method described in a previous paper.¹⁰ From 0.0289 g. of barium carbonate which had an activity of 0.163 mc./mg. and an isotope ratio of 52.6%, 85.3 g. of active styrene was obtained after successive dilutions in each step. Radioactivity of the monomer was found to be 13.4 μ c./g. by a comparison of its activity to that of standard reference sample of radioactive benzoic acid. The overall radioactive yield of total synthesis was about 24%. The monomer was further diluted before use with about eleven times of ordinary styrene to give a suitable activity.

All monomers were stored in a refrigerator with a small amount of *p*-*tert*-butyl catechol and distilled before use. The distilled monomer was kept overnight with calcium hydride in a refrigerator and degassed immediately before use.

Polymerization

Triisobutylaluminum was purified by distillation of a commercial product, b.p. 53°C./0.6 mm. and stored in a glass-stoppered flask filled with nitrogen, the ground joint being greased with Apiezon grease. A suspension of titanium trichloride in toluene, which was ground in a vibratory ball mill, was kindly supplied by Union Carbide Metals Company. The concentration of the suspension was determined to be 0.15 g. solid/g. of suspension by evaporation of the solvent in vacuum.

Polymerization was carried out in a sealed ampule. An ampule was heated in an oven at about 110°C. overnight and stoppered with a self-sealing rubber cap while hot, and flushed with prepurified nitrogen through a hypodermic needle. Titanium trichloride, triisobutylaluminum, and degassed heptane were injected by the use of a hypodermic syringe in this order. The ampule was weighed after each addition. While the ampule was being flushed with a slow stream of nitrogen through a hypodermic

needle, it was immersed in a Dry Ice-acetone bath, monomer was injected, and the ampule was sealed. Polymerization was carried out at 74–75°C. in an oil bath equipped with a rotating wheel.

Fractionation

A polymer was first divided into two parts, the soluble part in toluene at room temperature and the insoluble part. Extraction with toluene was carried out by digesting the polymer powder with toluene for several days with occasional shaking followed by centrifuging the residue, these procedures being repeated three times.

The soluble fraction in toluene was further fractionated by the usual precipitation method with methanol as a nonsolvent at 25°C. Fractionation of the residual part was carried out by dissolving the polymer in hot toluene (about 0.5%) followed by precipitation with methanol at 25°C.

In the case of the copolymerization product of styrene and *p*-fluorostyrene, the residual part was dissolved in hot tetrahydrofuran under nitrogen (about 0.5% solution) and precipitated successively with methanol at 30°C.

Radioactive Measurement

A xylene solution of a polymer having the concentration of about 10 mg./5 ml. solution was prepared by refluxing the mixture for 4 hr. under nitrogen. An aliquot of the solution, 5 ml., was pipetted into a scintillation counting cup equipped with ground glass cover, and added with 5 ml. of 0.6% solution of 2,5-diphenyloxazole in xylene. The cup was kept overnight in a desiccator over Drierite and before counting. The ground glass was greased with silicone grease.

Radioactivity was measured by an EKCO 612 scintillation counter at –17°C. and an EKCO N53. Scaler at PM voltage 1150 and bias 12.5 v. The counting efficiency of this instrument under this condition was estimated to be 74% by counting a reference standard source. The reference standard source, C¹⁴-labeled benzoic acid, having activity of 1.81 $\mu\text{c./g.}$ was the product of Tracerlab, Inc. Background was 1.9–2.0 counts/sec. Activity of an unknown sample was compared with a standard sample of thermally polymerized polystyrene- α -C¹⁴, which was obtained from the same batch of radioactive styrene at low conversion.

Determination of Copolymer Composition

Calculation of the copolymer composition was based upon a linear relationship between count rate and the amount of radioactive styrene units, which had been preliminarily proved to be valid under the present conditions. Errors in the determination of composition were estimated with 95% confidence.

Copolymer compositions of styrene-*p*-fluorostyrene copolymer were calculated based on fluorine analysis.

We gratefully acknowledge the support given by the Wright Air Development Division, Dayton, Ohio, under Contract No. AF33(616)-6866.

The authors also appreciate the helpful suggestions in radioactive analysis given by Dr. Joseph Steigman of the Polytechnic Institute of Brooklyn.

References

1. Overberger, C. G., and E. B. Davidson, *J. Polymer Sci.*, **62**, 23 (1962).
2. Carrick, W. L., F. J. Karol, G. L. Karapinka, and J. J. Smith, *J. Am. Chem. Soc.*, **82**, 1503 (1960).
3. Natta, G., and G. Crespi, *Chim. e ind. (Milan)*, **41**, 23 (1959).
4. Natta, G., G. Mazzanti, A. Valvassori, and G. Pajaro, *Chim. e ind. (Milan)*, **39**, 733 (1957).
5. Natta, G., G. Mazzanti, A. Valvassori, and G. Sartori, *Chim. e ind. (Milan)*, **40**, 717 (1958).
6. Reding, F. P., and E. R. Walter, *J. Polymer Sci.*, **37**, 555 (1959).
7. Murahashi, S., S. Nozakura, and M. Sumi, *Bull. Chem. Soc. Japan*, **33**, 1170 (1960).
8. Natta, G., F. Danusso, and D. Sianesi, *Makromol. Chem.*, **30**, 238 (1959).
9. Hodes, W., and A. Drucker, *J. Polymer Sci.*, **39**, 549 (1959).
10. Overberger, C. G., and F. Ang, *J. Am. Chem. Soc.*, **82**, 929 (1960).
11. Danusso, F., and D. Sianesi, *Makromol. Chem.*, **28**, 253 (1958).
12. Hodnett, E. M., and A. W. Jensen, *J. Polymer Sci.*, **43**, 183 (1960).
13. Mowry, R., M. Renoll, and W. Huber, *J. Am. Chem. Soc.*, **68**, 1105 (1946).
14. Hirschberg, Y., *J. Am. Chem. Soc.*, **71**, 3241 (1949).
15. Bachman, G. B., and L. L. Lewis, *J. Am. Chem. Soc.*, **69**, 2022 (1947).

Résumé

On a copolymérisé le styrène avec le *p*-*tert*-butyl-, *o*-méthyl-2,6-diméthyl-, et le *p*-fluorostyrène employant comme catalyseur l'aluminium alcoyle-trichlorure de titane. La composition globale du produit montrait que les styrènes substitués étaient moins réactionnels que prévu pour un mécanisme conventionnel radicalaire ou ionique en solution. Cette constatation faisait supposer une interaction stérique spéciale de l'avant-dernière unité pour ce système hétérogène. Un copolymère styrène-*p*-*tert*-butylstyrène a été fractionné. On en déduit que celui-ci était composé de deux ou plus de copolymères de différentes compositions. Une situation similaire reste valable pour les autres cas, excepté pour le 2,6-diméthylstyrène, qui ne forme ni homopolymère ni copolymère. On a expliqué les résultats en acceptant ou bien la multiactivité du catalyseur, due à des différences d'activité locale ou un processus contrôlé par la diffusion.

Zusammenfassung

Copolymerisation von Styrol mit *p*-*tert*-Butyl-, *o*-Methyl-, 2,6-Dimethyl- und *p*-Fluorstyrol wurde mit Aluminiumalkyl-Titaniumtrichlorid als Katalysator durchgeführt. Die Bruttozusammensetzung der Polymerisate zeigte, dass substituierte Styrole eine geringere Reaktivität besitzen, als für den normalen Radikal- oder Ionenmechanismus in Lösung zu erwarten ist. Dieser Umstand führte zu der Annahme einer speziellen sterischen Einwirkung der vorletzten Monomereinheit auf den Wachstumsschritt in diesem heterogenen System. Die Fraktionierung eines Styrol-*p*-*tert*-Butylstyrolcopolymeren zeigte, dass es aus zwei oder mehr Copolymeren mit verschiedener Zusammensetzung besteht. Eine ähnliche Lage besteht für die anderen Fälle mit Ausnahme von 2,6-Dimethylstyrol, welches weder Homopolymere noch Copolymere lieferte. Zur Erklärung wurde entweder eine durch Unterschiede in den aktiven Stellen bedingte Multiaktivität des Katalysators oder ein diffusionskontrollierten Vorgang angenommen.

Received February 27, 1962

Differential Thermal Analysis of High Polymers.

VI. Comments on Some Material and Experimental Factors

BACON KE,* *Research Department, Amoco Chemicals Corporation, Whiting, Indiana*

Synopsis

Some factors in the differential thermal analysis (DTA) of high polymers were studied. A newly designed, small cell assembly was used in most of the work. The thermal history and, to a lesser extent, the molecular weight affect the size and shape of the thermogram, depending on the amount of crystallinity and the distribution of crystallite sizes in the polymer. Interference due to oxidation should be prevented in the characterization of a thermally unstable polymer. Large sample quantity may lead to multiple peaks in the thermogram. High heating rates result in more intense peaks but also shift peak positions. Thermogram profiles become distorted when the temperature-sensing thermocouple is placed in the sample.

INTRODUCTION

Recent applications of differential thermal analysis (DTA) have demonstrated its usefulness for studying both the physical states and various transition phenomena in high polymers.¹ Experimental factors in DTA have already been extensively reported for ordinary inorganic and organic materials.² Additional factors, however, are involved in polymeric materials because of the unusual molecular structure and associated properties of long-chain molecules. Some of the experimental factors pertaining to high polymers have been investigated. A simple cell assembly for studying melted polymer samples has been developed.

EXPERIMENTAL

Materials

Most experiments were conducted with the commercial high density polyethylene, Marlex 6000, Type 15. Polymethylenes of widely different molecular weights, corresponding to inherent viscosities of 1 and 12, respectively, were prepared from diazomethane with boron triethyl catalyst. Poly-4-methylpentene-1 was prepared with the use of titanium trichloride and triethylaluminum as the catalyst. Finely powdered MgO was used as the reference material.

* Present address: C. F. Kettering Research Laboratory, Yellow Springs, Ohio.

Apparatus and Procedure

The apparatus consists of a cell assembly, a differential thermocouple, a temperature programmer, and an x - y recorder plus a d.c. preamplifier. The cell assembly and procedure described earlier¹ were used for poly-4-methylpentene-1. A smaller cell assembly was used in all other experiments.

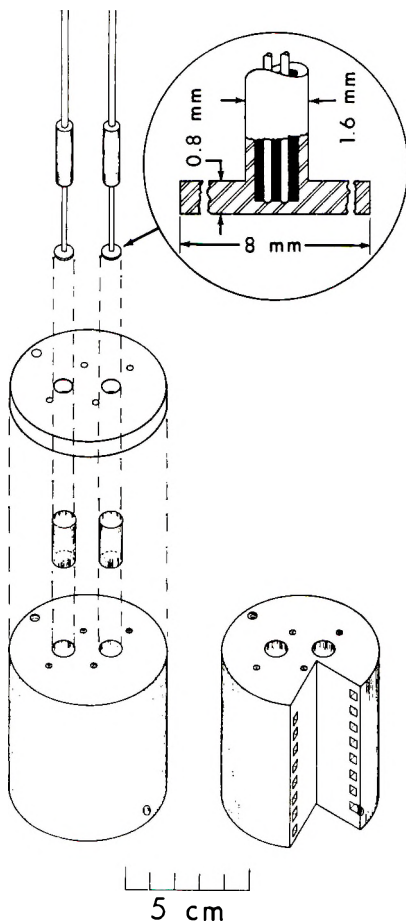


Fig. 1. Small cell assembly.

The smaller cell assembly, shown in the exploded view in Figure 1, consisted of a differential thermocouple (inset), two sample cells, a metal block for heating and cooling, and a heating mantle (not shown). The sample cells—thin-walled glass petticups, 10 mm. in diameter and 14 mm. high (Fisher Scientific)—are suitable for temperatures commonly used in polymer work. The stainless-steel block, 6.7 cm. in diameter and 5.3 cm. high, has two symmetrically located wells to hold the glass sample cells. Four other holes, 1.6 mm. in diameter, symmetrically located in the block, are

used for other accessory thermocouples. The block was made by pressing a $\frac{1}{8}$ in.-thick stainless-steel cylinder onto an inner block with $\frac{1}{8} \times \frac{1}{8}$ in. grooves on its surface. Cold air was passed through the spiral channel formed near the surface of the pressed block for controlled cooling experiments. Glass-Col heating mantles (250 cc. beaker size) were used up to 400°C. A 0.7 cm.-thick Transite disk having hole arrangement identical with that of the metal block was used as a mechanical shield and thermal insulator.

Besides the sheath-type thermocouples described previously,¹ disk-type thermocouples were also used, as shown in Figure 1. The metal disk conducts the heat uniformly between the polymer and the thermocouple junction. The stainless-steel disk, 0.8 mm. thick and 8 mm. in diameter, was welded to the thermocouple junction tip protected by a stainless-steel tubing, 1.6 mm. in diameter, as shown in the inset of Figure 1. The disk-type iron-Constantan thermocouples were made to order by Aero Research (Chicago) and can be obtained by ordering P/N T-5195-1BJ8A as matched pairs. They gave a practically straight horizontal line between room temperature and 200°C. when tested in the small cell block with the cells either empty or filled with equal amounts of a reference material.

The temperature programmer was a stepless proportioning temperature controller driven by a clock motor and appropriate gears.¹ A Moseley Model-5S Autograf *x-y* recorder was used for recording the thermograms. The preamplifier was a transistorized galvanometer (Kintel Model -204A). The temperature differential on the *y* axis was amplified 10³-fold; 1 in. of chart distance corresponds to 2°C.

SOME MATERIAL AND EXPERIMENTAL FACTORS

Some major factors in DTA, particularly those related to high polymers, have been investigated. The factors may be divided into those that depend on the sample and those that depend on the experimental procedure. Among the material factors studied are: the degree of crystallinity, either connected with the thermal history of the sample or molecular-weight entanglement, and the phenomena associated with thermal instability. Among the experimental factors studied are: the amount of material used, the heating (or cooling) rates, and the placement of the temperature (*X* axis)-driving thermocouple.

Effect of Thermal History or Molecular Weight on Crystallinity

Because the thermal history and molecular weight influence the crystalline state, e.g., degree of crystallinity, crystallite-size distribution, of crystalline high polymers, these variables should be specified in evaluating thermograms. It has been shown³ by DTA that in such semicrystalline polymers as polyesters the effect of thermal history is very pronounced. The effect of molecular weight on crystallinity is usually less pronounced than that of thermal treatments. The effects of molecular weight on crystallinity of low

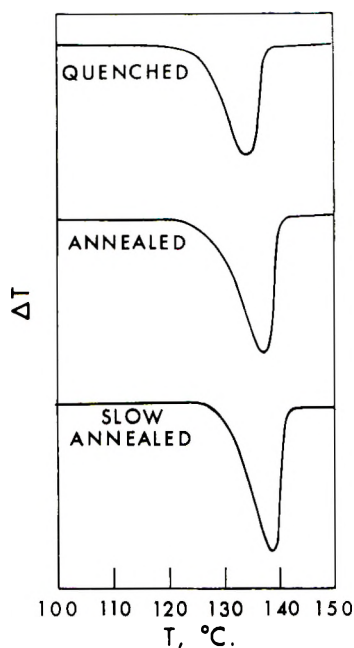


Fig. 2. Effect of thermal history on the melting thermogram of Marlex.

density⁴ and high density polyethylenes,⁵ as well as high density polyethylene fractions,⁶ have been reported.

A Marlex sample rapidly quenched from the melt in a cold air stream gave a thermogram noticeably different from that of one annealed, as shown in Figure 2. The thermogram of the rapidly quenched sample has a melting peak at 134°C., three degrees lower than that of the same sample melted and cooled at 1°C./min. The peak area is smaller by a little over 10%, and the initial departure from the thermogram baseline occurs about 7°C. lower. Marlex annealed and cooled more slowly at 0.1°C./min. gave a melting point at 138.5°C. and also a higher initial melting temperature. In the order of lowering cooling rates used here, the corresponding density value of the same Marlex sample were 0.959, 0.961, and 0.973 g./cc., respectively. The differences in the three thermograms obtained from the same sample but subjected to different thermal treatments indicate that the 2°C./min. heating rate is fast enough that no substantial recrystallization occurred during heating.

The effect of molecular weight on crystallinity is shown in Figure 3. Unfractionated polymethylene samples of inherent viscosities 1 and 12, or weight-average molecular weights of approximately 40,000 and 2,000,000, respectively, were identically treated by melting and then cooling at 0.1°C./min., and their thermograms are shown in Figure 3. The polymethylene of lower molecular weight yielded a narrow sharp peak at 136°C., whereas that of extremely high molecular weight with about 0.5% Santonox stabilizer present gave a slightly broader and shallower peak at 139°C. The peak

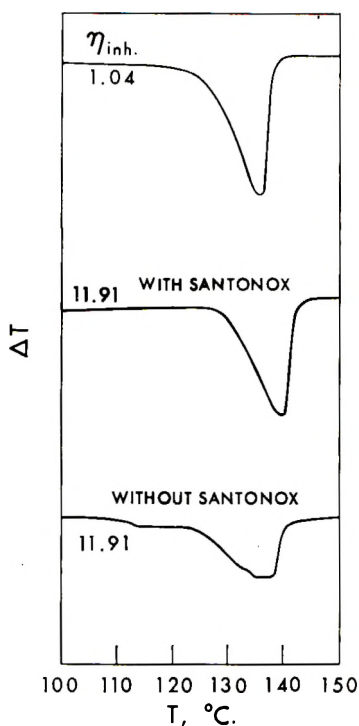


Fig. 3. Thermograms of polymethylenes of two widely different molecular weights.

area of the latter thermogram is smaller than that of the former. Without a stabilizer, the high molecular weight polymethylene yielded an even shallower thermogram; a premelting band started near 115°C ., and a peak occurred near 136°C .. Presumably some degradation resulted from the high temperature used in pressing the disk from the extremely elastic polymer of high molecular weight. Although the example in Figure 3 is rather extreme, it shows that supplementary information is often helpful or even necessary in interpreting DTA results.

Thermal Oxidation

Many high polymers oxidize at elevated temperatures. When DTA is used to characterize polymers, such oxidation reactions should be avoided if possible.

As an illustration, the thermograms of an isotactic poly-4-methylpentene-1 with and without an antioxidant are shown in Figure 4. With 1% Santonox, the polymer gave a well defined melting peak at 238°C .; without the antioxidant, the polymer also gave a melting peak at the same temperature but with a smaller peak area. Also, a pronounced exothermic peak appeared, starting at 178°C ., and peaking at 186°C ., which presumably represents an oxidation reaction. This behavior agrees with the recent finding⁷ that poly-4-methylpentene-1, among other polyolefins, has a

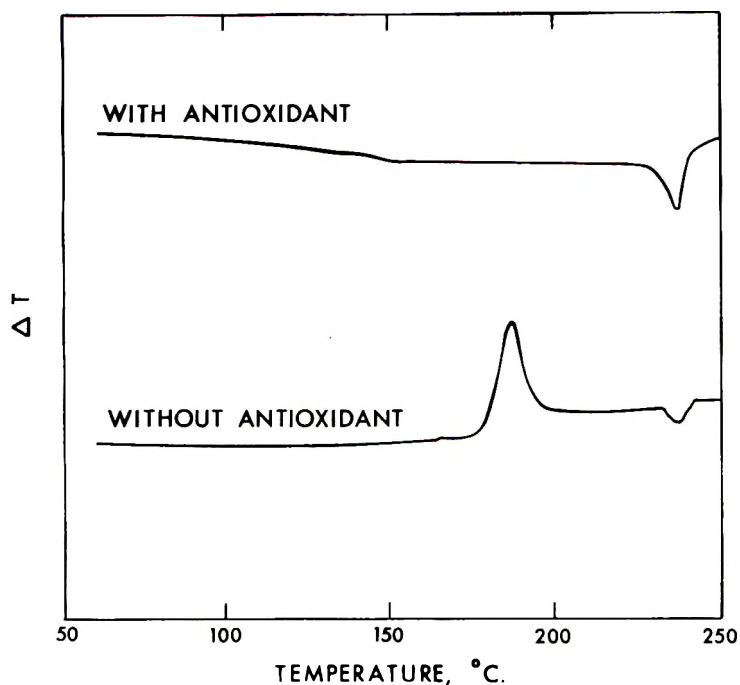


Fig. 4. Thermograms of poly-4-methylene-1 with and without antioxidant.

very high reactivity toward oxygen. It may also be related to the complex peak of an unknown character around 180°C. recently observed in the mechanical loss factor curve.⁸

In most polyolefin work, a trace amount of antioxidant is added to eliminate undesirable peaks that may complicate the thermogram interpretation. Using controlled atmosphere also prevents oxidation.^{9,10}

Sample Quantity

Experiments made with 0.05, 0.10, 0.15, 0.20, and 0.30 g. Marlex 6015 resulted in the thermograms shown in Figure 5. All samples were melt-pressed and annealed. As the cell diameter is fixed, different sample quantities gave different thicknesses of the polymer disks. For instance, 0.05 g. Marlex yields a disk slightly less than 1 mm. thick. Up to 0.15 g., the thermogram has a single peak at 137°C., which agrees well with the maximum melting temperature obtained by hot-stage microscopy on the same material annealed in a similar manner. With 0.20 g., the thermogram has a shoulder at 137°C., but the final peak shifts to 140.5°C. At 0.30 g., the peak is shifted even higher (141.5°C.), with a shoulder remaining near 137°C. Moreover at 0.20 g. or higher, the peak broadens considerably. Although the peak areas increase with more polymer, the relationship deviates increasingly from direct proportionality at higher sample levels.

Because of the dynamic nature of DTA and the low thermal conductivity of high polymers, a temperature gradient is likely to develop within a larger

size sample at relatively high heating rates. The multiple peaks produced by samples of 0.20 g. or more clearly indicate this to be the case. Although one peak always occurred near 137–138°C., at large sample quantities, the

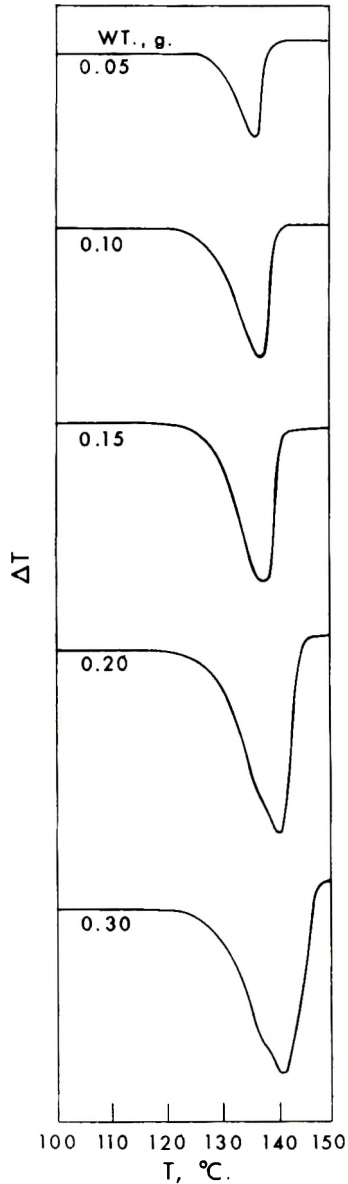


Fig. 5. Effect of sample quantity on the thermogram of Marlex.

final peak was shifted to higher temperatures. The shift represents a time lag in the melting of certain portions of the sample rather than an actual higher temperature required for melting. Hence, it would seem desirable

to use the smallest possible quantity of material sufficient to produce a detectable thermal effect.

Heating Rate

Annealed Marlex samples were heated at four different rates (1–4°C./min.); the thermograms are shown in Figure 6. Peak areas and heights are given in Table I.

The peak areas are directly proportional to the heating rates. Mathematically, the peak area is represented by $\int \Delta T dT$, where ΔT is the temperature differential and T the temperature, which varies linearly with time. An identical numerical value, therefore, should be obtained from this integral function at all four heating rates. The peak height or the maxi-

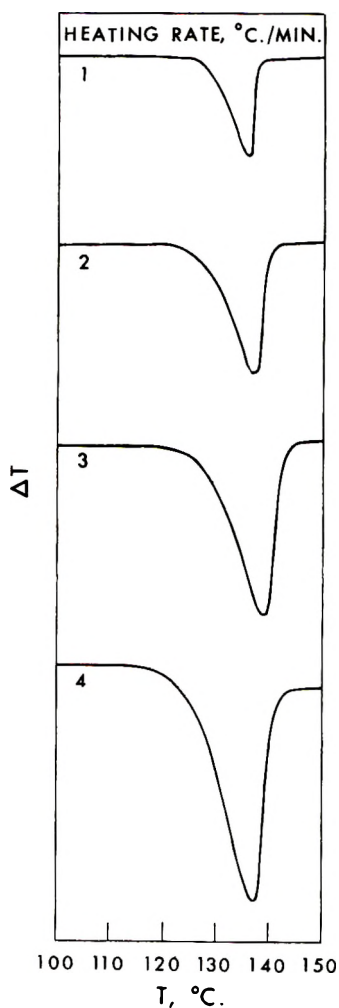


Fig. 6. Effect of heating rate on the thermogram of Marlex

TABLE I

Rate, °C./min.	Peak temp., °C.	Peak area, cm. ²	Peak height, °C.
1	136.7	2.1	2.0
2	137.0	3.9	2.8
3	138.4	6.0	4.0
4	139.0	8.0	4.5

imum temperature differential, however, does not follow the linear relationship. This means that not ΔT alone, but the entire integral function, $\int \Delta T dT$, or the peak area, more correctly represents the heat of transition. At the four heating rates studied, the peak temperature of the thermograms shifted slightly. The shift in peak position can again be ascribed to a time lag in the completion of the melting process rather than an actual higher temperature required.

In DTA work, heating rates from 0.5 to 100°C./min. have been used;² the commonly used heating rates range from 8 to 15°C./min. High heating rates usually produce more intense peaks; however, the peak positions are also shifted toward higher temperatures. Although peak temperature varies slightly in a narrow range of heating rates, the more correct transition temperature is obviously obtained at a lower heating rate.

In general, the melting points estimated from the peak position can be expected to agree well with the so-called maximum melting point of a polymer—the temperature at which the last trace of crystallinity disappears—determined by hot-stage microscopy. In broad crystallite distribution, where a small percentage of large crystallites persists far beyond the majority of the crystallites, the melting point determined by the optical method is likely to be higher than that measured by the thermogram peak position.¹¹ In such cases, the return from the peak to the baseline becomes slower, and the correct melting point may have to be estimated from some point beyond the peak position.

The dynamic nature of DTA and sometimes the sensitivity of the measuring system may demand the use of a sufficient amount of material and a finite heating rate. In such cases, a correction may be needed to obtain melting points approximating the equilibrium temperatures obtained by other methods. The correction can be made by simply extrapolating experimental data to low sample quantity and low heating rate.

Placement of the Temperature-Sensing Thermocouple

In the DTA literature, a wide variety of practices on the placement of the temperature-measuring thermocouple can be found. Among the possible locations are the heating bath or block, the sample, or the reference.² In our previous work, the temperature-sensing thermocouple was placed in the heating block. At the relatively low heating rates of 1–2°C./min., the temperatures of the bath, the sample, and the reference material are practically identical.

The effect of thermocouple placement on the thermogram profile was studied by examining two annealed Marlex samples, 0.10 g. each. A small iron-Constantan-thermocouple bead made from 30-gauge wires was placed on the bottom of the cell while the polymer disk was being melt-pressed and annealed. The thermogram obtained by using the thermocouple bead placed in the polymer sample as the temperature-sensing or x axis-driving thermocouple is shown in Figure 7A. A regular thermogram obtained by using a temperature-sensing thermocouple inserted in the block is shown in Figure 7B. Both arrangements have an identical thermocouple bead imbedded in the sample, except that in the latter, the thermocouple served only as a dummy. For comparison purposes, the actual

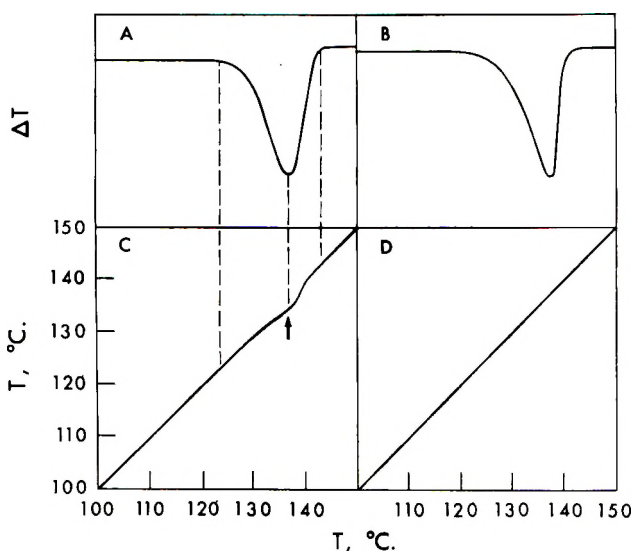


Fig. 7. Effects of placement of the temperature-sensing thermocouple on the thermogram of Marlex.

temperatures of the sample and the reference (or block) were also recorded as a function of the block temperature and are shown below the corresponding thermograms.

In melting, heat absorption in the sample causes a cooling effect or a temperature lag, as seen in Figure 7C. When a thermocouple is imbedded in the sample, this lag would result in a slight distortion of the thermogram profile, as seen from Figures 7A and 7B. When the melting thermogram profiles are used as a first approximation for the crystallite-size distribution or change in crystallinity as a function of temperature, such distortions make the estimations less valid. Much greater peak distortion could result from placing the x axis-driving thermocouple in the sample when heated at a higher rate. It has recently been shown that at 10°C./min. heating rate, the entire endothermic peak could even be bent toward the left, especially when a fine-gauge wire was used.¹²

The x axis-driving thermocouple may be placed in the sample if only a constant, single-point transition temperature is the subject of interest.¹² However, placement in the block or reference would be more likely to yield a meaningful melting profile as well as precise and reproducible transition temperatures.

References

1. Ke, B., in *Organic Analysis*, Vol. 4, John Mitchell, Jr., I. M. Kolthoff, E. S. Proskauer, and A. Weissberger, Eds., Interscience, New York, 1960.
2. Smothers, W. J., and Y. Chiang, *Differential Thermal Analysis: Theory and Practice*, Chemical Publishing Co., New York, 1958.
3. Ke, B., *J. Appl. Polymer Sci.*, **6**, 624 (1962).
4. Richards, R. B., *J. Appl. Chem.*, **1**, 370 (1951).
5. Burch, G. N. B., E. B. Feild, F. H. McTigue, and H. M. Spurlin, *SPE J.*, **13**, 34 (1957).
6. Tung, L. H., and S. Buckser, *J. Am. Chem. Soc.*, **62**, 1530 (1958).
7. Winslow, F. H., and W. Matreyek, paper presented at the 141st meeting of the American Chemical Society, Washington, D. C., March 1962.
8. Griffith, J. H., and B. G. Rånby, *J. Polymer Sci.*, **44**, 369 (1960).
9. Danusso, F., and G. Polizzotti, *Chim. Ind. (Milan)*, **44**, 241 (1962).
10. Nechitailo, N. A., I. M. Tolchinskiĭ, and P. I. Sanin, *Plasticheskie Massy*, **7**, 3 (1960).
11. Ke, B., *J. Polymer Sci.*, **42**, 15 (1960).
12. Vassallo, D. A., and J. C. Harden, *Anal. Chem.*, **34**, 132 (1962).

Résumé

On a étudié certains facteurs de l'analyse thermique différentielle (DTA) de hauts polymères. Dans la plupart de ces travaux on a employé un nouvel appareil avec un petit récipient. L'histoire thermique, et moins fort, le poids moléculaire, ont une influence sur les dimensions et la forme du thermogramme, qui est fonction du degré de cristallinité et de la distribution des cristallites de dimensions différentes dans le polymère. Des interférences qui sont dues à l'oxydation des polymères thermiquement instables, doivent être empêchées. Un échantillon en grande quantité peut faire apparaître plusieurs pics dans le thermogramme. Un chauffage intense augmente l'intensité des pics mais change aussi leur place. Le profil du thermogramme est altéré quand on place le thermocouple dans l'échantillon même.

Zusammenfassung

Einige bei der Differentialthermoanalyse (DTA) von Hochpolymeren auftretenden Grössen wurden untersucht. Eine neu entworfene Kleinzellenanordnung wurde im grössten Teil der Arbeit verwendet. Die thermische Vorgeschichte und, in geringerem Ausmass, das Molekulargewicht haben Einfluss auf Grösse und Gestalt des Thermogramms, das durch die Menge des kristallinen Anteils und die Kristallitgrössenverteilung im Polymeren bestimmt wird. Bei der Charakterisierung eines thermisch instabilen Polymeren sollten Vorkehrungen gegen Störungen durch Oxydation getroffen werden. Eine gross Probenmenge kann zu Mehrfachspitzen im Thermogramm führen. Hohe Erhitzungsgeschwindigkeit führt zu intensiveren Spitzen, verschiebt aber auch die Lage der Spitze. Bei Anbringung des Thermolement-Temperaturfühlers in der Probe wird das Thermogrammprofil verzerrt.

Received September 26, 1962

Some Novel Effects in Solution Polymerization*

D. B. ANDERSON, G. M. BURNETT, and A. C. GOWAN,
Department of Chemistry, University of Aberdeen, Old Aberdeen, Scotland

Synopsis

The polymerization of methyl methacrylate initiated by 2,2'-azoisobutyronitrile in the presence of halogenated benzenes and naphthalene has been investigated. In each case the order of reaction with respect to monomer is apparently of an order less than unity. Suggestions as to the possible participation of the solvent in the initiation process are discussed and shown to be in agreement with experimental measurements.

The effect of solvent on the rate and course of radical polymerization has been studied by a number of investigators.¹⁻¹¹ In all of these instances varying orders of reaction with respect to monomer have been reported and in time it was realized that the simple transfer reaction between growing polymer radical and solvent molecule gave rise to new free radicals which could participate in the termination reaction. Direct measurements of the polymerization of vinyl acetate in benzene have shown that the contribution from the interaction of transfer radical and growing radical is significant even at 95% monomer concentration.¹²

This paper describes another effect of solvent participation which has not been previously reported. Early work had demonstrated that vinyl acetate and benzene form a copolymer¹³ and that bromobenzene is apparently not incorporated in polystyrene formed in bromobenzene solution.¹⁴ The copolymerization of benzene with vinyl acetate and also methyl methacrylate has been confirmed¹⁵ with the use of ¹⁴C benzene and the absence of bromobenzene when polymer is formed in such solutions has been verified. Rate measurements in bromobenzene and related solvents have revealed anomalous effects which for methyl methacrylate give an apparent order of reaction of less than unity with respect to monomer. Similar results are recorded for the addition of naphthalene.

Experimental

Monomers. These were freed from stabilizers, washed and dried, and distilled in an inert atmosphere. Before use, samples were prepolymerized to about 4% conversion and distilled under high vacuum conditions.

Solvents. These were thoroughly dried and distilled through efficient fractionating columns. Samples labelled with ¹⁴C were obtained from U.K.A.E.A., Amersham.

* Presented at the IUPAC International Symposium on Macromolecular Chemistry, Moscow, June 1960.

Initiators. These were purified by recrystallization from the usual solvents or by distillation where applicable. The purified samples were stored at low temperature.

The reactions were followed by dilatometrically duplicate runs being used by filling two or more dilatometers with identical mixtures. All manipulations were carried out under high vacuum in rigorously oxygen-free conditions. The experimental procedure was similar to that used by Burnett and Loan.⁸

The method assay of radioactive polymeric samples was essentially the same as that used by Bevington et al.¹⁴

Results

The fractional rates of conversion of methyl methacrylate in benzene and bromobenzene solutions are compared in Figure 1, the reactions being carried out at 60° in the presence of 2,2'-azoisobutyronitrile (AZBN) (1.66 g./l.). It will be clearly seen that while in benzene solution the rate of reaction is close to first order with respect to monomer over quite a wide range of concentration, this is not true for bromobenzene for which there is a maximum in the curve. At any given monomer concentration the rate of reaction is proportional to the square root of the initiator concentration in accord with the concept of radical interaction as the chain termination reaction.

The effect of substituent was studied, with the results shown in Table I. It will be noted that the effect increases with decreasing electronegativity of the substituent.

Very similar behavior is noted when naphthalene is added in varying

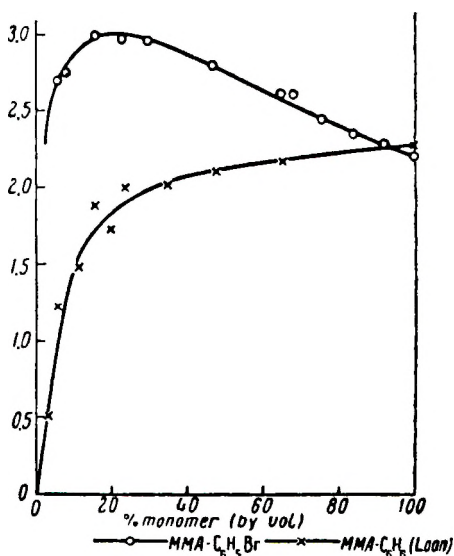


Fig. 1. Polymerization of methyl methacrylate in benzene and bromobenzene at 60° with AZBN (1.66 g./l.) as initiator. Ordinate: rate, %/min. $\times 10$.

TABLE I
Relative Rates of Conversion in Halogenobenzene Solution
(Monomer, methyl methacrylate, 22.4 mole-%;
initiator, AZBN, 1.66 g./l.; temperature, 60°)

Solvent	Rate, %/min.
None (bulk)	0.221
Benzene	0.19
Chlorobenzene	0.253
Bromobenzene	0.295
Iodobenzene	0.346

proportions to methyl methacrylate (Fig. 2), although in this case the curve is convex to the monomer axis. It is not possible to investigate the whole curve, owing to saturation of the solution, so that the point at 30% monomer is very likely to be in error.

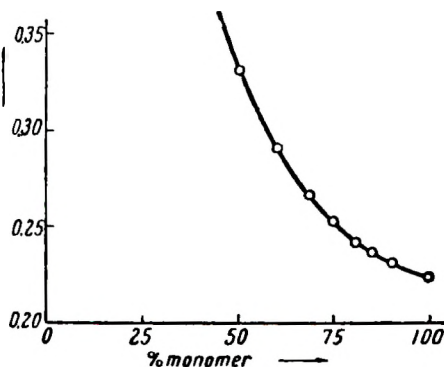


Fig. 2. Polymerization of methyl methacrylate in presence of naphthalene at 60° with AZBN (1.66 g./l.) as initiator. Ordinate: rate, %/min.

In all the systems so far described, AZBN was used as initiator and, since it was likely that the effect was brought about by participation of solvent in the initiation step, the effect with other initiators was examined. The initiators used were benzoyl peroxide (BP), di-*tert*-butyl peroxide (DTBP), and azocyclohexyl nitrile (AHN). In all cases the results conformed to the pattern already described, except for methyl methacrylate-naphthalene-BP, for which the reaction was of first order with respect to monomer (Fig. 3).

If the effect is the result of increased rate of production of free radicals by the initiator under the influence of solvent, then this should be detectable by measurement of the initiator efficiency in the manner advocated by Bevington et al.¹⁷ In the case of methacrylate-naphthalene-azo initiator systems, variation of the efficiency of initiation was noted. This measurement was based on the assumption that the rate of decomposition of the initiator was independent of the presence of naphthalene. Equally it could be interpreted as an increase in the rate of initiator decomposition. Results are set out in Table II.

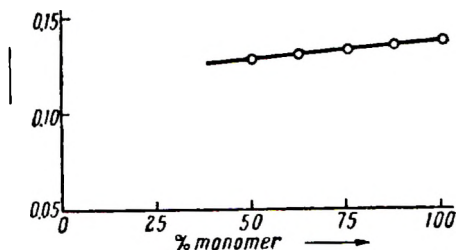


Fig. 3. Polymerization of methyl methacrylate in presence of naphthalene at 60° with BP as initiator. Ordinate: rate, %/min.

TABLE II
Initiation Efficiencies for Methacrylate Polymerization in Various Solvents

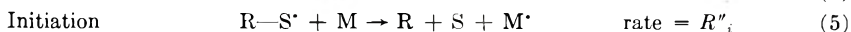
Methacrylate, %	Rate, mole l. ⁻¹ sec. ⁻¹	Efficiency, <i>e</i>
<i>C</i> ₁₀ <i>H</i> ₈ —AZBN (1.67 g./l.)		
100	3.32	0.38
84	2.95	0.44
75	2.82	0.49
60	2.51	0.57
<i>C</i> ₁₀ <i>H</i> ₈ —AHN (10 g./l.)		
100	8.10	0.39/ <i>k</i> _d
75	6.89	0.48/ <i>k</i> _d
50	5.31	0.56/ <i>k</i> _d
<i>C</i> ₆ <i>H</i> ₅ Br—AZBN		
100	—	0.38
70	—	0.42
23	—	0.37
23 (<i>C</i> ₆ <i>H</i> ₅ Cl)	—	0.39
23 (<i>C</i> ₆ <i>H</i> ₅ I)	—	0.40

Discussion

Of the results reported above the following are of greatest significance.

1. Increase in fractional rate with dilution, i.e., order of reaction < 1.
2. In no case are solvent fragments incorporated in the polymer.
3. The behavior depends on the initiator type.
4. Initiator efficiency (or decomposition rate) is not always affected.

In devising any scheme to account for the phenomenon it is necessary to consider all of these factors. Kinetically speaking, a satisfactory scheme can be devised in the following manner:



In order to accord with experiment, (3) must be independent of monomer and of (4). Competition between (3) and (4) for R' could increase the initiation rate but would lead to a diminution of the amount of nitrile present in the polymer at high dilutions. The direct initiation rate, *R'*_{*i*},

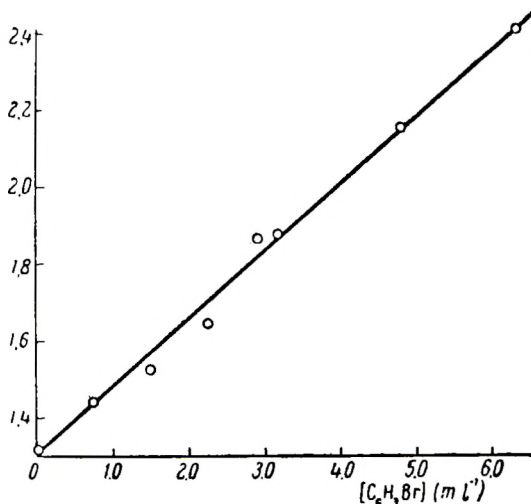


Fig. 4. Rate of polymerization as a function of solvent concentration for the system methyl methacrylate–bromobenzene–AZBN. Ordinate: R_f^2 (sec.⁻² × 10⁴).

is proportional to AZBN concentration while solvent initiation, R''_i , is proportional to both AZBN and solvent concentrations, so that total initiation rate is:

$$R_i = k'(AZBN) + k''(AZBN)(S)$$

where $k' = 2ek_a$, k_a being the rate constant for (1). If the rate of polymerization is proportional to monomer concentration then the fractional rate R_f is given by

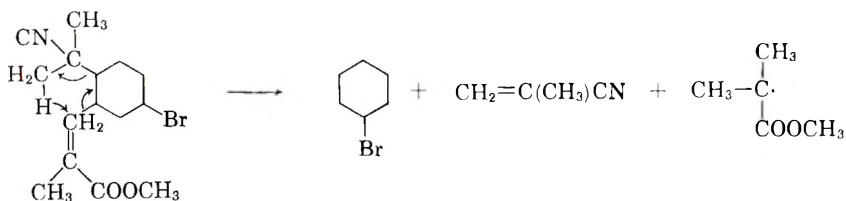
$$R_f = k_p k_t^{-1/2} R_i^{1/2} \quad (6)$$

or, substituting for R_i

$$R_f^2 = k_p^2 k_t^{-1} (AZBN) [k' + k''(S)]$$

For bromobenzene as solvent, the plot of R_f^2 against (S) with $(AZBN)$ constant should therefore be linear with the slope/intercept ratio = k''/k' . The relevant data are plotted in Figure 4, the linearity of which is obvious and one may deduce that $k''/k' = 1.7 \times 10^{-10}$ mole⁻¹ l. and so $k'' = 1.8 \times 10^{-5}$ mole⁻¹ l. sec.⁻¹. It is of some importance that, according to Basu et al.,¹⁸ the rate of thermal polymerization of methyl methacrylate in halogeno benzenes is independent of the solvent.

Although the scheme as outlined does agree with the rate measurements, the precise chemistry remains obscure. It is, however, possible to visualize that initiator radical add to bromobenzene in the *para* position, to give a new radical species which could add monomer at the *meta* position to Br and give:



Alternatively, the radical adduct $R-S^{\cdot}$ could abstract hydrogen from (or donate to) monomer, to initiate a new chain. Any of these possibilities would give the required experimental observations.

With naphthalene systems the interpretation has to be varied somewhat, since in most instances with azo initiators there is an increased incorporation of initiator in the polymer but there is no concomitant increase in naphthalene incorporation. These two facts are irreconcilable in the above scheme, but so far no satisfactory alternative has been evolved.

So far the effect described is confined to methyl methacrylate monomer and no similar effect is found for vinyl acetate. Further substitution of tetralin for naphthalene indicates that the methacrylate polymerization reverts to the benzene case.

The authors wish to thank the University of Aberdeen, Monsanto Chemicals (D.B.A.), and the Department of Scientific and Industrial Research (A.C.G.) for financial support during the prosecution of this work.

References

1. Schulz, Husemann, *Z. phys. Chem.*, **B39**, 246 (1938).
2. Medvedev, Kameniskaya, *Acta physicochim.*, **13**, 565 (1940).
3. Mark, Josefowitz, *Polymer Bull.*, **1**, 140 (1945).
4. Maetheson, *J. Chem. Phys.*, **13**, 584 (1945).
5. Burnett, Melville, *Discussions Faraday Soc.*, **2**, 327 (1947).
6. Tkachenko, Khomikovskii, Medvedev, *Zh. fiz. khimii*, **25**, 823 (1951).
7. Conix, Smets, *J. Polymer Sci.*, **10**, 525 (1953).
8. Burnett, Loan, *Trans. Faraday Soc.*, **51**, 214, 219, 226 (1955).
9. Allen, Merrett, Scanlan, *Trans. Faraday Soc.*, **51**, 95 (1955).
10. Jenkins, *J. Polymer Sci.*, **29**, 245 (1958).
11. Jenkins, *Trans. Faraday Soc.*, **54**, 1885 (1958).
12. Burnett, Elder, unpublished results.
13. Peebles, Stockmayer, *J. Am. Chem. Soc.*, **75**, 2278 (1953).
14. Mayo, *J. Am. Chem. Soc.*, **75**, 6133 (1953).
15. Anderson, Burnett, unpublished results.
16. Bevington, Guzman, Melville, *Proc. Roy. Soc.*, **A221**, 437 (1954).
17. Bevington, Bradbury, Burnett, *J. Polymer Sci.*, **12**, 469 (1954).
18. Basu, Sen, Palit, *Proc. Roy. Soc.*, **A202**, 485 (1950).

Résumé

On a étudié la polymérisation du méthacrylate de méthyle initiée par le 2,2'-azoisobutyronitrile en présence de benzène et naphthalène halogénés. Dans chaque cas l'ordre apparent de la réaction par rapport au monomère est inférieur à l'unité. Des hypothèses faisant intervenir le solvant dans le processus d'initiation sont soumises à la discussion; elles s'accordent avec les mesures expérimentales.

Zusammenfassung

Die Polymerisation von Methylmethacrylat wurde bei Anregung mit 2,2'-Azobutyronitril in Gegenwart von halogenierten Benzolen und Naphthalin untersucht. In allen Fällen ist die Ordnung der Reaktion in bezug auf das Monomere offenbar kleiner als eins. Eine Teilnahme des Lösungsmittels am Startvorgang wird als möglich betrachtet. Eine solche Annahme steht mit den Versuchsergebnissen in Übereinstimmung.

BOOK REVIEW

N. G. GAYLORD, Editor

Makromolekulare Stoffe. Part I, Vol. XIV. Methoden der Organischen Chemie (Houben-Weyl), E. MÜLLER, Ed., Georg Thieme Verlag, Stuttgart, 1961. lxiv + 1360 pp. \$71.75.

This book is the first part of Volume 14 of the renowned Houben-Weyl series on the methods of organic chemistry. In keeping with the emphasis in this whole series, the primary interest of the authors is in methods of preparation and in reactions, i.e., in this case in the organic aspects of polymer chemistry. Unlike some other books in this field, the task of presenting preparative methods is approached in the grand manner. The treatment is designed to be a comprehensive account of laboratory procedures and industrial processes. The presentation is so thorough that, in spite of the enormous size of this book, it covers only the preparation of polymers of vinyl and divinyl compounds. Part II, to be published later, will be concerned with polycondensation, ring-opening polymerization, reactions and characterization of polymers.

The book begins with a discussion of the nomenclature and terminology of polymer chemistry. (The reviewer was pleased to note that the German word "Blockpolymerisation" no longer refers to bulk polymerization, but now has the same meaning as in English.) Two long chapters explain bulk and solution polymerization, and heterogeneous-phase polymerization. The discussion is illustrated with diagrams of apparatus and numerous detailed polymerization procedures. Important equations are presented, but the emphasis is on the preparative methods rather than on theory. The book concludes with a chapter of over 600 pages dealing with special methods of polymerization for the most important monomers.

In a book of this size it is a difficult task to assess the comprehensiveness of the topics studied. It is felt that, on the whole, the authors have succeeded admirably in covering all important subject matter. Even the lesser topics are not neglected; the discussion of allyl compounds is excellent. However, the reviewer would have liked to see a more detailed coverage of propylene and the higher straight-chain olefins, which are given only five pages as compared to 52 for polyethylene.

This book gives ample evidence of careful editorial work. There are numerous references, some as recent as 1961 (a remarkable feat!). The subject index is 55 pages long and there is a detailed table of contents. A useful feature is a list of books on polymer chemistry presented in chronological order. The printing, paper, and binding are excellent.

Contributors to Part I are as follows: H. Logemann, H. Bartl, J. Nógrádi, K. Bodenbenner, H. Wilms, G. Pieper, and H. Gröne of *Farbenfabriken Bayer*; W. Kern, R. C. Schulz, H. Cherdron, and V. Jaacks of *University of Mainz*; E. Trommsdorf, F. Kollinsky, R. Kretz, H. Rauch-Puntigam, H. Schreiber, G. Schröder, K. Tessmar, T. Völker, and A. Wohnhas of *Röhm & Haas, G. m. b. H.*; W. Franke, H. Weber, K. Kopetz, and O. Glosaner of *Chemische Werke Hüls*; and H. Güterbock of *Badische Anilin- und Soda-fabrik*.

This book will be of great value to every laboratory concerned with the preparation of polymers.

Norbert M. Bikales

Gaylord Associates Inc.
Newark, New Jersey

ERRATA

The Dependence of the Stereospecific Action of the Complex Catalyst $\alpha\text{-TiCl}_3\text{-Me}(\text{C}_2\text{H}_5)_n$ during the Polymerization of α -Olefins on the Metal in the Metalloorganic Compound

(article in *J. Polymer Sci.*, **62**, S104-S105, 1962)

By A. P. FIRSOR, B. N. KASHPROV, YU. V. KISSIN, and N. M. CHIRKOV
Academy of Sciences, U.S.S.R., Moscow, U.S.S.R.

On page S104 the 2nd line in the article should read "... the catalyst $\alpha\text{-TiCl}_3\text{-Me}(\text{C}_2\text{H}_5)_n$], ..."

On page S105 in Table I under Fraction II, delete the comma after cold.

The 2nd author in reference 2 is J. Pasquon.

The 2nd author of the article is B. N. Kashpozov.

Rheology of Polytetrafluoroethylene

(article in *J. Polymer Sci.*, **A1**, 483-489, 1963)

By A. V. TOBOLSKY, D. KATZ, and M. TAKAHASHI
Frick Chemical Laboratory, Princeton University, Princeton, New Jersey

On page 486, Figure 4 lower abscissa scale should read as follows:

220, 240, 260, 280

$T - T_g$ ($^{\circ}\text{K.}$)

Studies on the Configuration and Conformation of Vinyl-Type Polymers. II. Temperature Dependence of the Infrared Spectrum of Polyvinyl Chloride in Solution and Stereoregularity

(article in *J. Polymer Sci.*, **57**, 383-393, 1962)

By MASATAMI TAKEDA and KAZUYOSHI IIMURA
Department of Chemistry, Tokyo College of Science, Kagurazaka, Shinjuku-ku, Tokyo, Japan

On page 393, line 25: the value of 10.3 should read 0.3.

Some Mechanical Aspects of the Swelling and Shrinking of Polymeric Solids. Part I. External and Internal Restraints

(article in *J. Polymer Sci.*, **58**, 821-837, 1962)

By B. ROSEN
Westinghouse Electric Corp., Research Laboratories, Churchill Boro, Pittsburgh, Pennsylvania

On page 827, our k in the Flory equation implies the modulus of rigidity.

On page 829, the lower mechanical model of Figure 3 should be maintained at the same strain as that in the upper model.

On pages 831-832, for $e - t/\tau$, read $\exp\{-t/\tau\}$.

On pages 836-837, the English synopsis, which differs from those in French and German, should be regarded as the appropriate one.